Bivalve Biomineralization in a Changing Climate: Investigating Marine Mussel Calcification Patterns over Seasons to Millennia

By

VERONICA PADILLA VRIESMAN

DISSERTATION

Submitted in partial satisfaction of the requirements for the degree of

DOCTOR OF PHILOSOPHY

in

Earth and Planetary Sciences

in the

OFFICE OF GRADUATE STUDIES

of the

UNIVERSITY OF CALIFORNIA

DAVIS

Approved:

Sandra Carlson

Tessa Hill

David Gold

Committee in Charge

2022

## Table of Contents

**Appendices**

**Acknowledgements**

I would like to thank my co-advisors, Sandy Carlson and Tessa Hill, for their scientific guidance, professional mentorship, and compassion. I have learned so much from both of them. I would also like to thank David Gold for his support as both a committee member and a co-instructor. I am grateful that he was always very supportive of graduate student endeavors. I am also deeply grateful to all of the people who provided access to samples, space, tools, and equipment. Among them, I would especially like to thank Greg Baxter for making superb thin sections, Jackie Sones for providing access to intertidal mussels in the Bodega Marine Reserve, Ann Russell for offering me Bodega Bay mussel shells, Elizabeth Bullard for sharing San Diego mussels with me, and John Grimsich for helping to run the SEM and EBSD at UC Berkeley. I am so appreciative of my supportive and talented lab mates in the Ocean Climate Lab both past and present. I especially would like to acknowledge Lena Capece, Cait Livsey, and Alyssa Griffin for their friendship. I want to thank the students and mentees that I have had the pleasure to work with and learn from over the past few years. My friends and family provided so much support, encouragement, and laughter – which is critical for navigating graduate school during a global pandemic. I especially want to thank my cousins, Hector and Erin Vallejo, and my goddaughter, Juliana, for always being there for me throughout this journey. I am deeply grateful to my mom and dad for their infinite love, support, and interest in my work. They have always made me feel like I can do anything. Finally, I want to thank my incredible partner, Z, for the joy, perspective, confidence, and levity that he helps bring to each day. He and our two cats, Bagheera and T'Challa, are wonderfully supportive study companions. This dissertation is dedicated to the memory of my grandparents, Dionicio and Martina Padilla.

**Abstract**

The California mussel (*Mytilus californianus*) is an ecologically and culturally important bivalve mollusc species that provides a habitat for hundreds of other taxa throughout rocky intertidal environments along the Pacific Coast of North America. *Mytilus californianus* is a well-studied organism in the fields of coastal archaeology and marine ecology, but an improved understanding of its shell structure, life-history traits, and calcification patterns could provide valuable insights paleo-seasonality or paleoceanography of Holocene coastal environments. Here, I investigated shell characteristics of *M. californianus* across a variety of spatial and temporal scales in order to assess and optimize its utility as a biogenic archive. By applying morphometrics, optical microscopy, and geochemical data-synthesis methods to modern, historic, and Holocene *M. californianus* shells collected throughout the California Current System, I established relationships between growth banding and seasonality, documented the influence of micro-habitat on shell growth, characterized stable isotopic variability over seasonal, ontogenetic, and millennial scales, and identified regional differences in calcification patterns. I present evidence for rapidly shifting calcification patterns in northern California mussels from the early 2000s to 2020, including thinner inner calcite layers and lowered contrast between dark-light growth bands. Shifting shell characteristics were correlated with greater temperature extremes, heightened temperature variability, and more intense upwelling in the past few years relative to the early 2000s. Northern populations of *M. californianus* preferentially grow their shells during stable, moderate periods (mean monthly temperature near 13°C) with low variability (< 5 C° seasonal temperature range), as indicated by calcite-rich light bands. I then expanded the geographic and temporal scope to characterize geochemical variability of *M. californianus* shells throughout southern California over millennial scales. By synthesizing the

ample published stable isotope records from archaeological mussel shells of the Channel Islands, California, I found that individual analysis of complete stable isotope profiles of many shells offers more valuable paleobiological and paleo-seasonal insights, including an $\delta^{18}O$-inferred annual seawater temperature range of ~ 5°C in the Channel Islands. Collectively, stable isotope data from mussels revealed both millennial-scale isotopic variability indicative of Holocene warm-cool oscillations and an east-west temperature gradient characteristic of the modern-day Channel Islands. However, *M. californianus* shells exhibited highly variable intra-individual $\delta^{18}O$ values depending on micro-environment and ontogeny, complicating the use of aggregated stable oxygen and carbon isotope data from many individuals as an annually resolved climate proxy. Finally, I investigated changes in shell morphology, growth banding, and microstructure over the twentieth century in *M. californianus* shells from the southern portion of the California Current System (Santa Barbara through Baja California Sur). Shell thickness, morphology, the percentage of calcite-rich light bands, and the contrast between dark-light banding remained unchanged throughout all study sites in southern California and the Baja California peninsula. It is likely that southern populations of *M. californianus* are adapted to warmer conditions, while mussels from regions farther north in the California Current System may be more susceptible to warming waters. *Mytilus californianus* is a complex yet useful archive of environmental variability. Its shell records its environment over seasonal to millennial scales, depending on a variety of factors such as ontogenetic age, tidal position, and the sampling technique. I conclude that *M. californianus* can serve as a valuable record when multiple approaches are applied in tandem: analysis of the growth band pattern, ontogenetic stable isotope profiles, shell morphometrics, and microstructural imaging in one individual, and then across multiple individuals from many sites through time.

## Chapter 1

## Investigating controls of shell growth features in a foundation bivalve species: seasonal trends and decadal changes in the California mussel


### Abstract

Marine bivalve mollusk shells can offer valuable insights into past oceanographic variability and seasonality. Given its ecological and archaeological significance, *Mytilus californianus* (California mussel) presents the opportunity to examine seasonal and decadal changes recorded in its shell over centuries to millennia. While dark–light growth bands in *M. californianus* shells could be advantageous for reconstructing past environments, uncertainties remain regarding shell structure, environmental controls of dark–light band formation, and the amount of time represented by a dark–light pair. By analyzing a suite of *M. californianus* shells collected in 2002, 2003, 2019, and 2020 from Bodega Bay, California, we describe the mineralogical composition; establish relationships among growth band pattern; micro-environment; and collection season; and compare shell structure and growth band expression between the archival (2002–2003) and modern (2019–2020) shells. We identified three mineralogical layers in *M. californianus*: an outer prismatic calcite layer, a middle aragonite layer, and a secondary inner prismatic calcite layer, which makes *M. californianus* the only *Mytilus* species to precipitate a secondary calcite layer. Within the inner calcite layer, light bands are strongly correlated with winter collection months and could be used to reconstruct periods with moderate, stable temperatures and minimal upwelling. Additionally, modern shells have significantly thinner inner calcite layers and more poorly expressed growth bands than the archival shells, although we also show that growth band contrast is strongly influenced by

micro–environment. *Mytilus californianus* from northern California is calcifying differently, and apparently more slowly, than it was 20 years ago.

## 1 Introduction

Marine bivalve shells offer a complex yet valuable record to explore questions about paleo– and modern seasonal extremes since many bivalve species can record ambient conditions as they calcify (Jones and Quitmyer, 1996; Wanamaker Jr. et al., 2006; Welsh et al., 2011; Schöne and Gillikin, 2013; Trofimova et al., 2021). Detailed paleoenvironmental, paleoceanographic, and anthropological information can be extracted from shell growth records over multiple timescales depending on the species' shell growth rate, the accuracy of ontogenetic age estimates, and the periodicity of the growth band pattern within the shell (Hallmann et al., 2013; Jazwa and Kennett, 2016; Cannon and Burchell, 2017). Seasonally resolved shell growth features allow for the approximation of historic baselines of temperature variability, the comparison of inferred paleo–temperature extremes to modern temperature ranges, and the prediction of climatic changes on organisms and ecosystems, which are typically controlled more strongly by extremes (Sydeman et al., 2014; Poloczanska et al., 2016; Mellin et al., 2016) than they are by average conditions. During calcification, both environmental and biological factors influence shell characteristics and chemistry differently depending on the species (Table 1). Light bands in bivalve shells represent increments of normal growth, while dark bands indicate slow or stunted growth during periods of stressful or sub-optimal conditions (Lutz and Rhoads, 1977; Killam and Clapham, 2018). Dark banding is possibly the product of increased organic material relative to calcium carbonate production during anaerobic conditions, or the visual representation of changes to the crystal microfabric when calcification occurs more slowly. In either case, however, dark bands are associated with reduced calcification. Using this

relationship, we aim to link environmental conditions with growth band coloration to investigate the timing and periodicity of dark–light band formation in marine mussel shells from northern California, and determine whether there are spatial or temporal differences in growth patterns. In order to interpret the shell growth features of a particular species as a paleo–seasonal or paleoceanographic archive, a clear understanding of the environmental parameters influencing the appearance of the growth band pattern and the timing of shell growth is required. For example, the well–studied bivalve species *Arctica islandica* has served as a reliable climate record with sub–seasonal resolution for high–latitude marine environments because it has been determined to be long–lived (~ 500 or more years) (Butler et al., 2013). Schöne et al. (2005a) and Schöne (2013) concluded that *A. islandica* produces annual and daily growth lines that form continually throughout the year. One individual provides high–resolution environmental information and seasonal extremes for multiple centuries within a single shell (Weidman et al., 1994; Schöne et al., 2005a; Schöne, 2013). While *A. islandica* is a unique archive due to its longevity and regularity, the relationships between environmental parameters and shell growth features should be tested in other, more distantly related bivalve species to optimize the paleoceanographic utility of fossil, archaeological, and historic specimens.

### 1.1 *Mytilus californianus* as a study organism

One species of interest for the northeastern Pacific Coast is *Mytilus californianus* (California mussel), an ecologically and culturally significant intertidal species that spans 20° of latitude ranging from the Aleutian Islands of Alaska to Baja California in northern Mexico (Paine, 1974). *Mytilus californianus* is a foundation species in rocky intertidal environments, playing a critical role in structuring and maintaining the intertidal community. It provides a habitat for ~ 300 interstitial species, filters detritus from seawater during feeding, and serves as a

food source for a variety of predators (Paine, 1974; Smith et al., 2009; Connor et al., 2016). *Mytilus californianus* shells are abundant in coastal California shell middens that span the terminal Pleistocene (~ 12 000 BP) through the late Holocene in age; many Indigenous communities, including the Coast Miwok, Island Chumash, and Salinan peoples, harvested California mussels as a critical or even primary food source (Jones and Richman, 1995; Jones and Kennett 1999; Kennedy, 2004; Kennedy et al., 2005; Braje et al., 2007; 2011; 2012; Campbell and Braje, 2015). Shellfish collection remains an important element of Traditional Ecological Knowledge and is still practiced by Indigenous communities along the West Coast of North America (Lepofsky et al., 2015). Given its prevalence in the archaeological record and abundance in modern intertidal ecosystems, *M. californianus* provides the opportunity to reconstruct coastal environments at various temporal scales and explore variation in shell growth features in a single species over the past ~ 12 000 years from multiple northeastern Pacific Coast sites. However, our understanding of shell structure and calcification rates and timing in *M. californianus* is highly variable and site-specific (e.g., Blanchette et al. 2007; Smith et al. 2009; Ford et al. 2010), hindering interpretations in fields ranging from archaeology to paleoceanography.

In order to accurately interpret *M. californianus* shell growth features – and to determine whether *M. californianus* can serve as a reliable paleoarchive – we analyzed the shell morphology, mineralogical layering, and growth band pattern of 40 specimens collected over various seasons in 2002, 2003, 2019, and 2020 in conjunction with sea surface temperature (SST) records and upwelling indices for the same location (Bodega Bay, California, 38.3332° N, 123.0481° W). We aimed to first characterize the shell structure and mineralogical layering of *M. californianus*, and then focused closely on the growth band pattern in order to investigate

environmental controls on shell growth and address the following questions: (1) What is the influence of micro–environment (tidal position and habitat type) on the visual expression of growth bands in *M. californianus* shells from Bodega Bay? (2) What is the influence of oceanographic conditions (SST and upwelling intensity) on the coloration (dark or light) of growth bands? (3) Are there temporal or periodic environmental trends (seasonal, annual, or decadal) influencing shell growth patterns (growth band expression and coloration of growth bands)?

## 2 Methods

### 2.1 Oceanographic setting

Bodega Bay, California is located approximately 100 km north of San Francisco Bay in the central portion of the California Current System (CCS). Oceanographically, Bodega Bay experiences strong seasonal cycles: a spring–early-summer (March to July) upwelling season with low mean monthly SSTs (~ 10 to 12°C), a late-summer–fall relaxation season (August to November) with reduced upwelling and relatively warmer monthly SSTs (~ 13 to 15°C), and a cool winter (December through February) with heavy precipitation and moderate SSTs (García–Reyes and Largier, 2010; 2012). The CCS comprises the dominant south–flowing California Current, the subsurface north–flowing California Undercurrent, and the seasonal north–flowing Davidson Current present at the sea surface in winter (Hickey and Banas, 2003). The geometry of the California coastline interacts with the CCS to produce different temperature regimes in northern and southern California; north of Point Conception, the coastline is roughly parallel to alongshore winds, resulting in high Ekman transport and strong upwelling near the coast (Huyer, 1983; Checkley and Barth, 2009). Interannual and decadal regional variability within the CCS is largely driven by El Niño Southern Oscillation (ENSO) and Pacific Decadal Oscillation (PDO)

(García–Reyes and Largier, 2012). In addition to ENSO and PDO phases, local–scale coastal variability on the order of meters to a few kilometers is controlled by local surface warming and wind stress (Dever and Lentz, 1994; García–Reyes and Largier, 2012).

For this study, three intertidal collection locations were chosen: Horseshoe Cove (a protected marine environment in Bodega Marine Reserve, BMR), an open–coast BMR site (350 m north of Horseshoe Cove), and a third site at Portuguese Beach (an open–coast site 7 km north of BMR). All three collection locations are located along Sonoma Coast, west and northwest of Bodega Harbor. Sonoma Coast is considered one oceanographic region since it is part of the same upwelling cell within the CCS (Largier et al., 1993; Wing et al., 1995), and 7 km of alongshore separation results in the same coastal SST and upwelling patterns at BMR and Portuguese Beach (John Largier, pers. comm., 2021).

**2.2 Specimen collection and preparation**

To examine the environmental and temporal factors influencing growth band patterns, we analyzed shell growth features from 40 *M. californianus* samples (n = 27 shells from 2019 and 2020; n = 13 shells collected in 2002 and 2003). Specimens were categorized as either modern (collected in 2019–2020) or archival (collected in 2002–2003). On 18 January 2019, nine initial *M. californianus* individuals were hand–collected from the intertidal zone of Horseshoe Cove (38.33325° N, 123.0480571° W) during low tide (–1.13 m) (Fig. 1) with written permission from BMR. Live specimens were collected along a 6 m transect: three specimens from high intertidal position (HIP) 0 m from shore, three specimens from middle intertidal position (MIP) 3 m from shore, and three specimens from low intertidal position (LIP) 6 m from shore. Specimens were immediately sacrificed by scraping soft tissue from the shells. Valves were scrubbed with hydrogen peroxide to remove epibionts, rinsed with deionized water, oven–dried at 40°C for 30

minutes, and air–dried overnight. Additional specimen collections took place on 11 July 2019 and 6 June 2020 at BMR. As previously, shells were hand–collected by intertidal position at Horseshoe Cove and from the open–coast BMR site in order to compare shells from a variety of micro–environments: tidal position (HIP, MIP, LIP) and habitat type (open–coast or protected). Both BMR collection sites experience marine rather than estuarine conditions; mean daily salinity at BMR was 33.4 ± 0.34 (1 SD) PSU in 2018.

Additionally, 13 archival *M. californianus* shells live–collected at Portuguese Beach on 10 May 2002, 19 July 2002, 1 December 2002, 23 December 2002, and 7 September 2003 were included for temporal comparisons. Portuguese Beach is an open–coast, rocky intertidal site ~ 7 km north of the BMR collection locations. All 13 Portuguese Beach specimens were collected from the MIP by Michael A. Kennedy for dissertation research with the Department of Anthropology of the University of California, Davis (Kennedy, 2004).

A thin section was prepared from one valve of each *M. californianus* specimen. Valves were cut along the axis of maximum growth (Fig. 2) using a Buehler Isomet saw with a 0.3 mm diamond wafering blade. Shell cross sections were mounted to an extra-large (50 x 75 mm) glass slide with epoxy and cured at 80°C. Cross sections were polished with a Buehler PetroThin saw and then polished repeatedly using diamond suspension, colloidal alumina suspension, and microcloth until each shell cross section was polished to a uniform thickness of 300 μm. Shell thin sections were immersed in Mutvei's solution at a temperature of 37°C for 15 minutes under constant stirring (Schöne et al., 2005b). Mutvei's solution stains organic–rich material with blue pigment and exposes mineralized growth increments, revealing the prismatic or tabular crystallographic microstructure of each calcium carbonate layer (Schöne et al., 2005b). After

treating samples with Mutvei's solution, each thin section was rinsed with deionized water and air-dried overnight.

**2.3 Analysis of shell characteristics**

Six shell characteristics were measured in each specimen: shell length (as shown in Fig. 2), maximum valve cross–sectional thickness, the thickness of the innermost calcium carbonate layer, the color of the final growth band, the width of the final growth band, and the standardized gray–value variance as a proxy for growth band contrast. The shell length of each whole valve was measured parallel to the hinge using digital calipers (0.1 mm accuracy) to estimate the relative ontogenetic age of each individual (i.e., longer shells lived longer), although no time–calibrated estimate of age from shell length exists for northern *M. californianus* individuals. Thin sections were examined both before and after Mutvei's treatment with an Olympus BH2 light microscope equipped with both transmitted and reflected light sources and attached camera with ScopePhoto software. Using Fiji imaging software (formerly ImageJ, available at https://imagej.net/software/fiji, last access: 10 August 2021), each shell's cross–sectional thickness was measured digitally near the umbo at the region of interest (Fig. 2b). Thin sections were photographed for analysis in Fiji in order to visually identify mineralogical layers and quantify (count and measure) dark–light growth bands. The thickness of the innermost calcium carbonate layer was also measured digitally at the region of interest near the umbo from oldest to youngest shell material (Fig. 2b). Photomicrographs taken of the region of interest were converted to 8 bit images for each specimen. In some cases, it was difficult to visually determine the color of the terminal band; to supplement visual inspection, gray values were obtained from the 8 bit image through a transect of dark-light banding at the region of interest (Katayama and Isshiki, 2007; Fig. 2b). Using the transect tool and the "Plot Profile" command in Fiji, we

obtained a grayscale profile and gray values for each transect of all 40 specimen images. To determine the proportion of light banding in each individual specimen and confirm the coloration of the terminal band, gray values greater than each individual's mean gray value were considered light bands, and gray values less than each individual's mean were considered dark bands. The percent of light bands was calculated as (total light band amount (mm)/(total dark + light band amount (mm) x 100%. Microsoft Excel was used to calculate and standardize each specimen's gray–value variance as a proxy for band expression; a higher standardized gray–value variance indicated greater contrast (strong visual expression) between dark–light bands, while low standardized gray–value variance indicated low contrast (weak visual expression) between dark–light bands. We expected greater contrast (higher gray-value variance) to correspond to more "normal" growth patterns (i.e., alternating deposition of distinguishable dark and light layers) and lower contrast (lower gray-value variance) to correspond to more disturbances or intervals of halted growth (i.e., more dark banding or little difference between dark and light bands).

Shell growth features were analyzed statistically using the Kruskal–Wallis rank sum test to compare shell thickness to length ratios, Welch's *t* test to compare gray–value variance and percent of light bands across specimens, and Pearson's chi–square test with Yates' continuity correction to assess relationships between the color of the terminal band and collection season. All statistical analyses were performed in R.

**2.4 Analysis of environmental data**

We accessed daily Bodega Bay SST data for the decades 1995–2004 and 2011–2020 provided by the Bodega Ocean Observing Node (BOON) Shorestation Seawater Observations from the Bodega Marine Laboratory of the University of California, Davis. Since warm (or cool) conditions occur synchronously during the same weeks or months along the Sonoma Coast,

BOON data are regionally representative of all three collection sites. SST datasets were averaged to generate monthly, seasonal, and annual mean temperature profiles. Daily SSTs for the 30 days prior to mussel collection dates were plotted for all eight collection dates to examine temperature conditions over the final month of each individual's lifespan.

Upwelling conditions for the same periods were assessed using the Coastal Upwelling Transport Index (CUTI) and Biologically Effective Upwelling Transport Index (BEUTI) for 38° N (Jacox et al., 2018). CUTI represents the rate of vertical water volume transported per second per meter of coastline at each 1° of latitude along the U.S. West Coast and incorporates impacts of Ekman pumping and cross–shore geostrophic flow (Jacox et al., 2018). CUTI was used as a measure of physical upwelling strength. BEUTI, a measure of vertical nitrate flux (Jacox et al., 2018), was used as an indicator of productivity in the surface waters. BEUTI and CUTI are typically positively correlated, but both indices were used and compared here since physical water transport and nutrient flux can become decoupled in the CCS during alongshore advection or anomalous oceanographic events (e.g., coastal–trapped wave propagation) (Jacox et al., 2018; Renault et al., 2016). Additionally, both CUTI and BEUTI were considered in case of disproportionate or separate influences of each metric on mussel shell growth.

Both daily data and a 14 d running mean were plotted to characterize environmental conditions for all three datasets (SST, BEUTI, CUTI) for the study periods 1995–2004 and 2011–2020 (Figs. S1, S2 in the Supplement). We calculated the standard deviation ($\sigma$) and plotted $y = \pm 1\sigma$ for SST records and $y = \pm 2\sigma$ for upwelling records to approximate typical ranges of variability for each decade–long study period. We chose to examine 10-year-long windows of time at daily resolution for three reasons: (1) to gauge intra–annual and interannual environmental variability at the study area, (2) to account for the decadal scale variability of

PDO, and (3) to examine environmental conditions over the typical lifespan of intertidal *M. californianus*. While the full lifespan of *M. californianus* is unknown, individuals have been known to live up to 11 years (McCoy et al., 2011; Pfister et al., 2011) and even hypothesized to be capable of surviving 50–100 years in undisturbed settings (Suchanek, 1981), although this has not been tested or documented in the literature. We chose ocean records spanning a decade over the years that these shells were collected to provide reasonable environmental context for shell growth patterns for individuals of various and unknown ages.

In addition to examining SST data over daily, monthly, seasonal, and annual scales, we also calculated the cumulative average SST of each month for all years in each study period (e.g., all January months over 1995–2004) to characterize the annual temperature cycle at Bodega Bay for each decade (Fig. S3). To assess any changes in SST and upwelling between the two decade long study periods, we performed a two–sample *t* test to identify any significant differences between means and an *F* test of equality of variances. All oceanographic data were analyzed and plotted in R.

## 3 Results

### 3.1 Shell characteristics: mineralogical layering

When examined under light microscope, all 40 Bodega Bay *M. californianus* specimens (n = 13 from 2002 and 2003; n = 27 from 2019 and 2020) exhibited three mineralogical layers: outer prismatic calcite, a thin middle layer of nacreous aragonite, and a secondary inner layer of calcite (Fig. 3). The outer prismatic layer made up each shell's exterior, protected by a very thin protein–rich periostracum. The periostracum was partially or mostly worn away from wave exposure in all of our specimens. The outermost calcite layer grows as ventral margin extension, adding to the shell length by terminal accretion, as evidenced by the direction of the faint, thin

growth bands in this layer (Fig. 3c). The outer calcite layer was the only layer to extend consistently throughout the shell from the umbo to the commissure. The aragonite layer appeared to cut through the middle of the cross–section, separating the inner and outer calcite layers (Fig. 3b). The composition of the umbo was primarily aragonite, although the proportion of aragonite to calcite in the umbo varied across specimens.

In thin section, the aragonite layer was visually distinct from the fan– and blade–like prisms characteristic of biogenic calcite. Faint banding did appear in portions of the aragonite layer; in some specimens, the banding appeared continuous with the dark–light banding in the inner calcite layer (Fig. 3b). The nacreous aragonite layer began at or near the umbo toward the outer margin of the shell but did not extend all the way to the commissure in any specimen. Under plane-polarized light, the aragonite layer appeared brown in color and contained tabular crystals oriented parallel to the shell's surface. The innermost layer of prismatic calcite near the anterior margin was microstructurally similar to the outer calcite layer, although the inward growth direction of the inner calcite layer adds to the shell thickness rather than shell length. The inner calcite layer was also the only layer to contain thick, strongly expressed dark–light-band pairs (Fig. 3a). The most recently formed growth band, or terminal band, is the innermost band distal to the outer calcite layer.

Shell morphology is controlled in part by the growth rates of each mineralogical layer, since the inner calcite layer contributes mainly to valve thickness and the outer calcite layer contributes mainly to shell length. There was a statistically significant positive relationship between the inner calcite layer and shell length (linear regression, $R^2 = 0.36$, $p < 0.001$, $F_{1,38} = 21.49$, Inner calcite thickness (mm) = 0.03 * Shell length (mm) – 0.06)).

Thick dark–light growth band pairs were present in the inner calcite layer (Fig. 3a) and faint, indistinguishable bands appeared in the outer calcite layer (Fig. 3c). The inner calcite layer of all specimens contained an average of three growth band pairs, ranging from 0 to 10 pairs per specimen, while the bands in the outer calcite layer were unquantifiable due to their faint and inconsistent expression. Growth band contrast (visual distinction between dark and light banding) and pattern (number of band pairs, color of terminal band, and band thickness) varied widely across specimens (Table S1). Standardized gray–value variance was used as a proxy for growth band contrast. Mean standardized gray–value variance of all specimens (n = 40) was 0.0 with a standard deviation of 1.0. High standardized gray–value variance is a quantitative indicator of a high contrast between dark and light bands, interpreted as strongly expressed banding. Conversely, low standardized gray–value variance is an indicator of low dark–light-band contrast, interpreted as weakly expressed banding (see Fig. S4 for examples of high- and low-contrast banding).

To determine whether inner calcite dark–light banding continues to form throughout ontogeny, we used shell length as an indicator of relative ontogenetic age. We applied reduced major axis (RMA) regression to assess the relationship between dark–light-band pairs and shell length (Fig. 4). We found weakly positive and statistically significant correlation between shell length and dark–light band pairs with greater variance among larger (older) individuals (RMA regression, $R^2 = 0.39$; $p < 0.001$, Number of dark–light pairs = 0.14 * shell length (mm) – 4.9). Across all specimens, there was no statistically significant relationship between standardized gray–value variance (an indicator of growth band contrast) and shell length (Pearson's correlation, $p = 0.15$). Shell characteristics for all specimens are provided in Table S1.

**3.2 Micro–environment and growth band contrast**

Standardized gray–value variance varied depending on the micro–environment (i.e., tidal position, habitat) (Fig. 5). Growth band contrast was first compared among specimens collected from a protected cove environment (Horseshoe Cove) and the open–coast sites (BMR and Portuguese Beach) (Fig. 5a). Specimens from open–coast habitats had a lower and broader range of gray–value variance (mean ± σ = 0.37 ± 1.26, n = 17) than cove specimens (mean ± σ = – 0.27 ± 0.66, n = 23). Nearly all specimens with high growth band contrast (standardized gray–value variance > 1) were collected from an open–coast habitat, although this relationship was not statistically significant (Welch two–sample *t*–test, t = – 1.91, p = 0.07).

Specimens were also categorized by intertidal position (LIP, MIP, HIP) (Fig. 5b). All specimens collected from LIP and HIP had low gray–value variances (ranging from –1.1 to 0.59, n = 13). Specimens with the highest contrast in gray values were collected from the MIP (ranging from –0.97 to 2.88, n = 27). Even when archival shells were excluded (all archival shells were collected from MIP), the modern shells displayed the same patterns, with the greatest range and highest standardized gray–value variance still found in MIP specimens only (Fig. S5).

**3.3 Oceanographic conditions and growth band pattern**

Thirteen specimens precipitated a light terminal band. Out of these 13 specimens, 10 were collected during months with average monthly SST between 12.75 and 13.5°C (Fig. 6a) and 11 were collected during seasons with a seasonal range in daily SST within 5°C (Fig. 6b). Out of all 40 shells, 27 shells had a dark terminal band, and 24 of these were collected during months with monthly SST either lower than 12.75°C or higher than 13.5°C. All six specimens collected during a month with monthly average SST ≤ 12°C had a dark terminal band, and 22 out of 24 specimens collected during months cooler than 12.75°C had a dark terminal band (Fig. 6a).

In addition to monthly and seasonal SST patterns, daily SST for the final 30 days of each individual's life were plotted (Figure 7). Collection dates in December 2002 were preceded by extremely steady daily temperatures between 12.5 and 13°C (n = 4 mussels, and 3 of these specimens had a light terminal band) (Figs. 7c, d). Oscillating warm-cool daily temperatures occurred in July 2002, September 2003, and June 2020 and were closely associated with dark terminal bands (Figs. 7 b, e, h). An extreme warm spike to 20°C occurred over the course of a 3 d long heatwave in July 2019 (Fig. 7g) and all six specimens collected following this event had a dark terminal band. Instrumental error occurred in May 2002, so it was not possible to connect the three specimens with dark terminal bands collected during that month with daily temperature trends (Fig. 7a). Seven out of nine specimens collected in January 2019 had a light terminal band despite a 3 d long temperature spike from 12.5°C up to ~ 16.25°C (Fig. 7f).

The color and width of the terminal band were also assessed in relation to upwelling conditions expressed as BEUTI and CUTI. Of the 13 shells with light terminal bands, 10 appeared in shells collected during months with negative BEUTI and CUTI values. Out of the 27 shells with a dark terminal band, 24 were collected during months where CUTI values were 0.5 or greater and BEUTI values were greater than 5.0. Patterns were similar for both BEUTI and CUTI (Fig. S6.) and strongly covaried with monthly SST (i.e., intense upwelling produces cool conditions while relaxed upwelling produces warm conditions).

**3.4 Temporal trends of shell growth features**

On a sub–annual scale, dark–light band pairs in the inner calcite layer displayed a strong relationship with season of collection in both modern shells (n = 27, collected in 2019 and 2020) and archival shells (n = 13, collected in 2002 and 2003). Of the 21 mussels collected in summer months with increasing temperatures, 19 had a dark band that precipitated as the terminal band

(90.5 %). Of the 13 mussels collected in winter months with stable temperatures, 10 had a light band that precipitated last (76.9 %). Only six mussels were collected during spring and fall (n = 3 each), but all of the shells collected in the spring have a dark band that precipitated as the terminal band and two out of three of the shells collected in fall have a dark band that precipitated as the terminal band (Table S1). We identified a statistically significant relationship between season of collection and color of the terminal band (chi–square test, $\chi^2 = 18.193$; df = 3, p = 0.0004).

Decade–specific growth trends were assessed by comparing shell characteristics between archival and modern shells. We compared gray–value variance measurements, inner calcite layer thickness to valve length ratios, and the percent of light bands per shell (Fig. 8). The standardized gray–value variance was significantly lower in modern shells than in the archival shells (Welch's two–sample *t* test, t = 2.27; df = 14.68; p = 0.039; Fig. 8a). The standardized ratios of the inner calcite thickness relative to the shell length were significantly lower in modern shells than they were in shells collected in 2002 and 2003 (Kruskal–Wallis rank sum test, $p < 0.05$) (Fig. 8b).

There was no statistical difference between the percent of light bands in archival versus modern shells (Welch's two sample *t* test, p = 0.5) (Fig. S7). The percent of light bands ranged from 0.15 to 0.61 in all specimens, with a mean of 0.43 and a median of 0.46.

**3.5 Evaluation of oceanographic data**

Using BOON SST data for Bodega Bay and monthly upwelling indices at 38° N from BEUTI and CUTI, we assessed daily, monthly, seasonal, and annual conditions for the study periods 1995–2004 and 2011–2020 to provide environmental context for the archival and modern shells, respectively. Over both study periods, the lowest SSTs occurred in April through

June and the warmest months of the year were August through November (Fig. S3). Temperatures changed drastically from April through July, with SST shifting from one annual extreme (< 10° C) to another (~ 16° C) within a 3-month period (Fig. S1). The coolest season of both study periods was spring of 2002 while the warmest season was winter of 2002 (Table 2). Summers recorded higher daily temperature variability ($\sigma > 1.5$) than winter and spring months ($\sigma < 1$).

Comparing the two study periods revealed no significant difference in mean monthly or annual SST values between the 1995–2004 period and 2011–2020 period (Two–sample *t*–test, p = 0.12 and 0.58, respectively). However, greater variance in SST occurred in the more recent study period (F–test, F = 0.6499; $df_{num} = 3140$, $df_{denom} = 3630$; $p < 0.001$). The mean annual SST was at or below 12.5°C from 1999 to 2004 and near or above 12.5°C from 2014 to 2020 (Fig. 9).

Both the archival and modern upwelling indices recorded weak upwelling during winter with low productivity (Fig. S8). Spring and early summer (March through June) is characterized by strong upwelling and high productivity, reflected by high BEUTI and CUTI values. Comparisons between upwelling indices revealed a significant difference in mean monthly CUTI values (two–sample *t* test, t = –3.3339; df = 7669; p = 0.0008) and variance values (F–test, F = 1.1503; $df_{num} = 4017$, $df_{denom} = 3652$; $p < 0.001$) with higher averages and greater variance occurring in the more recent study period (Fig. S2). The same shift was present in the BEUTI record for both average values (Two–sample *t* test, t = –5.5299; df = 7669; $p < 0.001$) and variance (*F* test, F = 0.902; $df_{num} = 4017$, $df_{denom} = 3652$; p = 0.001), with significantly higher means and greater variance of BEUTI values in 2011–2020 than in 1995–2004.

## 4 Discussion

### 4.1 Interpreting mineralogical layering and growth bands

Visual inspection under a reflected-light microscope showed three distinguishable mineralogical layers in Bodega Bay specimens (Fig. 3), regardless of collection location or shell length. The mineralogical layering of *M. californianus* was first described based on visual inspection and X-ray diffraction (XRD) analysis six decades ago (Dodd, 1963; 1964) and had not been re–examined in the literature prior to this study, leading to inconsistencies in the *M. californianus* literature. While all *Mytilus* congeners precipitate both calcite and aragonite in two distinct layers in their shell (Taylor et al., 1969), *M. californianus* is the only *Mytilus* species known to precipitate a secondary layer of calcite. A few previous *M. californianus* studies (e.g., McCoy et al. 2011, 2018; Pfister et al. 2011, 2016) noted the presence of a secondary inner layer of calcite, as initially described by Dodd (1964) and corroborated by the specimens analyzed here, but *M. californianus* shell mineralogy is often described or assumed to be bi–layered, with an outer calcite layer and an inner aragonite layer only.

The dark–light bands within the inner calcite layer of *M. californianus* have a different appearance from growth lines in many other well–studied bivalve species. Growth bands in *M. californianus* are thick bands alternating between dark and light increments, rather than thin lines that demarcate periods of accretionary growth. For example, in *Arctica islandica* and *Saxidomus gigantea*, thin growth lines result from growth cessation and reliably represent growth shutdown during winter, while light increments represent shell growth over the rest of the year (Schöne et al., 2005a; Hallmann et al., 2009; Burchell et al., 2013). Growth lines are understood to represent points at which calcification ceased and subsequently resumed, but formation of dark–light banding is more complex. The dark–light bands in *M. californianus* are more comparable to those found in *Crassostrea virginica*, which are described as alternating dark and light increments visible in cross–section (Kirby et al., 1998; Andrus and Crowe, 2000; Surge et al.,

2001; Zimmt et al., 2019; Table 1). Dark–light bands could represent alternating periods of shell deposition during aerobic and anaerobic respiration, with light bands forming during aerobiosis and dark bands forming during anaerobiosis (Lutz and Rhoads, 1977; Gordon and Carriker, 1978; McCoy et al., 2011). Under optimal conditions, such as during immersion or moderate to warm temperatures, *M. californianus* gapes and respires aerobically, and during sub–optimal conditions, such as during aerial exposure and/or extreme temperatures, *M. californianus* closes its valves and respires anaerobically (Bayne et al., 1976; Connor and Gracey, 2011; Connor et al., 2016). During anaerobiosis, glucose and aspartate ferment, resulting in the production of alanine and succinate, which is then converted to propionate if anaerobic conditions persist for several days (Connor and Gracey, 2011). Succinate is an acidic end–product of anaerobiosis, which may contribute to the production of an organic–rich dark band in the shell's inner calcite layer (McCoy et al., 2011). While it has been suggested that *M. californianus* partially dissolves its own shell during anaerobiosis in order to neutralize the acidic end–products of its own metabolism (Gordon and Carriker, 1978; McCoy et al., 2011), other sclerochronological studies have dismissed the anaerobiosis-dissolution theory to argue instead that the growth band pattern in bivalve mollusks is the visual result of fluctuating calcification rates and changes in crystallographic size and orientation (Schöne and Surge, 2012). While the mechanism that produces dark bands in *M. californianus* has not been identified, dark bands could be (1) dissolution bands, (2) organic–rich bands, (3) the visual expression of slow calcite biomineralization during sub–optimal growing conditions, or (4) a combination of multiple processes. Further investigation of the relationships (if any) among anaerobiosis, dissolution, and growth features in intertidal bivalves like *M. californianus* would help elucidate the mechanism of growth band formation in greater detail.

Because the physiological process behind dark band formation is unknown, it remains unclear if one pair of dark–light bands reliably represents 1 year in Bodega Bay specimens, as has been documented in populations of *M. californianus* from Tatoosh Island and Seattle, Washington (McCoy et al. 2011, 2018; Pfister et al. 2011, 2016). If dark bands in the inner calcite layer were to form annually in response to temperature cycles, then individuals of the same size class (and therefore age cohort) should have the same number of dark–light band pairs. Shell growth rate monitoring of *M. californianus* individuals from Bodega Bay and other northern California coastal sites has shown that individual shells < 80 mm long can grow between 0 and 1 mm per month (Smith et al., 2009). A young individual with an initial size of 10 mm growing 1 mm per month would grow ~ 30 mm in 30 months, or 2.5 years. This individual would be 40 mm long with 2.5 dark–light pairs after 2.5 years. While multiple specimens analyzed here did follow these estimates (Fig. 4), many individuals contain far fewer dark–light band pairs than their shell length would indicate, so it would not be possible to visually cross–date, as can be done in other bivalve species (e.g., *Panopea abrupta*) (Black et al., 2008).

The statistically significant positive correlation between shell length (a relative proxy for ontogenetic age) and dark–light band pairs within the inner calcite layer (RMA regression, $R^2 = 0.39$, $p < 0.001$; Fig. 4) suggests that *M. californianus* shells continue to form dark–light bands in the inner calcite layer as the shell grows posteriorly (i.e., the inner calcite layer thickens as the outer calcite layer lengthens throughout ontogeny). However, constraining calcification rates for *M. californianus* from northern California is complicated by slow shell growth rates (Smith et al. 2009) and the lack of a reliable ontogenetic age estimate based on shell length. Previous shell growth studies have focused on the fast–growing southern California *M. californianus* populations (Blanchette et al., 2007; Smith et al., 2009; Ford et al., 2010; Connor and Robles,

2015). An early study conducted 8 decades ago used 1000 mussels growing in La Jolla, California to estimate that an average *M. californianus* shell is ~ 80 mm long after 1 year (Coe and Fox, 1944). However, the latitudinal gradient and local oceanographic differences are strong indicators that the shell-length-based age estimate for southern California mussels is not applicable to northern California mussels, where seawater is significantly cooler and upwelling is more intense. In addition to geographic and oceanographic differences, environmental changes that have occurred in the ~ 80 years since the study necessitate an updated and site–specific estimate of *M. californianus* shell growth rate. Extremely low shell ventral margin-extension rates have been reported for *M. californianus* at Bodega Bay (~ 0 mm per month) (Smith et al., 2009) and the coast of Washington (~ 1 mm per month) (Paine, 1976). We found further evidence for markedly lower growth rates for northern *M. californianus* shells as a result of our collection methodology (Text S1 in the Supplement). The disparity between shell growth rates for northern and southern California mussel populations also influences the age at sexual maturity (Suchanek, 1981). Individuals from southern California reach sexual maturity at ~ 15–25 mm long, or approximately four months after settlement (Coe and Fox, 1944; Jones and Richman, 1995), but the shell length and age at sexual maturity are unknown and certainly different for slower growing northern California mussel shells.

**4.2 Relationships between the environment and growth band patterns**

We observed relationships between the micro–environment and growth band contrast, with open-coast and MIP specimens containing more strongly expressed dark–light bands than specimens collected from cove or extreme (LIP or HIP) tidal environments (Fig. 5). High standardized gray–value variance was again found only in MIP specimens even when all archival shells were excluded from analysis (since all archival shells are from the MIP at Portuguese

Beach; Fig. S5). The similarity in gray–value variance patterns across all sets of MIP specimens indicates that growth band contrast is more strongly controlled by subtle differences in micro-environment (e.g., aerial immersion time) than by the alongshore coastal oceanographic gradient of the Sonoma Coast. Such differences emphasize the importance of small-scale, within-site variation of calcification patterns for *M. californianus*, as previously presented by Thakar et al. (2017) and Connor and Robles (2015), for regions like Sonoma Coast with locally uniform oceanographic patterns. However, in regions with high alongshore variability or locally asynchronous warm/cool periods, differences in local oceanography would also play an important role in influencing calcification patterns. For example, there are significant differences in *M. californianus* shell growth rates just north and south of Point Conception in southern California, where SSTs and wave exposure vary strongly despite geographic proximity (Blanchette et al., 2007).

In addition to micro–environmental variation, we found relationships between broader oceanographic conditions and shell growth features. Shells collected during months with strong upwelling and high productivity were more likely to have a dark band that precipitated most recently (Fig. S6), indicating that strong upwelling and resultant high food availability does not necessarily cause faster shell growth in *M. californianus* from northern California. Low temperatures induced by upwelling may outweigh the effects of high food availability on calcification rate. Temperature – rather than upwelling and food availability – has been previously identified as the primary factor of shell growth rate for *M. californianus* populations in southern California in field studies (Phillips, 2005; Blanchette et al., 2007). We contribute an additional line of evidence for SST as the strongest control over growth rate in both archival and modern northern *M. californianus* shells and we suggest that SST stability (or variability) has a

stronger influence on growth band coloration and growth rate than absolute temperature (Fig. 6). While previous studies have suggested that food availability is not a strong driver of calcification for *M. californianus* because of the lack of relationship between chlorophyll *a* and shell growth (Phillips, 2005; Blanchette et al., 2007), it is also possible that upwelling–associated low pH can expose mussels to more acidic conditions in their habitats (Feely et al., 2008; Rose et al., 2020). Periods with heavy upwelling in the CCS could hinder calcification or even alter the proportion of shell calcite to aragonite in response to changes in the calcium carbonate saturation state (Bullard et al., 2021). While the heavy upwelling in the CCS offers a natural laboratory for examining low pH conditions, it may become increasingly difficult to disentangle the impacts of anthropogenic ocean acidification and upwelling–induced low pH on *M. californianus*, given that wind–driven upwelling has increased along the coast of California in recent decades due to intensifying onshore–offshore atmospheric pressure gradients associated with rising temperatures (García–Reyes and Largier, 2010). Evidence of decadal-scale intensification of upwelling appeared here in the CUTI and BEUTI records.

**4.3 Interpreting temporal trends of growth features**

Using the season of collection for each shell, we identified a significant relationship between the season and terminal band color, and specifically between winter and light bands (Fig. 6b). While winter is typically the time of year that bivalves in the northern hemisphere experience growth slowdown and produce a dark line (Killam and Clapham, 2018, and references therein), our findings from *M. californianus* support the hypothesis that mussels grow their shell optimally during warmer periods (up to a point) given that December at Bodega Bay has higher mean monthly SST and more stable daily SSTs than March through June, making winter months generally warmer than spring months and much less variable than summer months

(Table 2; Fig. 6b). We interpret the light band found in the majority of winter–collected shells as an indicator of fast (calcium carbonate–rich) growth (Schöne and Surge, 2012) occurring during optimal growth conditions for northern California mussel populations when SST is moderate and stable. Dark (slow–growth) bands were closely associated with spring–early summer, or during cooler or highly variable periods (Figs. 6, 7). Dark bands were also found in all specimens that experienced an extreme 3 d long heat wave (20°C) that occurred a week prior to their collection (Fig. 7g), indicating that *M. californianus* growth rate slows during variable, cold, or extremely high SSTs. Despite the strong correlation between season and band color, dark–light bands cannot necessarily be used as an indicator of lifespan because the dynamic oceanographic regime at Bodega Bay could result in multiple growth slowdowns within the span of one annual cycle. However, dark bands could potentially be used to reconstruct extreme or variable conditions while light bands could serve as indicators of stable and moderate periods.

In addition to seasonal variability at Bodega Bay, the intertidal zone experiences extreme environmental variation (temperature and submergence time) on daily and biweekly scales. While tidal cycling does not contribute to the number of dark–light bands in the inner calcite layer (i.e., mussels experience hundreds to thousands of high–low tidal cycles but contain only three dark–light band pairs on average), tidal variability could play a role in growth band contrast since intertidal position (LIP, MIP, HIP) and standardized gray–value variance were related (Fig. 5). LIP and HIP specimens experience tidal extremes for the longest periods of time (immersion and exposure, respectively) and have low-contrast growth bands. MIP specimens have a wide range of standardized gray–value variance, but all specimens with strongly expressed bands were collected from the MIP only, perhaps because they experienced tidal extremes for shorter periods of time than LIP and HIP specimens.

We calculated the percentage of light bands across all specimens to compare the time spent growing normally (light bands) versus abnormally (dark bands). The average percent of light bands across all specimens was 43 % and no specimen had a light-band percentage greater than 61 % (Fig. S7). If dark bands precipitate more slowly than light bands yet represent half or more than half of the inner calcite layer of all specimens, then Bodega Bay specimens spend more of their lives experiencing hindered growth rather than normal growth. Interestingly, northern California mussel populations seem to grow their shell during faster "growing windows" when conditions are moderate to warm and stable, but they calcify slowly for a longer period of the year and spend most of their lives experiencing slow–growth conditions. While most light bands are associated with winter (December and January), it is possible that the warmest time of year at Bodega Bay (August through October) could also be part of the growing window for northern California populations of *M. californianus*, but we did not have enough shells collected in fall months available (n = 3) to confirm this. Out of the three fall–collected shells, one specimen did have a light band that precipitated most recently, which does suggest that fast growth and light band precipitation can occur during the warm fall months, or during any period of the year with sustained conditions that match the optimal range for shell growth. At Bodega Bay, sustained optimal growth conditions are less likely to occur during spring and early summer because of cold and highly variable SST conditions controlled by the seasonal upwelling regime.

We also observed a statistically significant decline in inner calcite thickness to shell length ratios from the archival to the modern specimens, indicating that mussel shells growing in the same location nearly 2 decades apart are thinner relative to their length (Fig. 8b). Both the cross–sectional valve thickness and the thickness of the inner calcite layer have declined overall

relative to shell length. The valve thinning could indicate a slowed rate of calcification, that the inner calcite layer now grows for a shorter period of time in the life of the animal, or even that the length of life is declining in modern specimens. Evidence for rapid and recent shell thinning has also been found in Washington *M. californianus* populations, where cross–sectional shell thickness in modern mussels is significantly thinner than both archival (collected in the 1960s–1970s) and archaeological mussel shells (~ 2420–1000 cal BP) (Pfister et al., 2016). In addition to shell thinning, we found that growth bands in modern shells had significantly lower dark–light band contrast than the archival shells (Fig. 8a). This provides a new line of evidence for recent changes in shell microstructure occurring in the past 15 years, in addition to previous evidence of increased crystallographic disorder in modern *M. californianus* shells relative to archival and archaeological shells from Washington (McCoy et al., 2018) and a reduction in aragonite deposition relative to calcite in recent *M. californianus* shells from southern California (Bullard et al., 2021). Due to limitations in the length and availability of oceanographic data sets, we did not aim to link changes in shell growth and the dark–light band pattern to anthropogenic ocean acidification or lower pH in response to increased CCS upwelling, although SSTs were higher and more variable and upwelling was significantly stronger in 2011–2020 than in 1995–2004. We suggest that the weakened growth band expression and decline in inner calcite thickness ratios in the modern shells could be responses to warmer-than-average conditions and/or low pH conditions associated with stronger upwelling, which can be further explored by applying well–developed geochemical proxies to reconstruct conditions recorded by mussel shells (e.g., $\delta^{18}O_{[shell]}$ – SST). However, the primary challenge with sampling the inner calcite layer for stable isotope analysis is the fine–resolution sampling required; the inner calcite layer is ~ 2 mm thick (mean of n = 40) and individual bands can be extremely thin (on the order of micrometers).

### 4.4 Potential factors contributing to variability of shell growth features

Given that temperature and upwelling conditions are nested within temporal trends (interannual variability and periodic oceanographic phases), we expected and found significant differences in shell growth patterns between the archival and the modern shells. We observed a high degree of variability in growth band pattern and inner calcite thickness to shell length ratios in both modern and archival specimen categories (Fig. 8). Even when standardized, the variance of inner calcite thickness to shell length ratio across all specimens was high ($\sigma^2 = 7.77$), indicating that there is a range of growth rates and dark–light-band formation rates even among specimens experiencing the same or highly similar environmental conditions along the Sonoma Coast. While the three collection sites experience synchronous warm or cool periods, it is possible that small-scale oceanographic variability results in different shell growth patterns at the BMR versus Portuguese Beach open-coast collection sites. However, we found evidence to suggest that relative (rather than absolute) temperature variability is a stronger influence over shell growth patterns (Figs. 6 and 7). Another possible source of variability is the uneven sampling distributions due to the archival specimens available and restrictions on modern sample collection during the COVID–19 pandemic. Regardless of sample size, a certain degree of growth pattern variability is expected depending on the plasticity among individual organisms and on the micro–environment within and across populations. If dark–light banding is mediated by a physiological response to environmental conditions (e.g., a metabolism that alternates between anaerobic and aerobic respiration depending on SST), there can be varying physiological responses among individuals due to micro–environmental gradients in SST or immersion time in the highly variable intertidal zone (Connor and Robles, 2015; Thakar et al., 2017). For food availability, tidal position is a minor factor since functional–submergence time

(the time required for an individual to gape its valves and effectively filter–feed) is uniform across intertidal positions (LIP, MIP, HIP) for *M. californianus* (Connor et al., 2016). While low tide and low temperatures have been suggested as conditions that trigger a switch to anaerobic respiration in *M. californianus* (Connor and Gracey, 2011; McCoy et al., 2011), the temperature threshold for anaerobiosis is unknown and is likely to differ depending on the population's latitude and local oceanographic parameters. For example, northern California mussel populations experience cooler conditions and a narrower range of temperatures (~ 10–13.5°C mean monthly SST) than southern California mussels, which have been observed to grow most rapidly between 15 and 19°C (Smith et al., 2009). Temperatures approaching 19°C could be outside the range of tolerance for populations from northern California given that SSTs rarely exceed 19°C at Bodega Bay; the BOON SST record documents only 3 d warmer than 19°C over both decade–long study periods. The north–south SST gradient in California may result in slow growth and more frequent dark band formation for northern mussel populations, and optimal growth and light band formation — and perhaps a greater overall percentage of light bands — for warm–water acclimated southern California mussel populations. A latitudinal gradient in shell growth rate, and therefore growth band pattern, controlled by the CCS' variable upwelling regime is explained by the high plasticity in physiological responses to oceanographic conditions in *M. californianus* (Dahlhoff and Menge, 1996).

**5 Conclusions**

We identified three mineralogical layers in *M. californianus*: an outer calcite layer with faint indistinguishable banding, a thin nacreous aragonite middle layer, and an inner calcite layer that grows inward, precipitating dark–light band pairs. The improved understanding of shell layering and growth directionality has important implications for paleoceanography and

archaeology, which require geochemical subsampling approaches and proxy equations tailored to growth direction and the specific calcium carbonate polymorph. Within the genus *Mytilus*, the inner calcite layer is unique to *M. californianus* and may be a useful layer for the reconstruction of extreme conditions and determination of season of collection due to strongly expressed growth banding, although the contrast between dark–light bands is variable and dependent on tidal position and habitat type.

We documented a strongly positive and statistically significant correlation among light bands and winter collection months, moderate SST (average monthly SST between 12.75 and 13.5°C and average seasonal temperature of ~ 12°C), and weak upwelling (CUTI and BEUTI < 0) at Bodega Bay, indicating that light bands are more likely to precipitate during growing windows with relatively constant SSTs. Slower or halted growth, recorded as dark bands, is more likely to occur during spring through early summer, or when conditions are highly variable or locally extreme, although it is uncertain which conditions are considered "extreme" for intertidal *M. californianus* populations in northern California. We also found that low temperatures may result in slow shell growth and dark band formation even during periods of upwelling–induced productivity. Interestingly, most specimens analyzed here contained a greater percentage of dark bands than light bands, suggesting that the growth slowdown period is longer than the growing window for Bodega Bay mussels and that mussels spend more of the year – and more of their lives – experiencing hindered growth rather than normal growth.

A shift in calcification patterns from archival (2002–2003) to modern (2019–2020) mussels is also documented here. The statistically significant decline in growth band contrast and inner-calcite thickness to shell length ratios indicates that *M. californianus* is growing more slowly or calcifying less in 2019–2020 than this species was less than 2 decades ago at the same

location. The spatial and temporal variability of *M. californianus* shell growth from Bodega Bay highlights the need for future site–specific calibration of growth band patterns and comparisons through time. Given that *M. californianus* is an ecologically important foundation species and its shell appears to respond to and sensitively record environmental changes, analysis of the relationships among shell growth features, environmental conditions (SST, pH, and upwelling), and community ecology should be investigated to assess whether these shifts in calcification patterns will have negative impacts for *M. californianus* and the biologically rich intertidal community that this species supports.

**Original Publication and Data Availability**

This chapter is reproduced from the original publication: Vriesman, V.P., Carlson, S.J. and Hill, T.M., 2022. Investigating controls of shell growth features in a foundation bivalve species: seasonal trends and decadal changes in the California mussel. *Biogeosciences*, *19*(2), pp.329-346. https://doi.org/10.5194/bg-19-329-2022. All shell data collected for this paper are available in the Supplementary Information. BOON data are available online at https://boon.ucdavis.edu/ and all upwelling (CUTI and BEUTI) data are available online at https://oceanview.pfeg.noaa.gov/products/upwelling/cutibeuti and https://mjacox.com/upwelling-indices/.

**Acknowledgements**

This material is based upon work supported by the National Science Graduate Research Fellowship under Grant No. 2036201. We thank Jackie Sones for access and assistance at the Bodega Marine Reserve and Zachary Oretsky for assisting with mussel collection. We thank Ann Russell for providing access to archival mussel shells. All thin sections were prepared by Greg Baxter. Leslie Garcia helped to calibrate scales for thin section images. John Largier provided

helpful input about Sonoma Coast oceanography. Thoughtful reviews by Daniel Killam and Alan Wanamaker Jr. improved this manuscript.

## Tables

**Table 1**. Chemical and microstructural growth features recorded in bivalve shells and their environmental and biological influences. Species examples are not exhaustive.

| Shell feature | Environmental influences | Biological influences | Species examples |
|---|---|---|---|
| Light banding | Representative of warm temperatures (summer), high tide, high food availability, or conditions that allow for normal growth | Aerobic metabolism, faster calcification rate | *Mercenaria mercenaria* (Lutz and Rhoads, 1977); *Crassostrea virginica* (Surge et al., 2001) |
| Dark banding | Representative of cold temperatures (winter), low tide, low food availability, or conditions that impede normal growth | Anaerobic metabolism; slower calcification rate | *Mercenaria mercenaria* (Lutz and Rhoads, 1977); *Crassostrea virginica* (Surge et al., 2001) |
| $\delta^{18}O$ | Inversely correlated with seawater temperature and positively correlated with salinity | Growth slowdown or shutdown prevents the shell from recording the full annual range of $\delta^{18}O$–inferred SST | *M. californianus* (Ford et al., 2010); *M. galloprovincialis* (Zhao et al., 2019*)*; *Pecten maximus* (Freitas at al., 2012); *Saxidomus gigantea* (Hallmann et al. 2009) |
| $\delta^{13}C$ | Inversely correlated with upwelling strength; upwelling delivers remineralized $^{12}C$ to surface waters | Metabolic carbon is incorporated into $\delta^{13}C_{shell}$ during respiration; photosymbiosis | *M. californianus* (Killingley and Berger, 1979; Pfister et al., 2011; Ferguson et al., 2013); *Tridacna* species (Killam et al., 2020) |
| Mg/Ca | Positively correlated with seawater temperature | Strong and positive relationship between Mg/Ca and growth rate; physiological controls over elemental incorporation | *M. californianus* (Ford et al., 2010); *M. edulis* (Wanamaker Jr. et al., 2008); *M. trossulus* (Klein et al., 1996); *Pinna nobilis* (Freitas et al., 2005) |
| Ba/Ca | Inversely correlated with salinity; freshwater input proxy due to higher [Ba] in rivers relative to seawater | Potential remobilization of Ba stored in tissue during spawning | *M. edulis* (Gillikin et al., 2006); *Ruditapes philippinarum* (Poulain et al., 2015) |

**Table 2**. Seasonally averaged SST (°C) for the specific collection season of each mussel (n = 40 over eight collection dates across seven different seasons) and standard deviation for each calendar season of the study period. Spring = March through May; summer = June through August; winter = November through January, fall = September through November.

| Season | Mean seasonal SST (°C) | σ |
|---|---|---|
| Spring 2002 | 10.9 | 0.88 |
| Summer 2002 | 11.8 | 1.72 |
| Winter 2002 | 13.2 | 0.38 |
| Fall 2003 | 12.6 | 1.09 |
| Winter 2019 | 13.1 | 0.93 |
| Summer 2019 | 13.1 | 1.83 |
| Summer 2020 | 13.1 | 1.73 |

## Figures

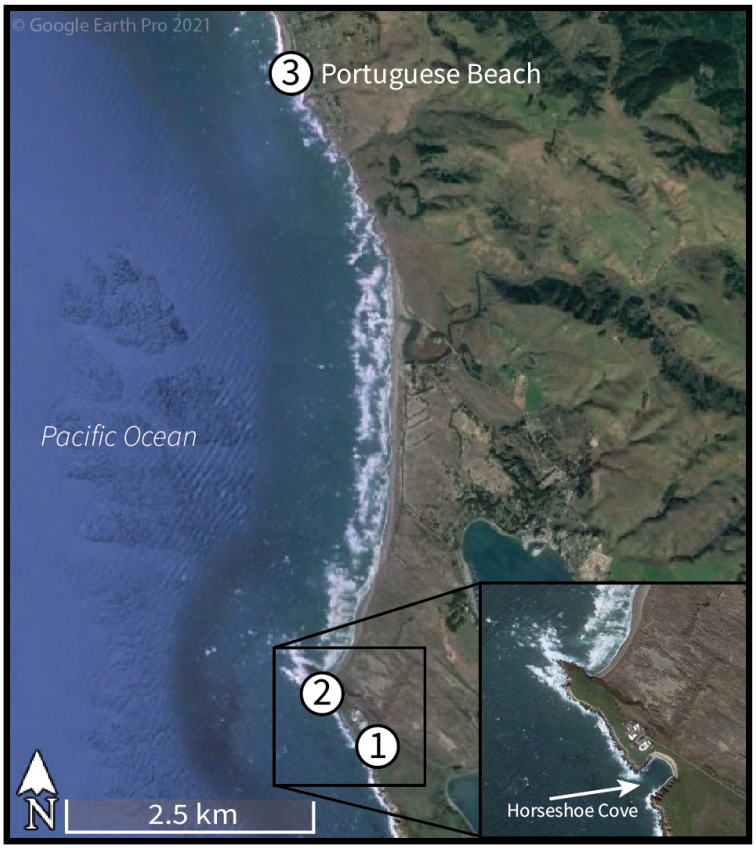


**Figure 1**. Intertidal collection sites at Bodega Bay, California along Sonoma Coast. Sites 1 and 2 are located within Bodega Marine Reserve and site 3 is located at Portuguese Beach. Modern shells were collected alive in 2019 and 2020 at sites 1 and 2 (Horseshoe Cove and the open-coast site, respectively). Archival shells were collected alive 7 km north at Portuguese Beach in 2002 and 2003. © Google Earth Pro 2021.

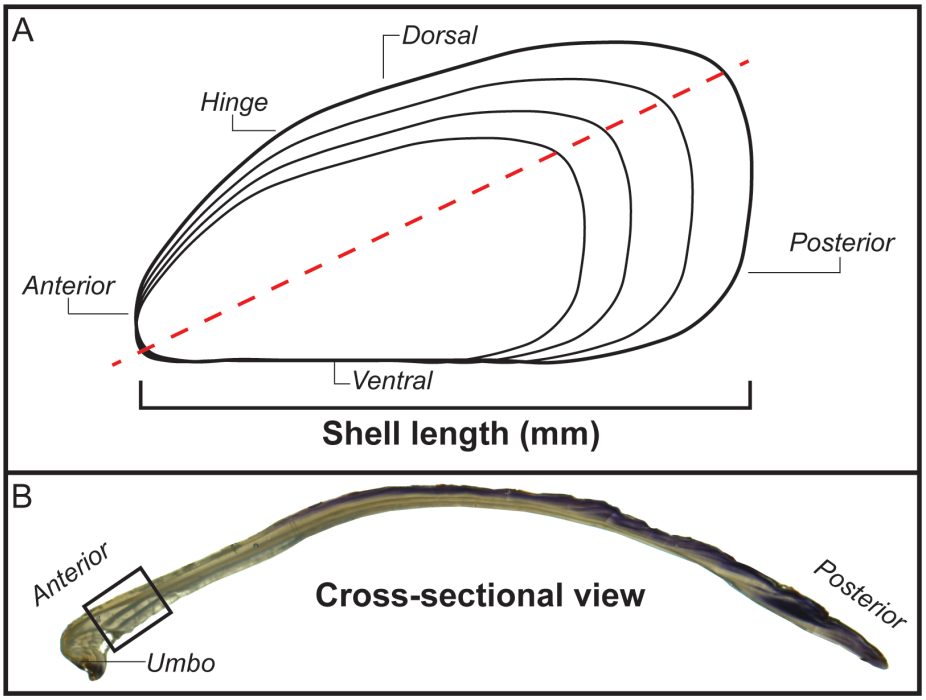


**Figure 2.** Anatomy of *M. californianus* whole valve and cross section. (a) Line drawing of whole valve showing where shell length was measured. Red dashed line denotes maximum growth axis along which the valve was cut to prepare a thin section. (b) Cross-sectional photograph of a shell taken under a microscope with reflected light. Black box denotes region of interest where the maximum valve cross-sectional thickness, the thickness of the innermost calcium carbonate layer, the color of the final growth band, and the width of the final growth band were measured or noted for all specimens.

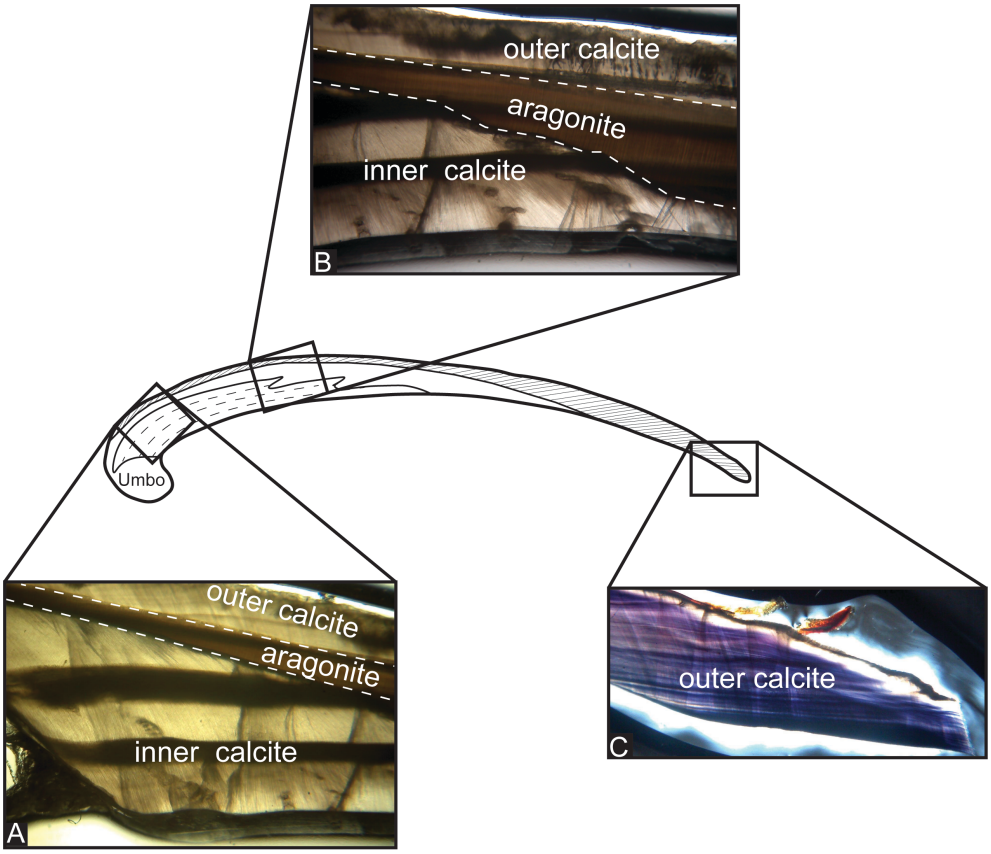


**Figure 3.** Shell structure and mineralogical layering in *M. californianus*. (a) Photo taken under light microscope focused at the region of interest showing the three mineralogical layers. Dashed lines indicate boundaries between inner calcite, aragonite, and outer calcite layers. (b) Photo taken towards the middle of the cross section showing that the inner calcite layer tapers to an end. (c) Photo taken at the posterior margin of the cross section at the commissure, where the outer calcite layer is the only layer present.

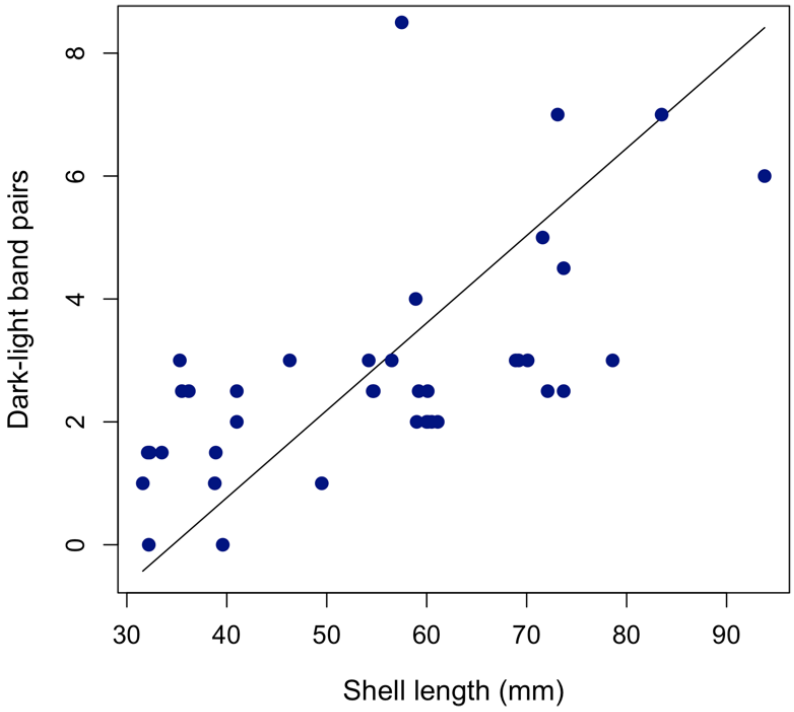


**Figure 4.** Relationship between shell length and number of growth band pairs for all 40 shells with an RMA regression line plotted; Number of dark-light pairs = 0.14 * shell length (mm) – 4.9.

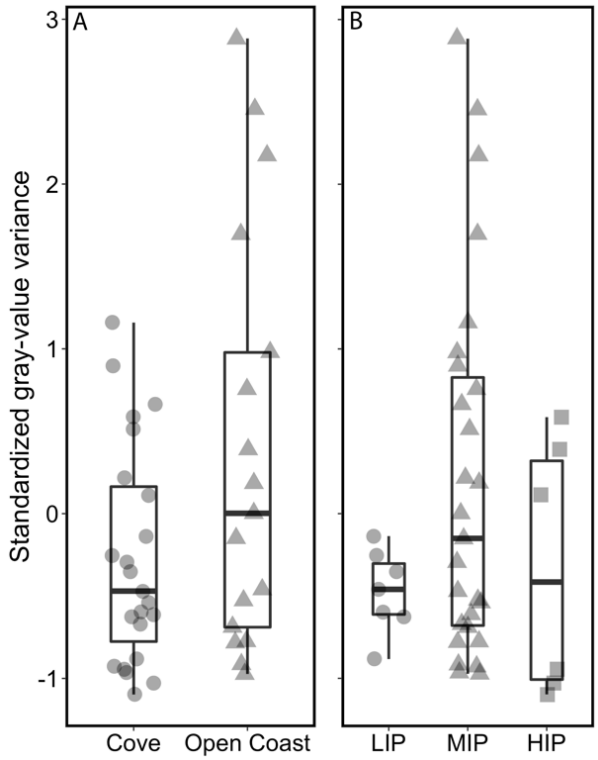

**Figure 5.** Relationships between micro-habitat and standardized gray-value variance as a proxy for growth band contrast. High standardized gray-value variance is indicative of high contrast between dark and light bands. (a) Cove specimens are from Horseshoe Cove at BMR and open-coast specimens are from an open-coast site within BMR and Portuguese Beach. (b) Relationships between intertidal position (LIP: low intertidal position; MIP: middle intertidal position; HIP: high intertidal position) and standardized gray-value variance for all 40 specimens.

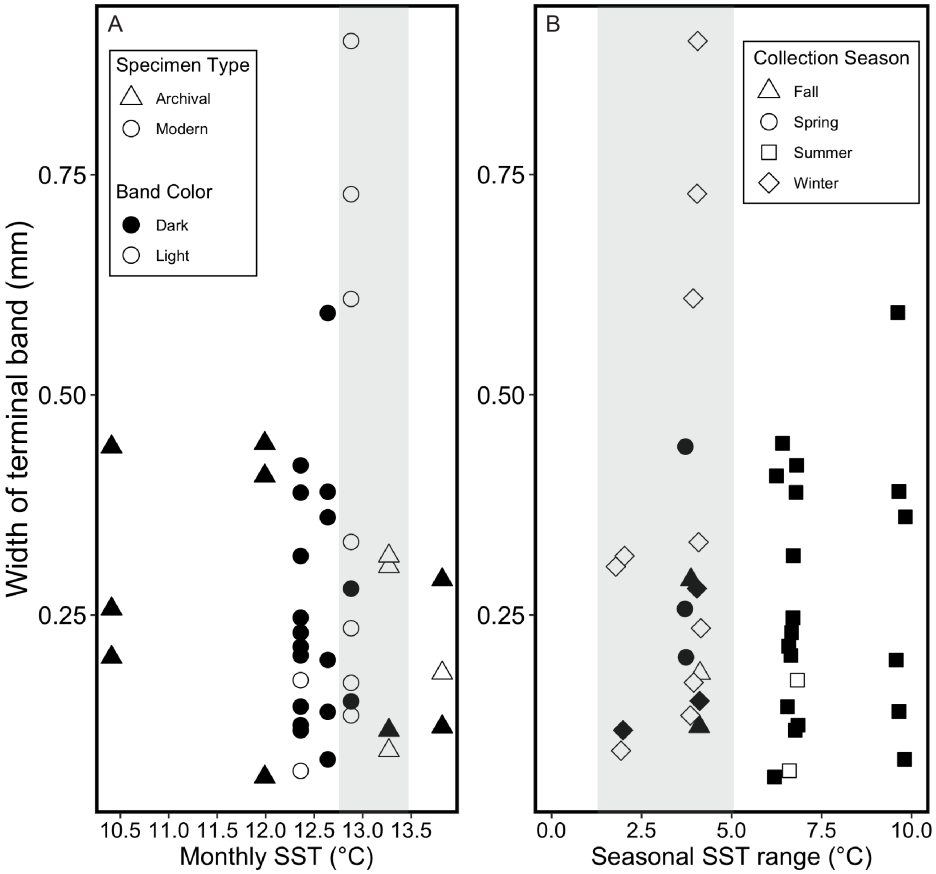


**Figure 6.** Relationships between SST, width of the terminal band, color of the terminal band, specimen type, and collection season for all 40 specimens. Filled (black) points represent dark terminal bands and open (white) points represent light terminal bands in both plots. (a) Relationships between mean monthly SST during the month of collection, color of the terminal band, and width of the terminal band. Shaded bar represents approximate monthly SST range over which most specimens are associated with light terminal bands (12.75-13.5°C). Specimen type specified with point shapes (see legend A). (b) Relationships between the seasonal SST range (mean daily SST maximum – mean daily SST minimum for each season of collection), color of the terminal band, and width of the terminal band. Shaded bar highlights that most terminal light bands are associated with a seasonal SST range < 5°C. Collection season specified with point shapes (see legend **b**).

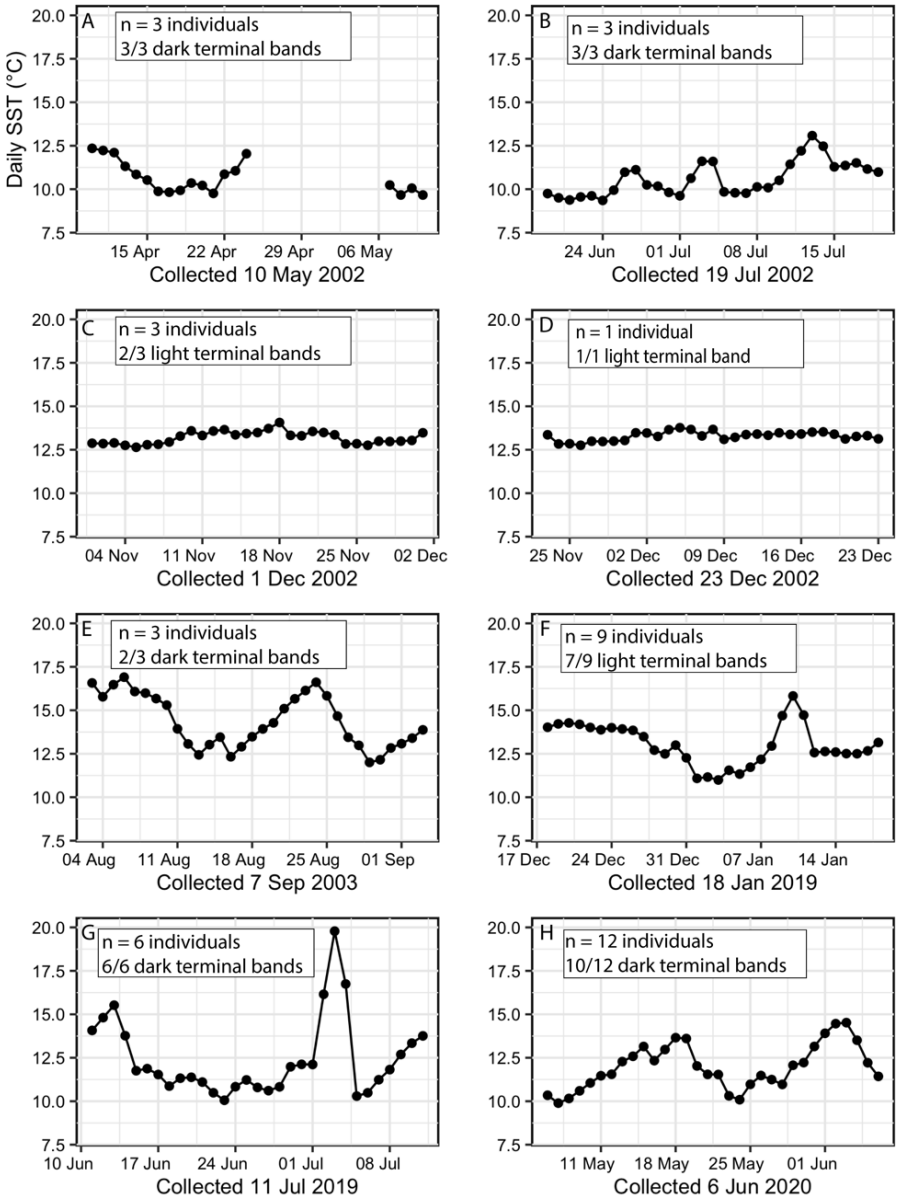


**Figure 7.** Daily temperatures for the 30 d prior to the collection date for all 40 specimens. Each plot features the number of specimens collected on that date and the majority terminal-band color. (a) Instrumental error occurred in May 2002. (b) Daily temperatures oscillating between cooler (~ 9°C) and warmer (~ 13°C) in July 2002. (c, d) Consistent daily temperatures between 12.25°C and 12.5° in December 2002. (e) Sinusoidal daily temperatures oscillating between ~12° and 17.5°C in September 2003. (f) Daily temperatures prior to 18 January 2019 collection date were consistent for two weeks before slight cooling and three days of warming. (g) Highly variable daily temperatures and a 3 d extreme warm spike in July 2019. (h) Daily temperatures oscillating between cooler (~ 10 °C) and warmer (~ 15 °C) in June 2020.

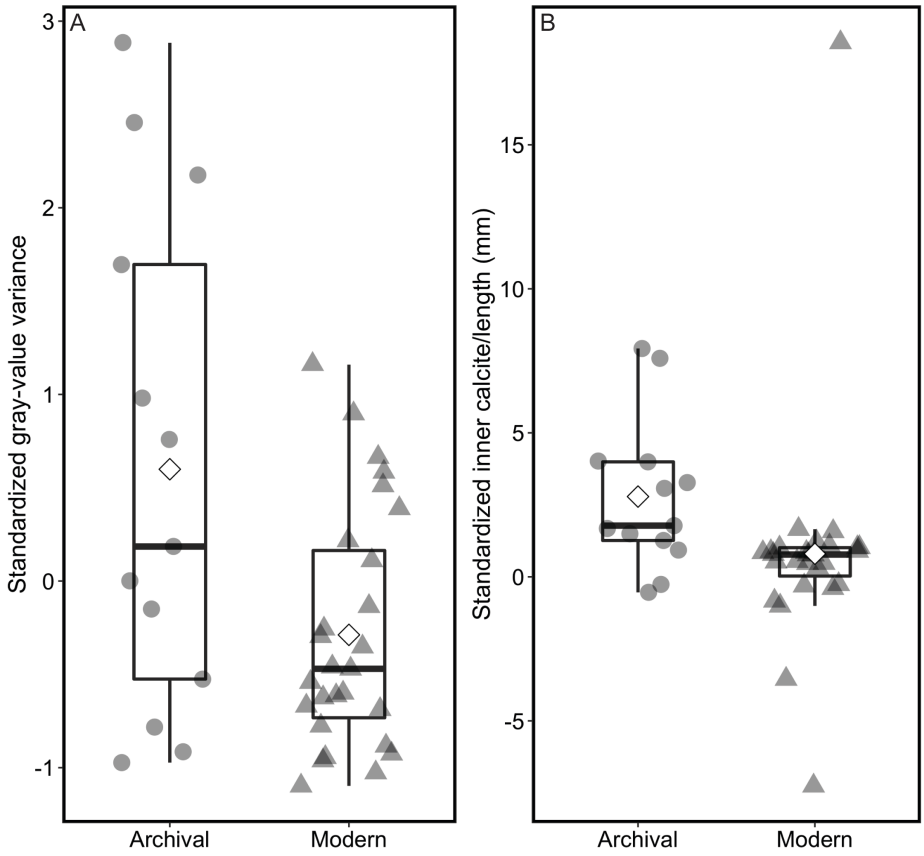


**Figure 8.** Box plot showing the range of standardized ratio of inner calcite thickness to shell length in archival and modern specimens. White diamond denotes mean.

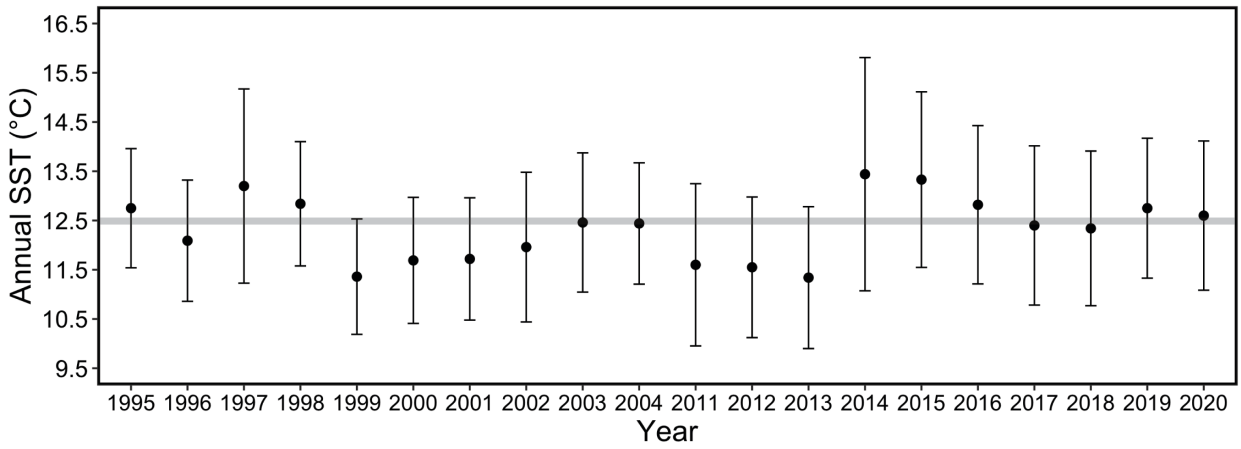


**Figure 9.** Mean annual SST for each year of the study period. Error bars represent standard deviation of daily temperatures over the course of each year. Shaded bar plotted at 12.5°C for ease of visual comparison across annual means from 1995 to 2004 and 2011 to 2020.

## Supplementary Information

This supplement contains eight (8) supplemental figures, one (1) supplementary text, and one (1) supplementary table.

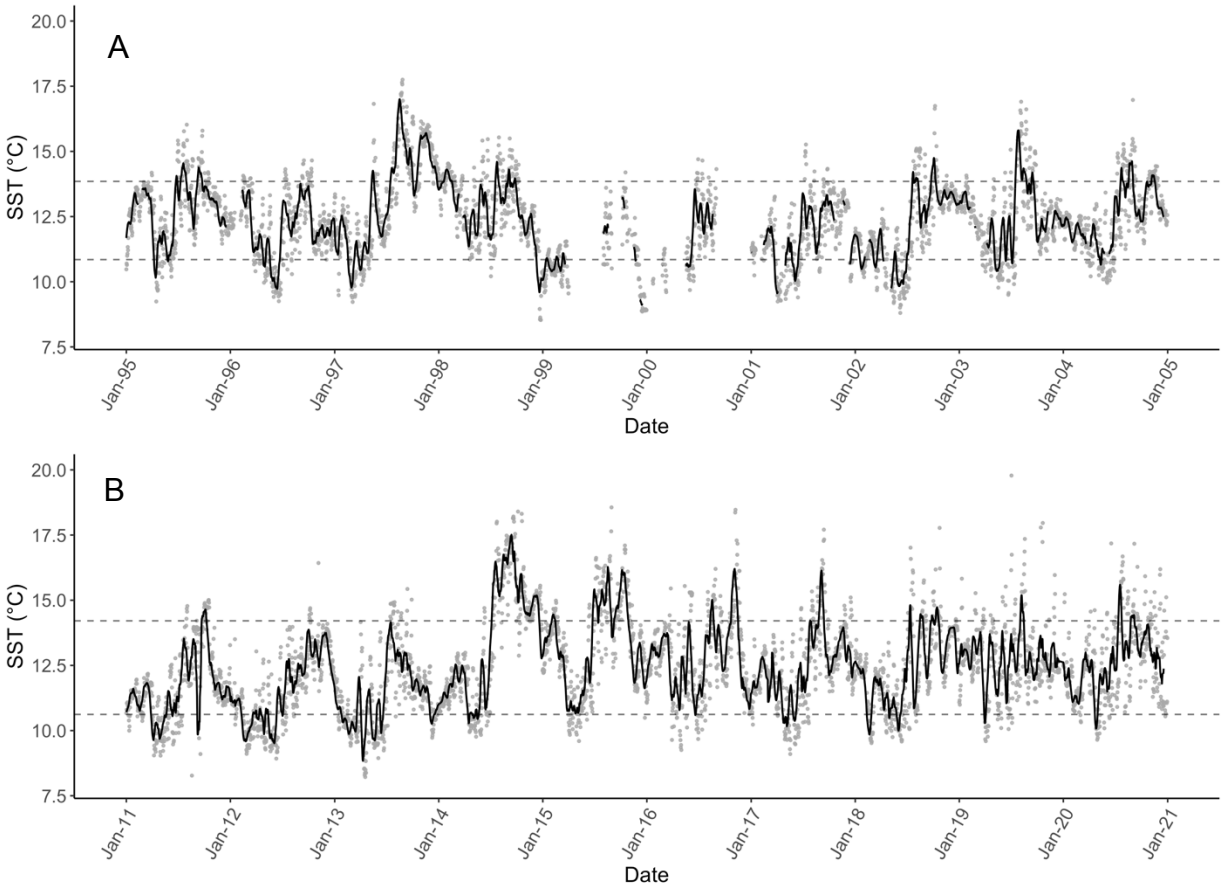


**Figure S1.** Sea surface temperature (SST) records from Bodega Ocean Observing Node (BOON) for the two study periods. Gray points represent daily SST and solid black lines represent 14-day running mean. Points within the dashed region fall within 2σ of the average daily temperature for each 10-year-long study period. (a) SST record from January 1995 through December 2004. Missing data points in 1999 2000 were due to instrumental malfunction. (b) SST record from January 2011 through December 2020.

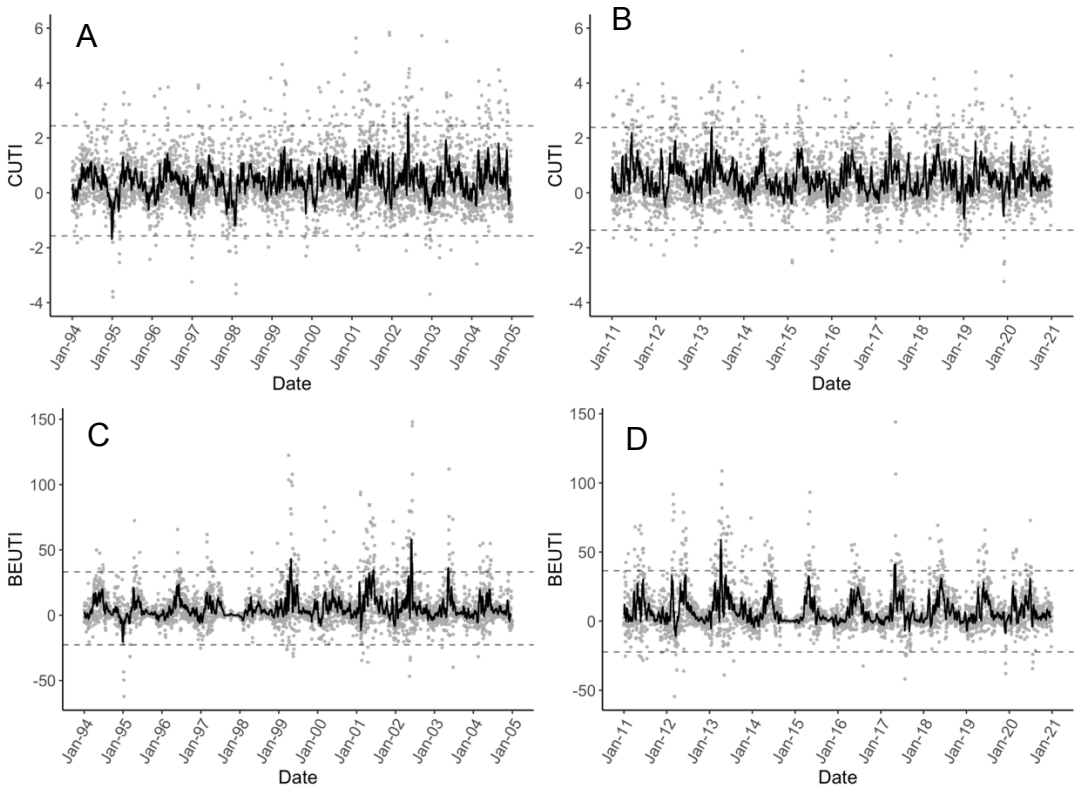


**Figure S2.** Coastal Upwelling Transport Index (CUTI) and Biologically Effective Upwelling Transport Index (BEUTI) from Jacox et al. (2018) accessible at https://mjacox.com/upwelling-indices/. Gray dots represent daily indices and **solid** black lines represent a 14-day running mean. Points within the dashed region fall within 1σ of the average daily index for each upwelling index of each 10-year-long study period. (a) CUTI record from January 1994 through December 2004. (b) CUTI record from January 2011 through December 2020. (c) BEUTI record from January 1994 through December 2004. (d) BEUTI record from January 2011 through December 2020.

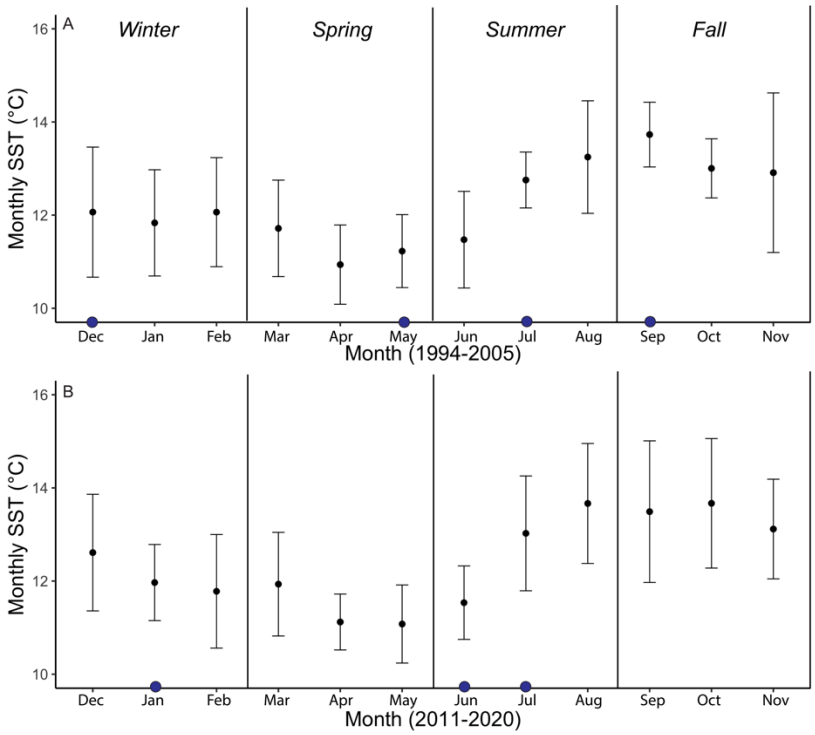


**Figure S3.** Aggregated monthly SST (°C) for both study periods to identify monthly and seasonal trends. Blue circles on x-axes represent months during which mussels were collected. (a) SST averaged for all months 1995-2004 (e.g., Jan = mean SST of all January months from 1995-2004). (b) SST averaged for all months 2011-2020 (e.g., Jan = mean SST of all January months from 2011-2020).

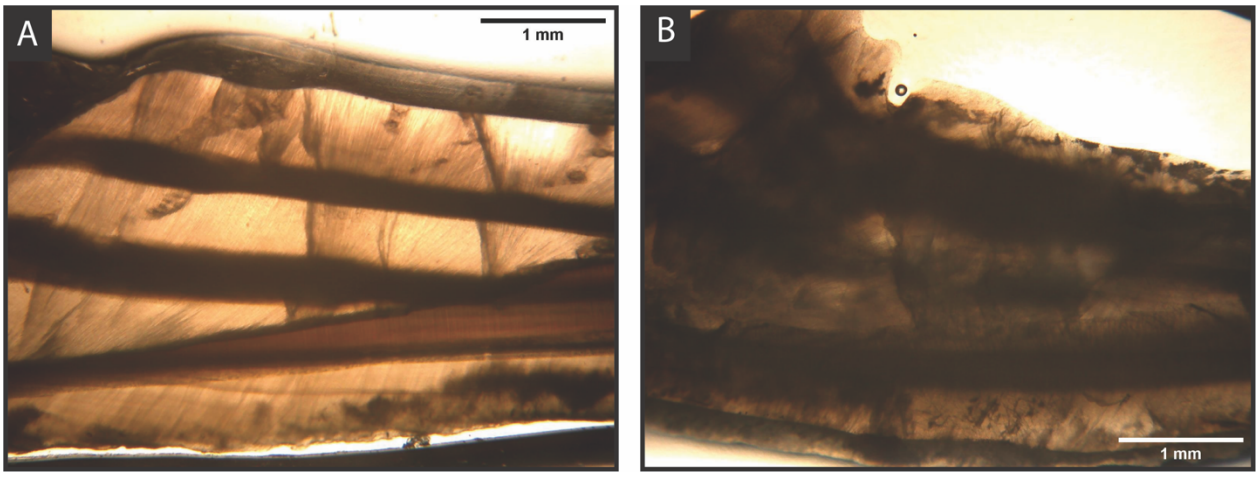


**Figure S4.** Photomicrographs taken in the region of interest for two *M. californianus* specimens polished to a uniform thickness (300 μm) to measure contrast between dark and light bands. (a) An example of high contrast between dark-light growth bands (standardized gray-value variance

= 2.89) in the inner calcite layer. (b) An example of low contrast between dark-light growth bands in a different specimen (standardized gray-value variance = -0.78).

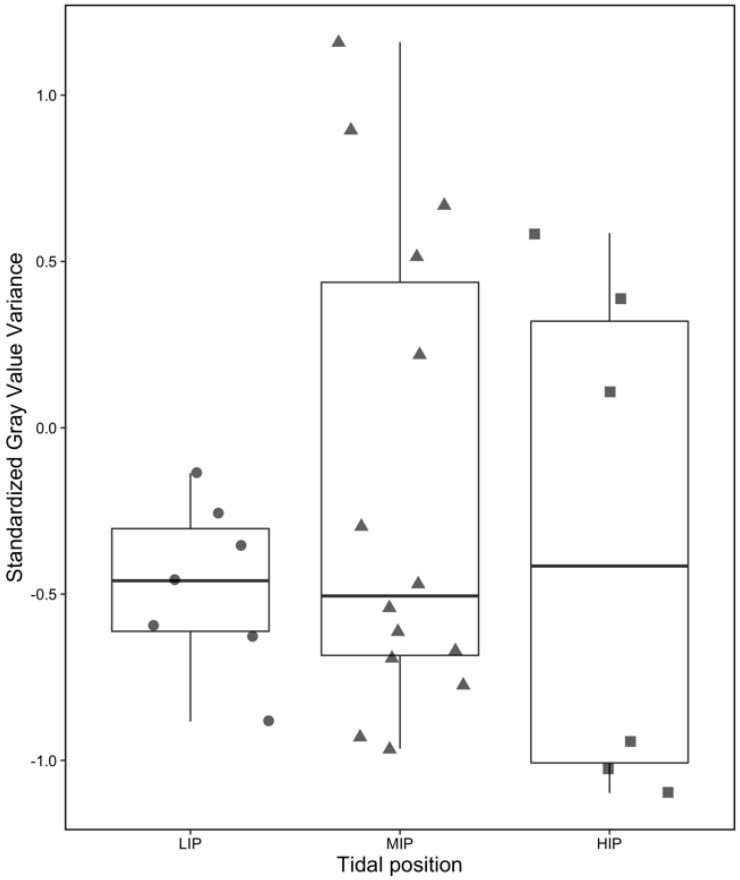


**Figure S5.** Box plot showing standardized gray value variance in modern specimens only (n = 27). Archival specimens were excluded in this plot since all archival specimens were collected from MIP.

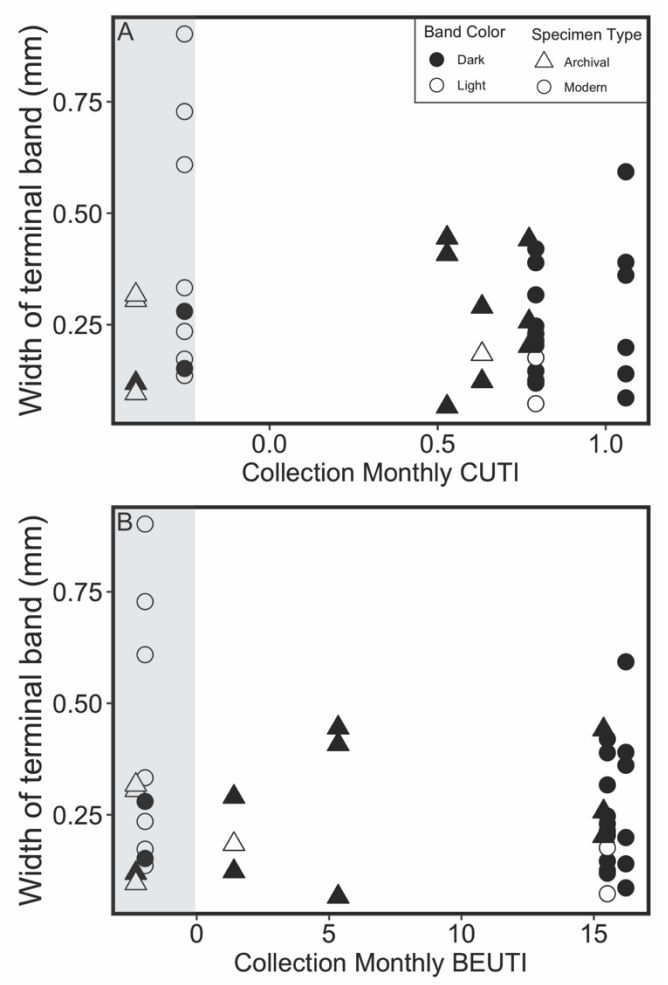


**Figure S6.** Monthly CUTI and BEUTI values for each specimen. Gray bar denotes range over which all but three specimens precipitated a light terminal band.

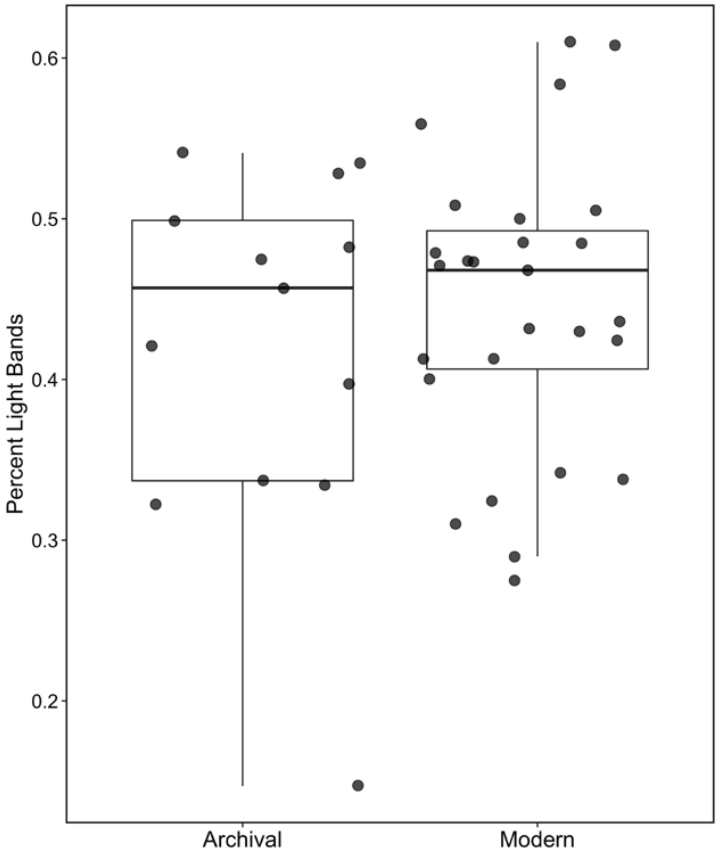


**Figure S7.** Box plot showing the percentage of light bands in archival and modern specimens. No statistically significant difference in percent of light bands between archival and modern shells.

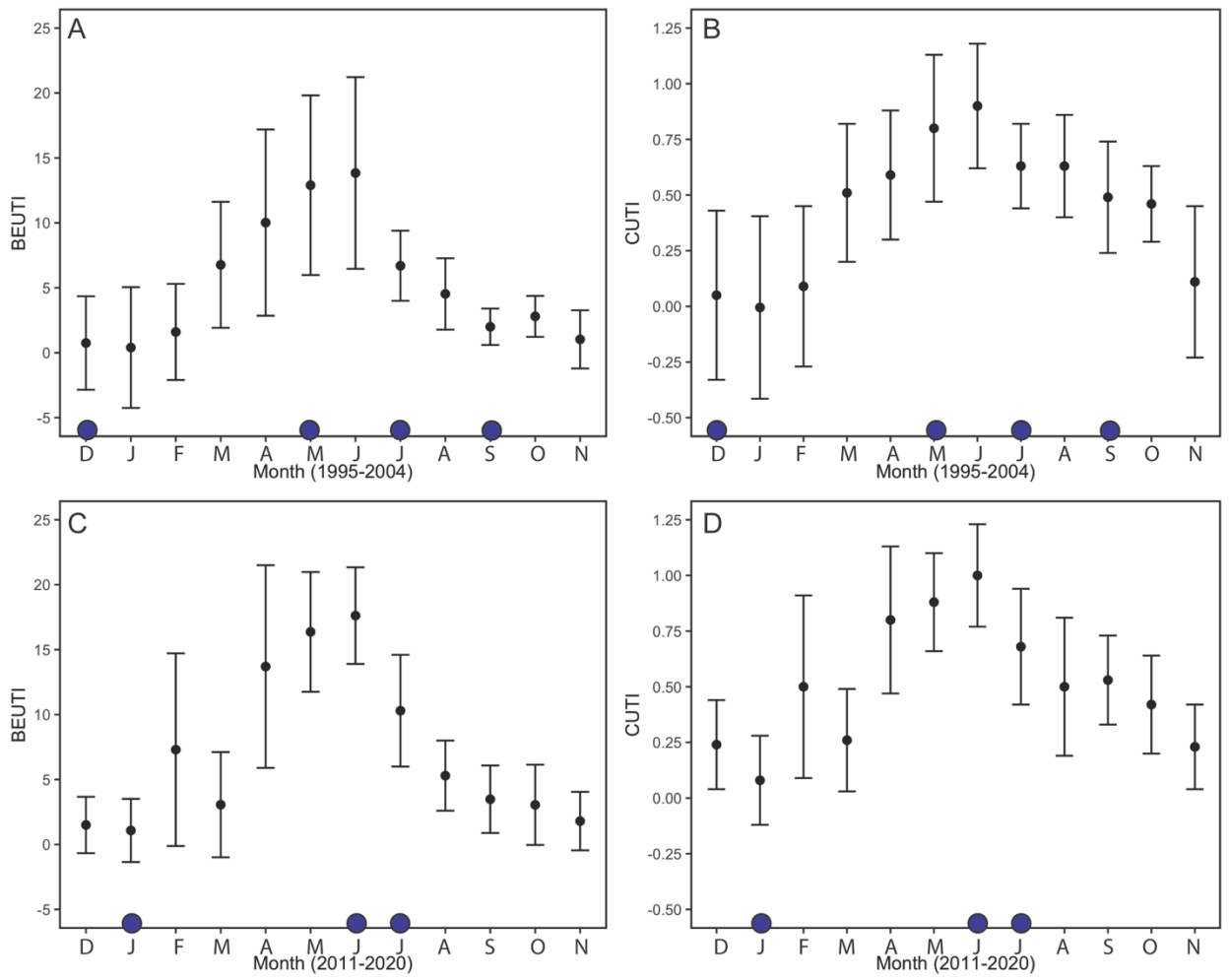


**Figure S8.** Aggregated monthly upwelling indices for both study periods to identify monthly and seasonal trends. Blue circles on x-axes represent months during which mussels were collected. (a) BEUTI averaged for all months 1995-2004 (e.g., Jan = mean BEUTI of all January months from 1994-2005). (b) CUTI averaged for all months 1995-2004 (e.g., Jan = mean CUTI of all January months from 2011-2020). (c) BEUTI averaged for all months 2011-2020 (e.g., Jan = mean BEUTI of all January months from 1994-2005). (d) CUTI averaged for all months 2011-2020 (e.g., Jan = mean CUTI of all January months from 2011-2020).

**Text S1.** The *M. californianus* individuals collected from Horseshoe Cove in June 2020 had been identified and tagged with gel nail polish in December 2019 to ensure that future collections occurred at the same micro-environment within the cove. We selected and tagged 10 shells that

were > 30 mm long to minimize sample loss from dislodgement or predation of smaller juvenile shells. The eight remaining tagged individuals were collected in June 2020 with terminal shell lengths ranging from 32.3 to 41 mm (average estimated ventral margin growth rates of 6.5 mm over the course of six months, or ~ 1.1 mm per month). This supports our interpretation that an 80 mm long shell = one-year old *M. californianus* (Coe and Fox, 1942) is not applicable or reasonable for northern California mussels.

**Table S2.** Shell characteristics for all 40 specimens in the study.

| Specimen ID | Collection date | Tidal pos. | Habitat | Shell length (mm) | Cross-sectional thickness (mm) | Inner calcite thickness (mm) | Std. gray value variance | Final growth band color |
|---|---|---|---|---|---|---|---|---|
| 51002A | 5/10/02 | Mid | Open coast | 60.00 | 2.36 | 1.81 | -0.53 | Dark |
| 51002B | 5/10/02 | Mid | Open coast | 60.50 | 2.94 | 2.37 | 0.19 | Dark |
| PB51002 | 5/10/02 | Mid | Open coast | 73.70 | 4.30 | 2.63 | -0.46 | Dark |
| PB71902 | 7/19/02 | Mid | Open coast | 54.60 | 3.10 | 1.25 | -0.92 | Dark |
| 71902B | 7/19/02 | Mid | Open coast | 60.10 | 3.29 | 2.02 | -0.15 | Dark |
| 71902A | 7/19/02 | Mid | Open coast | 61.10 | 2.63 | 1.66 | 2.45 | Dark |
| PB120102 | 12/1/02 | Mid | Open coast | 58.90 | 3.30 | 2.27 | 1.70 | Dark |
| 12102B | 12/1/02 | Mid | Open coast | 59.20 | 3.30 | 1.96 | 2.88 | Light |
| 12102A | 12/1/02 | Mid | Open coast | 60.10 | 3.09 | 1.93 | 0.98 | Light |
| PB122302 | 12/23/02 | Mid | Open coast | 69.20 | 2.60 | 1.34 | -0.78 | Light |
| 90703B | 9/7/03 | Mid | Open coast | 54.70 | 2.56 | 1.19 | 2.17 | Light |
| PB90703 | 9/7/03 | Mid | Open coast | 57.50 | 2.60 | 1.77 | -0.97 | Dark |
| 90703A | 9/7/03 | Mid | Open coast | 59.00 | 3.29 | 2.70 | 0.76 | Dark |
| BBL119 | 1/18/19 | Low | Cove | 32.20 | 2.00 | 0.81 | -0.26 | Light |
| BBLX19 | 1/18/19 | Low | Cove | 39.60 | 2.30 | 0.90 | -0.35 | Light |
| BBLY19 | 1/18/19 | Low | Cove | 41.00 | 2.00 | 1.26 | -0.88 | Light |
| BBMX19 | 1/18/19 | Mid | Cove | 46.30 | 3.70 | 3.02 | 1.16 | Light |
| BBH119 | 1/18/19 | High | Cove | 49.50 | 2.40 | 1.07 | -1.03 | Light |
| BBH219 | 1/18/19 | High | Cove | 54.20 | 3.40 | 2.05 | 0.59 | Light |

| | | | | | | | | |
|---|---|---|---|---|---|---|---|---|
| BBMY19 | 1/18/19 | Mid | Cove | 56.50 | 3.70 | 2.13 | 0.51 | Light |
| BBM319 | 1/18/19 | Mid | Cove | 68.90 | 3.60 | 2.37 | 0.67 | Dark |
| BBH319 | 1/18/19 | High | Cove | 70.10 | 3.60 | 1.50 | -0.94 | Dark |
| BB7114 | 7/11/19 | Mid | Cove | 72.10 | 2.51 | 1.92 | -0.67 | Dark |
| BB7116 | 7/11/19 | Mid | Cove | 73.10 | 2.85 | 2.15 | -0.61 | Dark |
| BB7113 | 7/11/19 | Mid | Cove | 76.60 | 3.20 | 3.59 | 0.22 | Dark |
| BB7111 | 7/11/19 | Mid | Cove | 78.60 | 2.55 | 1.38 | -0.54 | Dark |
| BB7112 | 7/11/19 | Mid | Cove | 83.50 | 3.10 | 2.77 | -0.47 | Dark |
| BB7115 | 7/11/19 | Mid | Cove | 93.80 | 4.00 | 3.46 | 0.90 | Dark |
| OCM220 | 6/6/20 | Mid | Open coast | 31.60 | 1.00 | 0.36 | -0.69 | Dark |
| OCM320 | 6/6/20 | Mid | Open coast | 32.10 | 1.30 | 0.44 | -0.78 | Dark |
| BBMB20 | 6/6/20 | Mid | Cove | 32.30 | 1.30 | 0.66 | -0.29 | Light |
| BBLB20 | 6/6/20 | Low | Cove | 33.50 | 1.00 | 0.38 | -0.63 | Dark |
| BBMA20 | 6/6/20 | Mid | Cove | 35.30 | 1.80 | 1.61 | -0.93 | Dark |
| BBMC20 | 6/6/20 | Mid | Cove | 35.50 | 1.80 | 0.80 | -0.96 | Light |
| BBHC20 | 6/6/20 | High | Cove | 36.20 | 1.80 | 0.63 | -1.10 | Dark |
| BBHA20 | 6/6/20 | High | Cove | 38.80 | 1.90 | 0.31 | 0.11 | Dark |
| BBLA20 | 6/6/20 | Low | Cove | 38.90 | 1.50 | 0.90 | -0.14 | Dark |
| BBLC20 | 6/6/20 | Low | Cove | 41.00 | 1.20 | 0.66 | -0.60 | Dark |
| OCMM20 | 6/6/20 | High | Open coast | 71.60 | 2.70 | 1.88 | 0.39 | Dark |
| OCLL20 | 6/6/20 | Low | Open coast | 73.70 | 3.50 | 2.42 | 0.00 | Dark |

## References


Andrus, C. F. T. and Crowe, D. E.: Geochemical analysis of Crassostrea virginica as a method to determine season of capture, J. Archaeol. Sci., 27, 33–42, https://doi.org/10.1006/jasc.1999.0417, 2000.

Bayne, B. L., Bayne, C. J., Carefoot, T. C., and Thompson, R. J.: The physiological ecology of Mytilus californianus Conrad, Oecologia, 22, 211–228, https://doi.org/10.1007/BF00344793, 1976.

Black, B. A. B. A., Gillespie, D. C. G. C., MacLellan, S. E. M. E., and Hand, C. M. H. M.: Establishing highly accurate production-age data using the tree-ring technique of crossdating: a case study for Pacific geoduck (Panopea abrupta), Can. J. Fish. Aquat., https://doi.org/10.1139/F08-158, 2008.

Blanchette, C. A., Helmuth, B., and Gaines, S. D.: Spatial patterns of growth in the mussel, Mytilus californianus, across a major oceanographic and biogeographic boundary at Point Conception, California, USA, J. Exp. Mar. Bio. Ecol., 340, 126–148, https://doi.org/10.1016/j.jembe.2006.09.022, 2007.

Bodega Ocean Observing Node: Shorestation Seawater Data, BML Seawater Temperature Daily, 1995-2004 and 2011-2020, Bodega Ocean Observing Node [data set], available at https://boon.ucdavis.edu/data-access/products/seawater/bml_seawater_temperature_daily (last access: November 2020), 2021.

Braje, T.J., Kennett, D.J., Erlandson, J.M., and Culleton, B.J.: Human impacts on nearshore shellfish taxa: a 7,000 year record from Santa Rosa Island, California, Am. Antiq. 72, 735–756, https://doi.org/10.2307/25470443, 2007.

Braje, T. J., Rick, T. C., and Erlandson, J. M.: A trans-Holocene historical ecological record of shellfish harvesting on California's Northern Channel Islands, Quat. Int., 264, 109–120, https://doi.org/10.1016/j.quaint.2011.09.011, 2012.

Braje, T. J., Rick, T. C., Willis, L. M., and Erlandson, J. M.: Shellfish and the Chumash: marine invertebrates and complex hunter-gatherers on late Holocene San Miguel Island, California, North American Archaeologist, 32, 267–290, https://doi.org/10.2190/NA.32.3.c, 2011.

Bullard, E.M., Torres, I., Ren, T., Graeve, O.A., and Roy, K.: Shell mineralogy of a foundational marine species, Mytilus californianus, over half a century in a changing ocean, Proc. Natl. Acad. Sci., 118, 3, https://doi.org/10.1073/pnas.2004769118, 2021.

Burchell, M., Cannon, A., Hallmann, N., Schwarcz, H. P., and Schöne, B. R.: Refining estimates for the season of shellfish collection on the Pacific Northwest Coast: applying high-resolution stable oxygen isotope analysis and sclerochronology, Archaeometry, 55, 258–276, https://doi.org/10.1111/j.1475-4754.2012.00684.x, 2013.

Butler, P.G., Wanamaker J.R., A.D., Scourse, J.D., Richardson, C.A., and Reynolds, D.J.: Variability of marine climate on the North Icelandic Shelf in a 1356-year proxy archive based on growth increments in the bivalve Arctica islandica, Palaeogeogr. Palaeoclimatol. Palaeoecol., 373, 141–151, https://doi: 10.1016/j.palaeo.2012.01.016, 2013.

Campbell, B. and Braje, T.J.: Estimating California mussel (Mytilus californianus) size from hinge fragments: a methodological application in historical ecology, J. Archaeol. Sci., 58, 167–174, https://doi.org/10.1016/j.jas.2015.02.007, 2015.

Cannon, A. and Burchell, M.: Reconciling oxygen isotope sclerochronology with interpretations

of millennia of seasonal shellfish collection on the Pacific Northwest Coast, Quat. Int., 427, 184–191, https://doi.org/10.1016/j.quaint.2016.02.037, 2017.
Checkley, D. M. and Barth, J. A.: Patterns and processes in the California Current System, Prog. Oceanogr., 83, 49–64, https://doi.org/10.1016/j.pocean.2009.07.028, 2009.
Coe, W. R. and Fox, D. L.: Biology of the California sea-mussel (Mytilus californianus). iii. Environmental conditions and rate of growth, The Biological Bulletin, 87, 59–72, https://doi.org/10.2307/1538129, 1944.
Connor, K. M. and Gracey, A. Y.: High-resolution analysis of metabolic cycles in the intertidal mussel Mytilus californianus, Am. J. Physiol. Regul. Integr. Comp. Physiol., 302, R103–R111, https://doi.org/10.1152/ajpregu.00453.2011, 2011.
Connor, K. M. and Robles, C. D.: Within-site variation of growth rates and terminal sizes in Mytilus californianus along wave exposure and tidal gradients, The Biological Bulletin, 228, 39–51, https://doi.org/10.1086/BBLv228n1p39, 2015.
Connor, K. M., Sung, A., Garcia, N. S., Gracey, A. Y., and German, D. P.: Modulation of digestive physiology and biochemistry in Mytilus californianus in response to feeding level acclimation and microhabitat, Biol. Open, 5, 1200–1210, https://doi.org/10.1242/bio.019430, 2016.
Dahlhoff, E. and Menge, B.: Influence of phytoplankton concentration and wave exposure on the ecophysiology of Mytilus californianus, Mar. Ecol. Prog. Ser., 144, 97–107, https://doi.org/10.3354/meps144097, 1996.
Dever, E.P. and Lentz, S.J.: Heat and salt balances over the northern California shelf in winter and spring, J. Geophys. Res., 99, 16001–16017, https://doi.org/10.1029/94JC01228, 1994.
Dodd, J.R.: Paleoecological implications of shell mineralogy in two pelecypod species, J. Geol. 71, 1–11, https://www.jstor.org/stable/30069360, 1963.
Dodd, J. R.: Environmentally controlled variation in the shell structure of a pelecypod species, J. Paleontol., 9, 1065–1071, http://www.jstor.org/stable/1301640, 1964.
Feely, R. A., Sabine, C. L., Hernandez-Ayon, J. M., Ianson, D., and Hales, B.: Evidence for upwelling of corrosive "acidified" water onto the continental shelf, Science, 320, 1490–1492, https://doi.org/10.1126/science.1155676, 2008.
Ferguson, J. E., Johnson, K. R., Santos, G., Meyer, L., and Tripati, A.: Investigating $\delta^{13}C$ and $\Delta^{14}C$ within *Mytilus californianus* shells as proxies of upwelling intensity: $\delta^{13}C$ AND $\Delta^{14}C$ in Mytilus shells, Geochem. Geophys. 14, 1856–1865, https://doi.org/10.1002/ggge.20090, 2013.
Ford, H. L., Schellenberg, S. A., Becker, B. J., Deutschman, D. L., Dyck, K. A., and Koch, P. L.: Evaluating the skeletal chemistry of *Mytilus californianus* as a temperature proxy: Effects of microenvironment and ontogeny, Paleoceanography, 25, https://doi.org/10.1029/2008PA001677, 2010.
Freitas, P., Clarke, L. J., Kennedy, H., and Richardson, C.: The potential of combined Mg/Ca and $\delta^{18}O$ measurements within the shell of the bivalve Pecten maximus to estimate seawater $\delta^{18}O$ composition, Chem. Geol., 291, 286–293, https://doi.org/10.1016/j.chemgeo.2011.10.023, 2012.
Freitas, P., Clarke, L. J., Kennedy, H., Richardson, C., and Abrantes, F.: Mg/Ca, Sr/Ca, and stable-isotope ($\delta^{18}O$ and $\delta^{13}C$) ratio profiles from the fan mussel *Pinna nobilis*: seasonal records and temperature relationships: Pinna nobilis ratio profiles, Geochem. Geophys., 6, https://doi.org/10.1029/2004GC000872, 2005.

García-Reyes, M. and Largier, J.: Observations of increased wind-driven coastal upwelling off central California, J. Geophys. Res.,115, https://doi.org/10.1029/2009JC005576, 2010.
García-Reyes, M. and Largier, J. L.: Seasonality of coastal upwelling off central and northern California: New insights, including temporal and spatial variability, J. Geophys. Res. 117, https://doi.org/10.1029/2011JC007629, 2012.
Gillikin, D. P., Dehairs, F., Lorrain, A., Steenmans, D., Baeyens, W., and André, L.: Barium uptake into the shells of the common mussel (Mytilus edulis) and the potential for estuarine paleo-chemistry reconstruction, Geochim. Cosmochim. Acta, 70, 395–407, https://doi.org/10.1016/j.gca.2005.09.015, 2006.
Gordon, J. and Carriker M.R.: Growth lines in a bivalve mollusk: subdaily patterns and dissolution of the shell, Science, 202(4367), 519–521, https://doi.org/10.1126/science.202.4367.519, 1978.
Hallmann, N., Burchell, M., Schöne, B. R., Irvine, G. V., and Maxwell, D.: High-resolution sclerochronological analysis of the bivalve mollusk Saxidomus gigantea from Alaska and British Columbia: techniques for revealing environmental archives and archaeological seasonality, J. Archaeol. Sci., 36, 2353–2364, https://doi.org/10.1016/j.jas.2009.06.018, 2009.
Hallmann, N., Burchell, M., Brewster, N., Martindale, A., and Schöne, B. R.: Holocene climate and seasonality of shell collection at the Dundas Islands Group, northern British Columbia, Canada—A bivalve sclerochronological approach, Palaeogeog., Palaeoclimatol., Palaeoecol., 373, 163–172, https://doi.org/10.1016/j.palaeo.2011.12.019, 2013.
Hickey, B. M. and Banas, N. S.: Oceanography of the U.S. Pacific Northwest coastal ocean and estuaries with application to coastal ecology, Estuaries, 26, 1010–1031, https://doi.org/10.1007/BF02803360, 2003.
Huyer, A.: Coastal upwelling in the California Current system, Prog. Oceangr., 12, 259–284, https://doi.org/10.1016/0079-6611(83)90010-1, 1983.
Jacox, M. G., Edwards, C. A., Hazen, E. L., and Bograd, S. J.: Coastal upwelling revisited: Ekman, Bakun, and improved upwelling indices for the U.S. West Coast, J. Geophys. Res. Oceans, 123, 7332–7350, https://doi.org/10.1029/2018JC014187, 2018.
Jazwa, C. S. and Kennett, D. J.: Sea mammal hunting and site seasonality on western San Miguel Island, California, J. Calif. Gt. Basin Anthropol., 36, 2, https://escholarship.org/uc/item/4pr7f4qb, 2016.
Jones, T. L. and Kennett, D. J.: Late Holocene Sea Temperatures along the Central California Coast, Quat. Res., 51, 74–82, https://doi.org/10.1006/qres.1998.2000, 1999.
Jones, D. S. and Quitmyer, I. R.: Marking time with bivalve shells: oxygen isotopes and season of annual increment formation, Palaios, 11, 340–346, https://doi.org/10.2307/3515244, 1996.
Jones, T. L. and Richman, J. R.: On mussels: *Mytilus californianus* as a prehistoric resource, North American Archaeologist, 16, 33–58, https://doi.org/10.2190/G5TT-YFHP-JE6A-P2TX, 1995.
Katayama, S. and Isshiki, T.: Variation in otolith macrostructure of Japanese flounder (Paralicthys olivaceus): A method to discriminate between wild and released fish, 57, 0–186, https://doi.org/10.1016/j.seares.2006.09.006, 2007.
Kennedy, M.A.: An investigation of hunter–gatherer shellfish foraging practices: archaeological

and geochemical evidence from Bodega Bay, California, Ph.D. thesis, University of California, Davis, USA, 3171887, 2004.
Kennedy, M. A., Russell, A. D., and Guilderson, T. P.: A radiocarbon chronology of hunter-gatherer occupation from Bodega Bay, California, USA, Radiocarbon, 47, 265–293, https://doi.org/10.1017/S0033822200019779, 2005.
Killam, D. E. and Clapham, M. E.: Identifying the ticks of bivalve shell clocks: seasonal growth in relation to temperature and food supply, Palaios, 33, 228–236, https://doi.org/10.2110/palo.2017.072, 2018.
Killam, D., Thomas, R., Al-Najjar, T., and Clapham, M.: Interspecific and intrashell stable isotope variation among the Red Sea giant clams, Geochem., Geophys., 21, e2019GC008669, https://doi.org/10.1029/2019GC00869, 2020.
Killingley, J. S. and Berger, W. H.: Stable isotopes in a mollusk shell: detection of upwelling events, Science, 205, 186–188, https://doi.org/10.1126/science.205.4402.186, 1979.
Kirby, M. X., Soniat, T. M., and Spero, H. J.: Stable isotope sclerochronology of Pleistocene and Recent oyster shells (Crassostrea virginica), Palaios, 13, 560–569, https://doi.org/10.2307/3515347, 1998.
Klein, R. T., Lohmann, K. C., and Thayer, C. W.: Bivalve skeletons record sea-surface temperature and $\delta^{18}O$ via Mg/Ca and $^{18}O/^{16}O$ ratios, Geology, 24, 5, 415–418, https://doi.org/10.1130/0091-7613(1996)024<0415:BSRSST>2.3.CO;2, 1996.
Largier, J. L., Magnell, B. A., and Winant, C. D.: Subtidal circulation over the northern California shelf, J. Geophys. Res. Oceans, 98, 18147–18179, https://doi.org/10.1029/93JC01074, 1993.
Lepofsky, D., Smith, N. F., Cardinal, N., Harper, J., Morris, M., Gitla, E. W., Bouchard, R., Kennedy, D. I. D., Salomon, A. K., Puckett, M., and Rowell, K.: ancient shellfish mariculture on the northwest coast of North America, Am. Antiq., 80, 236–259, https://doi.org/10.7183/0002-7316.80.2.236, 2015.
Lutz, R. A. and Rhoads, D. C.: Anaerobiosis and a theory of growth line formation, Science, 198, 1222–1227, https://doi.org/10.1126/science.198.4323.1222, 1977.
McCoy, S. J., Kamenos, N. A., Chung, P., Wootton, T. J., and Pfister, C. A.: A mineralogical record of ocean change: decadal and centennial patterns in the California mussel, Glob. Change Biol., 24, 2554–2562, https://doi.org/10.1111/gcb.14013, 2018.
McCoy, S. J., Robinson, L. F., Pfister, C. A., Wootton, J. T., and Shimizu, N.: Exploring B/Ca as a pH proxy in bivalves: relationships between Mytilus californianus B/Ca and environmental data from the northeast Pacific, Biogeosciences 8, 2567–2579, https://doi.org/10.5194/bg-8-2567-2011, 2011.
Mellin, C., Mouillot, D., Kulbicki, M., McClanahan, T. R., Vigliola, L., Bradshaw, C. J. A., Brainard, R. E., Chabanet, P., Edgar, G. J., Fordham, D. A., Friedlander, A. M., Parravicini, V., Sequeira, A. M. M., Stuart-Smith, R. D., Wantiez, L., and Caley, M. J.: Humans and seasonal climate variability threaten large-bodied coral reef fish with small ranges, Nature, 7, 10491, https://doi.org/10.1038/ncomms10491, 2016.
NOAA Fisheries - Southwest Fisheries Science Center: Environmental Research Division: New West Coast Upwelling Indices, NOAA Fisheries - Southwest Fisheres Science Center [data set], available at: https://oceanview.pfeg.noaa.gov/products/upwelling/dnld (last access: January 2022), 2018.
Paine, R. T.: Intertidal community structure, Oecologia, 15, 93–120,

https://doi.org/10.1007/BF00345739, 1974.
Paine, R. T.: Size-Limited Predation: an observational and experimental approach with the Mytilus-Pisaster interaction, Ecology 57, 858–873, https://doi.org/10.2307/1941053, 1976.
Pfister, C. A., McCoy, S. J., Wootton, J. T., Martin, P. A., Colman, A. S., and Archer, D.: Rapid environmental change over the past decade revealed by isotopic analysis of the California mussel in the northeast Pacific, PLoS ONE, 6, e25766, https://doi.org/10.1371/journal.pone.0025766, 2011.
Pfister, C. A., Roy, K., Wootton, J. T., McCoy, S. J., Paine, R. T., Suchanek, T. H., and Sanford, E.: Historical baselines and the future of shell calcification for a foundation species in a changing ocean, Proc. Royal Soc. B: Biol. Sci., 283, 20160392, https://doi.org/10.1098/rspb.2016.0392, 2016.
Phillips, N. E.: Growth of filter-feeding benthic invertebrates from a region with variable upwelling intensity, Mar. Ecol. Prog. Ser., 295, 79–89, https://doi.org/10.3354/meps295079, 2005.
Poloczanska, E. S., Burrows, M. T., Brown, C. J., García Molinos, J., Halpern, B. S., Hoegh-Guldberg, O., Kappel, C. V., Moore, P. J., Richardson, A. J., Schoeman, D. S., and Sydeman, W. J.: Responses of marine organisms to climate change across oceans, Front. Mar. Sci., 3, https://doi.org/10.3389/fmars.2016.00062, 2016.
Poulain, C., Gillikin, D. P., Thébault, J., Munaron, J. M., Bohn, M., Robert, R., Paulet, Y.-M., and Lorrain, A.: An evaluation of Mg/Ca, Sr/Ca, and Ba/Ca ratios as environmental proxies in aragonite bivalve shells, Chem. Geol., 396, 42–50, https://doi.org/10.1016/j.chemgeo.2014.12.019, 2015.
Renault, L., Deutsch, C., McWilliams, J. C., Frenzel, H., Liang, J.-H., and Colas, F.: Partial decoupling of primary productivity from upwelling in the California Current system, Nature, 9, 505–508, https://doi.org/10.1038/ngeo2722, 2016.
Rose, J. M., Blanchette, C. A., Chan, F., Gouhier, T. C., Raimondi, P. T., Sanford, E., and Menge, B. A.: Biogeography of ocean acidification: Differential field performance of transplanted mussels to upwelling-driven variation in carbonate chemistry, PLoS One, 15, e0234075, https://doi.org/10.1371/journal.pone.0234075, 2020.
Schöne, B. R.: Arctica islandica (Bivalvia): a unique paleoenvironmental archive of the northern North Atlantic Ocean, Glob. Planet. Change 111, 199–225, https://doi.org/10.1016/j.gloplacha.2013.09.013, 2013.
Schöne, B. R., Dunca, E., Fiebig, J., and Pfeiffer, M.: Mutvei's solution: an ideal agent for resolving microgrowth structures of biogenic carbonates, Palaeogeogr., Palaeoclimatol., Palaeoecol., 228, 149–166, https://doi.org/10.1016/j.palaeo.2005.03.054, 2005b.
Schöne, B.R. and Gillikin, D.P.: Unraveling environmental histories from skeletal diaries — Advances in sclerochronology, Palaeogeogr., Palaeoclimatol., Palaeoecol., 373, 1–5, https://doi.org/10.1016/j.palaeo.2012.11.026, 2013.
Schöne, B. R., Houk, S. D., Castro, A. D. F., Fiebig, J., Oschmann, W., Kröncke, I., Dreyer, W., and Gosselck, F.: Daily growth rates in shells of Arctica islandica: assessing sub-seasonal environmental controls on a long-lived bivalve mollusk, Palaios, 20, 78–92, https://doi.org/10.2110/palo.2003.p03-101, 2005a.
Schöne, B.R. and Surge, D.M.: Part N, Revised, Volume 1, Chapter 14: bivalve sclerochronology and geochemistry, Treatise online, 46, 1–23, 2012.
Smith, J. R., Fong, P., and Ambrose, R. F.: Spatial patterns in recruitment and growth of the

mussel Mytilus californianus (Conrad) in southern and northern California, USA, two regions with differing oceanographic conditions, J. Sea Res. 61, 165–173, https://doi.org/10.1016/j.seares.2008.10.009, 2009.
Suchanek, T. H.: The role of disturbance in the evolution of life history strategies in the intertidal mussels Mytilus edulis and Mytilus californianus, Oecologia, 50, 143–152, https://doi.org/10.1007/BF00348028, 1981.
Surge, D., Lohmann, K. C., and Dettman, D. L.: Controls on isotopic chemistry of the American oyster, Crassostrea virginica: implications for growth patterns, Palaeogeogr., Palaeoclimatol., Palaeoecol., 172, 283–296, https://doi.org/10.1016/S0031-0182(01)00303-0, 2001.
Sydeman, W. J., García-Reyes, M., Schoeman, D. S., Rykaczewski, R. R., Thompson, S. A., Black, B. A., and Bograd, S. J.: Climate change and wind intensification in coastal upwelling ecosystems, Science, 345, 77–80, https://doi.org/10.1126/science.1251635, 2014.
Taylor, J. D., Kennedy, W.J., and Hall, A.: The Shell Structure and Mineralogy of the Bivalvia: Introduction. Nuculacea-Trigonacea, Bull. Br. Mus. (Nat. Hist.), Zool., 3, 1–125, 1969.
Thakar, H. B., Glassow, M. A., and Blanchette, C.: Reconsidering evidence of human impacts: Implications of within-site variation of growth rates in Mytilus californianus along tidal gradients, Quat. Int., 427, 151–159, https://doi.org/10.1016/j.quaint.2015.10.018, 2017.
Trofimova, T., Andersson, C., Bonitz, F.G.W., Pederson, L.E.R., and Schöne, B.R.: Reconstructing early Holocene seasonal bottom-water temperatures in the northern North Sea using stable isotope records of Arctica islandica shells, Palaeogeog., Palaeoclimatol., Palaeoecol. 567, 110242, https://doi.org/10.1016/j.palaeo.2021.110242, 2021.
Wanamaker Jr., A.D., Kreutz, K.J., Borns Jr., H.W., Introne, D.S., Feindel, S., and Barber, B.J.: An aquaculture-based method for calibrated bivalve isotope paleothermometry, Geochem. Geophys., 7, 9, https://doi.org/10.1029/2005GC001189, 2006.
Wanamaker Jr., A.D., Kreutz, K.J., Wilson, T., Borns, H.W., Introne, D.S., and Feindel, S.: Experimentally determined Mg/Ca and Sr/Ca ratios in juvenile bivalve calcite for Mytilus edulis: implications for paleotemperature reconstructions, Geo-Marine Letters, 28(5–6), 359-368, https://doi.org/10.1007/s00367-008-0112-8, 2008.
Weidman, C., Jones, G.A., and Lohmann, K.C.: The long–lived mollusk Arctica islandica: a new https://doi.org/10.1029/94JC01882, 1994.
Welsh, K., Elliot, M., Tudhope, A., Ayling, B., Chappell, J.: Giant bivalves (Tridacna gigas) as –4, 266–270, https://doi.org/10.1016/j.epsl.2011.05.032, 2011.
Wing, S. R., Largier, J. L., Botsford, L. W., and Quinn, J. F.: Settlement and transport of benthic invertebrates in an intermittent upwelling region, Limnol. Oceanogr., 40, 316–329, https://doi.org/10.4319/lo.1995.40.2.0316, 1995.
Zhao, L., Shirai, K., Murakami-Sugihara, N., Higuchi, T., Sakamoto, T. T., Miyajima, T., and Tanaka, K.: retrospective monitoring of salinity in coastal waters with mussel shells, Sci. Total Environ., 671, 666–675, https://doi.org/10.1016/j.scitotenv.2019.03.405, 2019.
Zimmt, J. B., Lockwood, R., Andrus, C. F. T., and Herbert, G. S.: Sclerochronological basis for growth band counting: A reliable technique for life-span determination of Crassostrea virginica from the mid-Atlantic United States, Palaeogeogr., Palaeoclimatol., Palaeoecol., 516, 54–63, https://doi.org/10.1016/j.palaeo.2018.11.029, 2019.

## Chapter 2

## Coastal climate variability and seasonality recorded by an intertidal mussel species: insights from 9000 years of synthesized stable isotope data


### Abstract

Understanding past coastal climate variability is valuable for contextualizing modern changes in coastal settings, yet existing Holocene paleoceanographic records for the North American Pacific Coast commonly come from offshore marine sediments and may not represent the dynamic coastal environment. A potential archive of climate variability for the west coast of North America is the intertidal mussel species *Mytilus californianus*. Archaeologists have collected copious stable isotopic ($\delta^{18}O$ and $\delta^{13}C$) data from $^{14}C$-dated *M. californianus* shells to study human history at California's Channel Islands. When analyzed together, these isotopic data produce windows into a 9000-year-long record of Holocene isotopic variability. Here we synthesize over 6000 $\delta^{18}O$ and $\delta^{13}C$ data points from 13 published studies of *M. californianus* shells to characterize shell isotopic variability across ontogenetic, geographic, seasonal, and millennial scales. We aim to evaluate whether *M. californianus*, an intertidal bivalve mollusc: (1) records broad regional Holocene climate signals (e.g., warm/cool periods, freshwater flood events, etc.) and (2) contributes novel information about Holocene paleo-seasonality for coastal southern California. Synthesized data from *M. californianus* stable isotope profiles with five or more subsamples per shell show that this species records environmental information ranging from seasonal to millennial scales, depending on the number of individual shells and subsample resolution. Individual shells record seasonal scale processes, including an inferred annual temperature range of ~ 5°C. Collectively, the mussel record contains millennial-scale climate patterns, including warm-cool oscillations and an overall 0.52‰ depletion in shell $\delta^{18}O$ from

8800 BP to the present. Lastly, the mussel archive also reflects local-scale oceanographic variability in the form of a warmer coastal mainland shell $\delta^{18}O$ signature of -0.32‰ compared to the offshore Channel Islands cooler $\delta^{18}O_{shell}$ signature of 0.33‰. While this species is a promising coastal archive, we emphasize the need for high-resolution subsampling from multiple individuals to accurately infer broader climate patterns recorded by a single species over time.

## 1 Introduction

Anthropogenic changes in sea surface temperature (SST), ocean chemistry, and carbon cycling have been documented in nearshore surface waters globally [1–3]. Changing environmental conditions are particularly threatening to coastal ecosystems, which are highly sensitive to sea-level rise, storms, nutrient runoff, and ecological regime shifts [4–7]. Vulnerability of nearshore ecosystems to environmental perturbation is amplified by the cultural and economic importance of coastlines, which have been densely populated sites of human-environment interactions for thousands of years [8,9]. At present, the social and economic relevance of coastal zones continues to expand; nearly half of the global population is expected to live within 100 km of a coastline within the next decade [6,10,11]. As such, coastal archives of past climate and ecological change are of particular importance for understanding past natural baselines and estimating the onset of human impacts within coastal systems [8,12–14]. Biogenic coastal archives can reveal valuable information about broader scale climate oscillations [15–18] to supplement the vast collections of offshore archives, such as deeper marine sediments and corals, and terrestrial archives, such as speleothems, lake records, and ice cores [19–24].

Here, we address the need for high-resolution archives of coastal regions by investigating a potential record of Holocene environmental variability for the Pacific Coast of North America: *Mytilus californianus* (California mussel). *Mytilus californianus* is a promising archive of

regional coastal climate for California, USA due to its abundance and consistent presence in the archaeological record [25]. In order to assess the utility of *M. californianus* as a regional climate archive and determine whether this species contributes useful information about Holocene seasonality and climate variability for coastal California, we synthesize published stable isotope records from Holocene-aged *M. californianus* shells to document and characterize variability across both spatial (e.g., islands versus mainland) and temporal scales (e.g., seasonal versus millennial) and compare the mussel record to documented paleo-records for this same time interval and region. By analyzing ontogenetic, geographic, seasonal, and millennial scales of stable isotope variability, we contribute a newly synthesized 9000-year-long, snapshot-based spatio-temporal record of *M. californianus*. The data and synthesis provided here contribute to Holocene paleoceanography while reducing the need for further invasive sampling from culturally significant midden sites [26,27]. Extensive shell material from the northern Channel Islands has already been sampled and analyzed for stable isotopes, and these data are now integrated and analyzed in a format that is useful for paleoceanographic purposes.

### 1.1 Ecology and natural history of *Mytilus californianus*

*Mytilus californianus* is dominant in modern rocky intertidal ecosystems spanning 25° of latitude along the northeastern Pacific Coast (Aleutian Islands of Alaska, USA to Baja California, Mexico) [28]. As a foundation species, *M. californianus* forms a habitat for hundreds of marine taxa, provides a food source for coastal predators, and filters particulate matter from the intertidal water column [28–30]. *Mytilus californianus* is dominant in exposed, open-ocean environments with heavy wave action due to its strong, tri-layered shell and thicker byssal threads relative to its congeners [31,32]. Because of its widespread biogeographic distribution and its contributions to biological diversity, *M. californianus* has been a classic study organism

in the fields of intertidal ecology and marine invertebrate physiology since the mid-20th century [28,31,33–41]. Despite the attention *M. californianus* has received, its life history traits remain enigmatic; its lifespan is uncertain, although it is thought to range from 10 to 100 years depending on environmental conditions and disturbance levels [31,42]. Shell growth rate is variable across both micro-scale (e.g., tidal) and macro-scale (e.g., latitudinal) gradients that control conditions such as water temperature, wave action, and immersion time [29,40,43]. Estimating shell growth rate and lifespan is further complicated by the lack of time-calibrated periodic growth bands [44]. Despite these complexities, previous studies have constrained growth patterns of *M. californianus* for southern populations specifically; Ford et al. found that the *M. californianus* shell length grew continuously over the course of a 382-day outplant experiment in San Diego, which is advantageous for reconstructing minimum and maximum temperatures over the course of a year [42]. Additionally, Ferguson et al. (2013) found evidence for continuous calcification without growth shutdown in *M. californianus* throughout the year at sites in southern California, USA and Baja California, Mexico [45]. There is also general agreement in the mytilid literature that adult *M. californianus* shells accrete approximately 2-5 mm at their terminal growth margin per month in southern Californian environments [25,31,34] where they grow more rapidly in temperatures ranging from 15° to 19°C in particular [29]. Continuous annual growth patterns and the relationship between temperature and growth rate are specific to southern California since the upwelling and temperature regimes differ dramatically for regions north of Point Conception, resulting in significantly slower growth rates for marine calcifying biota in the central and northern portions of the California Current System [29,40,44,46].

### 1.2 Archaeological record of *Mytilus californianus*

In addition to its ecological value, *M. californianus* has been a culturally relevant species and major food source for Indigenous peoples throughout the Holocene. *Mytilus californianus* shells are found in northeastern Pacific Coast shell middens at a higher density than any other bivalve species. This species is particularly abundant in the shell middens of the Channel Islands, California, USA due to the populous Chumash civilizations that inhabited southern California throughout the Holocene [25,47,48]. Prior to European colonization, the Chumash peoples of present-day southern California had established 22 major villages on Santa Cruz, San Miguel, and Santa Rosa Islands, built extensive trade networks within and among coastal California and all nine Channel Islands, and established the largest populations known among hunter-gatherer civilizations according to published records [49]. The dominant presence of *M. californianus* shells in Channel Islands' shell middens of all ages indicates that the Chumash groups heavily and continuously harvested *M. californianus* as a significant food source throughout the Holocene [48,50]. Exceptional preservation of Channel Islands' shell middens has attracted the attention of archaeologists and anthropologists for the past two centuries, producing an extensive collection of *M. californianus* shells extracted from shell middens. Archaeologists commonly apply stable isotopic analysis to midden shells to reconstruct the season of harvest, which is useful for investigating questions about human migration patterns, site usage, and cultural traditions [51–55]. As such, the ample stable isotope records from archeological *M. californianus* shells have the potential to provide an archive of coastal climate variability and seasonality. The vast previously-excavated collections of archaeological shells in general have valuable potential for paleoceanographic purposes, and here we apply and test this for *M. californianus* from the Channel Islands middens in particular.

### 1.3 Shell chemistry of *Mytilus californianus*

Species-specific relationships between $\delta^{18}O_{shell}$ and sea surface temperature (SST) and $\delta^{13}C_{shell}$ and upwelling of nutrient-rich waters allow for paleoenvironmental reconstruction from biogenic carbonates. When sampled serially along the ontogenetic growth trajectory (from umbo to commissure), $\delta^{18}O_{shell}$ has been found to be a reliable record of mean annual temperature and mean annual temperature ranges in modern *M. californianus* shells from San Diego, with a slight and consistent enrichment in $^{18}O$ by 0.2 to 0.5‰ relative to predicted $\delta^{18}O_{equilibrium}$ [42]. Interpretation of $\delta^{13}C_{shell}$ is more complex and inconsistent due to the incorporation of metabolic (respired) carbon in the shell mineral. In molluscs, $\delta^{13}C_{shell}$ typically decreases with ontogenetic age [56]. For *Mytilus* in particular, up to 10% of isotopically light respired carbon can be incorporated into the shell during calcification and metabolic rate can vary throughout ontogeny [45,57], hindering the use of $\delta^{13}C_{shell}$ profiles as direct proxies of their environment. However, significant shifts in $\delta^{13}C_{shell}$ through time can also indicate broad changes in ocean carbonate chemistry, as documented by a negative trend in modern $\delta^{13}C_{shell}$ in *M. californianus* from Washington relative to $\delta^{13}C_{shell}$ of *M. californianus* shells collected decades and millennia prior to the 21st century [58]. In addition to assessing long-term changes in ocean carbonate chemistry, $\delta^{13}C_{shell}$ profiles from multiple individuals from the same locality could be used to track short-term, upwelling-driven changes in ocean chemistry on a seasonal scale since upwelled water delivers isotopically light respired carbon and nutrients to the surface [45,59], although the relationship between $\delta^{13}C_{shell}$ and $\delta^{13}C$ of dissolved inorganic carbon (DIC) of seawater is inconsistent [45,60,61]. While Killingley and Berger (1979) found remarkable correlation and covariation between upwelling indices and $\delta^{13}C_{shell}$ for San Diego *M.*

*californianus* shells, more recent work did not find these patterns in modern *M. californianus* shells from the same locality [45,59].

Diagenesis is a potential concern for interpretations of stable isotope and trace element data from archaeological or fossilized carbonates. All non-modern *M. californianus* shells analyzed in the present study are from shell middens, which structurally and chemically favor preservation since shells on the edges of a midden deposit serve as a natural, carbonate-rich buffer to dissolution and barrier against crushing and erosion [62]. Additionally, *M. californianus* has an outer layer of calcite [44,63], which is less likely to be chemically altered since its trigonal crystal structure is more stable than that of the orthorhombic crystal structure of aragonite. All sub-samples analyzed here are from the outer calcite layer of *M. californianu*s shells, and all midden shell data were sourced from studies that methodically addressed diagenesis by performing X-ray diffraction analysis and/or HCl etching to identify and remove diagenetically altered carbonate from the shell surface before sampling for stable isotope analysis [64,65].

## 2 Methods

### 2.1 Study area

The California Current System (CCS) controls patterns of sea surface temperature (SST), upwelling intensity, and nutrient concentrations in southern California. The CCS comprises the cold California Current, the warm north-flowing California Undercurrent (subsurface), the warm north-flowing Davidson Current (surface), and the Southern California Eddy [46,66–68]. The dominant California Current flows southward along the coastline of northern California parallel to the alongshore winds, resulting in strong Ekman transport and intense upwelling near the coast of northern and central California [46,67]. South of Point Conception, the coastline morphology

changes such that the current no longer runs parallel to alongshore winds, which results in weaker Ekman transport and upwelling along southern California. The southern portion of the CCS is characterized by weak upwelling relative to central and northern portions of the CCS. The variability in upwelling intensity produces a warmer SST regime along the southern California coast. Wind forcing and upwelling is strongest during the summer in all portions of the CCS [46], but seasonal variability is less pronounced south of Point Conception, resulting in a warm zone and a weaker yet more stable upwelling regime off the coast of southern California.

In order to avoid capturing regionally different oceanographic signatures, this study uses only *M. californianus* shells collected in the southern portion of the CCS, south of Point Conception and north of Baja California (Fig 1). Specific collection sites are located on the northern Channel Islands (San Miguel Island, Santa Rosa Island, Santa Cruz Island, and Anacapa Island), Newport Beach, and San Diego. Channel Islands mussels were more likely to experience relatively lower temperatures from the cold California Current, [69], while mussels from Newport Beach and San Diego may have experienced warmer water on the order of ~ 3°C delivered by the California Undercurrent and Davidson Current (Fig 1). We separated Channel Islands shells from mainland California shells in order to determine whether the Channel Islands shells have higher mean $\delta^{18}O$ values related to cooler SSTs farther offshore.

The temperature differential between the islands and mainland sites is compounded by considerable small-scale oceanographic variability among the northern Channel Islands due to current activity, which produces a warm-cool SST gradient from east to west [69–72]. At Santa Cruz Island, for example, mean SSTs have been lower on the west coast than the southeast coast throughout the Holocene [72]. Mean SSTs at San Miguel Island are ~ 1 to 4°C lower than those at Anacapa Island [73]. In addition to small-scale spatial variability, seasonal patterns result in a

~ 5°C range of annual temperature variability [54,74]. For example, at Anacapa Island, SST alternates between warming (~ 16°C to 19°C) from late June through early September and cooling (~ 19°C to 15°C) from late September to early March [53]. Seasonal cycles are similar throughout the northern Channel Islands (i.e., cooling and warming periods occur relatively synchronously for all four islands) due to the seasonally driven upwelling regime [73].

### 2.2 *Mytilus californianus* shell records

We used Web of Science to search the relevant literature in geochemical, archaeological, paleoceanographic, and sclerochronological journals using the following keywords: California mussel, *Mytilus californianus*, stable isotope data, oxygen isotopes ($\delta^{18}O$), and carbon isotopes ($\delta^{13}C$). We included oxygen and carbon isotope data from *M. californianus* shells that met the following criteria for further meta-analysis and interpretation:

- all shells were definitively identified by the original authors as *M. californianus*
- all shells are sourced from southern California (south of Point Conception), including the Channel Islands, either live-collected from the intertidal zone or excavated from a coastal shell midden or outcrop
- all mussels lived during the Holocene (geologically younger than 11,700 years old)
- all shells have multiple (two or more) stable isotope subsamples per shell along the ontogenetic growth trajectory with a clear sampling direction (i.e., stable isotope data is presented according to direction of growth in order to infer the directionality of cooling versus warming trends in individual shell profiles)
- non-modern shells were examined with X-ray diffraction and/or treated with HCl etching to avoid diagenetically altered shell material

- non-modern shells were complete or nearly complete valves (no fragments, tools, or jewelry)
- non-modern shells were published with associated radiocarbon ages from a dated section of a midden to confidently place specimens in temporal context, ± 30 years
- modern shells had a known collection date (month/day/year) and latitude/longitude location provided

While our study criteria were designed to include modern, archaeological, and fossil specimens, we found no published records of stable isotope data from fossilized *M. californianus* shells from this region and time interval (but see Dodd (1966) for stable isotopic analysis of Pleistocene *Mytilus* shells [75]). We only used data sets that reported the full suite of raw $\delta^{18}O$ and $\delta^{13}C$ values collected for each individual rather than summary statistics. The resultant database contains 6036 oxygen and carbon stable isotope data points from 411 *M. californianus* shells extracted from 13 published studies (Appendix 1). The majority (10 of 13 studies) utilized archaeological shells to reconstruct patterns of early human settlement or foraging behavior [51–53,72,76–81], while the other three studies used modern *M. californianus* shells to calibrate stable isotope-based environmental proxies [42,45] or test the influence of micro-environment on shell geochemistry [42,74]. For each individual shell that met our criteria, we assigned it a unique shell ID, then entered $\delta^{18}O$ and $\delta^{13}C$ values for each subsample so that *n* rows with the same shell ID indicate *n* subsamples per individual shell. In addition to stable isotope data, associated information provided in the database are the number of subsamples, the citation of the primary publication, subsample label or distance along shell (mm), age in years before present (BP), specimen type (midden or modern), location (islands or mainland), site (specific island or city), latitude, and longitude. The subsample distance along the shell is relative to total shell

length. In most cases, the total shell length was not provided, although we included it whenever it was reported by primary authors (Appendix 1).

**2.3 Stable isotope sampling techniques used by primary authors**

Many archaeological studies apply the terminal growth band (TGB) sampling approach in order to infer the season of harvest [77–79,82]. For individual shells with fewer sub-samples (< 5) analyzed here, the primary authors performed TGB sub-sampling nearest the commissure. In order to determine whether $\delta^{18}O$-inferred SST was increasing (indicative of spring-summer) or decreasing (indicative of fall-winter) during the time of collection, primary authors drilled an additional one to three sub-samples of shell material that precipitated just before the TGB, a sampling approach written as TGB + n, where n = number of additional sub-samples [78,79]. For example, TGB + 1 indicates that one sub-sample was taken at the terminal growth band of the shell, and one additional sub-sample was drilled ~ 2 mm from the TGB, producing a two-sample profile of the individual shell. This short-profile sampling strategy is intended to capture the isotopic signature during the time at which the individual was harvested. Shell profiles included in our data synthesis range from 2 to 60 subsamples per individual, representing 2 to 118 mm worth of shell, respectively. Subsamples are spaced evenly, 1 to 3 mm apart, depending on the study. The spacing of subsamples for each individual is specified in our database whenever this information was reported by primary authors. This commonly used subsampling strategy is based on the estimate of ~ 2-3 mm of growth per 1-2 months in adult *M. californianus* shells growing in southern California [25,29,34,74,77].

**2.4 Categorization and analysis of shell records**

After compiling stable isotope data from all shells that met our criteria, we categorized them for analysis based on sample age, location, and sub-sampling strategy. For geographic

categorization, data were binned according to their individual site (San Miguel Island, Santa Rosa Island, Santa Cruz Island, Anacapa Island, San Diego, Newport Beach) and whether they were from an island or the mainland. For temporal comparisons, data were binned both by millennium (e.g., within past 1000 years, 2000, 3000, etc. up to 9000 BP) and by sub-epoch (early, mid, or late Holocene) according to the Holocene sub-epoch boundaries formally defined by Walker et al. (2019): early Holocene (11,750-8200 BP), mid Holocene (8200-4200 BP), and late Holocene (4200-0 BP) [83]. For late Holocene shell samples, we distinguished between sample types to compare late Holocene midden samples and late Holocene modern, live-collected samples (Appendix 1).

Lastly, individual shells were categorized for analysis based on subsampling strategy: long profiles (15-60 sub-samples per shell, or 28-118 mm of growth), medium length profiles (5-14 sub-samples per shell, or 8-26 mm of growth), and short shell profiles (2-4 sub-samples per shell, or the last 4-6 mm of growth per individual shell). Sampling strategies were categorized in this way for three reasons: (1) to focus on the longest and highest-resolution shell records to investigate life-history traits and the time-averaging effects of sampling methods, (2) to examine a full seasonal cycle or more in medium length and long shell profiles, and (3) to isolate short profiles, which only capture a season or less of growth and therefore would bias the record based on their season of collection. Using subsampling methods and the directionality of sampling described in each paper, we expressed all shell profiles in terms of "distance from growing margin" so that 0 mm represents the most recent shell material to precipitate, closest to the date of harvest or collection. Long profiles were analyzed to examine ontogenetic variability, identify seasonal isotopic trends, document the timing and location of $\delta^{18}O$ and $\delta^{13}C$ extreme values, and determine whether there is uniformity or high intra-individual variability in stable isotope

profiles. Both medium and long profiles (five or more subsamples containing multiple seasons of growth per shell) were used for geographic and millennial-scale analyses. Short profiles were used to examine whether *M. californianus* shells record sub-seasonal $\delta^{18}O$-inferred temperature variability and to investigate the influence of ontogenetic stage (shell length) on terminal edge $\delta^{18}O$ values. Lastly, we compared $\delta^{18}O$ profiles of different lengths for shells of the same $^{14}C$ age and from the same island to determine whether the length of the subsample profile impacts the interpretations of shell chemistry (S1 Fig).

For statistical methods, analysis of variance (ANOVA) was applied to modern shells to test differences between $\delta^{18}O_{shell}$ and $\delta^{13}C_{shell}$ values of island and mainland sites and across tidal heights, whenever tidal height data were available. Tukey HSD was used to determine which tidal heights were statistically different from one another in isotopic composition. ANOVA and Tukey HSD were also used to determine whether $\delta^{18}O_{shell}$ values were significantly different from one another over each millennium throughout the Holocene. Pearson correlation was used to test relationships between ontogenetic stage (total shell length) and growth margin $\delta^{18}O_{shell}$ and $\delta^{13}C_{shell}$ values whenever shell length data were available. All data analysis was performed in R [84].

### 2.5 Paleotemperature and $\delta^{18}O$ of seawater

In order to examine temperatures recorded by *M. californianus* through the Holocene, we applied the $\delta^{18}O$-SST equation developed by Epstein et al. (1953) [85] and calibrated for *M. californianus* by Killingley (1981) [86]:

$$SST(°C) = 16.4 - 4.2((\delta^{18}O_{calcite} - \delta^{18}O_w)) + 0.13((\delta^{18}O_{calcite} - \delta^{18}O_w))^2 \qquad (1)$$

The 13 papers analyzed here employed a variety of approaches for $\delta 18O_w$. Multiple studies [72,76,80] used the measured modern $\delta^{18}O_w$ value of -0.32‰ from a seawater sample collected

by Rick et al. (2006) off the eastern coast of Santa Rosa Island [52]. Three different studies used the $\delta^{18}O_w$ value of -0.32‰ but applied an ice-volume correction [53,78,79] for reconstruction of Holocene paleo-temperatures [87]. Two papers did not provide a $\delta^{18}O_w$ value. Since sea level has been relatively constant since 6000 BP [88,89], we applied an ice-volume correction to $\delta^{18}O_w$ for shells with a radiocarbon age older than 6000 BP only and used the modern $\delta^{18}O_w$ value of -0.32‰ for all other Channel Islands shells younger than 6000 BP. We used established relationships between sea-level change and $\delta^{18}O_w$; a 10 m increase in sea level results in a 0.1‰ change in $\delta^{18}O_w$ [90,91]. Assuming a linear change in ice volume during the early Holocene, sea level rose 10 m per millennium [88,89,91]. Therefore, we used $\delta^{18}O_w$ = -0.32‰ + 0.3‰ for mussel shells aged 9000-8000 BP, -0.32‰ + 0.2‰ for mussel shells aged 8000-7000 BP, and -0.32‰ + 0.1‰ for shells aged 7000-6000 BP (Table 1).

## 3 Results and Discussion

### 3.1 Ontogenetic variability

Of all individual profiles analyzed here, the *M. californianus* shell with the longest stable isotope profile was collected at Cuyler Harbor, San Miguel Island in 2005 CE [80]. The shell was serially sub-sampled every 2 mm at 60 points along the ontogenetic growth trajectory, representing 118 mm of shell growth [80]. The length and resolution of this record presented the best opportunity to examine ontogenetic variation; the next longest individual record from the Channel Islands has 25 subsamples spanning 48 mm of growth.

The San Miguel 2005 shell recorded an average $\delta^{13}C$ value of -0.51‰, an average $\delta^{18}O$ value of 0.53‰, and six identifiable annual cycles in its $\delta^{18}O$ profile (Fig 2). The $\delta^{18}O$ minima represent warm seasons recorded by the shell and match the instrumental temperature records from 2000-2005 included for comparison (Fig 2a): National Data Buoy Center (NDBC) Station

46054 located in the Santa Barbara Channel (34.273° N, 120.470° W) and Point Dume Shore Station Data provided by the Shore Stations Program at Scripps Institute of Oceanography (34.014° N, 118.822° W). Comparing annual temperature profiles to the $\delta^{18}O$ shell profile indicates that the amount of time represented by evenly spaced (2 mm) subsamples decreases as the shell ages (Figs 2a, b). In the years 2000 and 2001, earlier on in the individual's life, the subsamples represent sub-monthly resolution (i.e., ~ 14-18 subsamples capturing 12 months of growth). Following fast growth during earlier stages of life, growth reduction could be linked to the attainment of sexual maturity, when mussels reallocate a greater portion of energy from shell growth to gametogenesis [43,92]. In the final two years of the individual's life (2004 and 2005), one full annual cycle is captured within 6-7 subsamples (Fig 2b). This indicates that *M. californianus* slows its growth from ~ 2.5 mm per month earlier in its life to ~ 1 mm per month within a span of five years. Ontogenetic growth reduction amplifies the effect of time-averaging introduced by the sampling strategy, as shown by the less apparent annual cycles when local polynomial regression was applied to the $\delta^{18}O$ shell profile with evenly spaced samples (Fig 2c). When *M. californianus* is growing more slowly in later stages of ontogeny, more subsamples are required in order to capture environmental periodicity (e.g., temperature seasonality) since the individual is calcifying, and therefore recording, less in the same amount of time.

Since growth reduction throughout ontogeny has been well documented for accretionary carbonates [93–97], we predicted that the *M. californianus* $\delta^{18}O$ ontogenetic profile from umbo to commissure would contain the following features characteristic of ontogenetic patterns: (1) sinusoidal in shape, but increasingly cuspate as the individual aged, (2) a progressive decline in amplitude, (3) a progressive increase in frequency, and (4) a progressive decline in wavelength. As predicted, the $\delta^{18}O_{shell}$ profile was generally sinusoidal with sharp cusps marking the warm

seasons during the last three years of its life (Fig 2b). The cuspate shape of the $\delta^{18}O$ local minima suggests that growth slowdown occurred during warmer seasons more so than during the cooler seasons, particularly as the organism aged [97–99]. Generally, the frequency increased and the wavelength declined as expected. Interestingly, however, this individual's $\delta^{18}O$ profile did not exhibit an ontogenetic decline in seasonal amplitude (Fig 2d), as determined by calculating the difference between the local $\delta^{18}O$ extreme for each warm or cool season and the profile's midpoint $\delta^{18}O$ value (0.49‰). This results in six warm and six cool seasons over the six-year period recorded by this individual. As the organism aged, it continued to record seasonal cyclicity but recorded less sub-seasonal variability (Fig 2b). More closely spaced subsamples towards the terminal edge of the shell would help capture finer-scale variability (e.g., weekly to monthly) in an aging individual.

We also found a small overall increase in annual standard deviation of $\delta^{18}O_{shell}$ from 0.27‰ in 2000 to 0.39‰ in 2005 (Fig 2d). This increase was expected since a lower standard deviation earlier in life represents the lower short-term variation between temporally close samples, and a higher standard deviation later in life reflects the greater variability or larger temperature swings from subsample to subsample due to more temporal gaps in the carbonate record.

The ontogenetic $\delta^{13}C$ profile of the same individual from San Miguel Island was examined separately since $\delta^{13}C$ is a more complex proxy than $\delta^{18}O$ in biogenic carbonates due to the varying impacts of ocean circulation, upwelling, primary productivity, seawater DIC $\delta^{13}C$, and metabolic effects on $\delta^{13}C_{shell}$ profiles [45](Ferguson et al., 2013). In this individual, the ontogenetic $\delta^{13}C$ profile records six annual cycles with increasing frequency (Fig 3), which likely represent seasonal upwelling/relaxation oscillations in the Santa Barbara Channel. There

was an ontogenetic trend towards more positive $\delta^{13}C$ values (Fig 3), which does not fit the prediction that the organism incorporates a greater amount of isotopically light metabolic carbon as it ages, as found in other marine mussel species including *Pinna nobilis* and *Mytilus edulis* [100–102]. The unexpectedly positive $\delta^{13}C$ trend found in this individual is likely associated with ontogenetic growth reduction in this species. Slower shell growth and lower metabolic rates could result in reduced incorporation of respired carbon and therefore higher $\delta^{13}C_{shell}$ values with age [102].

Since previous studies of other mussel species identified ontogenetic de-coupling between environmental parameters and shell chemistry [100,101], we tested the relationship between ontogenetic stage (shell length) and growing edge $\delta^{18}O$ and $\delta^{13}C$ values in 76 *M. californianus* shells live-collected on the same day at Santa Rosa Island in August 2017 [74]. These 76 individuals were chosen for this analysis since this was the only data set to include shell length information for each individual. Shell length cannot be assumed from subsampling distance (e.g., 10 mm of shell subsamples could be from an individual of any shell length 10 mm or longer, thus providing only a minimum estimate of shell length). The primary authors sub-sampled each of these 76 individuals at three points spaced 1 mm apart at the terminal edge of the shell to produce a mean $\delta^{18}O_{shell}$ and mean $\delta^{13}C_{shell}$ value for the final 3 mm of growth for each shell [74]. These mean terminal edge values are time-averaged, representing ~1-3 months of growth depending on the ontogenetic age of the shell. Shell lengths ranged from 42.5 mm to 118.5 mm with a mean of 73.9 mm. The $\delta^{18}O_{shell}$ values ranged from -1.12‰ to 1.17‰, and $\delta^{13}C_{shell}$ values ranged from -1.56‰ to 0.34‰. We found no significant relationship between shell length and mean terminal edge $\delta^{18}O$ (Pearson correlation test, $t = -1.5613$, $df = 74$, $p = 0.1227$). Similarly, there was no significant relationship between shell length and mean growing

edge $\delta^{13}C$ (Pearson correlation test, t = 1.5254, df = 74, p = 0.1314). The lack of relationship between shell length and end-of-life $\delta^{18}O$ and $\delta^{13}C$ values is not necessarily an indication that ontogenetic patterns do not strongly influence shell chemistry; ontogenetic stable isotope profiles show a marked increase in frequency and a decrease in wavelength with age (Figs 2, 3). Longer shell profiles capturing more growth are required to reconstruct environmental cycles and disentangle ontogenetic effects.

### 3.2 Geographic variability

#### 3.2.1 Geographic comparison of modern shells

In analyzing all modern shells with five or more subsamples, we found a significant difference in shell chemistry between *M. californianus* shells collected from the Channel Islands versus mainland southern California (Fig 4, ANOVA, oxygen: p = 0.0, carbon: p = 0.0). In present-day conditions, weak wind forcing and the delivery of warm water by the northbound California Undercurrent and Davidson Current produce a significantly warmer regime along the Southern California Bight than farther offshore (Fig 1), and this pattern is reflected in *M. californianus* shell chemistry: lower $\delta^{18}O_{shell}$ values (mean ± 1σ = -0.32‰ ± 0.47‰) from the mainland sites (Newport Beach and San Diego) relative to higher δ18O values (mean ± 1σ = 0.33‰ ± 0.42‰) in the Channel Islands shells (Fig 4a). Additionally, the lower $\delta^{13}C$ values of Channel Islands shells indicate stronger upwelling conditions (Fig 4b) due to the islands' proximity and exposure to the California Current, while the south-facing coastline of the Southern California Bight is protected from intense wind forcing [46], resulting in weaker upwelling and higher $\delta^{13}C$ shell values.

#### 3.2.2 Geographic variability across all time intervals

Oxygen and carbon isotope data from all shells with five or more subsamples across all time intervals were used to calculate summary statistics for each site (San Miguel Island, Santa Rosa Island, Santa Cruz Island, Anacapa Island, Newport Beach, and San Diego) as shown in Table 2. Even across all time intervals, *M. californianus* collectively recorded warmer SSTs from west to east, with stepwise depletion in median $\delta^{18}O_{shell}$ from San Miguel Island to Anacapa Island (Fig 5a). Mussels from Newport Beach and San Diego recorded the warmest $\delta^{18}O_{shell}$ signatures. Despite most of its shell samples originating within the late Holocene, Santa Cruz Island had the widest range of $\delta^{18}O_{shell}$ values, which is likely a product of its location. The California Current delivers cool water to western Santa Cruz Island, while SSTs on the eastern portion of the island are influenced by the warmer Davidson Current and Southern California Countercurrent. The dynamic setting may result in greater $\delta^{18}O_{shell}$ variability for Santa Cruz Island mussels.

Among the Channel Islands shells, there is an implied increase in upwelling strength farther offshore, with San Miguel Island mussels recording the lowest $\delta^{13}C_{shell}$ values and Anacapa Island mussels recording the highest $\delta^{13}C_{shell}$ values (Fig 5b). Newport Beach and San Diego mussel shells were isotopically lighter than shells from the eastern Channel Islands, but since the mainland $\delta^{13}C_{shell}$ values represent modern mussels only (live-collected in the 2000s) and the island $\delta^{13}C_{shell}$ values represent all time points throughout the Holocene, this offset is likely a temporal rather than geographic trend. Recent increases in upwelling strength and greater nearshore productivity have been documented along coastal mainland California [103], which may be reflected in the modern mainland California $\delta^{13}C_{shell}$ values. Our dataset contains no modern $\delta^{13}C_{shell}$ values from Santa Cruz Island or Anacapa Island, but when comparing $\delta^{13}C_{shell}$ of modern shells only, Santa Rosa and San Miguel Island shells maintained lower $\delta^{13}C_{shell}$ values

than the modern mainland shells. It does not appear that the mainland mussels recorded significant terrestrial influences, such as terrestrial plant decomposition, river input, or agricultural runoff, since these factors would result in isotopically lighter carbon rather than the higher mainland $\delta^{13}C_{shell}$ values found here. Collectively, $\delta^{13}C_{shell}$ in intertidal mussels may serve as a better indicator of relative oceanographic conditions (e.g., salinity and upwelling) rather than terrestrial influences. However, the reliability of $\delta^{13}C$ as an environmental proxy is limited due to the significant and complex role of metabolic $\delta^{13}C$ incorporation into the shell [56].

**3.3 Millennial scale temperature variability by island**

We binned oxygen isotope data from shells with five or more subsamples by millennium for each island and converted these values to SST (°C) using Equation 1 to produce a record of temperature snapshots throughout the Holocene. Santa Rosa Island offered the most temporally continuous record with data points spanning every millennium from 9000 BP through the present (Fig 6). Temperatures recorded at Santa Rosa Island were highest (> 14°C) between 9000-8000 BP and lowest (11.67°C) between 4000-3000 BP (Table 3). Both the geologically oldest and youngest shells were from San Miguel Island (8800 BP and 2005 CE), allowing for a comparison between two snapshots at both ends of the record. San Miguel mean SST was low (11.99°C) during the early Holocene and was overall higher in 2005 CE (12.92°C), although these differences were not statistically significant, perhaps due to uneven distributions of data (two-way ANOVA, $p = 0.52$). Anacapa Island had only one snapshot at 3010 BP but recorded a wide range of temperatures (11.08°-24.76°C; Table 3). Oxygen isotope data from the three westernmost islands (San Miguel Island, Santa Rosa Island, and Santa Cruz Island) within 6000-5000 BP preserved the geographic east-west SST gradient that characterizes the northern Channel Islands today, indicating that mussels did not collectively record fine-scale changes in

California Current and sub-current forcing that other models and records have documented for 6000 BP [104]. The late Holocene is well represented at Santa Cruz Island with snapshots from the past three millennia. Calculated mean temperatures for each millennium at Santa Cruz Island exhibit warm-cool millennial scale variability: 14.13°C between 6000-5000 BP, 13.77°C between 3000-2000 BP, 14.23°C between 2000-1000 BP, 13.05° in midden shells from the past 1000 years, and 14.6°C in modern shells (Table 3). Temperature variability was highest at Santa Cruz Island within 2000-1000 BP ($\sigma$ = 2.71°C) and lowest at Santa Rosa Island within 3000-2000 BP ($\sigma$ = 1.34°C). Santa Cruz and Anacapa Islands record the highest overall maximum temperatures, all three of which occurred in the late Holocene (Table 3). San Miguel Island has the lowest overall minimum temperature (6.29°C) at 8800 BP.

**3.4 Seasonal variability**

Shells with long profiles (15 or more subsamples per individual) were used to examine seasonal oscillations. Oxygen isotope profiles recorded sinusoidal seasonal variability, with some individuals recording more pronounced seasonal extremes than others (Fig 7). Long-profile individuals (n = 28) ranged in geologic age from 8800 BP through 2005 CE, yet all recorded at least one annual cycle with a mean of 2.6 ± 0.83 (1$\sigma$) warm seasons. Inferred warm seasons serve as a way to estimate the age of an individual at the time of its death if the subsampling profile extends throughout the full ontogenetic trajectory of the shell. However, since the shells analyzed here are primarily archaeological shells harvested by humans, the inferred ~2.6 warm seasons indicates the age at which shells were typically harvested for consumption rather than the average lifespan of a mussel, which is likely to be much longer than two years.

On average, the 28 individuals recorded a calculated SST range of 5.4°C ($\delta^{18}O$ = 1.35‰), which matches the typical annual temperature range for nearshore waters surrounding the

Channel Islands [54,74]. The highest SST and greatest intra-individual seasonality were both recorded by an individual at 7315 BP. The warmer conditions recorded by this individual are consistent with the oxygen isotope record of *G. bulloides* planktic foraminifera at ODP Site 893 A/B in Santa Barbara Basin for this same age range [105]. All temperatures lower than 9.5°C were recorded between 5200 and 5099 BP, although this period is considered to be a warm interval for this region [105].

Seasonality of carbon isotope profiles is less distinguishable. Out of all 28 long-profile shells, only one had clear seasonal cycles that closely aligned with its oxygen isotope seasonal oscillations, while multiple individuals did exhibit generally covarying $\delta^{13}C$ and $\delta^{18}O$ profiles (S2 Fig). The individual with the strongest seasonal cycles is the shell collected in 2005 CE from San Miguel Island (Fig 2). In this individual, oxygen isotope minima (warm seasons) aligned remarkably well with carbon isotope minima (minimal upwelling) in the last 50 mm of the shell's life in particular (Fig 8). The strongly expressed seasonal $\delta^{13}C$ cycles in this individual are comparable to those found by Killingley and Berger (1979) in *M. californianus* shells from San Diego [59]. However, the vast majority (27 out of 28 individuals) lacked seasonally resolved $\delta^{13}C_{shell}$ profiles or exhibited misaligned $\delta^{13}C_{shell}$ and $\delta^{18}O_{shell}$ cycles, supporting previous conclusions that $\delta^{13}C$ is an unreliable proxy for upwelling [45].

While seasonality is visually apparent in a $\delta^{18}O_{shell}$ profile, the number of subsamples required to capture seasonal variability depends on the growth rate (and therefore ontogenetic age) of the individual. Typically, ~ 3 mm is thought to represent 1-2 months of growth, and 8-10 closely spaced subsamples are required to identify an annual cycle [51,74]. Although evenly spaced 2-3 mm increments is a conventional subsampling approach based on field observations of California mussels, we emphasize the need for consistently updated, long-term, and site-

specific field studies of *M. californianus* shell growth rates since this species exhibits highly variable growth rates across sites and through time [29,40,44]. Since we observed that profiles with five subsamples contained a local minimum and a local maximum in most of our oxygen isotope profiles (e.g., a warm season and a cool season), we used all individuals with five or more subsamples to infer trends over broader spatial and temporal scales (Figs 4-6). This greatly expanded our sample size (both n = number of individual shells and n = number of subsamples) and allowed for more temporal snapshots and geographic comparisons. Individuals with fewer than five subsamples were excluded from broader scale interpretations since these short, end-of-life profiles capture only a season or less of growth, which could bias a long-term record. For example, if an individual collected in late summer is sampled at three evenly spaced points at its growing margin, its subsamples would only capture summer warming. This individual would introduce bias into a long-term record by indicating that conditions were warmer during its lifespan, so it is important to consider the amount of time represented by the sampling distance.

Collectively, the *M. californianus* record is sensitive enough to record sub-annual and seasonal variability, but short profiles indicate that fine-resolution variability is difficult to extract from 2-4 subsamples from one margin of the shell. For example, out of the 76 *M. californianus* individuals live-collected at Santa Rosa Island in August 2017, only 48 record overall summer warming in the 2-mm long $\delta^{18}O_{shell}$ profile at the terminal margin [74] (S3 Fig). These individuals spanned a variety of ontogenetic ages as implied by the range in shell length (42.5 mm to 118.5 mm) and were collected at various tidal heights (0 m to 1 m) at 10 cm increments on the same day [74]. Sub-seasonal variability in oxygen isotope profiles may be less related to temperature and instead more closely tied to ontogenetic age, growth rate, tidal height, and the dynamic nature of the intertidal zone. Apparent sub-seasonal variability could also be a

product of time-averaging introduced during sampling. There was a significant difference in mean terminal $\delta^{18}O_{shell}$ related to tidal height (ANOVA, df = 2, F-value = 12.29, p = < 0.001), and there were statistically different mean terminal $\delta^{18}O_{shell}$ values among mussels collected from the low and high tidal positions (Tukey HSD, p = < 0.0001) and middle and high tidal positions (Tukey HSD, p = 0.03), but not among middle and low tidal positions (Tukey HSD, mid-low p = 0.13). Differences in δ18Oshell related to tidal height are likely due to submergence times; mussels in the high tidal position are submerged for less time, and therefore experience more growth reduction or interruption than mussels in lower tidal positions [43,44,74].

**3.5 Millennial scale variability**

Holocene climate in North America is characterized by millennial-scale temperature variability [106]. We aimed to determine whether the Channel Islands collectively experienced millennial-scale variability despite the local-scale oceanographic differences among the islands that appeared in our record (Fig 5). We categorized the $\delta^{18}O_{shell}$ data into 1000-year time bins using individuals with five or more subsamples (Fig 9), which revealed that median $\delta^{18}O_{shell}$ values oscillate every 1000 years, with the highest median $\delta^{18}O_{shell}$ values occurring during 9000-8000 BP and 7000-6000 BP (0.7‰ and 0.73‰, respectively) and the lowest median $\delta^{18}O$ value (0.05‰) occurring at the start of the late Holocene (4000-3000 BP). ANOVA and Tukey HSD revealed that millennial $\delta^{18}O_{shell}$ values were statistically different from the previous millennium, except for from 8000 to 7000 BP and 3000 to 2000 BP. The statistical relationships between each millennium are shown in the Supplementary Information (S4 Table). Median $\delta^{18}O_{shell}$ for modern (non-midden, live-collected) shells is 0.32‰, identical to median $\delta^{18}O_{shell}$ values from 6000-5000 BP and 2000-1000 BP and lower than the median $\delta^{18}O_{shell}$ value of six of the nine millennia since 9000 BP (Fig 9a). There has been an overall decline in collective median $\delta^{18}O_{shell}$

values from the early Holocene to the late Holocene, indicating overall warming and freshening over the three intervals (Fig 9b). Interestingly, the Channel Islands mussels collectively recorded millennial-scale climate signals in addition to finer-scale trends (e.g., ontogeny, seasonality, local oceanography, micro-habitat), indicating that *M. californianus* shells provide a multi-scaled view of past environmental variability.

**3.6 Comparison to regional climate records**

We generated a snapshot-based Holocene *M. californianus* stable isotope record and compared it to other published coeval climate records for the southern California region to determine whether this intertidal species is a comparable archive of broader climate patterns. We used all Channel Islands mussel shells with five or more subsamples to calculate median $\delta^{18}O_{shell}$ and $\delta^{13}C_{shell}$ values for each year of the record to generate 58 annual snapshots over the Holocene (Fig 10). These snapshots were plotted along with 1000-year $\delta^{18}O_{shell}$ medians (as in Fig 9a) as well as terrestrial precipitation records [107] (Fig 10a) and marine sediment core records [105,108] (Figs 10b, 10c) from southern California. The annually resolved *M. californianus* oxygen isotope record (Fig 10e) does not closely match inferred temperatures from $\delta^{18}O_{foraminifera}$ (Fig 10c) from varved sediments in the Santa Barbara Basin. The $\delta^{18}O$ mussel record implies long-term warming since 9000 BP, while the $\delta^{18}O_{foraminifera}$ record indicates cooling over the Holocene. Environmental differences between the offshore planktic foraminifera *G. bulloides* and the intertidal *M. californianus* could contribute to the misalignment between the two records. There are also significant differences between the temporal resolutions of each record; varved marine sediments provide a much more temporally continuous record than *M. californianus* shells, while *M. californianus* is a sparser record of longer-lived shells with nested seasonal resolution. Annual treatment of $\delta^{18}O_{shell}$ data, such as calculating an annual average or annual

median from multiple subsamples and individuals, may obscure the seasonal and ontogenetic patterns that we identified in individual shells. However, it is still useful to examine the full *M. californianus* record at coarser resolution using large sample sizes, as supported by the statistically significant millennial-scale oscillations and geographic trends that emerge when *M. californianus* shells are collectively analyzed (Figs 5, 9), and both the $\delta^{18}O_{shell}$ and $\delta^{18}O_{foraminifera}$ records underscore recent warming since ~ 1000 BP. In some cases, low annual $\delta^{18}O_{shell}$ values indicative of low-salinity conditions align remarkably well with Santa Barbara Basin flooding events [109], although the alignment is not consistent enough throughout the Holocene to indicate that mussels experience and record freshwater input pulses as they calcify (Fig 10e).

**4 Conclusions**

In *M. californianus*, stable isotope proxies have been applied most frequently by archaeologists to infer the seasonality of shellfish harvesting by Indigenous coastal communities, but $\delta^{18}O$ and $\delta^{13}C$ data from midden shells can also offer paleoceanographic insights, including pre-industrial ranges of chemical variability, oscillating warm/cool climate intervals, paleo-seasonal cycles, and geographic trends. Our synthesis of multiple published datasets reveals that archaeological *M. californianus* shells (1) collectively record local-scale temperature and upwelling patterns, (2) serve as an archive of temperature seasonality when the stable isotope subsampling approach captures multiple seasons of growth across many individuals, and (3) record millennial-scale variability characteristic of western North America over the Holocene. Mussel shell chemistry reflects the geographic warm-cool gradient between mainland southern California and the northern Channel Islands and records cooler temperatures from east to west within the Channel Islands, likely due to the competing influences of the cold California Current and the warmer California Undercurrent and Davidson Current.

Within individual shell profiles, we found that five subsamples per shell revealed a local $\delta^{18}O_{shell}$ maximum and a local $\delta^{18}O_{shell}$ minimum from which a winter low temperature and a summer high temperature can be inferred, respectively. While a five-sample profile appeared to record one annual temperature cycle, we emphasize the importance of collecting 10 or more serial subsamples along the growth trajectory of the shell in order to account for ontogenetic variation and capture multi-season or multi-year $\delta^{18}O_{shell}$ profiles. A longer $\delta^{18}O_{shell}$ profile allows for the identification of annual minima and maxima over multiple years, and sampling multiple individuals allows for the cross-correlation and corroboration of seasonal cycles within the same region. Season of harvest information will also be more reliable when there is a multi-seasonal or multi-annual context experienced by the mussel. Conversely, short $\delta^{18}O_{shell}$ and $\delta^{13}C_{shell}$ profiles comprising only a few subsamples at the terminal edge of the shell are less useful for regional climate reconstruction because they reflect shorter periods of time (e.g., weeks to months) and therefore lack the temporal duration required to reconstruct broader climate patterns occurring over multiple seasons or years. We also observed high $\delta^{18}O_{shell}$ variability among specimens growing at the same time and location, which reduces confidence in $\delta^{18}O$-inferred temperature calculations from shells with terminal-edge (TGB) sampling only.

The *M. californianus* stable isotope record is complex to interpret due to multiple environmental and biological influences on shell chemistry. These challenges are compounded by the dynamic nature of the intertidal micro-environment and the nested temporal scales (e.g., seasons within years within millennia) that must be disentangled to accurately interpret the record. As such, *M. californianus* provides different information from existing offshore proxy-based marine records and cannot be interpreted in the same way. However, it is possible to infer broader climate patterns from individual shells if high-resolution sub-sampling and large sample

sizes of individuals are feasible and available. When sampled in this way, archaeological *M. californianus* shells supplement existing climate records by providing seasonally resolved snapshots that are ~ 2-5 years in length, depending on their age and shell length at the date of harvest. We encourage the use of the vast collections of published stable isotopic data from archaeological shells as paleoceanographic and paleobiological archives, and we emphasize the value of compiling and utilizing meta-analyses of biogenic carbonate data to streamline usage for multiple disciplines while reducing the need for further invasive sampling of culturally significant sites.

**5 Land and Data Acknowledgment**

We acknowledge that this paper includes discussion of Indigenous peoples of California who have stewarded the land and sea for millennia. We aim to document biogeochemical variability through the lens of a culturally significant mollusc species without further destruction of culturally sacred sites, but we acknowledge that the data used here from previously published studies may have been originally acquired without consent from Indigenous peoples. We acknowledge the keepers of intergenerational Indigenous knowledge who maintain stories and data of the impacts of settler colonization on humans, ecosystems, and global climate. We direct readers to the open-source resource: https://native-land.ca/ as a starting point to identify the homelands of the diverse Indigenous peoples of this region. Finally, we encourage the use of existing data sets and the prioritization of noninvasive methods in accordance with intersectional values, perspectives, and ethics of multiple communities.

## Tables

**Table 1.** Treatment of $\delta^{18}O_w$ values depending on binned age range (years BP). Some papers spanned multiple millennia and are therefore listed more than once.

| Age range | Ice volume correction | $\delta^{18}O_w$ value used | $\delta^{18}O_{shell}$ data sources |
|---|---|---|---|
| 9000 - 8000 BP | 0.3‰ | -0.02‰ | Jew et al., 2013a; Jew et al., 2013b [78,79] |
| 8000 - 7000 BP | 0.2‰ | -0.12‰ | Robbins et al., 2013 [80] |
| 7000 - 6000 BP | 0.1‰ | -0.22‰ | Robbins et al., 2013 [80] |
| 6000 BP - 0 BP | None; measured by Rick et al. (2006) [52] | -0.32‰ | Glassow et al., 1994; Kennett, 1998; Rick et al., 2006; Ford et al., 2010; Glassow et al., 2012; Ferguson et al., 2013; Robbins et al., 2013; Jew and Rick, 2014; Jazwa and Kennett, 2016; Flores, 2017; Jazwa et al., 2020 [42,45,51–53,72,74,76,77,80,81] |

**Table 2.** Summary statistics for all shells with five or more subsamples, sorted by site.

| Site | Mean $\delta^{18}O$ | Min $\delta^{18}O$ | Max $\delta^{18}O$ | $\sigma$ $\delta^{18}O$ | Mean $\delta^{13}C$ | Min $\delta^{13}C$ | Max $\delta^{13}C$ | $\sigma$ $\delta^{13}C$ |
|---|---|---|---|---|---|---|---|---|
| San Miguel Island | 0.91 | -0.3 | 2.6 | 0.58 | -0.08 | -1.3 | 1.2 | 0.55 |
| Santa Rosa Island | 0.45 | -0.92 | 1.6 | 0.47 | 0.47 | -1.1 | 2.5 | 0.51 |
| Santa Cruz Island | 0.29 | -2.47 | 1.98 | 0.55 | 0.46 | -2.83 | 2.73 | 0.52 |
| Anacapa Island | -0.1 | -2.1 | 0.95 | 0.58 | 0.71 | -0.5 | 1.9 | 0.48 |
| Newport Beach | -0.5 | -1.6 | 0.58 | 0.45 | 0.24 | -0.81 | 0.96 | 0.38 |
| San Diego | -0.27 | -1.81 | 0.85 | 0.46 | 0.39 | -0.74 | 1.25 | 0.36 |

**Table 3.** Summary statistics for all shells with five or more subsamples, sorted by both island and millennium. SST was calculated by applying the equation from Epstein et al. (1953) modified for *M. californianus* by Killingley (1981). $\delta^{18}O$ reported in ‰ and SST is in °C.

| Island | Millennium | Mean $\delta^{18}O$ | σ $\delta^{18}O$ | Mean SST | σ SST | Max SST | Min SST |
|---|---|---|---|---|---|---|---|
| San Miguel Island | 9000 BP | 1.08 | 0.59 | 11.99 | 2.29 | 15.6 | 6.29 |
| | modern | 0.53 | 0.34 | 12.92 | 1.37 | 12.5 | 10.66 |
| Santa Rosa Island | 9000 BP | 0.41 | 0.48 | 14.64 | 1.94 | 18.45 | 9.94 |
| | 8000 BP | 0.36 | 0.56 | 14.47 | 2.28 | 19.84 | 11.51 |
| | 7000 BP | 0.67 | 0.36 | 12.78 | 1.46 | 16.78 | 9.97 |
| | 6000 BP | 0.36 | 0.49 | 13.62 | 1.98 | 18.1 | 10.28 |
| | 5000 BP | 0.52 | 0.42 | 13 | 1.68 | 17.16 | 9.98 |
| | 4000 BP | 0.85 | 0.36 | 11.67 | 1.39 | 13.48 | 9.41 |
| | 3000 BP | 0.55 | 0.38 | 12.85 | 1.34 | 15.35 | 10.74 |
| | 2000 BP | 0.25 | 0.43 | 14.06 | 1.74 | 18.1 | 10.39 |
| | 1000 BP | 0.43 | 0.5 | 13.36 | 2.05 | 17.63 | 10.16 |
| Santa Cruz Island | 6000 BP | 0.24 | 0.63 | 14.13 | 2.57 | 21.31 | 8.78 |
| | 3000 BP | 0.33 | 0.5 | 13.77 | 2.03 | 24.94 | 7.43 |
| | 2000 BP | 0.22 | 0.65 | 14.23 | 2.71 | 26.03 | 8.63 |
| | 1000 BP | 0.5 | 0.44 | 13.05 | 1.74 | 16.36 | 9.34 |
| | modern | 0.12 | 0.38 | 14.6 | 1.57 | 17.75 | 11.66 |
| Anacapa Island | 4000 BP | -0.19 | 0.6 | 15.6 | 2.52 | 24.76 | 11.0 |

## Figures

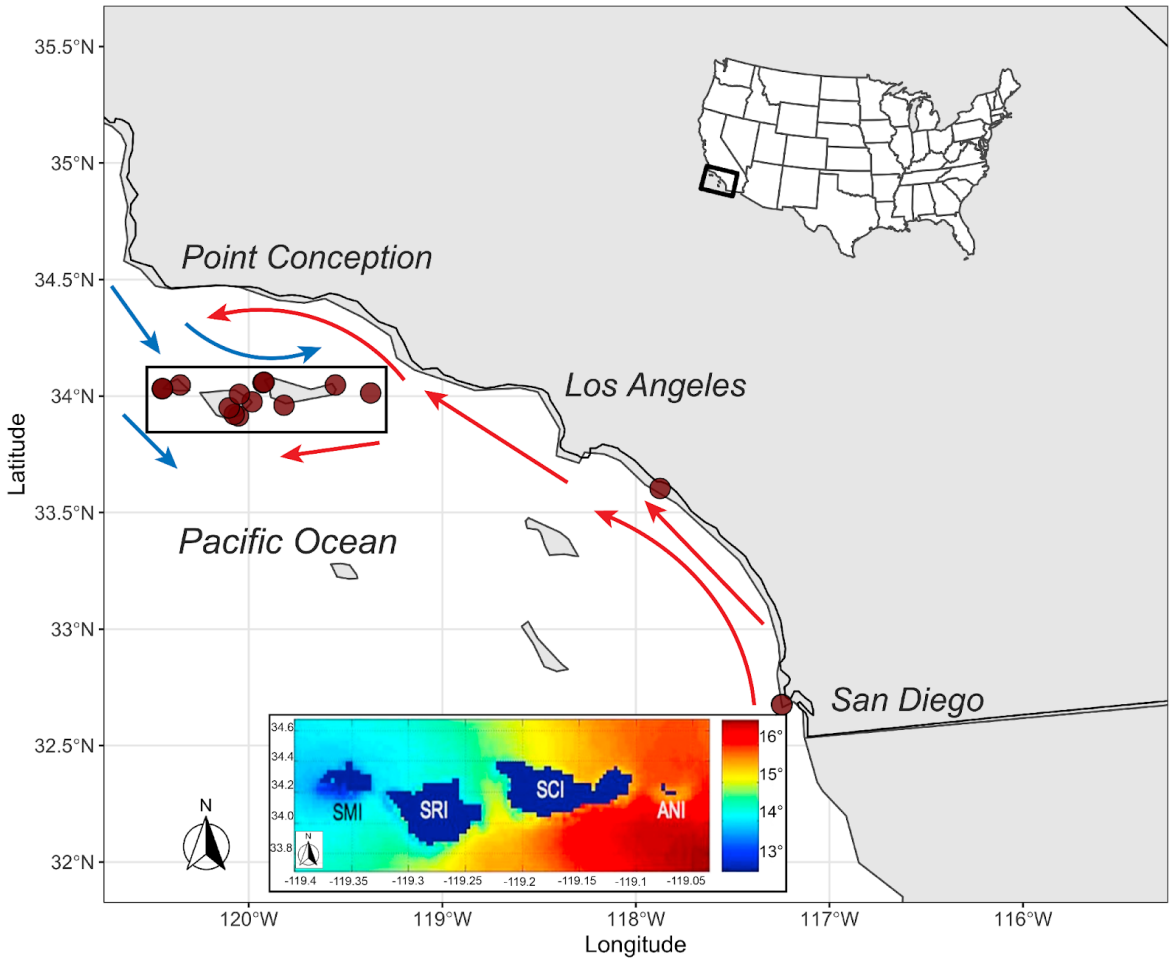


**Figure 1.** Map of southern California with collection sites plotted at northern Channel Islands (San Miguel Island, Santa Rosa Island, Santa Cruz Island, and Anacapa Island), Newport Beach, and San Diego. Black box around the northern Channel Islands corresponds to long-term mean SST Advanced Very High Resolution Radiometer (AVHRR) map of weekly mean SST from 1997 to 2002. Color scale on the right is in degrees Celsius. AVHRR map modified from Blanchette et al. (2006) and Flores (2017). [69,72]

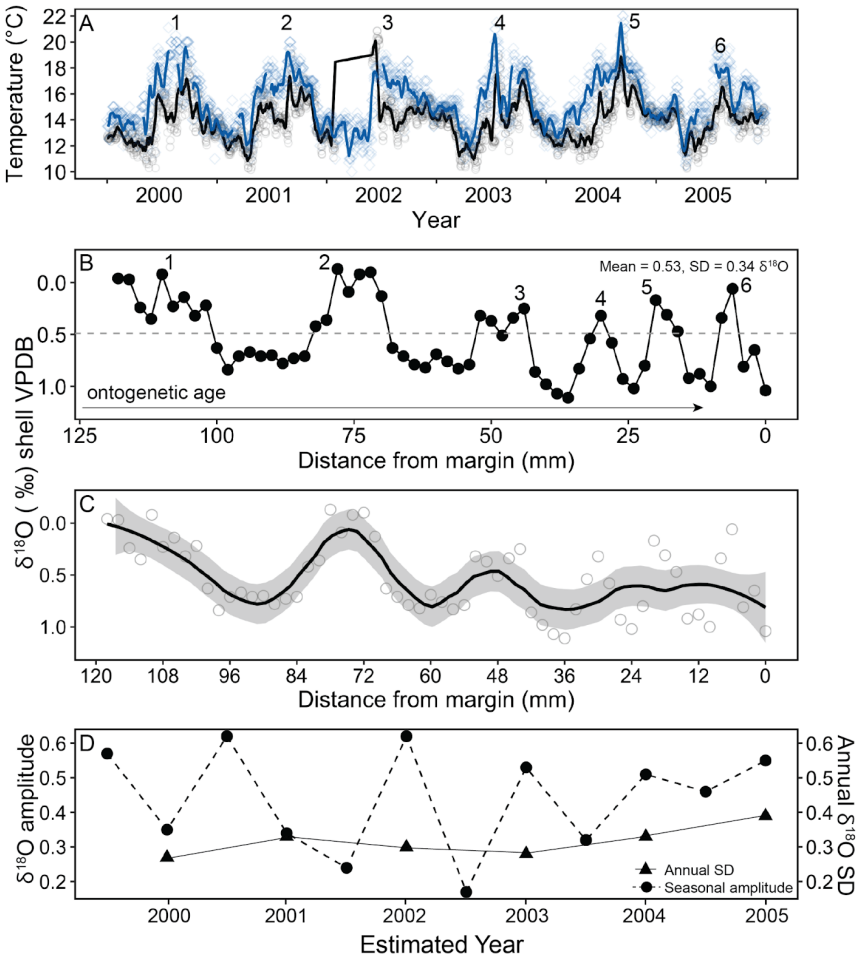


**Figure 2.** (A) Seawater temperature for 2000-2005. Black line is two-week running mean for NDBC Station 46054 in Santa Barbara Basin. Gray open circles are daily SST. Blue line is two-week running mean for Point Dume provided by the Shore Stations Program sponsored at Scripps Institution of Oceanography. Blue open circles are daily SST. Numbers represent SST extremes for each year of the record. (B) 120 mm of sampling $\delta^{18}O$ from a *M. californianus* shell collected in 2005 at San Miguel Island. Gray dashed line represents midpoint of 0.49‰. Numbers represent inferred seasonal extremes best matched with panel (A). (C) Local polynomial regression of $\delta^{18}O$ showing that modeled seasonal cycles become less apparent as the shell ages ontogenetically due to slower growth. Shaded region represents 95% confidence interval. (D) Calculated seasonal amplitude of $\delta^{18}O$ (dark circles and dashed line) and annual standard deviation of $\delta^{18}O$ (black triangles and solid line).

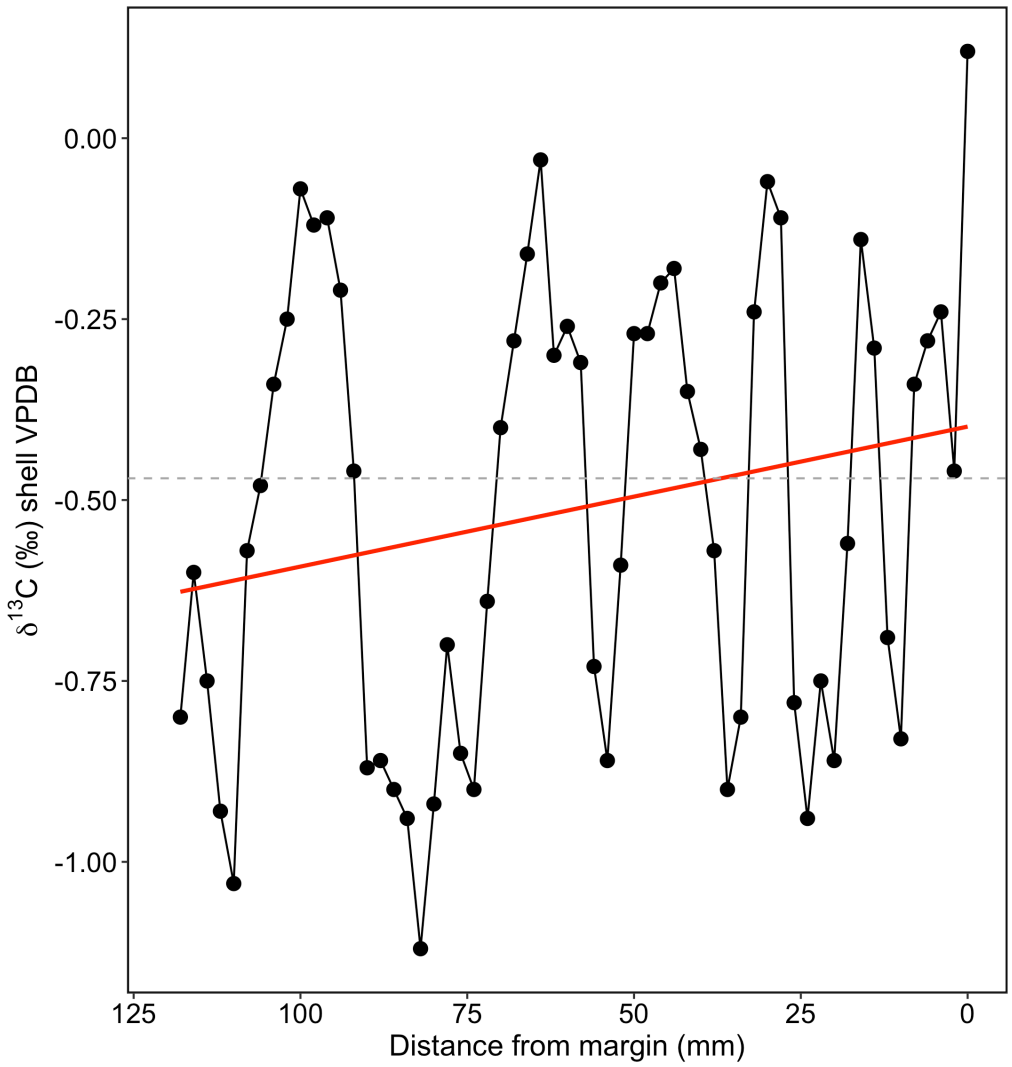


**Figure 3.** $\delta^{13}C$ profile of San Miguel Island *M. californianus* shell collected in 2005. X-axis represents ontogenetic growth from left to right (e.g., 0 mm is closest to time of death). Gray dashed line represents median $\delta^{13}C$ value of -0.47‰. Red line indicates ontogenetic trends towards positive $\delta^{13}C$ values.

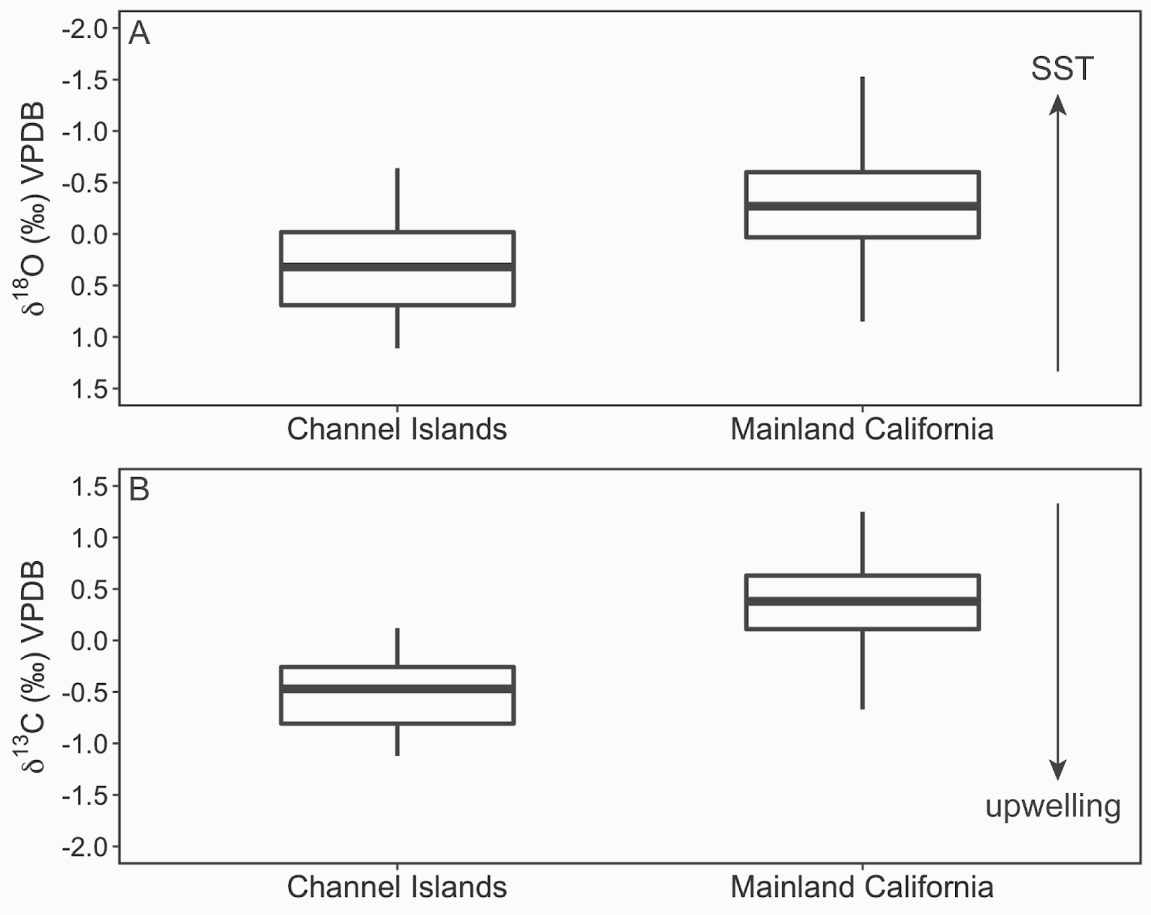


**Figure 4.** Box plots showing stable isotopic ranges of all modern shells by location. Channel Islands includes all data points from all modern shells with five or more subsamples from San Miguel Island and Santa Cruz Island. (No modern shells with > 5 subsamples from Anacapa or Santa Rosa Island.) Mainland California includes all data points from all modern shells with five or more subsamples from San Diego and Newport Beach. (A) Oxygen isotope range of modern $\delta^{18}O$ in Channel Islands vs. mainland shells. (B) Carbon isotope range of modern $\delta^{13}C$ in Channel Islands vs. mainland shells. (Oxygen: ANOVA, $p < 0.01$, Carbon: ANOVA, $p < 0.01$.).

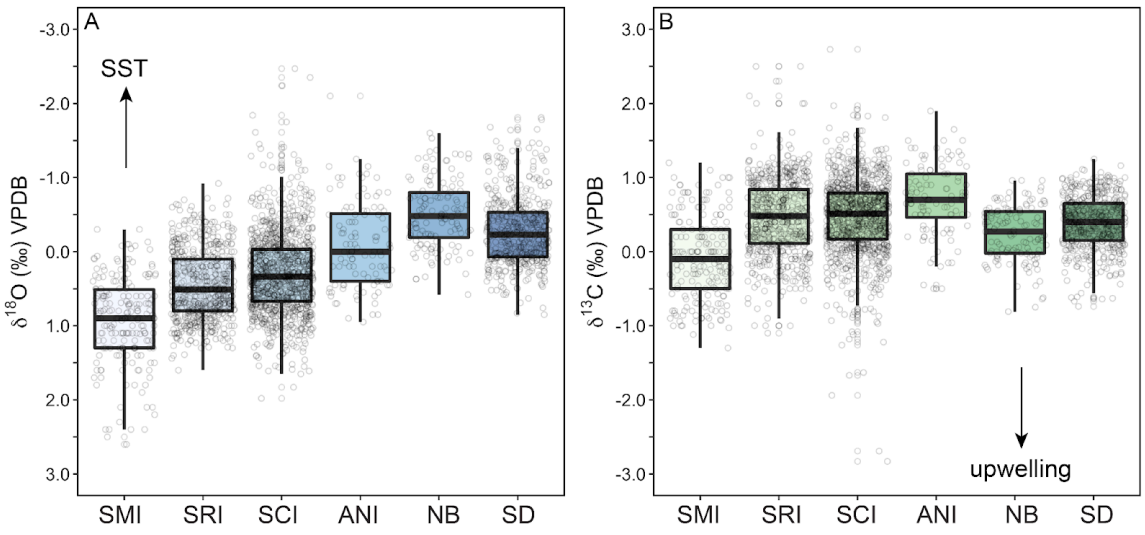


**Figure 5.** Box plots showing stable isotopic ranges of each site comprising all shells with five or more subsamples from all Holocene intervals. (A) Oxygen isotope data from all shells with five or more subsamples for San Miguel Island, Santa Rosa Island, Santa Cruz Island, Anacapa Island, Newport Beach, and San Diego. Y-axis is inverted to match directionality of temperature proxy as indicated by SST arrow. (B) Carbon isotope data from all shells with five or more subsamples for the same sites.

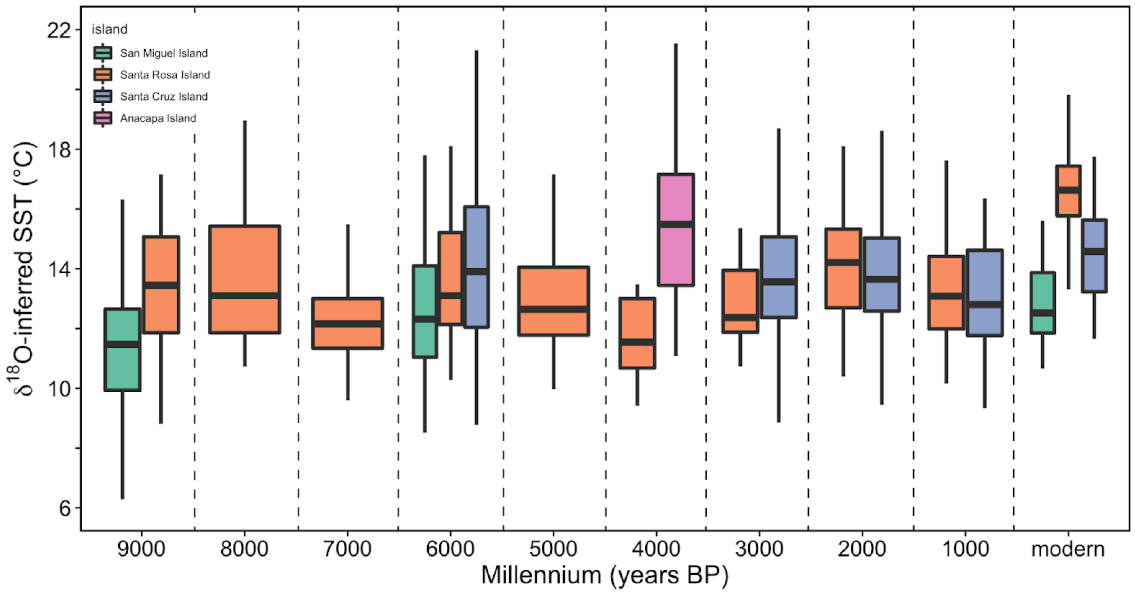


**Figure 6.** Millennial scale $\delta^{18}$O-inferred temperature variability for each island. Data were binned by millennium for each island to produce a range of temperature snapshots.

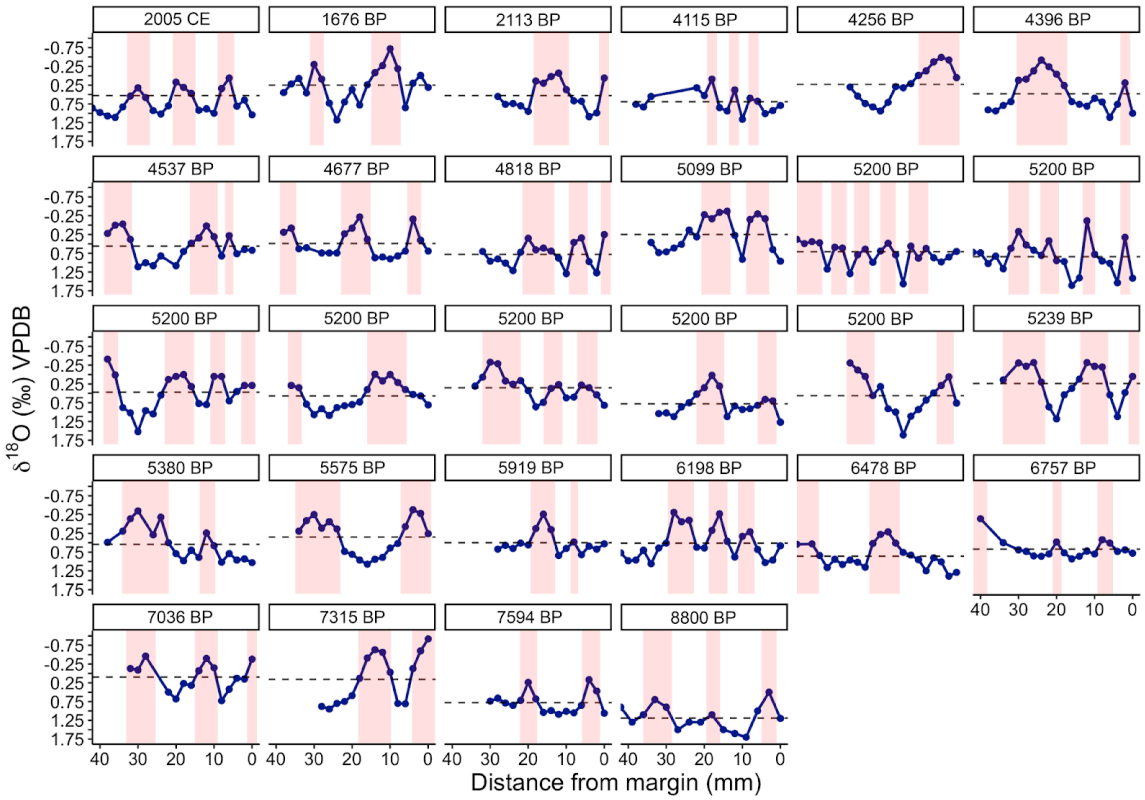


**Figure 7.** Individual oxygen isotope profiles of all 28 long profile shells (15+ subsamples) from Channel Islands. Each profile is from a unique shell with collection date or calibrated age in years before present (BP) labeled at the top of the plot. Dashed line represents mean oxygen isotope value recorded by each individual shell. Red shaded bars are estimations of warm seasons. Y-axis is inverted and the same for all plots.

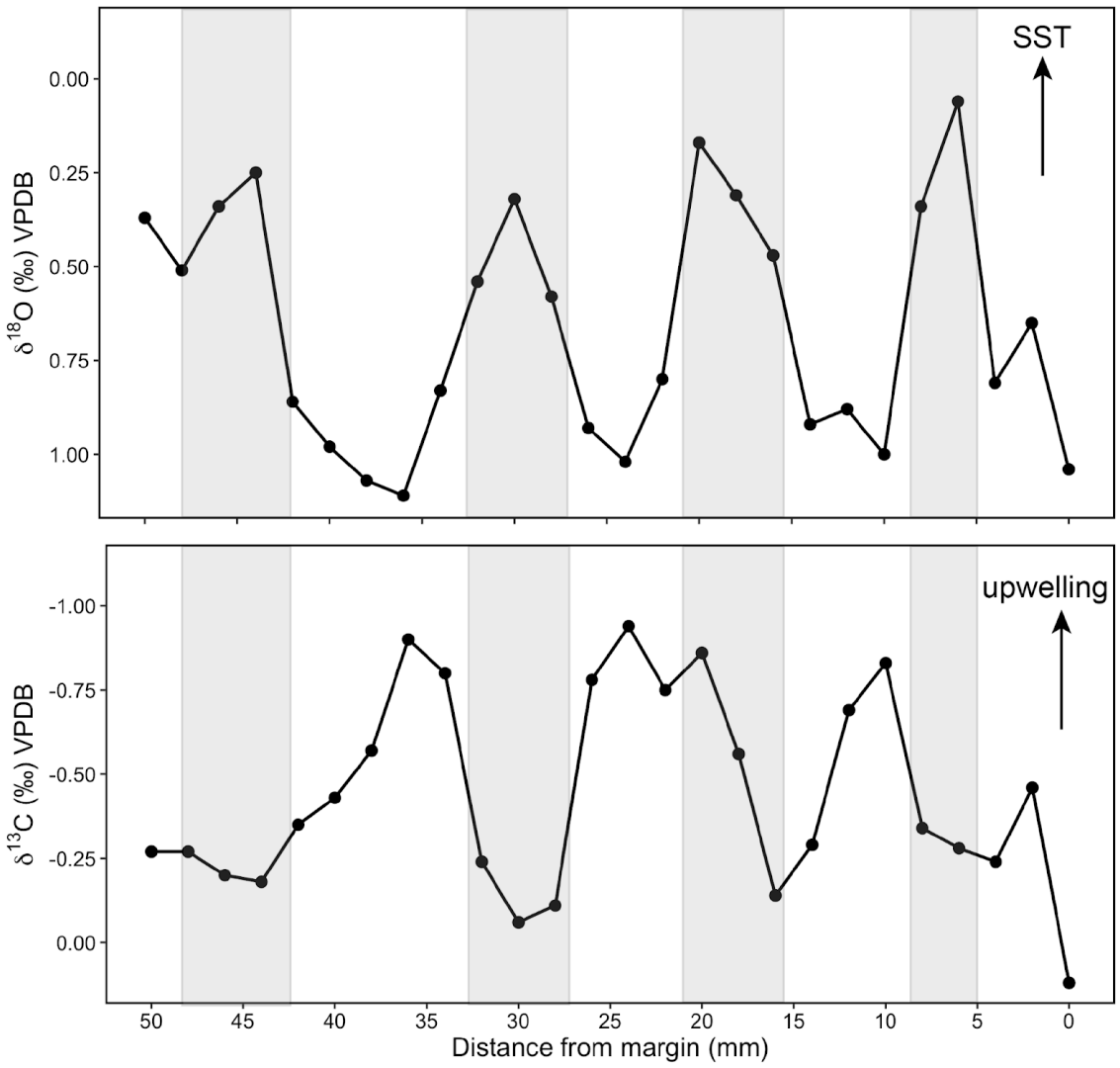


**Figure 8.** Last 50 mm of $\delta^{18}O$ and $\delta^{13}C$ profiles in a *M. californianus* shell collected from Santa Miguel Island in 2005 CE. In top plot ($\delta^{18}O$), y-axis is inverted to match directionality of temperature proxy as indicated by SST arrow. Gray bars in both plots denote $\delta^{18}O$-inferred warm seasons.

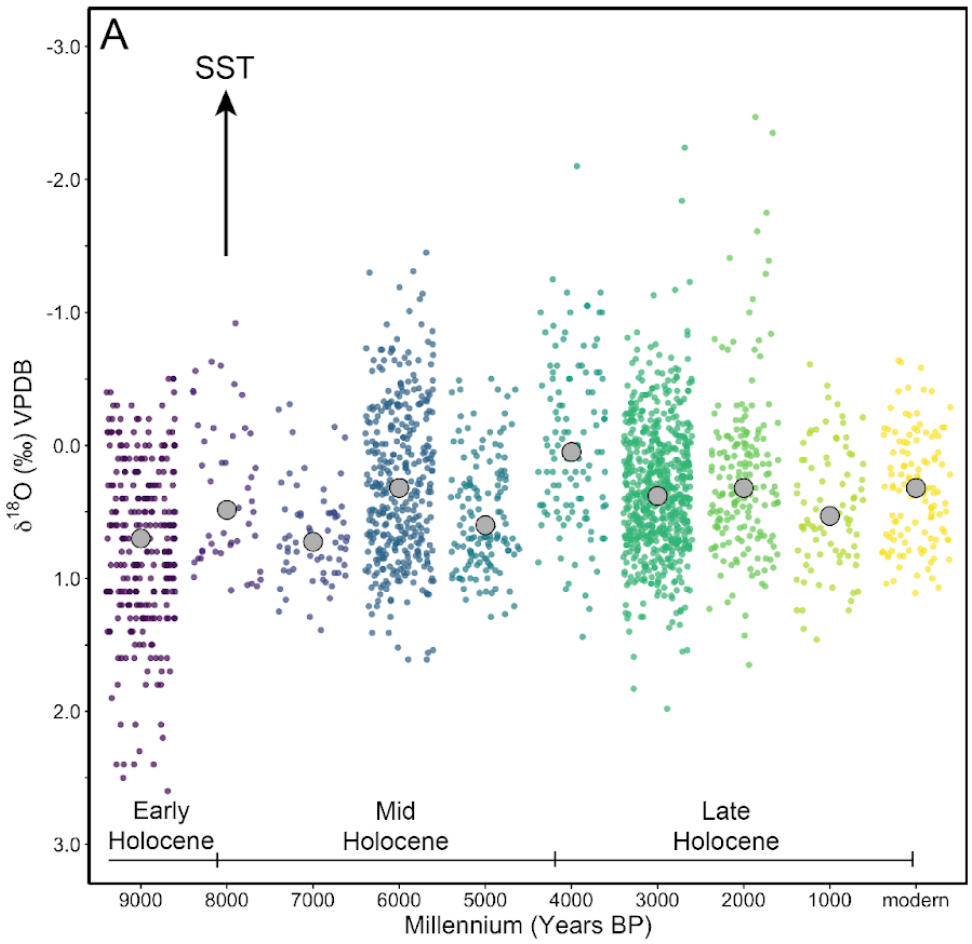
A
SST
-3.0
-2.0
-1.0
0.0
1.0
2.0
3.0
δ18O (‰) VPDB
Early Holocene
Mid Holocene
Late Holocene
9000
8000
7000
6000
5000
4000
3000
2000
1000
modern
Millennium (Years BP)

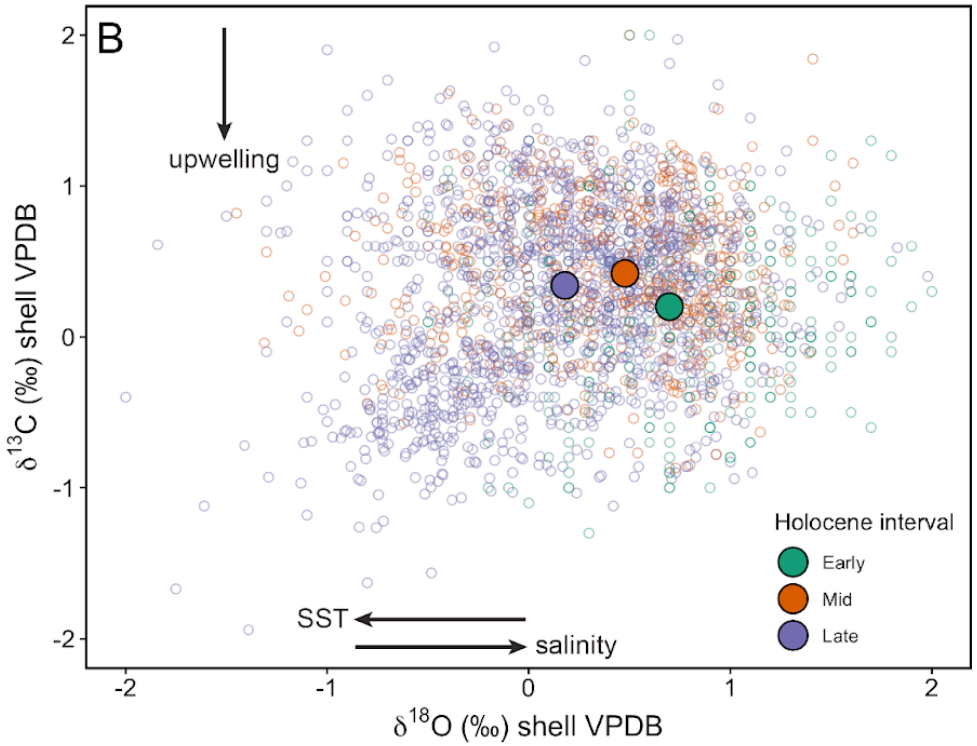
B
upwelling
2
1
0
-1
-2
δ13C (‰) shell VPDB
SST
salinity
Holocene interval
Early
Mid
Late
-2
-1
0
1
2
δ18O (‰) shell VPDB

**Figure 9.** All data points from all Channel Islands shells with five or more subsamples binned by time period. (A) Each time bin on the x-axis represents all samples within that millennium (e.g., 1000 represents all non-modern shells from 0-1000 BP, 2000 represents all shells from 1000-2000 BP, etc.). Modern shells (far right, in yellow) are included for comparison. These modern shells are also from the Channel Islands and contain five or more subsamples. Gray points denote median δ18O value of time bin. (B) All data points from Channel Islands shells in oxygen and carbon isotope space over the Holocene. Centroids (medians) are plotted for each sub-epoch. Seven outliers > 2‰ and < -2‰ were omitted from the plot.

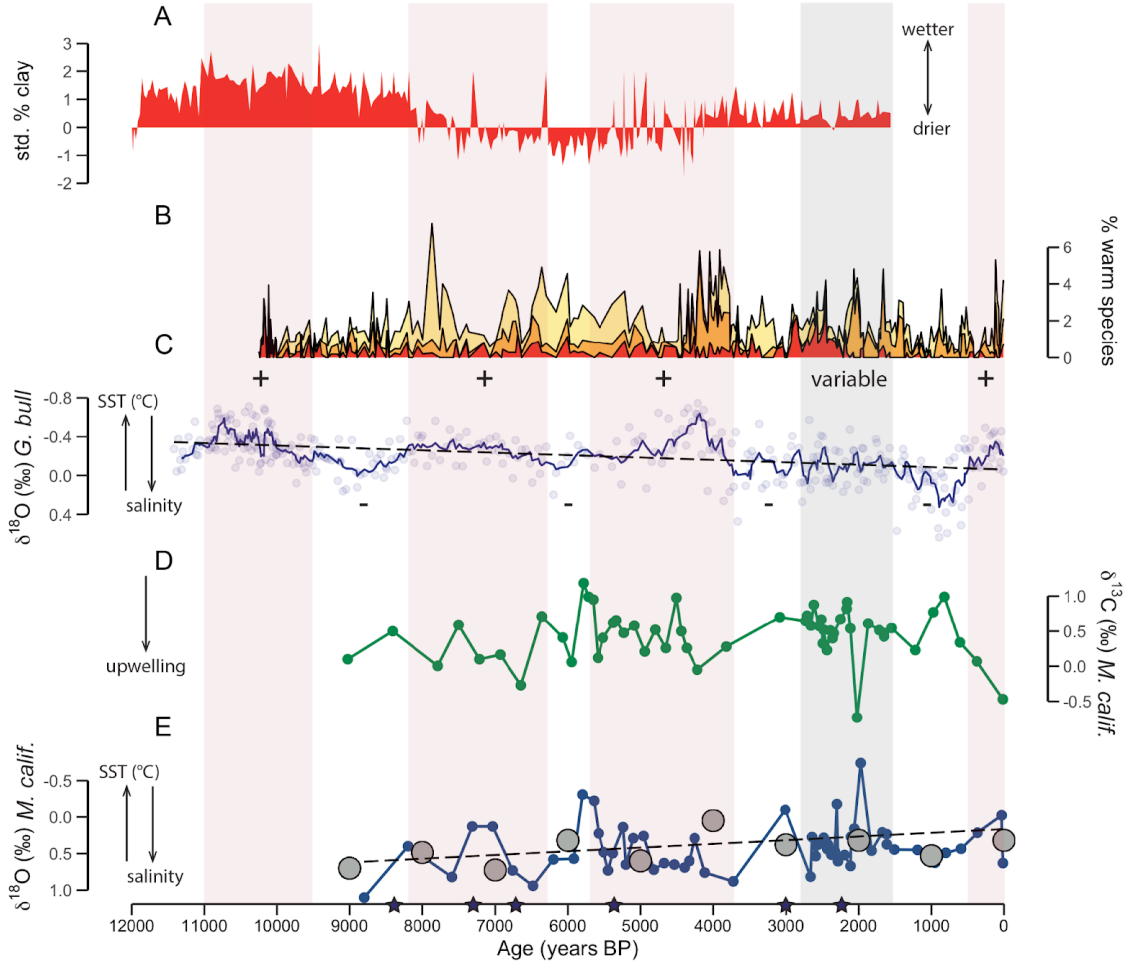


**Figure 10.** Age versus climate proxy data in calibrated years before present. (A) Standardized percent clay as a precipitation proxy from Silver Lake in the Central Mojave, California (Kirby et al., 2015). (B) Percentage of warm species (*Globigerinoides ruber* in orange, *Globoturborotalita rubescens* in red, and *Neogloboquadrina dutertrei* in yellow) from Santa Barbara Basin ODP Site 893 (Fisler and Hendy, 2008) [108]. (C) Oxygen isotope record from *Globigerina bulloides* planktic foraminifera at ODP Site 893 A/B (Kennett et al., 2007) [105]. Y-axis is inverted. Dashed line represents linear trend. (D) Carbon isotope record from *M.*

*californianus* shells analyzed in this study with 5 or more subsamples with median for each year of the record plotted. (E) Oxygen isotope record from *M. californianus* shells analyzed in this study with 5 or more subsamples with median for each year of the record plotted in blue. Y-axis is inverted. Dashed line represents linear trend. Large gray points represent 1000-year median $\delta^{18}O$ values as in Fig 9. Blue stars on x-axis denote timing of flood events identified from sediment cores in Santa Barbara Basin (Du et al., 2018) [109]. Shaded red bars denote warm periods and shaded gray bar denotes variable conditions inferred by Kennett et al. (2007) [105].

**Supplementary Information**

**S1 Figure.** Out of the all *M. californianus* shells synthesized here, there were only three cases where we could evaluate the impacts of subsampling strategy. We compared two mussels collected from the same site and with the same $^{14}C$ age (cal BP) with different subsampling strategies (short vs. long profiles, each one in a different individual). Top panels show longer profiles and bottom panels show short profiles. Each plot is a different individual. Blue horizontal line represents mean $\delta^{18}O$ value for that individual. The only cases where the mean $\delta^{18}O$ value is significantly different is for the two individuals from 5380 BP. Y-axes are reversed.

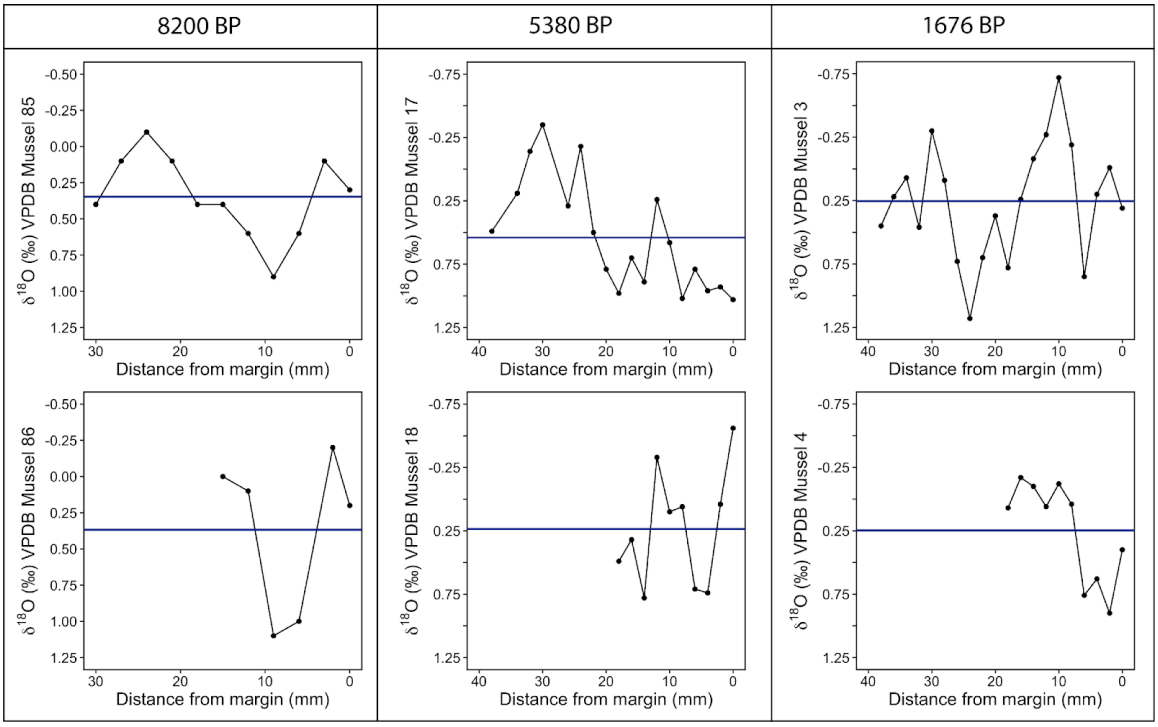


**S2 Figure.** Oxygen (blue) and carbon (green) isotope profiles for long-profile *M. californianus* shells from the Channel Islands of all ages. Each plot is an individual shell. This figure is comparable to Fig 7, which has $\delta^{18}O$ profiles for the same individuals plotted. This figure shows $\delta^{13}C$ profiles in addition.

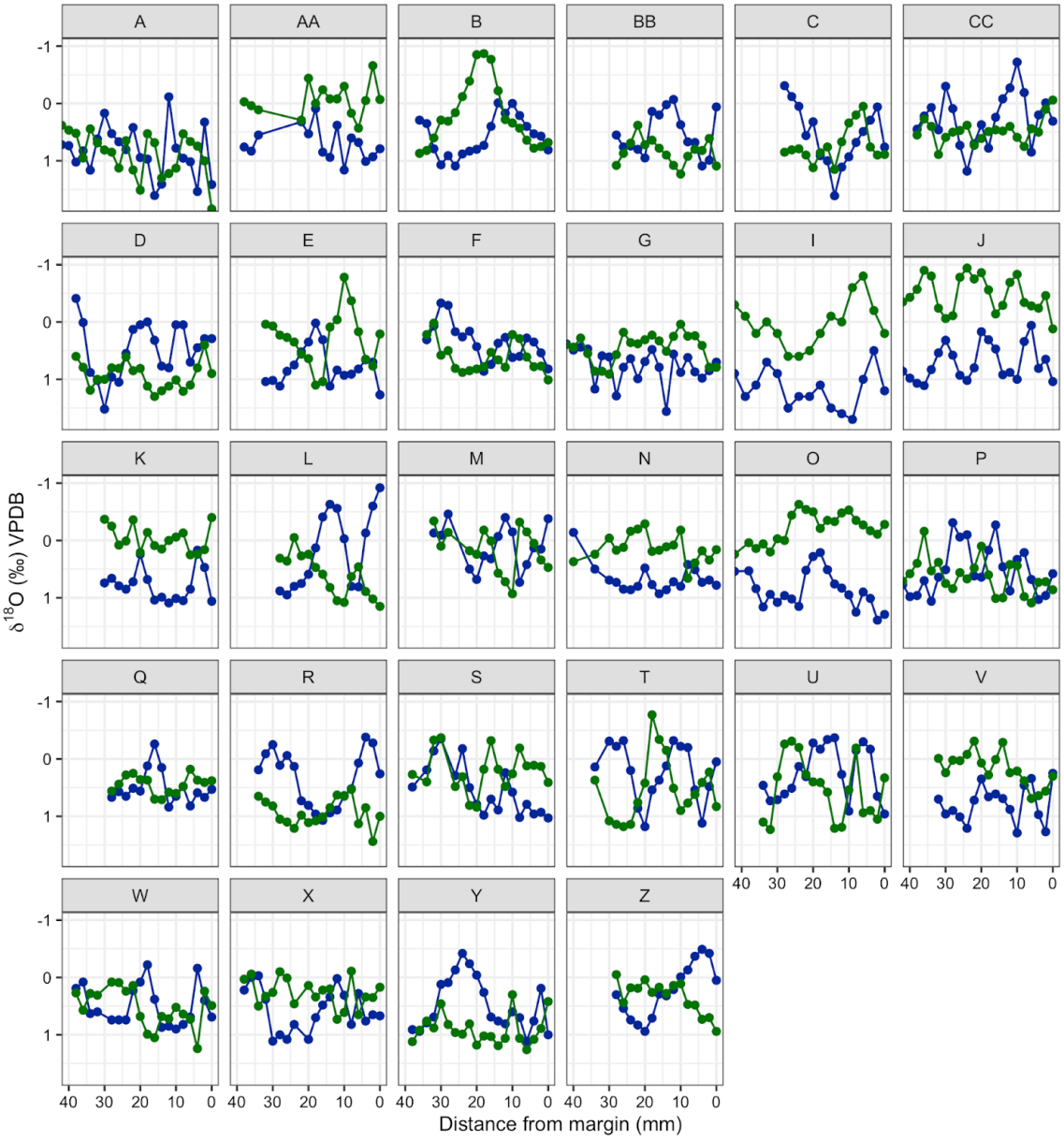


**S3 Figure.** Oxygen isotope profiles from the 76 individuals live-collected at Santa Rosa Island in August 2017 (Jazwa et al., 2020) [74]. Note that out of all 76 individuals, only 48 record overall summer warming. Both x- and y- axes are uniform for all individuals and y-axis is inverted to match directionality of temperature proxy (i.e., summer warming should appear as an increasing curve from left to right).

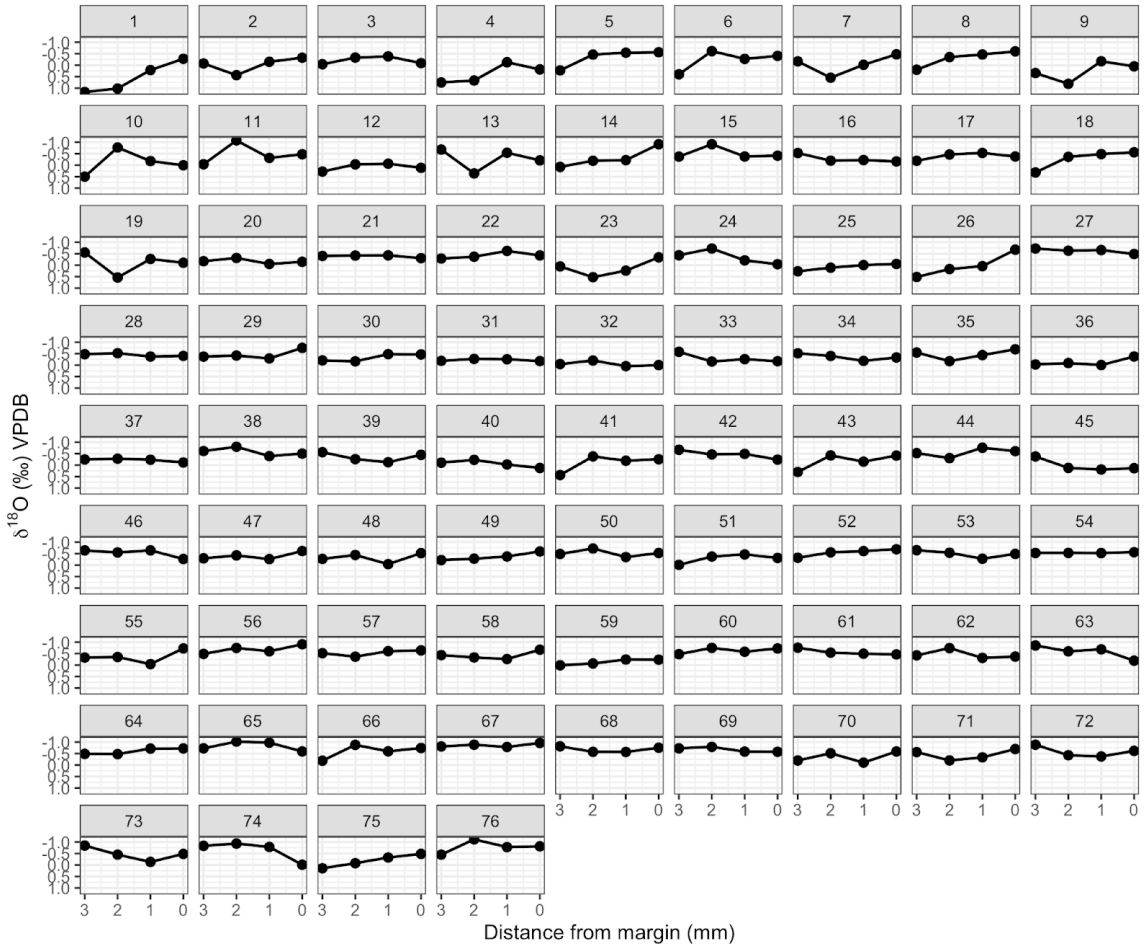


**S4 Table.** Statistical test results (ANOVA, Tukey HSD) of oxygen isotope data binned by millennia to identify significant changes occurring over millennial scales.

| Millennium Comparison (Year BP) | Difference | Lower | Upper | p-value |
|---|---|---|---|---|
| 1000-2000 | -0.36938959 | -0.51012044 | -0.22865873 | 0 |
| 1000-3000 | -0.48262339 | -0.57421929 | -0.39102749 | 0 |
| 1000-5000 | -0.6622544 | -0.81754606 | -0.50696274 | 0 |
| 1000-6000 | -0.43344712 | -0.5420085 | -0.32488574 | 0 |
| 1000-7000 | -0.81624042 | -1.03863233 | -0.5938485 | 0 |
| 1000-8000 | -0.50189259 | -0.76152431 | -0.24226086 | 0.0000001 |
| 1000-9000 | -0.89773295 | -1.01831315 | -0.77715275 | 0 |
| 2000-4000 | 0.22941004 | 0.02508188 | 0.4337382 | 0.0146938 |
| 2000-5000 | -0.29286481 | -0.48457084 | -0.10115879 | 0.0000777 |
| 2000-7000 | -0.44685083 | -0.69603723 | -0.19766443 | 0.000001 |
| 2000-9000 | -0.52834337 | -0.69319265 | -0.36349408 | 0 |
| 3000-4000 | 0.34264385 | 0.16847545 | 0.51681225 | 0 |

| | | | | |
|---|---|---|---|---|
| 3000-5000 | -0.17963101 | -0.33880335 | -0.02045866 | 0.0138082 |
| 3000-7000 | -0.33361702 | -0.55873587 | -0.10849817 | 0.0001528 |
| 3000-9000 | -0.41510956 | -0.54064808 | -0.28957104 | 0 |
| 4000-5000 | -0.52227486 | -0.73689154 | -0.30765817 | 0 |
| 4000-6000 | -0.29346757 | -0.47712594 | -0.10980921 | 0.0000264 |
| 4000-7000 | -0.67626087 | -0.94347424 | -0.4090475 | 0 |
| 4000-8000 | -0.36191304 | -0.66083353 | -0.06299256 | 0.0054686 |
| 4000-9000 | -0.75775341 | -0.94876232 | -0.56674449 | 0 |
| 5000-6000 | 0.22880728 | 0.0593033 | 0.39831126 | 0.000961 |
| 5000-9000 | -0.23547855 | -0.41292041 | -0.0580367 | 0.001296 |
| 6000-7000 | -0.3827933 | -0.61533203 | -0.15025457 | 0.0000122 |
| 6000-9000 | -0.46428583 | -0.60268989 | -0.32588177 | 0 |
| 8000-9000 | -0.39584036 | -0.66929739 | -0.12238334 | 0.000251 |
| 7000-8000 | 0.31434783 | -0.01685803 | 0.64555369 | 0.0785502 |
| 1000-4000 | -0.13997955 | -0.31060866 | 0.03064957 | 0.2102237 |
| 2000-3000 | -0.11323381 | -0.25823557 | 0.03176795 | 0.2710046 |
| 5000-7000 | -0.15398601 | -0.41167612 | 0.10370409 | 0.644971 |
| 5000-8000 | 0.16036181 | -0.13007693 | 0.45080055 | 0.738025 |
| 2000-8000 | -0.132503 | -0.41542408 | 0.15041807 | 0.8764606 |
| 3000-6000 | 0.04917627 | -0.06486717 | 0.16321972 | 0.9196979 |
| 2000-6000 | -0.06405753 | -0.22033061 | 0.09221554 | 0.9392879 |
| 7000-9000 | -0.08149254 | -0.31987935 | 0.15689428 | 0.9794916 |
| 6000-8000 | -0.06844547 | -0.33681971 | 0.19992877 | 0.9971079 |
| 3000-8000 | -0.0192692 | -0.28124051 | 0.24270212 | 0.9999998 |

## References


1. Abraham JP, Baringer M, Bindoff NL, Boyer T, Cheng LJ, Church JA, et al. A review of global ocean temperature observations: Implications for ocean heat content estimates and climate change. Rev Geophys. 2013;51: 450–483. doi:10.1002/rog.20022
2. Hutchins DA, Fu F. Microorganisms and ocean global change. Nature Microbiology. 2017;2: 1–11. doi:10.1038/nmicrobiol.2017.58
3. Bates NAR, Astor YM, Church MTJ, Currie K, Dore JE, Olafsson J, et al. A Time-Series View of Changing Surface Ocean Chemistry Due to Ocean Uptake of Anthropogenic $CO_2$ and Ocean Acidification. 2020; 17.
4. Scavia D, Field JC, Boesch DF, Buddemeier RW, Burkett V, Cayan DR, et al. Climate change impacts on U.S. Coastal and Marine Ecosystems. Estuaries. 2002;25: 149–164. doi:10.1007/BF02691304
5. Harley CDG, Randall Hughes A, Hultgren KM, Miner BG, Sorte CJB, Thornber CS, et al. The impacts of climate change in coastal marine systems. Ecology Letters. 2006;9: 228–241. doi:10.1111/j.1461-0248.2005.00871.x
6. Nguyen TTX, Bonetti J, Rogers K, Woodroffe CD. Indicator-based assessment of climate-change impacts on coasts: A review of concepts, methodological approaches and vulnerability indices. Ocean & Coastal Management. 2016;123: 18–43. doi:10.1016/j.ocecoaman.2015.11.022
7. Hewitt JE, Ellis JI, Thrush SF. Multiple stressors, nonlinear effects and the implications of climate change impacts on marine coastal ecosystems. Global Change Biology. 2016;22: 2665–2675. doi:10.1111/gcb.13176
8. Jackson JBC. Historical Overfishing and the Recent Collapse of Coastal Ecosystems. Science. 2001;293: 629–637. doi:10.1126/science.1059199
9. Lightfoot KG, Panich LM, Schneider TD, Gonzalez SL. European colonialism and the Anthropocene: A view from the Pacific Coast of North America. Anthropocene. 2013;4: 101–115. doi:10.1016/j.ancene.2013.09.002
10. Neumann B, Vafeidis AT, Zimmermann J, Nicholls RJ. Future Coastal Population Growth and Exposure to Sea-Level Rise and Coastal Flooding - A Global Assessment. PLOS ONE. 2015;10: e0118571. doi:10.1371/journal.pone.0118571
11. Martínez ML, Intralawan A, Vázquez G, Pérez-Maqueo O, Sutton P, Landgrave R. The coasts of our world: Ecological, economic and social importance. Ecological Economics. 2007;63: 254–272. doi:10.1016/j.ecolecon.2006.10.022
12. Tomašových A, Kidwell SM. Nineteenth-century collapse of a benthic marine ecosystem on the open continental shelf. Proceedings of the Royal Society B: Biological Sciences. 2017;284: 20170328. doi:10.1098/rspb.2017.0328
13. Leonard-Pingel JS, Kidwell SM, Tomaových A, Alexander CR, Cadien DB. Gauging benthic recovery from 20th century pollution on the southern California continental shelf using bivalves from sediment cores. Marine Ecology Progress Series. 2019;615: 101–119. doi:10.3354/meps12918
14. Meadows CA, Grebmeier JM, Kidwell SM. High-latitude benthic bivalve biomass and recent climate change: Testing the power of live-dead discordance in the Pacific Arctic. Deep Sea Research Part II: Topical Studies in Oceanography. 2019;162: 152–163. doi:10.1016/j.dsr2.2019.04.005
15. Jones DS, Quitmyer IR, Andrus CFT. Oxygen isotopic evidence for greater seasonality in

Holocene shells of Donax variabilis from Florida. Palaeogeography, Palaeoclimatology, Palaeoecology. 2005;228: 96–108. doi:10.1016/j.palaeo.2005.03.046
16. Fenger T, Surge D, Schöne B, Milner N. Sclerochronology and geochemical variation in limpet shells (Patella vulgata): A new archive to reconstruct coastal sea surface temperature. Geochemistry, Geophysics, Geosystems. 2007;8. doi:10.1029/2006GC001488
17. Pérez-Huerta A, Etayo-Cadavid MF, Andrus CFT, Jeffries TE, Watkins C, Street SC, et al. El Niño Impact on Mollusk Biomineralization–Implications for Trace Element Proxy Reconstructions and the Paleo-Archeological Record. PLOS ONE. 2013;8: e54274. doi:10.1371/journal.pone.0054274
18. Sandweiss DH, Andrus CFT, Kelley AR, Maasch KA, Reitz EJ, Roscoe PB. Archaeological climate proxies and the complexities of reconstructing Holocene El Niño in coastal Peru. PNAS. 2020;117: 8271–8279. doi:10.1073/pnas.1912242117
19. Oeschger H, Beer J, Siegenthaler U, Stauffer B, Dansgaard W, Langway C c. Late Glacial Climate History from Ice Cores. Climate Processes and Climate Sensitivity. American Geophysical Union (AGU); 1984. pp. 299–306. doi:10.1029/GM029p0299
20. Hendy IL, Kennett JP. Dansgaard-Oeschger Cycles and the California Current System: Planktonic foraminiferal response to rapid climate change in Santa Barbara Basin, Ocean Drilling Program Hole 893A. Paleoceanography. 2000;15: 30–42. doi:10.1029/1999PA000413
21. Barron JA, Heusser L, Herbert T, Lyle M. High-resolution climatic evolution of coastal northern California during the past 16,000 years: Climatic Evolution of Coastal California. Paleoceanography. 2003;18: n/a-n/a. doi:10.1029/2002PA000768
22. Cobb KM, Charles CD, Cheng H, Edwards RL. El Niño/Southern Oscillation and tropical Pacific climate during the last millennium. Nature. 2003;424: 271–276. doi:10.1038/nature01779
23. Kirby ME, Lund SP, Patterson WP, Anderson MA, Bird BW, Ivanovici L, et al. A Holocene record of Pacific Decadal Oscillation (PDO)-related hydrologic variability in Southern California (Lake Elsinore, CA). J Paleolimnol. 2010;44: 819–839. doi:10.1007/s10933-010-9454-0
24. Bernal JP, Lachniet M, McCulloch M, Mortimer G, Morales P, Cienfuegos E. A speleothem record of Holocene climate variability from southwestern Mexico. Quaternary Research. 2011;75: 104–113. doi:10.1016/j.yqres.2010.09.002
25. Jones TL, Richman JR. On Mussels: *Mytilus Californianus* as a Prehistoric Resource. North American Archaeologist. 1995;16: 33–58. doi:10.2190/G5TT-YFHP-JE6A-P2TX
26. Gonzalez SL. Indigenous Values and Methods in Archaeological Practice: Low-Impact Archaeology Through the Kashaya Pomo Interpretive Trail Project. American Antiquity. 2016;81: 533–549. doi:10.1017/S000273160000398X
27. Nelson, Peter PA. The Role of GPR in Community-Driven Compliance Archaeology with Tribal and Non-tribal Communities in Central California. Advances in Archaeological Practice. 2021;9: 215–225. doi:10.1017/aap.2021.14
28. Paine RT. Intertidal Community Structure. Experimental Studies on the Relationship between a Dominant Competitor and Its Principal Predator. Oecologia. 1974;15: 93–120.
29. Smith JR, Fong P, Ambrose RF. Spatial patterns in recruitment and growth of the mussel Mytilus californianus (Conrad) in southern and northern California, USA, two regions with differing oceanographic conditions. Journal of Sea Research. 2009;61: 165–173.

doi:10.1016/j.seares.2008.10.009
30. Connor KM, Sung A, Garcia NS, Gracey AY, German DP. Modulation of digestive physiology and biochemistry in Mytilus californianus in response to feeding level acclimation and microhabitat. Biology Open. 2016;5: 1200–1210. doi:10.1242/bio.019430
31. Suchanek TH. The role of disturbance in the evolution of life history strategies in the intertidal mussels Mytilus edulis and Mytilus californianus. Oecologia. 1981;50: 143–152. doi:10.1007/BF00348028
32. Bell EC, Gosline JM. Strategies for life in flow: tenacity, morphometry, and probability of dislodgment of two Mytilus species. Marine Ecology Progress Series. 1997;159: 197–208. doi:10.3354/meps159197
33. Young RT. The Distribution of the Mussel (Mytilus Californianus) in Relation to the Salinity of Its Environment. Ecology. 1941;22: 379–386. doi:10.2307/1930711
34. Coe WR, Fox DL. Biology of the california sea-mussel (mytilus californianus). iii. environmental conditions and rate of growth. The Biological Bulletin. 1944;87: 59–72. doi:10.2307/1538129
35. Dehnel PA. Growth rates in latitudinally and vertically separated populations of mytilus californianus. The Biological Bulletin. 1956;110: 43–53. doi:10.2307/1538891
36. Dodd JR. Paleoecological Implications of Shell Mineralogy in Two Pelecypod Species. The Journal of Geology. 1963;71: 1–11.
37. Bayne BL, Bayne CJ, Carefoot TC, Thompson RJ. The physiological ecology of Mytilus californianus Conrad. Oecologia. 1976;22: 211–228. doi:10.1007/BF00344793
38. Suchanek TH. The ecology of Mytilus edulis L. in exposed rocky intertidal communities. Journal of Experimental Marine Biology and Ecology. 1978;31: 105–120. doi:10.1016/0022-0981(78)90139-9
39. Dahlhoff E, Menge B. Influence of phytoplankton concentration and wave exposure on the ecophysiology of Mytilus californianus. Marine Ecology Progress Series. 1996;144: 97–107. doi:10.3354/meps144097
40. Blanchette CA, Helmuth B, Gaines SD. Spatial patterns of growth in the mussel, Mytilus californianus, across a major oceanographic and biogeographic boundary at Point Conception, California, USA. Journal of Experimental Marine Biology and Ecology. 2007;340: 126–148. doi:10.1016/j.jembe.2006.09.022
41. Jurgens LJ, Gaylord B. Edge effects reverse facilitation by a widespread foundation species. Scientific Reports. 2016;6: 37573. doi:10.1038/srep37573
42. Ford HL, Schellenberg SA, Becker BJ, Deutschman DL, Dyck KA, Koch PL. Evaluating the skeletal chemistry of *Mytilus californianus* as a temperature proxy: Effects of microenvironment and ontogeny: *MYTILUS* CHEMISTRY AS A TEMPERATURE PROXY. Paleoceanography. 2010;25. doi:10.1029/2008PA001677
43. Connor KM, Robles CD. Within-Site Variation of Growth Rates and Terminal Sizes in Mytilus californianus Along Wave Exposure and Tidal Gradients. The Biological Bulletin. 2015;228: 39–51. doi:10.1086/BBLv228n1p39
44. Vriesman VP, Carlson SJ, Hill TM. Investigating controls of shell growth features in a foundation bivalve species: seasonal trends and decadal changes in the California mussel. Biogeosciences. 2022;19: 329–346. doi:10.5194/bg-19-329-2022
45. Ferguson JE, Johnson KR, Santos G, Meyer L, Tripati A. Investigating $\delta^{13}C$ and $\Delta^{14}C$ within *Mytilus californianus* shells as proxies of upwelling intensity: $\delta^{13}C$ AND $\Delta^{14}C$ IN *MYTILUS* SHELLS. Geochemistry, Geophysics, Geosystems. 2013;14: 1856–1865.

doi:10.1002/ggge.20090
46. Checkley DM, Barth JA. Patterns and processes in the California Current System. Progress in Oceanography. 2009;83: 49–64. doi:10.1016/j.pocean.2009.07.028
47. Jones TL, Kennett DJ. Late Holocene Sea Temperatures along the Central California Coast. Quaternary Research. 1999;51: 74–82. doi:10.1006/qres.1998.2000
48. Thakar HB, Glassow MA, Blanchette C. Reconsidering evidence of human impacts: Implications of within-site variation of growth rates in Mytilus californianus along tidal gradients. Quaternary International. 2017;427: 151–159. doi:10.1016/j.quaint.2015.10.018
49. Rick TC. 8000 YEARS OF HUMAN SETTLEMENT AND LAND USE IN OLD RANCH CANYON, SANTA ROSA ISLAND, CALIFORNIA. : 12.
50. Braje TJ, Rick TC, Erlandson JM. A trans-Holocene historical ecological record of shellfish harvesting on California's Northern Channel Islands. Quaternary International. 2012;264: 109–120. doi:10.1016/j.quaint.2011.09.011
51. Glassow, Kennett, D.J., Kennett, J.P., Wilcoxon, L.R. Confirmation of Middle Holocene Ocean Cooling Inferred from Stable Isotopic Analysis of Prehistoric Shells. 1994.
52. Rick TC, Robbins JA, Ferguson KM. Stable Isotopes from Marine Shells, Ancient Environments, and Human Subsistence on Middle Holocene Santa Rosa Island, California, USA. The Journal of Island and Coastal Archaeology. 2006;1: 233–254. doi:10.1080/15564890600935480
53. Jew NP, Rick TC. Understanding the Occupation of Small Continental Islands: Seasonality and δ18O Evidence From Anacapa Island, California. The Journal of Island and Coastal Archaeology. 2014;9: 430–435. doi:10.1080/15564894.2013.861547
54. Jazwa CS, Braje TJ, Erlandson JM, Kennett DJ. Central place foraging and shellfish processing on California's Northern Channel Islands. Journal of Anthropological Archaeology. 2015;40: 33–47. doi:10.1016/j.jaa.2015.05.005
55. Schneider T, Panich L. Toms Point Archaeology: Investigating Native American History at Tomales Bay. Faculty Publications. 2017. Available: https://scholarcommons.scu.edu/anthro_fac_pubs/81
56. McConnaughey TA, Gillikin DP. Carbon isotopes in mollusk shell carbonates. Geo-Marine Letters. 2008;28: 287–299. doi:10.1007/s00367-008-0116-4
57. Gillikin DP, Dehairs F, Lorrain A, Steenmans D, Baeyens W, André L. Barium uptake into the shells of the common mussel (Mytilus edulis) and the potential for estuarine paleo-chemistry reconstruction. Geochimica et Cosmochimica Acta. 2006;70: 395–407. doi:10.1016/j.gca.2005.09.015
58. Pfister CA, McCoy SJ, Wootton JT, Martin PA, Colman AS, Archer D. Rapid Environmental Change over the Past Decade Revealed by Isotopic Analysis of the California Mussel in the Northeast Pacific. PLOS ONE. 2011;6: e25766. doi:10.1371/journal.pone.0025766
59. Killingley JS, Berger WH. Stable Isotopes in a Mollusk Shell: Detection of Upwelling Events. Science. 1979;205: 186–188. doi:10.1126/science.205.4402.186
60. Hinger EN, Santos GM, Druffel ERM, Griffin S. Carbon Isotope Measurements of Surface Seawater from a Time-Series Site Off Southern California. Radiocarbon. 2010;52: 69–89. doi:10.1017/S0033822200045045
61. Santos GM, Ferguson J, Acaylar K, Johnson KR, Griffin S, Druffel E. Δ14C and Δ13C of Seawater DIC as Tracers of Coastal Upwelling: A 5-Year Time Series from Southern California. Radiocarbon. 2011;53: 669–677. doi:10.1017/S0033822200039126

62. Andrus CFT. Shell midden sclerochronology. Quaternary Science Reviews. 2011;30: 2892–2905. doi:10.1016/j.quascirev.2011.07.016
63. Dodd JR. Environmentally Controlled Variation in the Shell Structure of a Pelecypod Species. : 9.
64. Bailey GN, Deith MR, Shackleton NJ. Oxygen Isotope Analysis and Seasonality Determinations: Limits and Potential of a New Technique. American Antiquity. 1983;48: 390–398. doi:10.2307/280460
65. Culleton BJ, Kennett DJ, Ingram BL, Erlandson JM, Southon JR. Intrashell Radiocarbon Variability in Marine Mollusks. Radiocarbon. 2006;48: 387–400. doi:10.1017/S0033822200038820
66. Hickey BM. The California current system—hypotheses and facts. Progress in Oceanography. 1979;8: 191–279. doi:10.1016/0079-6611(79)90002-8
67. Huyer A. Coastal upwelling in the California current system. Progress in Oceanography. 1983;12: 259–284. doi:10.1016/0079-6611(83)90010-1
68. Lynn RJ, Simpson JJ. The California Current system: The seasonal variability of its physical characteristics. Journal of Geophysical Research: Oceans. 1987;92: 12947–12966. doi:10.1029/JC092iC12p12947
69. Blanchette CA, Broitman BR, Gaines SD. Intertidal community structure and oceanographic patterns around Santa Cruz Island, CA, USA. Mar Biol. 2006;149: 689–701. doi:10.1007/s00227-005-0239-3
70. Hickey BM. Circulation over the Santa Monica-San Pedro Basin and Shelf. Progress in Oceanography. 1992;30: 37–115. doi:10.1016/0079-6611(92)90009-O
71. Blanchette CA, Raimondi PT, Broitman BR. SPATIAL PATTERNS OF INTERTIDAL COMMUNITY STRUCTURE ACROSS THE CALIFORNIA CHANNEL ISLANDS AND LINKS TO OCEAN TEMPERATURE. : 14.
72. Flores C. Importance of small-scale paleo-oceanographic conditions to interpret changes in size of California mussel ( Mytilus californianus ). Late Holocene, Santa Cruz island, California. Quaternary International. 2017;427: 137–150. doi:10.1016/j.quaint.2016.01.036
73. Kapsenberg L, Hofmann GE. Ocean pH time-series and drivers of variability along the northern Channel Islands, California, USA. Limnology and Oceanography. 2016;61: 953–968. doi:10.1002/lno.10264
74. Jazwa CS, Wolfe CA, Chu EY, Stull KE. The effects of vertical position in the intertidal zone on the δ18O and δ13C composition of Mytilus californianus shell carbonate. Journal of Archaeological Science: Reports. 2020;34: 102587. doi:10.1016/j.jasrep.2020.102587
75. ROBERT DODD J. Diagenetic Stability of Temperature-Sensitive Skeletal Properties in Mytilus from the Pleistocene of California. GSA Bulletin. 1966;77: 1213–1224. doi:10.1130/0016-7606(1966)77[1213:DSOTSP]2.0.CO;2
76. Glassow MA, Thakar HB, Kennett DJ. Red abalone collecting and marine water temperature during the Middle Holocene occupation of Santa Cruz Island, California. Journal of Archaeological Science. 2012;39: 2574–2582. doi:10.1016/j.jas.2012.03.017
77. Jazwa CS, Kennett DJ. Sea Mammal Hunting and Site Seasonality on Western San Miguel Island, California. Journal of California and Great Basin Anthropology. 2016;36: 23.
78. Jew a NP, Erlandson JM, Rick TC, Watts J. Shellfish, Seasonality, and Sedentism: δ18O Analysis of California Mussels from Early Holocene Shell Middens on San Miguel Island, California. : 12.

79. Jew b NP, Erlandson JM, Watts J, White FJ. Shellfish, Seasonality, and Stable Isotope Sampling: δ18O Analysis of Mussel Shells From an 8,800-Year-Old Shell Midden on California's Channel Islands. The Journal of Island and Coastal Archaeology. 2013;8: 170–189. doi:10.1080/15564894.2012.736917
80. Robbins JA, Ferguson KM, Gregory RT. A 7000-year sea-surface temperature record from CA-SRI-147, Santa Rosa Island, California, USA. The Holocene. 2013;23: 1008–1016. doi:10.1177/0959683613479619
81. Kennett, D.J. Behavioral ecology and the evolution of hunter-gatherer societies on the Northern Channel Islands, California - ProQuest. [cited 22 Apr 2022]. Available: https://www.proquest.com/openview/ba0c36daf0df1e158770444c1a79896b/1?pq-origsite=gscholar&cbl=18750&diss=y
82. Culleton BJ, Kennett DJ, Jones TL. Oxygen isotope seasonality in a temperate estuarine shell midden: a case study from CA-ALA-17 on the San Francisco Bay, California. Journal of Archaeological Science. 2009;36: 1354–1363. doi:10.1016/j.jas.2009.01.021
83. Walker M, Gibbard P, Head MJ, Berkelhammer M, Björck S, Cheng H, et al. Formal Subdivision of the Holocene Series/Epoch: A Summary. Journal of the Geological Society of India. 2019;93: 135–141. doi:10.1007/s12594-019-1141-9
84. R Core Team. R. 2021.
85. Epstein S, Buchsbaum R, Lowenstam HA, Urey HC. REVISED CARBONATE-WATER ISOTOPIC TEMPERATURE SCALE. GSA Bulletin. 1953;64: 1315–1326. doi:10.1130/0016-7606(1953)64[1315:RCITS]2.0.CO;2
86. Killingley JS. Seasonality of Mollusk Collecting Determined from O-18 Profiles of Midden Shells. American Antiquity. 1981;46: 152–158. doi:10.2307/279994
87. LeGrande AN, Schmidt GA. Sources of Holocene variability of oxygen isotopes in paleoclimate archives. Climate of the Past. 2009;5: 441–455. doi:10.5194/cp-5-441-2009
88. Bard E, Hamelin B, Arnold M, Montaggioni L, Cabioch G, Faure G, et al. Deglacial sea-level record from Tahiti corals and the timing of global meltwater discharge. Nature. 1996;382: 241–244. doi:10.1038/382241a0
89. Siddall M, Rohling EJ, Almogi-Labin A, Hemleben C, Meischner D, Schmelzer I, et al. Sea-level fluctuations during the last glacial cycle. Nature. 2003;423: 853–858. doi:10.1038/nature01690
90. Shackleton NJ, Opdyke ND. Oxygen Isotope and Palaeomagnetic Stratigraphy of Equatorial Pacific Core V28-238: Oxygen Isotope Temperatures and Ice Volumes on a 105 Year and 106 Year Scale*. Quaternary Research. 1973;3: 39–55. doi:10.1016/0033-5894(73)90052-5
91. White SM, Hill TM, Kennett JP, Behl RJ, Nicholson C. Millennial-scale variability to 735 ka: High-resolution climate records from Santa Barbara Basin, CA. Paleoceanography. 2013;28: 213–226. doi:10.1002/palo.20022
92. Rodhouse PG, McDonald JH, Newell RIE, Koehn RK. Gamete production, somatic growth and multiple-locus enzyme heterozygosity inMytilus edulis. Mar Biol. 1986;90: 209–214. doi:10.1007/BF00569129
93. Hall CA, Dollase WA, Corbató CE. Shell growth in Tivela stultorum (Mawe, 1823) and Callista chione (Linnaeus, 1758) (Bivalvia): annual periodicity, latitudinal differences, and diminution with age. Palaeogeography, Palaeoclimatology, Palaeoecology. 1974;15: 33–61. doi:10.1016/0031-0182(74)90036-4
94. Jones DS, Thompson I, Ambrose W. Age and growth rate determinations for the Atlantic

surf clam Spisula solidissima (Bivalvia: Mactracea), based on internal growth lines in shell cross-sections. Mar Biol. 1978;47: 63–70. doi:10.1007/BF00397019
95. IVANY LC, WILKINSON BH, JONES DS. Using Stable Isotopic Data to Resolve Rate and Duration of Growth throughout Ontogeny: An Example from the Surf Clam, Spisula solidissima. PALAIOS. 2003;18: 126–137. doi:10.1669/0883-1351(2003)18<126:USIDTR>2.0.CO;2
96. Schöne BR. The curse of physiology—challenges and opportunities in the interpretation of geochemical data from mollusk shells. Geo-Mar Lett. 2008;28: 269–285. doi:10.1007/s00367-008-0114-6
97. Ivany LC. Reconstructing Paleoseasonality from Accretionary Skeletal Carbonates—Challenges and Opportunities. The Paleontological Society Papers. 2012;18: 133–166. doi:10.1017/S108933260000259X
98. Jones DS, Arthur MA, Allard DJ. Sclerochronological records of temperature and growth from shells of Mercenaria mercenaria from Narragansett Bay, Rhode Island. Mar Biol. 1989;102: 225–234. doi:10.1007/BF00428284
99. GOODWIN DH, SCHÖNE BR, DETTMAN DL. Resolution and Fidelity of Oxygen Isotopes as Paleotemperature Proxies in Bivalve Mollusk Shells: Models and Observations. PALAIOS. 2003;18: 110–125. doi:10.1669/0883-1351(2003)18<110:RAFOOI>2.0.CO;2
100. Kennedy H, Richardson C, Duarte C, Kennedy D. Oxygen and carbon stable isotopic profiles of the fan mussel, Pinna nobilis, and reconstruction of sea surface temperatures in the Mediterranean. Marine Biology. 2001;139: 1115–1124. doi:10.1007/s002270100673
101. Freitas P, Clarke LJ, Kennedy H, Richardson C, Abrantes F. Mg/Ca, Sr/Ca, and stable-isotope ($\delta^{18}$O and $\delta^{13}$C) ratio profiles from the fan mussel *Pinna nobilis* : Seasonal records and temperature relationships: *PINNA NOBILIS* RATIO PROFILES. Geochemistry, Geophysics, Geosystems. 2005;6: n/a-n/a. doi:10.1029/2004GC000872
102. Gillikin DP, Lorrain A, Bouillon S, Willenz P, Dehairs F. Stable carbon isotopic composition of Mytilus edulis shells: relation to metabolism, salinity, δ13CDIC and phytoplankton. Organic Geochemistry. 2006;37: 1371–1382. doi:10.1016/j.orggeochem.2006.03.008
103. Snyder MA, Sloan LC, Diffenbaugh NS, Bell JL. Future climate change and upwelling in the California Current. Geophysical Research Letters. 2003;30. doi:10.1029/2003GL017647
104. Diffenbaugh NS, Ashfaq M. Response of California Current forcing to mid-Holocene insolation and sea surface temperatures. Paleoceanography. 2007;22. doi:10.1029/2006PA001382
105. Kennett DJ, Kennett JP, Erlandson JM, Cannariato KG. Human responses to Middle Holocene climate change on California's Channel Islands. Quaternary Science Reviews. 2007;26: 351–367. doi:10.1016/j.quascirev.2006.07.019
106. Viau AE, Gajewski K, Sawada MC, Fines P. Millennial-scale temperature variations in North America during the Holocene. Journal of Geophysical Research: Atmospheres. 2006;111. doi:10.1029/2005JD006031
107. Kirby ME, Knell EJ, Anderson WT, Lachniet MS, Palermo J, Eeg H, et al. Evidence for insolation and Pacific forcing of late glacial through Holocene climate in the Central Mojave Desert (Silver Lake, CA). Quaternary Research. 2015;84: 174–186. doi:10.1016/j.yqres.2015.07.003

108. Fisler J, Hendy IL. California Current System response to late Holocene climate cooling in southern California. Geophysical Research Letters. 2008;35: L09702. doi:10.1029/2008GL033902
109. Du X, Hendy I, Schimmelmann A. A 9000-year flood history for Southern California: A revised stratigraphy of varved sediments in Santa Barbara Basin. Marine Geology. 2018;397: 29–42. doi:10.1016/j.margeo.2017.11.014

## Chapter 3

## *Mytilus californianus* maintains consistent shell characteristics over a century of warming in the southern California Current System


### Abstract

Ocean warming and acidification due to anthropogenic carbon dioxide emissions have complex and variable impacts on the biomineralization patterns of marine calcifying taxa. Previous studies have shown that shifting calcification patterns are recorded through multiple shell characteristics, including shell morphology, microstructure, mineralogy, and growth band patterns. Environmentally driven shifts in calcification can develop over years to centuries, requiring a longer-term understanding of biomineralization patterns than laboratory- or field-based studies can provide. Here, we investigate the history of shell growth in *Mytilus californianus*, a critical foundation species that structures and supports biologically diverse intertidal environments spanning the west coast of North America. We evaluated archival *M. californianus* shells from sites within the southern portion of the California Current System to quantify changes in shell morphology, thickness, structure, and growth banding in 130 specimens collected with decadal frequency between 1913 and 2010. We paired shell growth data from morphometrics, optical microscopy, and preliminary microstructural analyses with instrumental temperature datasets from this same region. Despite increasingly warmer and more variable conditions in the southern CCS throughout the 20th century, none of the quantitative shell characteristics changed through time. *Mytilus californianus* shell features have remained quantitatively unchanged since 1913, although preliminary microstructural data suggests that crystal sizes may have become more variable. Our analysis provides historical evidence for generally stable and persistent shell growth characteristics throughout long-term warming trends,

indicating that southern populations of *M. californianus* may be more suited to cope with warming oceans than their northern counterparts. Results presented here highlight the value of species- and site-specific, multi-scaled investigations of shell growth through time in order to gauge resilience or sensitivity in the past and predict responses to ongoing and future changes.

## 1 Introduction

Anthropogenic carbon dioxide emissions are causing significant changes in ocean temperature and pH patterns globally (Doney et al., 2009; Abraham et al., 2013; Bates et al., 2020). Multiple meta-analyses and experimental observations have found that elevated temperatures and $pCO_2$ levels negatively impact many marine calcifying taxa by altering physiological processes and reducing calcification rates (Jokiel et al., 2008; Ries et al., 2009; Gaylord et al., 2011; Kroeker et al., 2013; Bednaršek et al., 2019; Figuerola et al., 2021; Hu et al., 2022). Shifts in calcification patterns have the potential to significantly alter ecosystem functioning (Kroeker et al., 2014; Nagelkerken and Connell, 2015; Hu et al., 2022), particularly when ecologically important species are adversely affected (Gaylord et al., 2011). However, given that biotic responses to ocean acidification (OA) and warming can be highly variable, it is difficult to quantify or predict the impacts of a changing ocean on marine calcifying taxa (Ries et al., 2009; Kroeker et al., 2010; 2013; Harvey et al., 2013). Similarly, the timescales over which organisms respond or adapt to changes are difficult to capture even in long-term experiments. While days- to weeks-long experimental laboratory observations are useful for documenting the immediate impacts of extreme conditions designed to mimic extreme warming or OA, a longer-term record of growth in ecologically important marine calcifying taxa is vital for accurately characterizing responses unfolding over decades to centuries. In an effort to better understand the timing and history of biological responses to changing climate conditions, some studies have

utilized museum collections of biogenic carbonates from the past century or longer to establish calcification baselines and examine changes in shell characteristics, including shell morphology, mineralogy, and microstructure, in modern species over the twentieth century (Pfister et al., 2016; Cross et al., 2018; McCoy et al., 2018; Bullard et al., 2021; Telesca et al., 2021).

Historic shells, or live-collected specimens with a known collection date preserved as archival samples, supplement the information gleaned from field monitoring studies and experimental observations by providing a longer context for changes in calcification over time scales relevant for ecological and evolutionary processes. Historic shells also allow for a closer examination of adaptive mechanisms through time; both gradual and sudden changes in shell characteristics indicate a shift in calcification patterns, which could have occurred either as an adverse response (i.e., vulnerability) or a compensatory response (i.e., resilience) to an environmental perturbation developing over years to decades (Telesca et al., 2021). As such, compiling long-term, multi-decadal records of a single species through time improves our ability to anticipate responses to ongoing and future changes.

One species of particular ecological and cultural significance for the west coast of North America is the marine mussel *Mytilus californianus*, a foundation species that dominates rocky intertidal environments from the Aleutian Islands of Alaska, USA to Baja California Sur, Mexico (Paine, 1974). As a critical member of intertidal communities, *M. californianus* provides a habitat for hundreds of encrusting species (Paine, 1974; Smith et al., 2009; Connor et al., 2016) and is therefore considered an ecosystem engineer for rocky environments throughout the northeastern Pacific Coast (Seed and Suchanek, 1992). Changes in *M. californianus* calcification patterns could have implications for its life history, including its body size and lifespan. Shifting calcification patterns could also have ecosystem-wide impacts if *M. californianus* shells become

thinner, smaller, or weaker – and therefore more vulnerable to predation or dislodgement on wave-swept rocky shores. *Mytilus californianus* precipitates both calcite and aragonite to form its tri–layered shell (Dodd,1964; Vriesman et al., 2022), so it is possible for the proportion of shell calcite relative to aragonite to shift in response to changes in carbonate chemistry (Bullard et al., 2021). Changing proportions of shell calcite and aragonite would also have implications for shell solubility and physical strength (Lin and Meyers, 2005; Ries, 2011).

Thus far, there are multiple lines of evidence for sudden shifts in *M. californianus* calcification patterns relative to the archaeological and historical record for this species (Table 1). For example, *M. californianus* shells collected at Tatoosh Island and Sand Point, Washington, USA in the 2010s are thinner with increased crystallographic disorder relative to both archival *M. californianus* shells collected in the 1970s and archaeological *M. californianus* shells excavated from a 2000-year-old midden at these same sites (Pfister et al., 2016; McCoy et al., 2018). In northern California, *M. californianus* shells are now thinner per unit length and have weaker contrast between dark-light growth bands than they did two decades ago (Vriesman et al., 2022). Laboratory experiments on *M. californianus* larvae indicated that higher $pCO_2$ levels that align with projections for the year 2100 (540-970 ppm) result in smaller, thinner, and weaker juvenile shells (Gaylord et al., 2011). A 60-year comparison of *M. californianus* shells from central and southern Californian localities suggested *M. californianus* individuals have precipitated more shell calcite relative to aragonite since the 1950s as seawater pH has decreased (Bullard et al., 2021). Here, we investigate the timing and degree to which *M. californianus* shells experienced shifts or reductions in calcification in the southern portion of the California Current System, as other studies of this species have found in northern California and Washington (Table 1).

Collectively, previous studies suggest that calcification patterns are changing in *M. californianus* after more than 2000 years of similarity and consistency in shell characteristics. However, changes in calcification patterns are not uniform across all populations and localities; for example, the shell thinning found in Washington specimens (Pfister et al., 2016) is in contrast to increased calcite production among mussels from central and southern California (Bullard et al., 2021). Although *M. californianus* is characterized by genetic homogeneity throughout its range, it may be responding to changing conditions in different ways due to regionally distinct oceanographic regimes and local acclimatization (Addison et al., 2008; Logan et al., 2012). The broad latitudinal distribution of *M. californianus* results in high oceanographic and climatic variability experienced by this species, particularly since the west coast of North America hosts an eastern boundary upwelling system and features diverse coastline morphologies; even small-scale local oceanographic differences can result in highly variable shell growth rates for this species (Blanchette and Gaines, 2007; Blanchette et al., 2007). Since our understanding of calcification history in *M. californianus* thus far is based upon single-year snapshots in time and spans over 38° of latitude encompassing vastly different oceanographic regimes, there is a need for further examination of the history and onset of biomineralogical changes in *M. californianus* in one broadly relevant coastal region.

To address this need, we investigated changes in shell morphology, shell structure, growth band patterning, and microstructural features in *M. californianus* individuals live-collected in the southern portion of the California Current System (CCS). This biomineralogical record spans every decade from 1913 to 2010. This is the longest biomineralogical record with decadal frequency in the *M. californianus* published literature thus far. We tested whether *M. californianus*, an ecologically and culturally valuable foundation species, exhibits signs of

reduced or altered calcification over the past century within the southern portion of the California Current System (Point Conception, California, USA through Baja California Sur, Mexico) in response to ocean warming and acidification. We predict that there has been a long-term reduction in calcification as indicated by thinner shells per unit length, a lower percentage of calcite-rich light banding, and increased crystallographic disorder in response to 20th century warming and ocean acidification in the southern portion of the California Current System. Alternatively, it is possible that southern California mussels will exhibit signs of consistent or even increased calcification to cope with changing climate conditions, as recently found in their European congener *M. edulis* (Telesca et al., 2021). Here we identify, characterize, and analyze shifts or consistencies in calcification in a critical foundation species in conjunction with temperature trends in the study area.

## 2 Materials and Methods

### 2.1 Study area and specimens

The southern portion of the California Current System (CCS) extends from Point Conception, California, USA (34.45 °N) to the Baja California peninsula of Mexico (~ 27.5 °N). The southern CCS is influenced by the cold, south-flowing California Current, the warm north-flowing Southern California Countercurrent, and the Southern Californian Eddy (Hickey, 1979; Huyer, 1983; Lynn and Simpson, 1987; Bograd and Lynn, 2003; Checkley and Barth, 2009; Kim and Cornuelle, 2015). The equatorward California Current is the dominant current in the region, flowing parallel to the coast of California until just north of San Diego, where it curves slightly eastward and then flows south past Baja California (Lynn and Bograd, 2002). The southern CCS is characterized by weaker seasonal upwelling and warmer sea surface temperatures relative to the central and northern portions of the CCS (Huyer, 1983; Checkley and Barth, 2009). Like all

of the CCS, the southern portion has experienced nearshore surface warming and OA over the past century (Bograd and Lynn, 2003; Osborne et al., 2020), and multiple instrumental and proxy-based records indicate that warming has escalated over the second half of the 20th century (Bograd and Lynn, 2003; di Lorenzo et al., 2005; Field et al., 2006). Additionally, increases in wind stress, upwelling strength, and anthropogenic ocean acidification have resulted in an estimated 0.21-unit decline in pH along the coast of San Diego since 1916 (Osborne et al., 2020).

The centennial warming and acidification trends are compounded by interannual to decadal scale variability in temperature and upwelling strength due to two dominant ocean-atmosphere modes, Pacific Decadal Oscillation (PDO) and El Niño Southern Oscillation (ENSO). ENSO cycles are nested within PDO phases, which alternate between positive (warm coastal water) and negative (cold coastal water) phases approximately every 20 to 30 years. ENSO oscillates between El Niño-like (warm SSTs and wetter conditions) and La Niña-like (cool SSTs and dry conditions) every two to seven years (Mantua et al., 1997; Lynn and Bograd, 2002; Mantua and Hare, 2002; Barron and Anderson, 2011).

To contextualize shell characteristics within 20th-century seawater temperature patterns throughout the study area, we accessed multiple sea surface temperature (SST) time series for sites along the southern CCS. We aimed to match the SST record and mussel collection years and locations as closely as possible, although sites along the Baja California peninsula did not have continuous SST monitoring available. In these cases, we used annual temperature data points from intertidal loggers and long-term trends from the literature (Sicard-González et al., 2012; IPCC, 2013; Helmuth et al., 2016). Specific SST record collection locations and durations are summarized in Table 2 and plotted along with mussel collection locations in Figure 1. Historic SST data were normally distributed and therefore analyzed with parametric linear

regression analysis, Welch two-sample t-tests, and the F-test of equality of variances using the programming language R.

We focus on the southern CCS due to its ecological and cultural value and its well-studied environmental history. The study area also offers extensive archives of *M. californianus* shells collected from southern California and the Baja California peninsula. In total, we accessed 130 specimens of *M. californianus* spanning every decade from the 1910s to 2010. One fossil Pleistocene specimen is included as an initial comparison. Aside from the Pleistocene sample, all of the mussels were originally live-collected from intertidal environments south of Point Conception from the California counties of Santa Barbara, Ventura, Los Angeles, Orange, and San Diego, and from the states of Baja California and Baja California Sur in Mexico (Figure 1; Table S1). Specimens were provided by the California Academy of Sciences, the University of California Museum of Paleontology, the Santa Barbara Museum of Natural History, the Natural History Museum of Los Angeles County, and researcher Elizabeth Bullard from Scripps Institute of Oceanography. Each shell had a known collection year and labeled locality (site name, latitude, and longitude). While the geographic range is somewhat broad (27.72°N to 34.47°N), this was necessary in order to obtain museum specimens from every single decade over a century. We restricted our range to include only the southern portion of the CCS, which is broadly governed by the same current patterns and periodic ocean modes (Checkley and Barth, 2009). In order to distinguish temporal trends from geographic patterns, we divided the study area into four sub-regions: (1) Santa Barbara and Ventura, (2) Greater Los Angeles, (3) San Diego and Baja California, and (4) Baja California Sur. We categorized each specimen by collection year, decade, sub-region, county, and locality. Shell characteristics were analyzed both temporally and spatially.

### 2.2 Shell morphology

One intact valve from each of the 130 individuals was selected for non-destructive morphological measurements. Whole valves with no remaining soft tissue and no or minimal epibionts were prioritized from museum collections. Digital calipers were used to measure shell dimensions to the nearest 0.1 mm. Shell length was measured from the umbo to commissure and shell width was measured at the widest distance from the dorsal to the ventral margin (Figure 2). The mass of each valve was measured to the nearest 0.1 g using an Acculab Precision Balance. A shell growth index was calculated for each specimen as the ratio between the log-transformed dry valve weight (g) and the log-transformed shell length (mm) (Grenier et al., 2020).

### 2.3 Optical microscopy

Fifty-one out of the 130 specimens were available for destructive analysis. In order to analyze mineralogical and microstructural shell characteristics, thin sections were prepared from these 51 specimens. Valves were cut longitudinally along the maximum growth trajectory (Figure 2) using a Buehler IsoMet saw equipped with a 0.3 mm diamond wafering blade. Cross sections were mounted to a glass slide and finely polished with colloidal alumina to a uniform thickness of 200 μm. All thin sections were examined and photographed using an Olympus BH2 microscope with an attached camera under both reflected and transmitted light. Using ImageJ software, the cross-sectional thickness of each shell was measured digitally at the thickest point adjacent to the umbo, where all mineralogical shell layers were present and dark-light growth banding was visible (Vriesman et al., 2022). Dark-light bands represent alternating periods of fast, calcite-rich growth (light bands) and slow, organic-rich growth (dark bands) (McCoy et al., 2011; Schöne and Surge, 2012; Killam and Clapham, 2018; Vriesman et al., 2022). Cross-sectional thicknesses were expressed relative to shell length and standardized in Excel.

Photomicrographs of each specimen were converted to 8-bit (grayscale) images in ImageJ in order to quantitatively analyze the growth band pattern in cross section. A transect perpendicular to the shell length was drawn through the dark-light growth banding in the inner shell layer. Gray values were obtained along this transect and exported to Excel in order to calculate the standardized gray-value variance for each specimen, used here as a proxy for the contrast between dark-light bands (Katayama and Isshiki, 2007; Vriesman et al., 2022). Light and dark bands were identified visually and supplemented with quantitative measurements; for each individual specimen, gray-value pixels above the mean were considered light bands and gray value pixels below the mean were considered dark bands. The percentage of light bands was estimated for each specimen by calculating the proportion of light bands out of the total banding: (total light band amount (mm) / total dark band + light band amount (mm) * 100 %)). Standardized gray-value variances and the percentages of light bands were compared among all 51 thin-sectioned specimens through time and across collection sites.

The Welch two-sample t-test, analysis of covariance (ANCOVA), and Tukey's HSD test were used to assess relationships between collection year, decade, sub-region, and standardized cross-sectional thickness per unit length since this shell characteristic was normally distributed. The non-parametric Kruskal-Wallis rank sum test was used to assess whether there were any significant changes in shell characteristics with non-normal distributions or measurements with values less than or equal to zero, such as the percentage of light bands and standardized gray-value variance. Shell characteristics with non-normal distributions and without negative values, such as dry valve weight and shell length, were log-transformed and then tested with a variety of regression analyses: multiple regression analysis (MRA), ordinary least squares regression (OLS), moving average analysis (MA), standardized major axis regression (SMA), and reduced

major axis regression (RMA). Geographic influences on shell shape (expressed as shell width/shell length) were evaluated using ANOVA. All statistical analyses were performed in R.

**2.4 SEM and EBSD analysis**

Three thin sections from the years 1913, 1956, and 2010 (n = 3 total) were chosen for microstructural analysis in order to determine whether crystal sizes and orientations have changed through time. Our methodology follows McCoy et al. (2018), which performed scanning electron microscopy with electron backscatter diffraction (SEM/EBSD) on *M. californianus* shells from Washington and found higher variability of calcite crystallographic orientations and smaller crystal sizes in shells collected in the 2010s despite consistent microstructural characteristics in shells from 2000 BP and the mid-20th century. McCoy et al. (2018) interpreted the sudden increase in crystallographic variability as evidence of calcification stress in response to acidifying conditions.

We performed EBSD on three *M. californianus* shells to determine whether southern specimens exhibit similar signs of calcification stress in response to warming and OA in the southern CCS. SEM/EBSD analyses were carried out on a Zeiss EVO-10 Variable Vacuum SEM in the Department of Earth and Planetary Science at UC Berkeley. SEM imaging was used to navigate towards the middle of the inner calcite layer adjacent to the shell's umbo to match the EBSD scanning sites for all three shells. Each finely polished thin section was analyzed under low-vacuum mode with a 70° stage tilt to optimize Kikuchi patterns produced by biogenic calcium carbonate crystals (Pérez-Huerta and Cusack, 2009). Prior to each EBSD scan, the diffraction patterns were indexed for both calcite and aragonite using OIM Analysis software from EDAX to confirm that the confidence index (CI) was near 0.1, indicating high accuracy for crystallographic orientation data of each indexed mineral. The electron probe was operated at 10

nA and the electron high tension (EHT) was set to 20 kV. Each scan is a 500 x 500 μm square grid imaged at ~ 200x magnification. Crystal size maps and crystallographic orientation maps were produced using OIM Analysis software. Adobe Illustrator was used to overlay crystallographic orientation maps over semi-transparent crystal boundary maps for each specimen to examine multiple microstructural properties at once. EBSD scans were compared to one another to identify differences in crystal size and orientations between 1913, 1956, and 2010.

## 3 Results

### 3.1 Study area warming trends

Coastal SST measurements from the past century highlight nearshore surface warming in the southern portion of the CCS. Linear regression analysis of each daily SST time series revealed significant increases in temperature over time for all locations with continuous data: (1) La Jolla SST; Linear regression: $R^2 = .03$, $F_{1,37046} = 1033$, $p < .000$, (2) Newport Beach SST; Linear regression: $R^2 = .004$, $F_{1,34026} = 131.9$, $p < .000$, (3) Santa Barbara SST; Linear regression: $R^2 = .01$, $F_{1,19933} = 242.6$, $p < .000$, (4) Point Dume SST; Linear regression: $R^2 = .001$, $F_{1,22347} = 17.39$, $p < .000$, (5) San Clemente SST; Linear regression, $R^2 = .03$, $F_{1,1984} = 531$, $p < .000$, (6) Station 46054 (Santa Barbara Basin) SST; Linear regression: $R^2 = .01$, $F_{1,2068} = 18.84$, $p < .000$). We plotted the five-year or one-year running mean for each SST dataset, depending on the length of the record, along with the regression line for the longest record (La Jolla, 1916 through present) to examine long-term warming and sub-decadal trends over the past century (Figure 3).

All five long-term records originating in 1965 or earlier have significantly higher mean temperatures since 1970 (Table 3): (1) La Jolla SST; Welch two-sample t-test: $t = 26.753$, $df = 3672$, $p < .000$, (2) Newport Beach SST; Welch two-sample t-test: $t = 7.4593$, df 7153.2, $p <$

.000, (3) Santa Barbara SST; Welch two-sample t-test: t = 11.712, df = 9481.2, p < .000), (4) Point Dume SST; Welch two-sample t-test: t = 7.4593, df = 7153.2, p < 0.000, and (5) San Clemente SST; Welch two-sample t-test: t = 4.278, df = 1995.2, p < 0.000. There were also statistically significant increases in daily temperature variance since 1970 at all long-term monitoring sites: (1) La Jolla SST; F-test: F = 1.079, $df_{num}$ = 18018, $df_{denom}$ = 19029, p < .000, (2) Newport Beach SST; F-test: F = 1.21, $df_{num}$ = 18166, $df_{denom}$ = 15861, p < .000, (3) Santa Barbara SST; F-test: F = 1.2661, $df_{num}$ = 14961, $df_{denom}$ = 4973, p < 0.000), (4) Point Dume SST; F-test: F = 1.3028, $df_{num}$ = 18074, $df_{denom}$ = 4274, p < .000, and (5) San Clemente SST; F-test: F = 1.126, $df_{num}$ = 17845, $df_{denom}$ = 1640, p = 0.001.

While there were no continuous time series temperature data available for the Baja California peninsula, SST monitoring and reconstructions estimate that coastal SST off of Baja California (27.5 N, 117.5 W) is 1.1°C warmer since the year 1901 (IPCC, 2013). We found recent annual SSTs measured by intertidal sensors for the Baja California peninsula (Sicard-González et al., 2012; Helmuth et al., 2016) to contextualize average temperatures for this region with the southern California SST time series (Figure 3).

**3.2 Shell characteristics: temporal patterns**

Non-destructive morphological measurements (n = 130 specimens) revealed that shell morphology did not change significantly over time. Multiple regression analysis of log-transformed shell length and width ratios found that shell width grows proportionally to shell length (slope = 0.91), but found no significant change in shell morphology since 1913 (Figure 4; Multiple regression analysis using Year and Sub-Region as factors, x = log(Length), y = log(Width): $F_{5,123}$ = 533.9, p < .000). The coefficients of multiple regression analysis are presented in Table S2. When sorted by decade, RMA regression analysis revealed highly

consistent slopes (width to length ratios) through time as long as each decade had a sample size larger than two individuals (Table S3). RMA analysis and all other regression analysis methods found shell width to length relationships with slopes close to 0.9, revealing proportional growth as the mussel ages and through time (Table 4, Figure S4).

Destructive analyses (n = 51 specimens) found that other quantitative shell characteristics did not change significantly through time (Figure 5). There was no statistically significant relationship between standardized cross-sectional thickness (measured at the thickest point adjacent to the umbo) per shell length and decade or sub-region (Kruskal-Wallis rank sum test: $p > 0.8$ for each decade and $p > 0.5$ for each sub-region). There was also no significant change in the percentage of light bands through time (Kruskal-Wallis rank sum test: $p = 0.39$ with Year as the factor; $p = 0.51$ with Decade as the factor). Lastly, the standardized gray-value variance did not change significantly over time (Kruskal-Wallis rank sum test: $p = 0.93$ with Year as the factor; $p = 0.78$ with Decade as the factor). Shell characteristics for each decade are summarized in Table 5.

Comparing photomicrographs of each thin section (n = 51) revealed no visually apparent changes in mineralogical layering through time (Figure 6). All specimens, including the Pleistocene shell (Figure S6), contained an inner prismatic calcite layer, a middle layer of aragonite, and an outer layer of calcite.

**3.3 Shell characteristics: geographic patterns**

Non-destructive morphological measurements (n = 130 specimens) found limited differences between shells collected from different sub-regions within the study area. There was a statistically significant difference in shell morphology through time as measured by log(width)/log(length) for two of the sub-regions in the study area ((1) Greater Los Angeles ($p =$

.048) and (2) San Diego and Baja California (p = 0.002), Multiple linear regression; Table S2, Figure S5).

Linear regression on shell growth indices (log(Mass (g))/log(Length (mm))) displayed an extremely slight negative trend through time (slope = -0.001382), although this was not statistically significant, nor did the growth indices vary significantly across sub-regions (p = 0.2; Figure 7). Shell growth indices are quite variable through time, but the late 1970s was a period with high growth indices for shells from all four sub-regions (Figure 7).

There was a statistically significant relationship between sub-region and shell shape when the temporal component was excluded from analyses (ANOVA: shell width/length with sub-region as the only factor, p = 0.0033). Shells from San Diego and Baja California had higher width to length ratios than shells from Santa Barbara and Ventura (Tukey HSD: p = 0.03) and shells from Baja California Sur had lower width to length ratios than shells from San Diego and Baja California (Tukey HSD: p = 0.04).

Destructive analyses (n = 51 specimens) found no further statistical difference between shell characteristics related to sub-region. Standardized cross-sectional thickness per shell length was not significantly different across sub-regions (ANOVA: p > 0.285). Similarly, the percentage of light bands and the standardized gray-value variance did not vary statistically throughout the study area (Kruskal-Wallis rank sum test: percentage of light bands, p = 0.133; standardized gray-value variance, p = 0.43). Shell characteristics for each sub-region are summarized in Table 6.

**3.4 Microstructural data (SEM/EBSD)**

EBSD scans of shells from 1913, 1956, and 2010 offer insight into crystallographic properties at the beginning, middle, and end of the 100-year study period. EBSD maps revealed

the crystallographic orientations, crystal size, and microstructural organization within the inner calcite layer of the three *M. californianus* specimens (Figure 8).

Mineralogic indexing in OIM Analysis software confirmed that EBSD scanning was performed within the inner calcite shell layer. The 1913 shell contained extremely well-organized microstructure; the elongate calcite crystals were very similar in size (Figure 8A) and form fan-like blades characteristic of biogenic calcite. Darker areas in the crystallographic map represent the absence of crystal backscatter in the dark, organic-rich, slow-growth bands. There is some variability in crystallographic orientation (Figure 8A) despite highly uniform crystal sizes. The 1956 shell also contained large, highly similar crystal sizes throughout the scan and crystallographic orientations were quite uniform (Figure 8B). The 2010 shell contained a greater variety of crystallographic orientations, more variability in crystal sizes, and smaller calcite crystals (Figure 8C).

**4 Discussion**

All long-term (pre-1965) continuous temperature records in southern California revealed significant overall warming since the start of each time series (Figure 3). Temperatures in the southern CCS have become warmer and more variable, aligning with both regional and global increases in the intensity and frequency of marine heatwaves over the past century (Oliver et al., 2018; Fumo et al., 2020). The plotted SST records are generally synchronous and covary over sub-decadal to decadal scales (Figure 3). Decadal variability is largely explained by the PDO, which accounts for up to 44% of temperature variability throughout the CCS, so high covariance across southern CCS SSTs was expected (Field et al., 2006). La Jolla experienced the warmest conditions throughout the record (mean of 17.23°C), while Santa Barbara, Point Dume, and Station 46054 (offshore in the Santa Barbara Basin) recorded the lowest temperatures for this

region (means of 15.93°C, 15.77°C, and 13.98°C, respectively). While all coastal records are closely aligned throughout the 20th century, there are two major periods where records diverge; firstly, there is a brief and abrupt gap between La Jolla and Newport Beach temperatures in 1950 after ~ 25 years of similar SSTs with strong covariance. Secondly, Point Dume and Santa Barbara experienced cooling in the early 2000s, while all other locations were warming. Since 2011, all long-term records show accelerated warming trends (0.13°C per year on average). Although Santa Barbara is the northernmost SST record, conditions at this location are warmer than Point Dume, which is ~ 100 km south of Santa Barbara. Conditions at Point Dume might appear cooler than Santa Barbara due to different collection methodologies by the Shore Stations Program between these two sites, or micro-differences related to coastline geometry. At Point Dume, daily SSTs were measured slightly offshore, west of the beach, to avoid capturing the effects of solar warming at the shoreline, while Santa Barbara temperatures were taken within the western end of the Santa Barbara Harbor. All continuous coastal SST records used here except for Point Dume were measured from piers or harbors. Seemingly cooler Point Dume waters may be a product of the collection location rather than a coastal oceanographic anomaly at this site.

The 1970s is considered a significant transitional period for the CCS both oceanographically and ecologically (McGowan et al., 2003; Field et al., 2006). There were significant differences between pre-1970 and post-1970 temperature patterns in all continuous, long-term records (Table 3). La Jolla, Newport Beach, Santa Barbara, Point Dume, and San Clemente all experienced higher mean SSTs and greater daily SST variability after the year 1970. Rising mean SSTs and more frequent event-scale processes, such as El Niño periods and positive-phase PDOs, can be major stressors to marine organisms (Oliver et al., 2018). Both

aerial and marine heat extremes can lead to severe metabolic stress and major die-offs in intertidal species in particular, including *M. californianus*. When low tide coincides with high aerial temperatures, intertidal organisms can experience desiccation, growth shutdown, and even mortality (Soon and Zheng, 2020). For example, *M. californianus* individuals growing in Bodega Bay in northern California responded to thermal stress during an extreme summer heatwave in July 2019 by slowing their growth rates and precipitating organic-rich dark bands instead of the light, calcite-rich bands that grow during moderate and stable temperature conditions (Vriesman et al., 2022). For this reason, we predicted that a regime shift towards significantly warmer conditions in the southern CCS would result in a marked shift in calcification patterns in *M. californianus*; we expected to find thinner shells per unit length and a lowered percentage of calcite-rich light banding in response to higher temperatures and estimated lower pH conditions in the southern CCS. However, the *M. californianus* samples analyzed here showed signs of remarkably stable or even elevated calcification (e.g., high shell growth indices in the 1970s).

None of the quantitative shell characteristics measured here, including shell morphology (Figure 4), cross-sectional thickness per shell length (Figure 5A), percentage of light bands (Figure 5B), gray-value variance (Figure 5C), and shell growth index (Figure 7) changed statistically significantly through time. Unlike *M. californianus* shells from Washington and northern California, mussels growing in the southern CCS exhibited biomineralogical consistency throughout the 20th century (Pfister et al., 2016; McCoy et al., 2018; Vriesman et al., 2022). Our results show that shell layering was visually consistent through time (Figure 6), with the prismatic inner calcite layer present in all 51 thin-sectioned samples. The inner calcite layer was present in archaeological *M. californianus* specimens from Washington dated to 2500 BP (Pfister et al., 2016), and here we found that the inner calcite layer is also present in a fossil

specimen of *M. californianus* (Figure S6). This species is the only *Mytilus* species to lay down an inner layer of calcite (Dodd, 1964; McCoy et al., 2018; Vriesman et al., 2022), so the evolutionary history and function of this additional layer is enigmatic. A previous study suggested that perhaps *M. californianus* began to precipitate a secondary calcite layer as a compensatory mechanism following the emergence of low-pH conditions driven by the seasonal upwelling regime within the CCS (McCoy et al., 2018), but the presence of this layer in a Pleistocene-aged *M. californianus* shell indicates that its shell structure predates the development of seasonal upwelling cycles in the CCS approximately 3500 years ago (Barron and Bukry, 2007).

Shell morphology was quantified by comparing log(shell width)/log(shell length) ratios in our samples; a high log(shell width)/log(shell length) ratio indicates a wider, shorter shell, while a low log(shell width)/log(shell length) ratio indicates a long, narrow shell. For a bivalve mollusc species, different shell shapes can have varying ecological implications (Johnson, 2020). For example, elongated valves with a longer ventral margin offer increased surface area for a mussel's benthic life mode, allowing *M. californianus* to attach itself more easily to rocky substrate along its ventral margin. *Mytilus californianus* also has very thick shells relative to other marine mussels, which provides protection from both shell-crushing predators and intense wave activity in the dynamic intertidal zone. The trade-off is that thick, heavy shells can inhibit locomotion, so *M. californianus* is relatively stationary once it is attached to substrate with its strong byssal threads (Harrington and Waite, 2007). If present, decadal variability or long-term changes in shell shape and size would have substantial ecological consequences for *M. californianus*, but shell morphology as measured here remained the same throughout the study period when all specimens were analyzed overall. There were, however, statistical differences in

shell morphology through time depending on sub-region; shells from Greater Los Angeles (n = 38, p = 0.048) and San Diego and Baja California (n = 68, p = 0.002) appeared to vary through time, while shells from the Santa Barbara and Ventura and Baja California Sur sub-regions did not change through time. When the temporal component is removed, there are statistically significant differences in shell morphology between shells collected from the two most distal sub-regions ((1) San Diego and Baja California and (2) Santa Barbara and Ventura) as well as between the two portions of the Baja California peninsula (Baja California and Baja California Sur). However, due to the limited numbers of museum specimens from Baja California Sur available (n = 5), it is possible that the morphological differences in shells from Baja California Sur are simply a product of uneven sampling distribution across sub-regions. Geographic differences had a stronger influence on shell shape than collection year or decade, but no other shell characteristic was significantly related to its collection sub-region. Site-specific studies of shell morphology through time with high sample sizes would help corroborate whether or not the two statistically significant geographic differences in shell shape are genuine trends, although it is challenging to access large numbers of museum specimens collected from a single locality.

Shell growth indices were quite variable through time and displayed no trends, except for markedly high shell growth indices for shells from all four sub-regions in the late 1970s (Figure 7), coeval with a warm shift in the CCS (Field et al., 2006). High growth indices are indicative of heavier, thicker shells per unit length (g $mm^{-1}$), so southern populations of *M. californianus* may have built more shell material during this period of rapid and substantial warming (Figures 3, 7). The relationship between elevated shell growth indices and high 1970s temperatures is different from documented shell growth-SST relationships for *M. californianus* in northern California, which preferentially grow their shell during moderately cool SST conditions, or during months

with mean temperatures near ~ 13 °C (Vriesman et al., 2022). However, southern California mussels have been reported to grow most rapidly in much warmer conditions (15 to 19°C) (Smith et al., 2009), indicating a regional or populational adaptation to different local conditions (e.g., temperature). Our results suggest a positive relationship between faster growth and higher temperatures for southern populations of *M. californianus* as long as temperatures do not exceed their thermal calcification threshold (~ 26°C) (Bayne et al., 1976).

Although 1970s warming aligned with a window of high shell growth indices, we saw no long-term trend indicating that mussel shell growth had increased as warming has progressed through time in the CCS. In our samples, standardized cross-sectional thickness per shell length, an indicator of overall shell thickness, did not increase or decrease through time (Figure 5A). Consistent shell thickness throughout the 20th century is in contrast to recent shell thinning and declining inner calcite layers in northern California and Washington specimens (Pfister et al., 2016; Vriesman et al., 2022), which is an additional line of evidence for a regional distinction in shell growth patterns. We suggest that there is a transitional zone between cool-water acclimated northern mussel populations and warm-water acclimated southern mussel populations, leading to dissimilar shell growth rates, ranges of optimal growth, and perhaps other life-history traits recorded in the shell. While this has not been tested for *M. californianus* shell growth, it is possible that the zone north of Monterey Bay is the boundary separating northern growth trends (cooler SSTs-faster growth) and southern growth trends (warm SSTs-faster growth) since this is an ecological boundary that demarcates biogeographic ranges of warm-water and cool-water taxa within the CCS (Sanford et al., 2019). This ecological transition zone could also be a calcification transition zone for a calcifying species that lives throughout multiple portions of the CCS.

In addition to shell morphology, shell structure, and shell thickness, the growth band pattern is also unchanged through time (Figure 5B, C). We quantified growth banding by calculating the percentage of light bands and measuring the standardized gray-value variance through a cross-sectional transect of dark-light banding near the umbo of every thin section (n = 51). We interpret the percentage of light bands as an indicator of how much time each individual spent growing normally (e.g., light bands represent fast, calcite-rich growth) (Schöne and Surge, 2012). The standardized gray-value variance is a quantitative indicator of growth band contrast; low gray-value variance implies very little difference between dark and light bands (e.g., poorly expressed or cloudy bands), while high gray-value variance implies greater differences between dark and light bands (e.g., strongly expressed, visually distinct bands). Together, these parameters (1) indicate whether a *M. californianus* individual is alternating between dark and light increments and (2) represent the amount of time the mussel spent calcifying normally versus slowly. While there is not yet an established baseline for the percentage of light bands in a shell precipitated by a typical *M. californianus* individual, the mean percentage of light bands in the specimens analyzed here (45%, n = 51) was strikingly similar to the mean percentage of light bands in 21st century *M. californianus* shells from Bodega Bay (43%, n = 40; Vriesman et al., 2022) despite the geographic and temporal differences between the two studies. The low percentage of light banding (< 50%) indicates that mussels – regardless of their length and ontogenetic age – have spent more of their lives growing slowly throughout the CCS for at least 120 years. Slow shell growth rates as inferred by low percentages of light banding may even be an evolutionary characteristic of this species since the single Pleistocene specimen analyzed here had 43% light bands. In addition to consistent light band percentages through space and time, we also found consistent contrast (standardized gray-value variance) between dark and light bands

throughout our specimens (Figure 5C), indicating that the growth band expression is not weakening through time in southern mussels. Growth bands are generally poorly expressed but visually apparent (see Figure 6 for representative examples of dark-light banding).

EBSD data from three shells collected in 1913, 1956, and 2010 indicate that microstructural characteristics are not as uniform through time as the quantitative shell characteristics measured here. Although shell morphology, shell structure, and the growth band pattern were consistent throughout the 20th century, qualitative EBSD data revealed greater crystallographic variability in 2010 than in 1913 and 1956 (Figure 8). The most recent shell (2010, San Diego) exhibited the widest variety of crystal sizes (Figure 8C), while the earliest non-Pleistocene shell in our study (1913, La Jolla) showed highly similar crystal sizes. All three shells showed some variability in crystallographic orientations, as was expected in biogenic calcite (McCoy et al., 2018). A previous study of *M. californianus* shells collected in Washington, USA also found a shift in microstructural properties, although only after ~ 2000 years of highly consistent microstructural patterns; shells from 2000 BP, the 1970s, and the early 2000s were similarly organized, and the microstructural shift did not appear until the 2010s (McCoy et al., 2018). Similarly, our results point to a potential shift in microstructural properties in the 2010s, although further EBSD analysis of a larger sample size of 20th- and 21st-century shells is required to confirm the timing and extent of the microstructural shift, if present at all. If crystallographic control has indeed declined in southern *M. californianus* shells, it is unclear whether this is a deleterious effect or an adaptive coping mechanism; reducing control of crystallography could be a sign of hindered calcification (vulnerability response), or it could be a way to calcify more quickly in response to changing temperature and/or pH conditions (compensatory response). Additionally, if shell thickness and mineralogy are maintained as

documented here, it is unknown if a shift in microstructural properties will have significant implications for *M. californianus*' life history and the ecosystems it supports, although it is likely that reduced crystallographic control could make *Mytilus* species more vulnerable to changing environments and increased predation pressure (Fitzer et al., 2014; 2016).

Although we found preliminary evidence for reduced crystallographic control through time, the majority of *M. californianus* shell characteristics analyzed here suggests that there are no significant changes in shell morphology, thickness, or growth band patterning during the 20th century within the southern portion of the CCS. While our results may differ from the declining calcification patterns identified by some previous studies on *M. californianus* (Table 1), our findings are consistent with other documented signs of stability and resilience in *M. californianus* itself, within the *Mytilus* genus, and across other marine calcifying taxa in temperate regions. For example, *M. californianus* shells collected at multiple sites along the California coast in 2017 and 2018 had significantly higher proportions of bulk shell calcite than shells collected from these same sites in 1958 through 1960 (Bullard et al., 2021). Similarly, the blue mussel *M. edulis* in coastal Belgium increased its calcification by precipitating thicker shell layers (both outer prismatic calcite and inner nacreous aragonite) over the past 120 years, despite long-term decreases in dissolved oxygen and elevated mean SSTs and summer maximum SSTs during this period (Telesca et al., 2021). In the brachiopod *Calloria inconspicua* from New Zealand, the vast majority of shell characteristics, including shell morphology, shell thickness, and shell elemental composition, were constant over the past 120 years despite ocean warming and higher $pCO_2$ through time at the study area (Cross et al., 2018).

Experimental studies, historical analyses, and meta-analyses confirm that marine calcifying taxa respond to changing environmental conditions differently depending on a variety

of factors ranging from genetics to geography (e.g., Kroeker et al., 2010; 2013). Our results further demonstrate that calcification responses can vary widely even within a single species, depending on the local oceanography and the rate of warming or OA in relation to baseline conditions for the region. For example, due to wind stress, coastline morphology, and upwelling patterns, the southern CCS experiences warmer waters than northern California and Washington, so southern populations of *M. californianus* may be less sensitive to anthropogenic warming, and therefore, calcification mechanisms and shell characteristics have remained stable. Similarly, mussel populations growing in intense upwelling regimes in northern California may be more acclimated to acidifying conditions, since upwelling-induced low pH is a natural seasonally-occurring phenomenon in this region. Local, population-specific acclimatization would also explain the OA-related shell thinning and heightened crystallographic disorder found in Washington *M. californianus* shells; Tatoosh Island and Sand Point, Washington (48°N) experience significantly less upwelling relative to the central portion of the CCS (~ 38°N), so Washington mussels were perhaps poorly adapted to low pH and more susceptible to long-term, anthropogenic OA trends (Pfister et al., 2011; 2016; Logan et al., 2012; Jacox et al., 2018; McCoy et al, 2018; Vriesman et al., 2022).

Assessing resilience or vulnerability to current and pending environmental changes is not only a species-specific concern; it is also dependent upon the specific locality and the population. Conspecific populations at different localities can have highly different calcification patterns. Further, high variability among our results alone suggests that factors not analyzed here, including micro-habitat (e.g., tidal position, thickness of mussel bed) and ontogenetic age may also influence responses to a changing climate across a population. For example, growth reduction has been tied to both ontogenetic processes and tidal height for *M. californianus* (Ford

et al., 2010; Connor and Robles, 2015; Jazwa et al., 2020). Variability induced by micro-scale biological and spatial conditions (e.g., ontogeny, tidal position) may dominate over broader, long-term trends when examining site- and population-specific calcification patterns. Across our suite of samples, we found no compelling evidence for shifting shell characteristics (either reduction or increases) due to collection year, decade, or site. However, such trends may emerge if we were able to analyze the same shell characteristics in a suite of ideal samples with known and uniform ontogenetic ages and tidal positions through time, although this is not necessarily feasible with existing museum collections.

## 5 Conclusions

Using museum collections of *M. californianus*, we found minimal evidence of shifting calcification patterns (neither increasing nor decreasing) in this species despite significant warming in the southern CCS over the 20th century. The majority of shell characteristics, particularly shell morphology, growth index (valve mass per shell length), valve cross-sectional thickness, percentage of light bands, and gray-value variance remained stable through time and across sites within the southern CCS. Shell layering was visually consistent (inner calcite, middle aragonite, outer calcite) throughout all shells, including the Pleistocene specimen. We interpret the unchanging shell characteristics as evidence for calcification persistence among the warm-water acclimated mussels in this region. However, qualitative microstructural analysis showed an increase in crystallographic disorder from 1913 and 1956 to 2010, although further analysis is required in order to confirm (1) whether a 2010s microstructural shift indeed occurred and (2) whether this microstructural shift is detrimental to *M. californianus* and the ecosystem it supports.

We encourage further investigations of temporal patterns in other regions of the CCS since mussels growing farther north may not be similarly adapted for warming conditions. Similarly, mussels that do not commonly experience naturally low-pH conditions (e.g., upwelling seasons) may be poorly adapted to anthropogenic OA conditions. *Mytilus californianus* is a critical foundation species that dominates intertidal zones throughout an expansive and oceanographically diverse coastline; understanding the ways in which its individuals and populations will respond to climate change across a variety of spatial and temporal scales is valuable for the hundreds of species that rely on *M. californianus* for habitat and protection, and consequently, the ecosystems and human communities that interact with and depend upon coastal environments. Beyond assessing collective responses to the impacts of climate change across marine calcifying taxa in laboratory and field settings, we encourage the application and synthesis of multi-scaled investigations (e.g., individual through population, annual through centennial, etc.) to quantify the history of calcification patterns in culturally, economically, and ecologically significant species.

**6 Acknowledgements**

We accessed seawater temperature data from the Shore Stations Program with current funding provided by the California Department of Parks and Recreation, Division of Boating and Waterways, Award #C1670003. Data are collected by staff aquarists and volunteers with the Birch Aquarium at Scripps. We thank Dr. Sara Hamilton of the Ocean Climate Lab for facilitating access to Shore Stations sea surface temperature data. Seawater temperature data were accessed from the National Oceanic and Atmospheric Administration's National Data Buoy Center Station 46054, owned and maintained by National Data Buoy Center 34.274 N 120.468 W (34°16'26" N 120°28'5" W). We are grateful to the following individuals and institutions for

providing mussel shells for this study: Invertebrate Zoology Senior Curatorial Assistant Elizabeth Kools at California Academy of Sciences, Senior Museum Scientist of Invertebrates Dr. Ashley Dineen at the UC Museum of Paleontology, Malacology Collections Manager Lindsey Groves at the Natural History Museum of Los Angeles County, Invertebrate Zoology Collection Manager Vanessa Delnavaz at the Santa Barbara Museum of Natural History, and PhD student Elizabeth Bullard from UC San Diego. Thin sections were prepared by Greg Baxter. Lupe Carrasco and Sebastian Westerink helped with photomicrograph scaling in ImageJ. SEM/EBSD analyses were performed with the assistance of John Grimsich at UC Berkeley. This research was supported by the Cordell Durrell Field Geology Fund (to Veronica Padilla Vriesman) and the National Science Foundation (nos. OCE 1832812 to Tessa M. Hill and 2036201 to Veronica Padilla Vriesman).

## Tables

**Table 1.** Summary of findings from published literature on calcification patterns of *M. californianus.*

| Reference | Location | Sample ages | Finding | Interpretation |
|---|---|---|---|---|
| Gaylord et al. (2011) | Bodega Marine Laboratory, California, USA | NA | Larvae growing in high $pCO_2$ conditions resulted in smaller, thinner, weaker juvenile shells | Projected reduction in calcification |
| Pfister et al. (2016); McCoy et al. (2018) | Washington, USA | 2000 BP, 1970s, 2010s | Thinner shells overall and relative to length in 2010s compared to 2000 BP and 1970s; increased crystallographic disorder in 2010s compared to 2000 BP and 1970s | Recent reduction in calcification |
| Bullard et al. (2021) | La Jolla, Corona del Mar, Avila Beach, California, USA | 1958, 1960, 2017, 2018 | Increased shell calcite precipitated relative to shell aragonite | Recent shift in calcification |
| Vriesman et al. (2022) | Bodega Bay, California, USA | 2002, 2003, 2019, 2020 | Thinner inner calcite layers and cross-sectional thicknesses relative to shell length, lowered contrast between dark-light growth bands in 2019-2020 relative to early 2000s | Recent reduction in calcification |

**Table 2.** Summary of continuous sea surface temperature record locations and durations for the study area. This table excludes annual SST data and long-term trends from Baja California and Baja California Sur since these are not continuous records. Historic SST records were accessed from the University of California, San Diego Scripps Institute of Oceanography Shore Stations Program (available at https://shorestations.ucsd.edu/, last accessed 27 April 2022) and the National Oceanic and Atmospheric Administration's National Data Buoy Center (available at https://www.ndbc.noaa.gov/, last accessed 27 April 2022).

| Record Name | Location | Record Length | Latitude | Longitude |
|---|---|---|---|---|
| SIO - Scripps Pier | La Jolla (San Diego) | 1916-2020 | 32.866198 | -117.254211 |
| San Clemente | San Clemente | 1965-2020 | 33.416193 | -117.618155 |
| San Clemente | Newport Beach | 1924-2020 | 33.607255 | -117.929179 |
| Point Dume | Point Dume | 1957-2021 | 34.017639 | -118.826212 |
| Santa Barbara | Santa Barbara | 1955-2020 | 34.402714 | -119.692695 |
| Station 46054 | Santa Barbara Basin | 2000-2005 | 34.272883 | -120.470103 |

**Table 3.** Summary statistics of each multi-year SST record in the study area. Table is ordered by the length of the record. All long-term records contain statistically significant increases in mean SST since 1970 ($p < .000$).

| Location | Record Length | Min (°C) | Max (°C) | Mean (°C) | σ | Pre-1970 Mean (°C) | Post-1970 Mean (°C) |
|---|---|---|---|---|---|---|---|
| La Jolla (San Diego) | 1916-2021 | 10.1 | 26.4 | 17.23 | 2.7 | 16.9 | 17.64 |
| Newport Beach | 1924-2020 | 9.9 | 25.2 | 16.5 | 2.4 | 16.4 | 16.6 |
| Santa Barbara | 1955-2020 | 9.9 | 23.4 | 15.93 | 2.3 | 15.63 | 16.04 |
| Point Dume | 1956-2020 | 8.9 | 23.9 | 15.77 | 2.3 | 15.56 | 15.82 |
| San Clemente | 1965-2020 | 9.8 | 26.2 | 17.14 | 2.6 | 16.89 | 17.12 |
| Santa Barbara Basin | 2000-2005 | 9.97 | 20.85 | 13.98 | 1.72 | NA | NA |

**Table 4.** Results from all regression analysis methods: ordinary least squares (OLS), moving average (MA), standardized major axis (SMA), and reduced major axis (RMA).

| Method | y-intercept (*b*) | slope (m) | Angle (degrees) |
|---|---|---|---|
| OLS | -0.373 | 0.905 | 42.146 |
| MA | -0.457 | 0.926 | 42.809 |
| SMA | -0.464 | 0.928 | 42.863 |
| RMA | -0.478 | 0.932 | 42.969 |

**Table 5.** Summary statistics of destructive analyses for each quantitative shell characteristic sorted by decade. Mean denoted with $\bar{x}$ and standard deviation denoted with σ. Shell growth index is log(valve mass (g))/log(shell length (mm)).

| Decade | *n* (whole valves) | $\bar{x}$ shell growth index | σ shell growth index | *n* (thin sections) | $\bar{x}$ std. cross-sectional thickness per length | σ std. cross-sectional thickness per length | $\bar{x}$ std. gray-value variance | σ std. gray-value variance | $\bar{x}$ portion of light bands | σ portion of light bands |
|---|---|---|---|---|---|---|---|---|---|---|
| 1910 | 2 | 0.38 | 0.1 | 1 | 1.43 | NA | 0.3 | NA | 0.55 | NA |
| 1920 | 9 | 0.41 | 0.17 | 3 | -0.5 | 0.62 | -0.19 | 0.62 | 0.46 | 0.09 |
| 1930 | 9 | 0.3 | 0.19 | 3 | 0.03 | 0.58 | -0.68 | 0.3 | 0.46 | 0.02 |
| 1940 | 2 | 0.29 | 0.06 | 1 | -0.88 | NA | -0.46 | NA | 0.48 | NA |
| 1950 | 13 | 0.34 | 0.39 | 7 | -0.13 | 1.01 | -0.03 | 1.04 | 0.49 | 0.06 |
| 1960 | 16 | 0.2 | 0.39 | 4 | 0.04 | 0.33 | -0.41 | 0.3 | 0.42 | 0.06 |
| 1970 | 27 | 0.2 | 0.19 | 3 | 0.34 | 2.27 | 0.4 | 0.31 | 0.53 | 0.1 |
| 1980 | 4 | 0.63 | 0.39 | 2 | -0.07 | 0.33 | -0.73 | 0.95 | 0.52 | 0.12 |
| 1990 | 6 | 0.29 | 0.28 | 5 | -0.02 | 1.97 | 0.002 | 1.05 | 0.43 | 0.07 |
| 2000 | 7 | 0.27 | 0.15 | 2 | 0.17 | 0.14 | -0.43 | 0.65 | 0.42 | 0.05 |
| 2010 | 34 | 0.22 | 0.35 | 19 | 0.08 | 0.77 | 0.24 | 1.28 | 0.42 | 0.11 |
| Pleistocene | 1 | 0.25 | NA | 1 | -0.88 | NA | 1.13 | NA | 0.43 | NA |

**Table 6.** Summary statistics of destructive analyses for each quantitative shell characteristic sorted by sub-region. Mean denoted with $\bar{x}$ and standard deviation denoted with σ.

| Sub-region | *n* (whole valves) | $\bar{x}$ shell growth index | σ shell growth index | *n* (thin sections) | $\bar{x}$ std. cross-sectional thickness per length | σ std. cross-sectional thickness per length | $\bar{x}$ std. gray-value variance | σ std. gray-value variance | $\bar{x}$ portion of light bands | σ portion of light bands |
|---|---|---|---|---|---|---|---|---|---|---|
| Santa Barbara and Ventura | 19 | 0.47 | 0.32 | 6 | 0.41 | 0.85 | -0.46 | 0.59 | 0.44 | 0.09 |
| Greater Los Angeles | 38 | 0.28 | 0.37 | 16 | -0.42 | 0.64 | -0.12 | 0.86 | 0.44 | 0.12 |
| San Diego and Baja California | 68 | 0.37 | 0.3 | 27 | 0.21 | 1.06 | 0.13 | 1.15 | 0.44 | 0.07 |
| Baja California Sur | 5 | 0.48 | 0.3 | 2 | -0.53 | 2.39 | 0.56 | 0.13 | 0.58 | 0.03 |

**Figures**

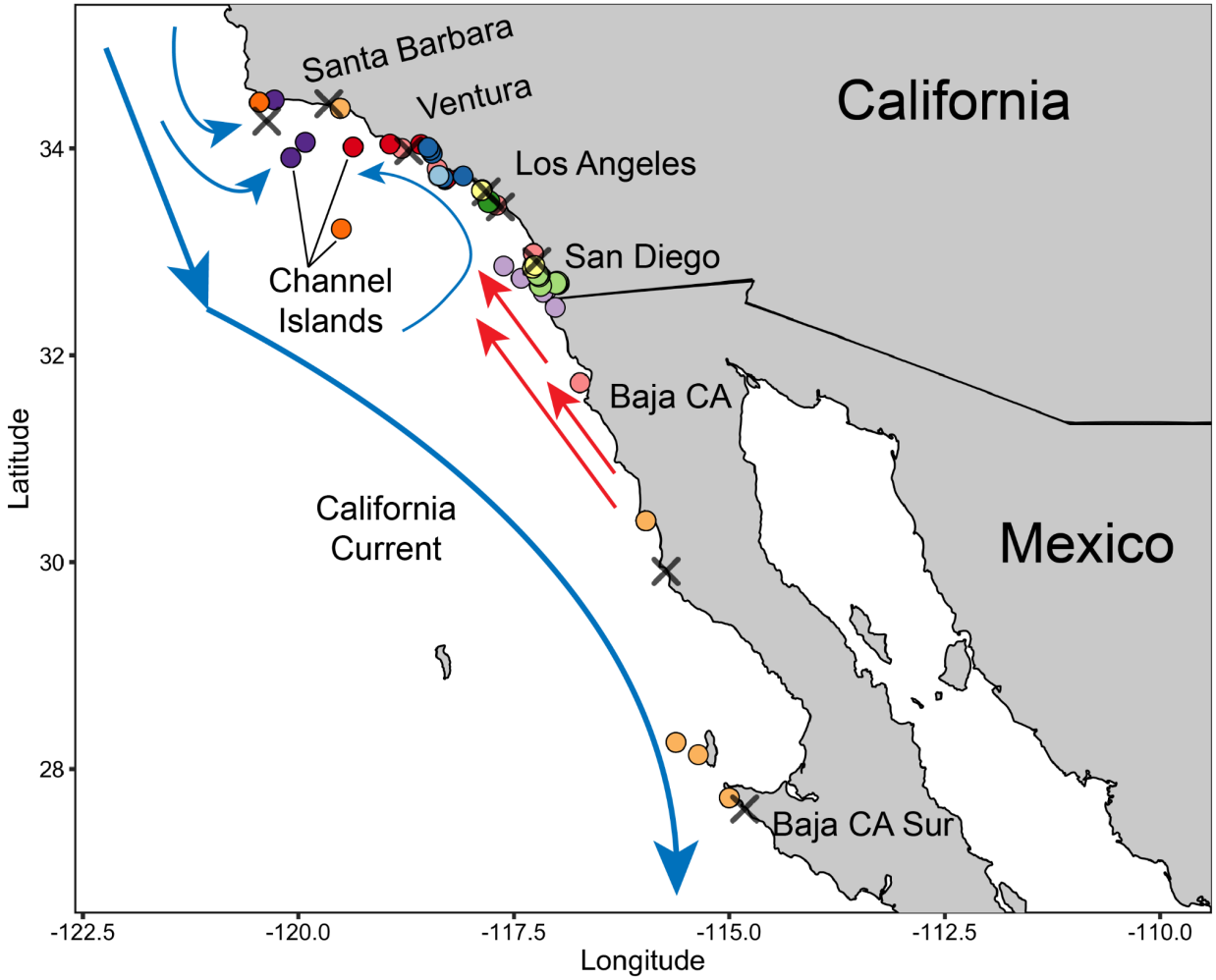


**Figure 1.** Map of *M. californianus* collection locations within the southern portion of the California Current System. The California Current (large blue arrow) flows southward along the coastline. The curved blue arrows represent the Southern Californian Eddy. The red arrows indicate the California Countercurrent. Each point color denotes the decade of collection: 1910s - light blue; 1920s - dark blue; 1930s - light green; 1940s - dark green; 1950s - pink; 1960s - red; 1970s - light orange; 1980s - dark orange; 1990s - light purple; 2000s - dark purple; 2010s - yellow. Sites with black X represent locations with SST data.

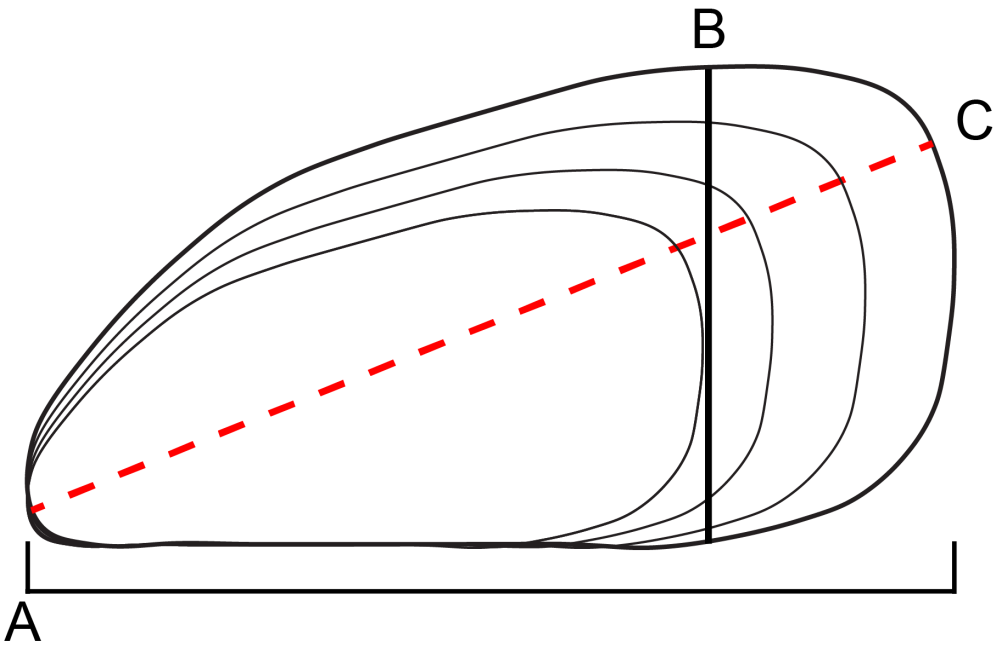


**Figure 2.** Sketch of valve showing where measurements were taken for each specimen (n = 130). (A) Line from anterior to posterior margin representing where shell length was measured with digital calipers parallel to hinge. (B) Line from dorsal to ventral margin showing where shell width was measured with digital calipers. (C) Red dashed line showing where shells (n = 51) were cut with a diamond saw to produce a thin section along the axis of maximum growth.

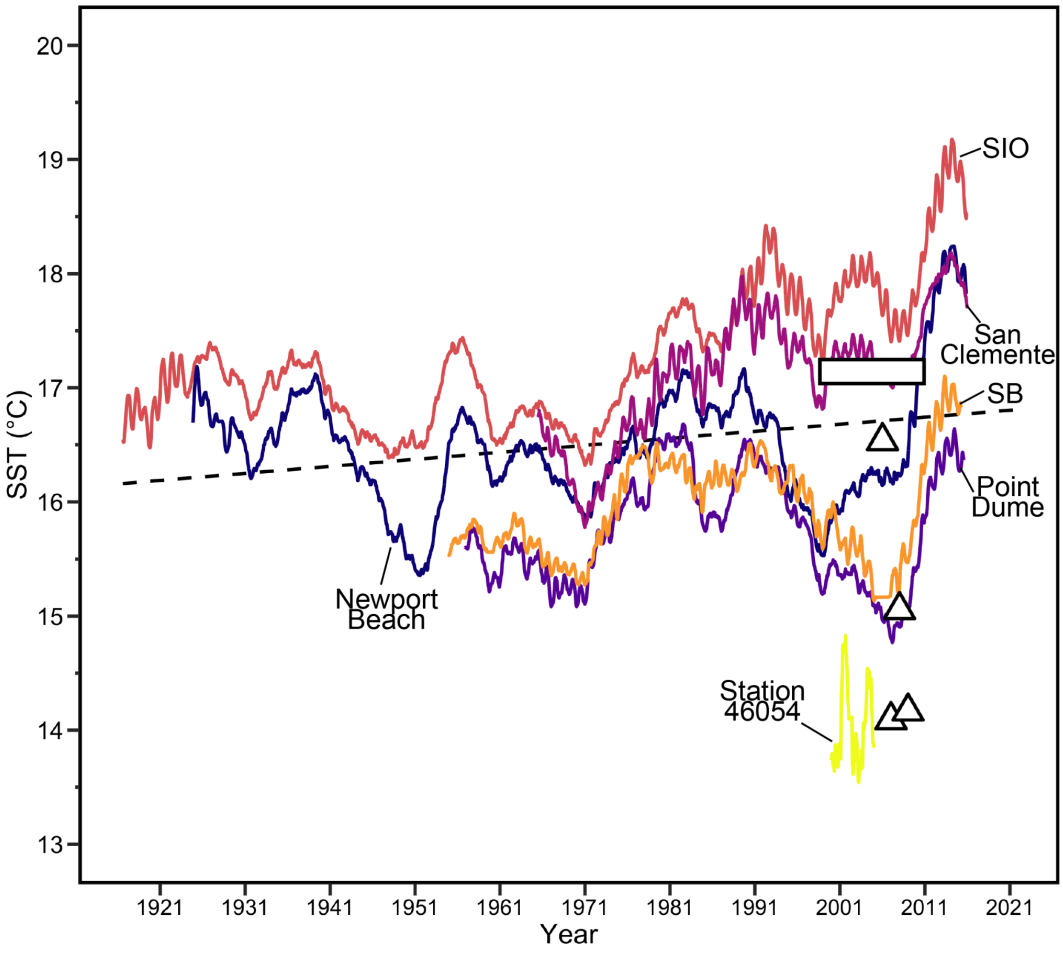


**Figure 3.** SST records for each site over time. Long-term records are plotted as a five-year running mean and the short-term record (Station 46054, Santa Barbara Basin, in yellow) is plotted with a one-year running mean. La Jolla (SIO) SST is in coral, Newport Beach SST is in navy, San Clemente SST is in magenta, Santa Barbara (SB) SST is in orange, and Point Dume is in purple (all labeled on plot). White triangles denote annually averaged intertidal SST measurements from loggers at Punta Baja, Baja California for 2006, 2007, 2009, and 2009 (Helmuth et al., 2016). White bar denotes mean SST from 2000 through 2011 at Bahía Tortugas, Baja California Sur (Sicard-González et al., 2012). Black dashed line is the regression line for the La Jolla (SIO) temperature record. All of these SST location sites are plotted on the map in Figure 1.

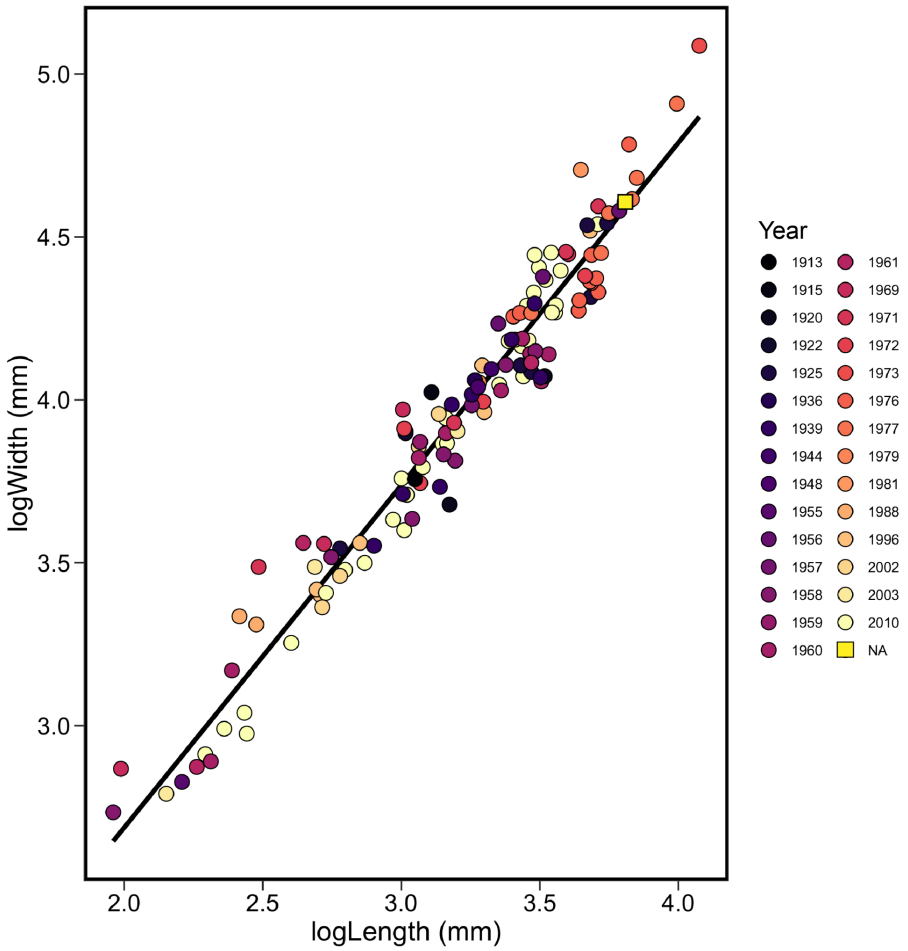


**Figure 4.** Relationships between log-transformed shell width and log-transformed shell length over the past 100 years. Each point is a unique specimen (n = 130) and each color represents a different year (30 different years) as shown in legend. Regression line represents the trend for all specimens. Year "NA" is the Pleistocene specimen.

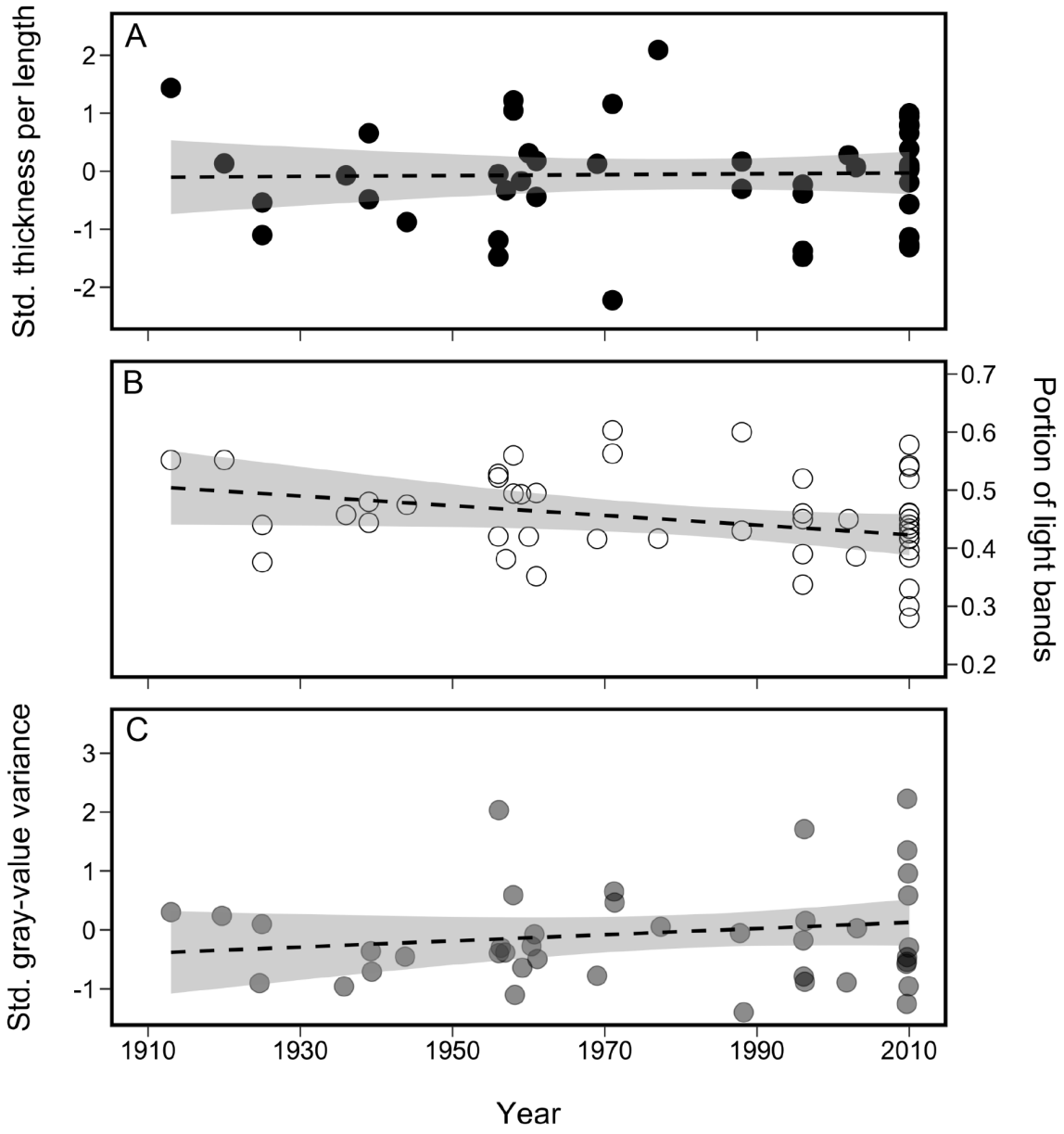


**Figure 5.** Quantitative *M. californianus* shell characteristics that have not changed significantly over the past century, including standardized cross-sectional thickness per shell length (A), portion of light bands in the inner calcite layer (B), and standardized gray-value variance of dark-light banding (C). Trend lines are plotted for each shell characteristic with a 95% confidence interval, although none of these are statistically significant linear trends.

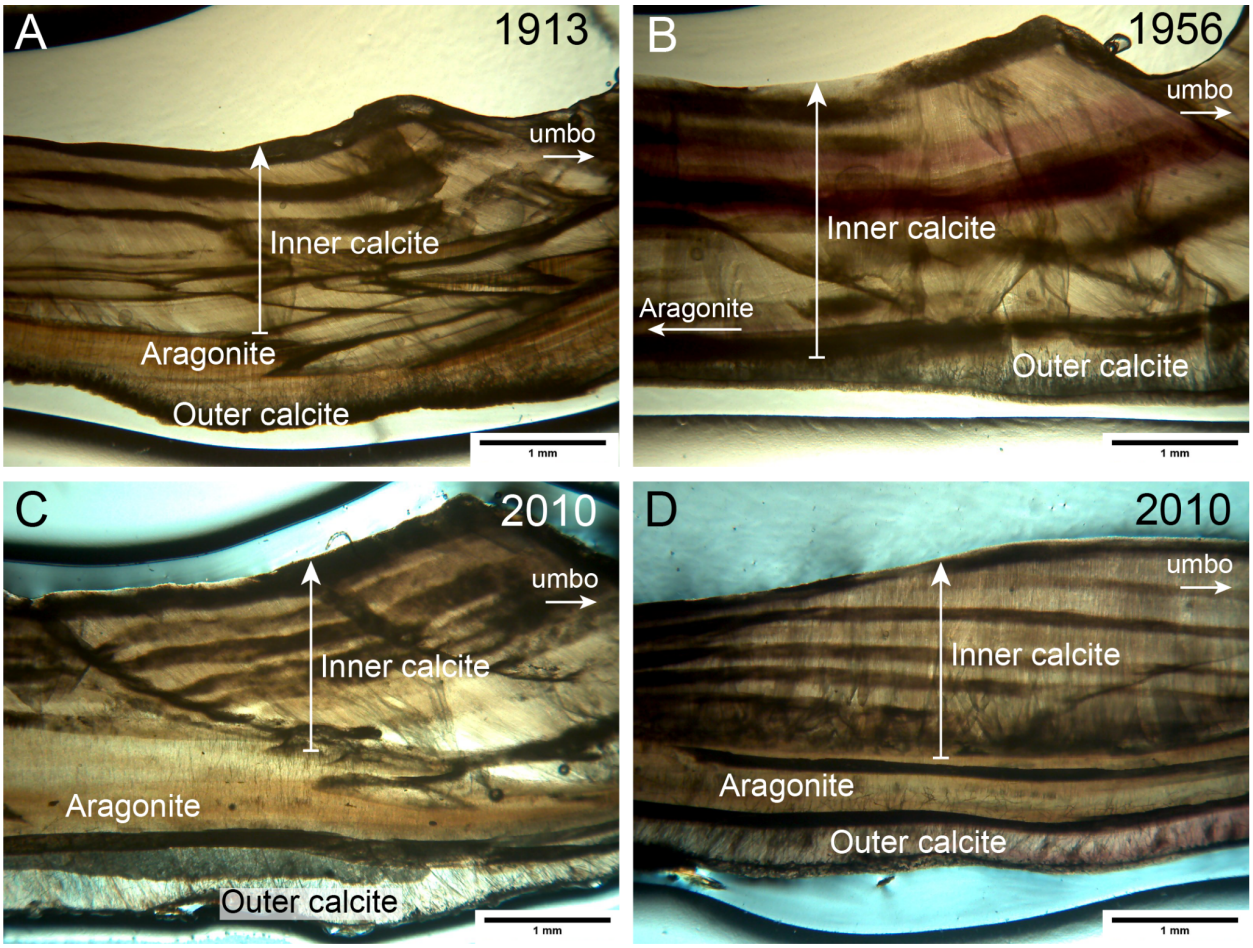


**Figure 6.** Photomicrographs of four cross-sectioned specimens collected from La Jolla in 1913 (A), Point Dume in 1956 (B), San Diego in 2010 (C), and another specimen from San Diego in 2010 (D). The aragonite and outer calcite layers are also visible, except for in (B), where the aragonite layer begins just to the left of the field of view. Each photo was taken adjacent to the umbo and focuses on the inner calcite layer with dark-light growth banding. The inner calcite layer grows inward as indicated by the white arrows. The youngest shell material is towards the top of each photo (i.e., the dark band at the inner layer of the shell was the last to precipitate for each specimen). The shell exterior is towards the bottom of each photo and the umbo is just to the right of the field of view for each specimen. Each scale bar is 1 mm.

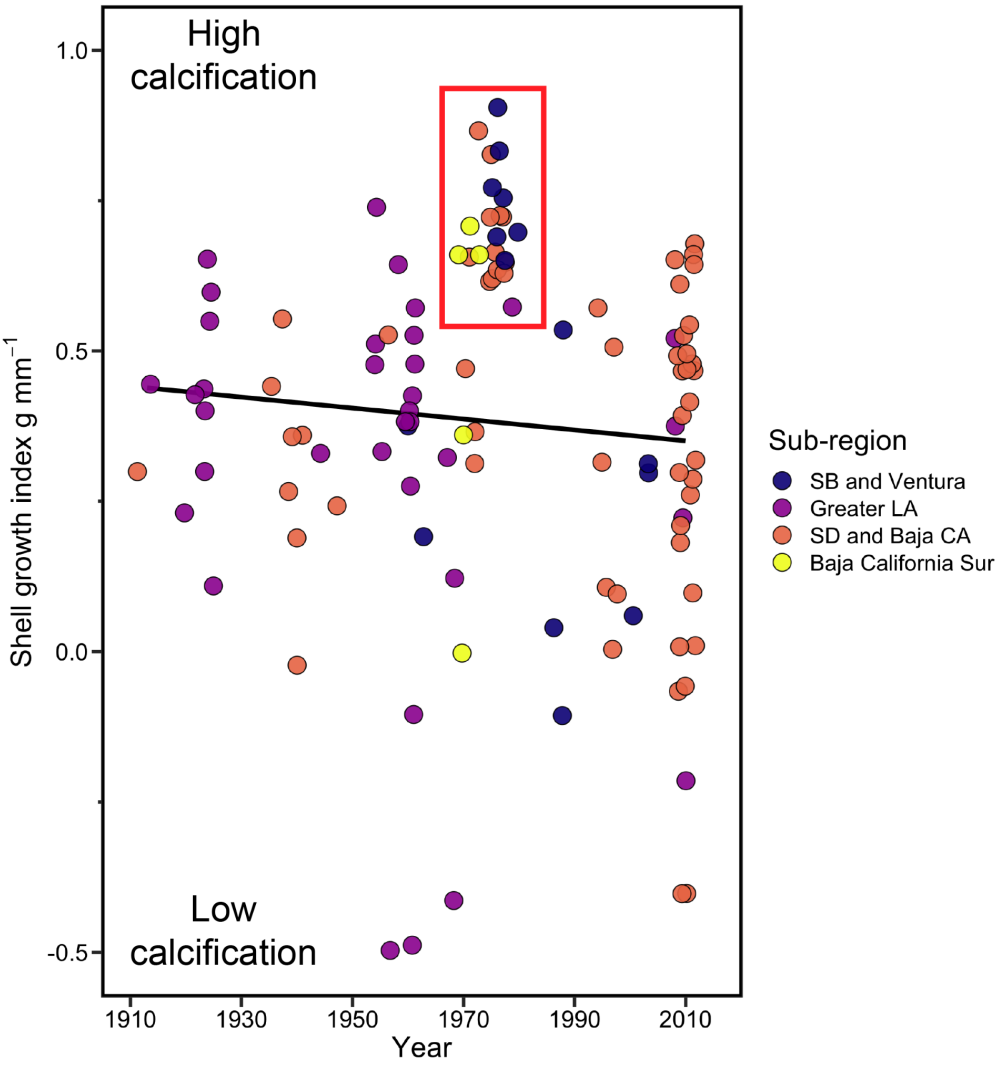


**Figure 7.** Shell growth indices of all specimens through time sorted by sub-region (see legend): Santa Barbara and Ventura (navy), Greater Los Angeles (magenta), San Diego and Baja California (coral), Baja California Sur (yellow). Black line plotted for all specimens and represents a non-significant negative slope (slope = -0.001382, p = 0.2). Red box highlights a period of high growth indices for all sub-regions.

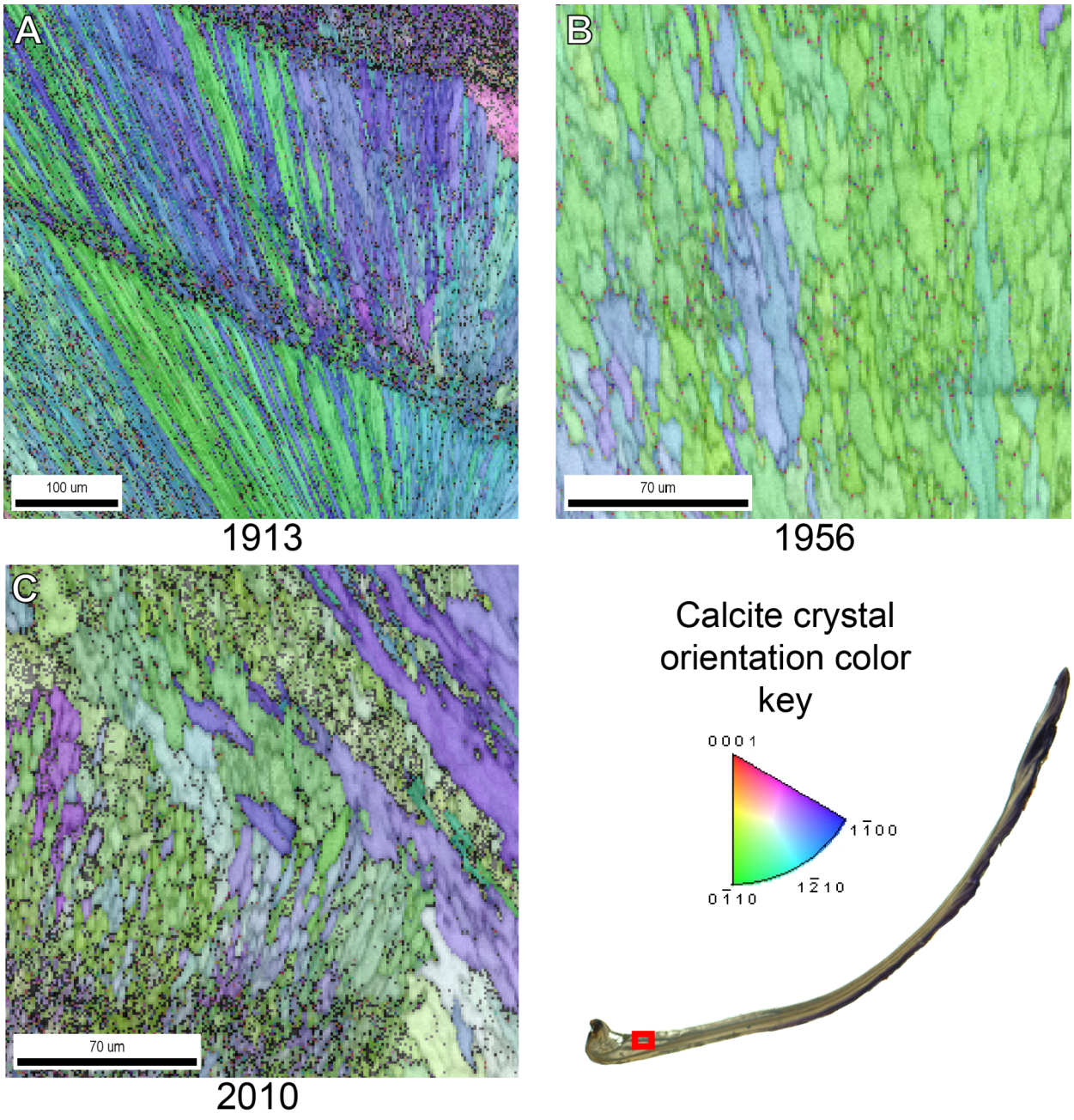


**Figure 8.** Electron backscatter diffraction (EBSD) scans within the center of the inner calcite layer adjacent to the umbo in three individuals, one collected in 1913 at La Jolla (A), another in 1956 at San Diego (B), and a third collected at Point Dume in 2010. Note that the scale bar is 100 µm for (A) and 70 µm for (B) and (C). The youngest shell material is towards the top of the image for each scan. The aragonite layer is below the field of view. Crystallographic orientations are shown relative to the {0001} plane, as shown in the calcite crystal orientation color key. Red box in the shell cross-section indicates where EBSD scans were performed.

**Supplementary Information**

**Table S1.** Summary of specimens used in this study and their sources, locations, and collection years.

| Sample Source (individual or institution name) | Collection Localities | Collection Years |
|---|---|---|
| Elizabeth Bullard, UC San Diego | La Jolla Tide Pools, Corona del Mar, SIO Pier Pilings, Dike Rock Tide Pools | 1996, 2010 |
| California Academy of Sciences, Invertebrate Zoology | Santa Monica Beach, Cabrillo Beach, Point Fermin, Anacapa Island, La Jolla, Dutch Harbor San Nicolas Island, Alegria, Fraser Point Santa Cruz Island, Johnsons Lee Santa Rosa Island, | 1925, 1960, 1961, 1973, 1981, 2002, 2003 |
| Natural History Museum of Los Angeles County, Malacology | Portuguese Bend Palos Verdes Peninsula, Venice Beach, White Point Palos Verdes Peninsula, Newport Beach Jetty, Carpinteria State Beach, Government Point, E Punta Azufre Baja California, Rocas Pináculo Islas San Benito Baja California, Piedra Colorada Isla Cedros, Punta Rompiente Baja California Sur | 1915, 1922, 1925, 1969, 1971, 1972, 1976, 1977, 1979, 1988 |
| Santa Barbara Museum of Natural History, Invertebrate Zoology | La Jolla, Playa del Rey, Anaheim Landing, North Island Coronado Jetty, South Laguna Beach, Point Dume, Palos Verdes, Whites Point, Corona del Mar, Point Fermin, Newport Mesa | 1913, 1920, 1936, 1944, 1956, 1957, 1959, 1960 |
| UC Museum of Paleontology, Invertebrates | Mission Bay, San Diego, Del Mar, Punta Banda, Dana Point, Solana Beach, Cabrillo Beach, Topanga Beach, Venice Beach | 1939, 1948, 1958, 1960, 1961 |

**Table S2.** Coefficients of multiple regression analysis (Year and Region as factors) for shell width to shell length relationships for all 130 shells measured.

| Independent (x) | Dependent (y) | slope (*m*) | SE | y-intercept (*b*) | *p*-value | $R^2$ |
|---|---|---|---|---|---|---|
| log(length) mm | log(width) mm | 0.91 | 0.68 | 0.06 | < .000 | 0.96 |

**Table S3.** Slopes of RMA regression lines for shell width to length ratios for each decade.

| Decade | slope (*m*) | number of shells | $r^2$ |
|---|---|---|---|
| 1910 | 0.22 | 2 | 1 |
| 1920 | 0.97 | 9 | 0.84 |
| 1930 | 0.85 | 9 | 0.85 |
| 1940 | 0.87 | 2 | 1 |
| 1950 | 0.94 | 13 | 0.97 |
| 1960 | 1.1 | 16 | 0.94 |
| 1970 | 0.98 | 27 | 0.9 |
| 1980 | 0.93 | 4 | 0.97 |
| 1990 | 0.89 | 6 | 0.99 |
| 2000 | 0.88 | 7 | 0.97 |
| 2010 | 0.84 | 34 | 0.98 |

**Figure S4.** RMA analysis shows proportional growth ($m$ = 0.93) between shell length and width for all specimens. Each point represents a single specimen and colors represent different decades (see legend). Red line represents the RMA regression line ($m$ = 0.93, $b$ = -0.48, angle = 42.97°) and gray lines indicate the confidence limits.

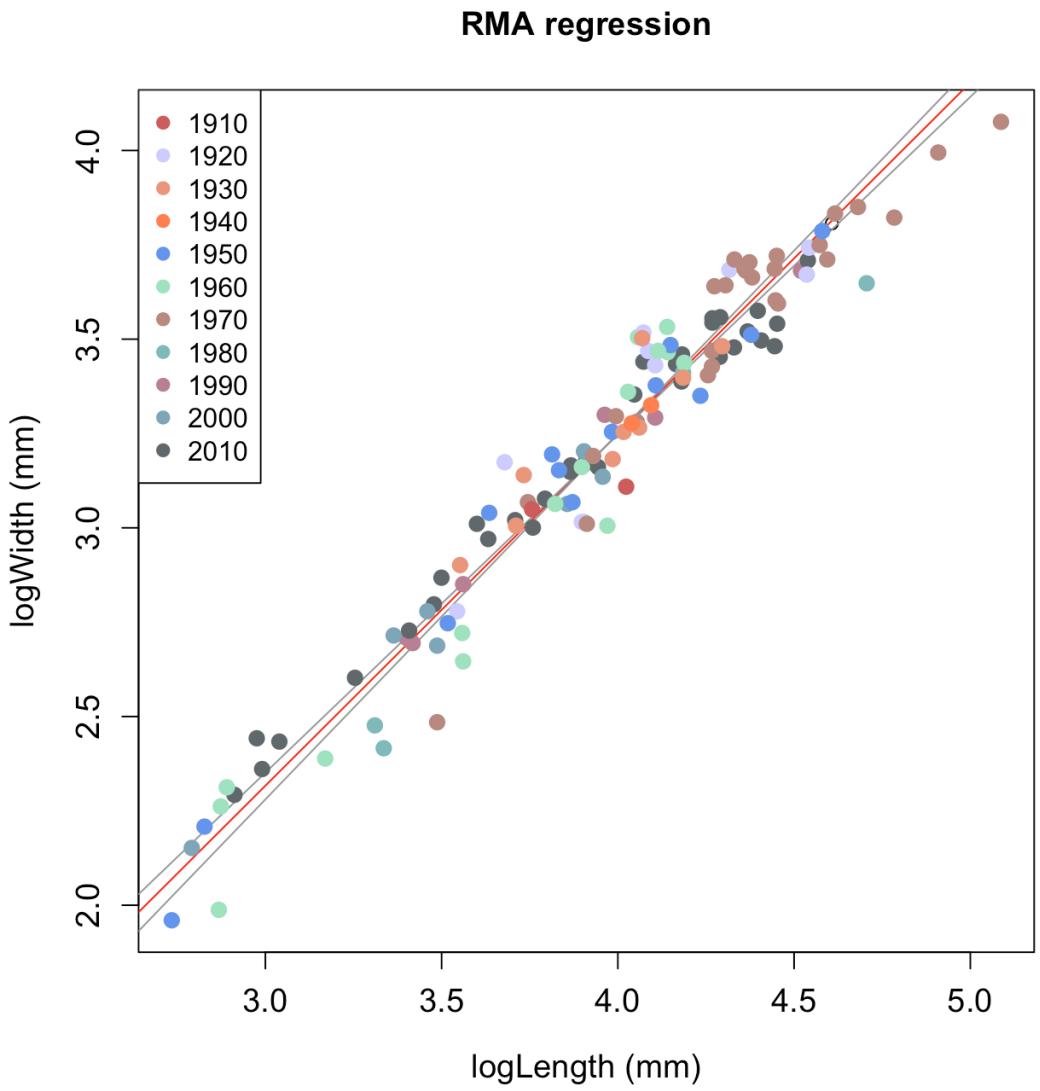

**Figure S5.** Relationships between log-transformed shell width and log-transformed shell length for all specimens. Each point is a unique specimen and each color represents a different sub-region of the study area (see legend). Regression line ($m$ = 0.91) represents the trend for all specimens, as in Figure 4.

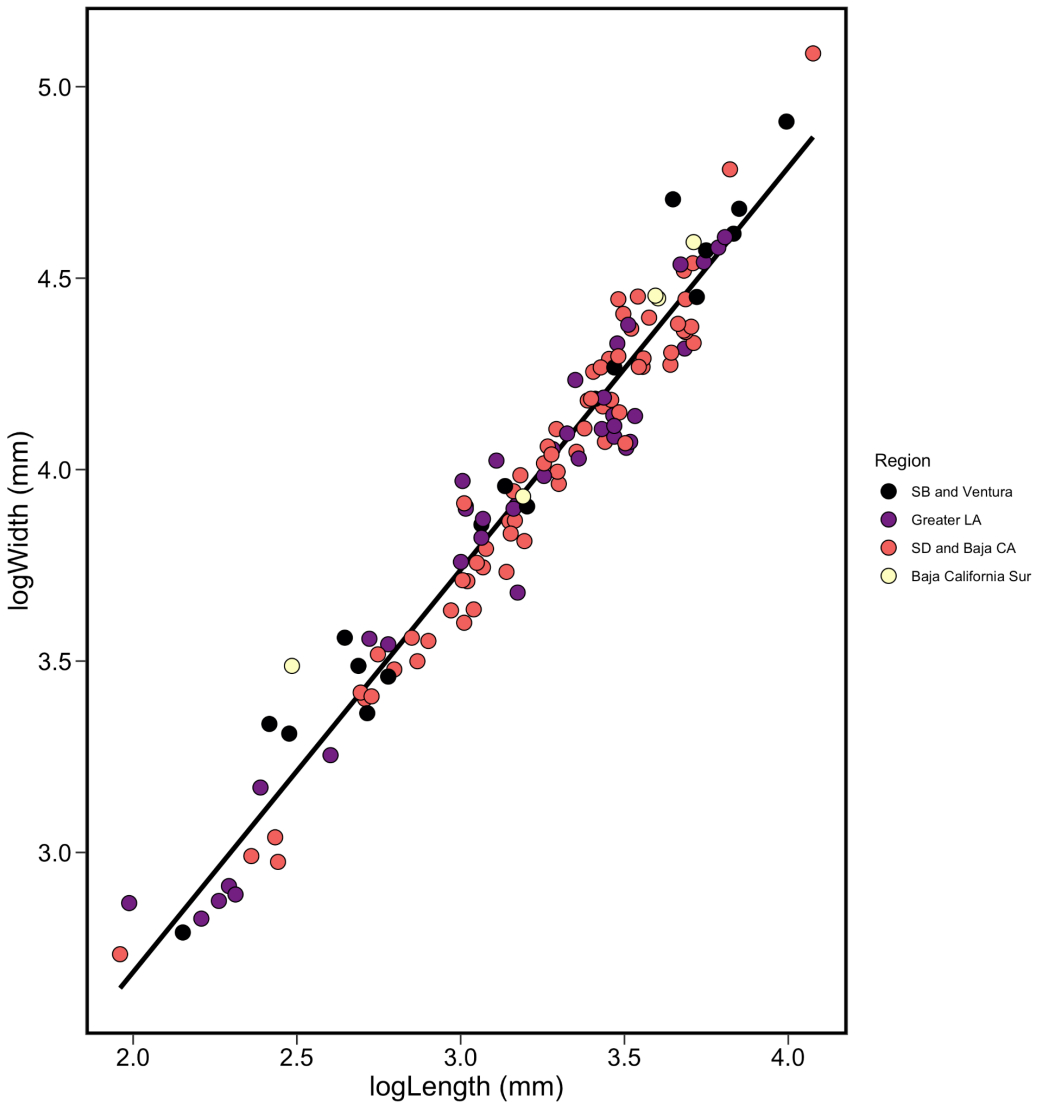

**Figure S6.** Cross-sectional view of the Pleistocene *M. californianus* specimen showing the presence of the inner calcite layer. Growth direction of the inner calcite layer is inward, as shown by the white arrow. The youngest shell material is towards the top of the image. The shell exterior is towards the bottom of the image.

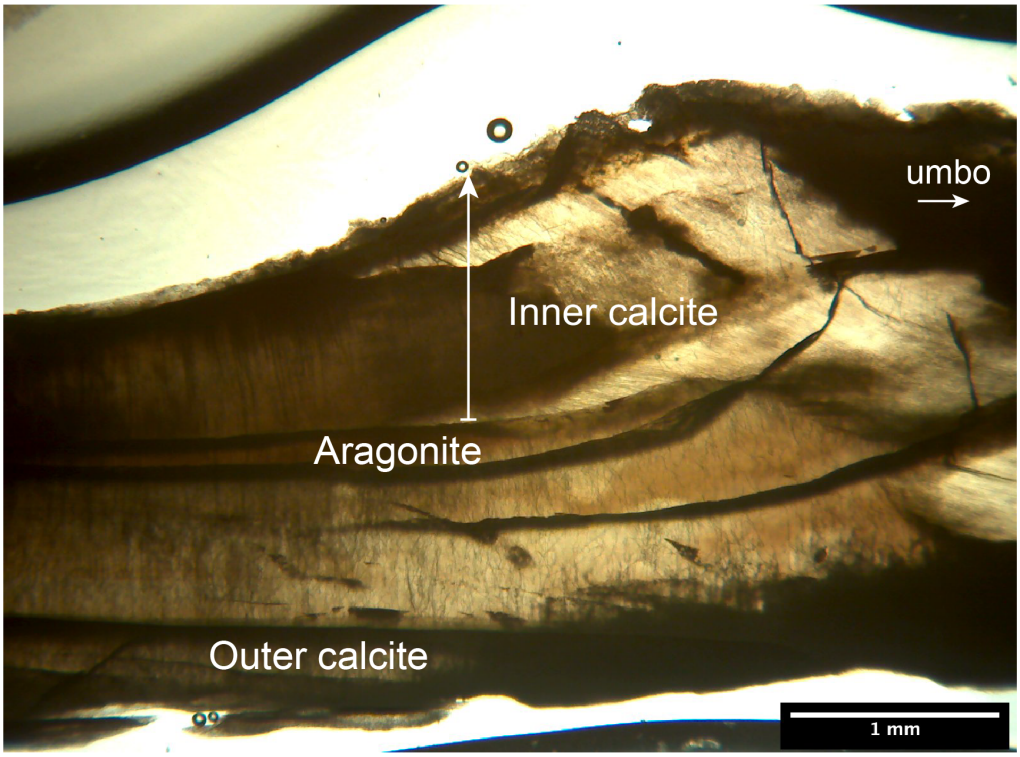

## References


Abraham, J.P., Baringer, M., Bindoff, N.L., Boyer, T., Cheng, L.J., Church, J.A., Conroy, J.L., Domingues, C.M., Fasullo, J.T., Gilson, J., Goni, G., Good, S.A., Gorman, J.M., Gouretski, V., Ishii, M., Johnson, G.C., Kizu, S., Lyman, J.M., Macdonald, A.M., Minkowycz, W.J., Moffitt, S.E., Palmer, M.D., Piola, A.R., Reseghetti, F., Schuckmann, K., Trenberth, K.E., Velicogna, I., and Willis, J.K., 2013. A review of global ocean temperature observations: Implications for ocean heat content estimates and climate change. *Reviews of Geophysics*, 51 (3), 450–483.

Addison, J.A., Ort, B.S., Mesa, K.A., and Pogson, G.H., 2008. Range-wide genetic homogeneity in the California sea mussel (Mytilus californianus): a comparison of allozymes, nuclear DNA markers, and mitochondrial DNA sequences. *Molecular Ecology*, 17 (19), 4222–4232.

Barron, J.A. and Anderson, L., 2011. Enhanced Late Holocene ENSO/PDO expression along the margins of the eastern North Pacific. *Quaternary International*, 235 (1–2), 3–12.

Barron, J.A. and Bukry, D., 2007. Development of the California Current during the past 12,000 yr based on diatoms and silicoflagellates. *Palaeogeography, Palaeoclimatology, Palaeoecology*, 248 (3), 313–338.

Bates, N.A.R., Astor, Y.M., Church, M.T.J., Currie, K., Dore, J.E., Olafsson, J., and Santana-Casiano, J.M., 2020. A Time-Series View of Changing Surface Ocean Chemistry Due to Ocean Uptake of Anthropogenic $CO_2$ and Ocean Acidification, 17.

Bayne, B.L., Bayne, C.J., Carefoot, T.C., and Thompson, R.J., 1976. The physiological ecology of Mytilus californianus Conrad. *Oecologia*, 22 (3), 211–228.

Bednaršek, N., Feely, R.A., Howes, E.L., Hunt, B.P.V., Kessouri, F., León, P., Lischka, S., Maas, A.E., McLaughlin, K., Nezlin, N.P., Sutula, M., and Weisberg, S.B., 2019. Systematic Review and Meta-Analysis Toward Synthesis of Thresholds of Ocean Acidification Impacts on Calcifying Pteropods and Interactions With Warming. *Frontiers in Marine Science*, 6.

Blanchette, C.A. and Gaines, S.D., 2007. Distribution, abundance, size and recruitment of the mussel, Mytilus californianus, across a major oceanographic and biogeographic boundary at Point Conception, California, USA. *Journal of Experimental Marine Biology and Ecology*, 340 (2), 268–279.

Blanchette, C.A., Helmuth, B., and Gaines, S.D., 2007. Spatial patterns of growth in the mussel, Mytilus californianus, across a major oceanographic and biogeographic boundary at Point Conception, California, USA. *Journal of Experimental Marine Biology and Ecology*, 340 (2), 126–148.

Bograd, S.J. and Lynn, R.J., 2003. Long-term variability in the Southern California Current System. *Deep Sea Research Part II: Topical Studies in Oceanography*, 50 (14), 2355–2370.

Bullard, E., 2021. Shell mineralogy of a foundational marine species, Mytilus californianus, over half a century in a changing ocean | PNAS [online]. Available from: https://www.pnas.org/content/118/3/e2004769118.short?casa_token=ohkRjpicGWgAAAAA:QQ0E3zvWP3jgeBlOh2RYdKd--8wG-12Kd_u6TI6TkmObZaJOu3faQjQbYe99hdnB6KtLF9_TCnRbUg0 [Accessed 16 Jul 2021].

Checkley, D.M. and Barth, J.A., 2009. Patterns and processes in the California Current System.

*Progress in Oceanography*, 83 (1), 49–64.
Connor, K.M. and Robles, C.D., 2015. Within-Site Variation of Growth Rates and Terminal Sizes in Mytilus californianus Along Wave Exposure and Tidal Gradients. *The Biological Bulletin*, 228 (1), 39–51.
Connor, K.M., Sung, A., Garcia, N.S., Gracey, A.Y., and German, D.P., 2016. Modulation of digestive physiology and biochemistry in Mytilus californianus in response to feeding level acclimation and microhabitat. *Biology Open*, 5 (9), 1200–1210.
Cross, E.L., Harper, E.M., and Peck, L.S., 2018. A 120-year record of resilience to environmental change in brachiopods. *Global Change Biology*, 24 (6), 2262–2271.
Dodd, J.R., 1964. Environmentally Controlled Variation in the Shell Structure of a Pelecypod Species, 9.
Doney, S.C., Fabry, V.J., Feely, R.A., and Kleypas, J.A., 2009. Ocean Acidification: The Other CO2 Problem. *Annual Review of Marine Science*, 1 (1), 169–192.
Field, D., Cayan, D., and Chavez, F., 2006. SECULAR WARMING IN THE CALIFORNIA CURRENT AND NORTH PACIFIC, 47, 17.
Figuerola, B., Hancock, A.M., Bax, N., Cummings, V.J., Downey, R., Griffiths, H.J., Smith, J., and Stark, J.S., 2021. A Review and Meta-Analysis of Potential Impacts of Ocean Acidification on Marine Calcifiers From the Southern Ocean. *Frontiers in Marine Science*, 8.
Fitzer, S.C., Chung, P., Maccherozzi, F., Dhesi, S.S., Kamenos, N.A., Phoenix, V.R., and Cusack, M., 2016. Biomineral shell formation under ocean acidification: a shift from order to chaos. *Scientific Reports*, 6 (1), 21076.
Fitzer, S.C., Phoenix, V.R., Cusack, M., and Kamenos, N.A., 2014. Ocean acidification impacts mussel control on biomineralisation. *Scientific Reports*, 4 (1), 6218.
Ford, H.L., Schellenberg, S.A., Becker, B.J., Deutschman, D.L., Dyck, K.A., and Koch, P.L., 2010. Evaluating the skeletal chemistry of *Mytilus californianus* as a temperature proxy: Effects of microenvironment and ontogeny: *MYTILUS* CHEMISTRY AS A TEMPERATURE PROXY. *Paleoceanography*, 25 (1).
Fumo, J.T., Carter, M.L., Flick, R.E., Rasmussen, L.L., Rudnick, D.L., and Iacobellis, S.F., 2020. Contextualizing Marine Heatwaves in the Southern California Bight Under Anthropogenic Climate Change. *Journal of Geophysical Research: Oceans*, 125 (5), e2019JC015674.
Gaylord, B., Hill, T.M., Sanford, E., Lenz, E.A., Jacobs, L.A., Sato, K.N., Russell, A.D., and Hettinger, A., 2011. Functional impacts of ocean acidification in an ecologically critical foundation species. *Journal of Experimental Biology*, 214 (15), 2586–2594.
Grenier, C., Román, R., Duarte, C., Navarro, J.M., Rodriguez-Navarro, A.B., and Ramajo, L., 2020. The combined effects of salinity and pH on shell biomineralization of the edible mussel Mytilus chilensis. *Environmental Pollution*, 263, 114555.
Harrington, M.J. and Waite, J.H., 2007. Holdfast heroics: comparing the molecular and mechanical properties of Mytilus californianus byssal threads. *Journal of Experimental Biology*, 210 (24), 4307–4318.
Harvey, B.P., Gwynn‐Jones, D., and Moore, P.J., 2013. Meta-analysis reveals complex marine biological responses to the interactive effects of ocean acidification and warming. *Ecology and Evolution*, 3 (4), 1016–1030.
Helmuth, B., Choi, F., Matzelle, A., Torossian, J.L., Morello, S.L., Mislan, K. a. S., Yamane, L., Strickland, D., Szathmary, P.L., Gilman, S.E., Tockstein, A., Hilbish, T.J., Burrows,

M.T., Power, A.M., Gosling, E., Mieszkowska, N., Harley, C.D.G., Nishizaki, M., Carrington, E., Menge, B., Petes, L., Foley, M.M., Johnson, A., Poole, M., Noble, M.M., Richmond, E.L., Robart, M., Robinson, J., Sapp, J., Sones, J., Broitman, B.R., Denny, M.W., Mach, K.J., Miller, L.P., O'Donnell, M., Ross, P., Hofmann, G.E., Zippay, M., Blanchette, C., Macfarlan, J.A., Carpizo-Ituarte, E., Ruttenberg, B., Peña Mejía, C.E., McQuaid, C.D., Lathlean, J., Monaco, C.J., Nicastro, K.R., and Zardi, G., 2016. Long-term, high frequency in situ measurements of intertidal mussel bed temperatures using biomimetic sensors. *Scientific Data*, 3 (1), 160087.

Hickey, B.M., 1979. The California current system—hypotheses and facts. *Progress in Oceanography*, 8 (4), 191–279.

Hu, N., Bourdeau, P.E., Harlos, C., Liu, Y., and Hollander, J., 2022. Meta-analysis reveals variance in tolerance to climate change across marine trophic levels. *Science of The Total Environment*, 154244.

Huyer, A., 1983. Coastal upwelling in the California current system. *Progress in Oceanography*, 12 (3), 259–284.

IPCC, 2013: *Climate Change 2013: The Physical Science Basis. Contribution of Working Group I to the Fifth Assessment Report of the Intergovernmental Panel on Climate Change* [Stocker, T.F., D. Qin, G.-K. Plattner, M. Tignor, S.K. Allen, J. Boschung, A. Nauels, Y. Xia, V. Bex and P.M. Midgley (eds.)]. Cambridge University Press, Cambridge, United Kingdom and New York, NY, USA, 1535 pp.

Jacox, M.G., Edwards, C.A., Hazen, E.L., and Bograd, S.J., 2018. Coastal Upwelling Revisited: Ekman, Bakun, and Improved Upwelling Indices for the U.S. West Coast. *Journal of Geophysical Research: Oceans*, 123 (10), 7332–7350.

Jazwa, C.S., Wolfe, C.A., Chu, E.Y., and Stull, K.E., 2020. The effects of vertical position in the intertidal zone on the $\delta^{18}O$ and $\delta^{13}C$ composition of Mytilus californianus shell carbonate. Journal of Archaeological Science: Reports (34): 102587.

Johnson, E.H., 2020. Experimental tests of bivalve shell shape reveal potential tradeoffs between mechanical and behavioral defenses. *Scientific Reports*, 10 (1), 19425.

Jokiel, P.L., Rodgers, K.S., Kuffner, I.B., Andersson, A.J., Cox, E.F., and Mackenzie, F.T., 2008. Ocean acidification and calcifying reef organisms: a mesocosm investigation. *Coral Reefs*, 27 (3), 473–483.

Katayama, S. and Isshiki, T., 2007. Variation in otolith macrostructure of Japanese flounder (Paralichthys olivaceus): A method to discriminate between wild and released fish. *Journal of Sea Research*, 57 (2), 180–186.

Killam, D.E. and Clapham, M.E., 2018. IDENTIFYING THE TICKS OF BIVALVE SHELL CLOCKS: SEASONAL GROWTH IN RELATION TO TEMPERATURE AND FOOD SUPPLY. *PALAIOS*, 33 (5), 228–236.

Kim, S.Y. and Cornuelle, B.D., 2015. Coastal ocean climatology of temperature and salinity off the Southern California Bight: Seasonal variability, climate index correlation, and linear trend. *Progress in Oceanography*, 138, 136–157.

Kroeker, K.J., Kordas, R.L., Crim, R., Hendriks, I.E., Ramajo, L., Singh, G.S., Duarte, C.M., and Gattuso, J.-P., 2013. Impacts of ocean acidification on marine organisms: quantifying sensitivities and interaction with warming. *Global Change Biology*, 19 (6), 1884–1896.

Kroeker, K.J., Kordas, R.L., Crim, R.N., and Singh, G.G., 2010. Meta-analysis reveals negative yet variable effects of ocean acidification on marine organisms. *Ecology Letters*, 13 (11), 1419–1434.

Kroeker, K.J., Sanford, E., Jellison, B.M., and Gaylord, B., 2014. Predicting the Effects of Ocean Acidification on Predator-Prey Interactions: A Conceptual Framework Based on Coastal Molluscs. *The Biological Bulletin*, 226 (3), 211–222.

Lin, A. and Meyers, M.A., 2005. Growth and structure in abalone shell. *Materials Science and Engineering: A*, 390 (1), 27–41.

Logan, C.A., Kost, L.E., and Somero, G.N., 2012. Latitudinal differences in Mytilus californianus thermal physiology. *Marine Ecology Progress Series*, 450, 93–105.

Lorenzo, E.D., Miller, A.J., Schneider, N., and McWilliams, J.C., 2005. The Warming of the California Current System: Dynamics and Ecosystem Implications. *Journal of Physical Oceanography*, 35 (3), 336–362.

Lynn, R.J. and Bograd, S.J., 2002. Dynamic evolution of the 1997–1999 El Niño–La Niña cycle in the southern California Current System. *Progress in Oceanography*, 54 (1), 59–75.

Lynn, R.J. and Simpson, J.J., 1987. The California Current system: The seasonal variability of its physical characteristics. *Journal of Geophysical Research: Oceans*, 92 (C12), 12947–12966.

Mantua, N.J. and Hare, S.R., 2002. The Pacific Decadal Oscillation. *Journal of Oceanography*, 58 (1), 35–44.

Mantua, N.J., Hare, S.R., Zhang, Y., Wallace, J.M., and Francis, R.C., 1997. A Pacific Interdecadal Climate Oscillation with Impacts on Salmon Production*. *Bulletin of the American Meteorological Society*, 78 (6), 1069–1080.

McCoy, S.J., Kamenos, N.A., Chung, P., Wootton, T.J., and Pfister, C.A., 2018. A mineralogical record of ocean change: Decadal and centennial patterns in the California mussel. *Global Change Biology*, 24 (6), 2554–2562.

McCoy, S.J., Robinson, L.F., Pfister, C.A., Wootton, J.T., and Shimizu, N., 2011. Exploring B/Ca as a pH proxy in bivalves: relationships between <I>Mytilus californianus</I> B/Ca and environmental data from the northeast Pacific. *Biogeosciences*, 8 (9), 2567–2579.

McGowan, J.A., Bograd, S.J., Lynn, R.J., and Miller, A.J., 2003. The biological response to the 1977 regime shift in the California Current. *Deep Sea Research Part II: Topical Studies in Oceanography*, 50 (14), 2567–2582.

Nagelkerken, I. and Connell, S.D., 2015. Global alteration of ocean ecosystem functioning due to increasing human $CO_2$ emissions. *Proceedings of the National Academy of Sciences*, 112 (43), 13272–13277.

Oliver, E.C.J., Donat, M.G., Burrows, M.T., Moore, P.J., Smale, D.A., Alexander, L.V., Benthuysen, J.A., Feng, M., Sen Gupta, A., Hobday, A.J., Holbrook, N.J., Perkins-Kirkpatrick, S.E., Scannell, H.A., Straub, S.C., and Wernberg, T., 2018. Longer and more frequent marine heatwaves over the past century. *Nature Communications*, 9 (1), 1324.

Osborne, E.B., Thunell, R.C., Gruber, N., Feely, R.A., and Benitez-Nelson, C.R., 2020. Decadal variability in twentieth-century ocean acidification in the California Current Ecosystem. *Nature Geoscience*, 13 (1), 43–49.

Paine, R.T., 1974. Intertidal Community Structure. Experimental Studies on the Relationship between a Dominant Competitor and Its Principal Predator. *Oecologia*, 15 (2), 93–120.

Pérez-Huerta, A. and Cusack, M., 2009. Optimizing Electron Backscatter Diffraction of Carbonate Biominerals—Resin Type and Carbon Coating. *Microscopy and Microanalysis*, 15 (3), 197–203.

Pfister, C.A., McCoy, S.J., Wootton, J.T., Martin, P.A., Colman, A.S., and Archer, D., 2011. Rapid Environmental Change over the Past Decade Revealed by Isotopic Analysis of the California Mussel in the Northeast Pacific. *PLOS ONE*, 6 (10), e25766.

Pfister, C.A., Roy, K., Wootton, J.T., McCoy, S.J., Paine, R.T., Suchanek, T.H., and Sanford, E., 2016. Historical baselines and the future of shell calcification for a foundation species in a changing ocean. *Proceedings of the Royal Society B: Biological Sciences*, 283 (1832), 20160392.

Ries, J.B., Cohen, A.L., and McCorkle, D.C., 2009. Marine calcifiers exhibit mixed responses to CO2-induced ocean acidification. *Geology*, 37 (12), 1131–1134.

Ries, J.B., 2011. Skeletal mineralogy in a high-CO2 world. *Journal of Experimental Marine Biology and Ecology*, 403 (1), 54–64.

Sanford, E., Sones, J.L., García-Reyes, M., Goddard, J.H.R., and Largier, J.L., 2019. Widespread shifts in the coastal biota of northern California during the 2014–2016 marine heatwaves. *Scientific Reports*, 9 (1), 4216.

Schöne, B.R. and Surge, D.M., 2012. PART N, REVISED, VOLUME 1, CHAPTER 14: BIVALVE SCLEROCHRONOLOGY AND GEOCHEMISTRY. *Treatise Online*, (46), 25.

Seed, R. and Suchanek, T., 1992. The Mussel Mytilus: Ecology, Physiology, Genetics and Culture. *Dev Aquac Fish Sci*, 25, 87–157.

Sicard -González, M.T., Tripp -Valdéz, M.A., Ocampo, L., Maeda -Martí-nez, A.N., and Lluch -Cota, S.E., 2012. Coastal sea surface temperature records along the Baja California Peninsula. *CICIMAR Oceánides*, 27 (2), 65–69.

Smith, J.R., Fong, P., and Ambrose, R.F., 2009. Spatial patterns in recruitment and growth of the mussel Mytilus californianus (Conrad) in southern and northern California, USA, two regions with differing oceanographic conditions. *Journal of Sea Research*, 61 (3), 165–173.

Soon, T.K. and Zheng, H., 2020. Climate Change and Bivalve Mass Mortality in Temperate Regions. *In*: P. de Voogt, ed. *Reviews of Environmental Contamination and Toxicology Volume 251*. Cham: Springer International Publishing, 109–129.

Telesca, L., Peck, L.S., Backeljau, T., Heinig, M.F., and Harper, E.M., 2021. A century of coping with environmental and ecological changes via compensatory biomineralization in mussels. *Global Change Biology*, 27 (3), 624–639.

Vriesman, V.P., Carlson, S.J., and Hill, T.M., 2022. Investigating controls of shell growth features in a foundation bivalve species: seasonal trends and decadal changes in the California mussel. *Biogeosciences*, 19 (2), 329–346.

## Appendices

**Appendix 1.** Appendix to Chapter 2. Table of all stable isotope data accessed and analyzed in Chapter 2. Shell ID refers to the unique label assigned to each individual shell in this study. N sub refers to the number of sub-samples measured for each individual shell. Primary ID was assigned by the primary authors of the study. Subsample refers to the subsample name assigned by primary authors or the subsampling distance along the growth trajectory (mm). Age (Year BP) is the geologic age of the mussel in years before present. Type refers to the sample type; Mod = modern live-collected mussel and Mid = archaeological midden shell. Setting refers to the coastal region of collection; Main = coastal mainland site and Island = Channel Island site.

| Shell ID | N sub samples | Primary citation | Primary ID | Subsample | Shell length (mm) | δ13C | δ18O | Age (Year BP) | Type | Site | Setting | Lat | Long |
|---|---|---|---|---|---|---|---|---|---|---|---|---|---|
| 1 | 31 | Ferguson et al., 2013 | NB Mussel 1 | CDMa-1 | | -0.75 | -0.58 | 10 | Mod | Newport Beach | Main | 33.6 | -117.9 |
| 1 | 31 | Ferguson et al., 2013 | NB Mussel 1 | CDMa-10 | | -0.62 | -0.38 | 10 | Mod | Newport Beach | Main | 33.6 | -117.9 |
| 1 | 31 | Ferguson et al., 2013 | NB Mussel 1 | CDMa-13 | | -0.23 | -0.23 | 10 | Mod | Newport Beach | Main | 33.6 | -117.9 |
| 1 | 31 | Ferguson et al., 2013 | NB Mussel 1 | CDMa-16 | | -0.46 | -0.21 | 10 | Mod | Newport Beach | Main | 33.6 | -117.9 |
| 1 | 31 | Ferguson et al., 2013 | NB Mussel 1 | CDMa-19 | | -0.13 | -0.31 | 10 | Mod | Newport Beach | Main | 33.6 | -117.9 |
| 1 | 31 | Ferguson et al., 2013 | NB Mussel 1 | CDMa-28 | | 0.21 | -0.39 | 11 | Mod | Newport Beach | Main | 33.6 | -117.9 |
| 1 | 31 | Ferguson et al., 2013 | NB Mussel 1 | CDMa-31 | | 0.24 | -0.67 | 11 | Mod | Newport Beach | Main | 33.6 | -117.9 |
| 1 | 31 | Ferguson et al., 2013 | NB Mussel 1 | CDMa-34 | | 0.05 | -1.26 | 11 | Mod | Newport Beach | Main | 33.6 | -117.9 |
| 1 | 31 | Ferguson et al., 2013 | NB Mussel 1 | CDMa-37 | | 0.27 | -1.23 | 11 | Mod | Newport Beach | Main | 33.6 | -117.9 |
| 1 | 31 | Ferguson et al., 2013 | NB Mussel 1 | CDMa-4 | | -0.81 | -0.09 | 10 | Mod | Newport Beach | Main | 33.6 | -117.9 |
| 1 | 31 | Ferguson et al., 2013 | NB Mussel 1 | CDMa-40 | | 0.13 | -1.60 | 11 | Mod | Newport Beach | Main | 33.6 | -117.9 |
| 1 | 31 | Ferguson et al., 2013 | NB Mussel 1 | CDMa-43 | | 0.64 | -1.23 | 11 | Mod | Newport Beach | Main | 33.6 | -117.9 |

| | | | | | | | | | | | | | |
|---|---|---|---|---|---|---|---|---|---|---|---|---|---|
| 1 | 31 | Ferguson et al., 2013 | NB Mussel 1 | CDMa-46 | | 0.87 | -1.09 | 11 | Mod | Newport Beach | Main | 33.6 | -117.9 |
| 1 | 31 | Ferguson et al., 2013 | NB Mussel 1 | CDMa-49 | | 0.56 | -0.88 | 11 | Mod | Newport Beach | Main | 33.6 | -117.9 |
| 1 | 31 | Ferguson et al., 2013 | NB Mussel 1 | CDMa-52 | | 0.02 | -0.56 | 11 | Mod | Newport Beach | Main | 33.6 | -117.9 |
| 1 | 31 | Ferguson et al., 2013 | NB Mussel 1 | CDMa-55 | | 0.05 | -0.58 | 11 | Mod | Newport Beach | Main | 33.6 | -117.9 |
| 1 | 31 | Ferguson et al., 2013 | NB Mussel 1 | CDMa-58 | | 0.13 | -0.27 | 11 | Mod | Newport Beach | Main | 33.6 | -117.9 |
| 1 | 31 | Ferguson et al., 2013 | NB Mussel 1 | CDMa-61 | | 0.45 | -0.50 | 11 | Mod | Newport Beach | Main | 33.6 | -117.9 |
| 1 | 31 | Ferguson et al., 2013 | NB Mussel 1 | CDMa-64 | | 0.41 | -0.37 | 11 | Mod | Newport Beach | Main | 33.6 | -117.9 |
| 1 | 31 | Ferguson et al., 2013 | NB Mussel 1 | CDMa-67 | | 0.65 | -0.15 | 11 | Mod | Newport Beach | Main | 33.6 | -117.9 |
| 1 | 31 | Ferguson et al., 2013 | NB Mussel 1 | CDMa-7 | | -0.64 | -0.10 | 10 | Mod | Newport Beach | Main | 33.6 | -117.9 |
| 1 | 31 | Ferguson et al., 2013 | NB Mussel 1 | CDMa-70 | | 0.37 | -0.03 | 11 | Mod | Newport Beach | Main | 33.6 | -117.9 |
| 1 | 31 | Ferguson et al., 2013 | NB Mussel 1 | CDMa-73 | | 0.23 | -0.21 | 11 | Mod | Newport Beach | Main | 33.6 | -117.9 |
| 1 | 31 | Ferguson et al., 2013 | NB Mussel 1 | CDMa-76 | | 0.22 | -0.29 | 12 | Mod | Newport Beach | Main | 33.6 | -117.9 |
| 1 | 31 | Ferguson et al., 2013 | NB Mussel 1 | CDMa-79 | | 0.13 | -0.07 | 12 | Mod | Newport Beach | Main | 33.6 | -117.9 |
| 1 | 31 | Ferguson et al., 2013 | NB Mussel 1 | CDMa-82 | | -0.17 | -0.50 | 12 | Mod | Newport Beach | Main | 33.6 | -117.9 |
| 1 | 31 | Ferguson et al., 2013 | NB Mussel 1 | CDMa-85 | | 0.00 | -0.77 | 12 | Mod | Newport Beach | Main | 33.6 | -117.9 |
| 1 | 31 | Ferguson et al., 2013 | NB Mussel 1 | CDMa-88 | | 0.05 | -1.11 | 12 | Mod | Newport Beach | Main | 33.6 | -117.9 |
| 1 | 31 | Ferguson et al., 2013 | NB Mussel 1 | CDMa-91 | | 0.09 | -1.31 | 12 | Mod | Newport Beach | Main | 33.6 | -117.9 |
| 1 | 31 | Ferguson et al., 2013 | NB Mussel 1 | CDMa-94 | | 0.10 | -1.53 | 12 | Mod | Newport Beach | Main | 33.6 | -117.9 |
| 1 | 31 | Ferguson et al., 2013 | NB Mussel 1 | CDMa-97 | | 0.39 | -1.32 | 12 | Mod | Newport Beach | Main | 33.6 | -117.9 |

| | | | | | | | | | | | | | |
|---|---|---|---|---|---|---|---|---|---|---|---|---|---|
| 2 | 54 | Ferguson et al., 2013 | NB Mussel 2 | CDMb-1 | | -0.40 | -0.32 | 10 | Mod | Newport Beach | Main | 33.6 | -117.9 |
| 2 | 54 | Ferguson et al., 2013 | NB Mussel 2 | CDMb-2 | | -0.47 | 0.18 | 10 | Mod | Newport Beach | Main | 33.6 | -117.9 |
| 2 | 54 | Ferguson et al., 2013 | NB Mussel 2 | CDMb-10 | | -0.28 | -0.58 | 11 | Mod | Newport Beach | Main | 33.6 | -117.9 |
| 2 | 54 | Ferguson et al., 2013 | NB Mussel 2 | CDMb-11 | | -0.10 | -0.24 | 11 | Mod | Newport Beach | Main | 33.6 | -117.9 |
| 2 | 54 | Ferguson et al., 2013 | NB Mussel 2 | CDMb-13 | | -0.18 | -0.19 | 11 | Mod | Newport Beach | Main | 33.6 | -117.9 |
| 2 | 54 | Ferguson et al., 2013 | NB Mussel 2 | CDMb-14 | | -0.09 | -0.07 | 11 | Mod | Newport Beach | Main | 33.6 | -117.9 |
| 2 | 54 | Ferguson et al., 2013 | NB Mussel 2 | CDMb-17 | | 0.02 | 0.11 | 11 | Mod | Newport Beach | Main | 33.6 | -117.9 |
| 2 | 54 | Ferguson et al., 2013 | NB Mussel 2 | CDMb-19 | | -0.06 | -0.24 | 11 | Mod | Newport Beach | Main | 33.6 | -117.9 |
| 2 | 54 | Ferguson et al., 2013 | NB Mussel 2 | CDMb-4 | | -0.18 | -0.04 | 11 | Mod | Newport Beach | Main | 33.6 | -117.9 |
| 2 | 54 | Ferguson et al., 2013 | NB Mussel 2 | CDMb-7 | | 0.46 | -1.35 | 11 | Mod | Newport Beach | Main | 33.6 | -117.9 |
| 2 | 54 | Ferguson et al., 2013 | NB Mussel 2 | CDMb-8 | | 0.55 | -1.01 | 11 | Mod | Newport Beach | Main | 33.6 | -117.9 |
| 2 | 54 | Ferguson et al., 2013 | NB Mussel 2 | CDMb-20 | | -0.08 | -0.32 | 12 | Mod | Newport Beach | Main | 33.6 | -117.9 |
| 2 | 54 | Ferguson et al., 2013 | NB Mussel 2 | CDMb-22 | | 0.16 | -0.63 | 12 | Mod | Newport Beach | Main | 33.6 | -117.9 |
| 2 | 54 | Ferguson et al., 2013 | NB Mussel 2 | CDMb-25 | | 0.40 | -0.80 | 12 | Mod | Newport Beach | Main | 33.6 | -117.9 |
| 2 | 54 | Ferguson et al., 2013 | NB Mussel 2 | CDMb-26 | | 0.46 | -0.96 | 12 | Mod | Newport Beach | Main | 33.6 | -117.9 |
| 2 | 54 | Ferguson et al., 2013 | NB Mussel 2 | CDMb-28 | | 0.19 | -1.32 | 12 | Mod | Newport Beach | Main | 33.6 | -117.9 |
| 2 | 54 | Ferguson et al., 2013 | NB Mussel 2 | CDMb-29 | | 0.17 | -1.25 | 12 | Mod | Newport Beach | Main | 33.6 | -117.9 |
| 2 | 54 | Ferguson et al., 2013 | NB Mussel 2 | CDMb-31 | | -0.03 | -0.97 | 12 | Mod | Newport Beach | Main | 33.6 | -117.9 |
| 2 | 54 | Ferguson et al., 2013 | NB Mussel 2 | CDMb-32 | | 0.15 | -0.51 | 12 | Mod | Newport Beach | Main | 33.6 | -117.9 |

| | | | | | | | | | | | | | |
|---|---|---|---|---|---|---|---|---|---|---|---|---|---|
| 2 | 54 | Ferguson et al., 2013 | NB Mussel 2 | CDMb-34 | | 0.00 | -0.73 | 12 | Mod | Newport Beach | Main | 33.6 | -117.9 |
| 2 | 54 | Ferguson et al., 2013 | NB Mussel 2 | CDMb-37 | | -0.16 | -0.73 | 12 | Mod | Newport Beach | Main | 33.6 | -117.9 |
| 2 | 54 | Ferguson et al., 2013 | NB Mussel 2 | CDMb-40 | | 0.00 | -0.55 | 12 | Mod | Newport Beach | Main | 33.6 | -117.9 |
| 2 | 54 | Ferguson et al., 2013 | NB Mussel 2 | CDMb-41 | | -0.02 | -0.35 | 12 | Mod | Newport Beach | Main | 33.6 | -117.9 |
| 2 | 54 | Ferguson et al., 2013 | NB Mussel 2 | CDMb-43 | | -0.02 | -0.30 | 12 | Mod | Newport Beach | Main | 33.6 | -117.9 |
| 2 | 54 | Ferguson et al., 2013 | NB Mussel 2 | CDMb-44 | | -0.03 | 0.06 | 12 | Mod | Newport Beach | Main | 33.6 | -117.9 |
| 2 | 54 | Ferguson et al., 2013 | NB Mussel 2 | CDMb-46 | | 0.06 | -0.14 | 12 | Mod | Newport Beach | Main | 33.6 | -117.9 |
| 2 | 54 | Ferguson et al., 2013 | NB Mussel 2 | CDMb-49 | | -0.05 | -0.04 | 12 | Mod | Newport Beach | Main | 33.6 | -117.9 |
| 2 | 54 | Ferguson et al., 2013 | NB Mussel 2 | CDMb-50 | | 0.12 | 0.02 | 12 | Mod | Newport Beach | Main | 33.6 | -117.9 |
| 2 | 54 | Ferguson et al., 2013 | NB Mussel 2 | CDMb-52 | | 0.04 | 0.08 | 12 | Mod | Newport Beach | Main | 33.6 | -117.9 |
| 2 | 54 | Ferguson et al., 2013 | NB Mussel 2 | CDMb-53 | | 0.02 | 0.14 | 12 | Mod | Newport Beach | Main | 33.6 | -117.9 |
| 2 | 54 | Ferguson et al., 2013 | NB Mussel 2 | CDMb-55 | | -0.01 | 0.58 | 12 | Mod | Newport Beach | Main | 33.6 | -117.9 |
| 2 | 54 | Ferguson et al., 2013 | NB Mussel 2 | CDMb-56 | | 0.01 | 0.15 | 12 | Mod | Newport Beach | Main | 33.6 | -117.9 |
| 2 | 54 | Ferguson et al., 2013 | NB Mussel 2 | CDMb-58 | | -0.18 | 0.34 | 12 | Mod | Newport Beach | Main | 33.6 | -117.9 |
| 2 | 54 | Ferguson et al., 2013 | NB Mussel 2 | CDMb-59 | | -0.05 | 0.37 | 12 | Mod | Newport Beach | Main | 33.6 | -117.9 |
| 2 | 54 | Ferguson et al., 2013 | NB Mussel 2 | CDMb-61 | | -0.17 | 0.37 | 12 | Mod | Newport Beach | Main | 33.6 | -117.9 |
| 2 | 54 | Ferguson et al., 2013 | NB Mussel 2 | CDMb-62 | | -0.21 | 0.30 | 12 | Mod | Newport Beach | Main | 33.6 | -117.9 |
| 2 | 54 | Ferguson et al., 2013 | NB Mussel 2 | CDMb-65 | | -0.07 | -0.10 | 13 | Mod | Newport Beach | Main | 33.6 | -117.9 |
| 2 | 54 | Ferguson et al., 2013 | NB Mussel 2 | CDMb-67 | | 0.39 | -0.70 | 13 | Mod | Newport Beach | Main | 33.6 | -117.9 |

| | | | | | | | | | | | | | |
|---|---|---|---|---|---|---|---|---|---|---|---|---|---|
| 2 | 54 | Ferguson et al., 2013 | NB Mussel 2 | CDMb-68 | | 0.36 | -0.95 | 13 | Mod | Newport Beach | Main | 33.6 | -117.9 |
| 2 | 54 | Ferguson et al., 2013 | NB Mussel 2 | CDMb-70 | | 0.29 | -1.27 | 13 | Mod | Newport Beach | Main | 33.6 | -117.9 |
| 2 | 54 | Ferguson et al., 2013 | NB Mussel 2 | CDMb-71 | | 0.41 | -1.03 | 13 | Mod | Newport Beach | Main | 33.6 | -117.9 |
| 2 | 54 | Ferguson et al., 2013 | NB Mussel 2 | CDMb-73 | | 0.47 | -0.90 | 13 | Mod | Newport Beach | Main | 33.6 | -117.9 |
| 2 | 54 | Ferguson et al., 2013 | NB Mussel 2 | CDMb-74 | | 0.53 | -0.72 | 13 | Mod | Newport Beach | Main | 33.6 | -117.9 |
| 2 | 54 | Ferguson et al., 2013 | NB Mussel 2 | CDMb-76 | | 0.57 | -0.47 | 13 | Mod | Newport Beach | Main | 33.6 | -117.9 |
| 2 | 54 | Ferguson et al., 2013 | NB Mussel 2 | CDMb-77 | | 0.37 | -0.56 | 13 | Mod | Newport Beach | Main | 33.6 | -117.9 |
| 2 | 54 | Ferguson et al., 2013 | NB Mussel 2 | CDMb-79 | | 0.13 | -0.34 | 13 | Mod | Newport Beach | Main | 33.6 | -117.9 |
| 2 | 54 | Ferguson et al., 2013 | NB Mussel 2 | CDMb-80 | | -0.11 | -0.25 | 13 | Mod | Newport Beach | Main | 33.6 | -117.9 |
| 2 | 54 | Ferguson et al., 2013 | NB Mussel 2 | CDMb-82 | | -0.24 | -0.05 | 13 | Mod | Newport Beach | Main | 33.6 | -117.9 |
| 2 | 54 | Ferguson et al., 2013 | NB Mussel 2 | CDMb-83 | | -0.24 | -0.03 | 13 | Mod | Newport Beach | Main | 33.6 | -117.9 |
| 2 | 54 | Ferguson et al., 2013 | NB Mussel 2 | CDMb-85 | | -0.20 | 0.09 | 13 | Mod | Newport Beach | Main | 33.6 | -117.9 |
| 2 | 54 | Ferguson et al., 2013 | NB Mussel 2 | CDMb-86 | | -0.15 | 0.02 | 13 | Mod | Newport Beach | Main | 33.6 | -117.9 |
| 2 | 54 | Ferguson et al., 2013 | NB Mussel 2 | CDMb-89 | | 0.17 | -0.68 | 14 | Mod | Newport Beach | Main | 33.6 | -117.9 |
| 2 | 54 | Ferguson et al., 2013 | NB Mussel 2 | CDMb-91 | | 0.38 | -0.69 | 14 | Mod | Newport Beach | Main | 33.6 | -117.9 |
| 2 | 54 | Ferguson et al., 2013 | NB Mussel 2 | CDMb-94 | | 0.55 | -0.59 | 14 | Mod | Newport Beach | Main | 33.6 | -117.9 |
| 3 | 19 | Ferguson et al., 2013 | NB Mussel 3 | CDM2-1 | | 0.82 | -0.38 | 11 | Mod | Newport Beach | Main | 33.6 | -117.9 |
| 3 | 19 | Ferguson et al., 2013 | NB Mussel 3 | CDM2-11 | | 0.69 | -0.72 | 11 | Mod | Newport Beach | Main | 33.6 | -117.9 |
| 3 | 19 | Ferguson et al., 2013 | NB Mussel 3 | CDM2-12 | | 0.59 | -0.92 | 11 | Mod | Newport Beach | Main | 33.6 | -117.9 |

| | | | | | | | | | | | | | |
|---|---|---|---|---|---|---|---|---|---|---|---|---|---|
| 3 | 19 | Ferguson et al., 2013 | NB Mussel 3 | CDM2-14 | | 0.71 | -0.82 | 11 | Mod | Newport Beach | Main | 33.6 | -117.9 |
| 3 | 19 | Ferguson et al., 2013 | NB Mussel 3 | CDM2-15 | | 0.64 | -0.82 | 11 | Mod | Newport Beach | Main | 33.6 | -117.9 |
| 3 | 19 | Ferguson et al., 2013 | NB Mussel 3 | CDM2-16 | | 0.96 | -0.48 | 11 | Mod | Newport Beach | Main | 33.6 | -117.9 |
| 3 | 19 | Ferguson et al., 2013 | NB Mussel 3 | CDM2-17 | | 0.96 | -0.44 | 11 | Mod | Newport Beach | Main | 33.6 | -117.9 |
| 3 | 19 | Ferguson et al., 2013 | NB Mussel 3 | CDM2-19 | | 0.72 | -0.09 | 11 | Mod | Newport Beach | Main | 33.6 | -117.9 |
| 3 | 19 | Ferguson et al., 2013 | NB Mussel 3 | CDM2-21 | | 0.73 | -0.28 | 11 | Mod | Newport Beach | Main | 33.6 | -117.9 |
| 3 | 19 | Ferguson et al., 2013 | NB Mussel 3 | CDM2-22 | | 0.62 | -0.25 | 11 | Mod | Newport Beach | Main | 33.6 | -117.9 |
| 3 | 19 | Ferguson et al., 2013 | NB Mussel 3 | CDM2-23 | | 0.72 | -0.27 | 11 | Mod | Newport Beach | Main | 33.6 | -117.9 |
| 3 | 19 | Ferguson et al., 2013 | NB Mussel 3 | CDM2-24 | | 0.52 | 0.03 | 11 | Mod | Newport Beach | Main | 33.6 | -117.9 |
| 3 | 19 | Ferguson et al., 2013 | NB Mussel 3 | CDM2-25 | | 0.59 | -0.45 | 11 | Mod | Newport Beach | Main | 33.6 | -117.9 |
| 3 | 19 | Ferguson et al., 2013 | NB Mussel 3 | CDM2-26 | | 0.69 | -0.22 | 11 | Mod | Newport Beach | Main | 33.6 | -117.9 |
| 3 | 19 | Ferguson et al., 2013 | NB Mussel 3 | CDM2-27 | | 0.53 | 0.06 | 11 | Mod | Newport Beach | Main | 33.6 | -117.9 |
| 3 | 19 | Ferguson et al., 2013 | NB Mussel 3 | CDM2-28 | | 0.59 | 0.00 | 11 | Mod | Newport Beach | Main | 33.6 | -117.9 |
| 3 | 19 | Ferguson et al., 2013 | NB Mussel 3 | CDM2-7 | | 0.36 | -0.73 | 11 | Mod | Newport Beach | Main | 33.6 | -117.9 |
| 3 | 19 | Ferguson et al., 2013 | NB Mussel 3 | CDM2-9 | | 0.34 | -0.23 | 11 | Mod | Newport Beach | Main | 33.6 | -117.9 |
| 3 | 19 | Ferguson et al., 2013 | NB Mussel 3 | CDM2-29 | | 0.72 | 0.01 | 12 | Mod | Newport Beach | Main | 33.6 | -117.9 |
| 4 | 21 | Ferguson et al., 2013 | NB Mussel 4 | CDM3-1 | | 0.52 | -0.64 | 11 | Mod | Newport Beach | Main | 33.6 | -117.9 |
| 4 | 21 | Ferguson et al., 2013 | NB Mussel 4 | CDM3-2 | | 0.48 | -0.85 | 11 | Mod | Newport Beach | Main | 33.6 | -117.9 |
| 4 | 21 | Ferguson et al., 2013 | NB Mussel 4 | CDM3-3 | | 0.50 | -0.72 | 11 | Mod | Newport Beach | Main | 33.6 | -117.9 |

| | | | | | | | | | | | | | |
|---|---|---|---|---|---|---|---|---|---|---|---|---|---|
| 4 | 21 | Ferguson et al., 2013 | NB Mussel 4 | CDM3-4 | | 0.51 | -0.51 | 11 | Mod | Newport Beach | Main | 33.6 | -117.9 |
| 4 | 21 | Ferguson et al., 2013 | NB Mussel 4 | CDM3-5 | | 0.46 | -0.48 | 11 | Mod | Newport Beach | Main | 33.6 | -117.9 |
| 4 | 21 | Ferguson et al., 2013 | NB Mussel 4 | CDM3-6 | | 0.54 | -0.40 | 11 | Mod | Newport Beach | Main | 33.6 | -117.9 |
| 4 | 21 | Ferguson et al., 2013 | NB Mussel 4 | CDM3-7 | | 0.41 | -0.39 | 11 | Mod | Newport Beach | Main | 33.6 | -117.9 |
| 4 | 21 | Ferguson et al., 2013 | NB Mussel 4 | CDM3-10 | | 0.31 | -0.75 | 12 | Mod | Newport Beach | Main | 33.6 | -117.9 |
| 4 | 21 | Ferguson et al., 2013 | NB Mussel 4 | CDM3-12* | | 0.35 | -0.75 | 12 | Mod | Newport Beach | Main | 33.6 | -117.9 |
| 4 | 21 | Ferguson et al., 2013 | NB Mussel 4 | CDM3-14 | | 0.56 | -1.02 | 12 | Mod | Newport Beach | Main | 33.6 | -117.9 |
| 4 | 21 | Ferguson et al., 2013 | NB Mussel 4 | CDM3-15 | | 0.54 | -1.26 | 12 | Mod | Newport Beach | Main | 33.6 | -117.9 |
| 4 | 21 | Ferguson et al., 2013 | NB Mussel 4 | CDM3-16 | | 0.64 | -1.12 | 12 | Mod | Newport Beach | Main | 33.6 | -117.9 |
| 4 | 21 | Ferguson et al., 2013 | NB Mussel 4 | CDM3-17 | | 0.69 | -1.37 | 12 | Mod | Newport Beach | Main | 33.6 | -117.9 |
| 4 | 21 | Ferguson et al., 2013 | NB Mussel 4 | CDM3-18 | | 0.80 | -0.98 | 12 | Mod | Newport Beach | Main | 33.6 | -117.9 |
| 4 | 21 | Ferguson et al., 2013 | NB Mussel 4 | CDM3-20 | | 0.96 | -1.15 | 12 | Mod | Newport Beach | Main | 33.6 | -117.9 |
| 4 | 21 | Ferguson et al., 2013 | NB Mussel 4 | CDM3-21 | | 0.78 | -0.93 | 12 | Mod | Newport Beach | Main | 33.6 | -117.9 |
| 4 | 21 | Ferguson et al., 2013 | NB Mussel 4 | CDM3-22 | | 0.79 | -0.75 | 12 | Mod | Newport Beach | Main | 33.6 | -117.9 |
| 4 | 21 | Ferguson et al., 2013 | NB Mussel 4 | CDM3-23 | | 0.68 | -0.61 | 12 | Mod | Newport Beach | Main | 33.6 | -117.9 |
| 4 | 21 | Ferguson et al., 2013 | NB Mussel 4 | CDM3-24 | | 0.57 | -0.44 | 12 | Mod | Newport Beach | Main | 33.6 | -117.9 |
| 4 | 21 | Ferguson et al., 2013 | NB Mussel 4 | CDM3-8 | | 0.40 | -0.44 | 12 | Mod | Newport Beach | Main | 33.6 | -117.9 |
| 4 | 21 | Ferguson et al., 2013 | NB Mussel 4 | CDM3-9 | | 0.41 | -0.50 | 12 | Mod | Newport Beach | Main | 33.6 | -117.9 |
| 5 | 8 | Flores 2017 | T1-1-A | 1.00 | | 0.04 | 0.56 | 595 | Mid | Santa Cruz Island | Island | 34.057 | -119.9 |

| | | | | | | | | | | | | | |
|---|---|---|---|---|---|---|---|---|---|---|---|---|---|
| 5 | 8 | Flores 2017 | T1-1-B | 2.00 | | -0.23 | 1.24 | 595 | Mid | Santa Cruz Island | Island | 34.057 | -119.9 |
| 5 | 8 | Flores 2017 | T1-1-C | 3.00 | | 0.05 | 1.07 | 595 | Mid | Santa Cruz Island | Island | 34.057 | -119.9 |
| 5 | 8 | Flores 2017 | T1-1-D | 4.00 | | 0.02 | 0.88 | 595 | Mid | Santa Cruz Island | Island | 34.057 | -119.9 |
| 5 | 8 | Flores 2017 | T1-1-E | 5.00 | | 0.10 | 1.03 | 595 | Mid | Santa Cruz Island | Island | 34.057 | -119.9 |
| 5 | 8 | Flores 2017 | T1-1-F | 6.00 | | -0.22 | 0.83 | 595 | Mid | Santa Cruz Island | Island | 34.057 | -119.9 |
| 5 | 8 | Flores 2017 | T1-1-G | 7.00 | | 0.34 | 0.79 | 595 | Mid | Santa Cruz Island | Island | 34.057 | -119.9 |
| 5 | 8 | Flores 2017 | T1-1-H | 8.00 | | 0.45 | 0.71 | 595 | Mid | Santa Cruz Island | Island | 34.057 | -119.9 |
| 6 | 8 | Flores 2017 | T1-2-A | 1.00 | | 1.19 | -0.09 | 595 | Mid | Santa Cruz Island | Island | 34.057 | -119.9 |
| 6 | 8 | Flores 2017 | T1-2-B | 2.00 | | 0.84 | -0.17 | 595 | Mid | Santa Cruz Island | Island | 34.057 | -119.9 |
| 6 | 8 | Flores 2017 | T1-2-C | 3.00 | | 0.92 | -0.02 | 595 | Mid | Santa Cruz Island | Island | 34.057 | -119.9 |
| 6 | 8 | Flores 2017 | T1-2-D | 4.00 | | 0.67 | 0.01 | 595 | Mid | Santa Cruz Island | Island | 34.057 | -119.9 |
| 6 | 8 | Flores 2017 | T1-2-E | 5.00 | | 0.43 | 0.47 | 595 | Mid | Santa Cruz Island | Island | 34.057 | -119.9 |
| 6 | 8 | Flores 2017 | T1-2-F | 6.00 | | 0.31 | 0.27 | 595 | Mid | Santa Cruz Island | Island | 34.057 | -119.9 |
| 6 | 8 | Flores 2017 | T1-2-G | 7.00 | | 0.34 | 0.17 | 595 | Mid | Santa Cruz Island | Island | 34.057 | -119.9 |
| 6 | 8 | Flores 2017 | T1-2-H | 8.00 | | 0.34 | 0.11 | 595 | Mid | Santa Cruz Island | Island | 34.057 | -119.9 |
| 7 | 8 | Flores 2017 | T1-3-A | 1.00 | | 0.04 | 0.61 | 595 | Mid | Santa Cruz Island | Island | 34.057 | -119.9 |
| 7 | 8 | Flores 2017 | T1-3-B | 2.00 | | 0.45 | 0.56 | 595 | Mid | Santa Cruz Island | Island | 34.057 | -119.9 |
| 7 | 8 | Flores 2017 | T1-3-C | 3.00 | | 0.59 | 0.51 | 595 | Mid | Santa Cruz Island | Island | 34.057 | -119.9 |
| 7 | 8 | Flores 2017 | T1-3-D | 4.00 | | 0.51 | 0.36 | 595 | Mid | Santa Cruz Island | Island | 34.057 | -119.9 |

| | | | | | | | | | | | | | |
|---|---|---|---|---|---|---|---|---|---|---|---|---|---|
| 7 | 8 | Flores 2017 | T1-3-E | 5.00 | | 0.53 | 0.40 | 595 | Mid | Santa Cruz Island | Island | 34.057 | -119.9 |
| 7 | 8 | Flores 2017 | T1-3-F | 6.00 | | 0.11 | 0.39 | 595 | Mid | Santa Cruz Island | Island | 34.057 | -119.9 |
| 7 | 8 | Flores 2017 | T1-3-G | 7.00 | | 0.24 | -0.06 | 595 | Mid | Santa Cruz Island | Island | 34.057 | -119.9 |
| 7 | 8 | Flores 2017 | T1-3-H | 8.00 | | 0.39 | 0.09 | 595 | Mid | Santa Cruz Island | Island | 34.057 | -119.9 |
| 8 | 9 | Flores 2017 | T10.1.B | 3.00 | | -1.94 | -1.39 | 1974 | Mid | Santa Cruz Island | Island | 34.057 | -119.9 |
| 8 | 9 | Flores 2017 | T10.1.C | 4.00 | | -1.12 | -1.61 | 1974 | Mid | Santa Cruz Island | Island | 34.057 | -119.9 |
| 8 | 9 | Flores 2017 | T10.1.D | 5.00 | | -0.72 | -1.41 | 1974 | Mid | Santa Cruz Island | Island | 34.057 | -119.9 |
| 8 | 9 | Flores 2017 | T10.1.E | 6.00 | | -0.73 | -0.30 | 1974 | Mid | Santa Cruz Island | Island | 34.057 | -119.9 |
| 8 | 9 | Flores 2017 | T10.1.F | 7.00 | | -1.63 | -0.80 | 1974 | Mid | Santa Cruz Island | Island | 34.057 | -119.9 |
| 8 | 9 | Flores 2017 | T10.1.G | 8.00 | | -1.67 | -1.75 | 1974 | Mid | Santa Cruz Island | Island | 34.057 | -119.9 |
| 8 | 9 | Flores 2017 | T10.1.H | 9.00 | | -0.93 | -1.29 | 1974 | Mid | Santa Cruz Island | Island | 34.057 | -119.9 |
| 9 | 8 | Flores 2017 | T10.2.A | 1.00 | | -0.64 | -0.74 | 1974 | Mid | Santa Cruz Island | Island | 34.057 | -119.9 |
| 9 | 8 | Flores 2017 | T10.2.B | 2.00 | | -0.58 | 0.16 | 1974 | Mid | Santa Cruz Island | Island | 34.057 | -119.9 |
| 9 | 8 | Flores 2017 | T10.2.C | 3.00 | | -0.24 | -0.22 | 1974 | Mid | Santa Cruz Island | Island | 34.057 | -119.9 |
| 9 | 8 | Flores 2017 | T10.2.D | 4.00 | | -0.23 | 0.37 | 1974 | Mid | Santa Cruz Island | Island | 34.057 | -119.9 |
| 9 | 8 | Flores 2017 | T10.2.E | 5.00 | | -0.06 | 0.32 | 1974 | Mid | Santa Cruz Island | Island | 34.057 | -119.9 |
| 9 | 8 | Flores 2017 | T10.2.F | 6.00 | | -0.15 | 0.37 | 1974 | Mid | Santa Cruz Island | Island | 34.057 | -119.9 |
| 9 | 8 | Flores 2017 | T10.2.G | 7.00 | | 0.14 | 0.19 | 1974 | Mid | Santa Cruz Island | Island | 34.057 | -119.9 |
| 9 | 8 | Flores 2017 | T10.2.H | 8.00 | | -0.24 | -0.07 | 1974 | Mid | Santa Cruz Island | Island | 34.057 | -119.9 |

| | | | | | | | | | | | | | |
|---|---|---|---|---|---|---|---|---|---|---|---|---|---|
| 10 | 10 | Flores 2017 | T10.3.B a | 3.00 | | -2.69 | -2.35 | 1974 | Mid | Santa Cruz Island | Island | 34.057 | -119.9 |
| 10 | 10 | Flores 2017 | T10.3.B b | 4.00 | | -2.83 | -2.47 | 1974 | Mid | Santa Cruz Island | Island | 34.057 | -119.9 |
| 10 | 10 | Flores 2017 | T10.3.C | 5.00 | | -1.26 | -0.84 | 1974 | Mid | Santa Cruz Island | Island | 34.057 | -119.9 |
| 10 | 10 | Flores 2017 | T10.3.D | 6.00 | | -1.22 | -0.72 | 1974 | Mid | Santa Cruz Island | Island | 34.057 | -119.9 |
| 10 | 10 | Flores 2017 | T10.3.E | 7.00 | | -0.95 | -0.49 | 1974 | Mid | Santa Cruz Island | Island | 34.057 | -119.9 |
| 10 | 10 | Flores 2017 | T10.3.F | 8.00 | | -1.18 | -1.10 | 1974 | Mid | Santa Cruz Island | Island | 34.057 | -119.9 |
| 10 | 10 | Flores 2017 | T10.3.G | 9.00 | | -0.37 | -0.67 | 1974 | Mid | Santa Cruz Island | Island | 34.057 | -119.9 |
| 10 | 10 | Flores 2017 | T10.3.H | 10.00 | | -0.56 | -1.00 | 1974 | Mid | Santa Cruz Island | Island | 34.057 | -119.9 |
| 11 | 8 | Flores 2017 | T12.1.A | 1.00 | | -0.81 | -0.03 | 2062 | Mid | Santa Cruz Island | Island | 34.057 | -119.9 |
| 11 | 8 | Flores 2017 | T12.1.B | 2.00 | | -0.85 | 0.05 | 2062 | Mid | Santa Cruz Island | Island | 34.057 | -119.9 |
| 11 | 8 | Flores 2017 | T12.1.C | 3.00 | | -0.89 | 0.11 | 2062 | Mid | Santa Cruz Island | Island | 34.057 | -119.9 |
| 11 | 8 | Flores 2017 | T12.1.D | 4.00 | | -0.37 | 0.40 | 2062 | Mid | Santa Cruz Island | Island | 34.057 | -119.9 |
| 11 | 8 | Flores 2017 | T12.1.E | 5.00 | | 0.33 | 0.10 | 2062 | Mid | Santa Cruz Island | Island | 34.057 | -119.9 |
| 11 | 8 | Flores 2017 | T12.1.F | 6.00 | | 0.86 | -0.62 | 2062 | Mid | Santa Cruz Island | Island | 34.057 | -119.9 |
| 11 | 8 | Flores 2017 | T12.1.G | 7.00 | | 0.82 | -0.85 | 2062 | Mid | Santa Cruz Island | Island | 34.057 | -119.9 |
| 11 | 8 | Flores 2017 | T12.1.H | 8.00 | | 0.33 | -0.58 | 2062 | Mid | Santa Cruz Island | Island | 34.057 | -119.9 |
| 12 | 8 | Flores 2017 | T12.2.A | 1.00 | | 0.37 | 0.13 | 2062 | Mid | Santa Cruz Island | Island | 34.057 | -119.9 |
| 12 | 8 | Flores 2017 | T12.2.B | 2.00 | | 0.90 | 0.20 | 2062 | Mid | Santa Cruz Island | Island | 34.057 | -119.9 |
| 12 | 8 | Flores 2017 | T12.2.C | 3.00 | | 0.42 | 0.63 | 2062 | Mid | Santa Cruz Island | Island | 34.057 | -119.9 |

| | | | | | | | | | | | | | |
|---|---|---|---|---|---|---|---|---|---|---|---|---|---|
| 12 | 8 | Flores 2017 | T12.2.D | 4.00 | | 0.51 | 0.75 | 2062 | Mid | Santa Cruz Island | Island | 34.057 | -119.9 |
| 12 | 8 | Flores 2017 | T12.2.E | 5.00 | | 0.74 | 0.88 | 2062 | Mid | Santa Cruz Island | Island | 34.057 | -119.9 |
| 12 | 8 | Flores 2017 | T12.2.F | 6.00 | | 0.58 | 0.31 | 2062 | Mid | Santa Cruz Island | Island | 34.057 | -119.9 |
| 12 | 8 | Flores 2017 | T12.2.G | 7.00 | | 0.54 | 0.23 | 2062 | Mid | Santa Cruz Island | Island | 34.057 | -119.9 |
| 12 | 8 | Flores 2017 | T12.2.H | 8.00 | | 0.02 | 0.12 | 2062 | Mid | Santa Cruz Island | Island | 34.057 | -119.9 |
| 13 | 8 | Flores 2017 | T12.3.A | 1.00 | | 0.31 | 0.13 | 2062 | Mid | Santa Cruz Island | Island | 34.057 | -119.9 |
| 13 | 8 | Flores 2017 | T12.3.B | 2.00 | | 0.54 | 0.20 | 2062 | Mid | Santa Cruz Island | Island | 34.057 | -119.9 |
| 13 | 8 | Flores 2017 | T12.3.C | 3.00 | | 0.87 | 0.19 | 2062 | Mid | Santa Cruz Island | Island | 34.057 | -119.9 |
| 13 | 8 | Flores 2017 | T12.3.D | 4.00 | | 1.05 | -0.05 | 2062 | Mid | Santa Cruz Island | Island | 34.057 | -119.9 |
| 13 | 8 | Flores 2017 | T12.3.E | 5.00 | | 0.92 | 0.42 | 2062 | Mid | Santa Cruz Island | Island | 34.057 | -119.9 |
| 13 | 8 | Flores 2017 | T12.3.F | 6.00 | | 0.65 | 0.54 | 2062 | Mid | Santa Cruz Island | Island | 34.057 | -119.9 |
| 13 | 8 | Flores 2017 | T12.3.G | 7.00 | | 0.62 | 0.33 | 2062 | Mid | Santa Cruz Island | Island | 34.057 | -119.9 |
| 13 | 8 | Flores 2017 | T12.3.H | 8.00 | | 1.04 | 0.02 | 2062 | Mid | Santa Cruz Island | Island | 34.057 | -119.9 |
| 14 | 8 | Flores 2017 | T13.1.A | 1.00 | | 0.61 | -0.45 | 2106 | Mid | Santa Cruz Island | Island | 34.057 | -119.9 |
| 14 | 8 | Flores 2017 | T13.1.B | 2.00 | | 0.49 | -0.04 | 2106 | Mid | Santa Cruz Island | Island | 34.057 | -119.9 |
| 14 | 8 | Flores 2017 | T13.1.C | 3.00 | | 0.67 | 0.81 | 2106 | Mid | Santa Cruz Island | Island | 34.057 | -119.9 |
| 14 | 8 | Flores 2017 | T13.1.D | 4.00 | | 0.74 | 0.65 | 2106 | Mid | Santa Cruz Island | Island | 34.057 | -119.9 |
| 14 | 8 | Flores 2017 | T13.1.E | 5.00 | | 0.93 | 0.68 | 2106 | Mid | Santa Cruz Island | Island | 34.057 | -119.9 |
| 14 | 8 | Flores 2017 | T13.1.F | 6.00 | | 0.93 | 0.04 | 2106 | Mid | Santa Cruz Island | Island | 34.057 | -119.9 |

| | | | | | | | | | | | | | |
|---|---|---|---|---|---|---|---|---|---|---|---|---|---|
| 14 | 8 | Flores 2017 | T13.1.G | 7.00 | | 1.06 | 0.18 | 2106 | Mid | Santa Cruz Island | Island | 34.057 | -119.9 |
| 14 | 8 | Flores 2017 | T13.1.H | 8.00 | | 1.05 | -0.25 | 2106 | Mid | Santa Cruz Island | Island | 34.057 | -119.9 |
| 15 | 8 | Flores 2017 | T13.2.A | 1.00 | | 1.18 | -0.03 | 2106 | Mid | Santa Cruz Island | Island | 34.057 | -119.9 |
| 15 | 8 | Flores 2017 | T13.2.B | 2.00 | | 0.21 | 0.42 | 2106 | Mid | Santa Cruz Island | Island | 34.057 | -119.9 |
| 15 | 8 | Flores 2017 | T13.2.C | 3.00 | | 0.57 | 0.68 | 2106 | Mid | Santa Cruz Island | Island | 34.057 | -119.9 |
| 15 | 8 | Flores 2017 | T13.2.D | 4.00 | | 1.13 | -0.03 | 2106 | Mid | Santa Cruz Island | Island | 34.057 | -119.9 |
| 15 | 8 | Flores 2017 | T13.2.E | 5.00 | | 0.93 | 0.02 | 2106 | Mid | Santa Cruz Island | Island | 34.057 | -119.9 |
| 15 | 8 | Flores 2017 | T13.2.F | 6.00 | | 0.74 | 0.24 | 2106 | Mid | Santa Cruz Island | Island | 34.057 | -119.9 |
| 15 | 8 | Flores 2017 | T13.2.G | 7.00 | | 0.46 | 0.40 | 2106 | Mid | Santa Cruz Island | Island | 34.057 | -119.9 |
| 15 | 8 | Flores 2017 | T13.2.H | 8.00 | | 0.41 | 0.74 | 2106 | Mid | Santa Cruz Island | Island | 34.057 | -119.9 |
| 16 | 8 | Flores 2017 | T13.3.A | 1.00 | | 1.22 | 0.13 | 2106 | Mid | Santa Cruz Island | Island | 34.057 | -119.9 |
| 16 | 8 | Flores 2017 | T13.3.B | 2.00 | | 0.94 | 0.60 | 2106 | Mid | Santa Cruz Island | Island | 34.057 | -119.9 |
| 16 | 8 | Flores 2017 | T13.3.C | 3.00 | | 0.23 | 0.39 | 2106 | Mid | Santa Cruz Island | Island | 34.057 | -119.9 |
| 16 | 8 | Flores 2017 | T13.3.D | 4.00 | | 0.61 | 0.40 | 2106 | Mid | Santa Cruz Island | Island | 34.057 | -119.9 |
| 16 | 8 | Flores 2017 | T13.3.E | 5.00 | | 1.04 | -0.38 | 2106 | Mid | Santa Cruz Island | Island | 34.057 | -119.9 |
| 16 | 8 | Flores 2017 | T13.3.F | 6.00 | | 1.25 | -0.01 | 2106 | Mid | Santa Cruz Island | Island | 34.057 | -119.9 |
| 16 | 8 | Flores 2017 | T13.3.G | 7.00 | | 1.16 | 0.32 | 2106 | Mid | Santa Cruz Island | Island | 34.057 | -119.9 |
| 16 | 8 | Flores 2017 | T13.3.H | 8.00 | | 0.90 | 0.30 | 2106 | Mid | Santa Cruz Island | Island | 34.057 | -119.9 |
| 17 | 8 | Flores 2017 | T15.1.A | 1.00 | | 0.12 | 0.09 | 2195 | Mid | Santa Cruz Island | Island | 34.057 | -119.9 |

| | | | | | | | | | | | | | |
|---|---|---|---|---|---|---|---|---|---|---|---|---|---|
| 17 | 8 | Flores 2017 | T15.1.B | 2.00 | | -0.14 | 0.49 | 2195 | Mid | Santa Cruz Island | Island | 34.057 | -119.9 |
| 17 | 8 | Flores 2017 | T15.1.C | 3.00 | | 0.80 | 0.30 | 2195 | Mid | Santa Cruz Island | Island | 34.057 | -119.9 |
| 17 | 8 | Flores 2017 | T15.1.D | 4.00 | | 0.77 | -0.09 | 2195 | Mid | Santa Cruz Island | Island | 34.057 | -119.9 |
| 17 | 8 | Flores 2017 | T15.1.E | 5.00 | | 0.77 | 0.12 | 2195 | Mid | Santa Cruz Island | Island | 34.057 | -119.9 |
| 17 | 8 | Flores 2017 | T15.1.F | 6.00 | | 0.67 | 0.24 | 2195 | Mid | Santa Cruz Island | Island | 34.057 | -119.9 |
| 17 | 8 | Flores 2017 | T15.1.G | 7.00 | | 0.88 | 0.71 | 2195 | Mid | Santa Cruz Island | Island | 34.057 | -119.9 |
| 17 | 8 | Flores 2017 | T15.1.H | 8.00 | | 0.96 | 0.35 | 2195 | Mid | Santa Cruz Island | Island | 34.057 | -119.9 |
| 18 | 8 | Flores 2017 | T15.2.A | 1.00 | | 0.51 | 0.11 | 2195 | Mid | Santa Cruz Island | Island | 34.057 | -119.9 |
| 18 | 8 | Flores 2017 | T15.2.B | 2.00 | | 0.48 | 0.57 | 2195 | Mid | Santa Cruz Island | Island | 34.057 | -119.9 |
| 18 | 8 | Flores 2017 | T15.2.C | 3.00 | | 0.44 | 0.91 | 2195 | Mid | Santa Cruz Island | Island | 34.057 | -119.9 |
| 18 | 8 | Flores 2017 | T15.2.D | 4.00 | | 0.69 | 0.64 | 2195 | Mid | Santa Cruz Island | Island | 34.057 | -119.9 |
| 18 | 8 | Flores 2017 | T15.2.E | 5.00 | | 1.00 | 0.04 | 2195 | Mid | Santa Cruz Island | Island | 34.057 | -119.9 |
| 18 | 8 | Flores 2017 | T15.2.F | 6.00 | | 0.78 | 0.16 | 2195 | Mid | Santa Cruz Island | Island | 34.057 | -119.9 |
| 18 | 8 | Flores 2017 | T15.2.G | 7.00 | | 0.28 | 0.68 | 2195 | Mid | Santa Cruz Island | Island | 34.057 | -119.9 |
| 18 | 8 | Flores 2017 | T15.2.H | 8.00 | | 0.30 | 0.64 | 2195 | Mid | Santa Cruz Island | Island | 34.057 | -119.9 |
| 19 | 8 | Flores 2017 | T15.3.A | 1.00 | | 0.66 | 0.66 | 2195 | Mid | Santa Cruz Island | Island | 34.057 | -119.9 |
| 19 | 8 | Flores 2017 | T15.3.B | 2.00 | | 0.84 | 0.55 | 2195 | Mid | Santa Cruz Island | Island | 34.057 | -119.9 |
| 19 | 8 | Flores 2017 | T15.3.C | 3.00 | | 0.67 | 0.74 | 2195 | Mid | Santa Cruz Island | Island | 34.057 | -119.9 |
| 19 | 8 | Flores 2017 | T15.3.D | 4.00 | | 1.03 | 0.25 | 2195 | Mid | Santa Cruz Island | Island | 34.057 | -119.9 |

| | | | | | | | | | | | | | |
|---|---|---|---|---|---|---|---|---|---|---|---|---|---|
| 19 | 8 | Flores 2017 | T15.3.E | 5.00 | | 0.66 | 0.55 | 2195 | Mid | Santa Cruz Island | Island | 34.057 | -119.9 |
| 19 | 8 | Flores 2017 | T15.3.F | 6.00 | | 0.46 | 0.78 | 2195 | Mid | Santa Cruz Island | Island | 34.057 | -119.9 |
| 19 | 8 | Flores 2017 | T15.3.G | 7.00 | | 0.63 | 0.71 | 2195 | Mid | Santa Cruz Island | Island | 34.057 | -119.9 |
| 19 | 8 | Flores 2017 | T15.3.H | 8.00 | | 0.77 | 0.39 | 2195 | Mid | Santa Cruz Island | Island | 34.057 | -119.9 |
| 20 | 8 | Flores 2017 | T17.1.A | 1.00 | | 0.30 | 0.97 | 2285 | Mid | Santa Cruz Island | Island | 34.057 | -119.9 |
| 20 | 8 | Flores 2017 | T17.1.B | 2.00 | | 0.22 | 0.78 | 2285 | Mid | Santa Cruz Island | Island | 34.057 | -119.9 |
| 20 | 8 | Flores 2017 | T17.1.C | 3.00 | | 0.26 | 0.47 | 2285 | Mid | Santa Cruz Island | Island | 34.057 | -119.9 |
| 20 | 8 | Flores 2017 | T17.1.D | 4.00 | | 0.57 | 0.00 | 2285 | Mid | Santa Cruz Island | Island | 34.057 | -119.9 |
| 20 | 8 | Flores 2017 | T17.1.E | 5.00 | | 0.64 | -0.19 | 2285 | Mid | Santa Cruz Island | Island | 34.057 | -119.9 |
| 20 | 8 | Flores 2017 | T17.1.F | 6.00 | | 0.45 | -0.01 | 2285 | Mid | Santa Cruz Island | Island | 34.057 | -119.9 |
| 20 | 8 | Flores 2017 | T17.1.G | 7.00 | | -0.17 | 0.41 | 2285 | Mid | Santa Cruz Island | Island | 34.057 | -119.9 |
| 20 | 8 | Flores 2017 | T17.1.H | 8.00 | | -0.45 | 0.60 | 2285 | Mid | Santa Cruz Island | Island | 34.057 | -119.9 |
| 21 | 8 | Flores 2017 | T17.2.A | 1.00 | | 0.39 | 1.22 | 2285 | Mid | Santa Cruz Island | Island | 34.057 | -119.9 |
| 21 | 8 | Flores 2017 | T17.2.B | 2.00 | | 0.44 | 0.78 | 2285 | Mid | Santa Cruz Island | Island | 34.057 | -119.9 |
| 21 | 8 | Flores 2017 | T17.2.C | 3.00 | | 0.52 | 0.91 | 2285 | Mid | Santa Cruz Island | Island | 34.057 | -119.9 |
| 21 | 8 | Flores 2017 | T17.2.D | 4.00 | | 0.94 | -0.04 | 2285 | Mid | Santa Cruz Island | Island | 34.057 | -119.9 |
| 21 | 8 | Flores 2017 | T17.2.E | 5.00 | | 0.78 | 0.18 | 2285 | Mid | Santa Cruz Island | Island | 34.057 | -119.9 |
| 21 | 8 | Flores 2017 | T17.2.F | 6.00 | | 0.34 | 0.33 | 2285 | Mid | Santa Cruz Island | Island | 34.057 | -119.9 |
| 21 | 8 | Flores 2017 | T17.2.G | 7.00 | | 0.69 | 0.61 | 2285 | Mid | Santa Cruz Island | Island | 34.057 | -119.9 |

| | | | | | | | | | | | | | |
|---|---|---|---|---|---|---|---|---|---|---|---|---|---|
| 21 | 8 | Flores 2017 | T17.2.H | 8.00 | | 0.26 | 0.61 | 2285 | Mid | Santa Cruz Island | Island | 34.057 | -119.9 |
| 22 | 8 | Flores 2017 | T17.3.A | 1.00 | | 0.78 | 1.08 | 2285 | Mid | Santa Cruz Island | Island | 34.057 | -119.9 |
| 22 | 8 | Flores 2017 | T17.3.B | 2.00 | | 0.79 | 0.77 | 2285 | Mid | Santa Cruz Island | Island | 34.057 | -119.9 |
| 22 | 8 | Flores 2017 | T17.3.C | 3.00 | | 0.59 | 0.72 | 2285 | Mid | Santa Cruz Island | Island | 34.057 | -119.9 |
| 22 | 8 | Flores 2017 | T17.3.D | 4.00 | | 0.99 | 0.21 | 2285 | Mid | Santa Cruz Island | Island | 34.057 | -119.9 |
| 22 | 8 | Flores 2017 | T17.3.E | 5.00 | | 0.91 | 0.01 | 2285 | Mid | Santa Cruz Island | Island | 34.057 | -119.9 |
| 22 | 8 | Flores 2017 | T17.3.F | 6.00 | | 0.49 | 0.40 | 2285 | Mid | Santa Cruz Island | Island | 34.057 | -119.9 |
| 22 | 8 | Flores 2017 | T17.3.G | 7.00 | | 0.15 | 0.74 | 2285 | Mid | Santa Cruz Island | Island | 34.057 | -119.9 |
| 22 | 8 | Flores 2017 | T17.3.H | 8.00 | | -0.40 | 0.79 | 2285 | Mid | Santa Cruz Island | Island | 34.057 | -119.9 |
| 23 | 8 | Flores 2017 | T18.1.A | 1.00 | | 0.28 | 0.33 | 2330 | Mid | Santa Cruz Island | Island | 34.057 | -119.9 |
| 23 | 8 | Flores 2017 | T18.1.B | 2.00 | | 0.50 | 0.52 | 2330 | Mid | Santa Cruz Island | Island | 34.057 | -119.9 |
| 23 | 8 | Flores 2017 | T18.1.C | 3.00 | | 0.38 | 0.49 | 2330 | Mid | Santa Cruz Island | Island | 34.057 | -119.9 |
| 23 | 8 | Flores 2017 | T18.1.D | 4.00 | | 0.08 | 0.75 | 2330 | Mid | Santa Cruz Island | Island | 34.057 | -119.9 |
| 23 | 8 | Flores 2017 | T18.1.E | 5.00 | | 0.52 | 1.09 | 2330 | Mid | Santa Cruz Island | Island | 34.057 | -119.9 |
| 23 | 8 | Flores 2017 | T18.1.F | 6.00 | | 0.41 | 0.72 | 2330 | Mid | Santa Cruz Island | Island | 34.057 | -119.9 |
| 23 | 8 | Flores 2017 | T18.1.G | 7.00 | | 0.55 | 0.35 | 2330 | Mid | Santa Cruz Island | Island | 34.057 | -119.9 |
| 23 | 8 | Flores 2017 | T18.1.H | 8.00 | | 0.73 | -0.13 | 2330 | Mid | Santa Cruz Island | Island | 34.057 | -119.9 |
| 24 | 8 | Flores 2017 | T18.2.A | 1.00 | | 0.55 | 0.75 | 2330 | Mid | Santa Cruz Island | Island | 34.057 | -119.9 |
| 24 | 8 | Flores 2017 | T18.2.B | 2.00 | | 0.19 | 0.91 | 2330 | Mid | Santa Cruz Island | Island | 34.057 | -119.9 |

| | | | | | | | | | | | | | |
|---|---|---|---|---|---|---|---|---|---|---|---|---|---|
| 24 | 8 | Flores 2017 | T18.2.C | 3.00 | | 0.70 | 0.13 | 2330 | Mid | Santa Cruz Island | Island | 34.057 | -119.9 |
| 24 | 8 | Flores 2017 | T18.2.D | 4.00 | | 0.11 | 0.48 | 2330 | Mid | Santa Cruz Island | Island | 34.057 | -119.9 |
| 24 | 8 | Flores 2017 | T18.2.E | 5.00 | | -0.29 | 0.92 | 2330 | Mid | Santa Cruz Island | Island | 34.057 | -119.9 |
| 24 | 8 | Flores 2017 | T18.2.F | 6.00 | | 0.30 | 0.81 | 2330 | Mid | Santa Cruz Island | Island | 34.057 | -119.9 |
| 24 | 8 | Flores 2017 | T18.2.G | 7.00 | | 0.45 | 0.66 | 2330 | Mid | Santa Cruz Island | Island | 34.057 | -119.9 |
| 24 | 8 | Flores 2017 | T18.2.H | 8.00 | | 0.50 | -0.41 | 2330 | Mid | Santa Cruz Island | Island | 34.057 | -119.9 |
| 25 | 8 | Flores 2017 | T18.3.A | 1.00 | | 0.87 | 0.68 | 2330 | Mid | Santa Cruz Island | Island | 34.057 | -119.9 |
| 25 | 8 | Flores 2017 | T18.3.B | 2.00 | | 0.49 | 0.46 | 2330 | Mid | Santa Cruz Island | Island | 34.057 | -119.9 |
| 25 | 8 | Flores 2017 | T18.3.C | 3.00 | | 0.86 | 0.24 | 2330 | Mid | Santa Cruz Island | Island | 34.057 | -119.9 |
| 25 | 8 | Flores 2017 | T18.3.D | 4.00 | | 0.74 | 0.01 | 2330 | Mid | Santa Cruz Island | Island | 34.057 | -119.9 |
| 25 | 8 | Flores 2017 | T18.3.E | 5.00 | | 0.97 | -0.35 | 2330 | Mid | Santa Cruz Island | Island | 34.057 | -119.9 |
| 25 | 8 | Flores 2017 | T18.3.F | 6.00 | | 1.04 | -0.42 | 2330 | Mid | Santa Cruz Island | Island | 34.057 | -119.9 |
| 25 | 8 | Flores 2017 | T18.3.G | 7.00 | | 0.82 | -0.39 | 2330 | Mid | Santa Cruz Island | Island | 34.057 | -119.9 |
| 25 | 8 | Flores 2017 | T18.3.H | 8.00 | | 0.81 | -0.52 | 2330 | Mid | Santa Cruz Island | Island | 34.057 | -119.9 |
| 26 | 8 | Flores 2017 | T19.1.A | 1.00 | | -0.20 | 0.63 | 2375 | Mid | Santa Cruz Island | Island | 34.057 | -119.9 |
| 26 | 8 | Flores 2017 | T19.1.B | 2.00 | | 0.29 | 1.03 | 2375 | Mid | Santa Cruz Island | Island | 34.057 | -119.9 |
| 26 | 8 | Flores 2017 | T19.1.C | 3.00 | | 0.86 | 0.73 | 2375 | Mid | Santa Cruz Island | Island | 34.057 | -119.9 |
| 26 | 8 | Flores 2017 | T19.1.D | 4.00 | | 0.73 | -0.17 | 2375 | Mid | Santa Cruz Island | Island | 34.057 | -119.9 |
| 26 | 8 | Flores 2017 | T19.1.E | 5.00 | | 0.41 | -0.33 | 2375 | Mid | Santa Cruz Island | Island | 34.057 | -119.9 |

| | | | | | | | | | | | | | |
|---|---|---|---|---|---|---|---|---|---|---|---|---|---|
| 26 | 8 | Flores 2017 | T19.1.F | 6.00 | | 0.14 | 0.17 | 2375 | Mid | Santa Cruz Island | Island | 34.057 | -119.9 |
| 26 | 8 | Flores 2017 | T19.1.G | 7.00 | | -0.38 | 0.87 | 2375 | Mid | Santa Cruz Island | Island | 34.057 | -119.9 |
| 26 | 8 | Flores 2017 | T19.1.H | 8.00 | | -0.53 | 0.92 | 2375 | Mid | Santa Cruz Island | Island | 34.057 | -119.9 |
| 27 | 8 | Flores 2017 | T19.2.A | 1.00 | | -0.10 | 0.54 | 2375 | Mid | Santa Cruz Island | Island | 34.057 | -119.9 |
| 27 | 8 | Flores 2017 | T19.2.B | 2.00 | | -0.13 | 0.77 | 2375 | Mid | Santa Cruz Island | Island | 34.057 | -119.9 |
| 27 | 8 | Flores 2017 | T19.2.C | 3.00 | | 0.11 | 0.36 | 2375 | Mid | Santa Cruz Island | Island | 34.057 | -119.9 |
| 27 | 8 | Flores 2017 | T19.2.D | 4.00 | | 0.10 | 0.17 | 2375 | Mid | Santa Cruz Island | Island | 34.057 | -119.9 |
| 27 | 8 | Flores 2017 | T19.2.E | 5.00 | | 0.27 | -0.24 | 2375 | Mid | Santa Cruz Island | Island | 34.057 | -119.9 |
| 27 | 8 | Flores 2017 | T19.2.F | 6.00 | | 0.31 | -0.40 | 2375 | Mid | Santa Cruz Island | Island | 34.057 | -119.9 |
| 27 | 8 | Flores 2017 | T19.2.G | 7.00 | | 0.37 | -0.28 | 2375 | Mid | Santa Cruz Island | Island | 34.057 | -119.9 |
| 27 | 8 | Flores 2017 | T19.2.H | 8.00 | | 0.32 | -0.21 | 2375 | Mid | Santa Cruz Island | Island | 34.057 | -119.9 |
| 28 | 8 | Flores 2017 | T19.3.A | 1.00 | | 0.52 | -0.02 | 2375 | Mid | Santa Cruz Island | Island | 34.057 | -119.9 |
| 28 | 8 | Flores 2017 | T19.3.B | 2.00 | | 0.51 | 0.41 | 2375 | Mid | Santa Cruz Island | Island | 34.057 | -119.9 |
| 28 | 8 | Flores 2017 | T19.3.C | 3.00 | | 0.01 | 0.49 | 2375 | Mid | Santa Cruz Island | Island | 34.057 | -119.9 |
| 28 | 8 | Flores 2017 | T19.3.D | 4.00 | | -0.07 | 0.57 | 2375 | Mid | Santa Cruz Island | Island | 34.057 | -119.9 |
| 28 | 8 | Flores 2017 | T19.3.E | 5.00 | | -0.33 | 0.86 | 2375 | Mid | Santa Cruz Island | Island | 34.057 | -119.9 |
| 28 | 8 | Flores 2017 | T19.3.F | 6.00 | | 0.19 | 0.62 | 2375 | Mid | Santa Cruz Island | Island | 34.057 | -119.9 |
| 28 | 8 | Flores 2017 | T19.3.G | 7.00 | | 0.50 | 0.64 | 2375 | Mid | Santa Cruz Island | Island | 34.057 | -119.9 |
| 28 | 8 | Flores 2017 | T19.3.H | 8.00 | | 0.48 | 0.56 | 2375 | Mid | Santa Cruz Island | Island | 34.057 | -119.9 |

| | | | | | | | | | | | | | |
|---|---|---|---|---|---|---|---|---|---|---|---|---|---|
| 29 | 8 | Flores 2017 | T2-1-A | 1.00 | | 1.23 | 0.01 | 1190 | Mid | Santa Cruz Island | Island | 34.057 | -119.9 |
| 29 | 8 | Flores 2017 | T2-1-B | 2.00 | | 0.45 | 0.22 | 1190 | Mid | Santa Cruz Island | Island | 34.057 | -119.9 |
| 29 | 8 | Flores 2017 | T2-1-C | 3.00 | | 0.15 | 0.54 | 1190 | Mid | Santa Cruz Island | Island | 34.057 | -119.9 |
| 29 | 8 | Flores 2017 | T2-1-D | 4.00 | | -0.28 | 0.94 | 1190 | Mid | Santa Cruz Island | Island | 34.057 | -119.9 |
| 29 | 8 | Flores 2017 | T2-1-E | 5.00 | | 0.21 | 0.66 | 1190 | Mid | Santa Cruz Island | Island | 34.057 | -119.9 |
| 29 | 8 | Flores 2017 | T2-1-F | 6.00 | | 0.53 | 0.49 | 1190 | Mid | Santa Cruz Island | Island | 34.057 | -119.9 |
| 29 | 8 | Flores 2017 | T2-1-G | 7.00 | | 0.58 | 0.37 | 1190 | Mid | Santa Cruz Island | Island | 34.057 | -119.9 |
| 29 | 8 | Flores 2017 | T2-1-H | 8.00 | | 0.41 | 0.14 | 1190 | Mid | Santa Cruz Island | Island | 34.057 | -119.9 |
| 30 | 8 | Flores 2017 | T2-2-A | 1.00 | | 0.42 | -0.19 | 1190 | Mid | Santa Cruz Island | Island | 34.057 | -119.9 |
| 30 | 8 | Flores 2017 | T2-2-B | 2.00 | | 0.41 | -0.05 | 1190 | Mid | Santa Cruz Island | Island | 34.057 | -119.9 |
| 30 | 8 | Flores 2017 | T2-2-C | 3.00 | | 0.27 | 0.09 | 1190 | Mid | Santa Cruz Island | Island | 34.057 | -119.9 |
| 30 | 8 | Flores 2017 | T2-2-D | 4.00 | | 0.05 | 0.41 | 1190 | Mid | Santa Cruz Island | Island | 34.057 | -119.9 |
| 30 | 8 | Flores 2017 | T2-2-E | 5.00 | | -0.05 | 0.51 | 1190 | Mid | Santa Cruz Island | Island | 34.057 | -119.9 |
| 30 | 8 | Flores 2017 | T2-2-F | 6.00 | | 0.14 | 0.35 | 1190 | Mid | Santa Cruz Island | Island | 34.057 | -119.9 |
| 30 | 8 | Flores 2017 | T2-2-G | 7.00 | | 0.06 | 0.56 | 1190 | Mid | Santa Cruz Island | Island | 34.057 | -119.9 |
| 30 | 8 | Flores 2017 | T2-2-H | 8.00 | | -0.09 | 0.83 | 1190 | Mid | Santa Cruz Island | Island | 34.057 | -119.9 |
| 31 | 8 | Flores 2017 | T2-3-A | 1.00 | | 0.25 | 0.88 | 1190 | Mid | Santa Cruz Island | Island | 34.057 | -119.9 |
| 31 | 8 | Flores 2017 | T2-3-B | 2.00 | | 0.34 | 0.24 | 1190 | Mid | Santa Cruz Island | Island | 34.057 | -119.9 |
| 31 | 8 | Flores 2017 | T2-3-C | 3.00 | | -0.19 | 0.77 | 1190 | Mid | Santa Cruz Island | Island | 34.057 | -119.9 |

| | | | | | | | | | | | | | |
|---|---|---|---|---|---|---|---|---|---|---|---|---|---|
| 31 | 8 | Flores 2017 | T2-3-D | 4.00 | | -0.24 | 0.98 | 1190 | Mid | Santa Cruz Island | Island | 34.057 | -119.9 |
| 31 | 8 | Flores 2017 | T2-3-E | 5.00 | | 0.19 | 0.72 | 1190 | Mid | Santa Cruz Island | Island | 34.057 | -119.9 |
| 31 | 8 | Flores 2017 | T2-3-F | 6.00 | | 0.49 | 0.50 | 1190 | Mid | Santa Cruz Island | Island | 34.057 | -119.9 |
| 31 | 8 | Flores 2017 | T2-3-G | 7.00 | | 0.30 | 0.06 | 1190 | Mid | Santa Cruz Island | Island | 34.057 | -119.9 |
| 31 | 8 | Flores 2017 | T2-3-H | 8.00 | | 0.04 | -0.07 | 1190 | Mid | Santa Cruz Island | Island | 34.057 | -119.9 |
| 32 | 8 | Flores 2017 | T20.1.A | 1.00 | | 0.07 | 0.88 | 2420 | Mid | Santa Cruz Island | Island | 34.057 | -119.9 |
| 32 | 8 | Flores 2017 | T20.1.B | 2.00 | | 0.02 | 0.95 | 2420 | Mid | Santa Cruz Island | Island | 34.057 | -119.9 |
| 32 | 8 | Flores 2017 | T20.1.C | 3.00 | | 0.35 | 0.55 | 2420 | Mid | Santa Cruz Island | Island | 34.057 | -119.9 |
| 32 | 8 | Flores 2017 | T20.1.D | 4.00 | | 0.27 | 0.40 | 2420 | Mid | Santa Cruz Island | Island | 34.057 | -119.9 |
| 32 | 8 | Flores 2017 | T20.1.E | 5.00 | | 0.33 | 0.49 | 2420 | Mid | Santa Cruz Island | Island | 34.057 | -119.9 |
| 32 | 8 | Flores 2017 | T20.1.F | 6.00 | | 0.24 | 0.68 | 2420 | Mid | Santa Cruz Island | Island | 34.057 | -119.9 |
| 32 | 8 | Flores 2017 | T20.1.G | 7.00 | | 0.52 | 0.45 | 2420 | Mid | Santa Cruz Island | Island | 34.057 | -119.9 |
| 32 | 8 | Flores 2017 | T20.1.H | 8.00 | | 0.57 | 0.04 | 2420 | Mid | Santa Cruz Island | Island | 34.057 | -119.9 |
| 33 | 8 | Flores 2017 | T20.2.A | 1.00 | | 0.20 | -0.02 | 2420 | Mid | Santa Cruz Island | Island | 34.057 | -119.9 |
| 33 | 8 | Flores 2017 | T20.2.B | 2.00 | | 0.10 | -0.03 | 2420 | Mid | Santa Cruz Island | Island | 34.057 | -119.9 |
| 33 | 8 | Flores 2017 | T20.2.C | 3.00 | | -0.02 | 0.16 | 2420 | Mid | Santa Cruz Island | Island | 34.057 | -119.9 |
| 33 | 8 | Flores 2017 | T20.2.D | 4.00 | | 0.10 | 0.52 | 2420 | Mid | Santa Cruz Island | Island | 34.057 | -119.9 |
| 33 | 8 | Flores 2017 | T20.2.E | 5.00 | | 0.03 | 0.51 | 2420 | Mid | Santa Cruz Island | Island | 34.057 | -119.9 |
| 33 | 8 | Flores 2017 | T20.2.F | 6.00 | | 0.08 | 0.70 | 2420 | Mid | Santa Cruz Island | Island | 34.057 | -119.9 |

| | | | | | | | | | | | | | |
|---|---|---|---|---|---|---|---|---|---|---|---|---|---|
| 33 | 8 | Flores 2017 | T20.2.G | 7.00 | | 0.06 | 0.77 | 2420 | Mid | Santa Cruz Island | Island | 34.057 | -119.9 |
| 33 | 8 | Flores 2017 | T20.2.H | 8.00 | | 0.13 | 1.13 | 2420 | Mid | Santa Cruz Island | Island | 34.057 | -119.9 |
| 34 | 8 | Flores 2017 | T20.3.A | 1.00 | | 0.74 | 0.30 | 2420 | Mid | Santa Cruz Island | Island | 34.057 | -119.9 |
| 34 | 8 | Flores 2017 | T20.3.B | 2.00 | | 0.87 | 0.19 | 2420 | Mid | Santa Cruz Island | Island | 34.057 | -119.9 |
| 34 | 8 | Flores 2017 | T20.3.C | 3.00 | | 0.16 | 1.13 | 2420 | Mid | Santa Cruz Island | Island | 34.057 | -119.9 |
| 34 | 8 | Flores 2017 | T20.3.D | 4.00 | | 0.51 | 0.91 | 2420 | Mid | Santa Cruz Island | Island | 34.057 | -119.9 |
| 34 | 8 | Flores 2017 | T20.3.E | 5.00 | | 0.89 | 0.68 | 2420 | Mid | Santa Cruz Island | Island | 34.057 | -119.9 |
| 34 | 8 | Flores 2017 | T20.3.F | 6.00 | | 1.26 | 0.21 | 2420 | Mid | Santa Cruz Island | Island | 34.057 | -119.9 |
| 34 | 8 | Flores 2017 | T20.3.G | 7.00 | | 1.03 | 0.17 | 2420 | Mid | Santa Cruz Island | Island | 34.057 | -119.9 |
| 34 | 8 | Flores 2017 | T20.3.H | 8.00 | | 0.97 | 0.19 | 2420 | Mid | Santa Cruz Island | Island | 34.057 | -119.9 |
| 35 | 8 | Flores 2017 | T21.1.A | 1.00 | | 0.10 | 0.46 | 2420 | Mid | Santa Cruz Island | Island | 34.057 | -119.9 |
| 35 | 8 | Flores 2017 | T21.1.B | 2.00 | | -0.37 | 0.56 | 2420 | Mid | Santa Cruz Island | Island | 34.057 | -119.9 |
| 35 | 8 | Flores 2017 | T21.1.C | 3.00 | | -0.03 | 1.03 | 2420 | Mid | Santa Cruz Island | Island | 34.057 | -119.9 |
| 35 | 8 | Flores 2017 | T21.1.D | 4.00 | | -0.55 | 1.03 | 2420 | Mid | Santa Cruz Island | Island | 34.057 | -119.9 |
| 35 | 8 | Flores 2017 | T21.1.E | 5.00 | | 0.36 | 0.98 | 2420 | Mid | Santa Cruz Island | Island | 34.057 | -119.9 |
| 35 | 8 | Flores 2017 | T21.1.F | 6.00 | | 0.65 | 0.89 | 2420 | Mid | Santa Cruz Island | Island | 34.057 | -119.9 |
| 35 | 8 | Flores 2017 | T21.1.G | 7.00 | | 0.58 | 0.71 | 2420 | Mid | Santa Cruz Island | Island | 34.057 | -119.9 |
| 35 | 8 | Flores 2017 | T21.1.H | 8.00 | | 0.89 | 0.70 | 2420 | Mid | Santa Cruz Island | Island | 34.057 | -119.9 |
| 36 | 8 | Flores 2017 | T21.2.A | 1.00 | | -0.32 | 0.99 | 2420 | Mid | Santa Cruz Island | Island | 34.057 | -119.9 |

| | | | | | | | | | | | | | |
|---|---|---|---|---|---|---|---|---|---|---|---|---|---|
| 36 | 8 | Flores 2017 | T21.2.B | 2.00 | | 0.66 | 1.03 | 2420 | Mid | Santa Cruz Island | Island | 34.057 | -119.9 |
| 36 | 8 | Flores 2017 | T21.2.C | 3.00 | | 0.91 | 0.83 | 2420 | Mid | Santa Cruz Island | Island | 34.057 | -119.9 |
| 36 | 8 | Flores 2017 | T21.2.D | 4.00 | | 0.90 | 0.57 | 2420 | Mid | Santa Cruz Island | Island | 34.057 | -119.9 |
| 36 | 8 | Flores 2017 | T21.2.E | 5.00 | | 0.85 | -0.07 | 2420 | Mid | Santa Cruz Island | Island | 34.057 | -119.9 |
| 36 | 8 | Flores 2017 | T21.2.F | 6.00 | | 0.41 | 0.16 | 2420 | Mid | Santa Cruz Island | Island | 34.057 | -119.9 |
| 36 | 8 | Flores 2017 | T21.2.G | 7.00 | | 0.24 | 0.28 | 2420 | Mid | Santa Cruz Island | Island | 34.057 | -119.9 |
| 36 | 8 | Flores 2017 | T21.2.H | 8.00 | | 0.34 | 0.67 | 2420 | Mid | Santa Cruz Island | Island | 34.057 | -119.9 |
| 37 | 8 | Flores 2017 | T21.3.A | 1.00 | | 0.99 | 0.40 | 2420 | Mid | Santa Cruz Island | Island | 34.057 | -119.9 |
| 37 | 8 | Flores 2017 | T21.3.B | 2.00 | | 1.07 | -0.50 | 2420 | Mid | Santa Cruz Island | Island | 34.057 | -119.9 |
| 37 | 8 | Flores 2017 | T21.3.C | 3.00 | | 0.69 | -0.24 | 2420 | Mid | Santa Cruz Island | Island | 34.057 | -119.9 |
| 37 | 8 | Flores 2017 | T21.3.D | 4.00 | | 0.66 | -0.19 | 2420 | Mid | Santa Cruz Island | Island | 34.057 | -119.9 |
| 37 | 8 | Flores 2017 | T21.3.E | 5.00 | | 0.22 | -0.13 | 2420 | Mid | Santa Cruz Island | Island | 34.057 | -119.9 |
| 37 | 8 | Flores 2017 | T21.3.F | 6.00 | | 0.13 | -0.01 | 2420 | Mid | Santa Cruz Island | Island | 34.057 | -119.9 |
| 37 | 8 | Flores 2017 | T21.3.G | 7.00 | | -0.02 | 0.20 | 2420 | Mid | Santa Cruz Island | Island | 34.057 | -119.9 |
| 37 | 8 | Flores 2017 | T21.3.H | 8.00 | | 0.15 | 0.39 | 2420 | Mid | Santa Cruz Island | Island | 34.057 | -119.9 |
| 38 | 8 | Flores 2017 | T23-1-A | 1.00 | | -0.25 | -0.03 | 2420 | Mid | Santa Cruz Island | Island | 34.057 | -119.9 |
| 38 | 8 | Flores 2017 | T23-1-B | 2.00 | | 0.33 | -0.07 | 2420 | Mid | Santa Cruz Island | Island | 34.057 | -119.9 |
| 38 | 8 | Flores 2017 | T23-1-C | 3.00 | | 0.17 | 0.13 | 2420 | Mid | Santa Cruz Island | Island | 34.057 | -119.9 |
| 38 | 8 | Flores 2017 | T23-1-D | 4.00 | | -0.33 | 0.62 | 2420 | Mid | Santa Cruz Island | Island | 34.057 | -119.9 |

| | | | | | | | | | | | | | |
|---|---|---|---|---|---|---|---|---|---|---|---|---|---|
| 38 | 8 | Flores 2017 | T23-1-E | 5.00 | | 0.56 | 0.01 | 2420 | Mid | Santa Cruz Island | Island | 34.057 | -119.9 |
| 38 | 8 | Flores 2017 | T23-1-F | 6.00 | | -0.05 | -0.14 | 2420 | Mid | Santa Cruz Island | Island | 34.057 | -119.9 |
| 38 | 8 | Flores 2017 | T23-1-G | 7.00 | | -0.21 | -0.04 | 2420 | Mid | Santa Cruz Island | Island | 34.057 | -119.9 |
| 38 | 8 | Flores 2017 | T23-1-H | 8.00 | | -0.29 | 0.26 | 2420 | Mid | Santa Cruz Island | Island | 34.057 | -119.9 |
| 39 | 8 | Flores 2017 | T23-2-A | 1.00 | | 0.77 | 0.23 | 2420 | Mid | Santa Cruz Island | Island | 34.057 | -119.9 |
| 39 | 8 | Flores 2017 | T23-2-B | 2.00 | | 0.36 | 0.64 | 2420 | Mid | Santa Cruz Island | Island | 34.057 | -119.9 |
| 39 | 8 | Flores 2017 | T23-2-C | 3.00 | | 0.52 | 0.58 | 2420 | Mid | Santa Cruz Island | Island | 34.057 | -119.9 |
| 39 | 8 | Flores 2017 | T23-2-D | 4.00 | | 0.70 | 0.22 | 2420 | Mid | Santa Cruz Island | Island | 34.057 | -119.9 |
| 39 | 8 | Flores 2017 | T23-2-E | 5.00 | | 0.79 | -0.20 | 2420 | Mid | Santa Cruz Island | Island | 34.057 | -119.9 |
| 39 | 8 | Flores 2017 | T23-2-F | 6.00 | | 0.63 | -0.24 | 2420 | Mid | Santa Cruz Island | Island | 34.057 | -119.9 |
| 39 | 8 | Flores 2017 | T23-2-G | 7.00 | | 0.54 | 0.03 | 2420 | Mid | Santa Cruz Island | Island | 34.057 | -119.9 |
| 39 | 8 | Flores 2017 | T23-2-H | 8.00 | | 0.32 | 0.23 | 2420 | Mid | Santa Cruz Island | Island | 34.057 | -119.9 |
| 40 | 8 | Flores 2017 | T23-3-A | 1.00 | | 0.35 | 0.82 | 2420 | Mid | Santa Cruz Island | Island | 34.057 | -119.9 |
| 40 | 8 | Flores 2017 | T23-3-B | 2.00 | | 0.60 | 0.85 | 2420 | Mid | Santa Cruz Island | Island | 34.057 | -119.9 |
| 40 | 8 | Flores 2017 | T23-3-C | 3.00 | | 0.72 | 0.84 | 2420 | Mid | Santa Cruz Island | Island | 34.057 | -119.9 |
| 40 | 8 | Flores 2017 | T23-3-D | 4.00 | | 0.54 | 0.58 | 2420 | Mid | Santa Cruz Island | Island | 34.057 | -119.9 |
| 40 | 8 | Flores 2017 | T23-3-E | 5.00 | | 0.62 | 0.13 | 2420 | Mid | Santa Cruz Island | Island | 34.057 | -119.9 |
| 40 | 8 | Flores 2017 | T23-3-F | 6.00 | | 0.36 | 0.25 | 2420 | Mid | Santa Cruz Island | Island | 34.057 | -119.9 |
| 40 | 8 | Flores 2017 | T23-3-G | 7.00 | | 0.23 | 0.39 | 2420 | Mid | Santa Cruz Island | Island | 34.057 | -119.9 |

| | | | | | | | | | | | | | |
|---|---|---|---|---|---|---|---|---|---|---|---|---|---|
| 40 | 8 | Flores 2017 | T23-3-H | 8.00 | | 0.28 | 0.64 | 2420 | Mid | Santa Cruz Island | Island | 34.057 | -119.9 |
| 41 | 8 | Flores 2017 | T24.1.A | 1.00 | | 0.69 | -0.08 | 2420 | Mid | Santa Cruz Island | Island | 34.057 | -119.9 |
| 41 | 8 | Flores 2017 | T24.1.B | 2.00 | | 0.16 | 1.00 | 2420 | Mid | Santa Cruz Island | Island | 34.057 | -119.9 |
| 41 | 8 | Flores 2017 | T24.1.C | 3.00 | | 0.38 | 0.94 | 2420 | Mid | Santa Cruz Island | Island | 34.057 | -119.9 |
| 41 | 8 | Flores 2017 | T24.1.D | 4.00 | | 0.31 | 0.05 | 2420 | Mid | Santa Cruz Island | Island | 34.057 | -119.9 |
| 41 | 8 | Flores 2017 | T24.1.E | 5.00 | | 0.69 | -0.01 | 2420 | Mid | Santa Cruz Island | Island | 34.057 | -119.9 |
| 41 | 8 | Flores 2017 | T24.1.F | 6.00 | | 0.78 | 0.09 | 2420 | Mid | Santa Cruz Island | Island | 34.057 | -119.9 |
| 41 | 8 | Flores 2017 | T24.1.G | 7.00 | | 0.59 | 0.29 | 2420 | Mid | Santa Cruz Island | Island | 34.057 | -119.9 |
| 41 | 8 | Flores 2017 | T24.1.H | 8.00 | | 0.48 | 0.48 | 2420 | Mid | Santa Cruz Island | Island | 34.057 | -119.9 |
| 42 | 8 | Flores 2017 | T24.2.A | 1.00 | | 0.19 | 0.85 | 2420 | Mid | Santa Cruz Island | Island | 34.057 | -119.9 |
| 42 | 8 | Flores 2017 | T24.2.B | 2.00 | | 0.12 | 0.37 | 2420 | Mid | Santa Cruz Island | Island | 34.057 | -119.9 |
| 42 | 8 | Flores 2017 | T24.2.C | 3.00 | | 0.33 | 0.71 | 2420 | Mid | Santa Cruz Island | Island | 34.057 | -119.9 |
| 42 | 8 | Flores 2017 | T24.2.D | 4.00 | | 0.23 | -0.04 | 2420 | Mid | Santa Cruz Island | Island | 34.057 | -119.9 |
| 42 | 8 | Flores 2017 | T24.2.E | 5.00 | | 0.17 | 0.43 | 2420 | Mid | Santa Cruz Island | Island | 34.057 | -119.9 |
| 42 | 8 | Flores 2017 | T24.2.F | 6.00 | | 0.04 | 0.44 | 2420 | Mid | Santa Cruz Island | Island | 34.057 | -119.9 |
| 42 | 8 | Flores 2017 | T24.2.G | 7.00 | | -0.15 | 0.38 | 2420 | Mid | Santa Cruz Island | Island | 34.057 | -119.9 |
| 42 | 8 | Flores 2017 | T24.2.H | 8.00 | | -0.15 | 0.55 | 2420 | Mid | Santa Cruz Island | Island | 34.057 | -119.9 |
| 43 | 8 | Flores 2017 | T24.3.A | 1.00 | | 0.39 | 0.85 | 2420 | Mid | Santa Cruz Island | Island | 34.057 | -119.9 |
| 43 | 8 | Flores 2017 | T24.3.B | 2.00 | | 0.93 | 0.20 | 2420 | Mid | Santa Cruz Island | Island | 34.057 | -119.9 |

| | | | | | | | | | | | | | |
|---|---|---|---|---|---|---|---|---|---|---|---|---|---|
| 43 | 8 | Flores 2017 | T24.3.C | 3.00 | | 1.13 | -0.14 | 2420 | Mid | Santa Cruz Island | Island | 34.057 | -119.9 |
| 43 | 8 | Flores 2017 | T24.3.D | 4.00 | | 0.91 | -0.09 | 2420 | Mid | Santa Cruz Island | Island | 34.057 | -119.9 |
| 43 | 8 | Flores 2017 | T24.3.E | 5.00 | | 0.58 | 0.77 | 2420 | Mid | Santa Cruz Island | Island | 34.057 | -119.9 |
| 43 | 8 | Flores 2017 | T24.3.F | 6.00 | | 0.61 | 0.72 | 2420 | Mid | Santa Cruz Island | Island | 34.057 | -119.9 |
| 43 | 8 | Flores 2017 | T24.3.G | 7.00 | | 0.99 | 0.32 | 2420 | Mid | Santa Cruz Island | Island | 34.057 | -119.9 |
| 43 | 8 | Flores 2017 | T24.3.H | 8.00 | | 1.06 | -0.02 | 2420 | Mid | Santa Cruz Island | Island | 34.057 | -119.9 |
| 44 | 8 | Flores 2017 | T25.1.A | 1.00 | | 0.39 | 0.64 | 2420 | Mid | Santa Cruz Island | Island | 34.057 | -119.9 |
| 44 | 8 | Flores 2017 | T25.1.B | 2.00 | | 0.50 | 0.71 | 2420 | Mid | Santa Cruz Island | Island | 34.057 | -119.9 |
| 44 | 8 | Flores 2017 | T25.1.C | 3.00 | | 0.56 | 0.62 | 2420 | Mid | Santa Cruz Island | Island | 34.057 | -119.9 |
| 44 | 8 | Flores 2017 | T25.1.D | 4.00 | | 0.61 | 0.60 | 2420 | Mid | Santa Cruz Island | Island | 34.057 | -119.9 |
| 44 | 8 | Flores 2017 | T25.1.E | 5.00 | | 0.57 | 0.63 | 2420 | Mid | Santa Cruz Island | Island | 34.057 | -119.9 |
| 44 | 8 | Flores 2017 | T25.1.F | 6.00 | | 0.50 | 0.27 | 2420 | Mid | Santa Cruz Island | Island | 34.057 | -119.9 |
| 44 | 8 | Flores 2017 | T25.1.G | 7.00 | | 0.63 | 0.61 | 2420 | Mid | Santa Cruz Island | Island | 34.057 | -119.9 |
| 44 | 8 | Flores 2017 | T25.1.H | 8.00 | | 0.65 | 0.30 | 2420 | Mid | Santa Cruz Island | Island | 34.057 | -119.9 |
| 45 | 8 | Flores 2017 | T25.2.A | 1.00 | | 0.69 | 0.22 | 2420 | Mid | Santa Cruz Island | Island | 34.057 | -119.9 |
| 45 | 8 | Flores 2017 | T25.2.B | 2.00 | | 0.54 | 0.48 | 2420 | Mid | Santa Cruz Island | Island | 34.057 | -119.9 |
| 45 | 8 | Flores 2017 | T25.2.C | 3.00 | | 0.57 | 0.53 | 2420 | Mid | Santa Cruz Island | Island | 34.057 | -119.9 |
| 45 | 8 | Flores 2017 | T25.2.D | 4.00 | | 0.63 | 0.45 | 2420 | Mid | Santa Cruz Island | Island | 34.057 | -119.9 |
| 45 | 8 | Flores 2017 | T25.2.E | 5.00 | | 0.80 | 0.13 | 2420 | Mid | Santa Cruz Island | Island | 34.057 | -119.9 |

| | | | | | | | | | | | | | |
|---|---|---|---|---|---|---|---|---|---|---|---|---|---|
| 45 | 8 | Flores 2017 | T25.2.F | 6.00 | | 0.63 | 0.28 | 2420 | Mid | Santa Cruz Island | Island | 34.057 | -119.9 |
| 45 | 8 | Flores 2017 | T25.2.G | 7.00 | | 0.67 | 0.30 | 2420 | Mid | Santa Cruz Island | Island | 34.057 | -119.9 |
| 45 | 8 | Flores 2017 | T25.2.H | 8.00 | | 0.50 | 0.38 | 2420 | Mid | Santa Cruz Island | Island | 34.057 | -119.9 |
| 46 | 8 | Flores 2017 | T25.3.A | 1.00 | | 0.67 | 0.72 | 2420 | Mid | Santa Cruz Island | Island | 34.057 | -119.9 |
| 46 | 8 | Flores 2017 | T25.3.B | 2.00 | | 0.76 | 0.42 | 2420 | Mid | Santa Cruz Island | Island | 34.057 | -119.9 |
| 46 | 8 | Flores 2017 | T25.3.C | 3.00 | | 0.59 | 1.01 | 2420 | Mid | Santa Cruz Island | Island | 34.057 | -119.9 |
| 46 | 8 | Flores 2017 | T25.3.D | 4.00 | | 0.90 | 0.44 | 2420 | Mid | Santa Cruz Island | Island | 34.057 | -119.9 |
| 46 | 8 | Flores 2017 | T25.3.E | 5.00 | | 0.51 | 0.37 | 2420 | Mid | Santa Cruz Island | Island | 34.057 | -119.9 |
| 46 | 8 | Flores 2017 | T25.3.F | 6.00 | | -0.03 | 0.12 | 2420 | Mid | Santa Cruz Island | Island | 34.057 | -119.9 |
| 46 | 8 | Flores 2017 | T25.3.G | 7.00 | | 0.26 | 0.34 | 2420 | Mid | Santa Cruz Island | Island | 34.057 | -119.9 |
| 46 | 8 | Flores 2017 | T25.3.H | 8.00 | | 0.41 | 0.14 | 2420 | Mid | Santa Cruz Island | Island | 34.057 | -119.9 |
| 47 | 8 | Flores 2017 | T26-1-A | 1.00 | | -0.16 | 0.65 | 2420 | Mid | Santa Cruz Island | Island | 34.057 | -119.9 |
| 47 | 8 | Flores 2017 | T26-1-B | 2.00 | | 0.11 | 0.72 | 2420 | Mid | Santa Cruz Island | Island | 34.057 | -119.9 |
| 47 | 8 | Flores 2017 | T26-1-C | 3.00 | | 0.45 | 0.77 | 2420 | Mid | Santa Cruz Island | Island | 34.057 | -119.9 |
| 47 | 8 | Flores 2017 | T26-1-D | 4.00 | | 0.54 | 0.52 | 2420 | Mid | Santa Cruz Island | Island | 34.057 | -119.9 |
| 47 | 8 | Flores 2017 | T26-1-E | 5.00 | | 0.63 | 0.71 | 2420 | Mid | Santa Cruz Island | Island | 34.057 | -119.9 |
| 47 | 8 | Flores 2017 | T26-1-F | 6.00 | | 0.69 | 0.55 | 2420 | Mid | Santa Cruz Island | Island | 34.057 | -119.9 |
| 47 | 8 | Flores 2017 | T26-1-G | 7.00 | | 0.66 | 0.37 | 2420 | Mid | Santa Cruz Island | Island | 34.057 | -119.9 |
| 47 | 8 | Flores 2017 | T26-1-H | 8.00 | | 0.61 | 0.19 | 2420 | Mid | Santa Cruz Island | Island | 34.057 | -119.9 |

| | | | | | | | | | | | | | |
|---|---|---|---|---|---|---|---|---|---|---|---|---|---|
| 48 | 8 | Flores 2017 | T26-2-A | 1.00 | | 1.01 | 0.21 | 2420 | Mid | Santa Cruz Island | Island | 34.057 | -119.9 |
| 48 | 8 | Flores 2017 | T26-2-B | 2.00 | | 1.30 | -0.19 | 2420 | Mid | Santa Cruz Island | Island | 34.057 | -119.9 |
| 48 | 8 | Flores 2017 | T26-2-C | 3.00 | | 0.97 | 0.07 | 2420 | Mid | Santa Cruz Island | Island | 34.057 | -119.9 |
| 48 | 8 | Flores 2017 | T26-2-D | 4.00 | | 1.07 | 0.06 | 2420 | Mid | Santa Cruz Island | Island | 34.057 | -119.9 |
| 48 | 8 | Flores 2017 | T26-2-E | 5.00 | | 1.09 | 0.11 | 2420 | Mid | Santa Cruz Island | Island | 34.057 | -119.9 |
| 48 | 8 | Flores 2017 | T26-2-F | 6.00 | | 1.14 | -0.07 | 2420 | Mid | Santa Cruz Island | Island | 34.057 | -119.9 |
| 48 | 8 | Flores 2017 | T26-2-G | 7.00 | | 1.24 | -0.16 | 2420 | Mid | Santa Cruz Island | Island | 34.057 | -119.9 |
| 48 | 8 | Flores 2017 | T26-2-H | 8.00 | | 0.94 | -0.18 | 2420 | Mid | Santa Cruz Island | Island | 34.057 | -119.9 |
| 49 | 8 | Flores 2017 | T26-3-A | 1.00 | | 0.79 | -0.26 | 2420 | Mid | Santa Cruz Island | Island | 34.057 | -119.9 |
| 49 | 8 | Flores 2017 | T26-3-B | 2.00 | | 0.54 | -0.54 | 2420 | Mid | Santa Cruz Island | Island | 34.057 | -119.9 |
| 49 | 8 | Flores 2017 | T26-3-C | 3.00 | | 0.58 | -0.26 | 2420 | Mid | Santa Cruz Island | Island | 34.057 | -119.9 |
| 49 | 8 | Flores 2017 | T26-3-D | 4.00 | | 0.35 | -0.26 | 2420 | Mid | Santa Cruz Island | Island | 34.057 | -119.9 |
| 49 | 8 | Flores 2017 | T26-3-E | 5.00 | | 0.17 | -0.27 | 2420 | Mid | Santa Cruz Island | Island | 34.057 | -119.9 |
| 49 | 8 | Flores 2017 | T26-3-F | 6.00 | | 0.08 | -0.01 | 2420 | Mid | Santa Cruz Island | Island | 34.057 | -119.9 |
| 49 | 8 | Flores 2017 | T26-3-G | 7.00 | | -0.25 | 0.56 | 2420 | Mid | Santa Cruz Island | Island | 34.057 | -119.9 |
| 49 | 8 | Flores 2017 | T26-3-H | 8.00 | | -0.29 | 0.65 | 2420 | Mid | Santa Cruz Island | Island | 34.057 | -119.9 |
| 50 | 8 | Flores 2017 | T27-1-A | 1.00 | | 0.59 | 0.15 | 2430 | Mid | Santa Cruz Island | Island | 34.057 | -119.9 |
| 50 | 8 | Flores 2017 | T27-1-B | 2.00 | | 0.75 | 0.51 | 2430 | Mid | Santa Cruz Island | Island | 34.057 | -119.9 |
| 50 | 8 | Flores 2017 | T27-1-C | 3.00 | | 0.64 | 0.15 | 2430 | Mid | Santa Cruz Island | Island | 34.057 | -119.9 |

| | | | | | | | | | | | | | |
|---|---|---|---|---|---|---|---|---|---|---|---|---|---|
| 50 | 8 | Flores 2017 | T27-1-D | 4.00 | | 0.34 | 0.78 | 2430 | Mid | Santa Cruz Island | Island | 34.057 | -119.9 |
| 50 | 8 | Flores 2017 | T27-1-E | 5.00 | | 0.84 | -0.09 | 2430 | Mid | Santa Cruz Island | Island | 34.057 | -119.9 |
| 50 | 8 | Flores 2017 | T27-1-F | 6.00 | | 0.27 | 0.42 | 2430 | Mid | Santa Cruz Island | Island | 34.057 | -119.9 |
| 50 | 8 | Flores 2017 | T27-1-G | 7.00 | | -0.01 | 0.86 | 2430 | Mid | Santa Cruz Island | Island | 34.057 | -119.9 |
| 50 | 8 | Flores 2017 | T27-1-H | 8.00 | | 0.06 | 0.97 | 2430 | Mid | Santa Cruz Island | Island | 34.057 | -119.9 |
| 51 | 8 | Flores 2017 | T27-2-A | 1.00 | | 0.77 | 0.51 | 2430 | Mid | Santa Cruz Island | Island | 34.057 | -119.9 |
| 51 | 8 | Flores 2017 | T27-2-B | 2.00 | | 1.23 | -0.01 | 2430 | Mid | Santa Cruz Island | Island | 34.057 | -119.9 |
| 51 | 8 | Flores 2017 | T27-2-C | 3.00 | | 0.52 | -0.02 | 2430 | Mid | Santa Cruz Island | Island | 34.057 | -119.9 |
| 51 | 8 | Flores 2017 | T27-2-D | 4.00 | | 0.28 | 0.31 | 2430 | Mid | Santa Cruz Island | Island | 34.057 | -119.9 |
| 51 | 8 | Flores 2017 | T27-2-E | 5.00 | | -0.14 | 0.46 | 2430 | Mid | Santa Cruz Island | Island | 34.057 | -119.9 |
| 51 | 8 | Flores 2017 | T27-2-F | 6.00 | | -0.03 | 0.68 | 2430 | Mid | Santa Cruz Island | Island | 34.057 | -119.9 |
| 51 | 8 | Flores 2017 | T27-2-G | 7.00 | | -0.01 | 0.47 | 2430 | Mid | Santa Cruz Island | Island | 34.057 | -119.9 |
| 51 | 8 | Flores 2017 | T27-2-H | 8.00 | | 0.27 | 0.77 | 2430 | Mid | Santa Cruz Island | Island | 34.057 | -119.9 |
| 52 | 8 | Flores 2017 | T27-3-A | 1.00 | | 0.17 | 0.22 | 2430 | Mid | Santa Cruz Island | Island | 34.057 | -119.9 |
| 52 | 8 | Flores 2017 | T27-3-B | 2.00 | | 0.22 | 0.52 | 2430 | Mid | Santa Cruz Island | Island | 34.057 | -119.9 |
| 52 | 8 | Flores 2017 | T27-3-C | 3.00 | | 0.38 | 0.51 | 2430 | Mid | Santa Cruz Island | Island | 34.057 | -119.9 |
| 52 | 8 | Flores 2017 | T27-3-D | 4.00 | | 0.31 | 0.54 | 2430 | Mid | Santa Cruz Island | Island | 34.057 | -119.9 |
| 52 | 8 | Flores 2017 | T27-3-E | 5.00 | | 0.02 | 0.23 | 2430 | Mid | Santa Cruz Island | Island | 34.057 | -119.9 |
| 52 | 8 | Flores 2017 | T27-3-F | 6.00 | | 0.50 | -0.15 | 2430 | Mid | Santa Cruz Island | Island | 34.057 | -119.9 |

| | | | | | | | | | | | | | |
|---|---|---|---|---|---|---|---|---|---|---|---|---|---|
| 52 | 8 | Flores 2017 | T27-3-G | 7.00 | | 0.58 | -0.17 | 2430 | Mid | Santa Cruz Island | Island | 34.057 | -119.9 |
| 52 | 8 | Flores 2017 | T27-3-H | 8.00 | | 0.53 | -0.05 | 2430 | Mid | Santa Cruz Island | Island | 34.057 | -119.9 |
| 53 | 8 | Flores 2017 | T5 1A | 1.00 | | 0.55 | 0.45 | 1507 | Mid | Santa Cruz Island | Island | 34.057 | -119.9 |
| 53 | 8 | Flores 2017 | T5 1B | 2.00 | | 0.32 | 0.68 | 1507 | Mid | Santa Cruz Island | Island | 34.057 | -119.9 |
| 53 | 8 | Flores 2017 | T5 1C | 3.00 | | 0.57 | 0.14 | 1507 | Mid | Santa Cruz Island | Island | 34.057 | -119.9 |
| 53 | 8 | Flores 2017 | T5 1D | 4.00 | | 0.30 | 0.62 | 1507 | Mid | Santa Cruz Island | Island | 34.057 | -119.9 |
| 53 | 8 | Flores 2017 | T5 1E | 5.00 | | 0.50 | 0.57 | 1507 | Mid | Santa Cruz Island | Island | 34.057 | -119.9 |
| 53 | 8 | Flores 2017 | T5 1F | 6.00 | | 0.65 | 0.70 | 1507 | Mid | Santa Cruz Island | Island | 34.057 | -119.9 |
| 53 | 8 | Flores 2017 | T5 1G | 7.00 | | 0.71 | 0.51 | 1507 | Mid | Santa Cruz Island | Island | 34.057 | -119.9 |
| 53 | 8 | Flores 2017 | T5 1H | 8.00 | | 0.84 | 0.62 | 1507 | Mid | Santa Cruz Island | Island | 34.057 | -119.9 |
| 54 | 8 | Flores 2017 | T5 2A | 1.00 | | 0.64 | 0.21 | 1507 | Mid | Santa Cruz Island | Island | 34.057 | -119.9 |
| 54 | 8 | Flores 2017 | T5 2B | 2.00 | | 0.35 | 0.55 | 1507 | Mid | Santa Cruz Island | Island | 34.057 | -119.9 |
| 54 | 8 | Flores 2017 | T5 2C | 3.00 | | 0.41 | 0.86 | 1507 | Mid | Santa Cruz Island | Island | 34.057 | -119.9 |
| 54 | 8 | Flores 2017 | T5 2D | 4.00 | | 0.56 | 0.61 | 1507 | Mid | Santa Cruz Island | Island | 34.057 | -119.9 |
| 54 | 8 | Flores 2017 | T5 2E | 5.00 | | 0.98 | 0.44 | 1507 | Mid | Santa Cruz Island | Island | 34.057 | -119.9 |
| 54 | 8 | Flores 2017 | T5 2F | 6.00 | | 0.84 | 0.35 | 1507 | Mid | Santa Cruz Island | Island | 34.057 | -119.9 |
| 54 | 8 | Flores 2017 | T5 2G | 7.00 | | 0.86 | 0.36 | 1507 | Mid | Santa Cruz Island | Island | 34.057 | -119.9 |
| 54 | 8 | Flores 2017 | T5 2H | 8.00 | | 0.63 | -0.06 | 1507 | Mid | Santa Cruz Island | Island | 34.057 | -119.9 |
| 55 | 8 | Flores 2017 | T5 3A | 1.00 | | 0.54 | 0.31 | 1507 | Mid | Santa Cruz Island | Island | 34.057 | -119.9 |

| | | | | | | | | | | | | | |
|---|---|---|---|---|---|---|---|---|---|---|---|---|---|
| 55 | 8 | Flores 2017 | T5 3B | 2.00 | | 0.61 | -0.12 | 1507 | Mid | Santa Cruz Island | Island | 34.057 | -119.9 |
| 55 | 8 | Flores 2017 | T5 3C | 3.00 | | 0.52 | 0.07 | 1507 | Mid | Santa Cruz Island | Island | 34.057 | -119.9 |
| 55 | 8 | Flores 2017 | T5 3D | 4.00 | | 0.36 | 0.43 | 1507 | Mid | Santa Cruz Island | Island | 34.057 | -119.9 |
| 55 | 8 | Flores 2017 | T5 3E | 5.00 | | 0.29 | 0.54 | 1507 | Mid | Santa Cruz Island | Island | 34.057 | -119.9 |
| 55 | 8 | Flores 2017 | T5 3F | 6.00 | | 0.18 | 0.37 | 1507 | Mid | Santa Cruz Island | Island | 34.057 | -119.9 |
| 55 | 8 | Flores 2017 | T5 3G | 7.00 | | 0.30 | 0.50 | 1507 | Mid | Santa Cruz Island | Island | 34.057 | -119.9 |
| 55 | 8 | Flores 2017 | T5 3H | 8.00 | | 0.30 | 0.43 | 1507 | Mid | Santa Cruz Island | Island | 34.057 | -119.9 |
| 56 | 8 | Flores 2017 | T6.1.A | 1.00 | | 0.87 | 0.46 | 1612 | Mid | Santa Cruz Island | Island | 34.057 | -119.9 |
| 56 | 8 | Flores 2017 | T6.1.B | 2.00 | | 0.30 | 0.87 | 1612 | Mid | Santa Cruz Island | Island | 34.057 | -119.9 |
| 56 | 8 | Flores 2017 | T6.1.C | 3.00 | | 0.00 | 1.23 | 1612 | Mid | Santa Cruz Island | Island | 34.057 | -119.9 |
| 56 | 8 | Flores 2017 | T6.1.D | 4.00 | | 0.53 | 1.13 | 1612 | Mid | Santa Cruz Island | Island | 34.057 | -119.9 |
| 56 | 8 | Flores 2017 | T6.1.E | 5.00 | | 0.48 | 0.62 | 1612 | Mid | Santa Cruz Island | Island | 34.057 | -119.9 |
| 56 | 8 | Flores 2017 | T6.1.F | 6.00 | | 1.08 | 0.35 | 1612 | Mid | Santa Cruz Island | Island | 34.057 | -119.9 |
| 56 | 8 | Flores 2017 | T6.1.G | 7.00 | | 0.76 | 0.14 | 1612 | Mid | Santa Cruz Island | Island | 34.057 | -119.9 |
| 56 | 8 | Flores 2017 | T6.1.H | 8.00 | | 0.54 | 0.35 | 1612 | Mid | Santa Cruz Island | Island | 34.057 | -119.9 |
| 57 | 8 | Flores 2017 | T6.2.A | 1.00 | | 0.67 | -0.15 | 1612 | Mid | Santa Cruz Island | Island | 34.057 | -119.9 |
| 57 | 8 | Flores 2017 | T6.2.B | 2.00 | | 0.69 | -0.31 | 1612 | Mid | Santa Cruz Island | Island | 34.057 | -119.9 |
| 57 | 8 | Flores 2017 | T6.2.C | 3.00 | | 0.47 | -0.09 | 1612 | Mid | Santa Cruz Island | Island | 34.057 | -119.9 |
| 57 | 8 | Flores 2017 | T6.2.D | 4.00 | | 0.22 | -0.05 | 1612 | Mid | Santa Cruz Island | Island | 34.057 | -119.9 |

| | | | | | | | | | | | | | |
|---|---|---|---|---|---|---|---|---|---|---|---|---|---|
| 57 | 8 | Flores 2017 | T6.2.E | 5.00 | | 0.01 | -0.05 | 1612 | Mid | Santa Cruz Island | Island | 34.057 | -119.9 |
| 57 | 8 | Flores 2017 | T6.2.F | 6.00 | | -0.22 | -0.02 | 1612 | Mid | Santa Cruz Island | Island | 34.057 | -119.9 |
| 57 | 8 | Flores 2017 | T6.2.G | 7.00 | | -0.29 | 0.13 | 1612 | Mid | Santa Cruz Island | Island | 34.057 | -119.9 |
| 57 | 8 | Flores 2017 | T6.2.H | 8.00 | | -0.51 | 0.31 | 1612 | Mid | Santa Cruz Island | Island | 34.057 | -119.9 |
| 58 | 8 | Flores 2017 | T6.3.A | 1.00 | | 0.55 | -0.10 | 1612 | Mid | Santa Cruz Island | Island | 34.057 | -119.9 |
| 58 | 8 | Flores 2017 | T6.3.B | 2.00 | | 0.15 | 0.82 | 1612 | Mid | Santa Cruz Island | Island | 34.057 | -119.9 |
| 58 | 8 | Flores 2017 | T6.3.C | 3.00 | | 0.60 | 0.34 | 1612 | Mid | Santa Cruz Island | Island | 34.057 | -119.9 |
| 58 | 8 | Flores 2017 | T6.3.D | 4.00 | | 0.68 | 0.38 | 1612 | Mid | Santa Cruz Island | Island | 34.057 | -119.9 |
| 58 | 8 | Flores 2017 | T6.3.E | 5.00 | | 0.72 | -0.12 | 1612 | Mid | Santa Cruz Island | Island | 34.057 | -119.9 |
| 58 | 8 | Flores 2017 | T6.3.F | 6.00 | | 0.46 | -0.31 | 1612 | Mid | Santa Cruz Island | Island | 34.057 | -119.9 |
| 58 | 8 | Flores 2017 | T6.3.G | 7.00 | | -0.30 | 0.16 | 1612 | Mid | Santa Cruz Island | Island | 34.057 | -119.9 |
| 58 | 8 | Flores 2017 | T6.3.H | 8.00 | | -0.49 | 0.36 | 1612 | Mid | Santa Cruz Island | Island | 34.057 | -119.9 |
| 59 | 8 | Flores 2017 | T8.1.A | 1.00 | | 0.54 | -0.01 | 1825 | Mid | Santa Cruz Island | Island | 34.057 | -119.9 |
| 59 | 8 | Flores 2017 | T8.1.B | 2.00 | | 0.01 | 0.96 | 1825 | Mid | Santa Cruz Island | Island | 34.057 | -119.9 |
| 59 | 8 | Flores 2017 | T8.1.C | 3.00 | | -0.02 | 0.50 | 1825 | Mid | Santa Cruz Island | Island | 34.057 | -119.9 |
| 59 | 8 | Flores 2017 | T8.1.D | 4.00 | | -0.15 | 0.85 | 1825 | Mid | Santa Cruz Island | Island | 34.057 | -119.9 |
| 59 | 8 | Flores 2017 | T8.1.E | 5.00 | | 0.50 | 0.41 | 1825 | Mid | Santa Cruz Island | Island | 34.057 | -119.9 |
| 59 | 8 | Flores 2017 | T8.1.F | 6.00 | | 0.21 | 0.68 | 1825 | Mid | Santa Cruz Island | Island | 34.057 | -119.9 |
| 59 | 8 | Flores 2017 | T8.1.G | 7.00 | | 0.39 | 0.75 | 1825 | Mid | Santa Cruz Island | Island | 34.057 | -119.9 |

| | | | | | | | | | | | | | |
|---|---|---|---|---|---|---|---|---|---|---|---|---|---|
| 59 | 8 | Flores 2017 | T8.1.H | 8.00 | | 0.30 | 0.01 | 1825 | Mid | Santa Cruz Island | Island | 34.057 | -119.9 |
| 60 | 8 | Flores 2017 | T8.2.A | 1.00 | | 0.30 | 0.65 | 1825 | Mid | Santa Cruz Island | Island | 34.057 | -119.9 |
| 60 | 8 | Flores 2017 | T8.2.B | 2.00 | | 0.64 | 0.07 | 1825 | Mid | Santa Cruz Island | Island | 34.057 | -119.9 |
| 60 | 8 | Flores 2017 | T8.2.C | 3.00 | | 0.45 | 0.43 | 1825 | Mid | Santa Cruz Island | Island | 34.057 | -119.9 |
| 60 | 8 | Flores 2017 | T8.2.D | 4.00 | | 0.58 | 0.68 | 1825 | Mid | Santa Cruz Island | Island | 34.057 | -119.9 |
| 60 | 8 | Flores 2017 | T8.2.E | 5.00 | | 0.86 | 0.72 | 1825 | Mid | Santa Cruz Island | Island | 34.057 | -119.9 |
| 60 | 8 | Flores 2017 | T8.2.F | 6.00 | | 1.08 | 0.35 | 1825 | Mid | Santa Cruz Island | Island | 34.057 | -119.9 |
| 60 | 8 | Flores 2017 | T8.2.G | 7.00 | | 1.13 | 0.08 | 1825 | Mid | Santa Cruz Island | Island | 34.057 | -119.9 |
| 60 | 8 | Flores 2017 | T8.2.H | 8.00 | | 0.36 | 0.38 | 1825 | Mid | Santa Cruz Island | Island | 34.057 | -119.9 |
| 61 | 8 | Flores 2017 | T8.3.A | 1.00 | | 0.87 | 0.61 | 1825 | Mid | Santa Cruz Island | Island | 34.057 | -119.9 |
| 61 | 8 | Flores 2017 | T8.3.B | 2.00 | | 1.28 | 0.22 | 1825 | Mid | Santa Cruz Island | Island | 34.057 | -119.9 |
| 61 | 8 | Flores 2017 | T8.3.C | 3.00 | | 1.18 | 0.49 | 1825 | Mid | Santa Cruz Island | Island | 34.057 | -119.9 |
| 61 | 8 | Flores 2017 | T8.3.D | 4.00 | | 1.38 | 0.04 | 1825 | Mid | Santa Cruz Island | Island | 34.057 | -119.9 |
| 61 | 8 | Flores 2017 | T8.3.E | 5.00 | | 1.23 | -0.01 | 1825 | Mid | Santa Cruz Island | Island | 34.057 | -119.9 |
| 61 | 8 | Flores 2017 | T8.3.F | 6.00 | | 1.29 | 0.16 | 1825 | Mid | Santa Cruz Island | Island | 34.057 | -119.9 |
| 61 | 8 | Flores 2017 | T8.3.G | 7.00 | | 1.17 | 0.61 | 1825 | Mid | Santa Cruz Island | Island | 34.057 | -119.9 |
| 61 | 8 | Flores 2017 | T8.3.H | 8.00 | | 1.24 | 0.56 | 1825 | Mid | Santa Cruz Island | Island | 34.057 | -119.9 |
| 62 | 8 | Flores 2017 | W.1.1.A | 1.00 | | 0.72 | 1.65 | 1610 | Mid | Santa Cruz Island | Island | 34.057 | -119.9 |
| 62 | 8 | Flores 2017 | W.1.1.B | 2.00 | | 0.61 | 0.76 | 1610 | Mid | Santa Cruz Island | Island | 34.057 | -119.9 |

| | | | | | | | | | | | | | |
|---|---|---|---|---|---|---|---|---|---|---|---|---|---|
| 62 | 8 | Flores 2017 | W.1.1.C | 3.00 | | 1.23 | 1.28 | 1610 | Mid | Santa Cruz Island | Island | 34.057 | -119.9 |
| 62 | 8 | Flores 2017 | W.1.1.D | 4.00 | | 1.52 | 0.92 | 1610 | Mid | Santa Cruz Island | Island | 34.057 | -119.9 |
| 62 | 8 | Flores 2017 | W.1.1.E | 5.00 | | 0.86 | -0.07 | 1610 | Mid | Santa Cruz Island | Island | 34.057 | -119.9 |
| 62 | 8 | Flores 2017 | W.1.1.F | 6.00 | | 0.24 | 0.14 | 1610 | Mid | Santa Cruz Island | Island | 34.057 | -119.9 |
| 62 | 8 | Flores 2017 | W.1.1.G | 7.00 | | 0.29 | 0.93 | 1610 | Mid | Santa Cruz Island | Island | 34.057 | -119.9 |
| 62 | 8 | Flores 2017 | W.1.1.H | 8.00 | | 0.43 | 0.98 | 1610 | Mid | Santa Cruz Island | Island | 34.057 | -119.9 |
| 63 | 8 | Flores 2017 | W.1.2.A | 1.00 | | 0.80 | 0.26 | 1610 | Mid | Santa Cruz Island | Island | 34.057 | -119.9 |
| 63 | 8 | Flores 2017 | W.1.2.B | 2.00 | | 0.07 | 0.24 | 1610 | Mid | Santa Cruz Island | Island | 34.057 | -119.9 |
| 63 | 8 | Flores 2017 | W.1.2.C | 3.00 | | 0.44 | 0.82 | 1610 | Mid | Santa Cruz Island | Island | 34.057 | -119.9 |
| 63 | 8 | Flores 2017 | W.1.2.D | 4.00 | | 0.43 | 1.43 | 1610 | Mid | Santa Cruz Island | Island | 34.057 | -119.9 |
| 63 | 8 | Flores 2017 | W.1.2.E | 5.00 | | 0.28 | 1.06 | 1610 | Mid | Santa Cruz Island | Island | 34.057 | -119.9 |
| 63 | 8 | Flores 2017 | W.1.2.F | 6.00 | | 0.84 | 0.32 | 1610 | Mid | Santa Cruz Island | Island | 34.057 | -119.9 |
| 63 | 8 | Flores 2017 | W.1.2.G | 7.00 | | 0.70 | 0.68 | 1610 | Mid | Santa Cruz Island | Island | 34.057 | -119.9 |
| 63 | 8 | Flores 2017 | W.1.2.H | 8.00 | | 0.63 | 0.45 | 1610 | Mid | Santa Cruz Island | Island | 34.057 | -119.9 |
| 64 | 8 | Flores 2017 | W.1.3.A | 1.00 | | -0.05 | -0.10 | 1610 | Mid | Santa Cruz Island | Island | 34.057 | -119.9 |
| 64 | 8 | Flores 2017 | W.1.3.B | 2.00 | | 0.06 | 1.04 | 1610 | Mid | Santa Cruz Island | Island | 34.057 | -119.9 |
| 64 | 8 | Flores 2017 | W.1.3.C | 3.00 | | 0.29 | 0.17 | 1610 | Mid | Santa Cruz Island | Island | 34.057 | -119.9 |
| 64 | 8 | Flores 2017 | W.1.3.D | 4.00 | | 0.42 | 0.11 | 1610 | Mid | Santa Cruz Island | Island | 34.057 | -119.9 |
| 64 | 8 | Flores 2017 | W.1.3.E | 5.00 | | 0.59 | 0.78 | 1610 | Mid | Santa Cruz Island | Island | 34.057 | -119.9 |

| | | | | | | | | | | | | | |
|---|---|---|---|---|---|---|---|---|---|---|---|---|---|
| 64 | 8 | Flores 2017 | W.1.3.F | 6.00 | | 0.13 | 0.05 | 1610 | Mid | Santa Cruz Island | Island | 34.057 | -119.9 |
| 64 | 8 | Flores 2017 | W.1.3.G | 7.00 | | -0.04 | 0.02 | 1610 | Mid | Santa Cruz Island | Island | 34.057 | -119.9 |
| 64 | 8 | Flores 2017 | W.1.3.H | 8.00 | | 0.29 | 0.08 | 1610 | Mid | Santa Cruz Island | Island | 34.057 | -119.9 |
| 65 | 8 | Flores 2017 | W.1.4.A | 1.00 | | 1.05 | -0.79 | 1610 | Mid | Santa Cruz Island | Island | 34.057 | -119.9 |
| 65 | 8 | Flores 2017 | W.1.4.B | 2.00 | | 0.82 | -0.78 | 1610 | Mid | Santa Cruz Island | Island | 34.057 | -119.9 |
| 65 | 8 | Flores 2017 | W.1.4.C | 3.00 | | -0.04 | -0.30 | 1610 | Mid | Santa Cruz Island | Island | 34.057 | -119.9 |
| 65 | 8 | Flores 2017 | W.1.4.D | 4.00 | | 0.34 | 0.43 | 1610 | Mid | Santa Cruz Island | Island | 34.057 | -119.9 |
| 65 | 8 | Flores 2017 | W.1.4.E | 5.00 | | 0.26 | 0.16 | 1610 | Mid | Santa Cruz Island | Island | 34.057 | -119.9 |
| 65 | 8 | Flores 2017 | W.1.4.F | 6.00 | | 0.62 | -0.24 | 1610 | Mid | Santa Cruz Island | Island | 34.057 | -119.9 |
| 65 | 8 | Flores 2017 | W.1.4.G | 7.00 | | 0.37 | 0.86 | 1610 | Mid | Santa Cruz Island | Island | 34.057 | -119.9 |
| 65 | 8 | Flores 2017 | W.1.4.H | 8.00 | | 0.25 | 0.57 | 1610 | Mid | Santa Cruz Island | Island | 34.057 | -119.9 |
| 66 | 8 | Flores 2017 | W.10.1.A | 1.00 | | 1.25 | 0.23 | 2590 | Mid | Santa Cruz Island | Island | 33.962 | -119.8 |
| 66 | 8 | Flores 2017 | W.10.1.B | 2.00 | | 0.84 | 0.37 | 2590 | Mid | Santa Cruz Island | Island | 33.962 | -119.8 |
| 66 | 8 | Flores 2017 | W.10.1.C | 3.00 | | 1.41 | -0.26 | 2590 | Mid | Santa Cruz Island | Island | 33.962 | -119.8 |
| 66 | 8 | Flores 2017 | W.10.1.D | 4.00 | | 1.35 | -0.49 | 2590 | Mid | Santa Cruz Island | Island | 33.962 | -119.8 |
| 66 | 8 | Flores 2017 | W.10.1.E | 5.00 | | 1.03 | -0.10 | 2590 | Mid | Santa Cruz Island | Island | 33.962 | -119.8 |
| 66 | 8 | Flores 2017 | W.10.1.F | 6.00 | | 0.98 | 0.15 | 2590 | Mid | Santa Cruz Island | Island | 33.962 | -119.8 |
| 66 | 8 | Flores 2017 | W.10.1.G | 7.00 | | 0.67 | 0.67 | 2590 | Mid | Santa Cruz Island | Island | 33.962 | -119.8 |
| 66 | 8 | Flores 2017 | W.10.1.H | 8.00 | | 0.86 | 1.07 | 2590 | Mid | Santa Cruz Island | Island | 33.962 | -119.8 |

| | | | | | | | | | | | | | |
|---|---|---|---|---|---|---|---|---|---|---|---|---|---|
| 67 | 8 | Flores 2017 | W.10.2.A | 1.00 | | 0.10 | 1.26 | 2590 | Mid | Santa Cruz Island | Island | 33.962 | -119.8 |
| 67 | 8 | Flores 2017 | W.10.2.B | 2.00 | | 0.11 | 0.65 | 2590 | Mid | Santa Cruz Island | Island | 33.962 | -119.8 |
| 67 | 8 | Flores 2017 | W.10.2.C | 3.00 | | -0.03 | 1.05 | 2590 | Mid | Santa Cruz Island | Island | 33.962 | -119.8 |
| 67 | 8 | Flores 2017 | W.10.2.D | 4.00 | | -0.31 | 0.91 | 2590 | Mid | Santa Cruz Island | Island | 33.962 | -119.8 |
| 67 | 8 | Flores 2017 | W.10.2.E | 5.00 | | 0.04 | 1.40 | 2590 | Mid | Santa Cruz Island | Island | 33.962 | -119.8 |
| 67 | 8 | Flores 2017 | W.10.2.F | 6.00 | | 0.09 | 0.43 | 2590 | Mid | Santa Cruz Island | Island | 33.962 | -119.8 |
| 67 | 8 | Flores 2017 | W.10.2.G | 7.00 | | 0.16 | 0.24 | 2590 | Mid | Santa Cruz Island | Island | 33.962 | -119.8 |
| 67 | 8 | Flores 2017 | W.10.2.H | 8.00 | | 0.23 | 0.76 | 2590 | Mid | Santa Cruz Island | Island | 33.962 | -119.8 |
| 68 | 8 | Flores 2017 | W.10.3.A | 1.00 | | 0.63 | -0.18 | 2590 | Mid | Santa Cruz Island | Island | 33.962 | -119.8 |
| 68 | 8 | Flores 2017 | W.10.3.B | 2.00 | | 0.18 | 0.27 | 2590 | Mid | Santa Cruz Island | Island | 33.962 | -119.8 |
| 68 | 8 | Flores 2017 | W.10.3.C | 3.00 | | 0.51 | 0.62 | 2590 | Mid | Santa Cruz Island | Island | 33.962 | -119.8 |
| 68 | 8 | Flores 2017 | W.10.3.D | 4.00 | | 0.53 | 0.74 | 2590 | Mid | Santa Cruz Island | Island | 33.962 | -119.8 |
| 68 | 8 | Flores 2017 | W.10.3.E | 5.00 | | 0.71 | 0.91 | 2590 | Mid | Santa Cruz Island | Island | 33.962 | -119.8 |
| 68 | 8 | Flores 2017 | W.10.3.F | 6.00 | | 0.77 | 0.08 | 2590 | Mid | Santa Cruz Island | Island | 33.962 | -119.8 |
| 68 | 8 | Flores 2017 | W.10.3.G | 7.00 | | 0.72 | 0.74 | 2590 | Mid | Santa Cruz Island | Island | 33.962 | -119.8 |
| 68 | 8 | Flores 2017 | W.10.3.H | 8.00 | | 0.93 | 0.73 | 2590 | Mid | Santa Cruz Island | Island | 33.962 | -119.8 |
| 69 | 8 | Flores 2017 | W.10.4.A | 1.00 | | 0.20 | 0.57 | 2590 | Mid | Santa Cruz Island | Island | 33.962 | -119.8 |
| 69 | 8 | Flores 2017 | W.10.4.B | 2.00 | | 0.41 | 0.69 | 2590 | Mid | Santa Cruz Island | Island | 33.962 | -119.8 |
| 69 | 8 | Flores 2017 | W.10.4.C | 3.00 | | 0.46 | 0.60 | 2590 | Mid | Santa Cruz Island | Island | 33.962 | -119.8 |

| | | | | | | | | | | | | | |
|---|---|---|---|---|---|---|---|---|---|---|---|---|---|
| 69 | 8 | Flores 2017 | W.10.4.D | 4.00 | | 0.50 | 0.50 | 2590 | Mid | Santa Cruz Island | Island | 33.962 | -119.8 |
| 69 | 8 | Flores 2017 | W.10.4.E | 5.00 | | 0.77 | -0.38 | 2590 | Mid | Santa Cruz Island | Island | 33.962 | -119.8 |
| 69 | 8 | Flores 2017 | W.10.4.F | 6.00 | | 0.68 | 0.28 | 2590 | Mid | Santa Cruz Island | Island | 33.962 | -119.8 |
| 69 | 8 | Flores 2017 | W.10.4.G | 7.00 | | 0.16 | 0.33 | 2590 | Mid | Santa Cruz Island | Island | 33.962 | -119.8 |
| 69 | 8 | Flores 2017 | W.10.4.H | 8.00 | | 0.94 | -0.35 | 2590 | Mid | Santa Cruz Island | Island | 33.962 | -119.8 |
| 70 | 8 | Flores 2017 | W.11.1.A | 1.00 | | 1.04 | 0.53 | 2660 | Mid | Santa Cruz Island | Island | 33.962 | -119.8 |
| 70 | 8 | Flores 2017 | W.11.1.B | 2.00 | | 0.86 | 1.27 | 2660 | Mid | Santa Cruz Island | Island | 33.962 | -119.8 |
| 70 | 8 | Flores 2017 | W.11.1.C | 3.00 | | 1.14 | 0.55 | 2660 | Mid | Santa Cruz Island | Island | 33.962 | -119.8 |
| 70 | 8 | Flores 2017 | W.11.1.D | 4.00 | | 0.83 | 0.84 | 2660 | Mid | Santa Cruz Island | Island | 33.962 | -119.8 |
| 70 | 8 | Flores 2017 | W.11.1.E | 5.00 | | 1.10 | 1.25 | 2660 | Mid | Santa Cruz Island | Island | 33.962 | -119.8 |
| 70 | 8 | Flores 2017 | W.11.1.F | 6.00 | | 1.05 | 0.20 | 2660 | Mid | Santa Cruz Island | Island | 33.962 | -119.8 |
| 70 | 8 | Flores 2017 | W.11.1.G | 7.00 | | 1.05 | 0.42 | 2660 | Mid | Santa Cruz Island | Island | 33.962 | -119.8 |
| 70 | 8 | Flores 2017 | W.11.1.H | 8.00 | | 0.94 | 0.79 | 2660 | Mid | Santa Cruz Island | Island | 33.962 | -119.8 |
| 71 | 8 | Flores 2017 | W.11.2.A | 1.00 | | 0.05 | 0.43 | 2660 | Mid | Santa Cruz Island | Island | 33.962 | -119.8 |
| 71 | 8 | Flores 2017 | W.11.2.B | 2.00 | | 0.35 | 0.31 | 2660 | Mid | Santa Cruz Island | Island | 33.962 | -119.8 |
| 71 | 8 | Flores 2017 | W.11.2.C | 3.00 | | 0.51 | 0.53 | 2660 | Mid | Santa Cruz Island | Island | 33.962 | -119.8 |
| 71 | 8 | Flores 2017 | W.11.2.D | 4.00 | | 0.02 | 1.35 | 2660 | Mid | Santa Cruz Island | Island | 33.962 | -119.8 |
| 71 | 8 | Flores 2017 | W.11.2.E | 5.00 | | 0.40 | 1.98 | 2660 | Mid | Santa Cruz Island | Island | 33.962 | -119.8 |
| 71 | 8 | Flores 2017 | W.11.2.F | 6.00 | | 0.35 | 1.59 | 2660 | Mid | Santa Cruz Island | Island | 33.962 | -119.8 |

| | | | | | | | | | | | | | |
|---|---|---|---|---|---|---|---|---|---|---|---|---|---|
| 71 | 8 | Flores 2017 | W.11.2.G | 7.00 | | 0.35 | 1.30 | 2660 | Mid | Santa Cruz Island | Island | 33.962 | -119.8 |
| 71 | 8 | Flores 2017 | W.11.2.H | 8.00 | | 0.43 | 0.40 | 2660 | Mid | Santa Cruz Island | Island | 33.962 | -119.8 |
| 72 | 8 | Flores 2017 | W.11.3.A | 1.00 | | 0.54 | 0.31 | 2660 | Mid | Santa Cruz Island | Island | 33.962 | -119.8 |
| 72 | 8 | Flores 2017 | W.11.3.B | 2.00 | | 0.68 | 0.88 | 2660 | Mid | Santa Cruz Island | Island | 33.962 | -119.8 |
| 72 | 8 | Flores 2017 | W.11.3.C | 3.00 | | 0.70 | 1.29 | 2660 | Mid | Santa Cruz Island | Island | 33.962 | -119.8 |
| 72 | 8 | Flores 2017 | W.11.3.D | 4.00 | | 0.34 | 0.91 | 2660 | Mid | Santa Cruz Island | Island | 33.962 | -119.8 |
| 72 | 8 | Flores 2017 | W.11.3.E | 5.00 | | 0.26 | 1.55 | 2660 | Mid | Santa Cruz Island | Island | 33.962 | -119.8 |
| 72 | 8 | Flores 2017 | W.11.3.F | 6.00 | | 0.59 | 1.83 | 2660 | Mid | Santa Cruz Island | Island | 33.962 | -119.8 |
| 72 | 8 | Flores 2017 | W.11.3.G | 7.00 | | 0.61 | 1.20 | 2660 | Mid | Santa Cruz Island | Island | 33.962 | -119.8 |
| 72 | 8 | Flores 2017 | W.11.3.H | 8.00 | | 0.74 | 0.84 | 2660 | Mid | Santa Cruz Island | Island | 33.962 | -119.8 |
| 73 | 8 | Flores 2017 | W.12.1.A | 1.00 | | 0.68 | 0.99 | 2660 | Mid | Santa Cruz Island | Island | 33.962 | -119.8 |
| 73 | 8 | Flores 2017 | W.12.1.B | 2.00 | | 0.38 | 0.14 | 2660 | Mid | Santa Cruz Island | Island | 33.962 | -119.8 |
| 73 | 8 | Flores 2017 | W.12.1.C | 3.00 | | 0.26 | 0.51 | 2660 | Mid | Santa Cruz Island | Island | 33.962 | -119.8 |
| 73 | 8 | Flores 2017 | W.12.1.D | 4.00 | | 0.87 | 0.18 | 2660 | Mid | Santa Cruz Island | Island | 33.962 | -119.8 |
| 73 | 8 | Flores 2017 | W.12.1.E | 5.00 | | 0.95 | 0.71 | 2660 | Mid | Santa Cruz Island | Island | 33.962 | -119.8 |
| 73 | 8 | Flores 2017 | W.12.1.F | 6.00 | | 1.15 | 0.88 | 2660 | Mid | Santa Cruz Island | Island | 33.962 | -119.8 |
| 73 | 8 | Flores 2017 | W.12.1.G | 7.00 | | 1.14 | 0.51 | 2660 | Mid | Santa Cruz Island | Island | 33.962 | -119.8 |
| 73 | 8 | Flores 2017 | W.12.1.H | 8.00 | | 0.61 | -1.84 | 2660 | Mid | Santa Cruz Island | Island | 33.962 | -119.8 |
| 74 | 8 | Flores 2017 | W.2.1.A | 1.00 | | 1.97 | 0.74 | 950 | Mid | Santa Cruz Island | Island | 33.962 | -119.8 |

| | | | | | | | | | | | | | |
|---|---|---|---|---|---|---|---|---|---|---|---|---|---|
| 74 | 8 | Flores 2017 | W.2.1.B | 2.00 | | 1.67 | 0.94 | 950 | Mid | Santa Cruz Island | Island | 33.962 | -119.8 |
| 74 | 8 | Flores 2017 | W.2.1.C | 3.00 | | 1.57 | 0.07 | 950 | Mid | Santa Cruz Island | Island | 33.962 | -119.8 |
| 74 | 8 | Flores 2017 | W.2.1.D | 4.00 | | 1.10 | -0.22 | 950 | Mid | Santa Cruz Island | Island | 33.962 | -119.8 |
| 74 | 8 | Flores 2017 | W.2.1.E | 5.00 | | 0.54 | 0.26 | 950 | Mid | Santa Cruz Island | Island | 33.962 | -119.8 |
| 74 | 8 | Flores 2017 | W.2.1.F | 6.00 | | 0.18 | 0.66 | 950 | Mid | Santa Cruz Island | Island | 33.962 | -119.8 |
| 74 | 8 | Flores 2017 | W.2.1.G | 7.00 | | 0.33 | 1.46 | 950 | Mid | Santa Cruz Island | Island | 33.962 | -119.8 |
| 74 | 8 | Flores 2017 | W.2.1.H | 8.00 | | 0.71 | 1.24 | 950 | Mid | Santa Cruz Island | Island | 33.962 | -119.8 |
| 75 | 8 | Flores 2017 | W.2.2.A | 1.00 | | 1.09 | 0.14 | 950 | Mid | Santa Cruz Island | Island | 33.962 | -119.8 |
| 75 | 8 | Flores 2017 | W.2.2.B | 2.00 | | 0.98 | 0.59 | 950 | Mid | Santa Cruz Island | Island | 33.962 | -119.8 |
| 75 | 8 | Flores 2017 | W.2.2.C | 3.00 | | 0.64 | 0.64 | 950 | Mid | Santa Cruz Island | Island | 33.962 | -119.8 |
| 75 | 8 | Flores 2017 | W.2.2.D | 4.00 | | 0.73 | 0.63 | 950 | Mid | Santa Cruz Island | Island | 33.962 | -119.8 |
| 75 | 8 | Flores 2017 | W.2.2.E | 5.00 | | 0.66 | 0.83 | 950 | Mid | Santa Cruz Island | Island | 33.962 | -119.8 |
| 75 | 8 | Flores 2017 | W.2.2.F | 6.00 | | 0.77 | 1.38 | 950 | Mid | Santa Cruz Island | Island | 33.962 | -119.8 |
| 75 | 8 | Flores 2017 | W.2.2.G | 7.00 | | 0.70 | 0.90 | 950 | Mid | Santa Cruz Island | Island | 33.962 | -119.8 |
| 75 | 8 | Flores 2017 | W.2.2.H | 8.00 | | 0.59 | 0.61 | 950 | Mid | Santa Cruz Island | Island | 33.962 | -119.8 |
| 76 | 8 | Flores 2017 | W.2.3.A | 1.00 | | 1.63 | -0.11 | 950 | Mid | Santa Cruz Island | Island | 33.962 | -119.8 |
| 76 | 8 | Flores 2017 | W.2.3.B | 2.00 | | 1.49 | -0.31 | 950 | Mid | Santa Cruz Island | Island | 33.962 | -119.8 |
| 76 | 8 | Flores 2017 | W.2.3.C | 3.00 | | 1.20 | -0.06 | 950 | Mid | Santa Cruz Island | Island | 33.962 | -119.8 |
| 76 | 8 | Flores 2017 | W.2.3.D | 4.00 | | 0.91 | 0.06 | 950 | Mid | Santa Cruz Island | Island | 33.962 | -119.8 |

| | | | | | | | | | | | | | |
|---|---|---|---|---|---|---|---|---|---|---|---|---|---|
| 76 | 8 | Flores 2017 | W.2.3.E | 5.00 | | 0.80 | 0.11 | 950 | Mid | Santa Cruz Island | Island | 33.962 | -119.8 |
| 76 | 8 | Flores 2017 | W.2.3.F | 6.00 | | 0.49 | 0.43 | 950 | Mid | Santa Cruz Island | Island | 33.962 | -119.8 |
| 76 | 8 | Flores 2017 | W.2.3.G | 7.00 | | 0.80 | 0.90 | 950 | Mid | Santa Cruz Island | Island | 33.962 | -119.8 |
| 76 | 8 | Flores 2017 | W.2.3.H | 8.00 | | 0.90 | 1.05 | 950 | Mid | Santa Cruz Island | Island | 33.962 | -119.8 |
| 77 | 8 | Flores 2017 | W.2.4.A | 1.00 | | 1.15 | -0.05 | 950 | Mid | Santa Cruz Island | Island | 33.962 | -119.8 |
| 77 | 8 | Flores 2017 | W.2.4.B | 2.00 | | 1.25 | 0.30 | 950 | Mid | Santa Cruz Island | Island | 33.962 | -119.8 |
| 77 | 8 | Flores 2017 | W.2.4.C | 3.00 | | 0.76 | 0.29 | 950 | Mid | Santa Cruz Island | Island | 33.962 | -119.8 |
| 77 | 8 | Flores 2017 | W.2.4.D | 4.00 | | 0.61 | 1.01 | 950 | Mid | Santa Cruz Island | Island | 33.962 | -119.8 |
| 77 | 8 | Flores 2017 | W.2.4.E | 5.00 | | 0.66 | 0.76 | 950 | Mid | Santa Cruz Island | Island | 33.962 | -119.8 |
| 77 | 8 | Flores 2017 | W.2.4.F | 6.00 | | 0.76 | 0.82 | 950 | Mid | Santa Cruz Island | Island | 33.962 | -119.8 |
| 77 | 8 | Flores 2017 | W.2.4.G | 7.00 | | 0.71 | 0.79 | 950 | Mid | Santa Cruz Island | Island | 33.962 | -119.8 |
| 77 | 8 | Flores 2017 | W.2.4.H | 8.00 | | 0.77 | 0.62 | 950 | Mid | Santa Cruz Island | Island | 33.962 | -119.8 |
| 78 | 8 | Flores 2017 | W.3.1.A | 1.00 | | 1.52 | -0.20 | 2300 | Mid | Santa Cruz Island | Island | 33.962 | -119.8 |
| 78 | 8 | Flores 2017 | W.3.1.B | 2.00 | | 1.37 | -0.16 | 2300 | Mid | Santa Cruz Island | Island | 33.962 | -119.8 |
| 78 | 8 | Flores 2017 | W.3.1.C | 3.00 | | 0.85 | 0.36 | 2300 | Mid | Santa Cruz Island | Island | 33.962 | -119.8 |
| 78 | 8 | Flores 2017 | W.3.1.D | 4.00 | | 0.42 | 0.54 | 2300 | Mid | Santa Cruz Island | Island | 33.962 | -119.8 |
| 78 | 8 | Flores 2017 | W.3.1.E | 5.00 | | 0.28 | 0.52 | 2300 | Mid | Santa Cruz Island | Island | 33.962 | -119.8 |
| 78 | 8 | Flores 2017 | W.3.1.F | 6.00 | | 0.09 | 0.43 | 2300 | Mid | Santa Cruz Island | Island | 33.962 | -119.8 |
| 78 | 8 | Flores 2017 | W.3.1.G | 7.00 | | 0.44 | -0.32 | 2300 | Mid | Santa Cruz Island | Island | 33.962 | -119.8 |

| | | | | | | | | | | | | | |
|---|---|---|---|---|---|---|---|---|---|---|---|---|---|
| 78 | 8 | Flores 2017 | W.3.1.H | 8.00 | | 0.82 | -0.32 | 2300 | Mid | Santa Cruz Island | Island | 33.962 | -119.8 |
| 79 | 8 | Flores 2017 | W.3.2.A | 1.00 | | 0.07 | 0.16 | 2300 | Mid | Santa Cruz Island | Island | 33.962 | -119.8 |
| 79 | 8 | Flores 2017 | W.3.2.B | 2.00 | | 0.73 | 0.58 | 2300 | Mid | Santa Cruz Island | Island | 33.962 | -119.8 |
| 79 | 8 | Flores 2017 | W.3.2.C | 3.00 | | 0.50 | 0.11 | 2300 | Mid | Santa Cruz Island | Island | 33.962 | -119.8 |
| 79 | 8 | Flores 2017 | W.3.2.D | 4.00 | | 0.48 | -0.41 | 2300 | Mid | Santa Cruz Island | Island | 33.962 | -119.8 |
| 79 | 8 | Flores 2017 | W.3.2.E | 5.00 | | 0.52 | -0.48 | 2300 | Mid | Santa Cruz Island | Island | 33.962 | -119.8 |
| 79 | 8 | Flores 2017 | W.3.2.F | 6.00 | | 0.32 | -0.56 | 2300 | Mid | Santa Cruz Island | Island | 33.962 | -119.8 |
| 79 | 8 | Flores 2017 | W.3.2.G | 7.00 | | 0.46 | -0.86 | 2300 | Mid | Santa Cruz Island | Island | 33.962 | -119.8 |
| 79 | 8 | Flores 2017 | W.3.2.H | 8.00 | | 0.38 | -0.55 | 2300 | Mid | Santa Cruz Island | Island | 33.962 | -119.8 |
| 80 | 8 | Flores 2017 | W.3.3.A | 1.00 | | 1.29 | -0.29 | 2300 | Mid | Santa Cruz Island | Island | 33.962 | -119.8 |
| 80 | 8 | Flores 2017 | W.3.3.B | 2.00 | | 0.69 | -1.23 | 2300 | Mid | Santa Cruz Island | Island | 33.962 | -119.8 |
| 80 | 8 | Flores 2017 | W.3.3.C | 3.00 | | 0.65 | 0.79 | 2300 | Mid | Santa Cruz Island | Island | 33.962 | -119.8 |
| 80 | 8 | Flores 2017 | W.3.3.D | 4.00 | | 0.06 | 0.57 | 2300 | Mid | Santa Cruz Island | Island | 33.962 | -119.8 |
| 80 | 8 | Flores 2017 | W.3.3.E | 5.00 | | 0.20 | 1.02 | 2300 | Mid | Santa Cruz Island | Island | 33.962 | -119.8 |
| 80 | 8 | Flores 2017 | W.3.3.F | 6.00 | | 0.12 | 0.94 | 2300 | Mid | Santa Cruz Island | Island | 33.962 | -119.8 |
| 80 | 8 | Flores 2017 | W.3.3.G | 7.00 | | 0.15 | 0.92 | 2300 | Mid | Santa Cruz Island | Island | 33.962 | -119.8 |
| 80 | 8 | Flores 2017 | W.3.3.H | 8.00 | | 0.15 | 0.91 | 2300 | Mid | Santa Cruz Island | Island | 33.962 | -119.8 |
| 81 | 8 | Flores 2017 | W.3.4.A | 1.00 | | 0.86 | -0.49 | 2300 | Mid | Santa Cruz Island | Island | 33.962 | -119.8 |
| 81 | 8 | Flores 2017 | W.3.4.B | 2.00 | | 0.60 | -0.57 | 2300 | Mid | Santa Cruz Island | Island | 33.962 | -119.8 |

| | | | | | | | | | | | | | |
|---|---|---|---|---|---|---|---|---|---|---|---|---|---|
| 81 | 8 | Flores 2017 | W.3.4.C | 3.00 | | 0.25 | -0.37 | 2300 | Mid | Santa Cruz Island | Island | 33.962 | -119.8 |
| 81 | 8 | Flores 2017 | W.3.4.D | 4.00 | | 0.04 | -0.74 | 2300 | Mid | Santa Cruz Island | Island | 33.962 | -119.8 |
| 81 | 8 | Flores 2017 | W.3.4.E | 5.00 | | 0.06 | -0.81 | 2300 | Mid | Santa Cruz Island | Island | 33.962 | -119.8 |
| 81 | 8 | Flores 2017 | W.3.4.F | 6.00 | | -0.24 | -0.26 | 2300 | Mid | Santa Cruz Island | Island | 33.962 | -119.8 |
| 81 | 8 | Flores 2017 | W.3.4.G | 7.00 | | -0.01 | 0.08 | 2300 | Mid | Santa Cruz Island | Island | 33.962 | -119.8 |
| 81 | 8 | Flores 2017 | W.3.4.H | 8.00 | | 0.06 | 0.25 | 2300 | Mid | Santa Cruz Island | Island | 33.962 | -119.8 |
| 82 | 8 | Flores 2017 | W.4.1.A | 1.00 | | -0.11 | -0.11 | 2480 | Mid | Santa Cruz Island | Island | 33.915 | -120.1 |
| 82 | 8 | Flores 2017 | W.4.1.B | 2.00 | | 0.71 | 0.95 | 2480 | Mid | Santa Cruz Island | Island | 33.915 | -120.1 |
| 82 | 8 | Flores 2017 | W.4.1.C | 3.00 | | 0.66 | -0.12 | 2480 | Mid | Santa Cruz Island | Island | 33.915 | -120.1 |
| 82 | 8 | Flores 2017 | W.4.1.D | 4.00 | | 0.52 | -0.10 | 2480 | Mid | Santa Cruz Island | Island | 33.915 | -120.1 |
| 82 | 8 | Flores 2017 | W.4.1.E | 5.00 | | 0.58 | 0.03 | 2480 | Mid | Santa Cruz Island | Island | 33.915 | -120.1 |
| 82 | 8 | Flores 2017 | W.4.1.F | 6.00 | | 0.10 | 0.31 | 2480 | Mid | Santa Cruz Island | Island | 33.915 | -120.1 |
| 82 | 8 | Flores 2017 | W.4.1G | 7.00 | | -0.42 | 0.45 | 2480 | Mid | Santa Cruz Island | Island | 33.915 | -120.1 |
| 82 | 8 | Flores 2017 | W.4.1H | 8.00 | | -0.04 | 0.70 | 2480 | Mid | Santa Cruz Island | Island | 33.915 | -120.1 |
| 83 | 8 | Flores 2017 | W.4.2A | 1.00 | | 1.16 | -1.17 | 2480 | Mid | Santa Cruz Island | Island | 33.915 | -120.1 |
| 83 | 8 | Flores 2017 | W.4.2B | 2.00 | | 0.87 | 0.01 | 2480 | Mid | Santa Cruz Island | Island | 33.915 | -120.1 |
| 83 | 8 | Flores 2017 | W.4.2C | 3.00 | | 0.80 | 0.70 | 2480 | Mid | Santa Cruz Island | Island | 33.915 | -120.1 |
| 83 | 8 | Flores 2017 | W.4.2D | 4.00 | | 0.98 | -0.43 | 2480 | Mid | Santa Cruz Island | Island | 33.915 | -120.1 |
| 83 | 8 | Flores 2017 | W.4.2E | 5.00 | | 1.07 | 0.34 | 2480 | Mid | Santa Cruz Island | Island | 33.915 | -120.1 |

| | | | | | | | | | | | | | |
|---|---|---|---|---|---|---|---|---|---|---|---|---|---|
| 83 | 8 | Flores 2017 | W.4.2F | 6.00 | | 0.98 | 0.44 | 2480 | Mid | Santa Cruz Island | Island | 33.915 | -120.1 |
| 83 | 8 | Flores 2017 | W.4.2G | 7.00 | | -0.81 | -2.24 | 2480 | Mid | Santa Cruz Island | Island | 33.915 | -120.1 |
| 83 | 8 | Flores 2017 | W.4.2H | 8.00 | | 1.10 | 1.15 | 2480 | Mid | Santa Cruz Island | Island | 33.915 | -120.1 |
| 84 | 8 | Flores 2017 | W.4.3A | 1.00 | | 0.05 | 0.97 | 2480 | Mid | Santa Cruz Island | Island | 33.915 | -120.1 |
| 84 | 8 | Flores 2017 | W.4.3B | 2.00 | | 0.07 | 1.54 | 2480 | Mid | Santa Cruz Island | Island | 33.915 | -120.1 |
| 84 | 8 | Flores 2017 | W.4.3C | 3.00 | | 0.32 | 0.32 | 2480 | Mid | Santa Cruz Island | Island | 33.915 | -120.1 |
| 84 | 8 | Flores 2017 | W.4.3D | 4.00 | | -0.15 | 0.67 | 2480 | Mid | Santa Cruz Island | Island | 33.915 | -120.1 |
| 84 | 8 | Flores 2017 | W.4.3E | 5.00 | | -0.08 | 1.37 | 2480 | Mid | Santa Cruz Island | Island | 33.915 | -120.1 |
| 84 | 8 | Flores 2017 | W.4.3F | 6.00 | | 0.06 | 1.33 | 2480 | Mid | Santa Cruz Island | Island | 33.915 | -120.1 |
| 84 | 8 | Flores 2017 | W.4.3G | 7.00 | | 0.23 | 1.19 | 2480 | Mid | Santa Cruz Island | Island | 33.915 | -120.1 |
| 84 | 8 | Flores 2017 | W.4.3H | 8.00 | | 0.11 | 1.13 | 2480 | Mid | Santa Cruz Island | Island | 33.915 | -120.1 |
| 85 | 8 | Flores 2017 | W.4.4A | 1.00 | | 0.63 | 1.29 | 2480 | Mid | Santa Cruz Island | Island | 33.915 | -120.1 |
| 85 | 8 | Flores 2017 | W.4.4B | 2.00 | | 0.19 | 0.40 | 2480 | Mid | Santa Cruz Island | Island | 33.915 | -120.1 |
| 85 | 8 | Flores 2017 | W.4.4C | 3.00 | | -0.04 | 0.55 | 2480 | Mid | Santa Cruz Island | Island | 33.915 | -120.1 |
| 85 | 8 | Flores 2017 | W.4.4D | 4.00 | | -0.07 | 1.26 | 2480 | Mid | Santa Cruz Island | Island | 33.915 | -120.1 |
| 85 | 8 | Flores 2017 | W.4.4E | 5.00 | | 0.34 | 1.24 | 2480 | Mid | Santa Cruz Island | Island | 33.915 | -120.1 |
| 85 | 8 | Flores 2017 | W.4.4F | 6.00 | | 0.37 | 0.76 | 2480 | Mid | Santa Cruz Island | Island | 33.915 | -120.1 |
| 85 | 8 | Flores 2017 | W.4.4G | 7.00 | | 0.18 | 0.11 | 2480 | Mid | Santa Cruz Island | Island | 33.915 | -120.1 |
| 85 | 8 | Flores 2017 | W.4.4H | 8.00 | | 0.55 | 0.24 | 2480 | Mid | Santa Cruz Island | Island | 33.915 | -120.1 |

| | | | | | | | | | | | | | |
|---|---|---|---|---|---|---|---|---|---|---|---|---|---|
| 86 | 8 | Flores 2017 | W.5.1A | 1.00 | | 0.99 | 0.36 | 2480 | Mid | Santa Cruz Island | Island | 33.915 | -120.1 |
| 86 | 8 | Flores 2017 | W.5.1B | 2.00 | | 0.72 | 0.26 | 2480 | Mid | Santa Cruz Island | Island | 33.915 | -120.1 |
| 86 | 8 | Flores 2017 | W.5.1C | 3.00 | | 0.71 | 0.47 | 2480 | Mid | Santa Cruz Island | Island | 33.915 | -120.1 |
| 86 | 8 | Flores 2017 | W.5.1D | 4.00 | | 0.60 | 0.74 | 2480 | Mid | Santa Cruz Island | Island | 33.915 | -120.1 |
| 86 | 8 | Flores 2017 | W.5.1E | 5.00 | | 0.57 | 0.67 | 2480 | Mid | Santa Cruz Island | Island | 33.915 | -120.1 |
| 86 | 8 | Flores 2017 | W.5.1F | 6.00 | | 0.92 | 0.60 | 2480 | Mid | Santa Cruz Island | Island | 33.915 | -120.1 |
| 86 | 8 | Flores 2017 | W.5.1G | 7.00 | | 0.95 | -0.05 | 2480 | Mid | Santa Cruz Island | Island | 33.915 | -120.1 |
| 86 | 8 | Flores 2017 | W.5.1H | 8.00 | | 0.68 | -0.33 | 2480 | Mid | Santa Cruz Island | Island | 33.915 | -120.1 |
| 87 | 8 | Flores 2017 | W.5.2A | 1.00 | | 0.59 | 0.26 | 2480 | Mid | Santa Cruz Island | Island | 33.915 | -120.1 |
| 87 | 8 | Flores 2017 | W.5.2B | 2.00 | | 0.38 | 0.44 | 2480 | Mid | Santa Cruz Island | Island | 33.915 | -120.1 |
| 87 | 8 | Flores 2017 | W.5.2C | 3.00 | | 1.13 | -0.06 | 2480 | Mid | Santa Cruz Island | Island | 33.915 | -120.1 |
| 87 | 8 | Flores 2017 | W.5.2D | 4.00 | | 0.73 | 0.03 | 2480 | Mid | Santa Cruz Island | Island | 33.915 | -120.1 |
| 87 | 8 | Flores 2017 | W.5.2E | 5.00 | | 0.21 | -0.08 | 2480 | Mid | Santa Cruz Island | Island | 33.915 | -120.1 |
| 87 | 8 | Flores 2017 | W.5.2F | 6.00 | | 0.62 | -0.23 | 2480 | Mid | Santa Cruz Island | Island | 33.915 | -120.1 |
| 87 | 8 | Flores 2017 | W.5.2G | 7.00 | | 0.73 | -0.13 | 2480 | Mid | Santa Cruz Island | Island | 33.915 | -120.1 |
| 87 | 8 | Flores 2017 | W.5.2H | 8.00 | | 0.64 | -0.66 | 2480 | Mid | Santa Cruz Island | Island | 33.915 | -120.1 |
| 88 | 8 | Flores 2017 | W.5.3A | 1.00 | | 0.50 | -0.65 | 2480 | Mid | Santa Cruz Island | Island | 33.915 | -120.1 |
| 88 | 8 | Flores 2017 | W.5.3B | 2.00 | | 0.63 | -0.65 | 2480 | Mid | Santa Cruz Island | Island | 33.915 | -120.1 |
| 88 | 8 | Flores 2017 | W.5.3C | 3.00 | | 0.11 | 0.10 | 2480 | Mid | Santa Cruz Island | Island | 33.915 | -120.1 |

| | | | | | | | | | | | | | |
|---|---|---|---|---|---|---|---|---|---|---|---|---|---|
| 88 | 8 | Flores 2017 | W.5.3D | 4.00 | | -0.42 | 0.51 | 2480 | Mid | Santa Cruz Island | Island | 33.915 | -120.1 |
| 88 | 8 | Flores 2017 | W.5.3E | 5.00 | | -0.51 | 0.65 | 2480 | Mid | Santa Cruz Island | Island | 33.915 | -120.1 |
| 88 | 8 | Flores 2017 | W.5.3F | 6.00 | | 0.05 | 0.32 | 2480 | Mid | Santa Cruz Island | Island | 33.915 | -120.1 |
| 88 | 8 | Flores 2017 | W.5.3G | 7.00 | | 0.63 | 0.06 | 2480 | Mid | Santa Cruz Island | Island | 33.915 | -120.1 |
| 88 | 8 | Flores 2017 | W.5.3H | 8.00 | | 0.83 | -0.22 | 2480 | Mid | Santa Cruz Island | Island | 33.915 | -120.1 |
| 89 | 8 | Flores 2017 | W.5.4A | 1.00 | | 0.43 | 0.35 | 2480 | Mid | Santa Cruz Island | Island | 33.915 | -120.1 |
| 89 | 8 | Flores 2017 | W.5.4B | 2.00 | | 0.68 | -0.11 | 2480 | Mid | Santa Cruz Island | Island | 33.915 | -120.1 |
| 89 | 8 | Flores 2017 | W.5.4C | 3.00 | | 1.03 | -0.18 | 2480 | Mid | Santa Cruz Island | Island | 33.915 | -120.1 |
| 89 | 8 | Flores 2017 | W.5.4D | 4.00 | | 0.49 | -0.43 | 2480 | Mid | Santa Cruz Island | Island | 33.915 | -120.1 |
| 89 | 8 | Flores 2017 | W.5.4E | 5.00 | | 0.37 | -0.22 | 2480 | Mid | Santa Cruz Island | Island | 33.915 | -120.1 |
| 89 | 8 | Flores 2017 | W.5.4F | 6.00 | | 0.60 | -0.35 | 2480 | Mid | Santa Cruz Island | Island | 33.915 | -120.1 |
| 89 | 8 | Flores 2017 | W.5.4G | 7.00 | | 0.59 | 0.03 | 2480 | Mid | Santa Cruz Island | Island | 33.915 | -120.1 |
| 89 | 8 | Flores 2017 | W.5.4H | 8.00 | | 0.87 | -0.09 | 2480 | Mid | Santa Cruz Island | Island | 33.915 | -120.1 |
| 90 | 8 | Flores 2017 | W.6.1A | 1.00 | | 0.52 | 0.23 | 2450 | Mid | Santa Cruz Island | Island | 33.915 | -120.1 |
| 90 | 8 | Flores 2017 | W.6.1B | 2.00 | | 1.31 | -0.68 | 2450 | Mid | Santa Cruz Island | Island | 33.915 | -120.1 |
| 90 | 8 | Flores 2017 | W.6.1C | 3.00 | | 1.58 | -0.44 | 2450 | Mid | Santa Cruz Island | Island | 33.915 | -120.1 |
| 90 | 8 | Flores 2017 | W.6.1D | 4.00 | | 1.36 | -0.17 | 2450 | Mid | Santa Cruz Island | Island | 33.915 | -120.1 |
| 90 | 8 | Flores 2017 | W.6.1E | 5.00 | | 1.10 | -0.03 | 2450 | Mid | Santa Cruz Island | Island | 33.915 | -120.1 |
| 90 | 8 | Flores 2017 | W.6.1F | 6.00 | | 1.06 | 0.12 | 2450 | Mid | Santa Cruz Island | Island | 33.915 | -120.1 |

| | | | | | | | | | | | | | |
|---|---|---|---|---|---|---|---|---|---|---|---|---|---|
| 90 | 8 | Flores 2017 | W.6.1G | 7.00 | | 0.69 | 0.15 | 2450 | Mid | Santa Cruz Island | Island | 33.915 | -120.1 |
| 90 | 8 | Flores 2017 | W.6.1H | 8.00 | | 0.69 | 0.51 | 2450 | Mid | Santa Cruz Island | Island | 33.915 | -120.1 |
| 91 | 8 | Flores 2017 | W.9.3.A | 1.00 | | 0.13 | -0.83 | 2640 | Mid | Santa Cruz Island | Island | 33.962 | -119.8 |
| 91 | 8 | Flores 2017 | W.9.3.B | 2.00 | | -0.97 | -1.13 | 2640 | Mid | Santa Cruz Island | Island | 33.962 | -119.8 |
| 91 | 8 | Flores 2017 | W.9.3.C | 3.00 | | 0.49 | -0.32 | 2640 | Mid | Santa Cruz Island | Island | 33.962 | -119.8 |
| 91 | 8 | Flores 2017 | W.9.3.D | 4.00 | | 0.29 | -0.14 | 2640 | Mid | Santa Cruz Island | Island | 33.962 | -119.8 |
| 91 | 8 | Flores 2017 | W.9.3.E | 5.00 | | 0.38 | 0.47 | 2640 | Mid | Santa Cruz Island | Island | 33.962 | -119.8 |
| 91 | 8 | Flores 2017 | W.9.3.F | 6.00 | | 0.95 | 0.40 | 2640 | Mid | Santa Cruz Island | Island | 33.962 | -119.8 |
| 91 | 8 | Flores 2017 | W.9.3.G | 7.00 | | 0.55 | -0.24 | 2640 | Mid | Santa Cruz Island | Island | 33.962 | -119.8 |
| 91 | 8 | Flores 2017 | W.9.3.H | 8.00 | | 0.82 | -0.28 | 2640 | Mid | Santa Cruz Island | Island | 33.962 | -119.8 |
| 92 | 8 | Flores 2017 | W.9.4.A | 1.00 | | 0.61 | 0.33 | 2640 | Mid | Santa Cruz Island | Island | 33.962 | -119.8 |
| 92 | 8 | Flores 2017 | W.9.4.B | 2.00 | | 0.71 | 0.08 | 2640 | Mid | Santa Cruz Island | Island | 33.962 | -119.8 |
| 92 | 8 | Flores 2017 | W.9.4.C | 3.00 | | 0.45 | 0.14 | 2640 | Mid | Santa Cruz Island | Island | 33.962 | -119.8 |
| 92 | 8 | Flores 2017 | W.9.4.D | 4.00 | | 0.21 | 0.10 | 2640 | Mid | Santa Cruz Island | Island | 33.962 | -119.8 |
| 92 | 8 | Flores 2017 | W.9.4.E | 5.00 | | 0.03 | 0.56 | 2640 | Mid | Santa Cruz Island | Island | 33.962 | -119.8 |
| 92 | 8 | Flores 2017 | W.9.4.F | 6.00 | | 0.11 | 0.27 | 2640 | Mid | Santa Cruz Island | Island | 33.962 | -119.8 |
| 92 | 8 | Flores 2017 | W.9.4.G | 7.00 | | 0.18 | 0.55 | 2640 | Mid | Santa Cruz Island | Island | 33.962 | -119.8 |
| 92 | 8 | Flores 2017 | W.9.4.H | 8.00 | | -0.13 | 0.48 | 2640 | Mid | Santa Cruz Island | Island | 33.962 | -119.8 |
| 93 | 8 | Flores 2017 | W.9.1.A | 1.00 | | 0.51 | -0.62 | 2640 | Mid | Santa Cruz Island | Island | 33.962 | -119.8 |

| | | | | | | | | | | | | | |
|---|---|---|---|---|---|---|---|---|---|---|---|---|---|
| 93 | 8 | Flores 2017 | W.9.1.B | 2.00 | | 0.89 | -0.19 | 2640 | Mid | Santa Cruz Island | Island | 33.962 | -119.8 |
| 93 | 8 | Flores 2017 | W.9.1.C | 3.00 | | 1.25 | 0.60 | 2640 | Mid | Santa Cruz Island | Island | 33.962 | -119.8 |
| 93 | 8 | Flores 2017 | W.9.1.D | 4.00 | | 0.73 | 0.72 | 2640 | Mid | Santa Cruz Island | Island | 33.962 | -119.8 |
| 93 | 8 | Flores 2017 | W.9.1.E | 5.00 | | 0.82 | 1.04 | 2640 | Mid | Santa Cruz Island | Island | 33.962 | -119.8 |
| 93 | 8 | Flores 2017 | W.9.1.F | 6.00 | | 1.36 | 0.46 | 2640 | Mid | Santa Cruz Island | Island | 33.962 | -119.8 |
| 93 | 8 | Flores 2017 | W.9.1.G | 7.00 | | 1.83 | 0.28 | 2640 | Mid | Santa Cruz Island | Island | 33.962 | -119.8 |
| 93 | 8 | Flores 2017 | W.9.1.H | 8.00 | | 1.81 | 0.70 | 2640 | Mid | Santa Cruz Island | Island | 33.962 | -119.8 |
| 94 | 8 | Flores 2017 | W.9.2.A | 1.00 | | 1.18 | 0.71 | 2640 | Mid | Santa Cruz Island | Island | 33.962 | -119.8 |
| 94 | 8 | Flores 2017 | W.9.2.B | 2.00 | | 1.37 | 0.60 | 2640 | Mid | Santa Cruz Island | Island | 33.962 | -119.8 |
| 94 | 8 | Flores 2017 | W.9.2.C | 3.00 | | 1.27 | 0.27 | 2640 | Mid | Santa Cruz Island | Island | 33.962 | -119.8 |
| 94 | 8 | Flores 2017 | W.9.2.D | 4.00 | | 0.60 | -0.76 | 2640 | Mid | Santa Cruz Island | Island | 33.962 | -119.8 |
| 94 | 8 | Flores 2017 | W.9.2.E | 5.00 | | 0.91 | -0.24 | 2640 | Mid | Santa Cruz Island | Island | 33.962 | -119.8 |
| 94 | 8 | Flores 2017 | W.9.2.F | 6.00 | | 1.23 | 0.62 | 2640 | Mid | Santa Cruz Island | Island | 33.962 | -119.8 |
| 94 | 8 | Flores 2017 | W.9.2.G | 7.00 | | 1.32 | 0.47 | 2640 | Mid | Santa Cruz Island | Island | 33.962 | -119.8 |
| 94 | 8 | Flores 2017 | W.9.2.H | 8.00 | | 1.24 | -0.14 | 2640 | Mid | Santa Cruz Island | Island | 33.962 | -119.8 |
| 95 | 8 | Flores 2017 | W.8.1.A | 1.00 | | 1.38 | 0.58 | 2550 | Mid | Santa Cruz Island | Island | 33.915 | -120.1 |
| 95 | 8 | Flores 2017 | W.8.1.B | 2.00 | | 1.57 | -0.07 | 2550 | Mid | Santa Cruz Island | Island | 33.915 | -120.1 |
| 95 | 8 | Flores 2017 | W.8.1.C | 3.00 | | 1.39 | -0.55 | 2550 | Mid | Santa Cruz Island | Island | 33.915 | -120.1 |
| 95 | 8 | Flores 2017 | W.8.1.D | 4.00 | | 1.63 | -0.39 | 2550 | Mid | Santa Cruz Island | Island | 33.915 | -120.1 |

| | | | | | | | | | | | | | |
|---|---|---|---|---|---|---|---|---|---|---|---|---|---|
| 95 | 8 | Flores 2017 | W.8.1.E | 5.00 | | 1.53 | -0.32 | 2550 | Mid | Santa Cruz Island | Island | 33.915 | -120.1 |
| 95 | 8 | Flores 2017 | W.8.1.F | 6.00 | | 1.13 | -0.23 | 2550 | Mid | Santa Cruz Island | Island | 33.915 | -120.1 |
| 95 | 8 | Flores 2017 | W.8.1.G | 7.00 | | 0.69 | 0.19 | 2550 | Mid | Santa Cruz Island | Island | 33.915 | -120.1 |
| 95 | 8 | Flores 2017 | W.8.1.H | 8.00 | | 0.83 | 0.41 | 2550 | Mid | Santa Cruz Island | Island | 33.915 | -120.1 |
| 96 | 8 | Flores 2017 | W.8.2.A | 1.00 | | 0.83 | 0.32 | 2550 | Mid | Santa Cruz Island | Island | 33.915 | -120.1 |
| 96 | 8 | Flores 2017 | W.8.2.B | 2.00 | | 0.59 | 0.36 | 2550 | Mid | Santa Cruz Island | Island | 33.915 | -120.1 |
| 96 | 8 | Flores 2017 | W.8.2.C | 3.00 | | 0.52 | 0.40 | 2550 | Mid | Santa Cruz Island | Island | 33.915 | -120.1 |
| 96 | 8 | Flores 2017 | W.8.2.D | 4.00 | | 0.22 | 0.46 | 2550 | Mid | Santa Cruz Island | Island | 33.915 | -120.1 |
| 96 | 8 | Flores 2017 | W.8.2.E | 5.00 | | 0.40 | 0.65 | 2550 | Mid | Santa Cruz Island | Island | 33.915 | -120.1 |
| 96 | 8 | Flores 2017 | W.8.2.F | 6.00 | | 0.71 | 1.01 | 2550 | Mid | Santa Cruz Island | Island | 33.915 | -120.1 |
| 96 | 8 | Flores 2017 | W.8.2.G | 7.00 | | 0.88 | 0.87 | 2550 | Mid | Santa Cruz Island | Island | 33.915 | -120.1 |
| 96 | 8 | Flores 2017 | W.8.2.H | 8.00 | | 0.72 | 0.69 | 2550 | Mid | Santa Cruz Island | Island | 33.915 | -120.1 |
| 97 | 8 | Flores 2017 | W.8.3.A | 1.00 | | -0.32 | 0.64 | 2550 | Mid | Santa Cruz Island | Island | 33.915 | -120.1 |
| 97 | 8 | Flores 2017 | W.8.3.B | 2.00 | | -0.46 | -0.49 | 2550 | Mid | Santa Cruz Island | Island | 33.915 | -120.1 |
| 97 | 8 | Flores 2017 | W.8.3.C | 3.00 | | -1.08 | -0.38 | 2550 | Mid | Santa Cruz Island | Island | 33.915 | -120.1 |
| 97 | 8 | Flores 2017 | W.8.3.D | 4.00 | | -0.78 | 0.29 | 2550 | Mid | Santa Cruz Island | Island | 33.915 | -120.1 |
| 97 | 8 | Flores 2017 | W.8.3.E | 5.00 | | -0.62 | -0.51 | 2550 | Mid | Santa Cruz Island | Island | 33.915 | -120.1 |
| 97 | 8 | Flores 2017 | W.8.3.F | 6.00 | | -0.01 | 0.06 | 2550 | Mid | Santa Cruz Island | Island | 33.915 | -120.1 |
| 97 | 8 | Flores 2017 | W.8.3.G | 7.00 | | 0.12 | -0.32 | 2550 | Mid | Santa Cruz Island | Island | 33.915 | -120.1 |

| | | | | | | | | | | | | | |
|---|---|---|---|---|---|---|---|---|---|---|---|---|---|
| 97 | 8 | Flores 2017 | W.8.3.H | 8.00 | | -0.11 | 0.29 | 2550 | Mid | Santa Cruz Island | Island | 33.915 | -120.1 |
| 98 | 8 | Flores 2017 | W.8.4.A | 1.00 | | 1.07 | 1.05 | 2550 | Mid | Santa Cruz Island | Island | 33.915 | -120.1 |
| 98 | 8 | Flores 2017 | W.8.4.B | 2.00 | | 1.15 | 0.15 | 2550 | Mid | Santa Cruz Island | Island | 33.915 | -120.1 |
| 98 | 8 | Flores 2017 | W.8.4.C | 3.00 | | 0.78 | 0.36 | 2550 | Mid | Santa Cruz Island | Island | 33.915 | -120.1 |
| 98 | 8 | Flores 2017 | W.8.4.D | 4.00 | | 0.74 | 0.70 | 2550 | Mid | Santa Cruz Island | Island | 33.915 | -120.1 |
| 98 | 8 | Flores 2017 | W.8.4.E | 5.00 | | 0.92 | 1.04 | 2550 | Mid | Santa Cruz Island | Island | 33.915 | -120.1 |
| 98 | 8 | Flores 2017 | W.8.4.F | 6.00 | | 1.03 | 0.74 | 2550 | Mid | Santa Cruz Island | Island | 33.915 | -120.1 |
| 98 | 8 | Flores 2017 | W.8.4.G | 7.00 | | 0.97 | -0.45 | 2550 | Mid | Santa Cruz Island | Island | 33.915 | -120.1 |
| 98 | 8 | Flores 2017 | W.8.4.H | 8.00 | | 1.14 | -0.01 | 2550 | Mid | Santa Cruz Island | Island | 33.915 | -120.1 |
| 99 | 8 | Flores 2017 | W.6.2A | 1.00 | | 0.73 | -0.51 | 2450 | Mid | Santa Cruz Island | Island | 33.915 | -120.1 |
| 99 | 8 | Flores 2017 | W.6.2B | 2.00 | | 0.11 | 0.05 | 2450 | Mid | Santa Cruz Island | Island | 33.915 | -120.1 |
| 99 | 8 | Flores 2017 | W.6.2C | 3.00 | | 0.03 | 0.39 | 2450 | Mid | Santa Cruz Island | Island | 33.915 | -120.1 |
| 99 | 8 | Flores 2017 | W.6.2D | 4.00 | | -0.01 | 0.76 | 2450 | Mid | Santa Cruz Island | Island | 33.915 | -120.1 |
| 99 | 8 | Flores 2017 | W6.2E | 5.00 | | 0.61 | 0.66 | 2450 | Mid | Santa Cruz Island | Island | 33.915 | -120.1 |
| 99 | 8 | Flores 2017 | W6.2F | 6.00 | | 0.43 | 0.79 | 2450 | Mid | Santa Cruz Island | Island | 33.915 | -120.1 |
| 99 | 8 | Flores 2017 | W6.2G | 7.00 | | 0.64 | 0.37 | 2450 | Mid | Santa Cruz Island | Island | 33.915 | -120.1 |
| 99 | 8 | Flores 2017 | W6.2H | 8.00 | | 0.90 | -0.19 | 2450 | Mid | Santa Cruz Island | Island | 33.915 | -120.1 |
| 100 | 8 | Flores 2017 | W6.3A | 1.00 | | 1.92 | -0.17 | 2450 | Mid | Santa Cruz Island | Island | 33.915 | -120.1 |
| 100 | 8 | Flores 2017 | W6.3B | 2.00 | | 1.17 | 0.28 | 2450 | Mid | Santa Cruz Island | Island | 33.915 | -120.1 |

| | | | | | | | | | | | | | |
|---|---|---|---|---|---|---|---|---|---|---|---|---|---|
| 100 | 8 | Flores 2017 | W6.3C | 3.00 | | 1.16 | 0.87 | 2450 | Mid | Santa Cruz Island | Island | 33.915 | -120.1 |
| 100 | 8 | Flores 2017 | W6.3D | 4.00 | | 1.45 | 1.10 | 2450 | Mid | Santa Cruz Island | Island | 33.915 | -120.1 |
| 100 | 8 | Flores 2017 | W6.3E | 5.00 | | 1.41 | -0.41 | 2450 | Mid | Santa Cruz Island | Island | 33.915 | -120.1 |
| 100 | 8 | Flores 2017 | W6.3F | 6.00 | | 0.86 | 0.70 | 2450 | Mid | Santa Cruz Island | Island | 33.915 | -120.1 |
| 100 | 8 | Flores 2017 | W6.3G | 7.00 | | 0.79 | -0.72 | 2450 | Mid | Santa Cruz Island | Island | 33.915 | -120.1 |
| 100 | 8 | Flores 2017 | W6.3H | 8.00 | | 0.42 | 0.41 | 2450 | Mid | Santa Cruz Island | Island | 33.915 | -120.1 |
| 101 | 8 | Flores 2017 | W6.4A | 1.00 | | 0.46 | 0.42 | 2450 | Mid | Santa Cruz Island | Island | 33.915 | -120.1 |
| 101 | 8 | Flores 2017 | W6.4B | 2.00 | | 0.89 | -0.41 | 2450 | Mid | Santa Cruz Island | Island | 33.915 | -120.1 |
| 101 | 8 | Flores 2017 | W6.4C | 3.00 | | 0.53 | 0.45 | 2450 | Mid | Santa Cruz Island | Island | 33.915 | -120.1 |
| 101 | 8 | Flores 2017 | W6.4D | 4.00 | | 0.84 | 0.60 | 2450 | Mid | Santa Cruz Island | Island | 33.915 | -120.1 |
| 101 | 8 | Flores 2017 | W6.4E | 5.00 | | 1.20 | -0.47 | 2450 | Mid | Santa Cruz Island | Island | 33.915 | -120.1 |
| 101 | 8 | Flores 2017 | W6.4F | 6.00 | | 0.70 | 0.63 | 2450 | Mid | Santa Cruz Island | Island | 33.915 | -120.1 |
| 101 | 8 | Flores 2017 | W6.4G | 7.00 | | 0.63 | 1.03 | 2450 | Mid | Santa Cruz Island | Island | 33.915 | -120.1 |
| 101 | 8 | Flores 2017 | W6.4H | 8.00 | | 0.84 | 0.66 | 2450 | Mid | Santa Cruz Island | Island | 33.915 | -120.1 |
| 102 | 8 | Flores 2017 | W7.1A | 1.00 | | 1.07 | 0.49 | 2450 | Mid | Santa Cruz Island | Island | 33.915 | -120.1 |
| 102 | 8 | Flores 2017 | W7.1B | 2.00 | | 2.73 | 0.22 | 2450 | Mid | Santa Cruz Island | Island | 33.915 | -120.1 |
| 102 | 8 | Flores 2017 | W7.1C | 3.00 | | 0.64 | 0.13 | 2450 | Mid | Santa Cruz Island | Island | 33.915 | -120.1 |
| 102 | 8 | Flores 2017 | W7.1D | 4.00 | | 0.79 | -0.36 | 2450 | Mid | Santa Cruz Island | Island | 33.915 | -120.1 |
| 102 | 8 | Flores 2017 | W7.1E | 5.00 | | 0.41 | -0.12 | 2450 | Mid | Santa Cruz Island | Island | 33.915 | -120.1 |

| | | | | | | | | | | | | | |
|---|---|---|---|---|---|---|---|---|---|---|---|---|---|
| 102 | 8 | Flores 2017 | W7.1F | 6.00 | | 0.43 | 0.38 | 2450 | Mid | Santa Cruz Island | Island | 33.915 | -120.1 |
| 102 | 8 | Flores 2017 | W7.1G | 7.00 | | 0.05 | 0.68 | 2450 | Mid | Santa Cruz Island | Island | 33.915 | -120.1 |
| 102 | 8 | Flores 2017 | W7.1H | 8.00 | | -0.19 | 0.79 | 2450 | Mid | Santa Cruz Island | Island | 33.915 | -120.1 |
| 103 | 8 | Flores 2017 | W7.2A | 1.00 | | -0.39 | 1.02 | 2450 | Mid | Santa Cruz Island | Island | 33.915 | -120.1 |
| 103 | 8 | Flores 2017 | W7.2B | 2.00 | | 0.04 | 0.59 | 2450 | Mid | Santa Cruz Island | Island | 33.915 | -120.1 |
| 103 | 8 | Flores 2017 | W7.2C | 3.00 | | 0.41 | 0.48 | 2450 | Mid | Santa Cruz Island | Island | 33.915 | -120.1 |
| 103 | 8 | Flores 2017 | W7.2D | 4.00 | | 0.59 | 0.29 | 2450 | Mid | Santa Cruz Island | Island | 33.915 | -120.1 |
| 103 | 8 | Flores 2017 | W7.2E | 5.00 | | 0.03 | 0.37 | 2450 | Mid | Santa Cruz Island | Island | 33.915 | -120.1 |
| 103 | 8 | Flores 2017 | W7.2F | 6.00 | | -0.16 | -0.10 | 2450 | Mid | Santa Cruz Island | Island | 33.915 | -120.1 |
| 103 | 8 | Flores 2017 | W7.2G | 7.00 | | -0.14 | 0.05 | 2450 | Mid | Santa Cruz Island | Island | 33.915 | -120.1 |
| 103 | 8 | Flores 2017 | W7.2H | 8.00 | | 0.59 | 0.00 | 2450 | Mid | Santa Cruz Island | Island | 33.915 | -120.1 |
| 104 | 25 | Ford et al., 2010 | 3L.01 | 3L.01.12 | | 0.85 | 0.28 | 15 | Mod | San Diego | Main | 32.664 | -117.2 |
| 104 | 25 | Ford et al., 2010 | 3L.01 | 3L.01.21 | | 0.36 | 0.34 | 15 | Mod | San Diego | Main | 32.664 | -117.2 |
| 104 | 25 | Ford et al., 2010 | 3L.01 | 3L.01.22 | | 0.26 | 0.24 | 15 | Mod | San Diego | Main | 32.664 | -117.2 |
| 104 | 25 | Ford et al., 2010 | 3L.01 | 3L.01.23 | | 0.41 | 0.47 | 15 | Mod | San Diego | Main | 32.664 | -117.2 |
| 104 | 25 | Ford et al., 2010 | 3L.01 | 3L.01.24 | | -0.07 | -0.17 | 15 | Mod | San Diego | Main | 32.664 | -117.2 |
| 104 | 25 | Ford et al., 2010 | 3L.01 | 3L.01.25 | | 0.44 | -0.09 | 15 | Mod | San Diego | Main | 32.664 | -117.2 |
| 104 | 25 | Ford et al., 2010 | 3L.01 | 3L.01.26 | | 0.42 | -0.21 | 15 | Mod | San Diego | Main | 32.664 | -117.2 |
| 104 | 25 | Ford et al., 2010 | 3L.01 | 3L.01.27 | | 0.35 | | 15 | Mod | San Diego | Main | 32.664 | -117.2 |
| 104 | 25 | Ford et al., 2010 | 3L.01 | 3L.01.28 | | 0.56 | -0.01 | 15 | Mod | San Diego | Main | 32.664 | -117.2 |
| 104 | 25 | Ford et al., 2010 | 3L.01 | 3L.01.30 | | 0.83 | 0.09 | 15 | Mod | San Diego | Main | 32.664 | -117.2 |
| 104 | 25 | Ford et al., 2010 | 3L.01 | 3L.01.31 | | 0.80 | -0.09 | 15 | Mod | San Diego | Main | 32.664 | -117.2 |
| 104 | 25 | Ford et al., 2010 | 3L.01 | 3L.01.33 | | 0.78 | -0.23 | 15 | Mod | San Diego | Main | 32.664 | -117.2 |

| | | | | | | | | | | | | | |
|---|---|---|---|---|---|---|---|---|---|---|---|---|---|
| 104 | 25 | Ford et al., 2010 | 3L.01 | 3L.01.34 | | 1.10 | -0.26 | 15 | Mod | San Diego | Main | 32.664 | -117.2 |
| 104 | 25 | Ford et al., 2010 | 3L.01 | 3L.01.36 | | 0.80 | -0.38 | 15 | Mod | San Diego | Main | 32.664 | -117.2 |
| 104 | 25 | Ford et al., 2010 | 3L.01 | 3L.01.6 | | 0.53 | -0.52 | 15 | Mod | San Diego | Main | 32.664 | -117.2 |
| 104 | 25 | Ford et al., 2010 | 3L.01 | 3L.01.6.1 | | 0.40 | -0.53 | 15 | Mod | San Diego | Main | 32.664 | -117.2 |
| 104 | 25 | Ford et al., 2010 | 3L.01 | 3L.01.6.2 | | 0.02 | -0.50 | 15 | Mod | San Diego | Main | 32.664 | -117.2 |
| 104 | 25 | Ford et al., 2010 | 3L.01 | 3L.01.6.3 | | 0.02 | 0.14 | 15 | Mod | San Diego | Main | 32.664 | -117.2 |
| 104 | 25 | Ford et al., 2010 | 3L.01 | 3L.01.6.4 | | -0.07 | -0.55 | 15 | Mod | San Diego | Main | 32.664 | -117.2 |
| 104 | 25 | Ford et al., 2010 | 3L.01 | 3L.01.6.5 | | 0.24 | -0.58 | 15 | Mod | San Diego | Main | 32.664 | -117.2 |
| 104 | 25 | Ford et al., 2010 | 3L.01 | 3L.01.7 | | 0.19 | -0.96 | 15 | Mod | San Diego | Main | 32.664 | -117.2 |
| 104 | 25 | Ford et al., 2010 | 3L.01 | 3L.01.7.1 | | -0.07 | -0.87 | 15 | Mod | San Diego | Main | 32.664 | -117.2 |
| 104 | 25 | Ford et al., 2010 | 3L.01 | 3L.01.7.2 | | 0.43 | -0.20 | 15 | Mod | San Diego | Main | 32.664 | -117.2 |
| 104 | 25 | Ford et al., 2010 | 3L.01 | 3L.01.7.3 | | 0.64 | -0.89 | 15 | Mod | San Diego | Main | 32.664 | -117.2 |
| 104 | 25 | Ford et al., 2010 | 3L.01 | 3L.01.7.4 | | 1.16 | -0.17 | 15 | Mod | San Diego | Main | 32.664 | -117.2 |
| 105 | 30 | Ford et al., 2010 | 3L.05 | 3L.05.1 | | 0.44 | -0.41 | 15 | Mod | San Diego | Main | 32.664 | -117.2 |
| 105 | 30 | Ford et al., 2010 | 3L.05 | 3L.05.12 | | 0.25 | -0.18 | 15 | Mod | San Diego | Main | 32.664 | -117.2 |
| 105 | 30 | Ford et al., 2010 | 3L.05 | 3L.05.13 | | 0.28 | 0.03 | 15 | Mod | San Diego | Main | 32.664 | -117.2 |
| 105 | 30 | Ford et al., 2010 | 3L.05 | 3L.05.14 | | 0.49 | 0.09 | 15 | Mod | San Diego | Main | 32.664 | -117.2 |
| 105 | 30 | Ford et al., 2010 | 3L.05 | 3L.05.15 | | 0.30 | 0.09 | 15 | Mod | San Diego | Main | 32.664 | -117.2 |
| 105 | 30 | Ford et al., 2010 | 3L.05 | 3L.05.16 | | 0.35 | -0.10 | 15 | Mod | San Diego | Main | 32.664 | -117.2 |
| 105 | 30 | Ford et al., 2010 | 3L.05 | 3L.05.17 | | 0.31 | -0.16 | 15 | Mod | San Diego | Main | 32.664 | -117.2 |
| 105 | 30 | Ford et al., 2010 | 3L.05 | 3L.05.19 | | 0.33 | -0.57 | 15 | Mod | San Diego | Main | 32.664 | -117.2 |
| 105 | 30 | Ford et al., 2010 | 3L.05 | 3L.05.2 | | 0.35 | -0.56 | 15 | Mod | San Diego | Main | 32.664 | -117.2 |
| 105 | 30 | Ford et al., 2010 | 3L.05 | 3L.05.20 | | 0.46 | -0.13 | 15 | Mod | San Diego | Main | 32.664 | -117.2 |
| 105 | 30 | Ford et al., 2010 | 3L.05 | 3L.05.21 | | 0.56 | -0.40 | 15 | Mod | San Diego | Main | 32.664 | -117.2 |
| 105 | 30 | Ford et al., 2010 | 3L.05 | 3L.05.22 | | 0.95 | -0.13 | 15 | Mod | San Diego | Main | 32.664 | -117.2 |
| 105 | 30 | Ford et al., 2010 | 3L.05 | 3L.05.23 | | 0.62 | -0.49 | 15 | Mod | San Diego | Main | 32.664 | -117.2 |
| 105 | 30 | Ford et al., 2010 | 3L.05 | 3L.05.24 | | 0.44 | -0.48 | 15 | Mod | San Diego | Main | 32.664 | -117.2 |
| 105 | 30 | Ford et al., 2010 | 3L.05 | 3L.05.26 | | 1.25 | -0.20 | 15 | Mod | San Diego | Main | 32.664 | -117.2 |

| | | | | | | | | | | | | | |
|---|---|---|---|---|---|---|---|---|---|---|---|---|---|
| 105 | 30 | Ford et al., 2010 | 3L.05 | 3L.05.27 | | 0.62 | -0.16 | 15 | Mod | San Diego | Main | 32.664 | -117.2 |
| 105 | 30 | Ford et al., 2010 | 3L.05 | 3L.05.28 | | 0.69 | -0.27 | 15 | Mod | San Diego | Main | 32.664 | -117.2 |
| 105 | 30 | Ford et al., 2010 | 3L.05 | 3L.05.29 | | 1.03 | -0.39 | 15 | Mod | San Diego | Main | 32.664 | -117.2 |
| 105 | 30 | Ford et al., 2010 | 3L.05 | 3L.05.30 | | 0.79 | 0.10 | 15 | Mod | San Diego | Main | 32.664 | -117.2 |
| 105 | 30 | Ford et al., 2010 | 3L.05 | 3L.05.31 | | 0.55 | 0.27 | 15 | Mod | San Diego | Main | 32.664 | -117.2 |
| 105 | 30 | Ford et al., 2010 | 3L.05 | 3L.05.32 | | 0.03 | 0.09 | 15 | Mod | San Diego | Main | 32.664 | -117.2 |
| 105 | 30 | Ford et al., 2010 | 3L.05 | 3L.05.33 | | 0.11 | 0.45 | 15 | Mod | San Diego | Main | 32.664 | -117.2 |
| 105 | 30 | Ford et al., 2010 | 3L.05 | 3L.05.34 | | 0.36 | 0.01 | 15 | Mod | San Diego | Main | 32.664 | -117.2 |
| 105 | 30 | Ford et al., 2010 | 3L.05 | 3L.05.35 | | 0.01 | 0.07 | 15 | Mod | San Diego | Main | 32.664 | -117.2 |
| 105 | 30 | Ford et al., 2010 | 3L.05 | 3L.05.37 | | 0.18 | 0.00 | 15 | Mod | San Diego | Main | 32.664 | -117.2 |
| 105 | 30 | Ford et al., 2010 | 3L.05 | 3L.05.38 | | 0.17 | -0.26 | 15 | Mod | San Diego | Main | 32.664 | -117.2 |
| 105 | 30 | Ford et al., 2010 | 3L.05 | 3L.05.39 | | 0.65 | -0.12 | 15 | Mod | San Diego | Main | 32.664 | -117.2 |
| 105 | 30 | Ford et al., 2010 | 3L.05 | 3L.05.40 | | 0.45 | 0.08 | 15 | Mod | San Diego | Main | 32.664 | -117.2 |
| 105 | 30 | Ford et al., 2010 | 3L.05 | 3L.05.43 | | 0.52 | 0.02 | 15 | Mod | San Diego | Main | 32.664 | -117.2 |
| 105 | 30 | Ford et al., 2010 | 3L.05 | 3L.05.6 | | 0.98 | -1.00 | 15 | Mod | San Diego | Main | 32.664 | -117.2 |
| 106 | 35 | Ford et al., 2010 | 3L.09 | 3L.09.01 | | -0.44 | -0.40 | 15 | Mod | San Diego | Main | 32.664 | -117.2 |
| 106 | 35 | Ford et al., 2010 | 3L.09 | 3L.09.02 | | -0.63 | -0.27 | 15 | Mod | San Diego | Main | 32.664 | -117.2 |
| 106 | 35 | Ford et al., 2010 | 3L.09 | 3L.09.03 | | -0.67 | -0.33 | 15 | Mod | San Diego | Main | 32.664 | -117.2 |
| 106 | 35 | Ford et al., 2010 | 3L.09 | 3L.09.04 | | -0.62 | -0.25 | 15 | Mod | San Diego | Main | 32.664 | -117.2 |
| 106 | 35 | Ford et al., 2010 | 3L.09 | 3L.09.05 | | -0.32 | 0.07 | 15 | Mod | San Diego | Main | 32.664 | -117.2 |
| 106 | 35 | Ford et al., 2010 | 3L.09 | 3L.09.06 | | -0.27 | 0.02 | 15 | Mod | San Diego | Main | 32.664 | -117.2 |
| 106 | 35 | Ford et al., 2010 | 3L.09 | 3L.09.07 | | -0.08 | -0.32 | 15 | Mod | San Diego | Main | 32.664 | -117.2 |
| 106 | 35 | Ford et al., 2010 | 3L.09 | 3L.09.08 | | 0.07 | -0.14 | 15 | Mod | San Diego | Main | 32.664 | -117.2 |
| 106 | 35 | Ford et al., 2010 | 3L.09 | 3L.09.09 | | 0.10 | -0.09 | 15 | Mod | San Diego | Main | 32.664 | -117.2 |
| 106 | 35 | Ford et al., 2010 | 3L.09 | 3L.09.10 | | -0.31 | -1.00 | 15 | Mod | San Diego | Main | 32.664 | -117.2 |
| 106 | 35 | Ford et al., 2010 | 3L.09 | 3L.09.11 | | 0.23 | -0.29 | 15 | Mod | San Diego | Main | 32.664 | -117.2 |
| 106 | 35 | Ford et al., 2010 | 3L.09 | 3L.09.13 | | 0.19 | -0.24 | 15 | Mod | San Diego | Main | 32.664 | -117.2 |
| 106 | 35 | Ford et al., 2010 | 3L.09 | 3L.09.15 | | 0.09 | 0.15 | 15 | Mod | San Diego | Main | 32.664 | -117.2 |

| | | | | | | | | | | | | | |
|---|---|---|---|---|---|---|---|---|---|---|---|---|---|
| 106 | 35 | Ford et al., 2010 | 3L.09 | 3L.09.16 | | 0.03 | 0.02 | 15 | Mod | San Diego | Main | 32.664 | -117.2 |
| 106 | 35 | Ford et al., 2010 | 3L.09 | 3L.09.17 | | -0.74 | -0.63 | 15 | Mod | San Diego | Main | 32.664 | -117.2 |
| 106 | 35 | Ford et al., 2010 | 3L.09 | 3L.09.19 | | -0.61 | 0.33 | 15 | Mod | San Diego | Main | 32.664 | -117.2 |
| 106 | 35 | Ford et al., 2010 | 3L.09 | 3L.09.21 | | 0.28 | 0.12 | 15 | Mod | San Diego | Main | 32.664 | -117.2 |
| 106 | 35 | Ford et al., 2010 | 3L.09 | 3L.09.23 | | 0.25 | 0.10 | 15 | Mod | San Diego | Main | 32.664 | -117.2 |
| 106 | 35 | Ford et al., 2010 | 3L.09 | 3L.09.24 | | 0.21 | 0.02 | 15 | Mod | San Diego | Main | 32.664 | -117.2 |
| 106 | 35 | Ford et al., 2010 | 3L.09 | 3L.09.25 | | 0.26 | -0.14 | 15 | Mod | San Diego | Main | 32.664 | -117.2 |
| 106 | 35 | Ford et al., 2010 | 3L.09 | 3L.09.26 | | 0.66 | -0.04 | 15 | Mod | San Diego | Main | 32.664 | -117.2 |
| 106 | 35 | Ford et al., 2010 | 3L.09 | 3L.09.27 | | 0.61 | 0.09 | 15 | Mod | San Diego | Main | 32.664 | -117.2 |
| 106 | 35 | Ford et al., 2010 | 3L.09 | 3L.09.28 | | 0.33 | 0.06 | 15 | Mod | San Diego | Main | 32.664 | -117.2 |
| 106 | 35 | Ford et al., 2010 | 3L.09 | 3L.09.29 | | 0.08 | 0.16 | 15 | Mod | San Diego | Main | 32.664 | -117.2 |
| 106 | 35 | Ford et al., 2010 | 3L.09 | 3L.09.31 | | 0.41 | 0.01 | 15 | Mod | San Diego | Main | 32.664 | -117.2 |
| 106 | 35 | Ford et al., 2010 | 3L.09 | 3L.09.33A | | 0.50 | -0.44 | 15 | Mod | San Diego | Main | 32.664 | -117.2 |
| 106 | 35 | Ford et al., 2010 | 3L.09 | 3L.09.35 | | 0.31 | -0.61 | 15 | Mod | San Diego | Main | 32.664 | -117.2 |
| 106 | 35 | Ford et al., 2010 | 3L.09 | 3L.09.36 | | 0.17 | -0.85 | 15 | Mod | San Diego | Main | 32.664 | -117.2 |
| 106 | 35 | Ford et al., 2010 | 3L.09 | 3L.09.37 | | 0.08 | -0.73 | 15 | Mod | San Diego | Main | 32.664 | -117.2 |
| 106 | 35 | Ford et al., 2010 | 3L.09 | 3L.09.38 | | -0.14 | -0.89 | 15 | Mod | San Diego | Main | 32.664 | -117.2 |
| 106 | 35 | Ford et al., 2010 | 3L.09 | 3L.09.39 | | -0.06 | -0.70 | 15 | Mod | San Diego | Main | 32.664 | -117.2 |
| 106 | 35 | Ford et al., 2010 | 3L.09 | 3L.09.41 | | 0.14 | -0.42 | 15 | Mod | San Diego | Main | 32.664 | -117.2 |
| 106 | 35 | Ford et al., 2010 | 3L.09 | 3L.09.43 | | -0.16 | -0.36 | 15 | Mod | San Diego | Main | 32.664 | -117.2 |
| 106 | 35 | Ford et al., 2010 | 3L.09 | 3L.09.44 | | -0.45 | -1.78 | 15 | Mod | San Diego | Main | 32.664 | -117.2 |
| 106 | 35 | Ford et al., 2010 | 3L.09 | 3L.09.45 | | 0.30 | -1.29 | 15 | Mod | San Diego | Main | 32.664 | -117.2 |
| 107 | 38 | Ford et al., 2010 | 3L.10 | 3L.10.1 | | 0.24 | -0.29 | 15 | Mod | San Diego | Main | 32.664 | -117.2 |
| 107 | 38 | Ford et al., 2010 | 3L.10 | 3L.10.10 | | -0.08 | -0.27 | 15 | Mod | San Diego | Main | 32.664 | -117.2 |
| 107 | 38 | Ford et al., 2010 | 3L.10 | 3L.10.11 | | -0.12 | -0.33 | 15 | Mod | San Diego | Main | 32.664 | -117.2 |
| 107 | 38 | Ford et al., 2010 | 3L.10 | 3L.10.13 | | 0.05 | -0.31 | 15 | Mod | San Diego | Main | 32.664 | -117.2 |
| 107 | 38 | Ford et al., 2010 | 3L.10 | 3L.10.14 | | 0.11 | -0.48 | 15 | Mod | San Diego | Main | 32.664 | -117.2 |
| 107 | 38 | Ford et al., 2010 | 3L.10 | 3L.10.15 | | 0.15 | -0.34 | 15 | Mod | San Diego | Main | 32.664 | -117.2 |

| | | | | | | | | | | | | | |
|---|---|---|---|---|---|---|---|---|---|---|---|---|---|
| 107 | 38 | Ford et al., 2010 | 3L.10 | 3L.10.16 | | 0.08 | -0.13 | 15 | Mod | San Diego | Main | 32.664 | -117.2 |
| 107 | 38 | Ford et al., 2010 | 3L.10 | 3L.10.17 | | 0.31 | -0.09 | 15 | Mod | San Diego | Main | 32.664 | -117.2 |
| 107 | 38 | Ford et al., 2010 | 3L.10 | 3L.10.18 | | 0.61 | -0.07 | 15 | Mod | San Diego | Main | 32.664 | -117.2 |
| 107 | 38 | Ford et al., 2010 | 3L.10 | 3L.10.19 | | 0.47 | 0.04 | 15 | Mod | San Diego | Main | 32.664 | -117.2 |
| 107 | 38 | Ford et al., 2010 | 3L.10 | 3L.10.2 | | 0.29 | -0.38 | 15 | Mod | San Diego | Main | 32.664 | -117.2 |
| 107 | 38 | Ford et al., 2010 | 3L.10 | 3L.10.20 | | 0.18 | 0.49 | 15 | Mod | San Diego | Main | 32.664 | -117.2 |
| 107 | 38 | Ford et al., 2010 | 3L.10 | 3L.10.21 | | 0.32 | 0.55 | 15 | Mod | San Diego | Main | 32.664 | -117.2 |
| 107 | 38 | Ford et al., 2010 | 3L.10 | 3L.10.22 | | -0.07 | 0.85 | 15 | Mod | San Diego | Main | 32.664 | -117.2 |
| 107 | 38 | Ford et al., 2010 | 3L.10 | 3L.10.23 | | 0.09 | 0.00 | 15 | Mod | San Diego | Main | 32.664 | -117.2 |
| 107 | 38 | Ford et al., 2010 | 3L.10 | 3L.10.24 | | 0.04 | -0.02 | 15 | Mod | San Diego | Main | 32.664 | -117.2 |
| 107 | 38 | Ford et al., 2010 | 3L.10 | 3L.10.25 | | 0.01 | 0.26 | 15 | Mod | San Diego | Main | 32.664 | -117.2 |
| 107 | 38 | Ford et al., 2010 | 3L.10 | 3L.10.26 | | 0.31 | 0.01 | 15 | Mod | San Diego | Main | 32.664 | -117.2 |
| 107 | 38 | Ford et al., 2010 | 3L.10 | 3L.10.27 | | 0.34 | -0.29 | 15 | Mod | San Diego | Main | 32.664 | -117.2 |
| 107 | 38 | Ford et al., 2010 | 3L.10 | 3L.10.28 | | 0.47 | 0.04 | 15 | Mod | San Diego | Main | 32.664 | -117.2 |
| 107 | 38 | Ford et al., 2010 | 3L.10 | 3L.10.29 | | 0.31 | 0.22 | 15 | Mod | San Diego | Main | 32.664 | -117.2 |
| 107 | 38 | Ford et al., 2010 | 3L.10 | 3L.10.3 | | 0.11 | -0.65 | 15 | Mod | San Diego | Main | 32.664 | -117.2 |
| 107 | 38 | Ford et al., 2010 | 3L.10 | 3L.10.31 | | 0.41 | 0.10 | 15 | Mod | San Diego | Main | 32.664 | -117.2 |
| 107 | 38 | Ford et al., 2010 | 3L.10 | 3L.10.4 | | 0.07 | -0.29 | 15 | Mod | San Diego | Main | 32.664 | -117.2 |
| 107 | 38 | Ford et al., 2010 | 3L.10 | 3L.10.41 | | 0.45 | -0.57 | 15 | Mod | San Diego | Main | 32.664 | -117.2 |
| 107 | 38 | Ford et al., 2010 | 3L.10 | 3L.10.42 | | 0.72 | -0.54 | 15 | Mod | San Diego | Main | 32.664 | -117.2 |
| 107 | 38 | Ford et al., 2010 | 3L.10 | 3L.10.43 | | 0.49 | -0.65 | 15 | Mod | San Diego | Main | 32.664 | -117.2 |
| 107 | 38 | Ford et al., 2010 | 3L.10 | 3L.10.44 | | 0.24 | -0.66 | 15 | Mod | San Diego | Main | 32.664 | -117.2 |
| 107 | 38 | Ford et al., 2010 | 3L.10 | 3L.10.45 | | 0.53 | -1.11 | 15 | Mod | San Diego | Main | 32.664 | -117.2 |
| 107 | 38 | Ford et al., 2010 | 3L.10 | 3L.10.5 | | 0.03 | -0.05 | 15 | Mod | San Diego | Main | 32.664 | -117.2 |
| 107 | 38 | Ford et al., 2010 | 3L.10 | 3L.10.6 | | -0.11 | -0.10 | 15 | Mod | San Diego | Main | 32.664 | -117.2 |
| 107 | 38 | Ford et al., 2010 | 3L.10 | 3L.10.7 | | -0.05 | 0.11 | 15 | Mod | San Diego | Main | 32.664 | -117.2 |
| 107 | 38 | Ford et al., 2010 | 3L.10 | 3L.10.8 | | -0.06 | 0.10 | 15 | Mod | San Diego | Main | 32.664 | -117.2 |
| 107 | 38 | Ford et al., 2010 | 3L.10 | 3L.10.9 | | -0.10 | -0.24 | 15 | Mod | San Diego | Main | 32.664 | -117.2 |

| | | | | | | | | | | | | | |
|---|---|---|---|---|---|---|---|---|---|---|---|---|---|
| 107 | 38 | Ford et al., 2010 | 3L.10 | 3L.10.34 | | 0.45 | -0.11 | 16 | Mod | San Diego | Main | 32.664 | -117.2 |
| 107 | 38 | Ford et al., 2010 | 3L.10 | 3L.10.37 | | 0.36 | -0.38 | 16 | Mod | San Diego | Main | 32.664 | -117.2 |
| 107 | 38 | Ford et al., 2010 | 3L.10 | 3L.10.38 | | 0.08 | -1.38 | 16 | Mod | San Diego | Main | 32.664 | -117.2 |
| 107 | 38 | Ford et al., 2010 | 3L.10 | 3L.10.40 | | 0.49 | -0.82 | 16 | Mod | San Diego | Main | 32.664 | -117.2 |
| 108 | 21 | Ford et al., 2010 | 3L.13 | 3L.13.1 | | 0.25 | -0.41 | 15 | Mod | San Diego | Main | 32.664 | -117.2 |
| 108 | 21 | Ford et al., 2010 | 3L.13 | 3L.13.10 | | 0.70 | 0.07 | 15 | Mod | San Diego | Main | 32.664 | -117.2 |
| 108 | 21 | Ford et al., 2010 | 3L.13 | 3L.13.11 | | 0.49 | -0.04 | 15 | Mod | San Diego | Main | 32.664 | -117.2 |
| 108 | 21 | Ford et al., 2010 | 3L.13 | 3L.13.12 | | 1.07 | -0.01 | 15 | Mod | San Diego | Main | 32.664 | -117.2 |
| 108 | 21 | Ford et al., 2010 | 3L.13 | 3L.13.13 | | 0.96 | 0.03 | 15 | Mod | San Diego | Main | 32.664 | -117.2 |
| 108 | 21 | Ford et al., 2010 | 3L.13 | 3L.13.14 | | 0.65 | 0.63 | 15 | Mod | San Diego | Main | 32.664 | -117.2 |
| 108 | 21 | Ford et al., 2010 | 3L.13 | 3L.13.15 | | 0.24 | 0.58 | 15 | Mod | San Diego | Main | 32.664 | -117.2 |
| 108 | 21 | Ford et al., 2010 | 3L.13 | 3L.13.17 | | 0.70 | 0.83 | 15 | Mod | San Diego | Main | 32.664 | -117.2 |
| 108 | 21 | Ford et al., 2010 | 3L.13 | 3L.13.18 | | 0.82 | 0.49 | 15 | Mod | San Diego | Main | 32.664 | -117.2 |
| 108 | 21 | Ford et al., 2010 | 3L.13 | 3L.13.19 | | 0.81 | 0.19 | 15 | Mod | San Diego | Main | 32.664 | -117.2 |
| 108 | 21 | Ford et al., 2010 | 3L.13 | 3L.13.20 | | 0.87 | 0.39 | 15 | Mod | San Diego | Main | 32.664 | -117.2 |
| 108 | 21 | Ford et al., 2010 | 3L.13 | 3L.13.21 | | 0.72 | 0.40 | 15 | Mod | San Diego | Main | 32.664 | -117.2 |
| 108 | 21 | Ford et al., 2010 | 3L.13 | 3L.13.3 | | -0.64 | -1.68 | 15 | Mod | San Diego | Main | 32.664 | -117.2 |
| 108 | 21 | Ford et al., 2010 | 3L.13 | 3L.13.5 | | 0.41 | 0.32 | 15 | Mod | San Diego | Main | 32.664 | -117.2 |
| 108 | 21 | Ford et al., 2010 | 3L.13 | 3L.13.6 | | 0.29 | -0.40 | 15 | Mod | San Diego | Main | 32.664 | -117.2 |
| 108 | 21 | Ford et al., 2010 | 3L.13 | 3L.13.7 | | 0.56 | 0.01 | 15 | Mod | San Diego | Main | 32.664 | -117.2 |
| 108 | 21 | Ford et al., 2010 | 3L.13 | 3L.13.23 | | 0.71 | 0.10 | 16 | Mod | San Diego | Main | 32.664 | -117.2 |
| 108 | 21 | Ford et al., 2010 | 3L.13 | 3L.13.24 | | 0.48 | -1.36 | 16 | Mod | San Diego | Main | 32.664 | -117.2 |
| 108 | 21 | Ford et al., 2010 | 3L.13 | 3L.13.25 | | 1.00 | -0.31 | 16 | Mod | San Diego | Main | 32.664 | -117.2 |
| 108 | 21 | Ford et al., 2010 | 3L.13 | 3L.13.26 | | 0.94 | -0.29 | 16 | Mod | San Diego | Main | 32.664 | -117.2 |
| 108 | 21 | Ford et al., 2010 | 3L.13 | 3L.13.28 | | 0.83 | -0.75 | 16 | Mod | San Diego | Main | 32.664 | -117.2 |
| 109 | 22 | Ford et al., 2010 | 3L.15 | 3L.15.13 | | 0.40 | -0.39 | 15 | Mod | San Diego | Main | 32.664 | -117.2 |
| 109 | 22 | Ford et al., 2010 | 3L.15 | 3L.15.13.1 | | 0.88 | 0.27 | 15 | Mod | San Diego | Main | 32.664 | -117.2 |
| 109 | 22 | Ford et al., 2010 | 3L.15 | 3L.15.13.2 | | 0.83 | 0.10 | 15 | Mod | San Diego | Main | 32.664 | -117.2 |

| | | | | | | | | | | | | | |
|---|---|---|---|---|---|---|---|---|---|---|---|---|---|
| 109 | 22 | Ford et al., 2010 | 3L.15 | 3L.15.5 | | 0.22 | -0.13 | 15 | Mod | San Diego | Main | 32.664 | -117.2 |
| 109 | 22 | Ford et al., 2010 | 3L.15 | 3L.15.5.1 | | 0.26 | 0.12 | 15 | Mod | San Diego | Main | 32.664 | -117.2 |
| 109 | 22 | Ford et al., 2010 | 3L.15 | 3L.15.5.2 | | 0.22 | 0.15 | 15 | Mod | San Diego | Main | 32.664 | -117.2 |
| 109 | 22 | Ford et al., 2010 | 3L.15 | 3L.15.5.3 | | 0.10 | -0.28 | 15 | Mod | San Diego | Main | 32.664 | -117.2 |
| 109 | 22 | Ford et al., 2010 | 3L.15 | 3L.15.5.4 | | 0.36 | -0.32 | 15 | Mod | San Diego | Main | 32.664 | -117.2 |
| 109 | 22 | Ford et al., 2010 | 3L.15 | 3L.15.5.5 | | 0.42 | -0.24 | 15 | Mod | San Diego | Main | 32.664 | -117.2 |
| 109 | 22 | Ford et al., 2010 | 3L.15 | 3L.15.5.6 | | 0.65 | -0.18 | 15 | Mod | San Diego | Main | 32.664 | -117.2 |
| 109 | 22 | Ford et al., 2010 | 3L.15 | 3L.15.6 | | 0.41 | -0.22 | 15 | Mod | San Diego | Main | 32.664 | -117.2 |
| 109 | 22 | Ford et al., 2010 | 3L.15 | 3L.15.6.1 | | 0.62 | -0.10 | 15 | Mod | San Diego | Main | 32.664 | -117.2 |
| 109 | 22 | Ford et al., 2010 | 3L.15 | 3L.15.6.2 | | 0.69 | 0.14 | 15 | Mod | San Diego | Main | 32.664 | -117.2 |
| 109 | 22 | Ford et al., 2010 | 3L.15 | 3L.15.6.3 | | 0.50 | 0.39 | 15 | Mod | San Diego | Main | 32.664 | -117.2 |
| 109 | 22 | Ford et al., 2010 | 3L.15 | 3L.15.6.4 | | 0.43 | -0.18 | 15 | Mod | San Diego | Main | 32.664 | -117.2 |
| 109 | 22 | Ford et al., 2010 | 3L.15 | 3L.15.13.3 | | 1.00 | 0.22 | 16 | Mod | San Diego | Main | 32.664 | -117.2 |
| 109 | 22 | Ford et al., 2010 | 3L.15 | 3L.15.21 | | 0.84 | 0.28 | 16 | Mod | San Diego | Main | 32.664 | -117.2 |
| 109 | 22 | Ford et al., 2010 | 3L.15 | 3L.15.21.1 | | 0.75 | 0.20 | 16 | Mod | San Diego | Main | 32.664 | -117.2 |
| 109 | 22 | Ford et al., 2010 | 3L.15 | 3L.15.21.2 | | 0.55 | -0.35 | 16 | Mod | San Diego | Main | 32.664 | -117.2 |
| 109 | 22 | Ford et al., 2010 | 3L.15 | 3L.15.21.3 | | 0.59 | -0.66 | 16 | Mod | San Diego | Main | 32.664 | -117.2 |
| 109 | 22 | Ford et al., 2010 | 3L.15 | 3L.15.21.4 | | 0.46 | -1.08 | 16 | Mod | San Diego | Main | 32.664 | -117.2 |
| 109 | 22 | Ford et al., 2010 | 3L.15 | 3L.15.25 | | 0.47 | -0.62 | 16 | Mod | San Diego | Main | 32.664 | -117.2 |
| 110 | 40 | Ford et al., 2010 | 3L.16 | 3L.16.1 | | 0.33 | -0.73 | 15 | Mod | San Diego | Main | 32.664 | -117.2 |
| 110 | 40 | Ford et al., 2010 | 3L.16 | 3L.16.10 | | 0.79 | -0.52 | 15 | Mod | San Diego | Main | 32.664 | -117.2 |
| 110 | 40 | Ford et al., 2010 | 3L.16 | 3L.16.11 | | 0.92 | 0.01 | 15 | Mod | San Diego | Main | 32.664 | -117.2 |
| 110 | 40 | Ford et al., 2010 | 3L.16 | 3L.16.12 | | 0.84 | 0.07 | 15 | Mod | San Diego | Main | 32.664 | -117.2 |
| 110 | 40 | Ford et al., 2010 | 3L.16 | 3L.16.13 | | 0.91 | 0.08 | 15 | Mod | San Diego | Main | 32.664 | -117.2 |
| 110 | 40 | Ford et al., 2010 | 3L.16 | 3L.16.14 | | 0.34 | -0.03 | 15 | Mod | San Diego | Main | 32.664 | -117.2 |
| 110 | 40 | Ford et al., 2010 | 3L.16 | 3L.16.15 | | 0.46 | 0.28 | 15 | Mod | San Diego | Main | 32.664 | -117.2 |
| 110 | 40 | Ford et al., 2010 | 3L.16 | 3L.16.16 | | 0.81 | -0.29 | 15 | Mod | San Diego | Main | 32.664 | -117.2 |
| 110 | 40 | Ford et al., 2010 | 3L.16 | 3L.16.17 | | 0.94 | 0.16 | 15 | Mod | San Diego | Main | 32.664 | -117.2 |

| | | | | | | | | | | | | | |
|---|---|---|---|---|---|---|---|---|---|---|---|---|---|
| 110 | 40 | Ford et al., 2010 | 3L.16 | 3L.16.18 | | 0.85 | 0.08 | 15 | Mod | San Diego | Main | 32.664 | -117.2 |
| 110 | 40 | Ford et al., 2010 | 3L.16 | 3L.16.20 | | 0.53 | -0.69 | 15 | Mod | San Diego | Main | 32.664 | -117.2 |
| 110 | 40 | Ford et al., 2010 | 3L.16 | 3L.16.21 | | 0.87 | -0.21 | 15 | Mod | San Diego | Main | 32.664 | -117.2 |
| 110 | 40 | Ford et al., 2010 | 3L.16 | 3L.16.22 | | 0.95 | -0.03 | 15 | Mod | San Diego | Main | 32.664 | -117.2 |
| 110 | 40 | Ford et al., 2010 | 3L.16 | 3L.16.23 | | 0.95 | -0.15 | 15 | Mod | San Diego | Main | 32.664 | -117.2 |
| 110 | 40 | Ford et al., 2010 | 3L.16 | 3L.16.24 | | 0.96 | -0.06 | 15 | Mod | San Diego | Main | 32.664 | -117.2 |
| 110 | 40 | Ford et al., 2010 | 3L.16 | 3L.16.25 | | 0.93 | 0.10 | 15 | Mod | San Diego | Main | 32.664 | -117.2 |
| 110 | 40 | Ford et al., 2010 | 3L.16 | 3L.16.26 | | 0.63 | -0.06 | 15 | Mod | San Diego | Main | 32.664 | -117.2 |
| 110 | 40 | Ford et al., 2010 | 3L.16 | 3L.16.28 | | 0.28 | -0.53 | 15 | Mod | San Diego | Main | 32.664 | -117.2 |
| 110 | 40 | Ford et al., 2010 | 3L.16 | 3L.16.29 | | 0.85 | 0.06 | 15 | Mod | San Diego | Main | 32.664 | -117.2 |
| 110 | 40 | Ford et al., 2010 | 3L.16 | 3L.16.3 | | 0.51 | -0.51 | 15 | Mod | San Diego | Main | 32.664 | -117.2 |
| 110 | 40 | Ford et al., 2010 | 3L.16 | 3L.16.30 | | 0.84 | 0.04 | 15 | Mod | San Diego | Main | 32.664 | -117.2 |
| 110 | 40 | Ford et al., 2010 | 3L.16 | 3L.16.31 | | 0.86 | 0.14 | 15 | Mod | San Diego | Main | 32.664 | -117.2 |
| 110 | 40 | Ford et al., 2010 | 3L.16 | 3L.16.33 | | 0.79 | 0.02 | 15 | Mod | San Diego | Main | 32.664 | -117.2 |
| 110 | 40 | Ford et al., 2010 | 3L.16 | 3L.16.4 | | 0.53 | -0.17 | 15 | Mod | San Diego | Main | 32.664 | -117.2 |
| 110 | 40 | Ford et al., 2010 | 3L.16 | 3L.16.5 | | 0.27 | -0.55 | 15 | Mod | San Diego | Main | 32.664 | -117.2 |
| 110 | 40 | Ford et al., 2010 | 3L.16 | 3L.16.6 | | 0.60 | -0.25 | 15 | Mod | San Diego | Main | 32.664 | -117.2 |
| 110 | 40 | Ford et al., 2010 | 3L.16 | 3L.16.7 | | 0.72 | -0.24 | 15 | Mod | San Diego | Main | 32.664 | -117.2 |
| 110 | 40 | Ford et al., 2010 | 3L.16 | 3L.16.8 | | 0.89 | -0.26 | 15 | Mod | San Diego | Main | 32.664 | -117.2 |
| 110 | 40 | Ford et al., 2010 | 3L.16 | 3L.16.9 | | 1.01 | -0.07 | 15 | Mod | San Diego | Main | 32.664 | -117.2 |
| 110 | 40 | Ford et al., 2010 | 3L.16 | 3L.16.34 | | 0.91 | 0.08 | 16 | Mod | San Diego | Main | 32.664 | -117.2 |
| 110 | 40 | Ford et al., 2010 | 3L.16 | 3L.16.35 | | 0.95 | -0.05 | 16 | Mod | San Diego | Main | 32.664 | -117.2 |
| 110 | 40 | Ford et al., 2010 | 3L.16 | 3L.16.36 | | 0.78 | -0.10 | 16 | Mod | San Diego | Main | 32.664 | -117.2 |
| 110 | 40 | Ford et al., 2010 | 3L.16 | 3L.16.37 | | 0.67 | -0.23 | 16 | Mod | San Diego | Main | 32.664 | -117.2 |
| 110 | 40 | Ford et al., 2010 | 3L.16 | 3L.16.38 | | 0.45 | -0.32 | 16 | Mod | San Diego | Main | 32.664 | -117.2 |
| 110 | 40 | Ford et al., 2010 | 3L.16 | 3L.16.39 | | 0.64 | -0.37 | 16 | Mod | San Diego | Main | 32.664 | -117.2 |
| 110 | 40 | Ford et al., 2010 | 3L.16 | 3L.16.41 | | 0.79 | -0.64 | 16 | Mod | San Diego | Main | 32.664 | -117.2 |
| 110 | 40 | Ford et al., 2010 | 3L.16 | 3L.16.42 | | 0.56 | -1.26 | 16 | Mod | San Diego | Main | 32.664 | -117.2 |

| | | | | | | | | | | | | | |
|---|---|---|---|---|---|---|---|---|---|---|---|---|---|
| 110 | 40 | Ford et al., 2010 | 3L.16 | 3L.16.43 | | 0.63 | -0.84 | 16 | Mod | San Diego | Main | 32.664 | -117.2 |
| 110 | 40 | Ford et al., 2010 | 3L.16 | 3L.16.44 | | 0.55 | -0.90 | 16 | Mod | San Diego | Main | 32.664 | -117.2 |
| 110 | 40 | Ford et al., 2010 | 3L.16 | 3L.16.45 | | 0.53 | -0.69 | 16 | Mod | San Diego | Main | 32.664 | -117.2 |
| 111 | 28 | Ford et al., 2010 | 3L.20 | 3L.20.01A | | 0.13 | -0.43 | 15 | Mod | San Diego | Main | 32.664 | -117.2 |
| 111 | 28 | Ford et al., 2010 | 3L.20 | 3L.20.02 | | 0.13 | -0.56 | 15 | Mod | San Diego | Main | 32.664 | -117.2 |
| 111 | 28 | Ford et al., 2010 | 3L.20 | 3L.20.04 | | -0.14 | -0.13 | 15 | Mod | San Diego | Main | 32.664 | -117.2 |
| 111 | 28 | Ford et al., 2010 | 3L.20 | 3L.20.05 | | -0.20 | 0.01 | 15 | Mod | San Diego | Main | 32.664 | -117.2 |
| 111 | 28 | Ford et al., 2010 | 3L.20 | 3L.20.06 | | -0.15 | 0.03 | 15 | Mod | San Diego | Main | 32.664 | -117.2 |
| 111 | 28 | Ford et al., 2010 | 3L.20 | 3L.20.07 | | -0.14 | -0.07 | 15 | Mod | San Diego | Main | 32.664 | -117.2 |
| 111 | 28 | Ford et al., 2010 | 3L.20 | 3L.20.08 | | -0.09 | -0.24 | 15 | Mod | San Diego | Main | 32.664 | -117.2 |
| 111 | 28 | Ford et al., 2010 | 3L.20 | 3L.20.09 | | 0.09 | -0.37 | 15 | Mod | San Diego | Main | 32.664 | -117.2 |
| 111 | 28 | Ford et al., 2010 | 3L.20 | 3L.20.10 | | 0.03 | -0.34 | 15 | Mod | San Diego | Main | 32.664 | -117.2 |
| 111 | 28 | Ford et al., 2010 | 3L.20 | 3L.20.11 | | -0.01 | -0.20 | 15 | Mod | San Diego | Main | 32.664 | -117.2 |
| 111 | 28 | Ford et al., 2010 | 3L.20 | 3L.20.12 | | 0.38 | -0.23 | 15 | Mod | San Diego | Main | 32.664 | -117.2 |
| 111 | 28 | Ford et al., 2010 | 3L.20 | 3L.20.14 | | 0.33 | -0.20 | 15 | Mod | San Diego | Main | 32.664 | -117.2 |
| 111 | 28 | Ford et al., 2010 | 3L.20 | 3L.20.15 | | 0.17 | 0.27 | 15 | Mod | San Diego | Main | 32.664 | -117.2 |
| 111 | 28 | Ford et al., 2010 | 3L.20 | 3L.20.16 | | 0.13 | 0.13 | 15 | Mod | San Diego | Main | 32.664 | -117.2 |
| 111 | 28 | Ford et al., 2010 | 3L.20 | 3L.20.17 | | -0.15 | 0.35 | 15 | Mod | San Diego | Main | 32.664 | -117.2 |
| 111 | 28 | Ford et al., 2010 | 3L.20 | 3L.20.18 | | -0.30 | 0.25 | 15 | Mod | San Diego | Main | 32.664 | -117.2 |
| 111 | 28 | Ford et al., 2010 | 3L.20 | 3L.20.19 | | -0.10 | 0.76 | 15 | Mod | San Diego | Main | 32.664 | -117.2 |
| 111 | 28 | Ford et al., 2010 | 3L.20 | 3L.20.20 | | 0.32 | 0.36 | 15 | Mod | San Diego | Main | 32.664 | -117.2 |
| 111 | 28 | Ford et al., 2010 | 3L.20 | 3L.20.21 | | 0.39 | 0.10 | 15 | Mod | San Diego | Main | 32.664 | -117.2 |
| 111 | 28 | Ford et al., 2010 | 3L.20 | 3L.20.22 | | 0.00 | -0.15 | 15 | Mod | San Diego | Main | 32.664 | -117.2 |
| 111 | 28 | Ford et al., 2010 | 3L.20 | 3L.20.24 | | 0.45 | -0.12 | 15 | Mod | San Diego | Main | 32.664 | -117.2 |
| 111 | 28 | Ford et al., 2010 | 3L.20 | 3L.20.25 | | 0.30 | -0.10 | 15 | Mod | San Diego | Main | 32.664 | -117.2 |
| 111 | 28 | Ford et al., 2010 | 3L.20 | 3L.20.26 | | 0.11 | 0.15 | 16 | Mod | San Diego | Main | 32.664 | -117.2 |
| 111 | 28 | Ford et al., 2010 | 3L.20 | 3L.20.27 | | 0.16 | 0.37 | 16 | Mod | San Diego | Main | 32.664 | -117.2 |
| 111 | 28 | Ford et al., 2010 | 3L.20 | 3L.20.28 | | 0.22 | 0.00 | 16 | Mod | San Diego | Main | 32.664 | -117.2 |

| | | | | | | | | | | | | | |
|---|---|---|---|---|---|---|---|---|---|---|---|---|---|
| 111 | 28 | Ford et al., 2010 | 3L.20 | 3L.20.29 | | 0.23 | -0.36 | 16 | Mod | San Diego | Main | 32.664 | -117.2 |
| 111 | 28 | Ford et al., 2010 | 3L.20 | 3L.20.30 | | 0.18 | -0.68 | 16 | Mod | San Diego | Main | 32.664 | -117.2 |
| 111 | 28 | Ford et al., 2010 | 3L.20 | 3L.20.31B | | 0.39 | -1.02 | 16 | Mod | San Diego | Main | 32.664 | -117.2 |
| 111 | 34 | Ford et al., 2010 | 3U.02 | 3U.02.1 | | 0.59 | -0.33 | 15 | Mod | San Diego | Main | 32.664 | -117.2 |
| 111 | 34 | Ford et al., 2010 | 3U.02 | 3U.02.1.1 | | 0.85 | -0.51 | 15 | Mod | San Diego | Main | 32.664 | -117.2 |
| 111 | 34 | Ford et al., 2010 | 3U.02 | 3U.02.1.2 | | 0.49 | -0.89 | 15 | Mod | San Diego | Main | 32.664 | -117.2 |
| 111 | 34 | Ford et al., 2010 | 3U.02 | 3U.02.16 | | 0.85 | -0.20 | 15 | Mod | San Diego | Main | 32.664 | -117.2 |
| 111 | 34 | Ford et al., 2010 | 3U.02 | 3U.02.16.1 | | 0.77 | 0.09 | 15 | Mod | San Diego | Main | 32.664 | -117.2 |
| 111 | 34 | Ford et al., 2010 | 3U.02 | 3U.02.16.2 | | 0.47 | 0.30 | 15 | Mod | San Diego | Main | 32.664 | -117.2 |
| 111 | 34 | Ford et al., 2010 | 3U.02 | 3U.02.16.3 | | 0.01 | 0.52 | 15 | Mod | San Diego | Main | 32.664 | -117.2 |
| 111 | 34 | Ford et al., 2010 | 3U.02 | 3U.02.16.4 | | -0.39 | 0.58 | 15 | Mod | San Diego | Main | 32.664 | -117.2 |
| 111 | 34 | Ford et al., 2010 | 3U.02 | 3U.02.16.5 | | 0.32 | 0.14 | 15 | Mod | San Diego | Main | 32.664 | -117.2 |
| 111 | 34 | Ford et al., 2010 | 3U.02 | 3U.02.19 | | -0.27 | 0.03 | 15 | Mod | San Diego | Main | 32.664 | -117.2 |
| 111 | 34 | Ford et al., 2010 | 3U.02 | 3U.02.19.1 | | -0.30 | 0.12 | 15 | Mod | San Diego | Main | 32.664 | -117.2 |
| 111 | 34 | Ford et al., 2010 | 3U.02 | 3U.02.19.2 | | 0.01 | 0.03 | 15 | Mod | San Diego | Main | 32.664 | -117.2 |
| 111 | 34 | Ford et al., 2010 | 3U.02 | 3U.02.19.3 | | 0.13 | -0.14 | 15 | Mod | San Diego | Main | 32.664 | -117.2 |
| 111 | 34 | Ford et al., 2010 | 3U.02 | 3U.02.2 | | 0.43 | -0.54 | 15 | Mod | San Diego | Main | 32.664 | -117.2 |
| 111 | 34 | Ford et al., 2010 | 3U.02 | 3U.02.2.1 | | 0.49 | -0.28 | 15 | Mod | San Diego | Main | 32.664 | -117.2 |
| 111 | 34 | Ford et al., 2010 | 3U.02 | 3U.02.2.2 | | -0.01 | -0.09 | 15 | Mod | San Diego | Main | 32.664 | -117.2 |
| 111 | 34 | Ford et al., 2010 | 3U.02 | 3U.02.2.3 | | 0.03 | -0.01 | 15 | Mod | San Diego | Main | 32.664 | -117.2 |
| 111 | 34 | Ford et al., 2010 | 3U.02 | 3U.02.2.4 | | -0.23 | -0.21 | 15 | Mod | San Diego | Main | 32.664 | -117.2 |
| 111 | 34 | Ford et al., 2010 | 3U.02 | 3U.02.24.1 | | 0.13 | 0.02 | 15 | Mod | San Diego | Main | 32.664 | -117.2 |
| 111 | 34 | Ford et al., 2010 | 3U.02 | 3U.02.24.2 | | 0.10 | 0.01 | 15 | Mod | San Diego | Main | 32.664 | -117.2 |
| 111 | 34 | Ford et al., 2010 | 3U.02 | 3U.02.8.1 | | -0.07 | -0.45 | 15 | Mod | San Diego | Main | 32.664 | -117.2 |
| 111 | 34 | Ford et al., 2010 | 3U.02 | 3U.02.8.2 | | -0.12 | -0.49 | 15 | Mod | San Diego | Main | 32.664 | -117.2 |
| 111 | 34 | Ford et al., 2010 | 3U.02 | 3U.02.8.4 | | 0.53 | -0.34 | 15 | Mod | San Diego | Main | 32.664 | -117.2 |
| 111 | 34 | Ford et al., 2010 | 3U.02 | 3U.02.24.3 | | 0.29 | 0.16 | 16 | Mod | San Diego | Main | 32.664 | -117.2 |
| 111 | 34 | Ford et al., 2010 | 3U.02 | 3U.02.28 | | 0.26 | 0.17 | 16 | Mod | San Diego | Main | 32.664 | -117.2 |

| | | | | | | | | | | | | | |
|---|---|---|---|---|---|---|---|---|---|---|---|---|---|
| 111 | 34 | Ford et al., 2010 | 3U.02 | 3U.02.28.1 | | 0.38 | 0.28 | 16 | Mod | San Diego | Main | 32.664 | -117.2 |
| 111 | 34 | Ford et al., 2010 | 3U.02 | 3U.02.28.2 | | 0.11 | -0.10 | 16 | Mod | San Diego | Main | 32.664 | -117.2 |
| 111 | 34 | Ford et al., 2010 | 3U.02 | 3U.02.28.3 | | 0.24 | -0.30 | 16 | Mod | San Diego | Main | 32.664 | -117.2 |
| 111 | 34 | Ford et al., 2010 | 3U.02 | 3U.02.32 | | 0.36 | -0.46 | 16 | Mod | San Diego | Main | 32.664 | -117.2 |
| 111 | 34 | Ford et al., 2010 | 3U.02 | 3U.02.32.1 | | 0.21 | -0.63 | 16 | Mod | San Diego | Main | 32.664 | -117.2 |
| 111 | 34 | Ford et al., 2010 | 3U.02 | 3U.02.32.2 | | 0.23 | -0.43 | 16 | Mod | San Diego | Main | 32.664 | -117.2 |
| 111 | 34 | Ford et al., 2010 | 3U.02 | 3U.02.32.3 | | 0.27 | -0.48 | 16 | Mod | San Diego | Main | 32.664 | -117.2 |
| 111 | 34 | Ford et al., 2010 | 3U.02 | 3U.02.32.4 | | 0.50 | -0.93 | 16 | Mod | San Diego | Main | 32.664 | -117.2 |
| 111 | 34 | Ford et al., 2010 | 3U.02 | 3U.02.36 | | 0.79 | -1.22 | 16 | Mod | San Diego | Main | 32.664 | -117.2 |
| 112 | 30 | Ford et al., 2010 | 3U.04 | 3U.04.1 | | 0.09 | -0.47 | 15 | Mod | San Diego | Main | 32.664 | -117.2 |
| 112 | 30 | Ford et al., 2010 | 3U.04 | 3U.04.11 | | -0.56 | -0.70 | 15 | Mod | San Diego | Main | 32.664 | -117.2 |
| 112 | 30 | Ford et al., 2010 | 3U.04 | 3U.04.12 | | -0.39 | -0.40 | 15 | Mod | San Diego | Main | 32.664 | -117.2 |
| 112 | 30 | Ford et al., 2010 | 3U.04 | 3U.04.13 | | -0.32 | -0.51 | 15 | Mod | San Diego | Main | 32.664 | -117.2 |
| 112 | 30 | Ford et al., 2010 | 3U.04 | 3U.04.14 | | -0.29 | -0.59 | 15 | Mod | San Diego | Main | 32.664 | -117.2 |
| 112 | 30 | Ford et al., 2010 | 3U.04 | 3U.04.15 | | -0.28 | -0.82 | 15 | Mod | San Diego | Main | 32.664 | -117.2 |
| 112 | 30 | Ford et al., 2010 | 3U.04 | 3U.04.16 | | -0.08 | -0.60 | 15 | Mod | San Diego | Main | 32.664 | -117.2 |
| 112 | 30 | Ford et al., 2010 | 3U.04 | 3U.04.17 | | 0.30 | -0.33 | 15 | Mod | San Diego | Main | 32.664 | -117.2 |
| 112 | 30 | Ford et al., 2010 | 3U.04 | 3U.04.18 | | 0.15 | -0.18 | 15 | Mod | San Diego | Main | 32.664 | -117.2 |
| 112 | 30 | Ford et al., 2010 | 3U.04 | 3U.04.19 | | -0.23 | 0.13 | 15 | Mod | San Diego | Main | 32.664 | -117.2 |
| 112 | 30 | Ford et al., 2010 | 3U.04 | 3U.04.2 | | 0.16 | -0.63 | 15 | Mod | San Diego | Main | 32.664 | -117.2 |
| 112 | 30 | Ford et al., 2010 | 3U.04 | 3U.04.20 | | -0.16 | 0.13 | 15 | Mod | San Diego | Main | 32.664 | -117.2 |
| 112 | 30 | Ford et al., 2010 | 3U.04 | 3U.04.21 | | -0.15 | -0.58 | 15 | Mod | San Diego | Main | 32.664 | -117.2 |
| 112 | 30 | Ford et al., 2010 | 3U.04 | 3U.04.23 | | 0.15 | -0.07 | 15 | Mod | San Diego | Main | 32.664 | -117.2 |
| 112 | 30 | Ford et al., 2010 | 3U.04 | 3U.04.24 | | -0.10 | -0.04 | 15 | Mod | San Diego | Main | 32.664 | -117.2 |
| 112 | 30 | Ford et al., 2010 | 3U.04 | 3U.04.25 | | -0.17 | 0.03 | 15 | Mod | San Diego | Main | 32.664 | -117.2 |
| 112 | 30 | Ford et al., 2010 | 3U.04 | 3U.04.26 | | 0.15 | 0.01 | 15 | Mod | San Diego | Main | 32.664 | -117.2 |
| 112 | 30 | Ford et al., 2010 | 3U.04 | 3U.04.27 | | 0.11 | 0.14 | 15 | Mod | San Diego | Main | 32.664 | -117.2 |
| 112 | 30 | Ford et al., 2010 | 3U.04 | 3U.04.28 | | 0.28 | 0.06 | 15 | Mod | San Diego | Main | 32.664 | -117.2 |

| | | | | | | | | | | | | | |
|---|---|---|---|---|---|---|---|---|---|---|---|---|---|
| 112 | 30 | Ford et al., 2010 | 3U.04 | 3U.04.6 | | 0.02 | -0.93 | 15 | Mod | San Diego | Main | 32.664 | -117.2 |
| 112 | 30 | Ford et al., 2010 | 3U.04 | 3U.04.7 | | -0.21 | -0.97 | 15 | Mod | San Diego | Main | 32.664 | -117.2 |
| 112 | 30 | Ford et al., 2010 | 3U.04 | 3U.04.9 | | -0.12 | -0.82 | 15 | Mod | San Diego | Main | 32.664 | -117.2 |
| 112 | 30 | Ford et al., 2010 | 3U.04 | 3U.04.29 | | 0.07 | 0.03 | 16 | Mod | San Diego | Main | 32.664 | -117.2 |
| 112 | 30 | Ford et al., 2010 | 3U.04 | 3U.04.30 | | 0.02 | 0.26 | 16 | Mod | San Diego | Main | 32.664 | -117.2 |
| 112 | 30 | Ford et al., 2010 | 3U.04 | 3U.04.31 | | 0.05 | 0.26 | 16 | Mod | San Diego | Main | 32.664 | -117.2 |
| 112 | 30 | Ford et al., 2010 | 3U.04 | 3U.04.34 | | -0.28 | -0.31 | 16 | Mod | San Diego | Main | 32.664 | -117.2 |
| 112 | 30 | Ford et al., 2010 | 3U.04 | 3U.04.35 | | 0.03 | -0.63 | 16 | Mod | San Diego | Main | 32.664 | -117.2 |
| 112 | 30 | Ford et al., 2010 | 3U.04 | 3U.04.36 | | 0.17 | -0.74 | 16 | Mod | San Diego | Main | 32.664 | -117.2 |
| 112 | 30 | Ford et al., 2010 | 3U.04 | 3U.04.37 | | -0.03 | -0.63 | 16 | Mod | San Diego | Main | 32.664 | -117.2 |
| 112 | 30 | Ford et al., 2010 | 3U.04 | 3U.04.38 | | 0.17 | -1.28 | 16 | Mod | San Diego | Main | 32.664 | -117.2 |
| 113 | 23 | Ford et al., 2010 | 3U.07 | 3U.07.01A | | 0.23 | -0.42 | 15 | Mod | San Diego | Main | 32.664 | -117.2 |
| 113 | 23 | Ford et al., 2010 | 3U.07 | 3U.07.04A | | 0.05 | -0.53 | 15 | Mod | San Diego | Main | 32.664 | -117.2 |
| 113 | 23 | Ford et al., 2010 | 3U.07 | 3U.07.05 | | 0.06 | -0.41 | 15 | Mod | San Diego | Main | 32.664 | -117.2 |
| 113 | 23 | Ford et al., 2010 | 3U.07 | 3U.07.06 | | 0.12 | -0.13 | 15 | Mod | San Diego | Main | 32.664 | -117.2 |
| 113 | 23 | Ford et al., 2010 | 3U.07 | 3U.07.07 | | 0.19 | -0.25 | 15 | Mod | San Diego | Main | 32.664 | -117.2 |
| 113 | 23 | Ford et al., 2010 | 3U.07 | 3U.07.08 | | 0.23 | -0.34 | 15 | Mod | San Diego | Main | 32.664 | -117.2 |
| 113 | 23 | Ford et al., 2010 | 3U.07 | 3U.07.09 | | 0.32 | -0.31 | 15 | Mod | San Diego | Main | 32.664 | -117.2 |
| 113 | 23 | Ford et al., 2010 | 3U.07 | 3U.07.10 | | 0.37 | -0.42 | 15 | Mod | San Diego | Main | 32.664 | -117.2 |
| 113 | 23 | Ford et al., 2010 | 3U.07 | 3U.07.11 | | 0.36 | -0.33 | 15 | Mod | San Diego | Main | 32.664 | -117.2 |
| 113 | 23 | Ford et al., 2010 | 3U.07 | 3U.07.12 | | 0.23 | 0.43 | 15 | Mod | San Diego | Main | 32.664 | -117.2 |
| 113 | 23 | Ford et al., 2010 | 3U.07 | 3U.07.13 | | 0.15 | 0.41 | 15 | Mod | San Diego | Main | 32.664 | -117.2 |
| 113 | 23 | Ford et al., 2010 | 3U.07 | 3U.07.14 | | 0.27 | 0.27 | 15 | Mod | San Diego | Main | 32.664 | -117.2 |
| 113 | 23 | Ford et al., 2010 | 3U.07 | 3U.07.15 | | 0.28 | 0.24 | 15 | Mod | San Diego | Main | 32.664 | -117.2 |
| 113 | 23 | Ford et al., 2010 | 3U.07 | 3U.07.16 | | | | 15 | Mod | San Diego | Main | 32.664 | -117.2 |
| 113 | 23 | Ford et al., 2010 | 3U.07 | 3U.07.17 | | 0.15 | 0.25 | 15 | Mod | San Diego | Main | 32.664 | -117.2 |
| 113 | 23 | Ford et al., 2010 | 3U.07 | 3U.07.18A | | 0.05 | 0.34 | 16 | Mod | San Diego | Main | 32.664 | -117.2 |
| 113 | 23 | Ford et al., 2010 | 3U.07 | 3U.07.19 | | 0.30 | 0.50 | 16 | Mod | San Diego | Main | 32.664 | -117.2 |

| | | | | | | | | | | | | | |
|---|---|---|---|---|---|---|---|---|---|---|---|---|---|
| 113 | 23 | Ford et al., 2010 | 3U.07 | 3U.07.20 | | 0.36 | 0.07 | 16 | Mod | San Diego | Main | 32.664 | -117.2 |
| 113 | 23 | Ford et al., 2010 | 3U.07 | 3U.07.21 | | 0.24 | -0.06 | 16 | Mod | San Diego | Main | 32.664 | -117.2 |
| 113 | 23 | Ford et al., 2010 | 3U.07 | 3U.07.22 | | 0.48 | -0.66 | 16 | Mod | San Diego | Main | 32.664 | -117.2 |
| 113 | 23 | Ford et al., 2010 | 3U.07 | 3U.07.23 | | 0.49 | -0.33 | 16 | Mod | San Diego | Main | 32.664 | -117.2 |
| 113 | 23 | Ford et al., 2010 | 3U.07 | 3U.07.24 | | 0.35 | -0.54 | 16 | Mod | San Diego | Main | 32.664 | -117.2 |
| 113 | 23 | Ford et al., 2010 | 3U.07 | 3U.07.25 | | 0.15 | -0.73 | 16 | Mod | San Diego | Main | 32.664 | -117.2 |
| 114 | 32 | Ford et al., 2010 | 3U.11 | 3U.11.10 | | 0.63 | -0.47 | 15 | Mod | San Diego | Main | 32.664 | -117.2 |
| 114 | 32 | Ford et al., 2010 | 3U.11 | 3U.11.11 | | 0.54 | -0.26 | 15 | Mod | San Diego | Main | 32.664 | -117.2 |
| 114 | 32 | Ford et al., 2010 | 3U.11 | 3U.11.12 | | 0.09 | -0.40 | 15 | Mod | San Diego | Main | 32.664 | -117.2 |
| 114 | 32 | Ford et al., 2010 | 3U.11 | 3U.11.13 | | -0.04 | 0.02 | 15 | Mod | San Diego | Main | 32.664 | -117.2 |
| 114 | 32 | Ford et al., 2010 | 3U.11 | 3U.11.14 | | 0.52 | 0.04 | 15 | Mod | San Diego | Main | 32.664 | -117.2 |
| 114 | 32 | Ford et al., 2010 | 3U.11 | 3U.11.15 | | 0.34 | -0.26 | 15 | Mod | San Diego | Main | 32.664 | -117.2 |
| 114 | 32 | Ford et al., 2010 | 3U.11 | 3U.11.16 | | 0.58 | -0.12 | 15 | Mod | San Diego | Main | 32.664 | -117.2 |
| 114 | 32 | Ford et al., 2010 | 3U.11 | 3U.11.17 | | 0.52 | -0.05 | 15 | Mod | San Diego | Main | 32.664 | -117.2 |
| 114 | 32 | Ford et al., 2010 | 3U.11 | 3U.11.18 | | 0.33 | -0.13 | 15 | Mod | San Diego | Main | 32.664 | -117.2 |
| 114 | 32 | Ford et al., 2010 | 3U.11 | 3U.11.19 | | 0.37 | -0.05 | 15 | Mod | San Diego | Main | 32.664 | -117.2 |
| 114 | 32 | Ford et al., 2010 | 3U.11 | 3U.11.2 | | 0.26 | -0.98 | 15 | Mod | San Diego | Main | 32.664 | -117.2 |
| 114 | 32 | Ford et al., 2010 | 3U.11 | 3U.11.20 | | 0.54 | 0.14 | 15 | Mod | San Diego | Main | 32.664 | -117.2 |
| 114 | 32 | Ford et al., 2010 | 3U.11 | 3U.11.21 | | 0.45 | 0.10 | 15 | Mod | San Diego | Main | 32.664 | -117.2 |
| 114 | 32 | Ford et al., 2010 | 3U.11 | 3U.11.3 | | 0.21 | -0.85 | 15 | Mod | San Diego | Main | 32.664 | -117.2 |
| 114 | 32 | Ford et al., 2010 | 3U.11 | 3U.11.4 | | 0.08 | -0.64 | 15 | Mod | San Diego | Main | 32.664 | -117.2 |
| 114 | 32 | Ford et al., 2010 | 3U.11 | 3U.11.5 | | 0.23 | -0.28 | 15 | Mod | San Diego | Main | 32.664 | -117.2 |
| 114 | 32 | Ford et al., 2010 | 3U.11 | 3U.11.6 | | 0.38 | -0.43 | 15 | Mod | San Diego | Main | 32.664 | -117.2 |
| 114 | 32 | Ford et al., 2010 | 3U.11 | 3U.11.7 | | 0.26 | -0.71 | 15 | Mod | San Diego | Main | 32.664 | -117.2 |
| 114 | 32 | Ford et al., 2010 | 3U.11 | 3U.11.8 | | 0.47 | -0.39 | 15 | Mod | San Diego | Main | 32.664 | -117.2 |
| 114 | 32 | Ford et al., 2010 | 3U.11 | 3U.11.9 | | 0.59 | -0.51 | 15 | Mod | San Diego | Main | 32.664 | -117.2 |
| 114 | 32 | Ford et al., 2010 | 3U.11 | 3U.11.22 | | 0.31 | -0.26 | 16 | Mod | San Diego | Main | 32.664 | -117.2 |
| 114 | 32 | Ford et al., 2010 | 3U.11 | 3U.11.23 | | -0.20 | -0.96 | 16 | Mod | San Diego | Main | 32.664 | -117.2 |

| | | | | | | | | | | | | | |
|---|---|---|---|---|---|---|---|---|---|---|---|---|---|
| 114 | 32 | Ford et al., 2010 | 3U.11 | 3U.11.24 | | 0.38 | 0.02 | 16 | Mod | San Diego | Main | 32.664 | -117.2 |
| 114 | 32 | Ford et al., 2010 | 3U.11 | 3U.11.25 | | 0.40 | 0.05 | 16 | Mod | San Diego | Main | 32.664 | -117.2 |
| 114 | 32 | Ford et al., 2010 | 3U.11 | 3U.11.26 | | 0.34 | -0.04 | 16 | Mod | San Diego | Main | 32.664 | -117.2 |
| 114 | 32 | Ford et al., 2010 | 3U.11 | 3U.11.27 | | 0.14 | -0.34 | 16 | Mod | San Diego | Main | 32.664 | -117.2 |
| 114 | 32 | Ford et al., 2010 | 3U.11 | 3U.11.28 | | 0.04 | -0.66 | 16 | Mod | San Diego | Main | 32.664 | -117.2 |
| 114 | 32 | Ford et al., 2010 | 3U.11 | 3U.11.29 | | 0.05 | -0.76 | 16 | Mod | San Diego | Main | 32.664 | -117.2 |
| 114 | 32 | Ford et al., 2010 | 3U.11 | 3U.11.30 | | 0.24 | -0.57 | 16 | Mod | San Diego | Main | 32.664 | -117.2 |
| 114 | 32 | Ford et al., 2010 | 3U.11 | 3U.11.31 | | 0.23 | -0.53 | 16 | Mod | San Diego | Main | 32.664 | -117.2 |
| 114 | 32 | Ford et al., 2010 | 3U.11 | 3U.11.32 | | 0.21 | -1.22 | 16 | Mod | San Diego | Main | 32.664 | -117.2 |
| 114 | 32 | Ford et al., 2010 | 3U.11 | 3U.11.33 | | 0.53 | -1.65 | 16 | Mod | San Diego | Main | 32.664 | -117.2 |
| 115 | 11 | Ford et al., 2010 | 3U.13 | 3U.13.1 | | 0.77 | -0.22 | 15 | Mod | San Diego | Main | 32.664 | -117.2 |
| 115 | 11 | Ford et al., 2010 | 3U.13 | 3U.13.10 | | 0.69 | 0.04 | 15 | Mod | San Diego | Main | 32.664 | -117.2 |
| 115 | 11 | Ford et al., 2010 | 3U.13 | 3U.13.11 | | 0.72 | 0.52 | 15 | Mod | San Diego | Main | 32.664 | -117.2 |
| 115 | 11 | Ford et al., 2010 | 3U.13 | 3U.13.12 | | 0.54 | 0.69 | 15 | Mod | San Diego | Main | 32.664 | -117.2 |
| 115 | 11 | Ford et al., 2010 | 3U.13 | 3U.13.15 | | 0.71 | 0.14 | 15 | Mod | San Diego | Main | 32.664 | -117.2 |
| 115 | 11 | Ford et al., 2010 | 3U.13 | 3U.13.16 | | 0.83 | 0.09 | 15 | Mod | San Diego | Main | 32.664 | -117.2 |
| 115 | 11 | Ford et al., 2010 | 3U.13 | 3U.13.2 | | 0.48 | -0.66 | 15 | Mod | San Diego | Main | 32.664 | -117.2 |
| 115 | 11 | Ford et al., 2010 | 3U.13 | 3U.13.3 | | 0.43 | -0.59 | 15 | Mod | San Diego | Main | 32.664 | -117.2 |
| 115 | 11 | Ford et al., 2010 | 3U.13 | 3U.13.8 | | 0.88 | 0.13 | 15 | Mod | San Diego | Main | 32.664 | -117.2 |
| 115 | 11 | Ford et al., 2010 | 3U.13 | 3U.13.21 | | 0.93 | 0.31 | 16 | Mod | San Diego | Main | 32.664 | -117.2 |
| 115 | 11 | Ford et al., 2010 | 3U.13 | 3U.13.23 | | 0.80 | 0.00 | 16 | Mod | San Diego | Main | 32.664 | -117.2 |
| 116 | 27 | Ford et al., 2010 | 3U.14 | 3U.14.01 | | 0.37 | -0.23 | 15 | Mod | San Diego | Main | 32.664 | -117.2 |
| 116 | 27 | Ford et al., 2010 | 3U.14 | 3U.14.02 | | | | 15 | Mod | San Diego | Main | 32.664 | -117.2 |
| 116 | 27 | Ford et al., 2010 | 3U.14 | 3U.14.03 | | 0.21 | -0.34 | 15 | Mod | San Diego | Main | 32.664 | -117.2 |
| 116 | 27 | Ford et al., 2010 | 3U.14 | 3U.14.04 | | 0.35 | -0.71 | 15 | Mod | San Diego | Main | 32.664 | -117.2 |
| 116 | 27 | Ford et al., 2010 | 3U.14 | 3U.14.05 | | 0.27 | -0.74 | 15 | Mod | San Diego | Main | 32.664 | -117.2 |
| 116 | 27 | Ford et al., 2010 | 3U.14 | 3U.14.06 | | -0.05 | -0.54 | 15 | Mod | San Diego | Main | 32.664 | -117.2 |
| 116 | 27 | Ford et al., 2010 | 3U.14 | 3U.14.07 | | -0.09 | -0.50 | 15 | Mod | San Diego | Main | 32.664 | -117.2 |

| | | | | | | | | | | | | | |
|---|---|---|---|---|---|---|---|---|---|---|---|---|---|
| 116 | 27 | Ford et al., 2010 | 3U.14 | 3U.14.08 | | 0.24 | -0.39 | 15 | Mod | San Diego | Main | 32.664 | -117.2 |
| 116 | 27 | Ford et al., 2010 | 3U.14 | 3U.14.09 | | 0.24 | -0.39 | 15 | Mod | San Diego | Main | 32.664 | -117.2 |
| 116 | 27 | Ford et al., 2010 | 3U.14 | 3U.14.10A | | 0.41 | -0.36 | 15 | Mod | San Diego | Main | 32.664 | -117.2 |
| 116 | 27 | Ford et al., 2010 | 3U.14 | 3U.14.11/12 | | 0.57 | -0.11 | 15 | Mod | San Diego | Main | 32.664 | -117.2 |
| 116 | 27 | Ford et al., 2010 | 3U.14 | 3U.14.13 | | 0.21 | 0.06 | 15 | Mod | San Diego | Main | 32.664 | -117.2 |
| 116 | 27 | Ford et al., 2010 | 3U.14 | 3U.14.14 | | 0.07 | 0.31 | 15 | Mod | San Diego | Main | 32.664 | -117.2 |
| 116 | 27 | Ford et al., 2010 | 3U.14 | 3U.14.15 | | 0.10 | 0.09 | 15 | Mod | San Diego | Main | 32.664 | -117.2 |
| 116 | 27 | Ford et al., 2010 | 3U.14 | 3U.14.16 | | 0.51 | 0.17 | 15 | Mod | San Diego | Main | 32.664 | -117.2 |
| 116 | 27 | Ford et al., 2010 | 3U.14 | 3U.14.17 | | 0.37 | 0.26 | 15 | Mod | San Diego | Main | 32.664 | -117.2 |
| 116 | 27 | Ford et al., 2010 | 3U.14 | 3U.14.18 | | 0.30 | 0.19 | 15 | Mod | San Diego | Main | 32.664 | -117.2 |
| 116 | 27 | Ford et al., 2010 | 3U.14 | 3U.14.19 | | 0.61 | 0.33 | 15 | Mod | San Diego | Main | 32.664 | -117.2 |
| 116 | 27 | Ford et al., 2010 | 3U.14 | 3U.14.20 | | 0.51 | 0.17 | 16 | Mod | San Diego | Main | 32.664 | -117.2 |
| 116 | 27 | Ford et al., 2010 | 3U.14 | 3U.14.21 | | 0.53 | 0.22 | 16 | Mod | San Diego | Main | 32.664 | -117.2 |
| 116 | 27 | Ford et al., 2010 | 3U.14 | 3U.14.22 | | 0.37 | -0.26 | 16 | Mod | San Diego | Main | 32.664 | -117.2 |
| 116 | 27 | Ford et al., 2010 | 3U.14 | 3U.14.23 | | 0.43 | -0.45 | 16 | Mod | San Diego | Main | 32.664 | -117.2 |
| 116 | 27 | Ford et al., 2010 | 3U.14 | 3U.14.24 | | 0.51 | -0.66 | 16 | Mod | San Diego | Main | 32.664 | -117.2 |
| 116 | 27 | Ford et al., 2010 | 3U.14 | 3U.14.25 | | 0.53 | -0.46 | 16 | Mod | San Diego | Main | 32.664 | -117.2 |
| 116 | 27 | Ford et al., 2010 | 3U.14 | 3U.14.26 | | 0.10 | -1.26 | 16 | Mod | San Diego | Main | 32.664 | -117.2 |
| 116 | 27 | Ford et al., 2010 | 3U.14 | 3U.14.27 | | 0.50 | -1.29 | 16 | Mod | San Diego | Main | 32.664 | -117.2 |
| 116 | 27 | Ford et al., 2010 | 3U.14 | 3U.14.28 | | 0.55 | -1.21 | 16 | Mod | San Diego | Main | 32.664 | -117.2 |
| 117 | 28 | Ford et al., 2010 | 3U.18 | 3U.18.15 | | 0.66 | 0.07 | 15 | Mod | San Diego | Main | 32.664 | -117.2 |
| 117 | 28 | Ford et al., 2010 | 3U.18 | 3U.18.15.1 | | 0.55 | 0.08 | 15 | Mod | San Diego | Main | 32.664 | -117.2 |
| 117 | 28 | Ford et al., 2010 | 3U.18 | 3U.18.15.2 | | 0.58 | 0.23 | 15 | Mod | San Diego | Main | 32.664 | -117.2 |
| 117 | 28 | Ford et al., 2010 | 3U.18 | 3U.18.15.3 | | 0.18 | 0.10 | 15 | Mod | San Diego | Main | 32.664 | -117.2 |
| 117 | 28 | Ford et al., 2010 | 3U.18 | 3U.18.15.4 | | 0.87 | 0.23 | 15 | Mod | San Diego | Main | 32.664 | -117.2 |
| 117 | 28 | Ford et al., 2010 | 3U.18 | 3U.18.15.5 | | 0.81 | 0.14 | 15 | Mod | San Diego | Main | 32.664 | -117.2 |
| 117 | 28 | Ford et al., 2010 | 3U.18 | 3U.18.8 | | 0.89 | -0.45 | 15 | Mod | San Diego | Main | 32.664 | -117.2 |
| 117 | 28 | Ford et al., 2010 | 3U.18 | 3U.18.8.1 | | 0.94 | -0.53 | 15 | Mod | San Diego | Main | 32.664 | -117.2 |

| | | | | | | | | | | | | | |
|---|---|---|---|---|---|---|---|---|---|---|---|---|---|
| 117 | 28 | Ford et al., 2010 | 3U.18 | 3U.18.8.2 | | 0.99 | -0.62 | 15 | Mod | San Diego | Main | 32.664 | -117.2 |
| 117 | 28 | Ford et al., 2010 | 3U.18 | 3U.18.8.3 | | 0.74 | -0.72 | 15 | Mod | San Diego | Main | 32.664 | -117.2 |
| 117 | 28 | Ford et al., 2010 | 3U.18 | 3U.18.8.4 | | 0.67 | -0.60 | 15 | Mod | San Diego | Main | 32.664 | -117.2 |
| 117 | 28 | Ford et al., 2010 | 3U.18 | 3U.18.8.5 | | 0.55 | -0.51 | 15 | Mod | San Diego | Main | 32.664 | -117.2 |
| 117 | 28 | Ford et al., 2010 | 3U.18 | 3U.18.8.6 | | 0.56 | -0.44 | 15 | Mod | San Diego | Main | 32.664 | -117.2 |
| 117 | 28 | Ford et al., 2010 | 3U.18 | 3U.18.9 | | 0.60 | -0.30 | 15 | Mod | San Diego | Main | 32.664 | -117.2 |
| 117 | 28 | Ford et al., 2010 | 3U.18 | 3U.18.9.1 | | 0.70 | -0.45 | 15 | Mod | San Diego | Main | 32.664 | -117.2 |
| 117 | 28 | Ford et al., 2010 | 3U.18 | 3U.18.9.2 | | 0.85 | -0.52 | 15 | Mod | San Diego | Main | 32.664 | -117.2 |
| 117 | 28 | Ford et al., 2010 | 3U.18 | 3U.18.9.3 | | 0.92 | -0.11 | 15 | Mod | San Diego | Main | 32.664 | -117.2 |
| 117 | 28 | Ford et al., 2010 | 3U.18 | 3U.18.9.4 | | 0.90 | -0.01 | 15 | Mod | San Diego | Main | 32.664 | -117.2 |
| 117 | 28 | Ford et al., 2010 | 3U.18 | 3U.18.9.5 | | 0.57 | 0.17 | 15 | Mod | San Diego | Main | 32.664 | -117.2 |
| 117 | 28 | Ford et al., 2010 | 3U.18 | 3U.18.9.6 | | 0.58 | 0.47 | 15 | Mod | San Diego | Main | 32.664 | -117.2 |
| 117 | 28 | Ford et al., 2010 | 3U.18 | 3U.18.9.7 | | 0.48 | 0.15 | 15 | Mod | San Diego | Main | 32.664 | -117.2 |
| 117 | 28 | Ford et al., 2010 | 3U.18 | 3U.18.9.8 | | 0.65 | 0.08 | 15 | Mod | San Diego | Main | 32.664 | -117.2 |
| 117 | 28 | Ford et al., 2010 | 3U.18 | 3U.18.24 | | 0.66 | 0.14 | 16 | Mod | San Diego | Main | 32.664 | -117.2 |
| 117 | 28 | Ford et al., 2010 | 3U.18 | 3U.18.24.1 | | 0.78 | 0.33 | 16 | Mod | San Diego | Main | 32.664 | -117.2 |
| 117 | 28 | Ford et al., 2010 | 3U.18 | 3U.18.24.2 | | 0.65 | 0.07 | 16 | Mod | San Diego | Main | 32.664 | -117.2 |
| 117 | 28 | Ford et al., 2010 | 3U.18 | 3U.18.24.3 | | 0.90 | -0.29 | 16 | Mod | San Diego | Main | 32.664 | -117.2 |
| 117 | 28 | Ford et al., 2010 | 3U.18 | 3U.18.24.4 | | 0.88 | -0.26 | 16 | Mod | San Diego | Main | 32.664 | -117.2 |
| 117 | 28 | Ford et al., 2010 | 3U.18 | 3U.18.30 | | 0.66 | -0.57 | 16 | Mod | San Diego | Main | 32.664 | -117.2 |
| 118 | 25 | Ford et al., 2010 | 3U.20 | 3U.20.1 | | 0.48 | -0.44 | 15 | Mod | San Diego | Main | 32.664 | -117.2 |
| 118 | 25 | Ford et al., 2010 | 3U.20 | 3U.20.10 | | 0.74 | 0.17 | 15 | Mod | San Diego | Main | 32.664 | -117.2 |
| 118 | 25 | Ford et al., 2010 | 3U.20 | 3U.20.11 | | 0.61 | 0.21 | 15 | Mod | San Diego | Main | 32.664 | -117.2 |
| 118 | 25 | Ford et al., 2010 | 3U.20 | 3U.20.12 | | | | 15 | Mod | San Diego | Main | 32.664 | -117.2 |
| 118 | 25 | Ford et al., 2010 | 3U.20 | 3U.20.2 | | 0.29 | -0.34 | 15 | Mod | San Diego | Main | 32.664 | -117.2 |
| 118 | 25 | Ford et al., 2010 | 3U.20 | 3U.20.3 | | 0.19 | -0.85 | 15 | Mod | San Diego | Main | 32.664 | -117.2 |
| 118 | 25 | Ford et al., 2010 | 3U.20 | 3U.20.4 | | 0.21 | -0.62 | 15 | Mod | San Diego | Main | 32.664 | -117.2 |
| 118 | 25 | Ford et al., 2010 | 3U.20 | 3U.20.5 | | 0.68 | -0.25 | 15 | Mod | San Diego | Main | 32.664 | -117.2 |

| | | | | | | | | | | | | | |
|---|---|---|---|---|---|---|---|---|---|---|---|---|---|
| 118 | 25 | Ford et al., 2010 | 3U.20 | 3U.20.6 | | 0.50 | -0.07 | 15 | Mod | San Diego | Main | 32.664 | -117.2 |
| 118 | 25 | Ford et al., 2010 | 3U.20 | 3U.20.7 | | 0.34 | 0.04 | 15 | Mod | San Diego | Main | 32.664 | -117.2 |
| 118 | 25 | Ford et al., 2010 | 3U.20 | 3U.20.8 | | 0.42 | 0.40 | 15 | Mod | San Diego | Main | 32.664 | -117.2 |
| 118 | 25 | Ford et al., 2010 | 3U.20 | 3U.20.9 | | 0.63 | 0.26 | 15 | Mod | San Diego | Main | 32.664 | -117.2 |
| 118 | 25 | Ford et al., 2010 | 3U.20 | 3U.20.13 | | 0.66 | 0.25 | 16 | Mod | San Diego | Main | 32.664 | -117.2 |
| 118 | 25 | Ford et al., 2010 | 3U.20 | 3U.20.14 | | 0.90 | 0.32 | 16 | Mod | San Diego | Main | 32.664 | -117.2 |
| 118 | 25 | Ford et al., 2010 | 3U.20 | 3U.20.15 | | 0.86 | 0.19 | 16 | Mod | San Diego | Main | 32.664 | -117.2 |
| 118 | 25 | Ford et al., 2010 | 3U.20 | 3U.20.16 | | 0.75 | 0.07 | 16 | Mod | San Diego | Main | 32.664 | -117.2 |
| 118 | 25 | Ford et al., 2010 | 3U.20 | 3U.20.17 | | 0.75 | 0.02 | 16 | Mod | San Diego | Main | 32.664 | -117.2 |
| 118 | 25 | Ford et al., 2010 | 3U.20 | 3U.20.18 | | 0.51 | -0.01 | 16 | Mod | San Diego | Main | 32.664 | -117.2 |
| 118 | 25 | Ford et al., 2010 | 3U.20 | 3U.20.19 | | 0.38 | -0.49 | 16 | Mod | San Diego | Main | 32.664 | -117.2 |
| 118 | 25 | Ford et al., 2010 | 3U.20 | 3U.20.20 | | 0.28 | -0.47 | 16 | Mod | San Diego | Main | 32.664 | -117.2 |
| 118 | 25 | Ford et al., 2010 | 3U.20 | 3U.20.21 | | 0.50 | -0.77 | 16 | Mod | San Diego | Main | 32.664 | -117.2 |
| 118 | 25 | Ford et al., 2010 | 3U.20 | 3U.20.22 | | 0.59 | -0.46 | 16 | Mod | San Diego | Main | 32.664 | -117.2 |
| 118 | 25 | Ford et al., 2010 | 3U.20 | 3U.20.23 | | 0.61 | -0.62 | 16 | Mod | San Diego | Main | 32.664 | -117.2 |
| 118 | 25 | Ford et al., 2010 | 3U.20 | 3U.20.24 | | 0.49 | -0.90 | 16 | Mod | San Diego | Main | 32.664 | -117.2 |
| 118 | 25 | Ford et al., 2010 | 3U.20 | 3U.20.25 | | 0.41 | -1.14 | 16 | Mod | San Diego | Main | 32.664 | -117.2 |
| 119 | 19 | Glassow et al., 1994 | 1 | 0 | | 0.68 | 0.81 | 5200 | Mid | Santa Cruz Island | Island | 34.06 | -119.9 |
| 119 | 19 | Glassow et al., 1994 | 1 | 2 | | 0.75 | 0.57 | 5200 | Mid | Santa Cruz Island | Island | 34.06 | -119.9 |
| 119 | 19 | Glassow et al., 1994 | 1 | 4 | | 0.78 | 0.53 | 5200 | Mid | Santa Cruz Island | Island | 34.06 | -119.9 |
| 119 | 19 | Glassow et al., 1994 | 1 | 6 | | 0.64 | 0.40 | 5200 | Mid | Santa Cruz Island | Island | 34.06 | -119.9 |
| 119 | 19 | Glassow et al., 1994 | 1 | 8 | | 0.43 | 0.21 | 5200 | Mid | Santa Cruz Island | Island | 34.06 | -119.9 |
| 119 | 19 | Glassow et al., 1994 | 1 | 10 | | 0.34 | 0.00 | 5200 | Mid | Santa Cruz Island | Island | 34.06 | -119.9 |
| 119 | 19 | Glassow et al., 1994 | 1 | 12 | | 0.28 | 0.17 | 5200 | Mid | Santa Cruz Island | Island | 34.06 | -119.9 |

| | | | | | | | | | | | | | |
|---|---|---|---|---|---|---|---|---|---|---|---|---|---|
| 119 | 19 | Glassow et al., 1994 | 1 | 14 | | -0.22 | -0.01 | 5200 | Mid | Santa Cruz Island | Island | 34.06 | -119.9 |
| 119 | 19 | Glassow et al., 1994 | 1 | 16 | | -0.77 | 0.40 | 5200 | Mid | Santa Cruz Island | Island | 34.06 | -119.9 |
| 119 | 19 | Glassow et al., 1994 | 1 | 18 | | -0.87 | 0.73 | 5200 | Mid | Santa Cruz Island | Island | 34.06 | -119.9 |
| 119 | 19 | Glassow et al., 1994 | 1 | 20 | | -0.85 | 0.80 | 5200 | Mid | Santa Cruz Island | Island | 34.06 | -119.9 |
| 119 | 19 | Glassow et al., 1994 | 1 | 22 | | -0.39 | 0.83 | 5200 | Mid | Santa Cruz Island | Island | 34.06 | -119.9 |
| 119 | 19 | Glassow et al., 1994 | 1 | 24 | | -0.12 | 0.88 | 5200 | Mid | Santa Cruz Island | Island | 34.06 | -119.9 |
| 119 | 19 | Glassow et al., 1994 | 1 | 26 | | 0.16 | 1.09 | 5200 | Mid | Santa Cruz Island | Island | 34.06 | -119.9 |
| 119 | 19 | Glassow et al., 1994 | 1 | 28 | | 0.31 | 0.91 | 5200 | Mid | Santa Cruz Island | Island | 34.06 | -119.9 |
| 119 | 19 | Glassow et al., 1994 | 1 | 30 | | 0.29 | 1.07 | 5200 | Mid | Santa Cruz Island | Island | 34.06 | -119.9 |
| 119 | 19 | Glassow et al., 1994 | 1 | 32 | | 0.60 | 0.79 | 5200 | Mid | Santa Cruz Island | Island | 34.06 | -119.9 |
| 119 | 19 | Glassow et al., 1994 | 1 | 34 | | 0.82 | 0.35 | 5200 | Mid | Santa Cruz Island | Island | 34.06 | -119.9 |
| 119 | 19 | Glassow et al., 1994 | 1 | 36 | | 0.87 | 0.29 | 5200 | Mid | Santa Cruz Island | Island | 34.06 | -119.9 |
| 120 | 20 | Glassow et al., 1994 | 2 | 0 | | 0.90 | 0.29 | 5200 | Mid | Santa Cruz Island | Island | 34.06 | -119.9 |
| 120 | 20 | Glassow et al., 1994 | 2 | 2 | | 0.40 | 0.29 | 5200 | Mid | Santa Cruz Island | Island | 34.06 | -119.9 |
| 120 | 20 | Glassow et al., 1994 | 2 | 4 | | 0.80 | 0.45 | 5200 | Mid | Santa Cruz Island | Island | 34.06 | -119.9 |
| 120 | 20 | Glassow et al., 1994 | 2 | 6 | | 1.10 | 0.70 | 5200 | Mid | Santa Cruz Island | Island | 34.06 | -119.9 |
| 120 | 20 | Glassow et al., 1994 | 2 | 8 | | 1.21 | 0.05 | 5200 | Mid | Santa Cruz Island | Island | 34.06 | -119.9 |
| 120 | 20 | Glassow et al., 1994 | 2 | 10 | | 1.01 | 0.05 | 5200 | Mid | Santa Cruz Island | Island | 34.06 | -119.9 |
| 120 | 20 | Glassow et al., 1994 | 2 | 12 | | 1.12 | 0.80 | 5200 | Mid | Santa Cruz Island | Island | 34.06 | -119.9 |

| | | | | | | | | | | | | | |
|---|---|---|---|---|---|---|---|---|---|---|---|---|---|
| 120 | 20 | Glassow et al., 1994 | 2 | 14 | | 1.20 | 0.77 | 5200 | Mid | Santa Cruz Island | Island | 34.06 | -119.9 |
| 120 | 20 | Glassow et al., 1994 | 2 | 16 | | 1.30 | 0.32 | 5200 | Mid | Santa Cruz Island | Island | 34.06 | -119.9 |
| 120 | 20 | Glassow et al., 1994 | 2 | 18 | | 1.12 | 0.00 | 5200 | Mid | Santa Cruz Island | Island | 34.06 | -119.9 |
| 120 | 20 | Glassow et al., 1994 | 2 | 20 | | 0.81 | 0.05 | 5200 | Mid | Santa Cruz Island | Island | 34.06 | -119.9 |
| 120 | 20 | Glassow et al., 1994 | 2 | 22 | | 0.85 | 0.13 | 5200 | Mid | Santa Cruz Island | Island | 34.06 | -119.9 |
| 120 | 20 | Glassow et al., 1994 | 2 | 24 | | 0.61 | 0.55 | 5200 | Mid | Santa Cruz Island | Island | 34.06 | -119.9 |
| 120 | 20 | Glassow et al., 1994 | 2 | 26 | | 0.81 | 1.05 | 5200 | Mid | Santa Cruz Island | Island | 34.06 | -119.9 |
| 120 | 20 | Glassow et al., 1994 | 2 | 28 | | 0.80 | 0.96 | 5200 | Mid | Santa Cruz Island | Island | 34.06 | -119.9 |
| 120 | 20 | Glassow et al., 1994 | 2 | 30 | | 1.00 | 1.52 | 5200 | Mid | Santa Cruz Island | Island | 34.06 | -119.9 |
| 120 | 20 | Glassow et al., 1994 | 2 | 32 | | 1.00 | 1.02 | 5200 | Mid | Santa Cruz Island | Island | 34.06 | -119.9 |
| 120 | 20 | Glassow et al., 1994 | 2 | 34 | | 1.19 | 0.88 | 5200 | Mid | Santa Cruz Island | Island | 34.06 | -119.9 |
| 120 | 20 | Glassow et al., 1994 | 2 | 36 | | 0.79 | 0.01 | 5200 | Mid | Santa Cruz Island | Island | 34.06 | -119.9 |
| 120 | 20 | Glassow et al., 1994 | 2 | 38 | | 0.60 | -0.41 | 5200 | Mid | Santa Cruz Island | Island | 34.06 | -119.9 |
| 121 | 18 | Glassow et al., 1994 | 3 | 0 | | 1.01 | 0.82 | 5200 | Mid | Santa Cruz Island | Island | 34.06 | -119.9 |
| 121 | 18 | Glassow et al., 1994 | 3 | 2 | | 0.77 | 0.54 | 5200 | Mid | Santa Cruz Island | Island | 34.06 | -119.9 |
| 121 | 18 | Glassow et al., 1994 | 3 | 4 | | 0.78 | 0.35 | 5200 | Mid | Santa Cruz Island | Island | 34.06 | -119.9 |
| 121 | 18 | Glassow et al., 1994 | 3 | 6 | | 0.61 | 0.28 | 5200 | Mid | Santa Cruz Island | Island | 34.06 | -119.9 |
| 121 | 18 | Glassow et al., 1994 | 3 | 8 | | 0.29 | 0.60 | 5200 | Mid | Santa Cruz Island | Island | 34.06 | -119.9 |
| 121 | 18 | Glassow et al., 1994 | 3 | 10 | | 0.22 | 0.62 | 5200 | Mid | Santa Cruz Island | Island | 34.06 | -119.9 |

| | | | | | | | | | | | | | |
|---|---|---|---|---|---|---|---|---|---|---|---|---|---|
| 121 | 18 | Glassow et al., 1994 | 3 | 12 | | 0.79 | 0.27 | 5200 | Mid | Santa Cruz Island | Island | 34.06 | -119.9 |
| 121 | 18 | Glassow et al., 1994 | 3 | 14 | | 0.66 | 0.37 | 5200 | Mid | Santa Cruz Island | Island | 34.06 | -119.9 |
| 121 | 18 | Glassow et al., 1994 | 3 | 16 | | 0.53 | 0.74 | 5200 | Mid | Santa Cruz Island | Island | 34.06 | -119.9 |
| 121 | 18 | Glassow et al., 1994 | 3 | 18 | | 0.78 | 0.86 | 5200 | Mid | Santa Cruz Island | Island | 34.06 | -119.9 |
| 121 | 18 | Glassow et al., 1994 | 3 | 20 | | 0.82 | 0.43 | 5200 | Mid | Santa Cruz Island | Island | 34.06 | -119.9 |
| 121 | 18 | Glassow et al., 1994 | 3 | 22 | | 0.85 | 0.16 | 5200 | Mid | Santa Cruz Island | Island | 34.06 | -119.9 |
| 121 | 18 | Glassow et al., 1994 | 3 | 24 | | 0.88 | 0.26 | 5200 | Mid | Santa Cruz Island | Island | 34.06 | -119.9 |
| 121 | 18 | Glassow et al., 1994 | 3 | 26 | | 0.81 | 0.17 | 5200 | Mid | Santa Cruz Island | Island | 34.06 | -119.9 |
| 121 | 18 | Glassow et al., 1994 | 3 | 28 | | 0.50 | -0.29 | 5200 | Mid | Santa Cruz Island | Island | 34.06 | -119.9 |
| 121 | 18 | Glassow et al., 1994 | 3 | 30 | | 0.58 | -0.33 | 5200 | Mid | Santa Cruz Island | Island | 34.06 | -119.9 |
| 121 | 18 | Glassow et al., 1994 | 3 | 32 | | 0.02 | 0.07 | 5200 | Mid | Santa Cruz Island | Island | 34.06 | -119.9 |
| 121 | 18 | Glassow et al., 1994 | 3 | 34 | | 0.22 | 0.31 | 5200 | Mid | Santa Cruz Island | Island | 34.06 | -119.9 |
| 122 | 22 | Glassow et al., 1994 | 25 | 0 | | 1.84 | 1.41 | 5200 | Mid | Santa Cruz Island | Island | 34.06 | -119.9 |
| 122 | 22 | Glassow et al., 1994 | 25 | 2 | | 1.00 | 0.33 | 5200 | Mid | Santa Cruz Island | Island | 34.06 | -119.9 |
| 122 | 22 | Glassow et al., 1994 | 25 | 4 | | 0.74 | 1.54 | 5200 | Mid | Santa Cruz Island | Island | 34.06 | -119.9 |
| 122 | 22 | Glassow et al., 1994 | 25 | 6 | | 0.66 | 1.02 | 5200 | Mid | Santa Cruz Island | Island | 34.06 | -119.9 |
| 122 | 22 | Glassow et al., 1994 | 25 | 8 | | 0.53 | 0.95 | 5200 | Mid | Santa Cruz Island | Island | 34.06 | -119.9 |
| 122 | 22 | Glassow et al., 1994 | 25 | 10 | | 1.13 | 0.78 | 5200 | Mid | Santa Cruz Island | Island | 34.06 | -119.9 |
| 122 | 22 | Glassow et al., 1994 | 25 | 12 | | 1.22 | -0.12 | 5200 | Mid | Santa Cruz Island | Island | 34.06 | -119.9 |

| | | | | | | | | | | | | | |
|---|---|---|---|---|---|---|---|---|---|---|---|---|---|
| 122 | 22 | Glassow et al., 1994 | 25 | 14 | | 1.30 | 1.41 | 5200 | Mid | Santa Cruz Island | Island | 34.06 | -119.9 |
| 122 | 22 | Glassow et al., 1994 | 25 | 16 | | 0.68 | 1.61 | 5200 | Mid | Santa Cruz Island | Island | 34.06 | -119.9 |
| 122 | 22 | Glassow et al., 1994 | 25 | 18 | | 0.53 | 0.97 | 5200 | Mid | Santa Cruz Island | Island | 34.06 | -119.9 |
| 122 | 22 | Glassow et al., 1994 | 25 | 20 | | 1.51 | 0.94 | 5200 | Mid | Santa Cruz Island | Island | 34.06 | -119.9 |
| 122 | 22 | Glassow et al., 1994 | 25 | 22 | | 1.16 | 0.42 | 5200 | Mid | Santa Cruz Island | Island | 34.06 | -119.9 |
| 122 | 22 | Glassow et al., 1994 | 25 | 24 | | 0.65 | 0.81 | 5200 | Mid | Santa Cruz Island | Island | 34.06 | -119.9 |
| 122 | 22 | Glassow et al., 1994 | 25 | 26 | | 1.13 | 0.67 | 5200 | Mid | Santa Cruz Island | Island | 34.06 | -119.9 |
| 122 | 22 | Glassow et al., 1994 | 25 | 28 | | 0.85 | 0.53 | 5200 | Mid | Santa Cruz Island | Island | 34.06 | -119.9 |
| 122 | 22 | Glassow et al., 1994 | 25 | 30 | | 0.81 | 0.17 | 5200 | Mid | Santa Cruz Island | Island | 34.06 | -119.9 |
| 122 | 22 | Glassow et al., 1994 | 25 | 32 | | 0.69 | 0.62 | 5200 | Mid | Santa Cruz Island | Island | 34.06 | -119.9 |
| 122 | 22 | Glassow et al., 1994 | 25 | 34 | | 0.44 | 1.16 | 5200 | Mid | Santa Cruz Island | Island | 34.06 | -119.9 |
| 122 | 22 | Glassow et al., 1994 | 25 | 36 | | 0.95 | 0.83 | 5200 | Mid | Santa Cruz Island | Island | 34.06 | -119.9 |
| 122 | 22 | Glassow et al., 1994 | 25 | 38 | | 0.52 | 1.02 | 5200 | Mid | Santa Cruz Island | Island | 34.06 | -119.9 |
| 122 | 22 | Glassow et al., 1994 | 25 | 40 | | 0.46 | 0.74 | 5200 | Mid | Santa Cruz Island | Island | 34.06 | -119.9 |
| 122 | 22 | Glassow et al., 1994 | 25 | 42 | | 0.38 | 0.72 | 5200 | Mid | Santa Cruz Island | Island | 34.06 | -119.9 |
| 123 | 15 | Glassow et al., 1994 | 1x | 0 | | 0.89 | 0.76 | 5200 | Mid | Santa Cruz Island | Island | 34.06 | -119.9 |
| 123 | 15 | Glassow et al., 1994 | 1x | 2 | | 0.90 | 0.06 | 5200 | Mid | Santa Cruz Island | Island | 34.06 | -119.9 |
| 123 | 15 | Glassow et al., 1994 | 1x | 4 | | 0.76 | 0.29 | 5200 | Mid | Santa Cruz Island | Island | 34.06 | -119.9 |
| 123 | 15 | Glassow et al., 1994 | 1x | 6 | | 0.05 | 0.49 | 5200 | Mid | Santa Cruz Island | Island | 34.06 | -119.9 |

| | | | | | | | | | | | | | |
|---|---|---|---|---|---|---|---|---|---|---|---|---|---|
| 123 | 15 | Glassow et al., 1994 | 1x | 8 | | 0.20 | 0.68 | 5200 | Mid | Santa Cruz Island | Island | 34.06 | -119.9 |
| 123 | 15 | Glassow et al., 1994 | 1x | 10 | | 0.34 | 0.93 | 5200 | Mid | Santa Cruz Island | Island | 34.06 | -119.9 |
| 123 | 15 | Glassow et al., 1994 | 1x | 12 | | 0.67 | 1.11 | 5200 | Mid | Santa Cruz Island | Island | 34.06 | -119.9 |
| 123 | 15 | Glassow et al., 1994 | 1x | 14 | | 1.15 | 1.61 | 5200 | Mid | Santa Cruz Island | Island | 34.06 | -119.9 |
| 123 | 15 | Glassow et al., 1994 | 1x | 16 | | 0.76 | 1.00 | 5200 | Mid | Santa Cruz Island | Island | 34.06 | -119.9 |
| 123 | 15 | Glassow et al., 1994 | 1x | 18 | | 0.86 | 0.91 | 5200 | Mid | Santa Cruz Island | Island | 34.06 | -119.9 |
| 123 | 15 | Glassow et al., 1994 | 1x | 20 | | 1.12 | 0.32 | 5200 | Mid | Santa Cruz Island | Island | 34.06 | -119.9 |
| 123 | 15 | Glassow et al., 1994 | 1x | 22 | | 0.90 | 0.56 | 5200 | Mid | Santa Cruz Island | Island | 34.06 | -119.9 |
| 123 | 15 | Glassow et al., 1994 | 1x | 24 | | 0.79 | 0.05 | 5200 | Mid | Santa Cruz Island | Island | 34.06 | -119.9 |
| 123 | 15 | Glassow et al., 1994 | 1x | 26 | | 0.81 | -0.12 | 5200 | Mid | Santa Cruz Island | Island | 34.06 | -119.9 |
| 123 | 15 | Glassow et al., 1994 | 1x | 28 | | 0.85 | -0.31 | 5200 | Mid | Santa Cruz Island | Island | 34.06 | -119.9 |
| 124 | 17 | Glassow et al., 1994 | 2x | 0 | | 0.21 | 1.27 | 5200 | Mid | Santa Cruz Island | Island | 34.06 | -119.9 |
| 124 | 17 | Glassow et al., 1994 | 2x | 2 | | 0.77 | 0.70 | 5200 | Mid | Santa Cruz Island | Island | 34.06 | -119.9 |
| 124 | 17 | Glassow et al., 1994 | 2x | 4 | | 0.65 | 0.66 | 5200 | Mid | Santa Cruz Island | Island | 34.06 | -119.9 |
| 124 | 17 | Glassow et al., 1994 | 2x | 6 | | 0.17 | 0.82 | 5200 | Mid | Santa Cruz Island | Island | 34.06 | -119.9 |
| 124 | 17 | Glassow et al., 1994 | 2x | 8 | | -0.37 | 0.91 | 5200 | Mid | Santa Cruz Island | Island | 34.06 | -119.9 |
| 124 | 17 | Glassow et al., 1994 | 2x | 10 | | -0.78 | 0.93 | 5200 | Mid | Santa Cruz Island | Island | 34.06 | -119.9 |
| 124 | 17 | Glassow et al., 1994 | 2x | 12 | | -0.04 | 0.84 | 5200 | Mid | Santa Cruz Island | Island | 34.06 | -119.9 |
| 124 | 17 | Glassow et al., 1994 | 2x | 14 | | 0.09 | 1.12 | 5200 | Mid | Santa Cruz Island | Island | 34.06 | -119.9 |

| | | | | | | | | | | | | | |
|---|---|---|---|---|---|---|---|---|---|---|---|---|---|
| 124 | 17 | Glassow et al., 1994 | 2x | 16 | | 1.04 | 0.31 | 5200 | Mid | Santa Cruz Island | Island | 34.06 | -119.9 |
| 124 | 17 | Glassow et al., 1994 | 2x | 18 | | 1.10 | 0.02 | 5200 | Mid | Santa Cruz Island | Island | 34.06 | -119.9 |
| 124 | 17 | Glassow et al., 1994 | 2x | 20 | | 0.64 | 0.35 | 5200 | Mid | Santa Cruz Island | Island | 34.06 | -119.9 |
| 124 | 17 | Glassow et al., 1994 | 2x | 22 | | 0.56 | 0.52 | 5200 | Mid | Santa Cruz Island | Island | 34.06 | -119.9 |
| 124 | 17 | Glassow et al., 1994 | 2x | 24 | | 0.35 | 0.75 | 5200 | Mid | Santa Cruz Island | Island | 34.06 | -119.9 |
| 124 | 17 | Glassow et al., 1994 | 2x | 26 | | 0.27 | 0.86 | 5200 | Mid | Santa Cruz Island | Island | 34.06 | -119.9 |
| 124 | 17 | Glassow et al., 1994 | 2x | 28 | | 0.23 | 1.12 | 5200 | Mid | Santa Cruz Island | Island | 34.06 | -119.9 |
| 124 | 17 | Glassow et al., 1994 | 2x | 30 | | 0.07 | 1.02 | 5200 | Mid | Santa Cruz Island | Island | 34.06 | -119.9 |
| 124 | 17 | Glassow et al., 1994 | 2x | 32 | | 0.04 | 1.04 | 5200 | Mid | Santa Cruz Island | Island | 34.06 | -119.9 |
| 125 | 25 | Glassow et al., 1994 | 3y | 0 | | 0.79 | 0.70 | 5200 | Mid | Santa Cruz Island | Island | 34.06 | -119.9 |
| 125 | 25 | Glassow et al., 1994 | 3y | 2 | | 0.79 | 0.85 | 5200 | Mid | Santa Cruz Island | Island | 34.06 | -119.9 |
| 125 | 25 | Glassow et al., 1994 | 3y | 4 | | 0.41 | 0.98 | 5200 | Mid | Santa Cruz Island | Island | 34.06 | -119.9 |
| 125 | 25 | Glassow et al., 1994 | 3y | 6 | | 0.24 | 0.87 | 5200 | Mid | Santa Cruz Island | Island | 34.06 | -119.9 |
| 125 | 25 | Glassow et al., 1994 | 3y | 8 | | 0.25 | 0.62 | 5200 | Mid | Santa Cruz Island | Island | 34.06 | -119.9 |
| 125 | 25 | Glassow et al., 1994 | 3y | 10 | | 0.04 | 0.88 | 5200 | Mid | Santa Cruz Island | Island | 34.06 | -119.9 |
| 125 | 25 | Glassow et al., 1994 | 3y | 12 | | 0.25 | 0.56 | 5200 | Mid | Santa Cruz Island | Island | 34.06 | -119.9 |
| 125 | 25 | Glassow et al., 1994 | 3y | 14 | | 0.51 | 1.56 | 5200 | Mid | Santa Cruz Island | Island | 34.06 | -119.9 |
| 125 | 25 | Glassow et al., 1994 | 3y | 16 | | 0.33 | 0.79 | 5200 | Mid | Santa Cruz Island | Island | 34.06 | -119.9 |
| 125 | 25 | Glassow et al., 1994 | 3y | 18 | | 0.23 | 0.48 | 5200 | Mid | Santa Cruz Island | Island | 34.06 | -119.9 |

| | | | | | | | | | | | | | |
|---|---|---|---|---|---|---|---|---|---|---|---|---|---|
| 125 | 25 | Glassow et al., 1994 | 3y | 20 | | 0.31 | 0.69 | 5200 | Mid | Santa Cruz Island | Island | 34.06 | -119.9 |
| 125 | 25 | Glassow et al., 1994 | 3y | 22 | | 0.38 | 0.99 | 5200 | Mid | Santa Cruz Island | Island | 34.06 | -119.9 |
| 125 | 25 | Glassow et al., 1994 | 3y | 24 | | 0.36 | 0.64 | 5200 | Mid | Santa Cruz Island | Island | 34.06 | -119.9 |
| 125 | 25 | Glassow et al., 1994 | 3y | 26 | | 0.18 | 0.79 | 5200 | Mid | Santa Cruz Island | Island | 34.06 | -119.9 |
| 125 | 25 | Glassow et al., 1994 | 3y | 28 | | 0.57 | 1.29 | 5200 | Mid | Santa Cruz Island | Island | 34.06 | -119.9 |
| 125 | 25 | Glassow et al., 1994 | 3y | 30 | | 0.91 | 0.61 | 5200 | Mid | Santa Cruz Island | Island | 34.06 | -119.9 |
| 125 | 25 | Glassow et al., 1994 | 3y | 32 | | 0.86 | 0.59 | 5200 | Mid | Santa Cruz Island | Island | 34.06 | -119.9 |
| 125 | 25 | Glassow et al., 1994 | 3y | 34 | | 0.86 | 1.17 | 5200 | Mid | Santa Cruz Island | Island | 34.06 | -119.9 |
| 125 | 25 | Glassow et al., 1994 | 3y | 36 | | 0.55 | 0.47 | 5200 | Mid | Santa Cruz Island | Island | 34.06 | -119.9 |
| 125 | 25 | Glassow et al., 1994 | 3y | 38 | | 0.28 | 0.44 | 5200 | Mid | Santa Cruz Island | Island | 34.06 | -119.9 |
| 125 | 25 | Glassow et al., 1994 | 3y | 40 | | 0.44 | 0.49 | 5200 | Mid | Santa Cruz Island | Island | 34.06 | -119.9 |
| 125 | 25 | Glassow et al., 1994 | 3y | 42 | | 0.40 | 0.38 | 5200 | Mid | Santa Cruz Island | Island | 34.06 | -119.9 |
| 125 | 25 | Glassow et al., 1994 | 3y | 44 | | 0.35 | 0.43 | 5200 | Mid | Santa Cruz Island | Island | 34.06 | -119.9 |
| 125 | 25 | Glassow et al., 1994 | 3y | 46 | | 0.32 | 0.26 | 5200 | Mid | Santa Cruz Island | Island | 34.06 | -119.9 |
| 125 | 25 | Glassow et al., 1994 | 3y | 48 | | 1.08 | 0.17 | 5200 | Mid | Santa Cruz Island | Island | 34.06 | -119.9 |
| 126 | 8 | Glassow et al., 2012 | Forneys 1 | 0.00 | | 0.14 | 0.29 | 5800 | Mid | Santa Cruz Island | Island | 33.961 | -119.8 |
| 126 | 8 | Glassow et al., 2012 | Forneys 1 | 2.00 | | 0.42 | -0.26 | 5800 | Mid | Santa Cruz Island | Island | 33.961 | -119.8 |
| 126 | 8 | Glassow et al., 2012 | Forneys 1 | 4.00 | | 0.47 | 0.14 | 5800 | Mid | Santa Cruz Island | Island | 33.961 | -119.8 |
| 126 | 8 | Glassow et al., 2012 | Forneys 1 | 6.00 | | 0.75 | -0.53 | 5800 | Mid | Santa Cruz Island | Island | 33.961 | -119.8 |

| | | | | | | | | | | | | | |
|---|---|---|---|---|---|---|---|---|---|---|---|---|---|
| 126 | 8 | Glassow et al., 2012 | Forneys 1 | 8.00 | | 0.45 | -0.01 | 5800 | Mid | Santa Cruz Island | Island | 33.961 | -119.8 |
| 126 | 8 | Glassow et al., 2012 | Forneys 1 | 10.00 | | 0.77 | -0.76 | 5800 | Mid | Santa Cruz Island | Island | 33.961 | -119.8 |
| 126 | 8 | Glassow et al., 2012 | Forneys 1 | 12.00 | | 0.67 | -0.86 | 5800 | Mid | Santa Cruz Island | Island | 33.961 | -119.8 |
| 126 | 8 | Glassow et al., 2012 | Forneys 1 | 14.00 | | 0.26 | -0.31 | 5800 | Mid | Santa Cruz Island | Island | 33.961 | -119.8 |
| 127 | 8 | Glassow et al., 2012 | Forneys 2 | 0.00 | | -0.20 | 0.35 | 5800 | Mid | Santa Cruz Island | Island | 33.961 | -119.8 |
| 127 | 8 | Glassow et al., 2012 | Forneys 2 | 2.00 | | -0.08 | -0.25 | 5800 | Mid | Santa Cruz Island | Island | 33.961 | -119.8 |
| 127 | 8 | Glassow et al., 2012 | Forneys 2 | 4.00 | | 0.24 | 0.09 | 5800 | Mid | Santa Cruz Island | Island | 33.961 | -119.8 |
| 127 | 8 | Glassow et al., 2012 | Forneys 2 | 6.00 | | -0.13 | -0.03 | 5800 | Mid | Santa Cruz Island | Island | 33.961 | -119.8 |
| 127 | 8 | Glassow et al., 2012 | Forneys 2 | 8.00 | | 0.02 | -0.48 | 5800 | Mid | Santa Cruz Island | Island | 33.961 | -119.8 |
| 127 | 8 | Glassow et al., 2012 | Forneys 2 | 10.00 | | 0.13 | -0.31 | 5800 | Mid | Santa Cruz Island | Island | 33.961 | -119.8 |
| 127 | 8 | Glassow et al., 2012 | Forneys 2 | 12.00 | | -0.14 | 0.12 | 5800 | Mid | Santa Cruz Island | Island | 33.961 | -119.8 |
| 127 | 8 | Glassow et al., 2012 | Forneys 2 | 14.00 | | 0.02 | -0.61 | 5800 | Mid | Santa Cruz Island | Island | 33.961 | -119.8 |
| 128 | 8 | Glassow et al., 2012 | Forneys 3 | 0.00 | | 0.61 | 0.07 | 5800 | Mid | Santa Cruz Island | Island | 33.961 | -119.8 |
| 128 | 8 | Glassow et al., 2012 | Forneys 3 | 2.00 | | 0.72 | -0.18 | 5800 | Mid | Santa Cruz Island | Island | 33.961 | -119.8 |
| 128 | 8 | Glassow et al., 2012 | Forneys 3 | 4.00 | | 0.52 | -0.39 | 5800 | Mid | Santa Cruz Island | Island | 33.961 | -119.8 |
| 128 | 8 | Glassow et al., 2012 | Forneys 3 | 6.00 | | 0.72 | -0.46 | 5800 | Mid | Santa Cruz Island | Island | 33.961 | -119.8 |
| 128 | 8 | Glassow et al., 2012 | Forneys 3 | 8.00 | | 0.75 | -0.41 | 5800 | Mid | Santa Cruz Island | Island | 33.961 | -119.8 |
| 128 | 8 | Glassow et al., 2012 | Forneys 3 | 10.00 | | 0.17 | -0.47 | 5800 | Mid | Santa Cruz Island | Island | 33.961 | -119.8 |
| 128 | 8 | Glassow et al., 2012 | Forneys 3 | 12.00 | | 0.09 | -0.33 | 5800 | Mid | Santa Cruz Island | Island | 33.961 | -119.8 |

| | | | | | | | | | | | | | |
|---|---|---|---|---|---|---|---|---|---|---|---|---|---|
| 128 | 8 | Glassow et al., 2012 | Forneys 3 | 14.00 | | 0.29 | -0.14 | 5800 | Mid | Santa Cruz Island | Island | 33.961 | -119.8 |
| 129 | 8 | Glassow et al., 2012 | Forneys 4 | 0.00 | | -0.16 | -0.08 | 5800 | Mid | Santa Cruz Island | Island | 33.961 | -119.8 |
| 129 | 8 | Glassow et al., 2012 | Forneys 4 | 2.00 | | 0.17 | -0.01 | 5800 | Mid | Santa Cruz Island | Island | 33.961 | -119.8 |
| 129 | 8 | Glassow et al., 2012 | Forneys 4 | 4.00 | | 0.05 | -0.68 | 5800 | Mid | Santa Cruz Island | Island | 33.961 | -119.8 |
| 129 | 8 | Glassow et al., 2012 | Forneys 4 | 6.00 | | 0.05 | -0.70 | 5800 | Mid | Santa Cruz Island | Island | 33.961 | -119.8 |
| 129 | 8 | Glassow et al., 2012 | Forneys 4 | 8.00 | | 0.25 | -0.61 | 5800 | Mid | Santa Cruz Island | Island | 33.961 | -119.8 |
| 129 | 8 | Glassow et al., 2012 | Forneys 4 | 10.00 | | 0.01 | 0.02 | 5800 | Mid | Santa Cruz Island | Island | 33.961 | -119.8 |
| 129 | 8 | Glassow et al., 2012 | Forneys 4 | 12.00 | | -0.02 | -0.24 | 5800 | Mid | Santa Cruz Island | Island | 33.961 | -119.8 |
| 129 | 8 | Glassow et al., 2012 | Forneys 4 | 14.00 | | 0.40 | -1.01 | 5800 | Mid | Santa Cruz Island | Island | 33.961 | -119.8 |
| 130 | 8 | Glassow et al., 2012 | Forneys 5 | 0.00 | | 0.23 | -0.10 | 5800 | Mid | Santa Cruz Island | Island | 33.961 | -119.8 |
| 130 | 8 | Glassow et al., 2012 | Forneys 5 | 2.00 | | 0.17 | -0.21 | 5800 | Mid | Santa Cruz Island | Island | 33.961 | -119.8 |
| 130 | 8 | Glassow et al., 2012 | Forneys 5 | 4.00 | | 0.04 | -0.06 | 5800 | Mid | Santa Cruz Island | Island | 33.961 | -119.8 |
| 130 | 8 | Glassow et al., 2012 | Forneys 5 | 6.00 | | 0.21 | -0.29 | 5800 | Mid | Santa Cruz Island | Island | 33.961 | -119.8 |
| 130 | 8 | Glassow et al., 2012 | Forneys 5 | 8.00 | | 0.16 | -0.40 | 5800 | Mid | Santa Cruz Island | Island | 33.961 | -119.8 |
| 130 | 8 | Glassow et al., 2012 | Forneys 5 | 10.00 | | 0.22 | -0.66 | 5800 | Mid | Santa Cruz Island | Island | 33.961 | -119.8 |
| 130 | 8 | Glassow et al., 2012 | Forneys 5 | 12.00 | | -0.06 | 0.10 | 5800 | Mid | Santa Cruz Island | Island | 33.961 | -119.8 |
| 130 | 8 | Glassow et al., 2012 | Forneys 5 | 14.00 | | 0.00 | -0.11 | 5800 | Mid | Santa Cruz Island | Island | 33.961 | -119.8 |
| 131 | 8 | Glassow et al., 2012 | Forneys 6 | 0.00 | | -0.07 | 0.46 | 5800 | Mid | Santa Cruz Island | Island | 33.961 | -119.8 |
| 131 | 8 | Glassow et al., 2012 | Forneys 6 | 2.00 | | 0.20 | -0.03 | 5800 | Mid | Santa Cruz Island | Island | 33.961 | -119.8 |

| | | | | | | | | | | | | | |
|---|---|---|---|---|---|---|---|---|---|---|---|---|---|
| 131 | 8 | Glassow et al., 2012 | Forneys 6 | 4.00 | | 0.07 | -0.05 | 5800 | Mid | Santa Cruz Island | Island | 33.961 | -119.8 |
| 131 | 8 | Glassow et al., 2012 | Forneys 6 | 6.00 | | -0.06 | -0.21 | 5800 | Mid | Santa Cruz Island | Island | 33.961 | -119.8 |
| 131 | 8 | Glassow et al., 2012 | Forneys 6 | 8.00 | | -0.20 | -0.29 | 5800 | Mid | Santa Cruz Island | Island | 33.961 | -119.8 |
| 131 | 8 | Glassow et al., 2012 | Forneys 6 | 10.00 | | 0.16 | -0.64 | 5800 | Mid | Santa Cruz Island | Island | 33.961 | -119.8 |
| 131 | 8 | Glassow et al., 2012 | Forneys 6 | 12.00 | | -0.48 | 0.28 | 5800 | Mid | Santa Cruz Island | Island | 33.961 | -119.8 |
| 131 | 8 | Glassow et al., 2012 | Forneys 6 | 14.00 | | -0.23 | -0.16 | 5800 | Mid | Santa Cruz Island | Island | 33.961 | -119.8 |
| 132 | 8 | Glassow et al., 2012 | Punta Arena 1 | 0.00 | | -0.48 | 0.19 | 5800 | Mid | Santa Cruz Island | Island | 33.961 | -119.8 |
| 132 | 8 | Glassow et al., 2012 | Punta Arena 1 | 2.00 | | -0.26 | 0.17 | 5800 | Mid | Santa Cruz Island | Island | 33.961 | -119.8 |
| 132 | 8 | Glassow et al., 2012 | Punta Arena 1 | 4.00 | | -0.05 | -0.73 | 5800 | Mid | Santa Cruz Island | Island | 33.961 | -119.8 |
| 132 | 8 | Glassow et al., 2012 | Punta Arena 1 | 6.00 | | -0.36 | -0.31 | 5800 | Mid | Santa Cruz Island | Island | 33.961 | -119.8 |
| 132 | 8 | Glassow et al., 2012 | Punta Arena 1 | 8.00 | | 0.09 | 0.00 | 5800 | Mid | Santa Cruz Island | Island | 33.961 | -119.8 |
| 132 | 8 | Glassow et al., 2012 | Punta Arena 1 | 10.00 | | 0.29 | -1.19 | 5800 | Mid | Santa Cruz Island | Island | 33.961 | -119.8 |
| 132 | 8 | Glassow et al., 2012 | Punta Arena 1 | 12.00 | | -0.09 | -0.30 | 5800 | Mid | Santa Cruz Island | Island | 33.961 | -119.8 |
| 132 | 8 | Glassow et al., 2012 | Punta Arena 1 | 14.00 | | 0.29 | -0.78 | 5800 | Mid | Santa Cruz Island | Island | 33.961 | -119.8 |
| 133 | 8 | Glassow et al., 2012 | Punta Arena 2 | 0.00 | | -0.39 | 0.28 | 5800 | Mid | Santa Cruz Island | Island | 33.961 | -119.8 |
| 133 | 8 | Glassow et al., 2012 | Punta Arena 2 | 2.00 | | 0.20 | -0.37 | 5800 | Mid | Santa Cruz Island | Island | 33.961 | -119.8 |
| 133 | 8 | Glassow et al., 2012 | Punta Arena 2 | 4.00 | | -0.31 | -0.05 | 5800 | Mid | Santa Cruz Island | Island | 33.961 | -119.8 |
| 133 | 8 | Glassow et al., 2012 | Punta Arena 2 | 6.00 | | 0.11 | -0.57 | 5800 | Mid | Santa Cruz Island | Island | 33.961 | -119.8 |
| 133 | 8 | Glassow et al., 2012 | Punta Arena 2 | 8.00 | | 0.03 | 0.21 | 5800 | Mid | Santa Cruz Island | Island | 33.961 | -119.8 |

| | | | | | | | | | | | | | |
|---|---|---|---|---|---|---|---|---|---|---|---|---|---|
| 133 | 8 | Glassow et al., 2012 | Punta Arena 2 | 10.00 | | 0.09 | -0.44 | 5800 | Mid | Santa Cruz Island | Island | 33.961 | -119.8 |
| 133 | 8 | Glassow et al., 2012 | Punta Arena 2 | 12.00 | | 0.18 | -1.10 | 5800 | Mid | Santa Cruz Island | Island | 33.961 | -119.8 |
| 133 | 8 | Glassow et al., 2012 | Punta Arena 2 | 14.00 | | -0.18 | -0.19 | 5800 | Mid | Santa Cruz Island | Island | 33.961 | -119.8 |
| 134 | 8 | Glassow et al., 2012 | Punta Arena 3 | 0.00 | | -0.44 | -0.80 | 5800 | Mid | Santa Cruz Island | Island | 33.961 | -119.8 |
| 134 | 8 | Glassow et al., 2012 | Punta Arena 3 | 2.00 | | -0.35 | -0.72 | 5800 | Mid | Santa Cruz Island | Island | 33.961 | -119.8 |
| 134 | 8 | Glassow et al., 2012 | Punta Arena 3 | 4.00 | | -0.04 | -0.49 | 5800 | Mid | Santa Cruz Island | Island | 33.961 | -119.8 |
| 134 | 8 | Glassow et al., 2012 | Punta Arena 3 | 6.00 | | -0.57 | -0.62 | 5800 | Mid | Santa Cruz Island | Island | 33.961 | -119.8 |
| 134 | 8 | Glassow et al., 2012 | Punta Arena 3 | 8.00 | | -0.38 | -0.64 | 5800 | Mid | Santa Cruz Island | Island | 33.961 | -119.8 |
| 134 | 8 | Glassow et al., 2012 | Punta Arena 3 | 10.00 | | 0.04 | -1.14 | 5800 | Mid | Santa Cruz Island | Island | 33.961 | -119.8 |
| 134 | 8 | Glassow et al., 2012 | Punta Arena 3 | 12.00 | | -0.12 | -0.91 | 5800 | Mid | Santa Cruz Island | Island | 33.961 | -119.8 |
| 134 | 8 | Glassow et al., 2012 | Punta Arena 3 | 14.00 | | -0.04 | -1.31 | 5800 | Mid | Santa Cruz Island | Island | 33.961 | -119.8 |
| 135 | 8 | Glassow et al., 2012 | Punta Arena 4 | 0.00 | | 0.57 | -0.31 | 5800 | Mid | Santa Cruz Island | Island | 33.961 | -119.8 |
| 135 | 8 | Glassow et al., 2012 | Punta Arena 4 | 2.00 | | -0.10 | -0.43 | 5800 | Mid | Santa Cruz Island | Island | 33.961 | -119.8 |
| 135 | 8 | Glassow et al., 2012 | Punta Arena 4 | 4.00 | | -0.32 | -0.73 | 5800 | Mid | Santa Cruz Island | Island | 33.961 | -119.8 |
| 135 | 8 | Glassow et al., 2012 | Punta Arena 4 | 6.00 | | -0.55 | -0.29 | 5800 | Mid | Santa Cruz Island | Island | 33.961 | -119.8 |
| 135 | 8 | Glassow et al., 2012 | Punta Arena 4 | 8.00 | | -0.01 | -0.42 | 5800 | Mid | Santa Cruz Island | Island | 33.961 | -119.8 |
| 135 | 8 | Glassow et al., 2012 | Punta Arena 4 | 10.00 | | 0.24 | -0.91 | 5800 | Mid | Santa Cruz Island | Island | 33.961 | -119.8 |
| 135 | 8 | Glassow et al., 2012 | Punta Arena 4 | 12.00 | | 0.51 | -0.72 | 5800 | Mid | Santa Cruz Island | Island | 33.961 | -119.8 |
| 135 | 8 | Glassow et al., 2012 | Punta Arena 4 | 14.00 | | -0.19 | 0.22 | 5800 | Mid | Santa Cruz Island | Island | 33.961 | -119.8 |

| | | | | | | | | | | | | | |
|---|---|---|---|---|---|---|---|---|---|---|---|---|---|
| 136 | 8 | Glassow et al., 2012 | Punta Arena 5 | 0.00 | | 0.00 | -0.42 | 5800 | Mid | Santa Cruz Island | Island | 33.961 | -119.8 |
| 136 | 8 | Glassow et al., 2012 | Punta Arena 5 | 2.00 | | -0.21 | -0.49 | 5800 | Mid | Santa Cruz Island | Island | 33.961 | -119.8 |
| 136 | 8 | Glassow et al., 2012 | Punta Arena 5 | 4.00 | | 0.82 | -1.45 | 5800 | Mid | Santa Cruz Island | Island | 33.961 | -119.8 |
| 136 | 8 | Glassow et al., 2012 | Punta Arena 5 | 6.00 | | 0.26 | -0.02 | 5800 | Mid | Santa Cruz Island | Island | 33.961 | -119.8 |
| 136 | 8 | Glassow et al., 2012 | Punta Arena 5 | 8.00 | | 0.04 | 0.29 | 5800 | Mid | Santa Cruz Island | Island | 33.961 | -119.8 |
| 136 | 8 | Glassow et al., 2012 | Punta Arena 5 | 10.00 | | 0.18 | 0.17 | 5800 | Mid | Santa Cruz Island | Island | 33.961 | -119.8 |
| 136 | 8 | Glassow et al., 2012 | Punta Arena 5 | 12.00 | | 0.31 | -0.27 | 5800 | Mid | Santa Cruz Island | Island | 33.961 | -119.8 |
| 136 | 8 | Glassow et al., 2012 | Punta Arena 5 | 14.00 | | 0.56 | -1.30 | 5800 | Mid | Santa Cruz Island | Island | 33.961 | -119.8 |
| 137 | 2 | Jazwa and Kennett 2016 | CA-SMI-528 | 1.00 | | | 0.15 | 5575 | Mid | San Miguel Island | Island | 34.031 | -120.4 |
| 137 | 2 | Jazwa and Kennett 2016 | CA-SMI-528 | 2.00 | | | 0.86 | 5575 | Mid | San Miguel Island | Island | 34.031 | -120.4 |
| 138 | 2 | Jazwa and Kennett 2016 | CA-SMI-528 | 1.00 | | | 0.33 | 5575 | Mid | San Miguel Island | Island | 34.031 | -120.4 |
| 138 | 2 | Jazwa and Kennett 2016 | CA-SMI-528 | 2.00 | | | 0.91 | 5575 | Mid | San Miguel Island | Island | 34.031 | -120.4 |
| 139 | 2 | Jazwa and Kennett 2016 | CA-SMI-528 | 1.00 | | | -0.05 | 5575 | Mid | San Miguel Island | Island | 34.031 | -120.4 |
| 139 | 2 | Jazwa and Kennett 2016 | CA-SMI-528 | 2.00 | | | 0.49 | 5575 | Mid | San Miguel Island | Island | 34.031 | -120.4 |
| 140 | 2 | Jazwa and Kennett 2016 | CA-SMI-528 | 1.00 | | | -0.12 | 5575 | Mid | San Miguel Island | Island | 34.031 | -120.4 |
| 140 | 2 | Jazwa and Kennett 2016 | CA-SMI-528 | 2.00 | | | 0.81 | 5575 | Mid | San Miguel Island | Island | 34.031 | -120.4 |

| | | | | | | | | | | | | | |
|---|---|---|---|---|---|---|---|---|---|---|---|---|---|
| 141 | 2 | Jazwa and Kennett 2016 | CA-SMI-528 | 2.00 | | | 0.11 | 5575 | Mid | San Miguel Island | Island | 34.031 | -120.4 |
| 141 | 2 | Jazwa and Kennett 2016 | CA-SMI-528 | 1.00 | | | 0.21 | 5575 | Mid | San Miguel Island | Island | 34.031 | -120.4 |
| 142 | 2 | Jazwa and Kennett 2016 | CA-SMI-528 | 1.00 | | | 0.23 | 5575 | Mid | San Miguel Island | Island | 34.031 | -120.4 |
| 142 | 2 | Jazwa and Kennett 2016 | CA-SMI-528 | 2.00 | | | 0.73 | 5575 | Mid | San Miguel Island | Island | 34.031 | -120.4 |
| 143 | 2 | Jazwa and Kennett 2016 | CA-SMI-528 | 1.00 | | | 0.28 | 5575 | Mid | San Miguel Island | Island | 34.031 | -120.4 |
| 143 | 2 | Jazwa and Kennett 2016 | CA-SMI-528 | 2.00 | | | 1.26 | 5575 | Mid | San Miguel Island | Island | 34.031 | -120.4 |
| 144 | 2 | Jazwa and Kennett 2016 | CA-SMI-528 | 2.00 | | | 0.33 | 5575 | Mid | San Miguel Island | Island | 34.031 | -120.4 |
| 144 | 2 | Jazwa and Kennett 2016 | CA-SMI-528 | 1.00 | | | 0.94 | 5575 | Mid | San Miguel Island | Island | 34.031 | -120.4 |
| 145 | 2 | Jazwa and Kennett 2016 | CA-SMI-528 | 2.00 | | | -0.04 | 5575 | Mid | San Miguel Island | Island | 34.031 | -120.4 |
| 145 | 2 | Jazwa and Kennett 2016 | CA-SMI-528 | 1.00 | | | 0.30 | 5575 | Mid | San Miguel Island | Island | 34.031 | -120.4 |
| 146 | 2 | Jazwa and Kennett 2016 | CA-SMI-528 | 1.00 | | | -0.32 | 5575 | Mid | San Miguel Island | Island | 34.031 | -120.4 |
| 146 | 2 | Jazwa and Kennett 2016 | CA-SMI-528 | 2.00 | | | 0.81 | 5575 | Mid | San Miguel Island | Island | 34.031 | -120.4 |
| 147 | 2 | Jazwa and Kennett 2016 | CA-SMI-528 | 1.00 | | | 0.16 | 5575 | Mid | San Miguel Island | Island | 34.031 | -120.4 |
| 147 | 2 | Jazwa and Kennett 2016 | CA-SMI-528 | 2.00 | | | 0.44 | 5575 | Mid | San Miguel Island | Island | 34.031 | -120.4 |

| | | | | | | | | | | | | | |
|---|---|---|---|---|---|---|---|---|---|---|---|---|---|
| 148 | 2 | Jazwa and Kennett 2016 | CA-SMI-528 | 2.00 | | | 0.23 | 5575 | Mid | San Miguel Island | Island | 34.031 | -120.4 |
| 148 | 2 | Jazwa and Kennett 2016 | CA-SMI-528 | 1.00 | | | 0.86 | 5575 | Mid | San Miguel Island | Island | 34.031 | -120.4 |
| 149 | 2 | Jazwa and Kennett 2016 | CA-SMI-528 | 1.00 | | | -0.05 | 5575 | Mid | San Miguel Island | Island | 34.031 | -120.4 |
| 149 | 2 | Jazwa and Kennett 2016 | CA-SMI-528 | 2.00 | | | 1.68 | 5575 | Mid | San Miguel Island | Island | 34.031 | -120.4 |
| 150 | 2 | Jazwa and Kennett 2016 | CA-SMI-528 | 1.00 | | | 0.41 | 5575 | Mid | San Miguel Island | Island | 34.031 | -120.4 |
| 150 | 2 | Jazwa and Kennett 2016 | CA-SMI-528 | 2.00 | | | 0.69 | 5575 | Mid | San Miguel Island | Island | 34.031 | -120.4 |
| 151 | 2 | Jazwa and Kennett 2016 | CA-SMI-528 | 1.00 | | | 0.35 | 5575 | Mid | San Miguel Island | Island | 34.031 | -120.4 |
| 151 | 2 | Jazwa and Kennett 2016 | CA-SMI-528 | 2.00 | | | 0.64 | 5575 | Mid | San Miguel Island | Island | 34.031 | -120.4 |
| 152 | 2 | Jazwa and Kennett 2016 | CA-SMI-528 | 1.00 | | | 0.50 | 5575 | Mid | San Miguel Island | Island | 34.031 | -120.4 |
| 152 | 2 | Jazwa and Kennett 2016 | CA-SMI-528 | 2.00 | | | 0.72 | 5575 | Mid | San Miguel Island | Island | 34.031 | -120.4 |
| 153 | 2 | Jazwa and Kennett 2016 | CA-SMI-528 | 1.00 | | | 0.57 | 5575 | Mid | San Miguel Island | Island | 34.031 | -120.4 |
| 153 | 2 | Jazwa and Kennett 2016 | CA-SMI-528 | 2.00 | | | 0.81 | 5575 | Mid | San Miguel Island | Island | 34.031 | -120.4 |
| 154 | 2 | Jazwa and Kennett 2016 | CA-SMI-528 | 1.00 | | | 1.01 | 5575 | Mid | San Miguel Island | Island | 34.031 | -120.4 |
| 154 | 2 | Jazwa and Kennett 2016 | CA-SMI-528 | 2.00 | | | 1.17 | 5575 | Mid | San Miguel Island | Island | 34.031 | -120.4 |

| | | | | | | | | | | | | | | |
|---|---|---|---|---|---|---|---|---|---|---|---|---|---|---|
| 155 | 2 | Jazwa and Kennett 2016 | CA-SMI-528 | 2.00 | | | 0.19 | 5575 | Mid | San Miguel Island | Island | 34.031 | -120.4 |
| 155 | 2 | Jazwa and Kennett 2016 | CA-SMI-528 | 1.00 | | | 0.26 | 5575 | Mid | San Miguel Island | Island | 34.031 | -120.4 |
| 156 | 2 | Jazwa and Kennett 2016 | CA-SMI-528 | 1.00 | | | 0.07 | 5575 | Mid | San Miguel Island | Island | 34.031 | -120.4 |
| 156 | 2 | Jazwa and Kennett 2016 | CA-SMI-528 | 2.00 | | | 0.47 | 5575 | Mid | San Miguel Island | Island | 34.031 | -120.4 |
| 157 | 2 | Jazwa and Kennett 2016 | CA-SMI-528 | 1.00 | | | 0.72 | 5575 | Mid | San Miguel Island | Island | 34.031 | -120.4 |
| 157 | 2 | Jazwa and Kennett 2016 | CA-SMI-528 | 2.00 | | | 1.12 | 5575 | Mid | San Miguel Island | Island | 34.031 | -120.4 |
| 158 | 2 | Jazwa and Kennett 2016 | CA-SMI-528 | 2.00 | | | 0.49 | 5575 | Mid | San Miguel Island | Island | 34.031 | -120.4 |
| 158 | 2 | Jazwa and Kennett 2016 | CA-SMI-528 | 1.00 | | | 1.02 | 5575 | Mid | San Miguel Island | Island | 34.031 | -120.4 |
| 159 | 2 | Jazwa and Kennett 2016 | CA-SMI-528 | 2.00 | | | 0.26 | 5575 | Mid | San Miguel Island | Island | 34.031 | -120.4 |
| 159 | 2 | Jazwa and Kennett 2016 | CA-SMI-528 | 1.00 | | | 0.27 | 5575 | Mid | San Miguel Island | Island | 34.031 | -120.4 |
| 160 | 2 | Jazwa and Kennett 2016 | CA-SMI-528 | 1.00 | | | 0.36 | 5575 | Mid | San Miguel Island | Island | 34.031 | -120.4 |
| 160 | 2 | Jazwa and Kennett 2016 | CA-SMI-528 | 2.00 | | | 1.03 | 5575 | Mid | San Miguel Island | Island | 34.031 | -120.4 |
| 161 | 2 | Jazwa and Kennett 2016 | CA-SMI-528 | 2.00 | | | 0.72 | 5575 | Mid | San Miguel Island | Island | 34.031 | -120.4 |
| 161 | 2 | Jazwa and Kennett 2016 | CA-SMI-528 | 1.00 | | | 0.99 | 5575 | Mid | San Miguel Island | Island | 34.031 | -120.4 |

| | | | | | | | | | | | | | |
|---|---|---|---|---|---|---|---|---|---|---|---|---|---|
| 162 | 2 | Jazwa and Kennett 2016 | CA-SMI-528 | 1.00 | | | 0.21 | 5575 | Mid | San Miguel Island | Island | 34.031 | -120.4 |
| 162 | 2 | Jazwa and Kennett 2016 | CA-SMI-528 | 2.00 | | | 0.76 | 5575 | Mid | San Miguel Island | Island | 34.031 | -120.4 |
| 163 | 2 | Jazwa and Kennett 2016 | CA-SMI-528 | 1.00 | | | 0.23 | 5575 | Mid | San Miguel Island | Island | 34.031 | -120.4 |
| 163 | 2 | Jazwa and Kennett 2016 | CA-SMI-528 | 2.00 | | | 0.65 | 5575 | Mid | San Miguel Island | Island | 34.031 | -120.4 |
| 164 | 2 | Jazwa and Kennett 2016 | CA-SMI-528 | 1.00 | | | -0.01 | 5575 | Mid | San Miguel Island | Island | 34.031 | -120.4 |
| 164 | 2 | Jazwa and Kennett 2016 | CA-SMI-528 | 2.00 | | | 0.57 | 5575 | Mid | San Miguel Island | Island | 34.031 | -120.4 |
| 165 | 2 | Jazwa and Kennett 2016 | CA-SMI-528 | 1.00 | | | -0.29 | 5575 | Mid | San Miguel Island | Island | 34.031 | -120.4 |
| 165 | 2 | Jazwa and Kennett 2016 | CA-SMI-528 | 2.00 | | | 0.71 | 5575 | Mid | San Miguel Island | Island | 34.031 | -120.4 |
| 166 | 2 | Jazwa and Kennett 2016 | CA-SMI-528 | 1.00 | | | -0.56 | 5575 | Mid | San Miguel Island | Island | 34.031 | -120.4 |
| 166 | 2 | Jazwa and Kennett 2016 | CA-SMI-528 | 2.00 | | | 0.67 | 5575 | Mid | San Miguel Island | Island | 34.031 | -120.4 |
| 167 | 2 | Jazwa and Kennett 2016 | CA-SMI-528 | 1.00 | | | 0.10 | 5575 | Mid | San Miguel Island | Island | 34.031 | -120.4 |
| 167 | 2 | Jazwa and Kennett 2016 | CA-SMI-528 | 2.00 | | | 1.53 | 5575 | Mid | San Miguel Island | Island | 34.031 | -120.4 |
| 168 | 2 | Jazwa and Kennett 2016 | CA-SMI-528 | 1.00 | | | -0.42 | 5575 | Mid | San Miguel Island | Island | 34.031 | -120.4 |
| 168 | 2 | Jazwa and Kennett 2016 | CA-SMI-528 | 2.00 | | | -0.22 | 5575 | Mid | San Miguel Island | Island | 34.031 | -120.4 |

| | | | | | | | | | | | | | |
|---|---|---|---|---|---|---|---|---|---|---|---|---|---|
| 169 | 2 | Jazwa and Kennett 2016 | CA-SMI-528 | 1.00 | | | 0.68 | 5575 | Mid | San Miguel Island | Island | 34.031 | -120.4 |
| 169 | 2 | Jazwa and Kennett 2016 | CA-SMI-528 | 2.00 | | | 1.14 | 5575 | Mid | San Miguel Island | Island | 34.031 | -120.4 |
| 170 | 2 | Jazwa and Kennett 2016 | CA-SMI-528 | 2.00 | | | -0.65 | 5575 | Mid | San Miguel Island | Island | 34.031 | -120.4 |
| 170 | 2 | Jazwa and Kennett 2016 | CA-SMI-528 | 1.00 | | | 1.07 | 5575 | Mid | San Miguel Island | Island | 34.031 | -120.4 |
| 171 | 2 | Jazwa and Kennett 2016 | CA-SMI-528 | 2.00 | | | 1.19 | 5575 | Mid | San Miguel Island | Island | 34.031 | -120.4 |
| 171 | 2 | Jazwa and Kennett 2016 | CA-SMI-528 | 1.00 | | | 1.57 | 5575 | Mid | San Miguel Island | Island | 34.031 | -120.4 |
| 172 | 2 | Jazwa and Kennett 2016 | CA-SMI-528 | 1.00 | | | 0.51 | 5575 | Mid | San Miguel Island | Island | 34.031 | -120.4 |
| 172 | 2 | Jazwa and Kennett 2016 | CA-SMI-528 | 2.00 | | | 0.54 | 5575 | Mid | San Miguel Island | Island | 34.031 | -120.4 |
| 173 | 2 | Jazwa and Kennett 2016 | CA-SMI-528 | 1.00 | | | 0.33 | 5575 | Mid | San Miguel Island | Island | 34.031 | -120.4 |
| 173 | 2 | Jazwa and Kennett 2016 | CA-SMI-528 | 2.00 | | | 1.38 | 5575 | Mid | San Miguel Island | Island | 34.031 | -120.4 |
| 174 | 2 | Jazwa and Kennett 2016 | CA-SMI-528 | 1.00 | | | 1.04 | 5575 | Mid | San Miguel Island | Island | 34.031 | -120.4 |
| 174 | 2 | Jazwa and Kennett 2016 | CA-SMI-528 | 2.00 | | | 1.14 | 5575 | Mid | San Miguel Island | Island | 34.031 | -120.4 |
| 175 | 2 | Jazwa and Kennett 2016 | CA-SMI-528_1 | 2.00 | | | 0.12 | 5575 | Mid | San Miguel Island | Island | 34.031 | -120.4 |
| 175 | 2 | Jazwa and Kennett 2016 | CA-SMI-528_1 | 1.00 | | | 0.23 | 5575 | Mid | San Miguel Island | Island | 34.031 | -120.4 |

| | | | | | | | | | | | | | |
|---|---|---|---|---|---|---|---|---|---|---|---|---|---|
| 176 | 2 | Jazwa and Kennett 2016 | CA-SMI-528_2 | 1.00 | | | -0.54 | 5575 | Mid | San Miguel Island | Island | 34.031 | -120.4 |
| 176 | 2 | Jazwa and Kennett 2016 | CA-SMI-528_2 | 2.00 | | | 0.17 | 5575 | Mid | San Miguel Island | Island | 34.031 | -120.4 |
| 177 | 2 | Jazwa and Kennett 2016 | CA-SMI-602 | 2.00 | | | 1.03 | 5575 | Mid | San Miguel Island | Island | 34.031 | -120.4 |
| 177 | 2 | Jazwa and Kennett 2016 | CA-SMI-602 | 1.00 | | | 1.04 | 5575 | Mid | San Miguel Island | Island | 34.031 | -120.4 |
| 178 | 2 | Jazwa and Kennett 2016 | CA-SMI-602 | 1.00 | | | 0.44 | 5575 | Mid | San Miguel Island | Island | 34.031 | -120.4 |
| 178 | 2 | Jazwa and Kennett 2016 | CA-SMI-602 | 2.00 | | | 0.80 | 5575 | Mid | San Miguel Island | Island | 34.031 | -120.4 |
| 179 | 2 | Jazwa and Kennett 2016 | CA-SMI-602 | 1.00 | | | -0.65 | 5575 | Mid | San Miguel Island | Island | 34.031 | -120.4 |
| 179 | 2 | Jazwa and Kennett 2016 | CA-SMI-602 | 2.00 | | | 0.13 | 5575 | Mid | San Miguel Island | Island | 34.031 | -120.4 |
| 180 | 2 | Jazwa and Kennett 2016 | CA-SMI-602 | 2.00 | | | 1.01 | 5575 | Mid | San Miguel Island | Island | 34.031 | -120.4 |
| 180 | 2 | Jazwa and Kennett 2016 | CA-SMI-602 | 1.00 | | | 1.15 | 5575 | Mid | San Miguel Island | Island | 34.031 | -120.4 |
| 181 | 2 | Jazwa and Kennett 2016 | CA-SMI-602 | 2.00 | | | 1.28 | 5575 | Mid | San Miguel Island | Island | 34.031 | -120.4 |
| 182 | 2 | Jazwa and Kennett 2016 | CA-SMI-602 | 1.00 | | | 1.43 | 5575 | Mid | San Miguel Island | Island | 34.031 | -120.4 |
| 183 | 2 | Jazwa and Kennett 2016 | CA-SMI-602 | 2.00 | | | 0.78 | 5575 | Mid | San Miguel Island | Island | 34.031 | -120.4 |
| 183 | 2 | Jazwa and Kennett 2016 | CA-SMI-602 | 1.00 | | | 1.01 | 5575 | Mid | San Miguel Island | Island | 34.031 | -120.4 |

| | | | | | | | | | | | | | | |
|---|---|---|---|---|---|---|---|---|---|---|---|---|---|---|
| 184 | 2 | Jazwa and Kennett 2016 | CA-SMI-602 | 2.00 | | | 1.00 | 5575 | Mid | San Miguel Island | Island | 34.031 | -120.4 |
| 184 | 2 | Jazwa and Kennett 2016 | CA-SMI-602 | 1.00 | | | 1.29 | 5575 | Mid | San Miguel Island | Island | 34.031 | -120.4 |
| 185 | 2 | Jazwa and Kennett 2016 | CA-SMI-602 | 2.00 | | | 0.85 | 5575 | Mid | San Miguel Island | Island | 34.031 | -120.4 |
| 185 | 2 | Jazwa and Kennett 2016 | CA-SMI-602 | 1.00 | | | 1.14 | 5575 | Mid | San Miguel Island | Island | 34.031 | -120.4 |
| 186 | 2 | Jazwa and Kennett 2016 | CA-SMI-602 | 2.00 | | | 0.83 | 5575 | Mid | San Miguel Island | Island | 34.031 | -120.4 |
| 186 | 2 | Jazwa and Kennett 2016 | CA-SMI-602 | 1.00 | | | 1.22 | 5575 | Mid | San Miguel Island | Island | 34.031 | -120.4 |
| 187 | 2 | Jazwa and Kennett 2016 | CA-SMI-602 | 1.00 | | | 0.40 | 5575 | Mid | San Miguel Island | Island | 34.031 | -120.4 |
| 187 | 2 | Jazwa and Kennett 2016 | CA-SMI-602 | 2.00 | | | 0.70 | 5575 | Mid | San Miguel Island | Island | 34.031 | -120.4 |
| 188 | 2 | Jazwa and Kennett 2016 | CA-SMI-602 | 1.00 | | | 0.89 | 5575 | Mid | San Miguel Island | Island | 34.031 | -120.4 |
| 189 | 2 | Jazwa and Kennett 2016 | CA-SMI-602 | 2.00 | | | 1.06 | 5575 | Mid | San Miguel Island | Island | 34.031 | -120.4 |
| 189 | 2 | Jazwa and Kennett 2016 | CA-SMI-602 | 1.00 | | | 0.32 | 5575 | Mid | San Miguel Island | Island | 34.031 | -120.4 |
| 190 | 2 | Jazwa and Kennett 2016 | CA-SMI-602 | 2.00 | | | 0.72 | 5575 | Mid | San Miguel Island | Island | 34.031 | -120.4 |
| 190 | 2 | Jazwa and Kennett 2016 | CA-SMI-602 | 2.00 | | | 0.81 | 5575 | Mid | San Miguel Island | Island | 34.031 | -120.4 |
| 191 | 2 | Jazwa and Kennett 2016 | CA-SMI-602 | 1.00 | | | 1.18 | 5575 | Mid | San Miguel Island | Island | 34.031 | -120.4 |

| | | | | | | | | | | | | | |
|---|---|---|---|---|---|---|---|---|---|---|---|---|---|
| 191 | 2 | Jazwa and Kennett 2016 | CA-SMI-602 | 2.00 | | | 0.81 | 5575 | Mid | San Miguel Island | Island | 34.031 | -120.4 |
| 192 | 2 | Jazwa and Kennett 2016 | CA-SMI-602 | 1.00 | | | 1.04 | 5575 | Mid | San Miguel Island | Island | 34.031 | -120.4 |
| 192 | 2 | Jazwa and Kennett 2016 | CA-SMI-602 | 2.00 | | | 1.18 | 5575 | Mid | San Miguel Island | Island | 34.031 | -120.4 |
| 193 | 4 | Jazwa et al., 2020 | 1_1 | 0 | 84.5 | -0.12 | -0.28 | 3 | Mod | Santa Rosa Island | Island | 34.008 | -120 |
| 193 | 4 | Jazwa et al., 2020 | 1_1 | 1 | 84.5 | -0.23 | 0.21 | 3 | Mod | Santa Rosa Island | Island | 34.008 | -120 |
| 193 | 4 | Jazwa et al., 2020 | 1_1 | 2 | 84.5 | -0.41 | 1.01 | 3 | Mod | Santa Rosa Island | Island | 34.008 | -120 |
| 193 | 4 | Jazwa et al., 2020 | 1_1 | 3 | 84.5 | -0.21 | 1.17 | 3 | Mod | Santa Rosa Island | Island | 34.008 | -120 |
| 194 | 4 | Jazwa et al., 2020 | 1_10 | 0 | 57.4 | -0.11 | 0.00 | 3 | Mod | Santa Rosa Island | Island | 34.008 | -120 |
| 194 | 4 | Jazwa et al., 2020 | 1_10 | 1 | 57.4 | -0.27 | -0.18 | 3 | Mod | Santa Rosa Island | Island | 34.008 | -120 |
| 194 | 4 | Jazwa et al., 2020 | 1_10 | 2 | 57.4 | -0.28 | -0.77 | 3 | Mod | Santa Rosa Island | Island | 34.008 | -120 |
| 194 | 4 | Jazwa et al., 2020 | 1_10 | 3 | 57.4 | -0.70 | 0.50 | 3 | Mod | Santa Rosa Island | Island | 34.008 | -120 |
| 195 | 4 | Jazwa et al., 2020 | 1_2 | 0 | 62.4 | -0.12 | -0.33 | 3 | Mod | Santa Rosa Island | Island | 34.008 | -120 |
| 195 | 4 | Jazwa et al., 2020 | 1_2 | 1 | 62.4 | -0.23 | -0.15 | 3 | Mod | Santa Rosa Island | Island | 34.008 | -120 |
| 195 | 4 | Jazwa et al., 2020 | 1_2 | 2 | 62.4 | -0.41 | 0.43 | 3 | Mod | Santa Rosa Island | Island | 34.008 | -120 |
| 195 | 4 | Jazwa et al., 2020 | 1_2 | 3 | 62.4 | -0.21 | -0.08 | 3 | Mod | Santa Rosa Island | Island | 34.008 | -120 |
| 196 | 4 | Jazwa et al., 2020 | 1_3 | 0 | 60.9 | -0.40 | -0.09 | 3 | Mod | Santa Rosa Island | Island | 34.008 | -120 |
| 196 | 4 | Jazwa et al., 2020 | 1_3 | 1 | 60.9 | -0.70 | -0.38 | 3 | Mod | Santa Rosa Island | Island | 34.008 | -120 |
| 196 | 4 | Jazwa et al., 2020 | 1_3 | 2 | 60.9 | -1.07 | -0.33 | 3 | Mod | Santa Rosa Island | Island | 34.008 | -120 |

| | | | | | | | | | | | | | |
|---|---|---|---|---|---|---|---|---|---|---|---|---|---|
| 196 | 4 | Jazwa et al., 2020 | 1_3 | 3 | 60.9 | 0.09 | -0.04 | 3 | Mod | Santa Rosa Island | Island | 34.008 | -120 |
| 197 | 4 | Jazwa et al., 2020 | 1_4 | 0 | 64.3 | 0.00 | 0.18 | 3 | Mod | Santa Rosa Island | Island | 34.008 | -120 |
| 197 | 4 | Jazwa et al., 2020 | 1_4 | 1 | 64.3 | -0.24 | -0.13 | 3 | Mod | Santa Rosa Island | Island | 34.008 | -120 |
| 197 | 4 | Jazwa et al., 2020 | 1_4 | 2 | 64.3 | -0.39 | 0.67 | 3 | Mod | Santa Rosa Island | Island | 34.008 | -120 |
| 197 | 4 | Jazwa et al., 2020 | 1_4 | 3 | 64.3 | -0.21 | 0.75 | 3 | Mod | Santa Rosa Island | Island | 34.008 | -120 |
| 198 | 4 | Jazwa et al., 2020 | 1_5 | 0 | 45.3 | -0.11 | -0.56 | 3 | Mod | Santa Rosa Island | Island | 34.008 | -120 |
| 198 | 4 | Jazwa et al., 2020 | 1_5 | 1 | 45.3 | 0.04 | -0.54 | 3 | Mod | Santa Rosa Island | Island | 34.008 | -120 |
| 198 | 4 | Jazwa et al., 2020 | 1_5 | 2 | 45.3 | -0.72 | -0.46 | 3 | Mod | Santa Rosa Island | Island | 34.008 | -120 |
| 198 | 4 | Jazwa et al., 2020 | 1_5 | 3 | 45.3 | -0.45 | 0.23 | 3 | Mod | Santa Rosa Island | Island | 34.008 | -120 |
| 199 | 4 | Jazwa et al., 2020 | 1_6 | 0 | 47.3 | 0.12 | -0.41 | 3 | Mod | Santa Rosa Island | Island | 34.008 | -120 |
| 199 | 4 | Jazwa et al., 2020 | 1_6 | 1 | 47.3 | -0.38 | -0.28 | 3 | Mod | Santa Rosa Island | Island | 34.008 | -120 |
| 199 | 4 | Jazwa et al., 2020 | 1_6 | 2 | 47.3 | -0.09 | -0.61 | 3 | Mod | Santa Rosa Island | Island | 34.008 | -120 |
| 199 | 4 | Jazwa et al., 2020 | 1_6 | 3 | 47.3 | -0.44 | 0.39 | 3 | Mod | Santa Rosa Island | Island | 34.008 | -120 |
| 200 | 4 | Jazwa et al., 2020 | 1_7 | 0 | 67.1 | -0.47 | -0.47 | 3 | Mod | Santa Rosa Island | Island | 34.008 | -120 |
| 200 | 4 | Jazwa et al., 2020 | 1_7 | 1 | 67.1 | -0.32 | -0.02 | 3 | Mod | Santa Rosa Island | Island | 34.008 | -120 |
| 200 | 4 | Jazwa et al., 2020 | 1_7 | 2 | 67.1 | -0.86 | 0.54 | 3 | Mod | Santa Rosa Island | Island | 34.008 | -120 |
| 200 | 4 | Jazwa et al., 2020 | 1_7 | 3 | 67.1 | -0.82 | -0.17 | 3 | Mod | Santa Rosa Island | Island | 34.008 | -120 |
| 201 | 4 | Jazwa et al., 2020 | 1_8 | 0 | 50.3 | -0.45 | -0.60 | 3 | Mod | Santa Rosa Island | Island | 34.008 | -120 |
| 201 | 4 | Jazwa et al., 2020 | 1_8 | 1 | 50.3 | -0.22 | -0.47 | 3 | Mod | Santa Rosa Island | Island | 34.008 | -120 |

| | | | | | | | | | | | | | |
|---|---|---|---|---|---|---|---|---|---|---|---|---|---|
| 201 | 4 | Jazwa et al., 2020 | 1_8 | 2 | 50.3 | -0.23 | -0.35 | 3 | Mod | Santa Rosa Island | Island | 34.008 | -120 |
| 201 | 4 | Jazwa et al., 2020 | 1_8 | 3 | 50.3 | -0.48 | 0.20 | 3 | Mod | Santa Rosa Island | Island | 34.008 | -120 |
| 202 | 4 | Jazwa et al., 2020 | 1_9 | 0 | 61.4 | -0.46 | 0.05 | 3 | Mod | Santa Rosa Island | Island | 34.008 | -120 |
| 202 | 4 | Jazwa et al., 2020 | 1_9 | 1 | 61.4 | -0.27 | -0.17 | 3 | Mod | Santa Rosa Island | Island | 34.008 | -120 |
| 202 | 4 | Jazwa et al., 2020 | 1_9 | 2 | 61.4 | -0.49 | 0.81 | 3 | Mod | Santa Rosa Island | Island | 34.008 | -120 |
| 202 | 4 | Jazwa et al., 2020 | 1_9 | 3 | 61.4 | -0.53 | 0.34 | 3 | Mod | Santa Rosa Island | Island | 34.008 | -120 |
| 203 | 4 | Jazwa et al., 2020 | 10_1 | 0 | 65.6 | -0.15 | -0.59 | 3 | Mod | Santa Rosa Island | Island | 34.008 | -120 |
| 203 | 4 | Jazwa et al., 2020 | 10_1 | 1 | 65.6 | -0.32 | -0.10 | 3 | Mod | Santa Rosa Island | Island | 34.008 | -120 |
| 203 | 4 | Jazwa et al., 2020 | 10_1 | 2 | 65.6 | -0.54 | -0.51 | 3 | Mod | Santa Rosa Island | Island | 34.008 | -120 |
| 203 | 4 | Jazwa et al., 2020 | 10_1 | 3 | 65.6 | -0.33 | -0.20 | 3 | Mod | Santa Rosa Island | Island | 34.008 | -120 |
| 204 | 4 | Jazwa et al., 2020 | 10_2 | 0 | 42.5 | -0.71 | -0.70 | 3 | Mod | Santa Rosa Island | Island | 34.008 | -120 |
| 204 | 4 | Jazwa et al., 2020 | 10_2 | 1 | 42.5 | -0.60 | -0.33 | 3 | Mod | Santa Rosa Island | Island | 34.008 | -120 |
| 204 | 4 | Jazwa et al., 2020 | 10_2 | 2 | 42.5 | -0.65 | -0.20 | 3 | Mod | Santa Rosa Island | Island | 34.008 | -120 |
| 204 | 4 | Jazwa et al., 2020 | 10_2 | 3 | 42.5 | -0.73 | -0.56 | 3 | Mod | Santa Rosa Island | Island | 34.008 | -120 |
| 205 | 4 | Jazwa et al., 2020 | 10_3 | 0 | 87.8 | -0.34 | -0.61 | 3 | Mod | Santa Rosa Island | Island | 34.008 | -120 |
| 205 | 4 | Jazwa et al., 2020 | 10_3 | 1 | 87.8 | -0.32 | -0.37 | 3 | Mod | Santa Rosa Island | Island | 34.008 | -120 |
| 205 | 4 | Jazwa et al., 2020 | 10_3 | 2 | 87.8 | -0.92 | -0.43 | 3 | Mod | Santa Rosa Island | Island | 34.008 | -120 |
| 205 | 4 | Jazwa et al., 2020 | 10_3 | 3 | 87.8 | -0.86 | -0.88 | 3 | Mod | Santa Rosa Island | Island | 34.008 | -120 |
| 206 | 4 | Jazwa et al., 2020 | 10_4 | 0 | 82.3 | -0.55 | -0.48 | 3 | Mod | Santa Rosa Island | Island | 34.008 | -120 |

| | | | | | | | | | | | | | |
|---|---|---|---|---|---|---|---|---|---|---|---|---|---|
| 206 | 4 | Jazwa et al., 2020 | 10_4 | 1 | 82.3 | -0.36 | -0.13 | 3 | Mod | Santa Rosa Island | Island | 34.008 | -120 |
| 206 | 4 | Jazwa et al., 2020 | 10_4 | 2 | 82.3 | -0.51 | -0.45 | 3 | Mod | Santa Rosa Island | Island | 34.008 | -120 |
| 206 | 4 | Jazwa et al., 2020 | 10_4 | 3 | 82.3 | -0.94 | -0.84 | 3 | Mod | Santa Rosa Island | Island | 34.008 | -120 |
| 207 | 4 | Jazwa et al., 2020 | 10_5 | 0 | 87.9 | 0.05 | -0.01 | 3 | Mod | Santa Rosa Island | Island | 34.008 | -120 |
| 207 | 4 | Jazwa et al., 2020 | 10_5 | 1 | 87.9 | -0.48 | -0.79 | 3 | Mod | Santa Rosa Island | Island | 34.008 | -120 |
| 207 | 4 | Jazwa et al., 2020 | 10_5 | 2 | 87.9 | -0.67 | -0.93 | 3 | Mod | Santa Rosa Island | Island | 34.008 | -120 |
| 207 | 4 | Jazwa et al., 2020 | 10_5 | 3 | 87.9 | -0.95 | -0.83 | 3 | Mod | Santa Rosa Island | Island | 34.008 | -120 |
| 208 | 4 | Jazwa et al., 2020 | 10_6 | 0 | 66.8 | -0.27 | -0.48 | 3 | Mod | Santa Rosa Island | Island | 34.008 | -120 |
| 208 | 4 | Jazwa et al., 2020 | 10_6 | 1 | 66.8 | -0.38 | -0.32 | 3 | Mod | Santa Rosa Island | Island | 34.008 | -120 |
| 208 | 4 | Jazwa et al., 2020 | 10_6 | 2 | 66.8 | -0.77 | -0.08 | 3 | Mod | Santa Rosa Island | Island | 34.008 | -120 |
| 208 | 4 | Jazwa et al., 2020 | 10_6 | 3 | 66.8 | -0.49 | 0.14 | 3 | Mod | Santa Rosa Island | Island | 34.008 | -120 |
| 209 | 4 | Jazwa et al., 2020 | 10_7 | 0 | 73.6 | -0.35 | -0.81 | 3 | Mod | Santa Rosa Island | Island | 34.008 | -120 |
| 209 | 4 | Jazwa et al., 2020 | 10_7 | 1 | 73.6 | -0.66 | -0.78 | 3 | Mod | Santa Rosa Island | Island | 34.008 | -120 |
| 209 | 4 | Jazwa et al., 2020 | 10_7 | 2 | 73.6 | -0.70 | -1.12 | 3 | Mod | Santa Rosa Island | Island | 34.008 | -120 |
| 209 | 4 | Jazwa et al., 2020 | 10_7 | 3 | 73.6 | -0.96 | -0.45 | 3 | Mod | Santa Rosa Island | Island | 34.008 | -120 |
| 210 | 4 | Jazwa et al., 2020 | 2_1 | 0 | 77.7 | -0.30 | -0.48 | 3 | Mod | Santa Rosa Island | Island | 34.008 | -120 |
| 210 | 4 | Jazwa et al., 2020 | 2_1 | 1 | 77.7 | -0.45 | -0.32 | 3 | Mod | Santa Rosa Island | Island | 34.008 | -120 |
| 210 | 4 | Jazwa et al., 2020 | 2_1 | 2 | 77.7 | -0.69 | -1.08 | 3 | Mod | Santa Rosa Island | Island | 34.008 | -120 |
| 210 | 4 | Jazwa et al., 2020 | 2_1 | 3 | 77.7 | -0.67 | -0.04 | 3 | Mod | Santa Rosa Island | Island | 34.008 | -120 |

| | | | | | | | | | | | | | |
|---|---|---|---|---|---|---|---|---|---|---|---|---|---|
| 211 | 4 | Jazwa et al., 2020 | 2_2 | 0 | 43.8 | -0.55 | 0.11 | 3 | Mod | Santa Rosa Island | Island | 34.008 | -120 |
| 211 | 4 | Jazwa et al., 2020 | 2_2 | 1 | 43.8 | -0.42 | -0.06 | 3 | Mod | Santa Rosa Island | Island | 34.008 | -120 |
| 211 | 4 | Jazwa et al., 2020 | 2_2 | 2 | 43.8 | -0.42 | -0.03 | 3 | Mod | Santa Rosa Island | Island | 34.008 | -120 |
| 211 | 4 | Jazwa et al., 2020 | 2_2 | 3 | 43.8 | -0.09 | 0.28 | 3 | Mod | Santa Rosa Island | Island | 34.008 | -120 |
| 212 | 4 | Jazwa et al., 2020 | 2_3 | 0 | 79 | 0.32 | -0.21 | 3 | Mod | Santa Rosa Island | Island | 34.008 | -120 |
| 212 | 4 | Jazwa et al., 2020 | 2_3 | 1 | 79 | -0.07 | -0.54 | 3 | Mod | Santa Rosa Island | Island | 34.008 | -120 |
| 212 | 4 | Jazwa et al., 2020 | 2_3 | 2 | 79 | -0.40 | 0.36 | 3 | Mod | Santa Rosa Island | Island | 34.008 | -120 |
| 212 | 4 | Jazwa et al., 2020 | 2_3 | 3 | 79 | -0.60 | -0.68 | 3 | Mod | Santa Rosa Island | Island | 34.008 | -120 |
| 213 | 4 | Jazwa et al., 2020 | 2_4 | 0 | 71 | -0.27 | -0.91 | 3 | Mod | Santa Rosa Island | Island | 34.008 | -120 |
| 213 | 4 | Jazwa et al., 2020 | 2_4 | 1 | 71 | -0.18 | -0.22 | 3 | Mod | Santa Rosa Island | Island | 34.008 | -120 |
| 213 | 4 | Jazwa et al., 2020 | 2_4 | 2 | 71 | -0.94 | -0.19 | 3 | Mod | Santa Rosa Island | Island | 34.008 | -120 |
| 213 | 4 | Jazwa et al., 2020 | 2_4 | 3 | 71 | -0.40 | 0.07 | 3 | Mod | Santa Rosa Island | Island | 34.008 | -120 |
| 214 | 4 | Jazwa et al., 2020 | 2_5 | 0 | 65.4 | -0.29 | -0.41 | 3 | Mod | Santa Rosa Island | Island | 34.008 | -120 |
| 214 | 4 | Jazwa et al., 2020 | 2_5 | 1 | 65.4 | -0.42 | -0.38 | 3 | Mod | Santa Rosa Island | Island | 34.008 | -120 |
| 214 | 4 | Jazwa et al., 2020 | 2_5 | 2 | 65.4 | -0.63 | -0.91 | 3 | Mod | Santa Rosa Island | Island | 34.008 | -120 |
| 214 | 4 | Jazwa et al., 2020 | 2_5 | 3 | 65.4 | -0.67 | -0.37 | 3 | Mod | Santa Rosa Island | Island | 34.008 | -120 |
| 215 | 4 | Jazwa et al., 2020 | 2_6 | 0 | 73.5 | -0.19 | -0.16 | 3 | Mod | Santa Rosa Island | Island | 34.008 | -120 |
| 215 | 4 | Jazwa et al., 2020 | 2_6 | 1 | 73.5 | -0.05 | -0.22 | 3 | Mod | Santa Rosa Island | Island | 34.008 | -120 |
| 215 | 4 | Jazwa et al., 2020 | 2_6 | 2 | 73.5 | 0.06 | -0.20 | 3 | Mod | Santa Rosa Island | Island | 34.008 | -120 |

| | | | | | | | | | | | | | |
|---|---|---|---|---|---|---|---|---|---|---|---|---|---|
| 215 | 4 | Jazwa et al., 2020 | 2_6 | 3 | 73.5 | -0.01 | -0.53 | 3 | Mod | Santa Rosa Island | Island | 34.008 | -120 |
| 216 | 4 | Jazwa et al., 2020 | 2_7 | 0 | 46.3 | -0.18 | -0.38 | 3 | Mod | Santa Rosa Island | Island | 34.008 | -120 |
| 216 | 4 | Jazwa et al., 2020 | 2_7 | 1 | 46.3 | -0.52 | -0.53 | 3 | Mod | Santa Rosa Island | Island | 34.008 | -120 |
| 216 | 4 | Jazwa et al., 2020 | 2_7 | 2 | 46.3 | -0.37 | -0.47 | 3 | Mod | Santa Rosa Island | Island | 34.008 | -120 |
| 216 | 4 | Jazwa et al., 2020 | 2_7 | 3 | 46.3 | -0.66 | -0.19 | 3 | Mod | Santa Rosa Island | Island | 34.008 | -120 |
| 217 | 4 | Jazwa et al., 2020 | 2_8 | 0 | 79.9 | -0.04 | -0.56 | 3 | Mod | Santa Rosa Island | Island | 34.008 | -120 |
| 217 | 4 | Jazwa et al., 2020 | 2_8 | 1 | 79.9 | -0.11 | -0.48 | 3 | Mod | Santa Rosa Island | Island | 34.008 | -120 |
| 217 | 4 | Jazwa et al., 2020 | 2_8 | 2 | 79.9 | -0.28 | -0.36 | 3 | Mod | Santa Rosa Island | Island | 34.008 | -120 |
| 217 | 4 | Jazwa et al., 2020 | 2_8 | 3 | 79.9 | -0.42 | 0.32 | 3 | Mod | Santa Rosa Island | Island | 34.008 | -120 |
| 218 | 4 | Jazwa et al., 2020 | 2_9 | 0 | 49.6 | 0.17 | -0.11 | 3 | Mod | Santa Rosa Island | Island | 34.008 | -120 |
| 218 | 4 | Jazwa et al., 2020 | 2_9 | 1 | 49.6 | -0.15 | -0.27 | 3 | Mod | Santa Rosa Island | Island | 34.008 | -120 |
| 218 | 4 | Jazwa et al., 2020 | 2_9 | 2 | 49.6 | -0.22 | 0.54 | 3 | Mod | Santa Rosa Island | Island | 34.008 | -120 |
| 218 | 4 | Jazwa et al., 2020 | 2_9 | 3 | 49.6 | -0.70 | -0.55 | 3 | Mod | Santa Rosa Island | Island | 34.008 | -120 |
| 219 | 4 | Jazwa et al., 2020 | 3_1 | 0 | 64.6 | 0.02 | -0.15 | 3 | Mod | Santa Rosa Island | Island | 34.008 | -120 |
| 219 | 4 | Jazwa et al., 2020 | 3_1 | 1 | 64.6 | 0.15 | -0.05 | 3 | Mod | Santa Rosa Island | Island | 34.008 | -120 |
| 219 | 4 | Jazwa et al., 2020 | 3_1 | 2 | 64.6 | -0.06 | -0.31 | 3 | Mod | Santa Rosa Island | Island | 34.008 | -120 |
| 219 | 4 | Jazwa et al., 2020 | 3_1 | 3 | 64.6 | -0.14 | -0.17 | 3 | Mod | Santa Rosa Island | Island | 34.008 | -120 |
| 220 | 4 | Jazwa et al., 2020 | 3_2 | 0 | 75.1 | -0.03 | -0.31 | 3 | Mod | Santa Rosa Island | Island | 34.008 | -120 |
| 220 | 4 | Jazwa et al., 2020 | 3_2 | 1 | 75.1 | -0.09 | -0.43 | 3 | Mod | Santa Rosa Island | Island | 34.008 | -120 |

| | | | | | | | | | | | | | |
|---|---|---|---|---|---|---|---|---|---|---|---|---|---|
| 220 | 4 | Jazwa et al., 2020 | 3_2 | 2 | 75.1 | -0.21 | -0.42 | 3 | Mod | Santa Rosa Island | Island | 34.008 | -120 |
| 220 | 4 | Jazwa et al., 2020 | 3_2 | 3 | 75.1 | -0.66 | -0.40 | 3 | Mod | Santa Rosa Island | Island | 34.008 | -120 |
| 221 | 4 | Jazwa et al., 2020 | 3_3 | 0 | 77.6 | 0.33 | -0.42 | 3 | Mod | Santa Rosa Island | Island | 34.008 | -120 |
| 221 | 4 | Jazwa et al., 2020 | 3_3 | 1 | 77.6 | -0.05 | -0.62 | 3 | Mod | Santa Rosa Island | Island | 34.008 | -120 |
| 221 | 4 | Jazwa et al., 2020 | 3_3 | 2 | 77.6 | 0.13 | -0.37 | 3 | Mod | Santa Rosa Island | Island | 34.008 | -120 |
| 221 | 4 | Jazwa et al., 2020 | 3_3 | 3 | 77.6 | -0.43 | -0.29 | 3 | Mod | Santa Rosa Island | Island | 34.008 | -120 |
| 222 | 4 | Jazwa et al., 2020 | 3_4 | 0 | 62.2 | -0.51 | -0.34 | 3 | Mod | Santa Rosa Island | Island | 34.008 | -120 |
| 222 | 4 | Jazwa et al., 2020 | 3_4 | 1 | 62.2 | -1.03 | 0.24 | 3 | Mod | Santa Rosa Island | Island | 34.008 | -120 |
| 222 | 4 | Jazwa et al., 2020 | 3_4 | 2 | 62.2 | -0.93 | 0.52 | 3 | Mod | Santa Rosa Island | Island | 34.008 | -120 |
| 222 | 4 | Jazwa et al., 2020 | 3_4 | 3 | 62.2 | -0.79 | 0.05 | 3 | Mod | Santa Rosa Island | Island | 34.008 | -120 |
| 223 | 4 | Jazwa et al., 2020 | 3_5 | 0 | 64.1 | -0.19 | -0.04 | 3 | Mod | Santa Rosa Island | Island | 34.008 | -120 |
| 223 | 4 | Jazwa et al., 2020 | 3_5 | 1 | 64.1 | -0.37 | -0.21 | 3 | Mod | Santa Rosa Island | Island | 34.008 | -120 |
| 223 | 4 | Jazwa et al., 2020 | 3_5 | 2 | 64.1 | -0.45 | -0.72 | 3 | Mod | Santa Rosa Island | Island | 34.008 | -120 |
| 223 | 4 | Jazwa et al., 2020 | 3_5 | 3 | 64.1 | -0.82 | -0.43 | 3 | Mod | Santa Rosa Island | Island | 34.008 | -120 |
| 224 | 4 | Jazwa et al., 2020 | 3_6 | 0 | 72.5 | -0.14 | -0.05 | 3 | Mod | Santa Rosa Island | Island | 34.008 | -120 |
| 224 | 4 | Jazwa et al., 2020 | 3_6 | 1 | 72.5 | -0.25 | 0.00 | 3 | Mod | Santa Rosa Island | Island | 34.008 | -120 |
| 224 | 4 | Jazwa et al., 2020 | 3_6 | 2 | 72.5 | -0.58 | 0.11 | 3 | Mod | Santa Rosa Island | Island | 34.008 | -120 |
| 224 | 4 | Jazwa et al., 2020 | 3_6 | 3 | 72.5 | -0.58 | 0.27 | 3 | Mod | Santa Rosa Island | Island | 34.008 | -120 |
| 225 | 4 | Jazwa et al., 2020 | 4_1 | 0 | 81.1 | -0.30 | -0.67 | 3 | Mod | Santa Rosa Island | Island | 34.008 | -120 |

| | | | | | | | | | | | | | |
|---|---|---|---|---|---|---|---|---|---|---|---|---|---|
| 225 | 4 | Jazwa et al., 2020 | 4_1 | 1 | 81.1 | 0.02 | 0.04 | 3 | Mod | Santa Rosa Island | Island | 34.008 | -120 |
| 225 | 4 | Jazwa et al., 2020 | 4_1 | 2 | 81.1 | -0.05 | 0.17 | 3 | Mod | Santa Rosa Island | Island | 34.008 | -120 |
| 225 | 4 | Jazwa et al., 2020 | 4_1 | 3 | 81.1 | -0.31 | 0.52 | 3 | Mod | Santa Rosa Island | Island | 34.008 | -120 |
| 226 | 4 | Jazwa et al., 2020 | 4_2 | 0 | 95.9 | -0.20 | -0.49 | 3 | Mod | Santa Rosa Island | Island | 34.008 | -120 |
| 226 | 4 | Jazwa et al., 2020 | 4_2 | 1 | 95.9 | -0.16 | -0.66 | 3 | Mod | Santa Rosa Island | Island | 34.008 | -120 |
| 226 | 4 | Jazwa et al., 2020 | 4_2 | 2 | 95.9 | -0.25 | -0.63 | 3 | Mod | Santa Rosa Island | Island | 34.008 | -120 |
| 226 | 4 | Jazwa et al., 2020 | 4_2 | 3 | 95.9 | -0.57 | -0.72 | 3 | Mod | Santa Rosa Island | Island | 34.008 | -120 |
| 227 | 4 | Jazwa et al., 2020 | 4_3 | 0 | 91.4 | 0.17 | -0.40 | 3 | Mod | Santa Rosa Island | Island | 34.008 | -120 |
| 227 | 4 | Jazwa et al., 2020 | 4_3 | 1 | 91.4 | -0.53 | -0.37 | 3 | Mod | Santa Rosa Island | Island | 34.008 | -120 |
| 227 | 4 | Jazwa et al., 2020 | 4_3 | 2 | 91.4 | -0.26 | -0.52 | 3 | Mod | Santa Rosa Island | Island | 34.008 | -120 |
| 227 | 4 | Jazwa et al., 2020 | 4_3 | 3 | 91.4 | -0.42 | -0.48 | 3 | Mod | Santa Rosa Island | Island | 34.008 | -120 |
| 228 | 4 | Jazwa et al., 2020 | 4_4 | 0 | 53.7 | -0.57 | -0.75 | 3 | Mod | Santa Rosa Island | Island | 34.008 | -120 |
| 228 | 4 | Jazwa et al., 2020 | 4_4 | 1 | 53.7 | -0.53 | -0.29 | 3 | Mod | Santa Rosa Island | Island | 34.008 | -120 |
| 228 | 4 | Jazwa et al., 2020 | 4_4 | 2 | 53.7 | -0.53 | -0.42 | 3 | Mod | Santa Rosa Island | Island | 34.008 | -120 |
| 228 | 4 | Jazwa et al., 2020 | 4_4 | 3 | 53.7 | -0.49 | -0.37 | 3 | Mod | Santa Rosa Island | Island | 34.008 | -120 |
| 229 | 4 | Jazwa et al., 2020 | 4_5 | 0 | 63.1 | -0.58 | -0.47 | 3 | Mod | Santa Rosa Island | Island | 34.008 | -120 |
| 229 | 4 | Jazwa et al., 2020 | 4_5 | 1 | 63.1 | -0.53 | -0.48 | 3 | Mod | Santa Rosa Island | Island | 34.008 | -120 |
| 229 | 4 | Jazwa et al., 2020 | 4_5 | 2 | 63.1 | -0.35 | -0.17 | 3 | Mod | Santa Rosa Island | Island | 34.008 | -120 |
| 229 | 4 | Jazwa et al., 2020 | 4_5 | 3 | 63.1 | -0.56 | -0.21 | 3 | Mod | Santa Rosa Island | Island | 34.008 | -120 |

| | | | | | | | | | | | | | |
|---|---|---|---|---|---|---|---|---|---|---|---|---|---|
| 230 | 4 | Jazwa et al., 2020 | 4_6 | 0 | 72.6 | -0.13 | -0.18 | 3 | Mod | Santa Rosa Island | Island | 34.008 | -120 |
| 230 | 4 | Jazwa et al., 2020 | 4_6 | 1 | 72.6 | -0.40 | -0.26 | 3 | Mod | Santa Rosa Island | Island | 34.008 | -120 |
| 230 | 4 | Jazwa et al., 2020 | 4_6 | 2 | 72.6 | -0.35 | -0.27 | 3 | Mod | Santa Rosa Island | Island | 34.008 | -120 |
| 230 | 4 | Jazwa et al., 2020 | 4_6 | 3 | 72.6 | -1.02 | -0.19 | 3 | Mod | Santa Rosa Island | Island | 34.008 | -120 |
| 231 | 4 | Jazwa et al., 2020 | 4_7 | 0 | 77.8 | 0.34 | 0.00 | 3 | Mod | Santa Rosa Island | Island | 34.008 | -120 |
| 231 | 4 | Jazwa et al., 2020 | 4_7 | 1 | 77.8 | 0.23 | 0.04 | 3 | Mod | Santa Rosa Island | Island | 34.008 | -120 |
| 231 | 4 | Jazwa et al., 2020 | 4_7 | 2 | 77.8 | -0.06 | -0.20 | 3 | Mod | Santa Rosa Island | Island | 34.008 | -120 |
| 231 | 4 | Jazwa et al., 2020 | 4_7 | 3 | 77.8 | -0.36 | -0.05 | 3 | Mod | Santa Rosa Island | Island | 34.008 | -120 |
| 232 | 4 | Jazwa et al., 2020 | 5_1 | 0 | 78.7 | -0.13 | -0.17 | 3 | Mod | Santa Rosa Island | Island | 34.008 | -120 |
| 232 | 4 | Jazwa et al., 2020 | 5_1 | 1 | 78.7 | -0.20 | -0.26 | 3 | Mod | Santa Rosa Island | Island | 34.008 | -120 |
| 232 | 4 | Jazwa et al., 2020 | 5_1 | 2 | 78.7 | -0.44 | -0.16 | 3 | Mod | Santa Rosa Island | Island | 34.008 | -120 |
| 232 | 4 | Jazwa et al., 2020 | 5_1 | 3 | 78.7 | -0.50 | -0.58 | 3 | Mod | Santa Rosa Island | Island | 34.008 | -120 |
| 233 | 4 | Jazwa et al., 2020 | 5_2 | 0 | 64.1 | -0.34 | -0.33 | 3 | Mod | Santa Rosa Island | Island | 34.008 | -120 |
| 233 | 4 | Jazwa et al., 2020 | 5_2 | 1 | 64.1 | -0.49 | -0.18 | 3 | Mod | Santa Rosa Island | Island | 34.008 | -120 |
| 233 | 4 | Jazwa et al., 2020 | 5_2 | 2 | 64.1 | -0.54 | -0.40 | 3 | Mod | Santa Rosa Island | Island | 34.008 | -120 |
| 233 | 4 | Jazwa et al., 2020 | 5_2 | 3 | 64.1 | -0.48 | -0.52 | 3 | Mod | Santa Rosa Island | Island | 34.008 | -120 |
| 234 | 4 | Jazwa et al., 2020 | 5_3 | 0 | 92.2 | 0.08 | -0.69 | 3 | Mod | Santa Rosa Island | Island | 34.008 | -120 |
| 234 | 4 | Jazwa et al., 2020 | 5_3 | 1 | 92.2 | 0.12 | -0.44 | 3 | Mod | Santa Rosa Island | Island | 34.008 | -120 |
| 234 | 4 | Jazwa et al., 2020 | 5_3 | 2 | 92.2 | -0.09 | -0.17 | 3 | Mod | Santa Rosa Island | Island | 34.008 | -120 |

| | | | | | | | | | | | | | |
|---|---|---|---|---|---|---|---|---|---|---|---|---|---|
| 234 | 4 | Jazwa et al., 2020 | 5_3 | 3 | 92.2 | -0.04 | -0.55 | 3 | Mod | Santa Rosa Island | Island | 34.008 | -120 |
| 235 | 4 | Jazwa et al., 2020 | 5_4 | 0 | 54.7 | -0.17 | -0.37 | 3 | Mod | Santa Rosa Island | Island | 34.008 | -120 |
| 235 | 4 | Jazwa et al., 2020 | 5_4 | 1 | 54.7 | -0.21 | 0.00 | 3 | Mod | Santa Rosa Island | Island | 34.008 | -120 |
| 235 | 4 | Jazwa et al., 2020 | 5_4 | 2 | 54.7 | -0.11 | -0.09 | 3 | Mod | Santa Rosa Island | Island | 34.008 | -120 |
| 235 | 4 | Jazwa et al., 2020 | 5_4 | 3 | 54.7 | -0.21 | -0.03 | 3 | Mod | Santa Rosa Island | Island | 34.008 | -120 |
| 236 | 4 | Jazwa et al., 2020 | 5_5 | 0 | 73.1 | -0.10 | -0.11 | 3 | Mod | Santa Rosa Island | Island | 34.008 | -120 |
| 236 | 4 | Jazwa et al., 2020 | 5_5 | 1 | 73.1 | -0.23 | -0.23 | 3 | Mod | Santa Rosa Island | Island | 34.008 | -120 |
| 236 | 4 | Jazwa et al., 2020 | 5_5 | 2 | 73.1 | -0.34 | -0.28 | 3 | Mod | Santa Rosa Island | Island | 34.008 | -120 |
| 236 | 4 | Jazwa et al., 2020 | 5_5 | 3 | 73.1 | -0.43 | -0.25 | 3 | Mod | Santa Rosa Island | Island | 34.008 | -120 |
| 237 | 4 | Jazwa et al., 2020 | 5_6 | 0 | 85.6 | -0.10 | -0.50 | 3 | Mod | Santa Rosa Island | Island | 34.008 | -120 |
| 237 | 4 | Jazwa et al., 2020 | 5_6 | 1 | 85.6 | -0.19 | -0.39 | 3 | Mod | Santa Rosa Island | Island | 34.008 | -120 |
| 237 | 4 | Jazwa et al., 2020 | 5_6 | 2 | 85.6 | -0.45 | -0.80 | 3 | Mod | Santa Rosa Island | Island | 34.008 | -120 |
| 237 | 4 | Jazwa et al., 2020 | 5_6 | 3 | 85.6 | -0.79 | -0.61 | 3 | Mod | Santa Rosa Island | Island | 34.008 | -120 |
| 238 | 4 | Jazwa et al., 2020 | 5_7 | 0 | 53.2 | -0.66 | -0.45 | 3 | Mod | Santa Rosa Island | Island | 34.008 | -120 |
| 238 | 4 | Jazwa et al., 2020 | 5_7 | 1 | 53.2 | -0.76 | -0.13 | 3 | Mod | Santa Rosa Island | Island | 34.008 | -120 |
| 238 | 4 | Jazwa et al., 2020 | 5_7 | 2 | 53.2 | -0.84 | -0.26 | 3 | Mod | Santa Rosa Island | Island | 34.008 | -120 |
| 238 | 4 | Jazwa et al., 2020 | 5_7 | 3 | 53.2 | -0.93 | -0.56 | 3 | Mod | Santa Rosa Island | Island | 34.008 | -120 |
| 239 | 4 | Jazwa et al., 2020 | 6_1 | 0 | 69 | -0.23 | 0.13 | 3 | Mod | Santa Rosa Island | Island | 34.008 | -120 |
| 239 | 4 | Jazwa et al., 2020 | 6_1 | 1 | 69 | -0.39 | -0.03 | 3 | Mod | Santa Rosa Island | Island | 34.008 | -120 |

| | | | | | | | | | | | | | |
|---|---|---|---|---|---|---|---|---|---|---|---|---|---|
| 239 | 4 | Jazwa et al., 2020 | 6_1 | 2 | 69 | -0.49 | -0.23 | 3 | Mod | Santa Rosa Island | Island | 34.008 | -120 |
| 239 | 4 | Jazwa et al., 2020 | 6_1 | 3 | 69 | -0.36 | -0.11 | 3 | Mod | Santa Rosa Island | Island | 34.008 | -120 |
| 240 | 4 | Jazwa et al., 2020 | 6_2 | 0 | 118.5 | -0.15 | -0.25 | 3 | Mod | Santa Rosa Island | Island | 34.008 | -120 |
| 240 | 4 | Jazwa et al., 2020 | 6_2 | 1 | 118.5 | -0.11 | -0.19 | 3 | Mod | Santa Rosa Island | Island | 34.008 | -120 |
| 240 | 4 | Jazwa et al., 2020 | 6_2 | 2 | 118.5 | -0.62 | -0.38 | 3 | Mod | Santa Rosa Island | Island | 34.008 | -120 |
| 240 | 4 | Jazwa et al., 2020 | 6_2 | 3 | 118.5 | -0.36 | 0.43 | 3 | Mod | Santa Rosa Island | Island | 34.008 | -120 |
| 241 | 4 | Jazwa et al., 2020 | 6_3 | 0 | 90.8 | -0.05 | -0.24 | 3 | Mod | Santa Rosa Island | Island | 34.008 | -120 |
| 241 | 4 | Jazwa et al., 2020 | 6_3 | 1 | 90.8 | -0.41 | -0.49 | 3 | Mod | Santa Rosa Island | Island | 34.008 | -120 |
| 241 | 4 | Jazwa et al., 2020 | 6_3 | 2 | 90.8 | -0.49 | -0.46 | 3 | Mod | Santa Rosa Island | Island | 34.008 | -120 |
| 241 | 4 | Jazwa et al., 2020 | 6_3 | 3 | 90.8 | -0.56 | -0.67 | 3 | Mod | Santa Rosa Island | Island | 34.008 | -120 |
| 242 | 4 | Jazwa et al., 2020 | 6_4 | 0 | 103.1 | -0.39 | -0.41 | 3 | Mod | Santa Rosa Island | Island | 34.008 | -120 |
| 242 | 4 | Jazwa et al., 2020 | 6_4 | 1 | 103.1 | -0.18 | -0.15 | 3 | Mod | Santa Rosa Island | Island | 34.008 | -120 |
| 242 | 4 | Jazwa et al., 2020 | 6_4 | 2 | 103.1 | -0.78 | -0.42 | 3 | Mod | Santa Rosa Island | Island | 34.008 | -120 |
| 242 | 4 | Jazwa et al., 2020 | 6_4 | 3 | 103.1 | -0.33 | 0.30 | 3 | Mod | Santa Rosa Island | Island | 34.008 | -120 |
| 243 | 4 | Jazwa et al., 2020 | 6_5 | 0 | 66.9 | 0.04 | -0.61 | 3 | Mod | Santa Rosa Island | Island | 34.008 | -120 |
| 243 | 4 | Jazwa et al., 2020 | 6_5 | 1 | 66.9 | 0.02 | -0.76 | 3 | Mod | Santa Rosa Island | Island | 34.008 | -120 |
| 243 | 4 | Jazwa et al., 2020 | 6_5 | 2 | 66.9 | -0.07 | -0.30 | 3 | Mod | Santa Rosa Island | Island | 34.008 | -120 |
| 243 | 4 | Jazwa et al., 2020 | 6_5 | 3 | 66.9 | -0.25 | -0.52 | 3 | Mod | Santa Rosa Island | Island | 34.008 | -120 |
| 244 | 4 | Jazwa et al., 2020 | 6_6 | 0 | 78.6 | 0.14 | 0.14 | 3 | Mod | Santa Rosa Island | Island | 34.008 | -120 |

| | | | | | | | | | | | | | |
|---|---|---|---|---|---|---|---|---|---|---|---|---|---|
| 244 | 4 | Jazwa et al., 2020 | 6_6 | 1 | 78.6 | 0.19 | 0.19 | 3 | Mod | Santa Rosa Island | Island | 34.008 | -120 |
| 244 | 4 | Jazwa et al., 2020 | 6_6 | 2 | 78.6 | 0.12 | 0.12 | 3 | Mod | Santa Rosa Island | Island | 34.008 | -120 |
| 244 | 4 | Jazwa et al., 2020 | 6_6 | 3 | 78.6 | -0.37 | -0.37 | 3 | Mod | Santa Rosa Island | Island | 34.008 | -120 |
| 245 | 4 | Jazwa et al., 2020 | 6_7 | 0 | 85.1 | 0.18 | -0.26 | 3 | Mod | Santa Rosa Island | Island | 34.008 | -120 |
| 245 | 4 | Jazwa et al., 2020 | 6_7 | 1 | 85.1 | -0.15 | -0.64 | 3 | Mod | Santa Rosa Island | Island | 34.008 | -120 |
| 245 | 4 | Jazwa et al., 2020 | 6_7 | 2 | 85.1 | -0.24 | -0.55 | 3 | Mod | Santa Rosa Island | Island | 34.008 | -120 |
| 245 | 4 | Jazwa et al., 2020 | 6_7 | 3 | 85.1 | -0.58 | -0.64 | 3 | Mod | Santa Rosa Island | Island | 34.008 | -120 |
| 246 | 4 | Jazwa et al., 2020 | 7_1 | 0 | 82.4 | -0.77 | -0.61 | 3 | Mod | Santa Rosa Island | Island | 34.008 | -120 |
| 246 | 4 | Jazwa et al., 2020 | 7_1 | 1 | 82.4 | -0.44 | -0.26 | 3 | Mod | Santa Rosa Island | Island | 34.008 | -120 |
| 246 | 4 | Jazwa et al., 2020 | 7_1 | 2 | 82.4 | -0.76 | -0.42 | 3 | Mod | Santa Rosa Island | Island | 34.008 | -120 |
| 246 | 4 | Jazwa et al., 2020 | 7_1 | 3 | 82.4 | -0.83 | -0.29 | 3 | Mod | Santa Rosa Island | Island | 34.008 | -120 |
| 247 | 4 | Jazwa et al., 2020 | 7_2 | 0 | 69.3 | -0.69 | -0.52 | 3 | Mod | Santa Rosa Island | Island | 34.008 | -120 |
| 247 | 4 | Jazwa et al., 2020 | 7_2 | 1 | 69.3 | -0.55 | -0.04 | 3 | Mod | Santa Rosa Island | Island | 34.008 | -120 |
| 247 | 4 | Jazwa et al., 2020 | 7_2 | 2 | 69.3 | -0.70 | -0.44 | 3 | Mod | Santa Rosa Island | Island | 34.008 | -120 |
| 247 | 4 | Jazwa et al., 2020 | 7_2 | 3 | 69.3 | -0.83 | -0.27 | 3 | Mod | Santa Rosa Island | Island | 34.008 | -120 |
| 248 | 4 | Jazwa et al., 2020 | 7_3 | 0 | 81.4 | -0.50 | -0.59 | 3 | Mod | Santa Rosa Island | Island | 34.008 | -120 |
| 248 | 4 | Jazwa et al., 2020 | 7_3 | 1 | 81.4 | -0.53 | -0.37 | 3 | Mod | Santa Rosa Island | Island | 34.008 | -120 |
| 248 | 4 | Jazwa et al., 2020 | 7_3 | 2 | 81.4 | -0.75 | -0.28 | 3 | Mod | Santa Rosa Island | Island | 34.008 | -120 |
| 248 | 4 | Jazwa et al., 2020 | 7_3 | 3 | 81.4 | -0.71 | -0.22 | 3 | Mod | Santa Rosa Island | Island | 34.008 | -120 |

| | | | | | | | | | | | | | |
|---|---|---|---|---|---|---|---|---|---|---|---|---|---|
| 249 | 4 | Jazwa et al., 2020 | 7_4 | 0 | 66.5 | -0.56 | -0.53 | 3 | Mod | Santa Rosa Island | Island | 34.008 | -120 |
| 249 | 4 | Jazwa et al., 2020 | 7_4 | 1 | 66.5 | -0.45 | -0.35 | 3 | Mod | Santa Rosa Island | Island | 34.008 | -120 |
| 249 | 4 | Jazwa et al., 2020 | 7_4 | 2 | 66.5 | -0.74 | -0.72 | 3 | Mod | Santa Rosa Island | Island | 34.008 | -120 |
| 249 | 4 | Jazwa et al., 2020 | 7_4 | 3 | 66.5 | -0.68 | -0.48 | 3 | Mod | Santa Rosa Island | Island | 34.008 | -120 |
| 250 | 4 | Jazwa et al., 2020 | 7_5 | 0 | 113.7 | -0.03 | -0.31 | 3 | Mod | Santa Rosa Island | Island | 34.008 | -120 |
| 250 | 4 | Jazwa et al., 2020 | 7_5 | 1 | 113.7 | -0.11 | -0.46 | 3 | Mod | Santa Rosa Island | Island | 34.008 | -120 |
| 250 | 4 | Jazwa et al., 2020 | 7_5 | 2 | 113.7 | -0.23 | -0.37 | 3 | Mod | Santa Rosa Island | Island | 34.008 | -120 |
| 250 | 4 | Jazwa et al., 2020 | 7_5 | 3 | 113.7 | 0.17 | -0.01 | 3 | Mod | Santa Rosa Island | Island | 34.008 | -120 |
| 251 | 4 | Jazwa et al., 2020 | 7_6 | 0 | 103.6 | -0.05 | -0.69 | 3 | Mod | Santa Rosa Island | Island | 34.008 | -120 |
| 251 | 4 | Jazwa et al., 2020 | 7_6 | 1 | 103.6 | -0.14 | -0.61 | 3 | Mod | Santa Rosa Island | Island | 34.008 | -120 |
| 251 | 4 | Jazwa et al., 2020 | 7_6 | 2 | 103.6 | -0.29 | -0.55 | 3 | Mod | Santa Rosa Island | Island | 34.008 | -120 |
| 251 | 4 | Jazwa et al., 2020 | 7_6 | 3 | 103.6 | -0.23 | -0.32 | 3 | Mod | Santa Rosa Island | Island | 34.008 | -120 |
| 252 | 4 | Jazwa et al., 2020 | 7_7 | 0 | 75.5 | 0.15 | -0.49 | 3 | Mod | Santa Rosa Island | Island | 34.008 | -120 |
| 252 | 4 | Jazwa et al., 2020 | 7_7 | 1 | 75.5 | -0.11 | -0.27 | 3 | Mod | Santa Rosa Island | Island | 34.008 | -120 |
| 252 | 4 | Jazwa et al., 2020 | 7_7 | 2 | 75.5 | 0.00 | -0.54 | 3 | Mod | Santa Rosa Island | Island | 34.008 | -120 |
| 252 | 4 | Jazwa et al., 2020 | 7_7 | 3 | 75.5 | -0.26 | -0.65 | 3 | Mod | Santa Rosa Island | Island | 34.008 | -120 |
| 253 | 4 | Jazwa et al., 2020 | 7_8 | 0 | 103.5 | -0.30 | -0.56 | 3 | Mod | Santa Rosa Island | Island | 34.008 | -120 |
| 253 | 4 | Jazwa et al., 2020 | 7_8 | 1 | 103.5 | -0.22 | -0.52 | 3 | Mod | Santa Rosa Island | Island | 34.008 | -120 |
| 253 | 4 | Jazwa et al., 2020 | 7_8 | 2 | 103.5 | -0.42 | -0.53 | 3 | Mod | Santa Rosa Island | Island | 34.008 | -120 |

| | | | | | | | | | | | | | |
|---|---|---|---|---|---|---|---|---|---|---|---|---|---|
| 253 | 4 | Jazwa et al., 2020 | 7_8 | 3 | 103.5 | -0.70 | -0.53 | 3 | Mod | Santa Rosa Island | Island | 34.008 | -120 |
| 254 | 4 | Jazwa et al., 2020 | 8_1 | 0 | 102.5 | -0.55 | -0.72 | 3 | Mod | Santa Rosa Island | Island | 34.008 | -120 |
| 254 | 4 | Jazwa et al., 2020 | 8_1 | 1 | 102.5 | -0.14 | -0.04 | 3 | Mod | Santa Rosa Island | Island | 34.008 | -120 |
| 254 | 4 | Jazwa et al., 2020 | 8_1 | 2 | 102.5 | -0.41 | -0.35 | 3 | Mod | Santa Rosa Island | Island | 34.008 | -120 |
| 254 | 4 | Jazwa et al., 2020 | 8_1 | 3 | 102.5 | -0.38 | -0.33 | 3 | Mod | Santa Rosa Island | Island | 34.008 | -120 |
| 255 | 4 | Jazwa et al., 2020 | 8_2 | 0 | 52.9 | -0.62 | -0.90 | 3 | Mod | Santa Rosa Island | Island | 34.008 | -120 |
| 255 | 4 | Jazwa et al., 2020 | 8_2 | 1 | 52.9 | -0.56 | -0.60 | 3 | Mod | Santa Rosa Island | Island | 34.008 | -120 |
| 255 | 4 | Jazwa et al., 2020 | 8_2 | 2 | 52.9 | -1.05 | -0.74 | 3 | Mod | Santa Rosa Island | Island | 34.008 | -120 |
| 255 | 4 | Jazwa et al., 2020 | 8_2 | 3 | 52.9 | -1.00 | -0.49 | 3 | Mod | Santa Rosa Island | Island | 34.008 | -120 |
| 256 | 4 | Jazwa et al., 2020 | 8_3 | 0 | 100.5 | -0.22 | -0.64 | 3 | Mod | Santa Rosa Island | Island | 34.008 | -120 |
| 256 | 4 | Jazwa et al., 2020 | 8_3 | 1 | 100.5 | -0.29 | -0.60 | 3 | Mod | Santa Rosa Island | Island | 34.008 | -120 |
| 256 | 4 | Jazwa et al., 2020 | 8_3 | 2 | 100.5 | -0.31 | -0.36 | 3 | Mod | Santa Rosa Island | Island | 34.008 | -120 |
| 256 | 4 | Jazwa et al., 2020 | 8_3 | 3 | 100.5 | -1.04 | -0.52 | 3 | Mod | Santa Rosa Island | Island | 34.008 | -120 |
| 257 | 4 | Jazwa et al., 2020 | 8_4 | 0 | 115.4 | -0.46 | -0.67 | 3 | Mod | Santa Rosa Island | Island | 34.008 | -120 |
| 257 | 4 | Jazwa et al., 2020 | 8_4 | 1 | 115.4 | -0.21 | -0.26 | 3 | Mod | Santa Rosa Island | Island | 34.008 | -120 |
| 257 | 4 | Jazwa et al., 2020 | 8_4 | 2 | 115.4 | -0.48 | -0.33 | 3 | Mod | Santa Rosa Island | Island | 34.008 | -120 |
| 257 | 4 | Jazwa et al., 2020 | 8_4 | 3 | 115.4 | -0.91 | -0.43 | 3 | Mod | Santa Rosa Island | Island | 34.008 | -120 |
| 258 | 4 | Jazwa et al., 2020 | 8_5 | 0 | 105.3 | -0.34 | -0.23 | 3 | Mod | Santa Rosa Island | Island | 34.008 | -120 |
| 258 | 4 | Jazwa et al., 2020 | 8_5 | 1 | 105.3 | -0.42 | -0.24 | 3 | Mod | Santa Rosa Island | Island | 34.008 | -120 |

| | | | | | | | | | | | | | |
|---|---|---|---|---|---|---|---|---|---|---|---|---|---|
| 258 | 4 | Jazwa et al., 2020 | 8_5 | 2 | 105.3 | -0.43 | -0.07 | 3 | Mod | Santa Rosa Island | Island | 34.008 | -120 |
| 258 | 4 | Jazwa et al., 2020 | 8_5 | 3 | 105.3 | -0.40 | 0.01 | 3 | Mod | Santa Rosa Island | Island | 34.008 | -120 |
| 259 | 4 | Jazwa et al., 2020 | 8_6 | 0 | 51.3 | -0.41 | -0.72 | 3 | Mod | Santa Rosa Island | Island | 34.008 | -120 |
| 259 | 4 | Jazwa et al., 2020 | 8_6 | 1 | 51.3 | -0.34 | -0.58 | 3 | Mod | Santa Rosa Island | Island | 34.008 | -120 |
| 259 | 4 | Jazwa et al., 2020 | 8_6 | 2 | 51.3 | -0.64 | -0.75 | 3 | Mod | Santa Rosa Island | Island | 34.008 | -120 |
| 259 | 4 | Jazwa et al., 2020 | 8_6 | 3 | 51.3 | -0.36 | -0.47 | 3 | Mod | Santa Rosa Island | Island | 34.008 | -120 |
| 260 | 4 | Jazwa et al., 2020 | 8_7 | 0 | 55.5 | -0.63 | -0.46 | 3 | Mod | Santa Rosa Island | Island | 34.008 | -120 |
| 260 | 4 | Jazwa et al., 2020 | 8_7 | 1 | 55.5 | -0.59 | -0.49 | 3 | Mod | Santa Rosa Island | Island | 34.008 | -120 |
| 260 | 4 | Jazwa et al., 2020 | 8_7 | 2 | 55.5 | -0.60 | -0.54 | 3 | Mod | Santa Rosa Island | Island | 34.008 | -120 |
| 260 | 4 | Jazwa et al., 2020 | 8_7 | 3 | 55.5 | -1.26 | -0.76 | 3 | Mod | Santa Rosa Island | Island | 34.008 | -120 |
| 261 | 4 | Jazwa et al., 2020 | 9_1 | 0 | 59.3 | -0.22 | -0.37 | 3 | Mod | Santa Rosa Island | Island | 34.008 | -120 |
| 261 | 4 | Jazwa et al., 2020 | 9_1 | 1 | 59.3 | -0.32 | -0.31 | 3 | Mod | Santa Rosa Island | Island | 34.008 | -120 |
| 261 | 4 | Jazwa et al., 2020 | 9_1 | 2 | 59.3 | -0.63 | -0.74 | 3 | Mod | Santa Rosa Island | Island | 34.008 | -120 |
| 261 | 4 | Jazwa et al., 2020 | 9_1 | 3 | 59.3 | -0.52 | -0.42 | 3 | Mod | Santa Rosa Island | Island | 34.008 | -120 |
| 262 | 4 | Jazwa et al., 2020 | 9_2 | 0 | 75.3 | -0.25 | -0.19 | 3 | Mod | Santa Rosa Island | Island | 34.008 | -120 |
| 262 | 4 | Jazwa et al., 2020 | 9_2 | 1 | 75.3 | -0.25 | -0.68 | 3 | Mod | Santa Rosa Island | Island | 34.008 | -120 |
| 262 | 4 | Jazwa et al., 2020 | 9_2 | 2 | 75.3 | -0.52 | -0.60 | 3 | Mod | Santa Rosa Island | Island | 34.008 | -120 |
| 262 | 4 | Jazwa et al., 2020 | 9_2 | 3 | 75.3 | -0.63 | -0.85 | 3 | Mod | Santa Rosa Island | Island | 34.008 | -120 |
| 263 | 4 | Jazwa et al., 2020 | 9_3 | 0 | 69.2 | -0.64 | -0.72 | 3 | Mod | Santa Rosa Island | Island | 34.008 | -120 |

| | | | | | | | | | | | | | |
|---|---|---|---|---|---|---|---|---|---|---|---|---|---|
| 263 | 4 | Jazwa et al., 2020 | 9_3 | 1 | 69.2 | -0.76 | -0.71 | 3 | Mod | Santa Rosa Island | Island | 34.008 | -120 |
| 263 | 4 | Jazwa et al., 2020 | 9_3 | 2 | 69.2 | -0.72 | -0.48 | 3 | Mod | Santa Rosa Island | Island | 34.008 | -120 |
| 263 | 4 | Jazwa et al., 2020 | 9_3 | 3 | 69.2 | -1.56 | -0.48 | 3 | Mod | Santa Rosa Island | Island | 34.008 | -120 |
| 264 | 4 | Jazwa et al., 2020 | 9_4 | 0 | 75.5 | -0.32 | -0.59 | 3 | Mod | Santa Rosa Island | Island | 34.008 | -120 |
| 264 | 4 | Jazwa et al., 2020 | 9_4 | 1 | 75.5 | -0.66 | -0.97 | 3 | Mod | Santa Rosa Island | Island | 34.008 | -120 |
| 264 | 4 | Jazwa et al., 2020 | 9_4 | 2 | 75.5 | -0.48 | -1.02 | 3 | Mod | Santa Rosa Island | Island | 34.008 | -120 |
| 264 | 4 | Jazwa et al., 2020 | 9_4 | 3 | 75.5 | -0.69 | -0.73 | 3 | Mod | Santa Rosa Island | Island | 34.008 | -120 |
| 265 | 4 | Jazwa et al., 2020 | 9_5 | 0 | 68.5 | -0.08 | -0.74 | 3 | Mod | Santa Rosa Island | Island | 34.008 | -120 |
| 265 | 4 | Jazwa et al., 2020 | 9_5 | 1 | 68.5 | -0.15 | -0.60 | 3 | Mod | Santa Rosa Island | Island | 34.008 | -120 |
| 265 | 4 | Jazwa et al., 2020 | 9_5 | 2 | 68.5 | -0.10 | -0.88 | 3 | Mod | Santa Rosa Island | Island | 34.008 | -120 |
| 265 | 4 | Jazwa et al., 2020 | 9_5 | 3 | 68.5 | -0.52 | -0.19 | 3 | Mod | Santa Rosa Island | Island | 34.008 | -120 |
| 266 | 4 | Jazwa et al., 2020 | 9_6 | 0 | 80.2 | -0.45 | -0.96 | 3 | Mod | Santa Rosa Island | Island | 34.008 | -120 |
| 266 | 4 | Jazwa et al., 2020 | 9_6 | 1 | 80.2 | -0.46 | -0.79 | 3 | Mod | Santa Rosa Island | Island | 34.008 | -120 |
| 266 | 4 | Jazwa et al., 2020 | 9_6 | 2 | 80.2 | -0.63 | -0.88 | 3 | Mod | Santa Rosa Island | Island | 34.008 | -120 |
| 266 | 4 | Jazwa et al., 2020 | 9_6 | 3 | 80.2 | -0.81 | -0.81 | 3 | Mod | Santa Rosa Island | Island | 34.008 | -120 |
| 267 | 4 | Jazwa et al., 2020 | 9_7 | 0 | 67.7 | -0.57 | -0.75 | 3 | Mod | Santa Rosa Island | Island | 34.008 | -120 |
| 267 | 4 | Jazwa et al., 2020 | 9_7 | 1 | 67.7 | -0.57 | -0.57 | 3 | Mod | Santa Rosa Island | Island | 34.008 | -120 |
| 267 | 4 | Jazwa et al., 2020 | 9_7 | 2 | 67.7 | -0.74 | -0.57 | 3 | Mod | Santa Rosa Island | Island | 34.008 | -120 |
| 267 | 4 | Jazwa et al., 2020 | 9_7 | 3 | 67.7 | -0.75 | -0.81 | 3 | Mod | Santa Rosa Island | Island | 34.008 | -120 |

| | | | | | | | | | | | | | |
|---|---|---|---|---|---|---|---|---|---|---|---|---|---|
| 268 | 4 | Jazwa et al., 2020 | 9_8 | 0 | 83.7 | -0.09 | -0.58 | 3 | Mod | Santa Rosa Island | Island | 34.008 | -120 |
| 268 | 4 | Jazwa et al., 2020 | 9_8 | 1 | 83.7 | -0.32 | -0.58 | 3 | Mod | Santa Rosa Island | Island | 34.008 | -120 |
| 268 | 4 | Jazwa et al., 2020 | 9_8 | 2 | 83.7 | -0.48 | -0.79 | 3 | Mod | Santa Rosa Island | Island | 34.008 | -120 |
| 268 | 4 | Jazwa et al., 2020 | 9_8 | 3 | 83.7 | -0.50 | -0.73 | 3 | Mod | Santa Rosa Island | Island | 34.008 | -120 |
| 269 | 5 | Jew and Rick 2014 | ANI-2-10a | 0.00 | | 1.40 | -1.00 | 3010 | Mid | Anacapa Island | Island | 34.013 | -119.4 |
| 269 | 5 | Jew and Rick 2014 | ANI-2-10b | 3.00 | | 0.85 | -1.05 | 3010 | Mid | Anacapa Island | Island | 34.013 | -119.4 |
| 269 | 5 | Jew and Rick 2014 | ANI-2-10c | 6.00 | | 1.20 | -1.00 | 3010 | Mid | Anacapa Island | Island | 34.013 | -119.4 |
| 269 | 5 | Jew and Rick 2014 | ANI-2-10d | 9.00 | | 0.94 | -0.30 | 3010 | Mid | Anacapa Island | Island | 34.013 | -119.4 |
| 269 | 5 | Jew and Rick 2014 | ANI-2-10e | 12.00 | | 0.55 | -0.10 | 3010 | Mid | Anacapa Island | Island | 34.013 | -119.4 |
| 270 | 5 | Jew and Rick 2014 | ANI-2-11a | 0.00 | | 1.30 | 0.40 | 3010 | Mid | Anacapa Island | Island | 34.013 | -119.4 |
| 270 | 5 | Jew and Rick 2014 | ANI-2-11b | 3.00 | | 0.20 | -0.55 | 3010 | Mid | Anacapa Island | Island | 34.013 | -119.4 |
| 270 | 5 | Jew and Rick 2014 | ANI-2-11c | 6.00 | | 0.75 | -0.80 | 3010 | Mid | Anacapa Island | Island | 34.013 | -119.4 |
| 270 | 5 | Jew and Rick 2014 | ANI-2-11d | 9.00 | | 0.50 | 0.20 | 3010 | Mid | Anacapa Island | Island | 34.013 | -119.4 |
| 270 | 5 | Jew and Rick 2014 | ANI-2-11e | 12.00 | | 0.65 | 0.55 | 3010 | Mid | Anacapa Island | Island | 34.013 | -119.4 |
| 271 | 5 | Jew and Rick 2014 | ANI-2-12a | 0.00 | | 1.25 | 0.30 | 3010 | Mid | Anacapa Island | Island | 34.013 | -119.4 |
| 271 | 5 | Jew and Rick 2014 | ANI-2-12b | 3.00 | | 1.05 | 0.60 | 3010 | Mid | Anacapa Island | Island | 34.013 | -119.4 |
| 271 | 5 | Jew and Rick 2014 | ANI-2-12c | 6.00 | | 0.80 | -0.05 | 3010 | Mid | Anacapa Island | Island | 34.013 | -119.4 |
| 271 | 5 | Jew and Rick 2014 | ANI-2-12d | 9.00 | | 0.80 | -0.85 | 3010 | Mid | Anacapa Island | Island | 34.013 | -119.4 |
| 271 | 5 | Jew and Rick 2014 | ANI-2-12e | 12.00 | | 0.60 | -0.05 | 3010 | Mid | Anacapa Island | Island | 34.013 | -119.4 |
| 272 | 5 | Jew and Rick 2014 | ANI-2-13a | 0.00 | | -0.50 | -2.10 | 3010 | Mid | Anacapa Island | Island | 34.013 | -119.4 |
| 272 | 5 | Jew and Rick 2014 | ANI-2-13b | 3.00 | | 0.90 | -0.55 | 3010 | Mid | Anacapa Island | Island | 34.013 | -119.4 |
| 272 | 5 | Jew and Rick 2014 | ANI-2-13c | 6.00 | | 0.55 | -0.85 | 3010 | Mid | Anacapa Island | Island | 34.013 | -119.4 |
| 272 | 5 | Jew and Rick 2014 | ANI-2-13d | 9.00 | | 0.15 | 0.20 | 3010 | Mid | Anacapa Island | Island | 34.013 | -119.4 |
| 272 | 5 | Jew and Rick 2014 | ANI-2-13e | 12.00 | | -0.20 | 0.20 | 3010 | Mid | Anacapa Island | Island | 34.013 | -119.4 |
| 273 | 5 | Jew and Rick 2014 | ANI-2-14a | 0.00 | | 0.25 | 0.20 | 3010 | Mid | Anacapa Island | Island | 34.013 | -119.4 |
| 273 | 5 | Jew and Rick 2014 | ANI-2-14b | 3.00 | | 0.35 | -0.90 | 3010 | Mid | Anacapa Island | Island | 34.013 | -119.4 |

| | | | | | | | | | | | | | |
|---|---|---|---|---|---|---|---|---|---|---|---|---|---|
| 273 | 5 | Jew and Rick 2014 | ANI-2-14c | 6.00 | | 0.75 | 0.20 | 3010 | Mid | Anacapa Island | Island | 34.013 | -119.4 |
| 273 | 5 | Jew and Rick 2014 | ANI-2-14d | 9.00 | | 0.20 | 0.40 | 3010 | Mid | Anacapa Island | Island | 34.013 | -119.4 |
| 273 | 5 | Jew and Rick 2014 | ANI-2-14e | 12.00 | | -0.45 | 0.85 | 3010 | Mid | Anacapa Island | Island | 34.013 | -119.4 |
| 274 | 5 | Jew and Rick 2014 | ANI-2-15a | 0.00 | | 1.05 | 0.90 | 3010 | Mid | Anacapa Island | Island | 34.013 | -119.4 |
| 274 | 5 | Jew and Rick 2014 | ANI-2-15b | 3.00 | | 0.95 | 0.45 | 3010 | Mid | Anacapa Island | Island | 34.013 | -119.4 |
| 274 | 5 | Jew and Rick 2014 | ANI-2-15c | 6.00 | | 0.85 | 0.00 | 3010 | Mid | Anacapa Island | Island | 34.013 | -119.4 |
| 274 | 5 | Jew and Rick 2014 | ANI-2-15d | 9.00 | | 0.55 | -0.10 | 3010 | Mid | Anacapa Island | Island | 34.013 | -119.4 |
| 274 | 5 | Jew and Rick 2014 | ANI-2-15e | 12.00 | | -0.15 | 0.45 | 3010 | Mid | Anacapa Island | Island | 34.013 | -119.4 |
| 275 | 5 | Jew and Rick 2014 | ANI-2-16a | 0.00 | | 0.30 | 0.55 | 3010 | Mid | Anacapa Island | Island | 34.013 | -119.4 |
| 275 | 5 | Jew and Rick 2014 | ANI-2-16b | 3.00 | | 0.65 | 0.45 | 3010 | Mid | Anacapa Island | Island | 34.013 | -119.4 |
| 275 | 5 | Jew and Rick 2014 | ANI-2-16c | 6.00 | | 0.85 | -0.20 | 3010 | Mid | Anacapa Island | Island | 34.013 | -119.4 |
| 275 | 5 | Jew and Rick 2014 | ANI-2-16d | 9.00 | | 0.30 | -0.35 | 3010 | Mid | Anacapa Island | Island | 34.013 | -119.4 |
| 275 | 5 | Jew and Rick 2014 | ANI-2-16e | 12.00 | | 0.35 | -0.50 | 3010 | Mid | Anacapa Island | Island | 34.013 | -119.4 |
| 276 | 5 | Jew and Rick 2014 | ANI-2-17a | 0.00 | | 0.95 | 0.70 | 3010 | Mid | Anacapa Island | Island | 34.013 | -119.4 |
| 276 | 5 | Jew and Rick 2014 | ANI-2-17b | 3.00 | | 0.80 | 0.65 | 3010 | Mid | Anacapa Island | Island | 34.013 | -119.4 |
| 276 | 5 | Jew and Rick 2014 | ANI-2-17c | 6.00 | | 0.75 | -0.40 | 3010 | Mid | Anacapa Island | Island | 34.013 | -119.4 |
| 276 | 5 | Jew and Rick 2014 | ANI-2-17d | 9.00 | | 0.50 | -0.15 | 3010 | Mid | Anacapa Island | Island | 34.013 | -119.4 |
| 276 | 5 | Jew and Rick 2014 | ANI-2-17e | 12.00 | | 0.30 | -0.55 | 3010 | Mid | Anacapa Island | Island | 34.013 | -119.4 |
| 277 | 5 | Jew and Rick 2014 | ANI-2-18a | 0.00 | | 1.90 | -1.00 | 3010 | Mid | Anacapa Island | Island | 34.013 | -119.4 |
| 277 | 5 | Jew and Rick 2014 | ANI-2-18b | 3.00 | | 1.50 | 0.00 | 3010 | Mid | Anacapa Island | Island | 34.013 | -119.4 |
| 277 | 5 | Jew and Rick 2014 | ANI-2-18c | 6.00 | | 1.40 | -0.50 | 3010 | Mid | Anacapa Island | Island | 34.013 | -119.4 |
| 277 | 5 | Jew and Rick 2014 | ANI-2-18d | 9.00 | | 1.30 | 0.00 | 3010 | Mid | Anacapa Island | Island | 34.013 | -119.4 |
| 277 | 5 | Jew and Rick 2014 | ANI-2-18e | 12.00 | | 1.10 | 0.70 | 3010 | Mid | Anacapa Island | Island | 34.013 | -119.4 |
| 278 | 5 | Jew and Rick 2014 | ANI-2-19a | 0.00 | | 1.40 | -0.20 | 3010 | Mid | Anacapa Island | Island | 34.013 | -119.4 |
| 278 | 5 | Jew and Rick 2014 | ANI-2-19b | 3.00 | | 1.30 | 0.10 | 3010 | Mid | Anacapa Island | Island | 34.013 | -119.4 |
| 278 | 5 | Jew and Rick 2014 | ANI-2-19c | 6.00 | | 1.10 | -0.30 | 3010 | Mid | Anacapa Island | Island | 34.013 | -119.4 |
| 278 | 5 | Jew and Rick 2014 | ANI-2-19d | 9.00 | | 1.30 | -0.60 | 3010 | Mid | Anacapa Island | Island | 34.013 | -119.4 |
| 278 | 5 | Jew and Rick 2014 | ANI-2-19e | 12.00 | | 0.90 | -0.60 | 3010 | Mid | Anacapa Island | Island | 34.013 | -119.4 |

| | | | | | | | | | | | | | |
|---|---|---|---|---|---|---|---|---|---|---|---|---|---|
| 279 | 9 | Jew and Rick 2014 | ANI-2-1a | 0 | | 1 | 0.2 | 3010 | Mid | San Miguel Island | Island | 34.013 | -119.4 |
| 279 | 9 | Jew and Rick 2014 | ANI-2-1b | 3 | | 1.1 | 0.05 | 3010 | Mid | San Miguel Island | Island | 34.013 | -119.4 |
| 279 | 9 | Jew and Rick 2014 | ANI-2-1c | 6 | | 1.35 | -0.5 | 3010 | Mid | San Miguel Island | Island | 34.013 | -119.4 |
| 279 | 9 | Jew and Rick 2014 | ANI-2-1d | 9 | | 0.8 | -0.25 | 3010 | Mid | San Miguel Island | Island | 34.013 | -119.4 |
| 279 | 9 | Jew and Rick 2014 | ANI-2-1e | 12 | | 0.5 | 0 | 3010 | Mid | San Miguel Island | Island | 34.013 | -119.4 |
| 279 | 9 | Jew and Rick 2014 | ANI-2-1f | 15 | | -0.15 | -0.5 | 3010 | Mid | San Miguel Island | Island | 34.013 | -119.4 |
| 279 | 9 | Jew and Rick 2014 | ANI-2-1g | 18 | | -0.1 | 0 | 3010 | Mid | San Miguel Island | Island | 34.013 | -119.4 |
| 279 | 9 | Jew and Rick 2014 | ANI-2-1h | 22 | | 0.65 | 0.3 | 3010 | Mid | San Miguel Island | Island | 34.013 | -119.4 |
| 279 | 9 | Jew and Rick 2014 | ANI-2-1i | 24 | | 0.7 | 0.85 | 3010 | Mid | San Miguel Island | Island | 34.013 | -119.4 |
| 280 | 5 | Jew and Rick 2014 | ANI-2-20a | 0.00 | | 1.50 | 0.50 | 3010 | Mid | Anacapa Island | Island | 34.013 | -119.4 |
| 280 | 5 | Jew and Rick 2014 | ANI-2-20b | 3.00 | | 0.60 | 0.10 | 3010 | Mid | Anacapa Island | Island | 34.013 | -119.4 |
| 280 | 5 | Jew and Rick 2014 | ANI-2-20c | 6.00 | | 0.70 | 0.60 | 3010 | Mid | Anacapa Island | Island | 34.013 | -119.4 |
| 280 | 5 | Jew and Rick 2014 | ANI-2-20d | 9.00 | | 0.50 | 0.40 | 3010 | Mid | Anacapa Island | Island | 34.013 | -119.4 |
| 280 | 5 | Jew and Rick 2014 | ANI-2-20e | 12.00 | | 0.70 | 0.20 | 3010 | Mid | Anacapa Island | Island | 34.013 | -119.4 |
| 281 | 5 | Jew and Rick 2014 | ANI-2-2a | 0.00 | | -0.50 | 0.60 | 3010 | Mid | Anacapa Island | Island | 34.013 | -119.4 |
| 281 | 5 | Jew and Rick 2014 | ANI-2-2b | 3.00 | | 0.00 | 0.30 | 3010 | Mid | Anacapa Island | Island | 34.013 | -119.4 |
| 281 | 5 | Jew and Rick 2014 | ANI-2-2c | 6.00 | | 0.50 | 0.05 | 3010 | Mid | Anacapa Island | Island | 34.013 | -119.4 |
| 281 | 5 | Jew and Rick 2014 | ANI-2-2d | 9.00 | | 0.15 | 0.45 | 3010 | Mid | Anacapa Island | Island | 34.013 | -119.4 |
| 281 | 5 | Jew and Rick 2014 | ANI-2-2e | 12.00 | | 0.20 | -1.00 | 3010 | Mid | Anacapa Island | Island | 34.013 | -119.4 |
| 282 | 5 | Jew and Rick 2014 | ANI-2-3a | 0.00 | | 0.90 | 0.25 | 3010 | Mid | Anacapa Island | Island | 34.013 | -119.4 |
| 282 | 5 | Jew and Rick 2014 | ANI-2-3b | 3.00 | | 0.60 | -0.75 | 3010 | Mid | Anacapa Island | Island | 34.013 | -119.4 |
| 282 | 5 | Jew and Rick 2014 | ANI-2-3c | 6.00 | | 0.75 | -1.05 | 3010 | Mid | Anacapa Island | Island | 34.013 | -119.4 |
| 282 | 5 | Jew and Rick 2014 | ANI-2-3d | 9.00 | | 0.70 | 0.05 | 3010 | Mid | Anacapa Island | Island | 34.013 | -119.4 |
| 282 | 5 | Jew and Rick 2014 | ANI-2-3e | 12.00 | | 0.15 | 0.05 | 3010 | Mid | Anacapa Island | Island | 34.013 | -119.4 |

| | | | | | | | | | | | | | |
|---|---|---|---|---|---|---|---|---|---|---|---|---|---|
| 283 | 5 | Jew and Rick 2014 | ANI-2-4a | 0.00 | | 1.50 | 0.25 | 3010 | Mid | Anacapa Island | Island | 34.013 | -119.4 |
| 283 | 5 | Jew and Rick 2014 | ANI-2-4b | 3.00 | | 1.25 | -0.10 | 3010 | Mid | Anacapa Island | Island | 34.013 | -119.4 |
| 283 | 5 | Jew and Rick 2014 | ANI-2-4c | 6.00 | | 1.00 | -1.15 | 3010 | Mid | Anacapa Island | Island | 34.013 | -119.4 |
| 283 | 5 | Jew and Rick 2014 | ANI-2-4d | 9.00 | | 0.65 | -0.80 | 3010 | Mid | Anacapa Island | Island | 34.013 | -119.4 |
| 283 | 5 | Jew and Rick 2014 | ANI-2-4e | 12.00 | | 0.70 | -0.55 | 3010 | Mid | Anacapa Island | Island | 34.013 | -119.4 |
| 284 | 5 | Jew and Rick 2014 | ANI-2-5a | 0.00 | | 1.15 | -0.25 | 3010 | Mid | Anacapa Island | Island | 34.013 | -119.4 |
| 284 | 5 | Jew and Rick 2014 | ANI-2-5b | 3.00 | | 0.90 | -1.25 | 3010 | Mid | Anacapa Island | Island | 34.013 | -119.4 |
| 284 | 5 | Jew and Rick 2014 | ANI-2-5c | 6.00 | | 0.50 | -0.60 | 3010 | Mid | Anacapa Island | Island | 34.013 | -119.4 |
| 284 | 5 | Jew and Rick 2014 | ANI-2-5d | 9.00 | | 0.30 | 0.10 | 3010 | Mid | Anacapa Island | Island | 34.013 | -119.4 |
| 284 | 5 | Jew and Rick 2014 | ANI-2-5e | 12.00 | | 1.35 | -0.20 | 3010 | Mid | Anacapa Island | Island | 34.013 | -119.4 |
| 285 | 5 | Jew and Rick 2014 | ANI-2-6a | 0.00 | | 0.60 | 0.55 | 3010 | Mid | Anacapa Island | Island | 34.013 | -119.4 |
| 285 | 5 | Jew and Rick 2014 | ANI-2-6b | 3.00 | | 0.80 | 0.45 | 3010 | Mid | Anacapa Island | Island | 34.013 | -119.4 |
| 285 | 5 | Jew and Rick 2014 | ANI-2-6c | 6.00 | | 1.25 | -0.60 | 3010 | Mid | Anacapa Island | Island | 34.013 | -119.4 |
| 285 | 5 | Jew and Rick 2014 | ANI-2-6d | 9.00 | | 1.65 | -0.75 | 3010 | Mid | Anacapa Island | Island | 34.013 | -119.4 |
| 285 | 5 | Jew and Rick 2014 | ANI-2-6e | 12.00 | | 0.75 | 0.45 | 3010 | Mid | Anacapa Island | Island | 34.013 | -119.4 |
| 286 | 5 | Jew and Rick 2014 | ANI-2-7a | 0.00 | | 1.15 | -0.40 | 3010 | Mid | Anacapa Island | Island | 34.013 | -119.4 |
| 286 | 5 | Jew and Rick 2014 | ANI-2-7b | 3.00 | | 0.65 | -0.20 | 3010 | Mid | Anacapa Island | Island | 34.013 | -119.4 |
| 286 | 5 | Jew and Rick 2014 | ANI-2-7c | 6.00 | | 1.00 | 0.55 | 3010 | Mid | Anacapa Island | Island | 34.013 | -119.4 |
| 286 | 5 | Jew and Rick 2014 | ANI-2-7d | 9.00 | | 1.20 | 0.50 | 3010 | Mid | Anacapa Island | Island | 34.013 | -119.4 |
| 286 | 5 | Jew and Rick 2014 | ANI-2-7e | 12.00 | | 1.15 | -0.45 | 3010 | Mid | Anacapa Island | Island | 34.013 | -119.4 |
| 287 | 5 | Jew and Rick 2014 | ANI-2-8a | 0.00 | | 0.25 | 0.70 | 3010 | Mid | Anacapa Island | Island | 34.013 | -119.4 |
| 287 | 5 | Jew and Rick 2014 | ANI-2-8b | 3.00 | | 0.65 | 0.50 | 3010 | Mid | Anacapa Island | Island | 34.013 | -119.4 |
| 287 | 5 | Jew and Rick 2014 | ANI-2-8c | 6.00 | | 0.70 | -0.40 | 3010 | Mid | Anacapa Island | Island | 34.013 | -119.4 |
| 287 | 5 | Jew and Rick 2014 | ANI-2-8d | 9.00 | | 0.00 | -1.15 | 3010 | Mid | Anacapa Island | Island | 34.013 | -119.4 |
| 287 | 5 | Jew and Rick 2014 | ANI-2-8e | 12.00 | | -0.15 | 0.15 | 3010 | Mid | Anacapa Island | Island | 34.013 | -119.4 |
| 288 | 5 | Jew and Rick 2014 | ANI-2-9a | 0.00 | | 0.50 | -0.50 | 3010 | Mid | Anacapa Island | Island | 34.013 | -119.4 |
| 288 | 5 | Jew and Rick 2014 | ANI-2-9b | 3.00 | | 0.25 | 0.35 | 3010 | Mid | Anacapa Island | Island | 34.013 | -119.4 |
| 288 | 5 | Jew and Rick 2014 | ANI-2-9c | 6.00 | | 0.50 | 0.95 | 3010 | Mid | Anacapa Island | Island | 34.013 | -119.4 |

| | | | | | | | | | | | | | |
|---|---|---|---|---|---|---|---|---|---|---|---|---|---|
| 288 | 5 | Jew and Rick 2014 | ANI-2-9d | 9.00 | | 0.85 | -0.25 | 3010 | Mid | Anacapa Island | Island | 34.013 | -119.4 |
| 288 | 5 | Jew and Rick 2014 | ANI-2-9e | 12.00 | | 0.30 | -0.10 | 3010 | Mid | Anacapa Island | Island | 34.013 | -119.4 |
| 289 | 6 | Jew et al., 2013a | 10Mc2a | 3 | | 0.2 | 1.2 | 8800 | Mid | San Miguel Island | Island | 34.032 | -120.4 |
| 289 | 6 | Jew et al., 2013a | 10Mc2b | 6 | | 0.5 | 1.1 | 8800 | Mid | San Miguel Island | Island | 34.032 | -120.4 |
| 289 | 6 | Jew et al., 2013a | 10Mc2c | 9 | | 0.9 | 0.6 | 8800 | Mid | San Miguel Island | Island | 34.032 | -120.4 |
| 289 | 6 | Jew et al., 2013a | 10Mc2d | 12 | | 0.8 | 0.3 | 8800 | Mid | San Miguel Island | Island | 34.032 | -120.4 |
| 289 | 6 | Jew et al., 2013a | 10Mc2e | 15 | | 0.9 | 0.6 | 8800 | Mid | San Miguel Island | Island | 34.032 | -120.4 |
| 289 | 6 | Jew et al., 2013a | 10Mc2f | 18 | | 0.1 | 0.5 | 8800 | Mid | San Miguel Island | Island | 34.032 | -120.4 |
| 290 | 6 | Jew et al., 2013a | 12Mc2a | 3 | | -0.4 | 0.9 | 8800 | Mid | San Miguel Island | Island | 34.032 | -120.4 |
| 290 | 6 | Jew et al., 2013a | 12Mc2b | 6 | | -0.7 | 1.1 | 8800 | Mid | San Miguel Island | Island | 34.032 | -120.4 |
| 290 | 6 | Jew et al., 2013a | 12Mc2c | 9 | | -0.4 | 1.3 | 8800 | Mid | San Miguel Island | Island | 34.032 | -120.4 |
| 290 | 6 | Jew et al., 2013a | 12Mc2d | 12 | | -0.1 | 1.6 | 8800 | Mid | San Miguel Island | Island | 34.032 | -120.4 |
| 290 | 6 | Jew et al., 2013a | 12Mc2e | 15 | | 0 | 1.3 | 8800 | Mid | San Miguel Island | Island | 34.032 | -120.4 |
| 290 | 6 | Jew et al., 2013a | 12Mc2f | 18 | | 0.2 | 1.3 | 8800 | Mid | San Miguel Island | Island | 34.032 | -120.4 |
| 291 | 6 | Jew et al., 2013a | 14Mc2a | 3 | | 0.4 | 0.7 | 8800 | Mid | San Miguel Island | Island | 34.032 | -120.4 |
| 291 | 6 | Jew et al., 2013a | 14Mc2b | 6 | | 0.8 | 1.3 | 8800 | Mid | San Miguel Island | Island | 34.032 | -120.4 |
| 291 | 6 | Jew et al., 2013a | 14Mc2c | 9 | | 0.8 | 0.8 | 8800 | Mid | San Miguel Island | Island | 34.032 | -120.4 |
| 291 | 6 | Jew et al., 2013a | 14Mc2d | 12 | | 0.4 | 0.6 | 8800 | Mid | San Miguel Island | Island | 34.032 | -120.4 |
| 291 | 6 | Jew et al., 2013a | 14Mc2e | 15 | | 0.5 | 1.8 | 8800 | Mid | San Miguel Island | Island | 34.032 | -120.4 |
| 291 | 6 | Jew et al., 2013a | 14Mc2f | 18 | | 0.3 | 1.1 | 8800 | Mid | San Miguel Island | Island | 34.032 | -120.4 |

| | | | | | | | | | | | | | |
|---|---|---|---|---|---|---|---|---|---|---|---|---|---|
| 292 | 6 | Jew et al., 2013a | 16Mc2a | 3 | | 0.8 | 0.8 | 8800 | Mid | San Miguel Island | Island | 34.032 | -120.4 |
| 292 | 6 | Jew et al., 2013a | 16Mc2b | 6 | | 1.1 | 0.4 | 8800 | Mid | San Miguel Island | Island | 34.032 | -120.4 |
| 292 | 6 | Jew et al., 2013a | 16Mc2c | 9 | | 1 | 0.6 | 8800 | Mid | San Miguel Island | Island | 34.032 | -120.4 |
| 292 | 6 | Jew et al., 2013a | 16Mc2d | 12 | | 0.5 | 1.2 | 8800 | Mid | San Miguel Island | Island | 34.032 | -120.4 |
| 292 | 6 | Jew et al., 2013a | 16Mc2e | 15 | | 0.7 | 0.9 | 8800 | Mid | San Miguel Island | Island | 34.032 | -120.4 |
| 292 | 6 | Jew et al., 2013a | 16Mc2f | 18 | | 1 | 0.6 | 8800 | Mid | San Miguel Island | Island | 34.032 | -120.4 |
| 293 | 6 | Jew et al., 2013a | 17Mc2a | 3 | | -0.1 | 0.8 | 8800 | Mid | San Miguel Island | Island | 34.032 | -120.4 |
| 293 | 6 | Jew et al., 2013a | 17Mc2b | 6 | | 0 | 1.4 | 8800 | Mid | San Miguel Island | Island | 34.032 | -120.4 |
| 293 | 6 | Jew et al., 2013a | 17Mc2c | 9 | | 0 | 1.3 | 8800 | Mid | San Miguel Island | Island | 34.032 | -120.4 |
| 293 | 6 | Jew et al., 2013a | 17Mc2d | 12 | | 0.5 | 1.2 | 8800 | Mid | San Miguel Island | Island | 34.032 | -120.4 |
| 293 | 6 | Jew et al., 2013a | 17Mc2e | 15 | | 1.2 | 1.8 | 8800 | Mid | San Miguel Island | Island | 34.032 | -120.4 |
| 293 | 6 | Jew et al., 2013a | 17Mc2f | 18 | | 0.6 | 0.3 | 8800 | Mid | San Miguel Island | Island | 34.032 | -120.4 |
| 294 | 6 | Jew et al., 2013a | 22Mc2a | 3 | | -0.8 | 0.1 | 8800 | Mid | San Miguel Island | Island | 34.032 | -120.4 |
| 294 | 6 | Jew et al., 2013a | 22Mc2b | 6 | | -1.3 | 0.3 | 8800 | Mid | San Miguel Island | Island | 34.032 | -120.4 |
| 294 | 6 | Jew et al., 2013a | 22Mc2c | 9 | | -0.4 | 1.2 | 8800 | Mid | San Miguel Island | Island | 34.032 | -120.4 |
| 294 | 6 | Jew et al., 2013a | 22Mc2d | 12 | | -0.1 | 1.8 | 8800 | Mid | San Miguel Island | Island | 34.032 | -120.4 |
| 294 | 6 | Jew et al., 2013a | 22Mc2e | 15 | | 0 | 1.5 | 8800 | Mid | San Miguel Island | Island | 34.032 | -120.4 |
| 294 | 6 | Jew et al., 2013a | 22Mc2f | 18 | | 0.1 | 1.1 | 8800 | Mid | San Miguel Island | Island | 34.032 | -120.4 |
| 295 | 6 | Jew et al., 2013a | 28Mc2a | 3 | | -1 | 0.2 | 8800 | Mid | San Miguel Island | Island | 34.032 | -120.4 |

| | | | | | | | | | | | | | |
|---|---|---|---|---|---|---|---|---|---|---|---|---|---|
| 295 | 6 | Jew et al., 2013a | 28Mc2b | 6 | | -0.5 | 1.4 | 8800 | Mid | San Miguel Island | Island | 34.032 | -120.4 |
| 295 | 6 | Jew et al., 2013a | 28Mc2c | 9 | | 0.6 | 2.1 | 8800 | Mid | San Miguel Island | Island | 34.032 | -120.4 |
| 295 | 6 | Jew et al., 2013a | 28Mc2d | 12 | | 0 | 0.5 | 8800 | Mid | San Miguel Island | Island | 34.032 | -120.4 |
| 295 | 6 | Jew et al., 2013a | 28Mc2e | 15 | | 0 | 0.7 | 8800 | Mid | San Miguel Island | Island | 34.032 | -120.4 |
| 295 | 6 | Jew et al., 2013a | 28Mc2f | 18 | | 0 | 1.8 | 8800 | Mid | San Miguel Island | Island | 34.032 | -120.4 |
| 296 | 6 | Jew et al., 2013a | 29Mc2a | 3 | | 0 | 2.4 | 8800 | Mid | San Miguel Island | Island | 34.032 | -120.4 |
| 296 | 6 | Jew et al., 2013a | 29Mc2b | 6 | | 0 | 2.4 | 8800 | Mid | San Miguel Island | Island | 34.032 | -120.4 |
| 296 | 6 | Jew et al., 2013a | 29Mc2c | 9 | | -0.8 | 0.7 | 8800 | Mid | San Miguel Island | Island | 34.032 | -120.4 |
| 296 | 6 | Jew et al., 2013a | 29Mc2d | 12 | | -0.1 | 0.1 | 8800 | Mid | San Miguel Island | Island | 34.032 | -120.4 |
| 296 | 6 | Jew et al., 2013a | 29Mc2e | 15 | | 0 | 1.2 | 8800 | Mid | San Miguel Island | Island | 34.032 | -120.4 |
| 296 | 6 | Jew et al., 2013a | 29Mc2f | 18 | | -0.1 | 1.6 | 8800 | Mid | San Miguel Island | Island | 34.032 | -120.4 |
| 297 | 6 | Jew et al., 2013a | 2Mc2a | 3 | | 0.7 | 1.1 | 8800 | Mid | San Miguel Island | Island | 34.032 | -120.4 |
| 297 | 6 | Jew et al., 2013a | 2Mc2b | 6 | | 0.3 | 1.6 | 8800 | Mid | San Miguel Island | Island | 34.032 | -120.4 |
| 297 | 6 | Jew et al., 2013a | 2Mc2c | 9 | | 1 | 1.1 | 8800 | Mid | San Miguel Island | Island | 34.032 | -120.4 |
| 297 | 6 | Jew et al., 2013a | 2Mc2d | 12 | | 1 | 0.9 | 8800 | Mid | San Miguel Island | Island | 34.032 | -120.4 |
| 297 | 6 | Jew et al., 2013a | 2Mc2e | 15 | | 0.3 | 1.6 | 8800 | Mid | San Miguel Island | Island | 34.032 | -120.4 |
| 297 | 6 | Jew et al., 2013a | 2Mc2f | 18 | | 0.9 | 0.9 | 8800 | Mid | San Miguel Island | Island | 34.032 | -120.4 |
| 298 | 6 | Jew et al., 2013a | 30Mc2a | 3 | | 0.1 | 1.7 | 8800 | Mid | San Miguel Island | Island | 34.032 | -120.4 |
| 298 | 6 | Jew et al., 2013a | 30Mc2b | 6 | | 0.7 | 2.6 | 8800 | Mid | San Miguel Island | Island | 34.032 | -120.4 |

| | | | | | | | | | | | | | |
|---|---|---|---|---|---|---|---|---|---|---|---|---|---|
| 298 | 6 | Jew et al., 2013a | 30Mc2c | 9 | | 0.8 | 2.2 | 8800 | Mid | San Miguel Island | Island | 34.032 | -120.4 |
| 298 | 6 | Jew et al., 2013a | 30Mc2d | 12 | | 0.9 | 1.5 | 8800 | Mid | San Miguel Island | Island | 34.032 | -120.4 |
| 298 | 6 | Jew et al., 2013a | 30Mc2e | 15 | | 0.1 | -0.3 | 8800 | Mid | San Miguel Island | Island | 34.032 | -120.4 |
| 298 | 6 | Jew et al., 2013a | 30Mc2f | 18 | | 0.3 | 0.6 | 8800 | Mid | San Miguel Island | Island | 34.032 | -120.4 |
| 299 | 6 | Jew et al., 2013a | 31Mc2a | 3 | | -1 | -0.1 | 8800 | Mid | San Miguel Island | Island | 34.032 | -120.4 |
| 299 | 6 | Jew et al., 2013a | 31Mc2b | 6 | | -1 | 0.9 | 8800 | Mid | San Miguel Island | Island | 34.032 | -120.4 |
| 299 | 6 | Jew et al., 2013a | 31Mc2c | 9 | | -0.1 | 2.1 | 8800 | Mid | San Miguel Island | Island | 34.032 | -120.4 |
| 299 | 6 | Jew et al., 2013a | 31Mc2d | 12 | | 0 | 2.1 | 8800 | Mid | San Miguel Island | Island | 34.032 | -120.4 |
| 299 | 6 | Jew et al., 2013a | 31Mc2e | 15 | | 0 | 1.3 | 8800 | Mid | San Miguel Island | Island | 34.032 | -120.4 |
| 299 | 6 | Jew et al., 2013a | 31Mc2f | 18 | | 0.3 | 1.7 | 8800 | Mid | San Miguel Island | Island | 34.032 | -120.4 |
| 300 | 6 | Jew et al., 2013a | 32Mc2a | 3 | | -0.5 | 1.6 | 8800 | Mid | San Miguel Island | Island | 34.032 | -120.4 |
| 300 | 6 | Jew et al., 2013a | 32Mc2b | 6 | | -0.2 | 1.3 | 8800 | Mid | San Miguel Island | Island | 34.032 | -120.4 |
| 300 | 6 | Jew et al., 2013a | 32Mc2c | 9 | | 0.6 | 2.5 | 8800 | Mid | San Miguel Island | Island | 34.032 | -120.4 |
| 300 | 6 | Jew et al., 2013a | 32Mc2d | 12 | | 0.1 | 1.1 | 8800 | Mid | San Miguel Island | Island | 34.032 | -120.4 |
| 300 | 6 | Jew et al., 2013a | 32Mc2e | 15 | | 0.4 | 1.1 | 8800 | Mid | San Miguel Island | Island | 34.032 | -120.4 |
| 300 | 6 | Jew et al., 2013a | 32Mc2f | 18 | | 0.4 | 1.6 | 8800 | Mid | San Miguel Island | Island | 34.032 | -120.4 |
| 301 | 6 | Jew et al., 2013a | 34Mc2a | 3 | | 0.4 | 2.3 | 8800 | Mid | San Miguel Island | Island | 34.032 | -120.4 |
| 301 | 6 | Jew et al., 2013a | 34Mc2b | 6 | | 0.7 | 2.4 | 8800 | Mid | San Miguel Island | Island | 34.032 | -120.4 |
| 301 | 6 | Jew et al., 2013a | 34Mc2c | 9 | | 0.6 | 0.6 | 8800 | Mid | San Miguel Island | Island | 34.032 | -120.4 |

| | | | | | | | | | | | | | |
|---|---|---|---|---|---|---|---|---|---|---|---|---|---|
| 301 | 6 | Jew et al., 2013a | 34Mc2d | 12 | | 0.6 | 0.9 | 8800 | Mid | San Miguel Island | Island | 34.032 | -120.4 |
| 301 | 6 | Jew et al., 2013a | 34Mc2e | 15 | | 0.3 | 1 | 8800 | Mid | San Miguel Island | Island | 34.032 | -120.4 |
| 301 | 6 | Jew et al., 2013a | 34Mc2f | 18 | | -0.2 | 1.1 | 8800 | Mid | San Miguel Island | Island | 34.032 | -120.4 |
| 302 | 6 | Jew et al., 2013a | 35Mc2a | 3 | | 0 | 1.4 | 8800 | Mid | San Miguel Island | Island | 34.032 | -120.4 |
| 302 | 6 | Jew et al., 2013a | 35Mc2b | 6 | | 0.5 | 0.4 | 8800 | Mid | San Miguel Island | Island | 34.032 | -120.4 |
| 302 | 6 | Jew et al., 2013a | 35Mc2c | 9 | | 0.2 | 0.6 | 8800 | Mid | San Miguel Island | Island | 34.032 | -120.4 |
| 302 | 6 | Jew et al., 2013a | 35Mc2d | 12 | | -0.3 | -0.3 | 8800 | Mid | San Miguel Island | Island | 34.032 | -120.4 |
| 302 | 6 | Jew et al., 2013a | 35Mc2e | 15 | | 0 | 0.4 | 8800 | Mid | San Miguel Island | Island | 34.032 | -120.4 |
| 302 | 6 | Jew et al., 2013a | 35Mc2f | 18 | | 0 | 0.8 | 8800 | Mid | San Miguel Island | Island | 34.032 | -120.4 |
| 303 | 6 | Jew et al., 2013a | 39Mc2a | 3 | | -0.5 | 0.1 | 8800 | Mid | San Miguel Island | Island | 34.032 | -120.4 |
| 303 | 6 | Jew et al., 2013a | 39Mc2b | 6 | | -0.9 | 0.2 | 8800 | Mid | San Miguel Island | Island | 34.032 | -120.4 |
| 303 | 6 | Jew et al., 2013a | 39Mc2c | 9 | | -1 | 0.2 | 8800 | Mid | San Miguel Island | Island | 34.032 | -120.4 |
| 303 | 6 | Jew et al., 2013a | 39Mc2d | 12 | | -0.6 | 0.7 | 8800 | Mid | San Miguel Island | Island | 34.032 | -120.4 |
| 303 | 6 | Jew et al., 2013a | 39Mc2e | 15 | | -0.1 | 1.4 | 8800 | Mid | San Miguel Island | Island | 34.032 | -120.4 |
| 303 | 6 | Jew et al., 2013a | 39Mc2f | 18 | | 0.1 | 0.9 | 8800 | Mid | San Miguel Island | Island | 34.032 | -120.4 |
| 304 | 6 | Jew et al., 2013a | 3Mc2a | 3 | | -0.5 | 1.1 | 8800 | Mid | San Miguel Island | Island | 34.032 | -120.4 |
| 304 | 6 | Jew et al., 2013a | 3Mc2b | 6 | | -0.2 | 1.5 | 8800 | Mid | San Miguel Island | Island | 34.032 | -120.4 |
| 304 | 6 | Jew et al., 2013a | 3Mc2c | 9 | | 0.5 | 2.4 | 8800 | Mid | San Miguel Island | Island | 34.032 | -120.4 |
| 304 | 6 | Jew et al., 2013a | 3Mc2d | 12 | | 0.6 | 1.9 | 8800 | Mid | San Miguel Island | Island | 34.032 | -120.4 |

| | | | | | | | | | | | | | |
|---|---|---|---|---|---|---|---|---|---|---|---|---|---|
| 304 | 6 | Jew et al., 2013a | 3Mc2e | 15 | | 0.2 | 1.1 | 8800 | Mid | San Miguel Island | Island | 34.032 | -120.4 |
| 304 | 6 | Jew et al., 2013a | 3Mc2f | 18 | | 0.8 | 0.8 | 8800 | Mid | San Miguel Island | Island | 34.032 | -120.4 |
| 305 | 6 | Jew et al., 2013a | 40Mc2a | 3 | | -0.2 | 0.9 | 8800 | Mid | San Miguel Island | Island | 34.032 | -120.4 |
| 305 | 6 | Jew et al., 2013a | 40Mc2b | 6 | | 0.2 | 1 | 8800 | Mid | San Miguel Island | Island | 34.032 | -120.4 |
| 305 | 6 | Jew et al., 2013a | 40Mc2c | 9 | | 0.3 | 0.5 | 8800 | Mid | San Miguel Island | Island | 34.032 | -120.4 |
| 305 | 6 | Jew et al., 2013a | 40Mc2d | 12 | | 0.8 | 0.4 | 8800 | Mid | San Miguel Island | Island | 34.032 | -120.4 |
| 305 | 6 | Jew et al., 2013a | 40Mc2e | 15 | | 0.2 | 0.6 | 8800 | Mid | San Miguel Island | Island | 34.032 | -120.4 |
| 305 | 6 | Jew et al., 2013a | 40Mc2f | 18 | | 0.2 | 1 | 8800 | Mid | San Miguel Island | Island | 34.032 | -120.4 |
| 306 | 6 | Jew et al., 2013a | 4Mc2a | 3 | | 0 | 0.6 | 8800 | Mid | San Miguel Island | Island | 34.032 | -120.4 |
| 306 | 6 | Jew et al., 2013a | 4Mc2b | 6 | | 0 | 1.4 | 8800 | Mid | San Miguel Island | Island | 34.032 | -120.4 |
| 306 | 6 | Jew et al., 2013a | 4Mc2c | 9 | | 0.3 | 1.3 | 8800 | Mid | San Miguel Island | Island | 34.032 | -120.4 |
| 306 | 6 | Jew et al., 2013a | 4Mc2d | 12 | | 0.7 | 1.1 | 8800 | Mid | San Miguel Island | Island | 34.032 | -120.4 |
| 306 | 6 | Jew et al., 2013a | 4Mc2e | 15 | | 0.7 | 0.9 | 8800 | Mid | San Miguel Island | Island | 34.032 | -120.4 |
| 306 | 6 | Jew et al., 2013a | 4Mc2f | 18 | | 0.8 | 0.8 | 8800 | Mid | San Miguel Island | Island | 34.032 | -120.4 |
| 307 | 6 | Jew et al., 2013a | 5Mc2a | 3 | | -0.4 | 0.3 | 8800 | Mid | San Miguel Island | Island | 34.032 | -120.4 |
| 307 | 6 | Jew et al., 2013a | 5Mc2b | 6 | | -0.7 | 0.6 | 8800 | Mid | San Miguel Island | Island | 34.032 | -120.4 |
| 307 | 6 | Jew et al., 2013a | 5Mc2c | 9 | | -0.7 | 1.1 | 8800 | Mid | San Miguel Island | Island | 34.032 | -120.4 |
| 307 | 6 | Jew et al., 2013a | 5Mc2d | 12 | | -0.8 | 1 | 8800 | Mid | San Miguel Island | Island | 34.032 | -120.4 |
| 307 | 6 | Jew et al., 2013a | 5Mc2e | 15 | | -0.5 | 1.3 | 8800 | Mid | San Miguel Island | Island | 34.032 | -120.4 |

| | | | | | | | | | | | | | |
|---|---|---|---|---|---|---|---|---|---|---|---|---|---|
| 307 | 6 | Jew et al., 2013a | 5Mc2f | 18 | | 0 | 0.7 | 8800 | Mid | San Miguel Island | Island | 34.032 | -120.4 |
| 308 | 6 | Jew et al., 2013a | 7Mc2a | 3 | | -0.2 | 0.1 | 8800 | Mid | San Miguel Island | Island | 34.032 | -120.4 |
| 308 | 6 | Jew et al., 2013a | 7Mc2b | 6 | | -0.7 | 0.3 | 8800 | Mid | San Miguel Island | Island | 34.032 | -120.4 |
| 308 | 6 | Jew et al., 2013a | 7Mc2c | 9 | | -0.6 | 0.9 | 8800 | Mid | San Miguel Island | Island | 34.032 | -120.4 |
| 308 | 6 | Jew et al., 2013a | 7Mc2d | 12 | | -0.3 | 1.2 | 8800 | Mid | San Miguel Island | Island | 34.032 | -120.4 |
| 308 | 6 | Jew et al., 2013a | 7Mc2e | 15 | | -0.4 | 1.2 | 8800 | Mid | San Miguel Island | Island | 34.032 | -120.4 |
| 308 | 6 | Jew et al., 2013a | 7Mc2f | 18 | | 0 | 1 | 8800 | Mid | San Miguel Island | Island | 34.032 | -120.4 |
| 309 | 2 | Jew et al., 2013a | Mc10a | 0 | | 1.2 | 1.5 | 8800 | Mid | San Miguel Island | Island | 34.032 | -120.4 |
| 309 | 2 | Jew et al., 2013a | Mc10b | 2 | | 0.2 | 1.1 | 8800 | Mid | San Miguel Island | Island | 34.032 | -120.4 |
| 310 | 2 | Jew et al., 2013a | Mc11a | 0 | | 0.5 | 0.4 | 8800 | Mid | San Miguel Island | Island | 34.032 | -120.4 |
| 310 | 2 | Jew et al., 2013a | Mc11b | 2 | | 0.2 | 1.9 | 8800 | Mid | San Miguel Island | Island | 34.032 | -120.4 |
| 311 | 2 | Jew et al., 2013a | Mc12a | 0 | | 0.7 | 1.7 | 8800 | Mid | San Miguel Island | Island | 34.032 | -120.4 |
| 311 | 2 | Jew et al., 2013a | Mc12b | 2 | | -0.3 | 0.5 | 8800 | Mid | San Miguel Island | Island | 34.032 | -120.4 |
| 312 | 2 | Jew et al., 2013a | Mc13a | 0 | | 0.5 | 0.9 | 8800 | Mid | San Miguel Island | Island | 34.032 | -120.4 |
| 312 | 2 | Jew et al., 2013a | Mc13b | 2 | | 0.4 | 1.5 | 8800 | Mid | San Miguel Island | Island | 34.032 | -120.4 |
| 313 | 2 | Jew et al., 2013a | Mc14a | 0 | | 0.8 | 1.7 | 8800 | Mid | San Miguel Island | Island | 34.032 | -120.4 |
| 313 | 2 | Jew et al., 2013a | Mc14b | 2 | | 0.4 | 1.6 | 8800 | Mid | San Miguel Island | Island | 34.032 | -120.4 |
| 314 | 2 | Jew et al., 2013a | Mc15a | 0 | | 1.3 | 1.7 | 8800 | Mid | San Miguel Island | Island | 34.032 | -120.4 |
| 314 | 2 | Jew et al., 2013a | Mc15b | 2 | | 0 | 0.4 | 8800 | Mid | San Miguel Island | Island | 34.032 | -120.4 |

| | | | | | | | | | | | | | |
|---|---|---|---|---|---|---|---|---|---|---|---|---|---|
| 315 | 2 | Jew et al., 2013a | Mc16a | 0 | | 1 | 0.8 | 8800 | Mid | San Miguel Island | Island | 34.032 | -120.4 |
| 315 | 2 | Jew et al., 2013a | Mc16b | 2 | | 0.4 | 1.5 | 8800 | Mid | San Miguel Island | Island | 34.032 | -120.4 |
| 316 | 2 | Jew et al., 2013a | Mc17a | 0 | | 0.7 | 1.3 | 8800 | Mid | San Miguel Island | Island | 34.032 | -120.4 |
| 316 | 2 | Jew et al., 2013a | Mc17b | 2 | | 0.2 | 0.5 | 8800 | Mid | San Miguel Island | Island | 34.032 | -120.4 |
| 317 | 2 | Jew et al., 2013a | Mc18a | 0 | | 0.1 | 1.1 | 8800 | Mid | San Miguel Island | Island | 34.032 | -120.4 |
| 317 | 2 | Jew et al., 2013a | Mc18b | 2 | | 0.2 | 0.7 | 8800 | Mid | San Miguel Island | Island | 34.032 | -120.4 |
| 318 | 2 | Jew et al., 2013a | Mc19a | 0 | | 1 | 1.1 | 8800 | Mid | San Miguel Island | Island | 34.032 | -120.4 |
| 318 | 2 | Jew et al., 2013a | Mc19b | 2 | | 0.4 | 0.9 | 8800 | Mid | San Miguel Island | Island | 34.032 | -120.4 |
| 319 | 2 | Jew et al., 2013a | Mc1a | 0 | | 0.7 | 1.4 | 8800 | Mid | San Miguel Island | Island | 34.032 | -120.4 |
| 319 | 2 | Jew et al., 2013a | Mc1b | 2 | | 0.1 | 1.2 | 8800 | Mid | San Miguel Island | Island | 34.032 | -120.4 |
| 320 | 2 | Jew et al., 2013a | Mc20a | 0 | | 0 | 0.9 | 8800 | Mid | San Miguel Island | Island | 34.032 | -120.4 |
| 320 | 2 | Jew et al., 2013a | Mc20b | 2 | | 0.1 | 1.4 | 8800 | Mid | San Miguel Island | Island | 34.032 | -120.4 |
| 321 | 17 | Jew et al., 2013a | Mc21a | 0 | | 0.2 | 1.2 | 8800 | Mid | San Miguel Island | Island | 34.032 | -120.4 |
| 321 | 17 | Jew et al., 2013a | Mc21b | 3 | | -0.2 | 0.5 | 8800 | Mid | San Miguel Island | Island | 34.032 | -120.4 |
| 321 | 17 | Jew et al., 2013a | Mc21c | 6 | | -0.8 | 1 | 8800 | Mid | San Miguel Island | Island | 34.032 | -120.4 |
| 321 | 17 | Jew et al., 2013a | Mc21d | 9 | | -0.6 | 1.7 | 8800 | Mid | San Miguel Island | Island | 34.032 | -120.4 |
| 321 | 17 | Jew et al., 2013a | Mc21e | 12 | | 0 | 1.6 | 8800 | Mid | San Miguel Island | Island | 34.032 | -120.4 |
| 321 | 17 | Jew et al., 2013a | Mc21f | 15 | | -0.1 | 1.5 | 8800 | Mid | San Miguel Island | Island | 34.032 | -120.4 |
| 321 | 17 | Jew et al., 2013a | Mc21g | 18 | | 0.2 | 1.1 | 8800 | Mid | San Miguel Island | Island | 34.032 | -120.4 |

| | | | | | | | | | | | | | |
|---|---|---|---|---|---|---|---|---|---|---|---|---|---|
| 321 | 17 | Jew et al., 2013a | Mc21h | 21 | | 0.5 | 1.3 | 8800 | Mid | San Miguel Island | Island | 34.032 | -120.4 |
| 321 | 17 | Jew et al., 2013a | Mc21i | 24 | | 0.6 | 1.3 | 8800 | Mid | San Miguel Island | Island | 34.032 | -120.4 |
| 321 | 17 | Jew et al., 2013a | Mc21j | 27 | | 0.6 | 1.5 | 8800 | Mid | San Miguel Island | Island | 34.032 | -120.4 |
| 321 | 17 | Jew et al., 2013a | Mc21k | 30 | | 0.2 | 0.9 | 8800 | Mid | San Miguel Island | Island | 34.032 | -120.4 |
| 321 | 17 | Jew et al., 2013a | Mc21l | 33 | | 0 | 0.7 | 8800 | Mid | San Miguel Island | Island | 34.032 | -120.4 |
| 321 | 17 | Jew et al., 2013a | Mc21m | 36 | | 0.2 | 1.1 | 8800 | Mid | San Miguel Island | Island | 34.032 | -120.4 |
| 321 | 17 | Jew et al., 2013a | Mc21n | 39 | | -0.1 | 1.3 | 8800 | Mid | San Miguel Island | Island | 34.032 | -120.4 |
| 321 | 17 | Jew et al., 2013a | Mc21o | 42 | | -0.3 | 0.9 | 8800 | Mid | San Miguel Island | Island | 34.032 | -120.4 |
| 321 | 17 | Jew et al., 2013a | Mc21p | 45 | | -0.3 | 1.3 | 8800 | Mid | San Miguel Island | Island | 34.032 | -120.4 |
| 321 | 17 | Jew et al., 2013a | Mc21q | 48 | | -0.1 | 1.4 | 8800 | Mid | San Miguel Island | Island | 34.032 | -120.4 |
| 322 | 2 | Jew et al., 2013a | Mc22a | 0 | | -0.2 | 0.5 | 8800 | Mid | San Miguel Island | Island | 34.032 | -120.4 |
| 322 | 2 | Jew et al., 2013a | Mc22b | 2 | | -0.3 | 0.3 | 8800 | Mid | San Miguel Island | Island | 34.032 | -120.4 |
| 323 | 2 | Jew et al., 2013a | Mc23a | 0 | | -0.2 | 0.1 | 8800 | Mid | San Miguel Island | Island | 34.032 | -120.4 |
| 323 | 2 | Jew et al., 2013a | Mc23b | 2 | | -0.3 | 0.3 | 8800 | Mid | San Miguel Island | Island | 34.032 | -120.4 |
| 324 | 2 | Jew et al., 2013a | Mc24a | 0 | | 0.2 | 0.4 | 8800 | Mid | San Miguel Island | Island | 34.032 | -120.4 |
| 324 | 2 | Jew et al., 2013a | Mc24b | 2 | | 0.1 | 0 | 8800 | Mid | San Miguel Island | Island | 34.032 | -120.4 |
| 325 | 2 | Jew et al., 2013a | Mc25a | 0 | | -0.2 | 0.4 | 8800 | Mid | San Miguel Island | Island | 34.032 | -120.4 |
| 325 | 2 | Jew et al., 2013a | Mc25b | 2 | | -0.8 | 0.2 | 8800 | Mid | San Miguel Island | Island | 34.032 | -120.4 |
| 326 | 2 | Jew et al., 2013a | Mc26a | 0 | | 0.1 | 0.5 | 8800 | Mid | San Miguel Island | Island | 34.032 | -120.4 |

| | | | | | | | | | | | | | |
|---|---|---|---|---|---|---|---|---|---|---|---|---|---|
| 326 | 2 | Jew et al., 2013a | Mc26b | 2 | | 0.5 | 0.6 | 8800 | Mid | San Miguel Island | Island | 34.032 | -120.4 |
| 327 | 2 | Jew et al., 2013a | Mc27a | 0 | | 0.1 | 0.5 | 8800 | Mid | San Miguel Island | Island | 34.032 | -120.4 |
| 327 | 2 | Jew et al., 2013a | Mc27b | 2 | | 0.1 | 0.6 | 8800 | Mid | San Miguel Island | Island | 34.032 | -120.4 |
| 328 | 2 | Jew et al., 2013a | Mc28a | 0 | | -0.1 | 0.3 | 8800 | Mid | San Miguel Island | Island | 34.032 | -120.4 |
| 328 | 2 | Jew et al., 2013a | Mc28b | 2 | | -0.6 | 0.6 | 8800 | Mid | San Miguel Island | Island | 34.032 | -120.4 |
| 329 | 2 | Jew et al., 2013a | Mc29a | 0 | | -0.1 | 0.5 | 8800 | Mid | San Miguel Island | Island | 34.032 | -120.4 |
| 329 | 2 | Jew et al., 2013a | Mc29b | 2 | | 0.1 | 0.3 | 8800 | Mid | San Miguel Island | Island | 34.032 | -120.4 |
| 330 | 2 | Jew et al., 2013a | Mc2a | 0 | | 0.3 | 0.8 | 8800 | Mid | San Miguel Island | Island | 34.032 | -120.4 |
| 330 | 2 | Jew et al., 2013a | Mc2b | 2 | | 0.1 | 1.7 | 8800 | Mid | San Miguel Island | Island | 34.032 | -120.4 |
| 331 | 2 | Jew et al., 2013a | Mc30a | 0 | | 0.1 | 0.3 | 8800 | Mid | San Miguel Island | Island | 34.032 | -120.4 |
| 331 | 2 | Jew et al., 2013a | Mc30b | 2 | | 0 | 0.7 | 8800 | Mid | San Miguel Island | Island | 34.032 | -120.4 |
| 332 | 2 | Jew et al., 2013a | Mc31a | 0 | | -0.4 | 0.1 | 8800 | Mid | San Miguel Island | Island | 34.032 | -120.4 |
| 332 | 2 | Jew et al., 2013a | Mc31b | 2 | | -0.7 | 0.2 | 8800 | Mid | San Miguel Island | Island | 34.032 | -120.4 |
| 333 | 2 | Jew et al., 2013a | Mc32a | 0 | | 0.5 | 0.6 | 8800 | Mid | San Miguel Island | Island | 34.032 | -120.4 |
| 333 | 2 | Jew et al., 2013a | Mc32b | 2 | | -0.6 | 0.2 | 8800 | Mid | San Miguel Island | Island | 34.032 | -120.4 |
| 334 | 2 | Jew et al., 2013a | Mc33a | 0 | | 1.4 | 0.5 | 8800 | Mid | San Miguel Island | Island | 34.032 | -120.4 |
| 334 | 2 | Jew et al., 2013a | Mc33b | 2 | | 0.8 | 0.4 | 8800 | Mid | San Miguel Island | Island | 34.032 | -120.4 |
| 335 | 2 | Jew et al., 2013a | Mc34a | 0 | | -0.1 | 0.4 | 8800 | Mid | San Miguel Island | Island | 34.032 | -120.4 |
| 335 | 2 | Jew et al., 2013a | Mc34b | 2 | | 0.4 | 0.8 | 8800 | Mid | San Miguel Island | Island | 34.032 | -120.4 |

| | | | | | | | | | | | | | |
|---|---|---|---|---|---|---|---|---|---|---|---|---|---|
| 336 | 2 | Jew et al., 2013a | Mc35a | 0 | | 0.8 | 0.8 | 8800 | Mid | San Miguel Island | Island | 34.032 | -120.4 |
| 336 | 2 | Jew et al., 2013a | Mc35b | 2 | | -0.6 | 0.9 | 8800 | Mid | San Miguel Island | Island | 34.032 | -120.4 |
| 337 | 2 | Jew et al., 2013a | Mc36a | 0 | | 0.2 | 0.4 | 8800 | Mid | San Miguel Island | Island | 34.032 | -120.4 |
| 337 | 2 | Jew et al., 2013a | Mc36b | 2 | | -0.9 | 0.7 | 8800 | Mid | San Miguel Island | Island | 34.032 | -120.4 |
| 338 | 2 | Jew et al., 2013a | Mc37a | 0 | | -0.2 | 0.6 | 8800 | Mid | San Miguel Island | Island | 34.032 | -120.4 |
| 338 | 2 | Jew et al., 2013a | Mc37b | 2 | | -0.6 | 0.9 | 8800 | Mid | San Miguel Island | Island | 34.032 | -120.4 |
| 339 | 2 | Jew et al., 2013a | Mc38a | 0 | | -0.1 | 0.4 | 8800 | Mid | San Miguel Island | Island | 34.032 | -120.4 |
| 339 | 2 | Jew et al., 2013a | Mc38b | 2 | | 0 | 0.2 | 8800 | Mid | San Miguel Island | Island | 34.032 | -120.4 |
| 340 | 2 | Jew et al., 2013a | Mc39a | 0 | | -0.2 | 0.1 | 8800 | Mid | San Miguel Island | Island | 34.032 | -120.4 |
| 340 | 2 | Jew et al., 2013a | Mc39b | 2 | | 0.6 | 1.1 | 8800 | Mid | San Miguel Island | Island | 34.032 | -120.4 |
| 341 | 2 | Jew et al., 2013a | Mc3a | 0 | | 0.4 | 0.8 | 8800 | Mid | San Miguel Island | Island | 34.032 | -120.4 |
| 341 | 2 | Jew et al., 2013a | Mc3b | 2 | | -0.2 | 1.1 | 8800 | Mid | San Miguel Island | Island | 34.032 | -120.4 |
| 342 | 2 | Jew et al., 2013a | Mc40a | 0 | | 0.3 | 0.7 | 8800 | Mid | San Miguel Island | Island | 34.032 | -120.4 |
| 342 | 2 | Jew et al., 2013a | Mc40b | 2 | | 0 | 0.2 | 8800 | Mid | San Miguel Island | Island | 34.032 | -120.4 |
| 343 | 2 | Jew et al., 2013a | Mc4a | 0 | | 0.4 | 1.4 | 8800 | Mid | San Miguel Island | Island | 34.032 | -120.4 |
| 343 | 2 | Jew et al., 2013a | Mc4b | 2 | | 0.4 | 1 | 8800 | Mid | San Miguel Island | Island | 34.032 | -120.4 |
| 344 | 2 | Jew et al., 2013a | Mc5a | 0 | | 0.5 | 1.5 | 8800 | Mid | San Miguel Island | Island | 34.032 | -120.4 |
| 344 | 2 | Jew et al., 2013a | Mc5b | 2 | | 0.1 | 0.9 | 8800 | Mid | San Miguel Island | Island | 34.032 | -120.4 |
| 345 | 2 | Jew et al., 2013a | Mc6a | 0 | | 0.3 | 1.2 | 8800 | Mid | San Miguel Island | Island | 34.032 | -120.4 |

| | | | | | | | | | | | | | |
|---|---|---|---|---|---|---|---|---|---|---|---|---|---|
| 345 | 2 | Jew et al., 2013a | Mc6b | 2 | | -0.3 | 0.8 | 8800 | Mid | San Miguel Island | Island | 34.032 | -120.4 |
| 346 | 2 | Jew et al., 2013a | Mc7a | 0 | | 0.1 | 0.8 | 8800 | Mid | San Miguel Island | Island | 34.032 | -120.4 |
| 346 | 2 | Jew et al., 2013a | Mc7b | 2 | | 0 | 1.1 | 8800 | Mid | San Miguel Island | Island | 34.032 | -120.4 |
| 347 | 2 | Jew et al., 2013a | Mc8a | 0 | | -0.1 | 0.9 | 8800 | Mid | San Miguel Island | Island | 34.032 | -120.4 |
| 347 | 2 | Jew et al., 2013a | Mc8b | 2 | | -0.1 | 1.1 | 8800 | Mid | San Miguel Island | Island | 34.032 | -120.4 |
| 348 | 2 | Jew et al., 2013a | Mc9a | 0 | | 0.2 | 0.7 | 8800 | Mid | San Miguel Island | Island | 34.032 | -120.4 |
| 348 | 2 | Jew et al., 2013a | Mc9b | 2 | | 0.3 | 2 | 8800 | Mid | San Miguel Island | Island | 34.032 | -120.4 |
| 349 | 6 | Jew et al., 2013b | 666-U1-10a | 0 | | 0.7 | 0.8 | 8200 | Mid | Santa Rosa Island | Island | 33.975 | -120 |
| 349 | 6 | Jew et al., 2013b | 666-U1-10b | 2 | | 0.5 | 0.5 | 8200 | Mid | Santa Rosa Island | Island | 33.975 | -120 |
| 349 | 6 | Jew et al., 2013b | 666-U1-10c | 6 | | 0 | 0.2 | 8200 | Mid | Santa Rosa Island | Island | 33.975 | -120 |
| 349 | 6 | Jew et al., 2013b | 666-U1-10d | 9 | | 0.2 | 0 | 8200 | Mid | Santa Rosa Island | Island | 33.975 | -120 |
| 349 | 6 | Jew et al., 2013b | 666-U1-10e | 12 | | 0.1 | 0 | 8200 | Mid | Santa Rosa Island | Island | 33.975 | -120 |
| 349 | 6 | Jew et al., 2013b | 666-U1-10f | 15 | | -0.1 | 0 | 8200 | Mid | Santa Rosa Island | Island | 33.975 | -120 |
| 350 | 6 | Jew et al., 2013b | 666-U1-11a | 0 | | 0.5 | 0.2 | 8200 | Mid | Santa Rosa Island | Island | 33.975 | -120 |
| 350 | 6 | Jew et al., 2013b | 666-U1-11b | 2 | | -0.1 | 1.3 | 8200 | Mid | Santa Rosa Island | Island | 33.975 | -120 |
| 350 | 6 | Jew et al., 2013b | 666-U1-11c | 6 | | 0.5 | 0.7 | 8200 | Mid | Santa Rosa Island | Island | 33.975 | -120 |
| 350 | 6 | Jew et al., 2013b | 666-U1-11d | 9 | | 0.8 | 1.1 | 8200 | Mid | Santa Rosa Island | Island | 33.975 | -120 |
| 350 | 6 | Jew et al., 2013b | 666-U1-11e | 12 | | 0.6 | 0.5 | 8200 | Mid | Santa Rosa Island | Island | 33.975 | -120 |
| 350 | 6 | Jew et al., 2013b | 666-U1-11f | 15 | | 0.8 | 0.8 | 8200 | Mid | Santa Rosa Island | Island | 33.975 | -120 |

| | | | | | | | | | | | | | |
|---|---|---|---|---|---|---|---|---|---|---|---|---|---|
| 351 | 6 | Jew et al., 2013b | 666-U1-12a | 0 | | 0.8 | 0 | 8200 | Mid | Santa Rosa Island | Island | 33.975 | -120 |
| 351 | 6 | Jew et al., 2013b | 666-U1-12b | 2 | | 0.5 | 0.4 | 8200 | Mid | Santa Rosa Island | Island | 33.975 | -120 |
| 351 | 6 | Jew et al., 2013b | 666-U1-12c | 6 | | 0.6 | 0.6 | 8200 | Mid | Santa Rosa Island | Island | 33.975 | -120 |
| 351 | 6 | Jew et al., 2013b | 666-U1-12d | 9 | | 0.8 | 1 | 8200 | Mid | Santa Rosa Island | Island | 33.975 | -120 |
| 351 | 6 | Jew et al., 2013b | 666-U1-12e | 12 | | 0.2 | 0.4 | 8200 | Mid | Santa Rosa Island | Island | 33.975 | -120 |
| 351 | 6 | Jew et al., 2013b | 666-U1-12f | 15 | | 0.6 | 1.1 | 8200 | Mid | Santa Rosa Island | Island | 33.975 | -120 |
| 352 | 6 | Jew et al., 2013b | 666-U1-13a | 0 | | 0.5 | 0.1 | 8200 | Mid | Santa Rosa Island | Island | 33.975 | -120 |
| 352 | 6 | Jew et al., 2013b | 666-U1-13b | 2 | | 0.5 | -0.2 | 8200 | Mid | Santa Rosa Island | Island | 33.975 | -120 |
| 352 | 6 | Jew et al., 2013b | 666-U1-13c | 6 | | 0.1 | -0.5 | 8200 | Mid | Santa Rosa Island | Island | 33.975 | -120 |
| 352 | 6 | Jew et al., 2013b | 666-U1-13d | 9 | | -0.1 | -0.1 | 8200 | Mid | Santa Rosa Island | Island | 33.975 | -120 |
| 352 | 6 | Jew et al., 2013b | 666-U1-13e | 12 | | -0.4 | 0.8 | 8200 | Mid | Santa Rosa Island | Island | 33.975 | -120 |
| 352 | 6 | Jew et al., 2013b | 666-U1-13f | 15 | | -0.3 | 1.1 | 8200 | Mid | Santa Rosa Island | Island | 33.975 | -120 |
| 353 | 6 | Jew et al., 2013b | 666-U1-18a | 0 | | 1 | 0.3 | 8200 | Mid | Santa Rosa Island | Island | 33.975 | -120 |
| 353 | 6 | Jew et al., 2013b | 666-U1-18b | 2 | | 1.1 | -0.4 | 8200 | Mid | Santa Rosa Island | Island | 33.975 | -120 |
| 353 | 6 | Jew et al., 2013b | 666-U1-18c | 6 | | 0.8 | -0.5 | 8200 | Mid | Santa Rosa Island | Island | 33.975 | -120 |
| 353 | 6 | Jew et al., 2013b | 666-U1-18d | 9 | | 0.3 | -0.4 | 8200 | Mid | Santa Rosa Island | Island | 33.975 | -120 |
| 353 | 6 | Jew et al., 2013b | 666-U1-18e | 12 | | 0.2 | 0.2 | 8200 | Mid | Santa Rosa Island | Island | 33.975 | -120 |
| 353 | 6 | Jew et al., 2013b | 666-U1-18f | 15 | | 0.7 | 1.1 | 8200 | Mid | Santa Rosa Island | Island | 33.975 | -120 |
| 354 | 6 | Jew et al., 2013b | 666-U1-1a | 0 | | 0.1 | -0.5 | 8200 | Mid | Santa Rosa Island | Island | 33.975 | -120 |

| | | | | | | | | | | | | | |
|---|---|---|---|---|---|---|---|---|---|---|---|---|---|
| 354 | 6 | Jew et al., 2013b | 666-U1-1b | 2 | | -0.9 | 0.7 | 8200 | Mid | Santa Rosa Island | Island | 33.975 | -120 |
| 354 | 6 | Jew et al., 2013b | 666-U1-1c | 6 | | -0.4 | -0.1 | 8200 | Mid | Santa Rosa Island | Island | 33.975 | -120 |
| 354 | 6 | Jew et al., 2013b | 666-U1-1d | 9 | | -0.7 | 0.7 | 8200 | Mid | Santa Rosa Island | Island | 33.975 | -120 |
| 354 | 6 | Jew et al., 2013b | 666-U1-1e | 12 | | -0.4 | 0.8 | 8200 | Mid | Santa Rosa Island | Island | 33.975 | -120 |
| 354 | 6 | Jew et al., 2013b | 666-U1-1f | 15 | | 0.4 | 0 | 8200 | Mid | Santa Rosa Island | Island | 33.975 | -120 |
| 355 | 11 | Jew et al., 2013b | 666-U1-20a | 0 | | 1 | 0.3 | 8200 | Mid | Santa Rosa Island | Island | 33.975 | -120 |
| 355 | 11 | Jew et al., 2013b | 666-U1-20b | 3 | | 0.5 | 0.1 | 8200 | Mid | Santa Rosa Island | Island | 33.975 | -120 |
| 355 | 11 | Jew et al., 2013b | 666-U1-20c | 6 | | 0.7 | 0.6 | 8200 | Mid | Santa Rosa Island | Island | 33.975 | -120 |
| 355 | 11 | Jew et al., 2013b | 666-U1-20d | 9 | | 1 | 0.9 | 8200 | Mid | Santa Rosa Island | Island | 33.975 | -120 |
| 355 | 11 | Jew et al., 2013b | 666-U1-20e | 12 | | 0.9 | 0.6 | 8200 | Mid | Santa Rosa Island | Island | 33.975 | -120 |
| 355 | 11 | Jew et al., 2013b | 666-U1-20f | 15 | | 0.7 | 0.4 | 8200 | Mid | Santa Rosa Island | Island | 33.975 | -120 |
| 355 | 11 | Jew et al., 2013b | 666-U1-20g | 18 | | 0.4 | 0.4 | 8200 | Mid | Santa Rosa Island | Island | 33.975 | -120 |
| 355 | 11 | Jew et al., 2013b | 666-U1-20h | 21 | | 0.5 | 0.1 | 8200 | Mid | Santa Rosa Island | Island | 33.975 | -120 |
| 355 | 11 | Jew et al., 2013b | 666-U1-20i | 24 | | 0.4 | -0.1 | 8200 | Mid | Santa Rosa Island | Island | 33.975 | -120 |
| 355 | 11 | Jew et al., 2013b | 666-U1-20j | 27 | | 0.3 | 0.1 | 8200 | Mid | Santa Rosa Island | Island | 33.975 | -120 |
| 355 | 11 | Jew et al., 2013b | 666-U1-20k | 30 | | -0.4 | 0.4 | 8200 | Mid | Santa Rosa Island | Island | 33.975 | -120 |
| 356 | 6 | Jew et al., 2013b | 666-U1-3a | 0 | | 0.8 | 0.3 | 8200 | Mid | Santa Rosa Island | Island | 33.975 | -120 |
| 356 | 6 | Jew et al., 2013b | 666-U1-3b | 2 | | 0.6 | 0.2 | 8200 | Mid | Santa Rosa Island | Island | 33.975 | -120 |
| 356 | 6 | Jew et al., 2013b | 666-U1-3c | 6 | | 0.9 | 1.2 | 8200 | Mid | Santa Rosa Island | Island | 33.975 | -120 |

| | | | | | | | | | | | | | |
|---|---|---|---|---|---|---|---|---|---|---|---|---|---|
| 356 | 6 | Jew et al., 2013b | 666-U1-3d | 9 | | 1.1 | 0.4 | 8200 | Mid | Santa Rosa Island | Island | 33.975 | -120 |
| 356 | 6 | Jew et al., 2013b | 666-U1-3e | 12 | | 0.9 | 0 | 8200 | Mid | Santa Rosa Island | Island | 33.975 | -120 |
| 356 | 6 | Jew et al., 2013b | 666-U1-3f | 15 | | 0.8 | -0.2 | 8200 | Mid | Santa Rosa Island | Island | 33.975 | -120 |
| 357 | 6 | Jew et al., 2013b | 666-U1-6a | 0 | | 1.1 | -0.1 | 8200 | Mid | Santa Rosa Island | Island | 33.975 | -120 |
| 357 | 6 | Jew et al., 2013b | 666-U1-6b | 2 | | 0.2 | 0.9 | 8200 | Mid | Santa Rosa Island | Island | 33.975 | -120 |
| 357 | 6 | Jew et al., 2013b | 666-U1-6c | 6 | | 0.4 | 1 | 8200 | Mid | Santa Rosa Island | Island | 33.975 | -120 |
| 357 | 6 | Jew et al., 2013b | 666-U1-6d | 9 | | 0.5 | 0.6 | 8200 | Mid | Santa Rosa Island | Island | 33.975 | -120 |
| 357 | 6 | Jew et al., 2013b | 666-U1-6e | 12 | | 0.3 | 0.2 | 8200 | Mid | Santa Rosa Island | Island | 33.975 | -120 |
| 357 | 6 | Jew et al., 2013b | 666-U1-6f | 15 | | 0.3 | 0 | 8200 | Mid | Santa Rosa Island | Island | 33.975 | -120 |
| 358 | 6 | Jew et al., 2013b | 666-U1-8a | 0 | | 0.7 | 0.6 | 8200 | Mid | Santa Rosa Island | Island | 33.975 | -120 |
| 358 | 6 | Jew et al., 2013b | 666-U1-8b | 2 | | 0.5 | -0.3 | 8200 | Mid | Santa Rosa Island | Island | 33.975 | -120 |
| 358 | 6 | Jew et al., 2013b | 666-U1-8c | 6 | | 0.3 | -0.2 | 8200 | Mid | Santa Rosa Island | Island | 33.975 | -120 |
| 358 | 6 | Jew et al., 2013b | 666-U1-8d | 9 | | 0 | -0.1 | 8200 | Mid | Santa Rosa Island | Island | 33.975 | -120 |
| 358 | 6 | Jew et al., 2013b | 666-U1-8e | 12 | | -0.2 | -0.1 | 8200 | Mid | Santa Rosa Island | Island | 33.975 | -120 |
| 358 | 6 | Jew et al., 2013b | 666-U1-8f | 15 | | -0.5 | 0.3 | 8200 | Mid | Santa Rosa Island | Island | 33.975 | -120 |
| 359 | 6 | Jew et al., 2013b | 666-U1-9a | 0 | | 0 | 1.2 | 8200 | Mid | Santa Rosa Island | Island | 33.975 | -120 |
| 359 | 6 | Jew et al., 2013b | 666-U1-9b | 2 | | 0 | 0.1 | 8200 | Mid | Santa Rosa Island | Island | 33.975 | -120 |
| 359 | 6 | Jew et al., 2013b | 666-U1-9c | 6 | | -1 | -0.2 | 8200 | Mid | Santa Rosa Island | Island | 33.975 | -120 |
| 359 | 6 | Jew et al., 2013b | 666-U1-9d | 9 | | -1.1 | 0 | 8200 | Mid | Santa Rosa Island | Island | 33.975 | -120 |

| | | | | | | | | | | | | | |
|---|---|---|---|---|---|---|---|---|---|---|---|---|---|
| 359 | 6 | Jew et al., 2013b | 666-U1-9e | 12 | | -1 | 0.7 | 8200 | Mid | Santa Rosa Island | Island | 33.975 | -120 |
| 359 | 6 | Jew et al., 2013b | 666-U1-9f | 15 | | -1 | 0.7 | 8200 | Mid | Santa Rosa Island | Island | 33.975 | -120 |
| 360 | 6 | Jew et al., 2013b | 666-U3-21a | 0 | | 0.2 | 0.2 | 8200 | Mid | Santa Rosa Island | Island | 33.975 | -120 |
| 360 | 6 | Jew et al., 2013b | 666-U3-21b | 2 | | -0.7 | -0.2 | 8200 | Mid | Santa Rosa Island | Island | 33.975 | -120 |
| 360 | 6 | Jew et al., 2013b | 666-U3-21c | 6 | | -0.5 | 1 | 8200 | Mid | Santa Rosa Island | Island | 33.975 | -120 |
| 360 | 6 | Jew et al., 2013b | 666-U3-21d | 9 | | -0.1 | 1.1 | 8200 | Mid | Santa Rosa Island | Island | 33.975 | -120 |
| 360 | 6 | Jew et al., 2013b | 666-U3-21e | 12 | | -0.2 | 0.1 | 8200 | Mid | Santa Rosa Island | Island | 33.975 | -120 |
| 360 | 6 | Jew et al., 2013b | 666-U3-21f | 15 | | 0 | 0 | 8200 | Mid | Santa Rosa Island | Island | 33.975 | -120 |
| 361 | 6 | Jew et al., 2013b | 666-U3-23a | 0 | | 1 | 0.5 | 8200 | Mid | Santa Rosa Island | Island | 33.975 | -120 |
| 361 | 6 | Jew et al., 2013b | 666-U3-23b | 2 | | 0.5 | -0.1 | 8200 | Mid | Santa Rosa Island | Island | 33.975 | -120 |
| 361 | 6 | Jew et al., 2013b | 666-U3-23c | 6 | | -0.4 | 0.4 | 8200 | Mid | Santa Rosa Island | Island | 33.975 | -120 |
| 361 | 6 | Jew et al., 2013b | 666-U3-23d | 9 | | -0.6 | 0.6 | 8200 | Mid | Santa Rosa Island | Island | 33.975 | -120 |
| 361 | 6 | Jew et al., 2013b | 666-U3-23e | 12 | | 0.5 | 1 | 8200 | Mid | Santa Rosa Island | Island | 33.975 | -120 |
| 361 | 6 | Jew et al., 2013b | 666-U3-23f | 15 | | 0.6 | 0.5 | 8200 | Mid | Santa Rosa Island | Island | 33.975 | -120 |
| 362 | 6 | Jew et al., 2013b | 666-U3-24a | 0 | | 1.2 | 0.7 | 8200 | Mid | Santa Rosa Island | Island | 33.975 | -120 |
| 362 | 6 | Jew et al., 2013b | 666-U3-24b | 2 | | 1.6 | 0.5 | 8200 | Mid | Santa Rosa Island | Island | 33.975 | -120 |
| 362 | 6 | Jew et al., 2013b | 666-U3-24c | 6 | | 0.2 | -0.3 | 8200 | Mid | Santa Rosa Island | Island | 33.975 | -120 |
| 362 | 6 | Jew et al., 2013b | 666-U3-24d | 9 | | -0.5 | 0.6 | 8200 | Mid | Santa Rosa Island | Island | 33.975 | -120 |
| 362 | 6 | Jew et al., 2013b | 666-U3-24e | 12 | | 0.5 | 0.5 | 8200 | Mid | Santa Rosa Island | Island | 33.975 | -120 |

| | | | | | | | | | | | | | |
|---|---|---|---|---|---|---|---|---|---|---|---|---|---|
| 362 | 6 | Jew et al., 2013b | 666-U3-24f | 15 | | 0.6 | 0.8 | 8200 | Mid | Santa Rosa Island | Island | 33.975 | -120 |
| 363 | 6 | Jew et al., 2013b | 666-U3-25a | 0 | | 1 | 0.3 | 8200 | Mid | Santa Rosa Island | Island | 33.975 | -120 |
| 363 | 6 | Jew et al., 2013b | 666-U3-25b | 2 | | 0.8 | -0.1 | 8200 | Mid | Santa Rosa Island | Island | 33.975 | -120 |
| 363 | 6 | Jew et al., 2013b | 666-U3-25c | 6 | | 0.4 | 0.5 | 8200 | Mid | Santa Rosa Island | Island | 33.975 | -120 |
| 363 | 6 | Jew et al., 2013b | 666-U3-25d | 9 | | 0.4 | 0.9 | 8200 | Mid | Santa Rosa Island | Island | 33.975 | -120 |
| 363 | 6 | Jew et al., 2013b | 666-U3-25e | 12 | | 0.7 | 0.6 | 8200 | Mid | Santa Rosa Island | Island | 33.975 | -120 |
| 363 | 6 | Jew et al., 2013b | 666-U3-25f | 15 | | 0.8 | 0.4 | 8200 | Mid | Santa Rosa Island | Island | 33.975 | -120 |
| 364 | 6 | Jew et al., 2013b | 666-U3-27a | 0 | | 0.7 | 0.1 | 8200 | Mid | Santa Rosa Island | Island | 33.975 | -120 |
| 364 | 6 | Jew et al., 2013b | 666-U3-27b | 2 | | 0.3 | 1.3 | 8200 | Mid | Santa Rosa Island | Island | 33.975 | -120 |
| 364 | 6 | Jew et al., 2013b | 666-U3-27c | 6 | | 0.5 | -0.1 | 8200 | Mid | Santa Rosa Island | Island | 33.975 | -120 |
| 364 | 6 | Jew et al., 2013b | 666-U3-27d | 9 | | 0 | 1 | 8200 | Mid | Santa Rosa Island | Island | 33.975 | -120 |
| 364 | 6 | Jew et al., 2013b | 666-U3-27e | 12 | | 1 | -0.4 | 8200 | Mid | Santa Rosa Island | Island | 33.975 | -120 |
| 364 | 6 | Jew et al., 2013b | 666-U3-27f | 15 | | 0.2 | 0.1 | 8200 | Mid | Santa Rosa Island | Island | 33.975 | -120 |
| 365 | 6 | Jew et al., 2013b | 666-U3-29a | 0 | | 2 | 0.6 | 8200 | Mid | Santa Rosa Island | Island | 33.975 | -120 |
| 365 | 6 | Jew et al., 2013b | 666-U3-29b | 2 | | 0.9 | 0 | 8200 | Mid | Santa Rosa Island | Island | 33.975 | -120 |
| 365 | 6 | Jew et al., 2013b | 666-U3-29c | 6 | | 0.4 | -0.2 | 8200 | Mid | Santa Rosa Island | Island | 33.975 | -120 |
| 365 | 6 | Jew et al., 2013b | 666-U3-29d | 9 | | 0.1 | 0.2 | 8200 | Mid | Santa Rosa Island | Island | 33.975 | -120 |
| 365 | 6 | Jew et al., 2013b | 666-U3-29e | 12 | | -0.1 | 0.4 | 8200 | Mid | Santa Rosa Island | Island | 33.975 | -120 |
| 365 | 6 | Jew et al., 2013b | 666-U3-29f | 15 | | 0.1 | 0.9 | 8200 | Mid | Santa Rosa Island | Island | 33.975 | -120 |

| | | | | | | | | | | | | | |
|---|---|---|---|---|---|---|---|---|---|---|---|---|---|
| 366 | 6 | Jew et al., 2013b | 666-U3-30a | 0 | | 1.3 | 0 | 8200 | Mid | Santa Rosa Island | Island | 33.975 | -120 |
| 366 | 6 | Jew et al., 2013b | 666-U3-30b | 2 | | 0.8 | 1.6 | 8200 | Mid | Santa Rosa Island | Island | 33.975 | -120 |
| 366 | 6 | Jew et al., 2013b | 666-U3-30c | 6 | | 0.6 | 0.7 | 8200 | Mid | Santa Rosa Island | Island | 33.975 | -120 |
| 366 | 6 | Jew et al., 2013b | 666-U3-30d | 9 | | 0.1 | 0.2 | 8200 | Mid | Santa Rosa Island | Island | 33.975 | -120 |
| 366 | 6 | Jew et al., 2013b | 666-U3-30e | 12 | | 0 | 0.1 | 8200 | Mid | Santa Rosa Island | Island | 33.975 | -120 |
| 366 | 6 | Jew et al., 2013b | 666-U3-30f | 15 | | -0.4 | 1.1 | 8200 | Mid | Santa Rosa Island | Island | 33.975 | -120 |
| 367 | 6 | Jew et al., 2013b | 666-U3-31a | 0 | | 2 | 0.5 | 8200 | Mid | Santa Rosa Island | Island | 33.975 | -120 |
| 367 | 6 | Jew et al., 2013b | 666-U3-31b | 2 | | 0.7 | 0.5 | 8200 | Mid | Santa Rosa Island | Island | 33.975 | -120 |
| 367 | 6 | Jew et al., 2013b | 666-U3-31c | 6 | | 0.9 | 0.9 | 8200 | Mid | Santa Rosa Island | Island | 33.975 | -120 |
| 367 | 6 | Jew et al., 2013b | 666-U3-31d | 9 | | 1.1 | 0.9 | 8200 | Mid | Santa Rosa Island | Island | 33.975 | -120 |
| 367 | 6 | Jew et al., 2013b | 666-U3-31e | 12 | | 1 | 0.3 | 8200 | Mid | Santa Rosa Island | Island | 33.975 | -120 |
| 367 | 6 | Jew et al., 2013b | 666-U3-31f | 15 | | 0.7 | 0 | 8200 | Mid | Santa Rosa Island | Island | 33.975 | -120 |
| 368 | 6 | Jew et al., 2013b | 666-U3-36a | 0 | | 1 | 0.5 | 8200 | Mid | Santa Rosa Island | Island | 33.975 | -120 |
| 368 | 6 | Jew et al., 2013b | 666-U3-36b | 2 | | 1 | -0.2 | 8200 | Mid | Santa Rosa Island | Island | 33.975 | -120 |
| 368 | 6 | Jew et al., 2013b | 666-U3-36c | 6 | | -0.1 | 1.1 | 8200 | Mid | Santa Rosa Island | Island | 33.975 | -120 |
| 368 | 6 | Jew et al., 2013b | 666-U3-36d | 9 | | 0.4 | 1 | 8200 | Mid | Santa Rosa Island | Island | 33.975 | -120 |
| 368 | 6 | Jew et al., 2013b | 666-U3-36e | 12 | | 0.4 | 0.8 | 8200 | Mid | Santa Rosa Island | Island | 33.975 | -120 |
| 368 | 6 | Jew et al., 2013b | 666-U3-36f | 15 | | 0.6 | 0.6 | 8200 | Mid | Santa Rosa Island | Island | 33.975 | -120 |
| 369 | 6 | Jew et al., 2013b | 666-U3-39a | 0 | | 0.2 | 0 | 8200 | Mid | Santa Rosa Island | Island | 33.975 | -120 |

| | | | | | | | | | | | | | |
|---|---|---|---|---|---|---|---|---|---|---|---|---|---|
| 369 | 6 | Jew et al., 2013b | 666-U3-39b | 2 | | 0.5 | 1.4 | 8200 | Mid | Santa Rosa Island | Island | 33.975 | -120 |
| 369 | 6 | Jew et al., 2013b | 666-U3-39c | 6 | | 0.4 | 1 | 8200 | Mid | Santa Rosa Island | Island | 33.975 | -120 |
| 369 | 6 | Jew et al., 2013b | 666-U3-39d | 9 | | -0.1 | 0.3 | 8200 | Mid | Santa Rosa Island | Island | 33.975 | -120 |
| 369 | 6 | Jew et al., 2013b | 666-U3-39e | 12 | | 0.1 | 1.2 | 8200 | Mid | Santa Rosa Island | Island | 33.975 | -120 |
| 369 | 6 | Jew et al., 2013b | 666-U3-39f | 15 | | 0.6 | 1.2 | 8200 | Mid | Santa Rosa Island | Island | 33.975 | -120 |
| 370 | 17 | Kennett 1998 | | 0 | | | 0.68 | 28 | Mod | Santa Cruz Island | Island | 34.047 | -119.6 |
| 370 | 17 | Kennett 1998 | | 2 | | | 0.44 | 28 | Mod | Santa Cruz Island | Island | 34.047 | -119.6 |
| 370 | 17 | Kennett 1998 | | 4 | | | 0.53 | 28 | Mod | Santa Cruz Island | Island | 34.047 | -119.6 |
| 370 | 17 | Kennett 1998 | | 6 | | | -0.14 | 28 | Mod | Santa Cruz Island | Island | 34.047 | -119.6 |
| 370 | 17 | Kennett 1998 | | 8 | | | 0.25 | 28 | Mod | Santa Cruz Island | Island | 34.047 | -119.6 |
| 370 | 17 | Kennett 1998 | | 10 | | | 0.57 | 28 | Mod | Santa Cruz Island | Island | 34.047 | -119.6 |
| 370 | 17 | Kennett 1998 | | 12 | | | 0.85 | 28 | Mod | Santa Cruz Island | Island | 34.047 | -119.6 |
| 370 | 17 | Kennett 1998 | | 14 | | | 0.50 | 28 | Mod | Santa Cruz Island | Island | 34.047 | -119.6 |
| 370 | 17 | Kennett 1998 | | 16 | | | 0.11 | 28 | Mod | Santa Cruz Island | Island | 34.047 | -119.6 |
| 370 | 17 | Kennett 1998 | | 18 | | | -0.28 | 28 | Mod | Santa Cruz Island | Island | 34.047 | -119.6 |
| 370 | 17 | Kennett 1998 | | 20 | | | 0.18 | 28 | Mod | Santa Cruz Island | Island | 34.047 | -119.6 |
| 370 | 17 | Kennett 1998 | | 22 | | | 0.54 | 28 | Mod | Santa Cruz Island | Island | 34.047 | -119.6 |
| 370 | 17 | Kennett 1998 | | 24 | | | 0.38 | 28 | Mod | Santa Cruz Island | Island | 34.047 | -119.6 |
| 370 | 17 | Kennett 1998 | | 26 | | | -0.07 | 28 | Mod | Santa Cruz Island | Island | 34.047 | -119.6 |

| | | | | | | | | | | | | | |
|---|---|---|---|---|---|---|---|---|---|---|---|---|---|
| 370 | 17 | Kennett 1998 | | 28 | | | 0.05 | 28 | Mod | Santa Cruz Island | Island | 34.047 | -119.6 |
| 370 | 17 | Kennett 1998 | | 30 | | | 0.16 | 28 | Mod | Santa Cruz Island | Island | 34.047 | -119.6 |
| 370 | 17 | Kennett 1998 | | 32 | | | 0.31 | 28 | Mod | Santa Cruz Island | Island | 34.047 | -119.6 |
| 371 | 20 | Kennett 1998 | | 0 | | | 0.14 | 33 | Mod | Santa Cruz Island | Island | 34.047 | -119.6 |
| 371 | 20 | Kennett 1998 | | 2 | | | 0.53 | 33 | Mod | Santa Cruz Island | Island | 34.047 | -119.6 |
| 371 | 20 | Kennett 1998 | | 4 | | | 0.29 | 33 | Mod | Santa Cruz Island | Island | 34.047 | -119.6 |
| 371 | 20 | Kennett 1998 | | 6 | | | 0.65 | 33 | Mod | Santa Cruz Island | Island | 34.047 | -119.6 |
| 371 | 20 | Kennett 1998 | | 8 | | | 0.12 | 33 | Mod | Santa Cruz Island | Island | 34.047 | -119.6 |
| 371 | 20 | Kennett 1998 | | 10 | | | -0.11 | 33 | Mod | Santa Cruz Island | Island | 34.047 | -119.6 |
| 371 | 20 | Kennett 1998 | | 12 | | | -0.14 | 33 | Mod | Santa Cruz Island | Island | 34.047 | -119.6 |
| 371 | 20 | Kennett 1998 | | 14 | | | 0.81 | 33 | Mod | Santa Cruz Island | Island | 34.047 | -119.6 |
| 371 | 20 | Kennett 1998 | | 16 | | | 0.27 | 33 | Mod | Santa Cruz Island | Island | 34.047 | -119.6 |
| 371 | 20 | Kennett 1998 | | 18 | | | -0.64 | 33 | Mod | Santa Cruz Island | Island | 34.047 | -119.6 |
| 371 | 20 | Kennett 1998 | | 20 | | | -0.16 | 33 | Mod | Santa Cruz Island | Island | 34.047 | -119.6 |
| 371 | 20 | Kennett 1998 | | 22 | | | 0.45 | 33 | Mod | Santa Cruz Island | Island | 34.047 | -119.6 |
| 371 | 20 | Kennett 1998 | | 24 | | | 0.30 | 33 | Mod | Santa Cruz Island | Island | 34.047 | -119.6 |
| 371 | 20 | Kennett 1998 | | 26 | | | -0.23 | 33 | Mod | Santa Cruz Island | Island | 34.047 | -119.6 |
| 371 | 20 | Kennett 1998 | | 28 | | | -0.41 | 33 | Mod | Santa Cruz Island | Island | 34.047 | -119.6 |
| 371 | 20 | Kennett 1998 | | 30 | | | -0.13 | 33 | Mod | Santa Cruz Island | Island | 34.047 | -119.6 |

| | | | | | | | | | | | | | |
|---|---|---|---|---|---|---|---|---|---|---|---|---|---|
| 371 | 20 | Kennett 1998 | | 32 | | | -0.03 | 33 | Mod | Santa Cruz Island | Island | 34.047 | -119.6 |
| 371 | 20 | Kennett 1998 | | 34 | | | -0.29 | 33 | Mod | Santa Cruz Island | Island | 34.047 | -119.6 |
| 371 | 20 | Kennett 1998 | | 36 | | | -0.02 | 33 | Mod | Santa Cruz Island | Island | 34.047 | -119.6 |
| 371 | 20 | Kennett 1998 | | 38 | | | 0.66 | 33 | Mod | Santa Cruz Island | Island | 34.047 | -119.6 |
| 372 | 20 | Kennett 1998 | | 0 | | | 0.47 | 33 | Mod | Santa Cruz Island | Island | 34.047 | -119.6 |
| 372 | 20 | Kennett 1998 | | 2 | | | 0.15 | 33 | Mod | Santa Cruz Island | Island | 34.047 | -119.6 |
| 372 | 20 | Kennett 1998 | | 4 | | | 0.22 | 33 | Mod | Santa Cruz Island | Island | 34.047 | -119.6 |
| 372 | 20 | Kennett 1998 | | 6 | | | 0.80 | 33 | Mod | Santa Cruz Island | Island | 34.047 | -119.6 |
| 372 | 20 | Kennett 1998 | | 8 | | | -0.24 | 33 | Mod | Santa Cruz Island | Island | 34.047 | -119.6 |
| 372 | 20 | Kennett 1998 | | 10 | | | -0.41 | 33 | Mod | Santa Cruz Island | Island | 34.047 | -119.6 |
| 372 | 20 | Kennett 1998 | | 12 | | | -0.10 | 33 | Mod | Santa Cruz Island | Island | 34.047 | -119.6 |
| 372 | 20 | Kennett 1998 | | 14 | | | 0.57 | 33 | Mod | Santa Cruz Island | Island | 34.047 | -119.6 |
| 372 | 20 | Kennett 1998 | | 16 | | | 0.52 | 33 | Mod | Santa Cruz Island | Island | 34.047 | -119.6 |
| 372 | 20 | Kennett 1998 | | 18 | | | 0.22 | 33 | Mod | Santa Cruz Island | Island | 34.047 | -119.6 |
| 372 | 20 | Kennett 1998 | | 20 | | | -0.12 | 33 | Mod | Santa Cruz Island | Island | 34.047 | -119.6 |
| 372 | 20 | Kennett 1998 | | 22 | | | -0.42 | 33 | Mod | Santa Cruz Island | Island | 34.047 | -119.6 |
| 372 | 20 | Kennett 1998 | | 24 | | | -0.10 | 33 | Mod | Santa Cruz Island | Island | 34.047 | -119.6 |
| 372 | 20 | Kennett 1998 | | 26 | | | -0.07 | 33 | Mod | Santa Cruz Island | Island | 34.047 | -119.6 |
| 372 | 20 | Kennett 1998 | | 28 | | | 0.05 | 33 | Mod | Santa Cruz Island | Island | 34.047 | -119.6 |

| | | | | | | | | | | | | | |
|---|---|---|---|---|---|---|---|---|---|---|---|---|---|
| 372 | 20 | Kennett 1998 | | 30 | | | 0.05 | 33 | Mod | Santa Cruz Island | Island | 34.047 | -119.6 |
| 372 | 20 | Kennett 1998 | | 32 | | | -0.24 | 33 | Mod | Santa Cruz Island | Island | 34.047 | -119.6 |
| 372 | 20 | Kennett 1998 | | 34 | | | -0.43 | 33 | Mod | Santa Cruz Island | Island | 34.047 | -119.6 |
| 372 | 20 | Kennett 1998 | | 36 | | | -0.62 | 33 | Mod | Santa Cruz Island | Island | 34.047 | -119.6 |
| 372 | 20 | Kennett 1998 | | 38 | | | -0.58 | 33 | Mod | Santa Cruz Island | Island | 34.047 | -119.6 |
| 373 | 5 | Rick et al., 2006 | CA-SRI-191 Santa Rosa Island | TMSRAM1cA | | 2.10 | 0.40 | 4330 | Mid | Santa Rosa Island | Island | 33.95 | -120.1 |
| 373 | 5 | Rick et al., 2006 | CA-SRI-191 Santa Rosa Island | TMSRAM1cB | | 2.00 | 0.50 | 4330 | Mid | Santa Rosa Island | Island | 33.95 | -120.1 |
| 373 | 5 | Rick et al., 2006 | CA-SRI-191 Santa Rosa Island | TMSRAM1cC | | 2.50 | 0.60 | 4330 | Mid | Santa Rosa Island | Island | 33.95 | -120.1 |
| 373 | 5 | Rick et al., 2006 | CA-SRI-191 Santa Rosa Island | TMSRAM1cE | | 2.50 | 0.70 | 4330 | Mid | Santa Rosa Island | Island | 33.95 | -120.1 |
| 373 | 5 | Rick et al., 2006 | CA-SRI-191 Santa Rosa Island | TMSRAM1cD | | 2.30 | 0.80 | 4330 | Mid | Santa Rosa Island | Island | 33.95 | -120.1 |
| 374 | 5 | Rick et al., 2006 | CA-SRI-191 Santa Rosa Island | SRI191U1Cm2cc1 | | 0.50 | 0.50 | 4330 | Mid | Santa Rosa Island | Island | 33.95 | -120.1 |
| 374 | 5 | Rick et al., 2006 | CA-SRI-191 Santa Rosa Island | SRI191U1Cm2cc3 | | 0.60 | 0.70 | 4330 | Mid | Santa Rosa Island | Island | 33.95 | -120.1 |
| 374 | 5 | Rick et al., 2006 | CA-SRI-191 Santa Rosa Island | SRI191U1Cm2cc2 | | 0.50 | 1.00 | 4330 | Mid | Santa Rosa Island | Island | 33.95 | -120.1 |

| | | | | | | | | | | | | | |
|---|---|---|---|---|---|---|---|---|---|---|---|---|---|
| 374 | 5 | Rick et al., 2006 | CA-SRI-191 Santa Rosa Island | SRI191U1Cm2cc4 | | 0.30 | 1.10 | 4330 | Mid | Santa Rosa Island | Island | 33.95 | -120.1 |
| 374 | 5 | Rick et al., 2006 | CA-SRI-191 Santa Rosa Island | SRI191U1Cm2cc5 | | 0.20 | 1.10 | 4330 | Mid | Santa Rosa Island | Island | 33.95 | -120.1 |
| 375 | 5 | Rick et al., 2006 | CA-SRI-191 Santa Rosa Island | SRI191U1Cm3cc1 | | 0.10 | 0.30 | 4330 | Mid | Santa Rosa Island | Island | 33.95 | -120.1 |
| 375 | 5 | Rick et al., 2006 | CA-SRI-191 Santa Rosa Island | SRI191U1Cm3cc5 | | 0.50 | 0.70 | 4330 | Mid | Santa Rosa Island | Island | 33.95 | -120.1 |
| 375 | 5 | Rick et al., 2006 | CA-SRI-191 Santa Rosa Island | SRI191U1Cm3cc2 | | 0.10 | 0.80 | 4330 | Mid | Santa Rosa Island | Island | 33.95 | -120.1 |
| 375 | 5 | Rick et al., 2006 | CA-SRI-191 Santa Rosa Island | SRI191U1Cm3cc4 | | 0.20 | 0.90 | 4330 | Mid | Santa Rosa Island | Island | 33.95 | -120.1 |
| 375 | 5 | Rick et al., 2006 | CA-SRI-191 Santa Rosa Island | SRI191U1Cm3cc3 | | 0.30 | 1.00 | 4330 | Mid | Santa Rosa Island | Island | 33.95 | -120.1 |
| 376 | 4 | Rick et al., 2006 | CA-SRI-191 Santa Rosa Island | TMSBSI1cD | | 0.60 | 0.10 | 4330 | Mid | Santa Rosa Island | Island | 33.95 | -120.1 |
| 376 | 4 | Rick et al., 2006 | CA-SRI-191 Santa Rosa Island | TMSBSI1cB | | 0.40 | 0.20 | 4330 | Mid | Santa Rosa Island | Island | 33.95 | -120.1 |
| 376 | 4 | Rick et al., 2006 | CA-SRI-191 Santa Rosa Island | TMSBSI1cC | | 0.50 | 0.30 | 4330 | Mid | Santa Rosa Island | Island | 33.95 | -120.1 |
| 376 | 4 | Rick et al., 2006 | CA-SRI-191 Santa Rosa Island | TMSBSI1cA | | 0.80 | 1.10 | 4330 | Mid | Santa Rosa Island | Island | 33.95 | -120.1 |

| | | | | | | | | | | | | | |
|---|---|---|---|---|---|---|---|---|---|---|---|---|---|
| 377 | 5 | Rick et al., 2006 | CA-SRI-191 Santa Rosa Island | TMSBSI2cD | | 0.60 | -0.50 | 4330 | Mid | Santa Rosa Island | Island | 33.95 | -120.1 |
| 377 | 5 | Rick et al., 2006 | CA-SRI-191 Santa Rosa Island | TMSBSI2cC | | 1.00 | -0.40 | 4330 | Mid | Santa Rosa Island | Island | 33.95 | -120.1 |
| 377 | 5 | Rick et al., 2006 | CA-SRI-191 Santa Rosa Island | TMSBSI2cA | | 0.90 | -0.10 | 4330 | Mid | Santa Rosa Island | Island | 33.95 | -120.1 |
| 377 | 5 | Rick et al., 2006 | CA-SRI-191 Santa Rosa Island | TMSBSI2cE | | 0.70 | 0.50 | 4330 | Mid | Santa Rosa Island | Island | 33.95 | -120.1 |
| 377 | 5 | Rick et al., 2006 | CA-SRI-191 Santa Rosa Island | TMSBSI2cB | | 0.50 | 1.00 | 4330 | Mid | Santa Rosa Island | Island | 33.95 | -120.1 |
| 378 | 5 | Rick et al., 2006 | CA-SRI-191 Santa Rosa Island | TMSBSI3cA | | -0.40 | -0.10 | 4330 | Mid | Santa Rosa Island | Island | 33.95 | -120.1 |
| 378 | 5 | Rick et al., 2006 | CA-SRI-191 Santa Rosa Island | TMSBSI3cB | | -0.20 | 0.30 | 4330 | Mid | Santa Rosa Island | Island | 33.95 | -120.1 |
| 378 | 5 | Rick et al., 2006 | CA-SRI-191 Santa Rosa Island | TMSBSI3cD | | 0.50 | 0.40 | 4330 | Mid | Santa Rosa Island | Island | 33.95 | -120.1 |
| 378 | 5 | Rick et al., 2006 | CA-SRI-191 Santa Rosa Island | TMSBSI3cC | | 0.80 | 0.60 | 4330 | Mid | Santa Rosa Island | Island | 33.95 | -120.1 |
| 378 | 5 | Rick et al., 2006 | CA-SRI-191 Santa Rosa Island | TMSBSI3cE | | 0.80 | 0.60 | 4330 | Mid | Santa Rosa Island | Island | 33.95 | -120.1 |
| 379 | 60 | Robbins et al., 2013 | Cuyler Harbor | 0.00 | | 0.12 | 1.04 | 15 | Mod | San Miguel Island | Island | 34.047 | -120.4 |
| 379 | 60 | Robbins et al., 2013 | Cuyler Harbor | 2.00 | | -0.46 | 0.65 | 15 | Mod | San Miguel Island | Island | 34.047 | -120.4 |

| | | | | | | | | | | | | | |
|---|---|---|---|---|---|---|---|---|---|---|---|---|---|
| 379 | 60 | Robbins et al., 2013 | Cuyler Harbor | 4.00 | | -0.24 | 0.81 | 15 | Mod | San Miguel Island | Island | 34.047 | -120.4 |
| 379 | 60 | Robbins et al., 2013 | Cuyler Harbor | 6.00 | | -0.28 | 0.06 | 15 | Mod | San Miguel Island | Island | 34.047 | -120.4 |
| 379 | 60 | Robbins et al., 2013 | Cuyler Harbor | 8.00 | | -0.34 | 0.34 | 15 | Mod | San Miguel Island | Island | 34.047 | -120.4 |
| 379 | 60 | Robbins et al., 2013 | Cuyler Harbor | 10.00 | | -0.83 | 1.00 | 15 | Mod | San Miguel Island | Island | 34.047 | -120.4 |
| 379 | 60 | Robbins et al., 2013 | Cuyler Harbor | 12.00 | | -0.69 | 0.88 | 15 | Mod | San Miguel Island | Island | 34.047 | -120.4 |
| 379 | 60 | Robbins et al., 2013 | Cuyler Harbor | 14.00 | | -0.29 | 0.92 | 15 | Mod | San Miguel Island | Island | 34.047 | -120.4 |
| 379 | 60 | Robbins et al., 2013 | Cuyler Harbor | 16.00 | | -0.14 | 0.47 | 15 | Mod | San Miguel Island | Island | 34.047 | -120.4 |
| 379 | 60 | Robbins et al., 2013 | Cuyler Harbor | 18.00 | | -0.56 | 0.31 | 15 | Mod | San Miguel Island | Island | 34.047 | -120.4 |
| 379 | 60 | Robbins et al., 2013 | Cuyler Harbor | 20.00 | | -0.86 | 0.17 | 15 | Mod | San Miguel Island | Island | 34.047 | -120.4 |
| 379 | 60 | Robbins et al., 2013 | Cuyler Harbor | 22.00 | | -0.75 | 0.80 | 15 | Mod | San Miguel Island | Island | 34.047 | -120.4 |
| 379 | 60 | Robbins et al., 2013 | Cuyler Harbor | 24.00 | | -0.94 | 1.02 | 15 | Mod | San Miguel Island | Island | 34.047 | -120.4 |
| 379 | 60 | Robbins et al., 2013 | Cuyler Harbor | 26.00 | | -0.78 | 0.93 | 15 | Mod | San Miguel Island | Island | 34.047 | -120.4 |
| 379 | 60 | Robbins et al., 2013 | Cuyler Harbor | 28.00 | | -0.11 | 0.58 | 15 | Mod | San Miguel Island | Island | 34.047 | -120.4 |
| 379 | 60 | Robbins et al., 2013 | Cuyler Harbor | 30.00 | | -0.06 | 0.32 | 15 | Mod | San Miguel Island | Island | 34.047 | -120.4 |
| 379 | 60 | Robbins et al., 2013 | Cuyler Harbor | 32.00 | | -0.24 | 0.54 | 15 | Mod | San Miguel Island | Island | 34.047 | -120.4 |
| 379 | 60 | Robbins et al., 2013 | Cuyler Harbor | 34.00 | | -0.80 | 0.83 | 15 | Mod | San Miguel Island | Island | 34.047 | -120.4 |
| 379 | 60 | Robbins et al., 2013 | Cuyler Harbor | 36.00 | | -0.90 | 1.11 | 15 | Mod | San Miguel Island | Island | 34.047 | -120.4 |
| 379 | 60 | Robbins et al., 2013 | Cuyler Harbor | 38.00 | | -0.57 | 1.07 | 15 | Mod | San Miguel Island | Island | 34.047 | -120.4 |
| 379 | 60 | Robbins et al., 2013 | Cuyler Harbor | 40.00 | | -0.43 | 0.98 | 15 | Mod | San Miguel Island | Island | 34.047 | -120.4 |

| | | | | | | | | | | | | | |
|---|---|---|---|---|---|---|---|---|---|---|---|---|---|
| 379 | 60 | Robbins et al., 2013 | Cuyler Harbor | 42.00 | | -0.35 | 0.86 | 15 | Mod | San Miguel Island | Island | 34.047 | -120.4 |
| 379 | 60 | Robbins et al., 2013 | Cuyler Harbor | 44.00 | | -0.18 | 0.25 | 15 | Mod | San Miguel Island | Island | 34.047 | -120.4 |
| 379 | 60 | Robbins et al., 2013 | Cuyler Harbor | 46.00 | | -0.20 | 0.34 | 15 | Mod | San Miguel Island | Island | 34.047 | -120.4 |
| 379 | 60 | Robbins et al., 2013 | Cuyler Harbor | 48.00 | | -0.27 | 0.51 | 15 | Mod | San Miguel Island | Island | 34.047 | -120.4 |
| 379 | 60 | Robbins et al., 2013 | Cuyler Harbor | 50.00 | | -0.27 | 0.37 | 15 | Mod | San Miguel Island | Island | 34.047 | -120.4 |
| 379 | 60 | Robbins et al., 2013 | Cuyler Harbor | 52.00 | | -0.59 | 0.32 | 15 | Mod | San Miguel Island | Island | 34.047 | -120.4 |
| 379 | 60 | Robbins et al., 2013 | Cuyler Harbor | 54.00 | | -0.86 | 0.79 | 15 | Mod | San Miguel Island | Island | 34.047 | -120.4 |
| 379 | 60 | Robbins et al., 2013 | Cuyler Harbor | 56.00 | | -0.73 | 0.83 | 15 | Mod | San Miguel Island | Island | 34.047 | -120.4 |
| 379 | 60 | Robbins et al., 2013 | Cuyler Harbor | 58.00 | | -0.31 | 0.76 | 15 | Mod | San Miguel Island | Island | 34.047 | -120.4 |
| 379 | 60 | Robbins et al., 2013 | Cuyler Harbor | 60.00 | | -0.26 | 0.69 | 15 | Mod | San Miguel Island | Island | 34.047 | -120.4 |
| 379 | 60 | Robbins et al., 2013 | Cuyler Harbor | 62.00 | | -0.30 | 0.82 | 15 | Mod | San Miguel Island | Island | 34.047 | -120.4 |
| 379 | 60 | Robbins et al., 2013 | Cuyler Harbor | 64.00 | | -0.03 | 0.79 | 15 | Mod | San Miguel Island | Island | 34.047 | -120.4 |
| 379 | 60 | Robbins et al., 2013 | Cuyler Harbor | 66.00 | | -0.16 | 0.71 | 15 | Mod | San Miguel Island | Island | 34.047 | -120.4 |
| 379 | 60 | Robbins et al., 2013 | Cuyler Harbor | 68.00 | | -0.28 | 0.63 | 15 | Mod | San Miguel Island | Island | 34.047 | -120.4 |
| 379 | 60 | Robbins et al., 2013 | Cuyler Harbor | 70.00 | | -0.40 | 0.13 | 15 | Mod | San Miguel Island | Island | 34.047 | -120.4 |
| 379 | 60 | Robbins et al., 2013 | Cuyler Harbor | 72.00 | | -0.64 | -0.10 | 15 | Mod | San Miguel Island | Island | 34.047 | -120.4 |
| 379 | 60 | Robbins et al., 2013 | Cuyler Harbor | 74.00 | | -0.90 | -0.08 | 15 | Mod | San Miguel Island | Island | 34.047 | -120.4 |
| 379 | 60 | Robbins et al., 2013 | Cuyler Harbor | 76.00 | | -0.85 | 0.09 | 15 | Mod | San Miguel Island | Island | 34.047 | -120.4 |
| 379 | 60 | Robbins et al., 2013 | Cuyler Harbor | 78.00 | | -0.70 | -0.13 | 15 | Mod | San Miguel Island | Island | 34.047 | -120.4 |

| | | | | | | | | | | | | | |
|---|---|---|---|---|---|---|---|---|---|---|---|---|---|
| 379 | 60 | Robbins et al., 2013 | Cuyler Harbor | 80.00 | | -0.92 | 0.36 | 15 | Mod | San Miguel Island | Island | 34.047 | -120.4 |
| 379 | 60 | Robbins et al., 2013 | Cuyler Harbor | 82.00 | | -1.12 | 0.42 | 15 | Mod | San Miguel Island | Island | 34.047 | -120.4 |
| 379 | 60 | Robbins et al., 2013 | Cuyler Harbor | 84.00 | | -0.94 | 0.71 | 15 | Mod | San Miguel Island | Island | 34.047 | -120.4 |
| 379 | 60 | Robbins et al., 2013 | Cuyler Harbor | 86.00 | | -0.90 | 0.73 | 15 | Mod | San Miguel Island | Island | 34.047 | -120.4 |
| 379 | 60 | Robbins et al., 2013 | Cuyler Harbor | 88.00 | | -0.86 | 0.78 | 15 | Mod | San Miguel Island | Island | 34.047 | -120.4 |
| 379 | 60 | Robbins et al., 2013 | Cuyler Harbor | 90.00 | | -0.87 | 0.70 | 15 | Mod | San Miguel Island | Island | 34.047 | -120.4 |
| 379 | 60 | Robbins et al., 2013 | Cuyler Harbor | 92.00 | | -0.46 | 0.71 | 15 | Mod | San Miguel Island | Island | 34.047 | -120.4 |
| 379 | 60 | Robbins et al., 2013 | Cuyler Harbor | 94.00 | | -0.21 | 0.67 | 15 | Mod | San Miguel Island | Island | 34.047 | -120.4 |
| 379 | 60 | Robbins et al., 2013 | Cuyler Harbor | 96.00 | | -0.11 | 0.71 | 15 | Mod | San Miguel Island | Island | 34.047 | -120.4 |
| 379 | 60 | Robbins et al., 2013 | Cuyler Harbor | 98.00 | | -0.12 | 0.84 | 15 | Mod | San Miguel Island | Island | 34.047 | -120.4 |
| 379 | 60 | Robbins et al., 2013 | Cuyler Harbor | 100.00 | | -0.07 | 0.63 | 15 | Mod | San Miguel Island | Island | 34.047 | -120.4 |
| 379 | 60 | Robbins et al., 2013 | Cuyler Harbor | 102.00 | | -0.25 | 0.22 | 15 | Mod | San Miguel Island | Island | 34.047 | -120.4 |
| 379 | 60 | Robbins et al., 2013 | Cuyler Harbor | 104.00 | | -0.34 | 0.32 | 15 | Mod | San Miguel Island | Island | 34.047 | -120.4 |
| 379 | 60 | Robbins et al., 2013 | Cuyler Harbor | 106.00 | | -0.48 | 0.14 | 15 | Mod | San Miguel Island | Island | 34.047 | -120.4 |
| 379 | 60 | Robbins et al., 2013 | Cuyler Harbor | 108.00 | | -0.57 | 0.23 | 15 | Mod | San Miguel Island | Island | 34.047 | -120.4 |
| 379 | 60 | Robbins et al., 2013 | Cuyler Harbor | 110.00 | | -1.03 | -0.08 | 15 | Mod | San Miguel Island | Island | 34.047 | -120.4 |
| 379 | 60 | Robbins et al., 2013 | Cuyler Harbor | 112.00 | | -0.93 | 0.35 | 15 | Mod | San Miguel Island | Island | 34.047 | -120.4 |
| 379 | 60 | Robbins et al., 2013 | Cuyler Harbor | 114.00 | | -0.75 | 0.24 | 15 | Mod | San Miguel Island | Island | 34.047 | -120.4 |
| 379 | 60 | Robbins et al., 2013 | Cuyler Harbor | 116.00 | | -0.60 | -0.03 | 15 | Mod | San Miguel Island | Island | 34.047 | -120.4 |

| | | | | | | | | | | | | | |
|---|---|---|---|---|---|---|---|---|---|---|---|---|---|
| 379 | 60 | Robbins et al., 2013 | Cuyler Harbor | 118.00 | | -0.80 | -0.04 | 15 | Mod | San Miguel Island | Island | 34.047 | -120.4 |
| 380 | 12 | Robbins et al., 2013 | SRI-147-10-20 | 6.00 | | 0.08 | -0.61 | 365 | Mid | Santa Rosa Island | Island | 33.921 | -120.1 |
| 380 | 12 | Robbins et al., 2013 | SRI-147-10-20 | 8.00 | | 0.06 | -0.45 | 365 | Mid | Santa Rosa Island | Island | 33.921 | -120.1 |
| 380 | 12 | Robbins et al., 2013 | SRI-147-10-20 | 2.00 | | 0.17 | -0.36 | 365 | Mid | Santa Rosa Island | Island | 33.921 | -120.1 |
| 380 | 12 | Robbins et al., 2013 | SRI-147-10-20 | 10.00 | | -0.07 | -0.21 | 365 | Mid | Santa Rosa Island | Island | 33.921 | -120.1 |
| 380 | 12 | Robbins et al., 2013 | SRI-147-10-20 | 4.00 | | 0.14 | -0.18 | 365 | Mid | Santa Rosa Island | Island | 33.921 | -120.1 |
| 380 | 12 | Robbins et al., 2013 | SRI-147-10-20 | 0.00 | | 0.10 | -0.12 | 365 | Mid | Santa Rosa Island | Island | 33.921 | -120.1 |
| 380 | 12 | Robbins et al., 2013 | SRI-147-10-20 | 12.00 | | -0.01 | 0.55 | 365 | Mid | Santa Rosa Island | Island | 33.921 | -120.1 |
| 380 | 12 | Robbins et al., 2013 | SRI-147-10-20 | 22.00 | | 0.24 | 0.63 | 365 | Mid | Santa Rosa Island | Island | 33.921 | -120.1 |
| 380 | 12 | Robbins et al., 2013 | SRI-147-10-20 | 16.00 | | -0.20 | 1.10 | 365 | Mid | Santa Rosa Island | Island | 33.921 | -120.1 |
| 380 | 12 | Robbins et al., 2013 | SRI-147-10-20 | 20.00 | | 0.30 | 1.11 | 365 | Mid | Santa Rosa Island | Island | 33.921 | -120.1 |
| 380 | 12 | Robbins et al., 2013 | SRI-147-10-20 | 18.00 | | -0.22 | 1.17 | 365 | Mid | Santa Rosa Island | Island | 33.921 | -120.1 |
| 380 | 12 | Robbins et al., 2013 | SRI-147-10-20 | 14.00 | | -0.04 | 1.24 | 365 | Mid | Santa Rosa Island | Island | 33.921 | -120.1 |
| 381 | 15 | Robbins et al., 2013 | SRI-147-100-110 | 18.00 | | 0.00 | 0.09 | 4115 | Mid | Santa Rosa Island | Island | 33.921 | -120.1 |
| 381 | 15 | Robbins et al., 2013 | SRI-147-100-110 | 22.00 | | 0.29 | 0.32 | 4115 | Mid | Santa Rosa Island | Island | 33.921 | -120.1 |
| 381 | 15 | Robbins et al., 2013 | SRI-147-100-110 | 12.00 | | -0.08 | 0.38 | 4115 | Mid | Santa Rosa Island | Island | 33.921 | -120.1 |
| 381 | 15 | Robbins et al., 2013 | SRI-147-100-110 | 20.00 | | -0.44 | 0.53 | 4115 | Mid | Santa Rosa Island | Island | 33.921 | -120.1 |
| 381 | 15 | Robbins et al., 2013 | SRI-147-100-110 | 34.00 | | 0.11 | 0.55 | 4115 | Mid | Santa Rosa Island | Island | 33.921 | -120.1 |
| 381 | 15 | Robbins et al., 2013 | SRI-147-100-110 | 8.00 | | 0.17 | 0.60 | 4115 | Mid | Santa Rosa Island | Island | 33.921 | -120.1 |

| | | | | | | | | | | | | | |
|---|---|---|---|---|---|---|---|---|---|---|---|---|---|
| 381 | 15 | Robbins et al., 2013 | SRI-147-100-110 | 6.00 | | 0.43 | 0.68 | 4115 | Mid | Santa Rosa Island | Island | 33.921 | -120.1 |
| 381 | 15 | Robbins et al., 2013 | SRI-147-100-110 | 38.00 | | -0.03 | 0.76 | 4115 | Mid | Santa Rosa Island | Island | 33.921 | -120.1 |
| 381 | 15 | Robbins et al., 2013 | SRI-147-100-110 | 0.00 | | -0.07 | 0.79 | 4115 | Mid | Santa Rosa Island | Island | 33.921 | -120.1 |
| 381 | 15 | Robbins et al., 2013 | SRI-147-100-110 | 36.00 | | 0.04 | 0.83 | 4115 | Mid | Santa Rosa Island | Island | 33.921 | -120.1 |
| 381 | 15 | Robbins et al., 2013 | SRI-147-100-110 | 16.00 | | -0.24 | 0.85 | 4115 | Mid | Santa Rosa Island | Island | 33.921 | -120.1 |
| 381 | 15 | Robbins et al., 2013 | SRI-147-100-110 | 2.00 | | -0.66 | 0.93 | 4115 | Mid | Santa Rosa Island | Island | 33.921 | -120.1 |
| 381 | 15 | Robbins et al., 2013 | SRI-147-100-110 | 14.00 | | -0.08 | 0.94 | 4115 | Mid | Santa Rosa Island | Island | 33.921 | -120.1 |
| 381 | 15 | Robbins et al., 2013 | SRI-147-100-110 | 4.00 | | -0.05 | 1.01 | 4115 | Mid | Santa Rosa Island | Island | 33.921 | -120.1 |
| 381 | 15 | Robbins et al., 2013 | SRI-147-100-110 | 10.00 | | -0.30 | 1.16 | 4115 | Mid | Santa Rosa Island | Island | 33.921 | -120.1 |
| 382 | 15 | Robbins et al., 2013 | SRI-147-110-120 | 4.00 | | 0.73 | -0.49 | 4256 | Mid | Santa Rosa Island | Island | 33.921 | -120.1 |
| 382 | 15 | Robbins et al., 2013 | SRI-147-110-120 | 2.00 | | 0.70 | -0.42 | 4256 | Mid | Santa Rosa Island | Island | 33.921 | -120.1 |
| 382 | 15 | Robbins et al., 2013 | SRI-147-110-120 | 6.00 | | 0.48 | -0.37 | 4256 | Mid | Santa Rosa Island | Island | 33.921 | -120.1 |
| 382 | 15 | Robbins et al., 2013 | SRI-147-110-120 | 8.00 | | 0.47 | -0.13 | 4256 | Mid | Santa Rosa Island | Island | 33.921 | -120.1 |
| 382 | 15 | Robbins et al., 2013 | SRI-147-110-120 | 10.00 | | 0.11 | -0.01 | 4256 | Mid | Santa Rosa Island | Island | 33.921 | -120.1 |
| 382 | 15 | Robbins et al., 2013 | SRI-147-110-120 | 0.00 | | 0.94 | 0.05 | 4256 | Mid | Santa Rosa Island | Island | 33.921 | -120.1 |
| 382 | 15 | Robbins et al., 2013 | SRI-147-110-120 | 12.00 | | 0.14 | 0.21 | 4256 | Mid | Santa Rosa Island | Island | 33.921 | -120.1 |
| 382 | 15 | Robbins et al., 2013 | SRI-147-110-120 | 16.00 | | 0.17 | 0.29 | 4256 | Mid | Santa Rosa Island | Island | 33.921 | -120.1 |
| 382 | 15 | Robbins et al., 2013 | SRI-147-110-120 | 28.00 | | -0.05 | 0.30 | 4256 | Mid | Santa Rosa Island | Island | 33.921 | -120.1 |
| 382 | 15 | Robbins et al., 2013 | SRI-147-110-120 | 14.00 | | 0.28 | 0.32 | 4256 | Mid | Santa Rosa Island | Island | 33.921 | -120.1 |

| | | | | | | | | | | | | | |
|---|---|---|---|---|---|---|---|---|---|---|---|---|---|
| 382 | 15 | Robbins et al., 2013 | SRI-147-110-120 | 26.00 | | 0.44 | 0.54 | 4256 | Mid | Santa Rosa Island | Island | 33.921 | -120.1 |
| 382 | 15 | Robbins et al., 2013 | SRI-147-110-120 | 18.00 | | 0.26 | 0.71 | 4256 | Mid | Santa Rosa Island | Island | 33.921 | -120.1 |
| 382 | 15 | Robbins et al., 2013 | SRI-147-110-120 | 24.00 | | 0.18 | 0.74 | 4256 | Mid | Santa Rosa Island | Island | 33.921 | -120.1 |
| 382 | 15 | Robbins et al., 2013 | SRI-147-110-120 | 22.00 | | 0.19 | 0.83 | 4256 | Mid | Santa Rosa Island | Island | 33.921 | -120.1 |
| 382 | 15 | Robbins et al., 2013 | SRI-147-110-120 | 20.00 | | 0.04 | 0.94 | 4256 | Mid | Santa Rosa Island | Island | 33.921 | -120.1 |
| 383 | 20 | Robbins et al., 2013 | SRI-147-120-130 | 24.00 | | 0.99 | -0.42 | 4396 | Mid | Santa Rosa Island | Island | 33.921 | -120.1 |
| 383 | 20 | Robbins et al., 2013 | SRI-147-120-130 | 22.00 | | 0.81 | -0.24 | 4396 | Mid | Santa Rosa Island | Island | 33.921 | -120.1 |
| 383 | 20 | Robbins et al., 2013 | SRI-147-120-130 | 26.00 | | 0.96 | -0.13 | 4396 | Mid | Santa Rosa Island | Island | 33.921 | -120.1 |
| 383 | 20 | Robbins et al., 2013 | SRI-147-120-130 | 20.00 | | 1.18 | -0.04 | 4396 | Mid | Santa Rosa Island | Island | 33.921 | -120.1 |
| 383 | 20 | Robbins et al., 2013 | SRI-147-120-130 | 28.00 | | 0.82 | 0.09 | 4396 | Mid | Santa Rosa Island | Island | 33.921 | -120.1 |
| 383 | 20 | Robbins et al., 2013 | SRI-147-120-130 | 30.00 | | 0.46 | 0.12 | 4396 | Mid | Santa Rosa Island | Island | 33.921 | -120.1 |
| 383 | 20 | Robbins et al., 2013 | SRI-147-120-130 | 2.00 | | 0.89 | 0.19 | 4396 | Mid | Santa Rosa Island | Island | 33.921 | -120.1 |
| 383 | 20 | Robbins et al., 2013 | SRI-147-120-130 | 18.00 | | 1.02 | 0.26 | 4396 | Mid | Santa Rosa Island | Island | 33.921 | -120.1 |
| 383 | 20 | Robbins et al., 2013 | SRI-147-120-130 | 10.00 | | 0.30 | 0.60 | 4396 | Mid | Santa Rosa Island | Island | 33.921 | -120.1 |
| 383 | 20 | Robbins et al., 2013 | SRI-147-120-130 | 16.00 | | 1.03 | 0.69 | 4396 | Mid | Santa Rosa Island | Island | 33.921 | -120.1 |
| 383 | 20 | Robbins et al., 2013 | SRI-147-120-130 | 32.00 | | 0.88 | 0.69 | 4396 | Mid | Santa Rosa Island | Island | 33.921 | -120.1 |
| 383 | 20 | Robbins et al., 2013 | SRI-147-120-130 | 8.00 | | 1.06 | 0.70 | 4396 | Mid | Santa Rosa Island | Island | 33.921 | -120.1 |
| 383 | 20 | Robbins et al., 2013 | SRI-147-120-130 | 14.00 | | 1.19 | 0.76 | 4396 | Mid | Santa Rosa Island | Island | 33.921 | -120.1 |
| 383 | 20 | Robbins et al., 2013 | SRI-147-120-130 | 4.00 | | 1.08 | 0.76 | 4396 | Mid | Santa Rosa Island | Island | 33.921 | -120.1 |

| | | | | | | | | | | | | | |
|---|---|---|---|---|---|---|---|---|---|---|---|---|---|
| 383 | 20 | Robbins et al., 2013 | SRI-147-120-130 | 34.00 | | 0.76 | 0.79 | 4396 | Mid | Santa Rosa Island | Island | 33.921 | -120.1 |
| 383 | 20 | Robbins et al., 2013 | SRI-147-120-130 | 12.00 | | 1.06 | 0.81 | 4396 | Mid | Santa Rosa Island | Island | 33.921 | -120.1 |
| 383 | 20 | Robbins et al., 2013 | SRI-147-120-130 | 38.00 | | 1.12 | 0.91 | 4396 | Mid | Santa Rosa Island | Island | 33.921 | -120.1 |
| 383 | 20 | Robbins et al., 2013 | SRI-147-120-130 | 36.00 | | 0.92 | 0.94 | 4396 | Mid | Santa Rosa Island | Island | 33.921 | -120.1 |
| 383 | 20 | Robbins et al., 2013 | SRI-147-120-130 | 0.00 | | 0.42 | 1.00 | 4396 | Mid | Santa Rosa Island | Island | 33.921 | -120.1 |
| 383 | 20 | Robbins et al., 2013 | SRI-147-120-130 | 6.00 | | 1.26 | 1.11 | 4396 | Mid | Santa Rosa Island | Island | 33.921 | -120.1 |
| 384 | 19 | Robbins et al., 2013 | SRI-147-130-140 | 34.00 | | 0.50 | -0.03 | 4537 | Mid | Santa Rosa Island | Island | 33.921 | -120.1 |
| 384 | 19 | Robbins et al., 2013 | SRI-147-130-140 | 36.00 | | -0.06 | 0.00 | 4537 | Mid | Santa Rosa Island | Island | 33.921 | -120.1 |
| 384 | 19 | Robbins et al., 2013 | SRI-147-130-140 | 12.00 | | 0.73 | 0.02 | 4537 | Mid | Santa Rosa Island | Island | 33.921 | -120.1 |
| 384 | 19 | Robbins et al., 2013 | SRI-147-130-140 | 38.00 | | 0.03 | 0.22 | 4537 | Mid | Santa Rosa Island | Island | 33.921 | -120.1 |
| 384 | 19 | Robbins et al., 2013 | SRI-147-130-140 | 6.00 | | 0.65 | 0.28 | 4537 | Mid | Santa Rosa Island | Island | 33.921 | -120.1 |
| 384 | 19 | Robbins et al., 2013 | SRI-147-130-140 | 10.00 | | 0.61 | 0.31 | 4537 | Mid | Santa Rosa Island | Island | 33.921 | -120.1 |
| 384 | 19 | Robbins et al., 2013 | SRI-147-130-140 | 14.00 | | 0.20 | 0.34 | 4537 | Mid | Santa Rosa Island | Island | 33.921 | -120.1 |
| 384 | 19 | Robbins et al., 2013 | SRI-147-130-140 | 32.00 | | 0.33 | 0.38 | 4537 | Mid | Santa Rosa Island | Island | 33.921 | -120.1 |
| 384 | 19 | Robbins et al., 2013 | SRI-147-130-140 | 16.00 | | 0.22 | 0.48 | 4537 | Mid | Santa Rosa Island | Island | 33.921 | -120.1 |
| 384 | 19 | Robbins et al., 2013 | SRI-147-130-140 | 2.00 | | 0.35 | 0.65 | 4537 | Mid | Santa Rosa Island | Island | 33.921 | -120.1 |
| 384 | 19 | Robbins et al., 2013 | SRI-147-130-140 | 0.00 | | 0.17 | 0.67 | 4537 | Mid | Santa Rosa Island | Island | 33.921 | -120.1 |
| 384 | 19 | Robbins et al., 2013 | SRI-147-130-140 | 18.00 | | 0.34 | 0.70 | 4537 | Mid | Santa Rosa Island | Island | 33.921 | -120.1 |
| 384 | 19 | Robbins et al., 2013 | SRI-147-130-140 | 4.00 | | 0.34 | 0.76 | 4537 | Mid | Santa Rosa Island | Island | 33.921 | -120.1 |

| | | | | | | | | | | | | | |
|---|---|---|---|---|---|---|---|---|---|---|---|---|---|
| 384 | 19 | Robbins et al., 2013 | SRI-147-130-140 | 24.00 | | 0.46 | 0.82 | 4537 | Mid | Santa Rosa Island | Island | 33.921 | -120.1 |
| 384 | 19 | Robbins et al., 2013 | SRI-147-130-140 | 8.00 | | -0.11 | 0.82 | 4537 | Mid | Santa Rosa Island | Island | 33.921 | -120.1 |
| 384 | 19 | Robbins et al., 2013 | SRI-147-130-140 | 28.00 | | -0.10 | 1.00 | 4537 | Mid | Santa Rosa Island | Island | 33.921 | -120.1 |
| 384 | 19 | Robbins et al., 2013 | SRI-147-130-140 | 20.00 | | 0.14 | 1.08 | 4537 | Mid | Santa Rosa Island | Island | 33.921 | -120.1 |
| 384 | 19 | Robbins et al., 2013 | SRI-147-130-140 | 26.00 | | 0.01 | 1.08 | 4537 | Mid | Santa Rosa Island | Island | 33.921 | -120.1 |
| 384 | 19 | Robbins et al., 2013 | SRI-147-130-140 | 30.00 | | 0.26 | 1.11 | 4537 | Mid | Santa Rosa Island | Island | 33.921 | -120.1 |
| 385 | 19 | Robbins et al., 2013 | SRI-147-140-150 | 18.00 | | 0.99 | -0.22 | 4677 | Mid | Santa Rosa Island | Island | 33.921 | -120.1 |
| 385 | 19 | Robbins et al., 2013 | SRI-147-140-150 | 4.00 | | 1.24 | -0.16 | 4677 | Mid | Santa Rosa Island | Island | 33.921 | -120.1 |
| 385 | 19 | Robbins et al., 2013 | SRI-147-140-150 | 20.00 | | 0.68 | 0.08 | 4677 | Mid | Santa Rosa Island | Island | 33.921 | -120.1 |
| 385 | 19 | Robbins et al., 2013 | SRI-147-140-150 | 36.00 | | 0.57 | 0.08 | 4677 | Mid | Santa Rosa Island | Island | 33.921 | -120.1 |
| 385 | 19 | Robbins et al., 2013 | SRI-147-140-150 | 38.00 | | 0.27 | 0.19 | 4677 | Mid | Santa Rosa Island | Island | 33.921 | -120.1 |
| 385 | 19 | Robbins et al., 2013 | SRI-147-140-150 | 22.00 | | 0.14 | 0.23 | 4677 | Mid | Santa Rosa Island | Island | 33.921 | -120.1 |
| 385 | 19 | Robbins et al., 2013 | SRI-147-140-150 | 16.00 | | 1.05 | 0.38 | 4677 | Mid | Santa Rosa Island | Island | 33.921 | -120.1 |
| 385 | 19 | Robbins et al., 2013 | SRI-147-140-150 | 2.00 | | 0.24 | 0.40 | 4677 | Mid | Santa Rosa Island | Island | 33.921 | -120.1 |
| 385 | 19 | Robbins et al., 2013 | SRI-147-140-150 | 32.00 | | 0.31 | 0.60 | 4677 | Mid | Santa Rosa Island | Island | 33.921 | -120.1 |
| 385 | 19 | Robbins et al., 2013 | SRI-147-140-150 | 34.00 | | 0.28 | 0.63 | 4677 | Mid | Santa Rosa Island | Island | 33.921 | -120.1 |
| 385 | 19 | Robbins et al., 2013 | SRI-147-140-150 | 6.00 | | 0.73 | 0.69 | 4677 | Mid | Santa Rosa Island | Island | 33.921 | -120.1 |
| 385 | 19 | Robbins et al., 2013 | SRI-147-140-150 | 0.00 | | 0.49 | 0.69 | 4677 | Mid | Santa Rosa Island | Island | 33.921 | -120.1 |
| 385 | 19 | Robbins et al., 2013 | SRI-147-140-150 | 24.00 | | 0.24 | 0.74 | 4677 | Mid | Santa Rosa Island | Island | 33.921 | -120.1 |

| | | | | | | | | | | | | | |
|---|---|---|---|---|---|---|---|---|---|---|---|---|---|
| 385 | 19 | Robbins et al., 2013 | SRI-147-140-150 | 26.00 | | 0.09 | 0.74 | 4677 | Mid | Santa Rosa Island | Island | 33.921 | -120.1 |
| 385 | 19 | Robbins et al., 2013 | SRI-147-140-150 | 28.00 | | 0.08 | 0.74 | 4677 | Mid | Santa Rosa Island | Island | 33.921 | -120.1 |
| 385 | 19 | Robbins et al., 2013 | SRI-147-140-150 | 8.00 | | 0.64 | 0.82 | 4677 | Mid | Santa Rosa Island | Island | 33.921 | -120.1 |
| 385 | 19 | Robbins et al., 2013 | SRI-147-140-150 | 12.00 | | 0.72 | 0.85 | 4677 | Mid | Santa Rosa Island | Island | 33.921 | -120.1 |
| 385 | 19 | Robbins et al., 2013 | SRI-147-140-150 | 14.00 | | 0.68 | 0.87 | 4677 | Mid | Santa Rosa Island | Island | 33.921 | -120.1 |
| 385 | 19 | Robbins et al., 2013 | SRI-147-140-150 | 10.00 | | 0.52 | 0.90 | 4677 | Mid | Santa Rosa Island | Island | 33.921 | -120.1 |
| 386 | 17 | Robbins et al., 2013 | SRI-147-150-160 | 0.00 | | 0.30 | 0.25 | 4818 | Mid | Santa Rosa Island | Island | 33.921 | -120.1 |
| 386 | 17 | Robbins et al., 2013 | SRI-147-150-160 | 6.00 | | 0.69 | 0.34 | 4818 | Mid | Santa Rosa Island | Island | 33.921 | -120.1 |
| 386 | 17 | Robbins et al., 2013 | SRI-147-150-160 | 20.00 | | 0.07 | 0.35 | 4818 | Mid | Santa Rosa Island | Island | 33.921 | -120.1 |
| 386 | 17 | Robbins et al., 2013 | SRI-147-150-160 | 8.00 | | 0.38 | 0.46 | 4818 | Mid | Santa Rosa Island | Island | 33.921 | -120.1 |
| 386 | 17 | Robbins et al., 2013 | SRI-147-150-160 | 16.00 | | 0.01 | 0.61 | 4818 | Mid | Santa Rosa Island | Island | 33.921 | -120.1 |
| 386 | 17 | Robbins et al., 2013 | SRI-147-150-160 | 18.00 | | 0.28 | 0.66 | 4818 | Mid | Santa Rosa Island | Island | 33.921 | -120.1 |
| 386 | 17 | Robbins et al., 2013 | SRI-147-150-160 | 14.00 | | -0.29 | 0.69 | 4818 | Mid | Santa Rosa Island | Island | 33.921 | -120.1 |
| 386 | 17 | Robbins et al., 2013 | SRI-147-150-160 | 32.00 | | -0.01 | 0.70 | 4818 | Mid | Santa Rosa Island | Island | 33.921 | -120.1 |
| 386 | 17 | Robbins et al., 2013 | SRI-147-150-160 | 22.00 | | -0.31 | 0.72 | 4818 | Mid | Santa Rosa Island | Island | 33.921 | -120.1 |
| 386 | 17 | Robbins et al., 2013 | SRI-147-150-160 | 12.00 | | 0.24 | 0.88 | 4818 | Mid | Santa Rosa Island | Island | 33.921 | -120.1 |
| 386 | 17 | Robbins et al., 2013 | SRI-147-150-160 | 28.00 | | 0.02 | 0.90 | 4818 | Mid | Santa Rosa Island | Island | 33.921 | -120.1 |
| 386 | 17 | Robbins et al., 2013 | SRI-147-150-160 | 30.00 | | 0.24 | 0.96 | 4818 | Mid | Santa Rosa Island | Island | 33.921 | -120.1 |
| 386 | 17 | Robbins et al., 2013 | SRI-147-150-160 | 4.00 | | 0.64 | 0.97 | 4818 | Mid | Santa Rosa Island | Island | 33.921 | -120.1 |

| | | | | | | | | | | | | | |
|---|---|---|---|---|---|---|---|---|---|---|---|---|---|
| 386 | 17 | Robbins et al., 2013 | SRI-147-150-160 | 26.00 | | 0.03 | 1.01 | 4818 | Mid | Santa Rosa Island | Island | 33.921 | -120.1 |
| 386 | 17 | Robbins et al., 2013 | SRI-147-150-160 | 24.00 | | -0.08 | 1.21 | 4818 | Mid | Santa Rosa Island | Island | 33.921 | -120.1 |
| 386 | 17 | Robbins et al., 2013 | SRI-147-150-160 | 2.00 | | 0.56 | 1.27 | 4818 | Mid | Santa Rosa Island | Island | 33.921 | -120.1 |
| 386 | 17 | Robbins et al., 2013 | SRI-147-150-160 | 10.00 | | 0.21 | 1.29 | 4818 | Mid | Santa Rosa Island | Island | 33.921 | -120.1 |
| 387 | 13 | Robbins et al., 2013 | SRI-147-160-170 | 22.00 | | 0.53 | -0.42 | 4958 | Mid | Santa Rosa Island | Island | 33.921 | -120.1 |
| 387 | 13 | Robbins et al., 2013 | SRI-147-160-170 | 24.00 | | 0.61 | -0.24 | 4958 | Mid | Santa Rosa Island | Island | 33.921 | -120.1 |
| 387 | 13 | Robbins et al., 2013 | SRI-147-160-170 | 20.00 | | 0.58 | -0.11 | 4958 | Mid | Santa Rosa Island | Island | 33.921 | -120.1 |
| 387 | 13 | Robbins et al., 2013 | SRI-147-160-170 | 14.00 | | 0.89 | -0.03 | 4958 | Mid | Santa Rosa Island | Island | 33.921 | -120.1 |
| 387 | 13 | Robbins et al., 2013 | SRI-147-160-170 | 12.00 | | 0.76 | 0.16 | 4958 | Mid | Santa Rosa Island | Island | 33.921 | -120.1 |
| 387 | 13 | Robbins et al., 2013 | SRI-147-160-170 | 6.00 | | 1.00 | 0.25 | 4958 | Mid | Santa Rosa Island | Island | 33.921 | -120.1 |
| 387 | 13 | Robbins et al., 2013 | SRI-147-160-170 | 16.00 | | 0.65 | 0.26 | 4958 | Mid | Santa Rosa Island | Island | 33.921 | -120.1 |
| 387 | 13 | Robbins et al., 2013 | SRI-147-160-170 | 8.00 | | 0.82 | 0.36 | 4958 | Mid | Santa Rosa Island | Island | 33.921 | -120.1 |
| 387 | 13 | Robbins et al., 2013 | SRI-147-160-170 | 18.00 | | 0.11 | 0.39 | 4958 | Mid | Santa Rosa Island | Island | 33.921 | -120.1 |
| 387 | 13 | Robbins et al., 2013 | SRI-147-160-170 | 0.00 | | 0.55 | 0.59 | 4958 | Mid | Santa Rosa Island | Island | 33.921 | -120.1 |
| 387 | 13 | Robbins et al., 2013 | SRI-147-160-170 | 4.00 | | 0.53 | 0.78 | 4958 | Mid | Santa Rosa Island | Island | 33.921 | -120.1 |
| 387 | 13 | Robbins et al., 2013 | SRI-147-160-170 | 10.00 | | 0.24 | 0.79 | 4958 | Mid | Santa Rosa Island | Island | 33.921 | -120.1 |
| 387 | 13 | Robbins et al., 2013 | SRI-147-160-170 | 2.00 | | 0.18 | 0.88 | 4958 | Mid | Santa Rosa Island | Island | 33.921 | -120.1 |
| 388 | 18 | Robbins et al., 2013 | SRI-147-170-180 | 14.00 | | 1.21 | -0.37 | 5099 | Mid | Santa Rosa Island | Island | 33.921 | -120.1 |
| 388 | 18 | Robbins et al., 2013 | SRI-147-170-180 | 16.00 | | 0.58 | -0.34 | 5099 | Mid | Santa Rosa Island | Island | 33.921 | -120.1 |

| | | | | | | | | | | | | | |
|---|---|---|---|---|---|---|---|---|---|---|---|---|---|
| 388 | 18 | Robbins et al., 2013 | SRI-147-170-180 | 6.00 | | 0.94 | -0.30 | 5099 | Mid | Santa Rosa Island | Island | 33.921 | -120.1 |
| 388 | 18 | Robbins et al., 2013 | SRI-147-170-180 | 20.00 | | 0.40 | -0.28 | 5099 | Mid | Santa Rosa Island | Island | 33.921 | -120.1 |
| 388 | 18 | Robbins et al., 2013 | SRI-147-170-180 | 4.00 | | 0.90 | -0.17 | 5099 | Mid | Santa Rosa Island | Island | 33.921 | -120.1 |
| 388 | 18 | Robbins et al., 2013 | SRI-147-170-180 | 18.00 | | 0.41 | -0.17 | 5099 | Mid | Santa Rosa Island | Island | 33.921 | -120.1 |
| 388 | 18 | Robbins et al., 2013 | SRI-147-170-180 | 8.00 | | -0.19 | -0.15 | 5099 | Mid | Santa Rosa Island | Island | 33.921 | -120.1 |
| 388 | 18 | Robbins et al., 2013 | SRI-147-170-180 | 24.00 | | -0.20 | 0.13 | 5099 | Mid | Santa Rosa Island | Island | 33.921 | -120.1 |
| 388 | 18 | Robbins et al., 2013 | SRI-147-170-180 | 12.00 | | 1.19 | 0.27 | 5099 | Mid | Santa Rosa Island | Island | 33.921 | -120.1 |
| 388 | 18 | Robbins et al., 2013 | SRI-147-170-180 | 22.00 | | 0.27 | 0.31 | 5099 | Mid | Santa Rosa Island | Island | 33.921 | -120.1 |
| 388 | 18 | Robbins et al., 2013 | SRI-147-170-180 | 34.00 | | 1.10 | 0.46 | 5099 | Mid | Santa Rosa Island | Island | 33.921 | -120.1 |
| 388 | 18 | Robbins et al., 2013 | SRI-147-170-180 | 26.00 | | -0.31 | 0.51 | 5099 | Mid | Santa Rosa Island | Island | 33.921 | -120.1 |
| 388 | 18 | Robbins et al., 2013 | SRI-147-170-180 | 28.00 | | -0.26 | 0.61 | 5099 | Mid | Santa Rosa Island | Island | 33.921 | -120.1 |
| 388 | 18 | Robbins et al., 2013 | SRI-147-170-180 | 2.00 | | 1.05 | 0.65 | 5099 | Mid | Santa Rosa Island | Island | 33.921 | -120.1 |
| 388 | 18 | Robbins et al., 2013 | SRI-147-170-180 | 30.00 | | 0.31 | 0.71 | 5099 | Mid | Santa Rosa Island | Island | 33.921 | -120.1 |
| 388 | 18 | Robbins et al., 2013 | SRI-147-170-180 | 32.00 | | 1.23 | 0.73 | 5099 | Mid | Santa Rosa Island | Island | 33.921 | -120.1 |
| 388 | 18 | Robbins et al., 2013 | SRI-147-170-180 | 10.00 | | 0.54 | 0.91 | 5099 | Mid | Santa Rosa Island | Island | 33.921 | -120.1 |
| 388 | 18 | Robbins et al., 2013 | SRI-147-170-180 | 0.00 | | 0.33 | 0.96 | 5099 | Mid | Santa Rosa Island | Island | 33.921 | -120.1 |
| 389 | 17 | Robbins et al., 2013 | SRI-147-180-190 | 26.00 | | 1.18 | -0.32 | 5239 | Mid | Santa Rosa Island | Island | 33.921 | -120.1 |
| 389 | 17 | Robbins et al., 2013 | SRI-147-180-190 | 12.00 | | 0.51 | -0.32 | 5239 | Mid | Santa Rosa Island | Island | 33.921 | -120.1 |
| 389 | 17 | Robbins et al., 2013 | SRI-147-180-190 | 30.00 | | 1.08 | -0.31 | 5239 | Mid | Santa Rosa Island | Island | 33.921 | -120.1 |

| | | | | | | | | | | | | | |
|---|---|---|---|---|---|---|---|---|---|---|---|---|---|
| 389 | 17 | Robbins et al., 2013 | SRI-147-180-190 | 28.00 | | 1.14 | -0.22 | 5239 | Mid | Santa Rosa Island | Island | 33.921 | -120.1 |
| 389 | 17 | Robbins et al., 2013 | SRI-147-180-190 | 10.00 | | 0.90 | -0.22 | 5239 | Mid | Santa Rosa Island | Island | 33.921 | -120.1 |
| 389 | 17 | Robbins et al., 2013 | SRI-147-180-190 | 8.00 | | 0.77 | -0.20 | 5239 | Mid | Santa Rosa Island | Island | 33.921 | -120.1 |
| 389 | 17 | Robbins et al., 2013 | SRI-147-180-190 | 0.00 | | 0.83 | 0.05 | 5239 | Mid | Santa Rosa Island | Island | 33.921 | -120.1 |
| 389 | 17 | Robbins et al., 2013 | SRI-147-180-190 | 14.00 | | -0.15 | 0.12 | 5239 | Mid | Santa Rosa Island | Island | 33.921 | -120.1 |
| 389 | 17 | Robbins et al., 2013 | SRI-147-180-190 | 34.00 | | 0.37 | 0.14 | 5239 | Mid | Santa Rosa Island | Island | 33.921 | -120.1 |
| 389 | 17 | Robbins et al., 2013 | SRI-147-180-190 | 24.00 | | 1.14 | 0.20 | 5239 | Mid | Santa Rosa Island | Island | 33.921 | -120.1 |
| 389 | 17 | Robbins et al., 2013 | SRI-147-180-190 | 16.00 | | -0.34 | 0.37 | 5239 | Mid | Santa Rosa Island | Island | 33.921 | -120.1 |
| 389 | 17 | Robbins et al., 2013 | SRI-147-180-190 | 2.00 | | 0.23 | 0.48 | 5239 | Mid | Santa Rosa Island | Island | 33.921 | -120.1 |
| 389 | 17 | Robbins et al., 2013 | SRI-147-180-190 | 6.00 | | 0.62 | 0.54 | 5239 | Mid | Santa Rosa Island | Island | 33.921 | -120.1 |
| 389 | 17 | Robbins et al., 2013 | SRI-147-180-190 | 18.00 | | -0.77 | 0.54 | 5239 | Mid | Santa Rosa Island | Island | 33.921 | -120.1 |
| 389 | 17 | Robbins et al., 2013 | SRI-147-180-190 | 22.00 | | 0.76 | 0.86 | 5239 | Mid | Santa Rosa Island | Island | 33.921 | -120.1 |
| 389 | 17 | Robbins et al., 2013 | SRI-147-180-190 | 4.00 | | 0.41 | 1.12 | 5239 | Mid | Santa Rosa Island | Island | 33.921 | -120.1 |
| 389 | 17 | Robbins et al., 2013 | SRI-147-180-190 | 20.00 | | 0.42 | 1.18 | 5239 | Mid | Santa Rosa Island | Island | 33.921 | -120.1 |
| 391 | 18 | Robbins et al., 2013 | SRI-147-190-200 | 30.00 | | -0.37 | -0.35 | 5380 | Mid | Santa Rosa Island | Island | 33.921 | -120.1 |
| 391 | 18 | Robbins et al., 2013 | SRI-147-190-200 | 24.00 | | 0.31 | -0.18 | 5380 | Mid | Santa Rosa Island | Island | 33.921 | -120.1 |
| 391 | 18 | Robbins et al., 2013 | SRI-147-190-200 | 32.00 | | -0.33 | -0.14 | 5380 | Mid | Santa Rosa Island | Island | 33.921 | -120.1 |
| 391 | 18 | Robbins et al., 2013 | SRI-147-190-200 | 34.00 | | 0.40 | 0.19 | 5380 | Mid | Santa Rosa Island | Island | 33.921 | -120.1 |
| 391 | 18 | Robbins et al., 2013 | SRI-147-190-200 | 12.00 | | 0.48 | 0.24 | 5380 | Mid | Santa Rosa Island | Island | 33.921 | -120.1 |

| | | | | | | | | | | | | | |
|---|---|---|---|---|---|---|---|---|---|---|---|---|---|
| 391 | 18 | Robbins et al., 2013 | SRI-147-190-200 | 26.00 | | 0.48 | 0.29 | 5380 | Mid | Santa Rosa Island | Island | 33.921 | -120.1 |
| 391 | 18 | Robbins et al., 2013 | SRI-147-190-200 | 38.00 | | 0.27 | 0.49 | 5380 | Mid | Santa Rosa Island | Island | 33.921 | -120.1 |
| 391 | 18 | Robbins et al., 2013 | SRI-147-190-200 | 22.00 | | 0.81 | 0.50 | 5380 | Mid | Santa Rosa Island | Island | 33.921 | -120.1 |
| 391 | 18 | Robbins et al., 2013 | SRI-147-190-200 | 10.00 | | 0.26 | 0.58 | 5380 | Mid | Santa Rosa Island | Island | 33.921 | -120.1 |
| 391 | 18 | Robbins et al., 2013 | SRI-147-190-200 | 16.00 | | -0.32 | 0.70 | 5380 | Mid | Santa Rosa Island | Island | 33.921 | -120.1 |
| 391 | 18 | Robbins et al., 2013 | SRI-147-190-200 | 20.00 | | 0.84 | 0.79 | 5380 | Mid | Santa Rosa Island | Island | 33.921 | -120.1 |
| 391 | 18 | Robbins et al., 2013 | SRI-147-190-200 | 6.00 | | 0.12 | 0.79 | 5380 | Mid | Santa Rosa Island | Island | 33.921 | -120.1 |
| 391 | 18 | Robbins et al., 2013 | SRI-147-190-200 | 14.00 | | 0.18 | 0.89 | 5380 | Mid | Santa Rosa Island | Island | 33.921 | -120.1 |
| 391 | 18 | Robbins et al., 2013 | SRI-147-190-200 | 2.00 | | 0.13 | 0.93 | 5380 | Mid | Santa Rosa Island | Island | 33.921 | -120.1 |
| 391 | 18 | Robbins et al., 2013 | SRI-147-190-200 | 4.00 | | 0.11 | 0.96 | 5380 | Mid | Santa Rosa Island | Island | 33.921 | -120.1 |
| 391 | 18 | Robbins et al., 2013 | SRI-147-190-200 | 18.00 | | 0.18 | 0.98 | 5380 | Mid | Santa Rosa Island | Island | 33.921 | -120.1 |
| 391 | 18 | Robbins et al., 2013 | SRI-147-190-200 | 8.00 | | -0.19 | 1.02 | 5380 | Mid | Santa Rosa Island | Island | 33.921 | -120.1 |
| 391 | 18 | Robbins et al., 2013 | SRI-147-190-200 | 0.00 | | 0.41 | 1.03 | 5380 | Mid | Santa Rosa Island | Island | 33.921 | -120.1 |
| 392 | 10 | Robbins et al., 2013 | SRI-147-190-200 | 0.00 | | 0.96 | -0.56 | 5380 | Mid | Santa Rosa Island | Island | 33.921 | -120.1 |
| 392 | 10 | Robbins et al., 2013 | SRI-147-190-200 | 12.00 | | 0.03 | -0.33 | 5380 | Mid | Santa Rosa Island | Island | 33.921 | -120.1 |
| 392 | 10 | Robbins et al., 2013 | SRI-147-190-200 | 2.00 | | 0.71 | 0.04 | 5380 | Mid | Santa Rosa Island | Island | 33.921 | -120.1 |
| 392 | 10 | Robbins et al., 2013 | SRI-147-190-200 | 8.00 | | 0.96 | 0.06 | 5380 | Mid | Santa Rosa Island | Island | 33.921 | -120.1 |
| 392 | 10 | Robbins et al., 2013 | SRI-147-190-200 | 10.00 | | 0.77 | 0.10 | 5380 | Mid | Santa Rosa Island | Island | 33.921 | -120.1 |
| 392 | 10 | Robbins et al., 2013 | SRI-147-190-200 | 16.00 | | 0.89 | 0.32 | 5380 | Mid | Santa Rosa Island | Island | 33.921 | -120.1 |

| | | | | | | | | | | | | | |
|---|---|---|---|---|---|---|---|---|---|---|---|---|---|
| 392 | 10 | Robbins et al., 2013 | SRI-147-190-200 | 18.00 | | 0.87 | 0.49 | 5380 | Mid | Santa Rosa Island | Island | 33.921 | -120.1 |
| 392 | 10 | Robbins et al., 2013 | SRI-147-190-200 | 6.00 | | 1.27 | 0.71 | 5380 | Mid | Santa Rosa Island | Island | 33.921 | -120.1 |
| 392 | 10 | Robbins et al., 2013 | SRI-147-190-200 | 4.00 | | 0.99 | 0.74 | 5380 | Mid | Santa Rosa Island | Island | 33.921 | -120.1 |
| 392 | 10 | Robbins et al., 2013 | SRI-147-190-200 | 14.00 | | 0.86 | 0.78 | 5380 | Mid | Santa Rosa Island | Island | 33.921 | -120.1 |
| 393 | 14 | Robbins et al., 2013 | SRI-147-20-30 | 6.00 | | 0.99 | 0.14 | 802 | Mid | Santa Rosa Island | Island | 33.921 | -120.1 |
| 393 | 14 | Robbins et al., 2013 | SRI-147-20-30 | 4.00 | | 0.97 | 0.22 | 802 | Mid | Santa Rosa Island | Island | 33.921 | -120.1 |
| 393 | 14 | Robbins et al., 2013 | SRI-147-20-30 | 16.00 | | 1.09 | 0.33 | 802 | Mid | Santa Rosa Island | Island | 33.921 | -120.1 |
| 393 | 14 | Robbins et al., 2013 | SRI-147-20-30 | 14.00 | | 1.14 | 0.41 | 802 | Mid | Santa Rosa Island | Island | 33.921 | -120.1 |
| 393 | 14 | Robbins et al., 2013 | SRI-147-20-30 | 0.00 | | 0.74 | 0.41 | 802 | Mid | Santa Rosa Island | Island | 33.921 | -120.1 |
| 393 | 14 | Robbins et al., 2013 | SRI-147-20-30 | 24.00 | | 0.94 | 0.45 | 802 | Mid | Santa Rosa Island | Island | 33.921 | -120.1 |
| 393 | 14 | Robbins et al., 2013 | SRI-147-20-30 | 18.00 | | 1.08 | 0.48 | 802 | Mid | Santa Rosa Island | Island | 33.921 | -120.1 |
| 393 | 14 | Robbins et al., 2013 | SRI-147-20-30 | 8.00 | | 0.92 | 0.50 | 802 | Mid | Santa Rosa Island | Island | 33.921 | -120.1 |
| 393 | 14 | Robbins et al., 2013 | SRI-147-20-30 | 12.00 | | 0.99 | 0.59 | 802 | Mid | Santa Rosa Island | Island | 33.921 | -120.1 |
| 393 | 14 | Robbins et al., 2013 | SRI-147-20-30 | 10.00 | | 1.07 | 0.61 | 802 | Mid | Santa Rosa Island | Island | 33.921 | -120.1 |
| 393 | 14 | Robbins et al., 2013 | SRI-147-20-30 | 22.00 | | 1.13 | 0.67 | 802 | Mid | Santa Rosa Island | Island | 33.921 | -120.1 |
| 393 | 14 | Robbins et al., 2013 | SRI-147-20-30 | 20.00 | | 1.05 | 0.80 | 802 | Mid | Santa Rosa Island | Island | 33.921 | -120.1 |
| 393 | 14 | Robbins et al., 2013 | SRI-147-20-30 | 28.00 | | 0.84 | 0.83 | 802 | Mid | Santa Rosa Island | Island | 33.921 | -120.1 |
| 393 | 14 | Robbins et al., 2013 | SRI-147-20-30 | 26.00 | | 0.74 | 0.83 | 802 | Mid | Santa Rosa Island | Island | 33.921 | -120.1 |
| 394 | 13 | Robbins et al., 2013 | SRI-147-200-210 | 4.00 | | 0.76 | 0.07 | 5445 | Mid | Santa Rosa Island | Island | 33.921 | -120.1 |

| | | | | | | | | | | | | | |
|---|---|---|---|---|---|---|---|---|---|---|---|---|---|
| 394 | 13 | Robbins et al., 2013 | SRI-147-200-210 | 2.00 | | 0.97 | 0.34 | 5445 | Mid | Santa Rosa Island | Island | 33.921 | -120.1 |
| 394 | 13 | Robbins et al., 2013 | SRI-147-200-210 | 16.00 | | -0.10 | 0.60 | 5445 | Mid | Santa Rosa Island | Island | 33.921 | -120.1 |
| 394 | 13 | Robbins et al., 2013 | SRI-147-200-210 | 0.00 | | 1.03 | 0.67 | 5445 | Mid | Santa Rosa Island | Island | 33.921 | -120.1 |
| 394 | 13 | Robbins et al., 2013 | SRI-147-200-210 | 6.00 | | 0.11 | 0.67 | 5445 | Mid | Santa Rosa Island | Island | 33.921 | -120.1 |
| 394 | 13 | Robbins et al., 2013 | SRI-147-200-210 | 18.00 | | -0.15 | 0.69 | 5445 | Mid | Santa Rosa Island | Island | 33.921 | -120.1 |
| 394 | 13 | Robbins et al., 2013 | SRI-147-200-210 | 26.00 | | 0.12 | 0.73 | 5445 | Mid | Santa Rosa Island | Island | 33.921 | -120.1 |
| 394 | 13 | Robbins et al., 2013 | SRI-147-200-210 | 22.00 | | -0.19 | 0.85 | 5445 | Mid | Santa Rosa Island | Island | 33.921 | -120.1 |
| 394 | 13 | Robbins et al., 2013 | SRI-147-200-210 | 14.00 | | 0.10 | 0.93 | 5445 | Mid | Santa Rosa Island | Island | 33.921 | -120.1 |
| 394 | 13 | Robbins et al., 2013 | SRI-147-200-210 | 12.00 | | 0.28 | 1.04 | 5445 | Mid | Santa Rosa Island | Island | 33.921 | -120.1 |
| 394 | 13 | Robbins et al., 2013 | SRI-147-200-210 | 8.00 | | 0.33 | 1.17 | 5445 | Mid | Santa Rosa Island | Island | 33.921 | -120.1 |
| 394 | 13 | Robbins et al., 2013 | SRI-147-200-210 | 10.00 | | 0.26 | 1.21 | 5445 | Mid | Santa Rosa Island | Island | 33.921 | -120.1 |
| 394 | 13 | Robbins et al., 2013 | SRI-147-200-210 | 24.00 | | -0.24 | 1.21 | 5445 | Mid | Santa Rosa Island | Island | 33.921 | -120.1 |
| 395 | 11 | Robbins et al., 2013 | SRI-147-210-220 | 0.00 | | 1.29 | -0.14 | 5510 | Mid | Santa Rosa Island | Island | 33.921 | -120.1 |
| 395 | 11 | Robbins et al., 2013 | SRI-147-210-220 | 2.00 | | 1.41 | -0.11 | 5510 | Mid | Santa Rosa Island | Island | 33.921 | -120.1 |
| 395 | 11 | Robbins et al., 2013 | SRI-147-210-220 | 12.00 | | 1.14 | 0.11 | 5510 | Mid | Santa Rosa Island | Island | 33.921 | -120.1 |
| 395 | 11 | Robbins et al., 2013 | SRI-147-210-220 | 10.00 | | 1.01 | 0.33 | 5510 | Mid | Santa Rosa Island | Island | 33.921 | -120.1 |
| 395 | 11 | Robbins et al., 2013 | SRI-147-210-220 | 14.00 | | 0.94 | 0.37 | 5510 | Mid | Santa Rosa Island | Island | 33.921 | -120.1 |
| 395 | 11 | Robbins et al., 2013 | SRI-147-210-220 | 22.00 | | 0.95 | 0.48 | 5510 | Mid | Santa Rosa Island | Island | 33.921 | -120.1 |
| 395 | 11 | Robbins et al., 2013 | SRI-147-210-220 | 18.00 | | 0.90 | 0.68 | 5510 | Mid | Santa Rosa Island | Island | 33.921 | -120.1 |

| | | | | | | | | | | | | | |
|---|---|---|---|---|---|---|---|---|---|---|---|---|---|
| 395 | 11 | Robbins et al., 2013 | SRI-147-210-220 | 8.00 | | 0.95 | 0.71 | 5510 | Mid | Santa Rosa Island | Island | 33.921 | -120.1 |
| 395 | 11 | Robbins et al., 2013 | SRI-147-210-220 | 16.00 | | 0.66 | 0.75 | 5510 | Mid | Santa Rosa Island | Island | 33.921 | -120.1 |
| 395 | 11 | Robbins et al., 2013 | SRI-147-210-220 | 6.00 | | 0.77 | 0.92 | 5510 | Mid | Santa Rosa Island | Island | 33.921 | -120.1 |
| 395 | 11 | Robbins et al., 2013 | SRI-147-210-220 | 4.00 | | 0.47 | 0.95 | 5510 | Mid | Santa Rosa Island | Island | 33.921 | -120.1 |
| 396 | 18 | Robbins et al., 2013 | SRI-147-220-230 | 4.00 | | 0.85 | -0.38 | 5575 | Mid | Santa Rosa Island | Island | 33.921 | -120.1 |
| 396 | 18 | Robbins et al., 2013 | SRI-147-220-230 | 2.00 | | 1.44 | -0.28 | 5575 | Mid | Santa Rosa Island | Island | 33.921 | -120.1 |
| 396 | 18 | Robbins et al., 2013 | SRI-147-220-230 | 30.00 | | 0.82 | -0.25 | 5575 | Mid | Santa Rosa Island | Island | 33.921 | -120.1 |
| 396 | 18 | Robbins et al., 2013 | SRI-147-220-230 | 32.00 | | 0.75 | -0.09 | 5575 | Mid | Santa Rosa Island | Island | 33.921 | -120.1 |
| 396 | 18 | Robbins et al., 2013 | SRI-147-220-230 | 26.00 | | 1.10 | -0.06 | 5575 | Mid | Santa Rosa Island | Island | 33.921 | -120.1 |
| 396 | 18 | Robbins et al., 2013 | SRI-147-220-230 | 6.00 | | 1.13 | 0.07 | 5575 | Mid | Santa Rosa Island | Island | 33.921 | -120.1 |
| 396 | 18 | Robbins et al., 2013 | SRI-147-220-230 | 28.00 | | 1.05 | 0.11 | 5575 | Mid | Santa Rosa Island | Island | 33.921 | -120.1 |
| 396 | 18 | Robbins et al., 2013 | SRI-147-220-230 | 24.00 | | 1.21 | 0.13 | 5575 | Mid | Santa Rosa Island | Island | 33.921 | -120.1 |
| 396 | 18 | Robbins et al., 2013 | SRI-147-220-230 | 34.00 | | 0.65 | 0.19 | 5575 | Mid | Santa Rosa Island | Island | 33.921 | -120.1 |
| 396 | 18 | Robbins et al., 2013 | SRI-147-220-230 | 0.00 | | 1.00 | 0.26 | 5575 | Mid | Santa Rosa Island | Island | 33.921 | -120.1 |
| 396 | 18 | Robbins et al., 2013 | SRI-147-220-230 | 8.00 | | 0.53 | 0.52 | 5575 | Mid | Santa Rosa Island | Island | 33.921 | -120.1 |
| 396 | 18 | Robbins et al., 2013 | SRI-147-220-230 | 10.00 | | 0.65 | 0.64 | 5575 | Mid | Santa Rosa Island | Island | 33.921 | -120.1 |
| 396 | 18 | Robbins et al., 2013 | SRI-147-220-230 | 22.00 | | 0.98 | 0.73 | 5575 | Mid | Santa Rosa Island | Island | 33.921 | -120.1 |
| 396 | 18 | Robbins et al., 2013 | SRI-147-220-230 | 20.00 | | 1.11 | 0.81 | 5575 | Mid | Santa Rosa Island | Island | 33.921 | -120.1 |
| 396 | 18 | Robbins et al., 2013 | SRI-147-220-230 | 12.00 | | 0.63 | 0.89 | 5575 | Mid | Santa Rosa Island | Island | 33.921 | -120.1 |

| | | | | | | | | | | | | | |
|---|---|---|---|---|---|---|---|---|---|---|---|---|---|
| 396 | 18 | Robbins et al., 2013 | SRI-147-220-230 | 14.00 | | 0.85 | 0.94 | 5575 | Mid | Santa Rosa Island | Island | 33.921 | -120.1 |
| 396 | 18 | Robbins et al., 2013 | SRI-147-220-230 | 18.00 | | 1.08 | 0.96 | 5575 | Mid | Santa Rosa Island | Island | 33.921 | -120.1 |
| 396 | 18 | Robbins et al., 2013 | SRI-147-220-230 | 16.00 | | 1.01 | 1.07 | 5575 | Mid | Santa Rosa Island | Island | 33.921 | -120.1 |
| 397 | 14 | Robbins et al., 2013 | SRI-147-230-240 | 22.00 | | 0.92 | -0.72 | 5640 | Mid | Santa Rosa Island | Island | 33.921 | -120.1 |
| 397 | 14 | Robbins et al., 2013 | SRI-147-230-240 | 24.00 | | 0.72 | -0.70 | 5640 | Mid | Santa Rosa Island | Island | 33.921 | -120.1 |
| 397 | 14 | Robbins et al., 2013 | SRI-147-230-240 | 26.00 | | 1.22 | -0.64 | 5640 | Mid | Santa Rosa Island | Island | 33.921 | -120.1 |
| 397 | 14 | Robbins et al., 2013 | SRI-147-230-240 | 18.00 | | 1.17 | -0.64 | 5640 | Mid | Santa Rosa Island | Island | 33.921 | -120.1 |
| 397 | 14 | Robbins et al., 2013 | SRI-147-230-240 | 20.00 | | 1.12 | -0.59 | 5640 | Mid | Santa Rosa Island | Island | 33.921 | -120.1 |
| 397 | 14 | Robbins et al., 2013 | SRI-147-230-240 | 4.00 | | 1.61 | -0.40 | 5640 | Mid | Santa Rosa Island | Island | 33.921 | -120.1 |
| 397 | 14 | Robbins et al., 2013 | SRI-147-230-240 | 16.00 | | 1.19 | -0.29 | 5640 | Mid | Santa Rosa Island | Island | 33.921 | -120.1 |
| 397 | 14 | Robbins et al., 2013 | SRI-147-230-240 | 2.00 | | 1.51 | -0.16 | 5640 | Mid | Santa Rosa Island | Island | 33.921 | -120.1 |
| 397 | 14 | Robbins et al., 2013 | SRI-147-230-240 | 14.00 | | 1.31 | 0.07 | 5640 | Mid | Santa Rosa Island | Island | 33.921 | -120.1 |
| 397 | 14 | Robbins et al., 2013 | SRI-147-230-240 | 6.00 | | 1.20 | 0.30 | 5640 | Mid | Santa Rosa Island | Island | 33.921 | -120.1 |
| 397 | 14 | Robbins et al., 2013 | SRI-147-230-240 | 12.00 | | 1.42 | 0.52 | 5640 | Mid | Santa Rosa Island | Island | 33.921 | -120.1 |
| 397 | 14 | Robbins et al., 2013 | SRI-147-230-240 | 0.00 | | 1.18 | 0.66 | 5640 | Mid | Santa Rosa Island | Island | 33.921 | -120.1 |
| 397 | 14 | Robbins et al., 2013 | SRI-147-230-240 | 8.00 | | 1.06 | 0.67 | 5640 | Mid | Santa Rosa Island | Island | 33.921 | -120.1 |
| 397 | 14 | Robbins et al., 2013 | SRI-147-230-240 | 10.00 | | 1.12 | 1.08 | 5640 | Mid | Santa Rosa Island | Island | 33.921 | -120.1 |
| 398 | 15 | Robbins et al., 2013 | SRI-147-240-250 | 16.00 | | 0.70 | -0.26 | 5919 | Mid | Santa Rosa Island | Island | 33.921 | -120.1 |
| 398 | 15 | Robbins et al., 2013 | SRI-147-240-250 | 18.00 | | 0.37 | 0.12 | 5919 | Mid | Santa Rosa Island | Island | 33.921 | -120.1 |

| | | | | | | | | | | | | | |
|---|---|---|---|---|---|---|---|---|---|---|---|---|---|
| 398 | 15 | Robbins et al., 2013 | SRI-147-240-250 | 14.00 | | 0.71 | 0.15 | 5919 | Mid | Santa Rosa Island | Island | 33.921 | -120.1 |
| 398 | 15 | Robbins et al., 2013 | SRI-147-240-250 | 8.00 | | 0.48 | 0.48 | 5919 | Mid | Santa Rosa Island | Island | 33.921 | -120.1 |
| 398 | 15 | Robbins et al., 2013 | SRI-147-240-250 | 22.00 | | 0.25 | 0.51 | 5919 | Mid | Santa Rosa Island | Island | 33.921 | -120.1 |
| 398 | 15 | Robbins et al., 2013 | SRI-147-240-250 | 0.00 | | 0.38 | 0.53 | 5919 | Mid | Santa Rosa Island | Island | 33.921 | -120.1 |
| 398 | 15 | Robbins et al., 2013 | SRI-147-240-250 | 20.00 | | 0.36 | 0.56 | 5919 | Mid | Santa Rosa Island | Island | 33.921 | -120.1 |
| 398 | 15 | Robbins et al., 2013 | SRI-147-240-250 | 26.00 | | 0.44 | 0.57 | 5919 | Mid | Santa Rosa Island | Island | 33.921 | -120.1 |
| 398 | 15 | Robbins et al., 2013 | SRI-147-240-250 | 4.00 | | 0.37 | 0.59 | 5919 | Mid | Santa Rosa Island | Island | 33.921 | -120.1 |
| 398 | 15 | Robbins et al., 2013 | SRI-147-240-250 | 10.00 | | 0.60 | 0.65 | 5919 | Mid | Santa Rosa Island | Island | 33.921 | -120.1 |
| 398 | 15 | Robbins et al., 2013 | SRI-147-240-250 | 24.00 | | 0.28 | 0.65 | 5919 | Mid | Santa Rosa Island | Island | 33.921 | -120.1 |
| 398 | 15 | Robbins et al., 2013 | SRI-147-240-250 | 28.00 | | 0.56 | 0.67 | 5919 | Mid | Santa Rosa Island | Island | 33.921 | -120.1 |
| 398 | 15 | Robbins et al., 2013 | SRI-147-240-250 | 2.00 | | 0.41 | 0.67 | 5919 | Mid | Santa Rosa Island | Island | 33.921 | -120.1 |
| 398 | 15 | Robbins et al., 2013 | SRI-147-240-250 | 6.00 | | 0.18 | 0.82 | 5919 | Mid | Santa Rosa Island | Island | 33.921 | -120.1 |
| 398 | 15 | Robbins et al., 2013 | SRI-147-240-250 | 12.00 | | 0.58 | 0.84 | 5919 | Mid | Santa Rosa Island | Island | 33.921 | -120.1 |
| 399 | 25 | Robbins et al., 2013 | SRI-147-250-260 | 28.00 | | 0.84 | -0.31 | 6198 | Mid | Santa Rosa Island | Island | 33.921 | -120.1 |
| 399 | 25 | Robbins et al., 2013 | SRI-147-250-260 | 16.00 | | 1.01 | -0.27 | 6198 | Mid | Santa Rosa Island | Island | 33.921 | -120.1 |
| 399 | 25 | Robbins et al., 2013 | SRI-147-250-260 | 24.00 | | 0.67 | -0.10 | 6198 | Mid | Santa Rosa Island | Island | 33.921 | -120.1 |
| 399 | 25 | Robbins et al., 2013 | SRI-147-250-260 | 26.00 | | 0.56 | -0.06 | 6198 | Mid | Santa Rosa Island | Island | 33.921 | -120.1 |
| 399 | 25 | Robbins et al., 2013 | SRI-147-250-260 | 18.00 | | 0.60 | 0.17 | 6198 | Mid | Santa Rosa Island | Island | 33.921 | -120.1 |
| 399 | 25 | Robbins et al., 2013 | SRI-147-250-260 | 8.00 | | 0.98 | 0.21 | 6198 | Mid | Santa Rosa Island | Island | 33.921 | -120.1 |

| | | | | | | | | | | | | | |
|---|---|---|---|---|---|---|---|---|---|---|---|---|---|
| 399 | 25 | Robbins et al., 2013 | SRI-147-250-260 | 48.00 | | 1.03 | 0.30 | 6198 | Mid | Santa Rosa Island | Island | 33.921 | -120.1 |
| 399 | 25 | Robbins et al., 2013 | SRI-147-250-260 | 10.00 | | 0.44 | 0.33 | 6198 | Mid | Santa Rosa Island | Island | 33.921 | -120.1 |
| 399 | 25 | Robbins et al., 2013 | SRI-147-250-260 | 14.00 | | 1.00 | 0.46 | 6198 | Mid | Santa Rosa Island | Island | 33.921 | -120.1 |
| 399 | 25 | Robbins et al., 2013 | SRI-147-250-260 | 46.00 | | 0.94 | 0.51 | 6198 | Mid | Santa Rosa Island | Island | 33.921 | -120.1 |
| 399 | 25 | Robbins et al., 2013 | SRI-147-250-260 | 30.00 | | 0.75 | 0.51 | 6198 | Mid | Santa Rosa Island | Island | 33.921 | -120.1 |
| 399 | 25 | Robbins et al., 2013 | SRI-147-250-260 | 44.00 | | 1.26 | 0.53 | 6198 | Mid | Santa Rosa Island | Island | 33.921 | -120.1 |
| 399 | 25 | Robbins et al., 2013 | SRI-147-250-260 | 0.00 | | 0.86 | 0.58 | 6198 | Mid | Santa Rosa Island | Island | 33.921 | -120.1 |
| 399 | 25 | Robbins et al., 2013 | SRI-147-250-260 | 22.00 | | 0.48 | 0.62 | 6198 | Mid | Santa Rosa Island | Island | 33.921 | -120.1 |
| 399 | 25 | Robbins et al., 2013 | SRI-147-250-260 | 32.00 | | 0.38 | 0.64 | 6198 | Mid | Santa Rosa Island | Island | 33.921 | -120.1 |
| 399 | 25 | Robbins et al., 2013 | SRI-147-250-260 | 20.00 | | 0.10 | 0.64 | 6198 | Mid | Santa Rosa Island | Island | 33.921 | -120.1 |
| 399 | 25 | Robbins et al., 2013 | SRI-147-250-260 | 6.00 | | 1.09 | 0.68 | 6198 | Mid | Santa Rosa Island | Island | 33.921 | -120.1 |
| 399 | 25 | Robbins et al., 2013 | SRI-147-250-260 | 36.00 | | -0.16 | 0.70 | 6198 | Mid | Santa Rosa Island | Island | 33.921 | -120.1 |
| 399 | 25 | Robbins et al., 2013 | SRI-147-250-260 | 42.00 | | 0.71 | 0.77 | 6198 | Mid | Santa Rosa Island | Island | 33.921 | -120.1 |
| 399 | 25 | Robbins et al., 2013 | SRI-147-250-260 | 12.00 | | 0.42 | 0.88 | 6198 | Mid | Santa Rosa Island | Island | 33.921 | -120.1 |
| 399 | 25 | Robbins et al., 2013 | SRI-147-250-260 | 2.00 | | 0.72 | 0.96 | 6198 | Mid | Santa Rosa Island | Island | 33.921 | -120.1 |
| 399 | 25 | Robbins et al., 2013 | SRI-147-250-260 | 38.00 | | 0.40 | 0.96 | 6198 | Mid | Santa Rosa Island | Island | 33.921 | -120.1 |
| 399 | 25 | Robbins et al., 2013 | SRI-147-250-260 | 40.00 | | 0.58 | 0.98 | 6198 | Mid | Santa Rosa Island | Island | 33.921 | -120.1 |
| 399 | 25 | Robbins et al., 2013 | SRI-147-250-260 | 4.00 | | 0.73 | 1.03 | 6198 | Mid | Santa Rosa Island | Island | 33.921 | -120.1 |
| 399 | 25 | Robbins et al., 2013 | SRI-147-250-260 | 34.00 | | 0.53 | 1.06 | 6198 | Mid | Santa Rosa Island | Island | 33.921 | -120.1 |

| | | | | | | | | | | | | | |
|---|---|---|---|---|---|---|---|---|---|---|---|---|---|
| 400 | 21 | Robbins et al., 2013 | SRI-147-260-270 | 18.00 | | -0.21 | 0.21 | 6478 | Mid | Santa Rosa Island | Island | 33.921 | -120.1 |
| 400 | 21 | Robbins et al., 2013 | SRI-147-260-270 | 20.00 | | -0.50 | 0.28 | 6478 | Mid | Santa Rosa Island | Island | 33.921 | -120.1 |
| 400 | 21 | Robbins et al., 2013 | SRI-147-260-270 | 16.00 | | -0.35 | 0.51 | 6478 | Mid | Santa Rosa Island | Island | 33.921 | -120.1 |
| 400 | 21 | Robbins et al., 2013 | SRI-147-260-270 | 22.00 | | -0.54 | 0.52 | 6478 | Mid | Santa Rosa Island | Island | 33.921 | -120.1 |
| 400 | 21 | Robbins et al., 2013 | SRI-147-260-270 | 38.00 | | 0.04 | 0.53 | 6478 | Mid | Santa Rosa Island | Island | 33.921 | -120.1 |
| 400 | 21 | Robbins et al., 2013 | SRI-147-260-270 | 42.00 | | 0.24 | 0.54 | 6478 | Mid | Santa Rosa Island | Island | 33.921 | -120.1 |
| 400 | 21 | Robbins et al., 2013 | SRI-147-260-270 | 14.00 | | -0.33 | 0.76 | 6478 | Mid | Santa Rosa Island | Island | 33.921 | -120.1 |
| 400 | 21 | Robbins et al., 2013 | SRI-147-260-270 | 12.00 | | -0.48 | 0.83 | 6478 | Mid | Santa Rosa Island | Island | 33.921 | -120.1 |
| 400 | 21 | Robbins et al., 2013 | SRI-147-260-270 | 36.00 | | 0.14 | 0.84 | 6478 | Mid | Santa Rosa Island | Island | 33.921 | -120.1 |
| 400 | 21 | Robbins et al., 2013 | SRI-147-260-270 | 6.00 | | -0.27 | 0.90 | 6478 | Mid | Santa Rosa Island | Island | 33.921 | -120.1 |
| 400 | 21 | Robbins et al., 2013 | SRI-147-260-270 | 32.00 | | 0.20 | 0.94 | 6478 | Mid | Santa Rosa Island | Island | 33.921 | -120.1 |
| 400 | 21 | Robbins et al., 2013 | SRI-147-260-270 | 10.00 | | -0.53 | 0.95 | 6478 | Mid | Santa Rosa Island | Island | 33.921 | -120.1 |
| 400 | 21 | Robbins et al., 2013 | SRI-147-260-270 | 28.00 | | 0.00 | 0.96 | 6478 | Mid | Santa Rosa Island | Island | 33.921 | -120.1 |
| 400 | 21 | Robbins et al., 2013 | SRI-147-260-270 | 4.00 | | -0.17 | 1.01 | 6478 | Mid | Santa Rosa Island | Island | 33.921 | -120.1 |
| 400 | 21 | Robbins et al., 2013 | SRI-147-260-270 | 26.00 | | -0.44 | 1.02 | 6478 | Mid | Santa Rosa Island | Island | 33.921 | -120.1 |
| 400 | 21 | Robbins et al., 2013 | SRI-147-260-270 | 30.00 | | -0.03 | 1.08 | 6478 | Mid | Santa Rosa Island | Island | 33.921 | -120.1 |
| 400 | 21 | Robbins et al., 2013 | SRI-147-260-270 | 24.00 | | -0.63 | 1.15 | 6478 | Mid | Santa Rosa Island | Island | 33.921 | -120.1 |
| 400 | 21 | Robbins et al., 2013 | SRI-147-260-270 | 34.00 | | 0.06 | 1.16 | 6478 | Mid | Santa Rosa Island | Island | 33.921 | -120.1 |
| 400 | 21 | Robbins et al., 2013 | SRI-147-260-270 | 8.00 | | -0.35 | 1.25 | 6478 | Mid | Santa Rosa Island | Island | 33.921 | -120.1 |

| | | | | | | | | | | | | | |
|---|---|---|---|---|---|---|---|---|---|---|---|---|---|
| 400 | 21 | Robbins et al., 2013 | SRI-147-260-270 | 0.00 | | -0.28 | 1.29 | 6478 | Mid | Santa Rosa Island | Island | 33.921 | -120.1 |
| 400 | 21 | Robbins et al., 2013 | SRI-147-260-270 | 2.00 | | -0.11 | 1.39 | 6478 | Mid | Santa Rosa Island | Island | 33.921 | -120.1 |
| 401 | 18 | Robbins et al., 2013 | SRI-147-270-280 | 40.00 | | 0.37 | -0.14 | 6757 | Mid | Santa Rosa Island | Island | 33.921 | -120.1 |
| 401 | 18 | Robbins et al., 2013 | SRI-147-270-280 | 8.00 | | 0.66 | 0.42 | 6757 | Mid | Santa Rosa Island | Island | 33.921 | -120.1 |
| 401 | 18 | Robbins et al., 2013 | SRI-147-270-280 | 20.00 | | -0.29 | 0.48 | 6757 | Mid | Santa Rosa Island | Island | 33.921 | -120.1 |
| 401 | 18 | Robbins et al., 2013 | SRI-147-270-280 | 34.00 | | 0.24 | 0.50 | 6757 | Mid | Santa Rosa Island | Island | 33.921 | -120.1 |
| 401 | 18 | Robbins et al., 2013 | SRI-147-270-280 | 6.00 | | 0.39 | 0.51 | 6757 | Mid | Santa Rosa Island | Island | 33.921 | -120.1 |
| 401 | 18 | Robbins et al., 2013 | SRI-147-270-280 | 2.00 | | 0.34 | 0.69 | 6757 | Mid | Santa Rosa Island | Island | 33.921 | -120.1 |
| 401 | 18 | Robbins et al., 2013 | SRI-147-270-280 | 30.00 | | -0.04 | 0.69 | 6757 | Mid | Santa Rosa Island | Island | 33.921 | -120.1 |
| 401 | 18 | Robbins et al., 2013 | SRI-147-270-280 | 12.00 | | 0.08 | 0.72 | 6757 | Mid | Santa Rosa Island | Island | 33.921 | -120.1 |
| 401 | 18 | Robbins et al., 2013 | SRI-147-270-280 | 4.00 | | 0.18 | 0.73 | 6757 | Mid | Santa Rosa Island | Island | 33.921 | -120.1 |
| 401 | 18 | Robbins et al., 2013 | SRI-147-270-280 | 28.00 | | 0.17 | 0.73 | 6757 | Mid | Santa Rosa Island | Island | 33.921 | -120.1 |
| 401 | 18 | Robbins et al., 2013 | SRI-147-270-280 | 18.00 | | 0.19 | 0.77 | 6757 | Mid | Santa Rosa Island | Island | 33.921 | -120.1 |
| 401 | 18 | Robbins et al., 2013 | SRI-147-270-280 | 0.00 | | 0.16 | 0.78 | 6757 | Mid | Santa Rosa Island | Island | 33.921 | -120.1 |
| 401 | 18 | Robbins et al., 2013 | SRI-147-270-280 | 10.00 | | -0.18 | 0.80 | 6757 | Mid | Santa Rosa Island | Island | 33.921 | -120.1 |
| 401 | 18 | Robbins et al., 2013 | SRI-147-270-280 | 22.00 | | -0.20 | 0.80 | 6757 | Mid | Santa Rosa Island | Island | 33.921 | -120.1 |
| 401 | 18 | Robbins et al., 2013 | SRI-147-270-280 | 26.00 | | 0.12 | 0.85 | 6757 | Mid | Santa Rosa Island | Island | 33.921 | -120.1 |
| 401 | 18 | Robbins et al., 2013 | SRI-147-270-280 | 14.00 | | 0.11 | 0.86 | 6757 | Mid | Santa Rosa Island | Island | 33.921 | -120.1 |
| 401 | 18 | Robbins et al., 2013 | SRI-147-270-280 | 24.00 | | -0.16 | 0.86 | 6757 | Mid | Santa Rosa Island | Island | 33.921 | -120.1 |

| | | | | | | | | | | | | | |
|---|---|---|---|---|---|---|---|---|---|---|---|---|---|
| 401 | 18 | Robbins et al., 2013 | SRI-147-270-280 | 16.00 | | 0.17 | 0.93 | 6757 | Mid | Santa Rosa Island | Island | 33.921 | -120.1 |
| 402 | 15 | Robbins et al., 2013 | SRI-147-280-290 | 28.00 | | -0.14 | -0.46 | 7036 | Mid | Santa Rosa Island | Island | 33.921 | -120.1 |
| 402 | 15 | Robbins et al., 2013 | SRI-147-280-290 | 12.00 | | 0.72 | -0.40 | 7036 | Mid | Santa Rosa Island | Island | 33.921 | -120.1 |
| 402 | 15 | Robbins et al., 2013 | SRI-147-280-290 | 0.00 | | 0.47 | -0.38 | 7036 | Mid | Santa Rosa Island | Island | 33.921 | -120.1 |
| 402 | 15 | Robbins et al., 2013 | SRI-147-280-290 | 10.00 | | 0.93 | -0.15 | 7036 | Mid | Santa Rosa Island | Island | 33.921 | -120.1 |
| 402 | 15 | Robbins et al., 2013 | SRI-147-280-290 | 32.00 | | -0.34 | -0.13 | 7036 | Mid | Santa Rosa Island | Island | 33.921 | -120.1 |
| 402 | 15 | Robbins et al., 2013 | SRI-147-280-290 | 30.00 | | 0.10 | -0.09 | 7036 | Mid | Santa Rosa Island | Island | 33.921 | -120.1 |
| 402 | 15 | Robbins et al., 2013 | SRI-147-280-290 | 14.00 | | 0.57 | -0.07 | 7036 | Mid | Santa Rosa Island | Island | 33.921 | -120.1 |
| 402 | 15 | Robbins et al., 2013 | SRI-147-280-290 | 4.00 | | 0.05 | 0.13 | 7036 | Mid | Santa Rosa Island | Island | 33.921 | -120.1 |
| 402 | 15 | Robbins et al., 2013 | SRI-147-280-290 | 2.00 | | 0.34 | 0.15 | 7036 | Mid | Santa Rosa Island | Island | 33.921 | -120.1 |
| 402 | 15 | Robbins et al., 2013 | SRI-147-280-290 | 18.00 | | -0.18 | 0.27 | 7036 | Mid | Santa Rosa Island | Island | 33.921 | -120.1 |
| 402 | 15 | Robbins et al., 2013 | SRI-147-280-290 | 16.00 | | 0.01 | 0.32 | 7036 | Mid | Santa Rosa Island | Island | 33.921 | -120.1 |
| 402 | 15 | Robbins et al., 2013 | SRI-147-280-290 | 6.00 | | -0.15 | 0.42 | 7036 | Mid | Santa Rosa Island | Island | 33.921 | -120.1 |
| 402 | 15 | Robbins et al., 2013 | SRI-147-280-290 | 22.00 | | 0.18 | 0.50 | 7036 | Mid | Santa Rosa Island | Island | 33.921 | -120.1 |
| 402 | 15 | Robbins et al., 2013 | SRI-147-280-290 | 20.00 | | 0.24 | 0.68 | 7036 | Mid | Santa Rosa Island | Island | 33.921 | -120.1 |
| 402 | 15 | Robbins et al., 2013 | SRI-147-280-290 | 8.00 | | -0.32 | 0.73 | 7036 | Mid | Santa Rosa Island | Island | 33.921 | -120.1 |
| 403 | 15 | Robbins et al., 2013 | SRI-147-290-300 | 0.00 | | 1.15 | -0.92 | 7315 | Mid | Santa Rosa Island | Island | 33.921 | -120.1 |
| 403 | 15 | Robbins et al., 2013 | SRI-147-290-300 | 14.00 | | 0.82 | -0.63 | 7315 | Mid | Santa Rosa Island | Island | 33.921 | -120.1 |
| 403 | 15 | Robbins et al., 2013 | SRI-147-290-300 | 2.00 | | 1.02 | -0.60 | 7315 | Mid | Santa Rosa Island | Island | 33.921 | -120.1 |

| | | | | | | | | | | | | | |
|---|---|---|---|---|---|---|---|---|---|---|---|---|---|
| 403 | 15 | Robbins et al., 2013 | SRI-147-290-300 | 12.00 | | 1.05 | -0.56 | 7315 | Mid | Santa Rosa Island | Island | 33.921 | -120.1 |
| 403 | 15 | Robbins et al., 2013 | SRI-147-290-300 | 16.00 | | 0.59 | -0.41 | 7315 | Mid | Santa Rosa Island | Island | 33.921 | -120.1 |
| 403 | 15 | Robbins et al., 2013 | SRI-147-290-300 | 4.00 | | 0.89 | -0.13 | 7315 | Mid | Santa Rosa Island | Island | 33.921 | -120.1 |
| 403 | 15 | Robbins et al., 2013 | SRI-147-290-300 | 10.00 | | 1.08 | -0.03 | 7315 | Mid | Santa Rosa Island | Island | 33.921 | -120.1 |
| 403 | 15 | Robbins et al., 2013 | SRI-147-290-300 | 18.00 | | 0.47 | 0.13 | 7315 | Mid | Santa Rosa Island | Island | 33.921 | -120.1 |
| 403 | 15 | Robbins et al., 2013 | SRI-147-290-300 | 20.00 | | 0.24 | 0.59 | 7315 | Mid | Santa Rosa Island | Island | 33.921 | -120.1 |
| 403 | 15 | Robbins et al., 2013 | SRI-147-290-300 | 22.00 | | 0.27 | 0.75 | 7315 | Mid | Santa Rosa Island | Island | 33.921 | -120.1 |
| 403 | 15 | Robbins et al., 2013 | SRI-147-290-300 | 8.00 | | 0.63 | 0.80 | 7315 | Mid | Santa Rosa Island | Island | 33.921 | -120.1 |
| 403 | 15 | Robbins et al., 2013 | SRI-147-290-300 | 24.00 | | -0.05 | 0.80 | 7315 | Mid | Santa Rosa Island | Island | 33.921 | -120.1 |
| 403 | 15 | Robbins et al., 2013 | SRI-147-290-300 | 6.00 | | 0.46 | 0.81 | 7315 | Mid | Santa Rosa Island | Island | 33.921 | -120.1 |
| 403 | 15 | Robbins et al., 2013 | SRI-147-290-300 | 28.00 | | 0.31 | 0.88 | 7315 | Mid | Santa Rosa Island | Island | 33.921 | -120.1 |
| 403 | 15 | Robbins et al., 2013 | SRI-147-290-300 | 26.00 | | 0.36 | 0.95 | 7315 | Mid | Santa Rosa Island | Island | 33.921 | -120.1 |
| 404 | 16 | Robbins et al., 2013 | SRI-147-300-310 | 4.00 | | 0.24 | 0.17 | 7594 | Mid | Santa Rosa Island | Island | 33.921 | -120.1 |
| 404 | 16 | Robbins et al., 2013 | SRI-147-300-310 | 20.00 | | 0.21 | 0.24 | 7594 | Mid | Santa Rosa Island | Island | 33.921 | -120.1 |
| 404 | 16 | Robbins et al., 2013 | SRI-147-300-310 | 2.00 | | 0.16 | 0.47 | 7594 | Mid | Santa Rosa Island | Island | 33.921 | -120.1 |
| 404 | 16 | Robbins et al., 2013 | SRI-147-300-310 | 28.00 | | -0.25 | 0.66 | 7594 | Mid | Santa Rosa Island | Island | 33.921 | -120.1 |
| 404 | 16 | Robbins et al., 2013 | SRI-147-300-310 | 18.00 | | -0.14 | 0.68 | 7594 | Mid | Santa Rosa Island | Island | 33.921 | -120.1 |
| 404 | 16 | Robbins et al., 2013 | SRI-147-300-310 | 22.00 | | -0.36 | 0.72 | 7594 | Mid | Santa Rosa Island | Island | 33.921 | -120.1 |
| 404 | 16 | Robbins et al., 2013 | SRI-147-300-310 | 30.00 | | -0.37 | 0.74 | 7594 | Mid | Santa Rosa Island | Island | 33.921 | -120.1 |

| | | | | | | | | | | | | | |
|---|---|---|---|---|---|---|---|---|---|---|---|---|---|
| 404 | 16 | Robbins et al., 2013 | SRI-147-300-310 | 26.00 | | 0.08 | 0.79 | 7594 | Mid | Santa Rosa Island | Island | 33.921 | -120.1 |
| 404 | 16 | Robbins et al., 2013 | SRI-147-300-310 | 6.00 | | 0.25 | 0.85 | 7594 | Mid | Santa Rosa Island | Island | 33.921 | -120.1 |
| 404 | 16 | Robbins et al., 2013 | SRI-147-300-310 | 24.00 | | 0.01 | 0.85 | 7594 | Mid | Santa Rosa Island | Island | 33.921 | -120.1 |
| 404 | 16 | Robbins et al., 2013 | SRI-147-300-310 | 14.00 | | 0.15 | 0.99 | 7594 | Mid | Santa Rosa Island | Island | 33.921 | -120.1 |
| 404 | 16 | Robbins et al., 2013 | SRI-147-300-310 | 10.00 | | -0.06 | 1.01 | 7594 | Mid | Santa Rosa Island | Island | 33.921 | -120.1 |
| 404 | 16 | Robbins et al., 2013 | SRI-147-300-310 | 16.00 | | 0.09 | 1.04 | 7594 | Mid | Santa Rosa Island | Island | 33.921 | -120.1 |
| 404 | 16 | Robbins et al., 2013 | SRI-147-300-310 | 8.00 | | -0.13 | 1.05 | 7594 | Mid | Santa Rosa Island | Island | 33.921 | -120.1 |
| 404 | 16 | Robbins et al., 2013 | SRI-147-300-310 | 0.00 | | -0.40 | 1.06 | 7594 | Mid | Santa Rosa Island | Island | 33.921 | -120.1 |
| 404 | 16 | Robbins et al., 2013 | SRI-147-300-310 | 12.00 | | 0.00 | 1.09 | 7594 | Mid | Santa Rosa Island | Island | 33.921 | -120.1 |
| 405 | 20 | Robbins et al., 2013 | SRI-147-40-50 | 10.00 | | 0.59 | -0.72 | 1676 | Mid | Santa Rosa Island | Island | 33.921 | -120.1 |
| 405 | 20 | Robbins et al., 2013 | SRI-147-40-50 | 30.00 | | 0.59 | -0.30 | 1676 | Mid | Santa Rosa Island | Island | 33.921 | -120.1 |
| 405 | 20 | Robbins et al., 2013 | SRI-147-40-50 | 12.00 | | 0.40 | -0.27 | 1676 | Mid | Santa Rosa Island | Island | 33.921 | -120.1 |
| 405 | 20 | Robbins et al., 2013 | SRI-147-40-50 | 8.00 | | 0.75 | -0.19 | 1676 | Mid | Santa Rosa Island | Island | 33.921 | -120.1 |
| 405 | 20 | Robbins et al., 2013 | SRI-147-40-50 | 14.00 | | 0.48 | -0.08 | 1676 | Mid | Santa Rosa Island | Island | 33.921 | -120.1 |
| 405 | 20 | Robbins et al., 2013 | SRI-147-40-50 | 2.00 | | 0.10 | -0.01 | 1676 | Mid | Santa Rosa Island | Island | 33.921 | -120.1 |
| 405 | 20 | Robbins et al., 2013 | SRI-147-40-50 | 34.00 | | 0.40 | 0.07 | 1676 | Mid | Santa Rosa Island | Island | 33.921 | -120.1 |
| 405 | 20 | Robbins et al., 2013 | SRI-147-40-50 | 28.00 | | 0.50 | 0.09 | 1676 | Mid | Santa Rosa Island | Island | 33.921 | -120.1 |
| 405 | 20 | Robbins et al., 2013 | SRI-147-40-50 | 4.00 | | 0.50 | 0.20 | 1676 | Mid | Santa Rosa Island | Island | 33.921 | -120.1 |
| 405 | 20 | Robbins et al., 2013 | SRI-147-40-50 | 36.00 | | 0.27 | 0.22 | 1676 | Mid | Santa Rosa Island | Island | 33.921 | -120.1 |

| | | | | | | | | | | | | | |
|---|---|---|---|---|---|---|---|---|---|---|---|---|---|
| 405 | 20 | Robbins et al., 2013 | SRI-147-40-50 | 16.00 | | 0.46 | 0.24 | 1676 | Mid | Santa Rosa Island | Island | 33.921 | -120.1 |
| 405 | 20 | Robbins et al., 2013 | SRI-147-40-50 | 0.00 | | -0.06 | 0.31 | 1676 | Mid | Santa Rosa Island | Island | 33.921 | -120.1 |
| 405 | 20 | Robbins et al., 2013 | SRI-147-40-50 | 20.00 | | 0.61 | 0.37 | 1676 | Mid | Santa Rosa Island | Island | 33.921 | -120.1 |
| 405 | 20 | Robbins et al., 2013 | SRI-147-40-50 | 38.00 | | 0.55 | 0.45 | 1676 | Mid | Santa Rosa Island | Island | 33.921 | -120.1 |
| 405 | 20 | Robbins et al., 2013 | SRI-147-40-50 | 32.00 | | 0.89 | 0.46 | 1676 | Mid | Santa Rosa Island | Island | 33.921 | -120.1 |
| 405 | 20 | Robbins et al., 2013 | SRI-147-40-50 | 22.00 | | 0.73 | 0.70 | 1676 | Mid | Santa Rosa Island | Island | 33.921 | -120.1 |
| 405 | 20 | Robbins et al., 2013 | SRI-147-40-50 | 26.00 | | 0.47 | 0.73 | 1676 | Mid | Santa Rosa Island | Island | 33.921 | -120.1 |
| 405 | 20 | Robbins et al., 2013 | SRI-147-40-50 | 18.00 | | 0.49 | 0.78 | 1676 | Mid | Santa Rosa Island | Island | 33.921 | -120.1 |
| 405 | 20 | Robbins et al., 2013 | SRI-147-40-50 | 6.00 | | 0.44 | 0.85 | 1676 | Mid | Santa Rosa Island | Island | 33.921 | -120.1 |
| 405 | 20 | Robbins et al., 2013 | SRI-147-40-50 | 24.00 | | 0.38 | 1.18 | 1676 | Mid | Santa Rosa Island | Island | 33.921 | -120.1 |
| 406 | 10 | Robbins et al., 2013 | SRI-147-40-50 | 16.00 | | 0.53 | -0.17 | 1676 | Mid | Santa Rosa Island | Island | 33.921 | -120.1 |
| 406 | 10 | Robbins et al., 2013 | SRI-147-40-50 | 10.00 | | 1.39 | -0.12 | 1676 | Mid | Santa Rosa Island | Island | 33.921 | -120.1 |
| 406 | 10 | Robbins et al., 2013 | SRI-147-40-50 | 14.00 | | 0.96 | -0.10 | 1676 | Mid | Santa Rosa Island | Island | 33.921 | -120.1 |
| 406 | 10 | Robbins et al., 2013 | SRI-147-40-50 | 8.00 | | 1.04 | 0.04 | 1676 | Mid | Santa Rosa Island | Island | 33.921 | -120.1 |
| 406 | 10 | Robbins et al., 2013 | SRI-147-40-50 | 12.00 | | 1.20 | 0.06 | 1676 | Mid | Santa Rosa Island | Island | 33.921 | -120.1 |
| 406 | 10 | Robbins et al., 2013 | SRI-147-40-50 | 18.00 | | 0.49 | 0.07 | 1676 | Mid | Santa Rosa Island | Island | 33.921 | -120.1 |
| 406 | 10 | Robbins et al., 2013 | SRI-147-40-50 | 0.00 | | 0.50 | 0.40 | 1676 | Mid | Santa Rosa Island | Island | 33.921 | -120.1 |
| 406 | 10 | Robbins et al., 2013 | SRI-147-40-50 | 4.00 | | 0.67 | 0.63 | 1676 | Mid | Santa Rosa Island | Island | 33.921 | -120.1 |
| 406 | 10 | Robbins et al., 2013 | SRI-147-40-50 | 6.00 | | 1.05 | 0.76 | 1676 | Mid | Santa Rosa Island | Island | 33.921 | -120.1 |

| | | | | | | | | | | | | | |
|---|---|---|---|---|---|---|---|---|---|---|---|---|---|
| 406 | 10 | Robbins et al., 2013 | SRI-147-40-50 | 2.00 | | 0.75 | 0.90 | 1676 | Mid | Santa Rosa Island | Island | 33.921 | -120.1 |
| 407 | 15 | Robbins et al., 2013 | SRI-147-50-60 | 12.00 | | 1.08 | -0.07 | 2113 | Mid | Santa Rosa Island | Island | 33.921 | -120.1 |
| 407 | 15 | Robbins et al., 2013 | SRI-147-50-60 | 14.00 | | 0.90 | 0.02 | 2113 | Mid | Santa Rosa Island | Island | 33.921 | -120.1 |
| 407 | 15 | Robbins et al., 2013 | SRI-147-50-60 | 0.00 | | 1.09 | 0.06 | 2113 | Mid | Santa Rosa Island | Island | 33.921 | -120.1 |
| 407 | 15 | Robbins et al., 2013 | SRI-147-50-60 | 18.00 | | 0.64 | 0.14 | 2113 | Mid | Santa Rosa Island | Island | 33.921 | -120.1 |
| 407 | 15 | Robbins et al., 2013 | SRI-147-50-60 | 16.00 | | 0.78 | 0.20 | 2113 | Mid | Santa Rosa Island | Island | 33.921 | -120.1 |
| 407 | 15 | Robbins et al., 2013 | SRI-147-50-60 | 10.00 | | 1.23 | 0.37 | 2113 | Mid | Santa Rosa Island | Island | 33.921 | -120.1 |
| 407 | 15 | Robbins et al., 2013 | SRI-147-50-60 | 28.00 | | 1.08 | 0.55 | 2113 | Mid | Santa Rosa Island | Island | 33.921 | -120.1 |
| 407 | 15 | Robbins et al., 2013 | SRI-147-50-60 | 8.00 | | 0.92 | 0.67 | 2113 | Mid | Santa Rosa Island | Island | 33.921 | -120.1 |
| 407 | 15 | Robbins et al., 2013 | SRI-147-50-60 | 6.00 | | 0.80 | 0.68 | 2113 | Mid | Santa Rosa Island | Island | 33.921 | -120.1 |
| 407 | 15 | Robbins et al., 2013 | SRI-147-50-60 | 24.00 | | 0.69 | 0.74 | 2113 | Mid | Santa Rosa Island | Island | 33.921 | -120.1 |
| 407 | 15 | Robbins et al., 2013 | SRI-147-50-60 | 26.00 | | 0.87 | 0.76 | 2113 | Mid | Santa Rosa Island | Island | 33.921 | -120.1 |
| 407 | 15 | Robbins et al., 2013 | SRI-147-50-60 | 22.00 | | 0.38 | 0.80 | 2113 | Mid | Santa Rosa Island | Island | 33.921 | -120.1 |
| 407 | 15 | Robbins et al., 2013 | SRI-147-50-60 | 20.00 | | 0.72 | 0.95 | 2113 | Mid | Santa Rosa Island | Island | 33.921 | -120.1 |
| 407 | 15 | Robbins et al., 2013 | SRI-147-50-60 | 2.00 | | 0.61 | 0.99 | 2113 | Mid | Santa Rosa Island | Island | 33.921 | -120.1 |
| 407 | 15 | Robbins et al., 2013 | SRI-147-50-60 | 4.00 | | 0.82 | 1.09 | 2113 | Mid | Santa Rosa Island | Island | 33.921 | -120.1 |
| 408 | 12 | Robbins et al., 2013 | SRI-147-60-70 | 10.00 | | 1.08 | 0.16 | 2550 | Mid | Santa Rosa Island | Island | 33.921 | -120.1 |
| 408 | 12 | Robbins et al., 2013 | SRI-147-60-70 | 20.00 | | 1.09 | 0.19 | 2550 | Mid | Santa Rosa Island | Island | 33.921 | -120.1 |
| 408 | 12 | Robbins et al., 2013 | SRI-147-60-70 | 4.00 | | 1.02 | 0.35 | 2550 | Mid | Santa Rosa Island | Island | 33.921 | -120.1 |

| | | | | | | | | | | | | | |
|---|---|---|---|---|---|---|---|---|---|---|---|---|---|
| 408 | 12 | Robbins et al., 2013 | SRI-147-60-70 | 22.00 | | 0.84 | 0.39 | 2550 | Mid | Santa Rosa Island | Island | 33.921 | -120.1 |
| 408 | 12 | Robbins et al., 2013 | SRI-147-60-70 | 0.00 | | 1.05 | 0.40 | 2550 | Mid | Santa Rosa Island | Island | 33.921 | -120.1 |
| 408 | 12 | Robbins et al., 2013 | SRI-147-60-70 | 12.00 | | 0.87 | 0.49 | 2550 | Mid | Santa Rosa Island | Island | 33.921 | -120.1 |
| 408 | 12 | Robbins et al., 2013 | SRI-147-60-70 | 2.00 | | 1.10 | 0.71 | 2550 | Mid | Santa Rosa Island | Island | 33.921 | -120.1 |
| 408 | 12 | Robbins et al., 2013 | SRI-147-60-70 | 14.00 | | 0.93 | 0.77 | 2550 | Mid | Santa Rosa Island | Island | 33.921 | -120.1 |
| 408 | 12 | Robbins et al., 2013 | SRI-147-60-70 | 8.00 | | 1.18 | 0.79 | 2550 | Mid | Santa Rosa Island | Island | 33.921 | -120.1 |
| 408 | 12 | Robbins et al., 2013 | SRI-147-60-70 | 18.00 | | 0.89 | 0.82 | 2550 | Mid | Santa Rosa Island | Island | 33.921 | -120.1 |
| 408 | 12 | Robbins et al., 2013 | SRI-147-60-70 | 6.00 | | 1.09 | 0.90 | 2550 | Mid | Santa Rosa Island | Island | 33.921 | -120.1 |
| 408 | 12 | Robbins et al., 2013 | SRI-147-60-70 | 16.00 | | 0.59 | 1.01 | 2550 | Mid | Santa Rosa Island | Island | 33.921 | -120.1 |
| 409 | 11 | Robbins et al., 2013 | SRI-147-90-100 | 20.00 | | -0.07 | 0.39 | 3724 | Mid | Santa Rosa Island | Island | 33.921 | -120.1 |
| 409 | 11 | Robbins et al., 2013 | SRI-147-90-100 | 18.00 | | -0.02 | 0.46 | 3724 | Mid | Santa Rosa Island | Island | 33.921 | -120.1 |
| 409 | 11 | Robbins et al., 2013 | SRI-147-90-100 | 6.00 | | 0.48 | 0.50 | 3724 | Mid | Santa Rosa Island | Island | 33.921 | -120.1 |
| 409 | 11 | Robbins et al., 2013 | SRI-147-90-100 | 8.00 | | 0.35 | 0.52 | 3724 | Mid | Santa Rosa Island | Island | 33.921 | -120.1 |
| 409 | 11 | Robbins et al., 2013 | SRI-147-90-100 | 4.00 | | 0.30 | 0.71 | 3724 | Mid | Santa Rosa Island | Island | 33.921 | -120.1 |
| 409 | 11 | Robbins et al., 2013 | SRI-147-90-100 | 16.00 | | 0.00 | 0.88 | 3724 | Mid | Santa Rosa Island | Island | 33.921 | -120.1 |
| 409 | 11 | Robbins et al., 2013 | SRI-147-90-100 | 2.00 | | 0.67 | 1.04 | 3724 | Mid | Santa Rosa Island | Island | 33.921 | -120.1 |
| 409 | 11 | Robbins et al., 2013 | SRI-147-90-100 | 10.00 | | 0.28 | 1.08 | 3724 | Mid | Santa Rosa Island | Island | 33.921 | -120.1 |
| 409 | 11 | Robbins et al., 2013 | SRI-147-90-100 | 14.00 | | 0.21 | 1.13 | 3724 | Mid | Santa Rosa Island | Island | 33.921 | -120.1 |
| 409 | 11 | Robbins et al., 2013 | SRI-147-90-100 | 12.00 | | 0.17 | 1.23 | 3724 | Mid | Santa Rosa Island | Island | 33.921 | -120.1 |

| | | | | | | | | | | | | | |
|---|---|---|---|---|---|---|---|---|---|---|---|---|---|
| 409 | 11 | Robbins et al., 2013 | SRI-147-90-100 | 0.00 | | 0.74 | 1.44 | 3724 | Mid | Santa Rosa Island | Island | 33.921 | -120.1 |
| 410 | 24 | Ferguson et al., 2013 | SD Mussel 1 | SD130a-10 | | 0.73 | -1.23 | 23 | Mod | San Diego | Main | 32.867 | -117.3 |
| 410 | 24 | Ferguson et al., 2013 | SD Mussel 1 | SD130a-11 | | 0.97 | -1.01 | 23 | Mod | San Diego | Main | 32.867 | -117.3 |
| 410 | 24 | Ferguson et al., 2013 | SD Mussel 1 | SD130a-12 | | 0.72 | -0.98 | 23 | Mod | San Diego | Main | 32.867 | -117.3 |
| 410 | 24 | Ferguson et al., 2013 | SD Mussel 1 | SD130a-13 | | 0.62 | -0.85 | 23 | Mod | San Diego | Main | 32.867 | -117.3 |
| 410 | 24 | Ferguson et al., 2013 | SD Mussel 1 | SD130a-14 | | 0.43 | -0.98 | 23 | Mod | San Diego | Main | 32.867 | -117.3 |
| 410 | 24 | Ferguson et al., 2013 | SD Mussel 1 | SD130a-16 | | 0.66 | -0.72 | 23 | Mod | San Diego | Main | 32.867 | -117.3 |
| 410 | 24 | Ferguson et al., 2013 | SD Mussel 1 | SD130a-17 | | 0.74 | -0.86 | 23 | Mod | San Diego | Main | 32.867 | -117.3 |
| 410 | 24 | Ferguson et al., 2013 | SD Mussel 1 | SD130a-18 | | 0.66 | -0.64 | 23 | Mod | San Diego | Main | 32.867 | -117.3 |
| 410 | 24 | Ferguson et al., 2013 | SD Mussel 1 | SD130a-19 | | 0.74 | -0.42 | 23 | Mod | San Diego | Main | 32.867 | -117.3 |
| 410 | 24 | Ferguson et al., 2013 | SD Mussel 1 | SD130a-20 | | 0.73 | -0.46 | 23 | Mod | San Diego | Main | 32.867 | -117.3 |
| 410 | 24 | Ferguson et al., 2013 | SD Mussel 1 | SD130a-22 | | 0.66 | -0.43 | 23 | Mod | San Diego | Main | 32.867 | -117.3 |
| 410 | 24 | Ferguson et al., 2013 | SD Mussel 1 | SD130a-24 | | 0.46 | 0.05 | 23 | Mod | San Diego | Main | 32.867 | -117.3 |
| 410 | 24 | Ferguson et al., 2013 | SD Mussel 1 | SD130a-26 | | 0.59 | -0.23 | 23 | Mod | San Diego | Main | 32.867 | -117.3 |
| 410 | 24 | Ferguson et al., 2013 | SD Mussel 1 | SD130a-27 | | 0.50 | 0.24 | 23 | Mod | San Diego | Main | 32.867 | -117.3 |
| 410 | 24 | Ferguson et al., 2013 | SD Mussel 1 | SD130a-28 | | 0.50 | 0.12 | 23 | Mod | San Diego | Main | 32.867 | -117.3 |
| 410 | 24 | Ferguson et al., 2013 | SD Mussel 1 | SD130a-30 | | 0.36 | 0.09 | 23 | Mod | San Diego | Main | 32.867 | -117.3 |
| 410 | 24 | Ferguson et al., 2013 | SD Mussel 1 | SD130a-31 | | 0.28 | 0.18 | 23 | Mod | San Diego | Main | 32.867 | -117.3 |
| 410 | 24 | Ferguson et al., 2013 | SD Mussel 1 | SD130a-32 | | 0.20 | 0.07 | 23 | Mod | San Diego | Main | 32.867 | -117.3 |

| | | | | | | | | | | | | | |
|---|---|---|---|---|---|---|---|---|---|---|---|---|---|
| 410 | 24 | Ferguson et al., 2013 | SD Mussel 1 | SD130a-33 | | 0.12 | -0.05 | 23 | Mod | San Diego | Main | 32.867 | -117.3 |
| 410 | 24 | Ferguson et al., 2013 | SD Mussel 1 | SD130a-34 | | 0.29 | 0.12 | 23 | Mod | San Diego | Main | 32.867 | -117.3 |
| 410 | 24 | Ferguson et al., 2013 | SD Mussel 1 | SD130a-5 | | 0.75 | -1.14 | 23 | Mod | San Diego | Main | 32.867 | -117.3 |
| 410 | 24 | Ferguson et al., 2013 | SD Mussel 1 | SD130a-7 | | 0.99 | -1.15 | 23 | Mod | San Diego | Main | 32.867 | -117.3 |
| 410 | 24 | Ferguson et al., 2013 | SD Mussel 1 | SD130a-8 | | 0.95 | -1.28 | 23 | Mod | San Diego | Main | 32.867 | -117.3 |
| 410 | 24 | Ferguson et al., 2013 | SD Mussel 1 | SD130a-9 | | 0.87 | -1.18 | 23 | Mod | San Diego | Main | 32.867 | -117.3 |
| 411 | 26 | Ferguson et al., 2013 | SD Mussel 2 | SD136-10 | | 1.04 | -1.38 | 23 | Mod | San Diego | Main | 32.867 | -117.3 |
| 411 | 26 | Ferguson et al., 2013 | SD Mussel 2 | SD136-11 | | 0.91 | -1.40 | 23 | Mod | San Diego | Main | 32.867 | -117.3 |
| 411 | 26 | Ferguson et al., 2013 | SD Mussel 2 | SD136-12 | | 0.60 | -1.33 | 23 | Mod | San Diego | Main | 32.867 | -117.3 |
| 411 | 26 | Ferguson et al., 2013 | SD Mussel 2 | SD136-13 | | 1.11 | -1.20 | 23 | Mod | San Diego | Main | 32.867 | -117.3 |
| 411 | 26 | Ferguson et al., 2013 | SD Mussel 2 | SD136-14 | | 0.94 | -1.46 | 23 | Mod | San Diego | Main | 32.867 | -117.3 |
| 411 | 26 | Ferguson et al., 2013 | SD Mussel 2 | SD136-15 | | 0.99 | -1.49 | 23 | Mod | San Diego | Main | 32.867 | -117.3 |
| 411 | 26 | Ferguson et al., 2013 | SD Mussel 2 | SD136-16 | | 0.88 | -1.47 | 23 | Mod | San Diego | Main | 32.867 | -117.3 |
| 411 | 26 | Ferguson et al., 2013 | SD Mussel 2 | SD136-19 | | 0.73 | -0.93 | 23 | Mod | San Diego | Main | 32.867 | -117.3 |
| 411 | 26 | Ferguson et al., 2013 | SD Mussel 2 | SD136-2 | | -0.33 | -1.04 | 23 | Mod | San Diego | Main | 32.867 | -117.3 |
| 411 | 26 | Ferguson et al., 2013 | SD Mussel 2 | SD136-21 | | 0.70 | -0.83 | 23 | Mod | San Diego | Main | 32.867 | -117.3 |
| 411 | 26 | Ferguson et al., 2013 | SD Mussel 2 | SD136-22 | | 0.76 | -0.72 | 23 | Mod | San Diego | Main | 32.867 | -117.3 |
| 411 | 26 | Ferguson et al., 2013 | SD Mussel 2 | SD136-24 | | 1.01 | -0.35 | 23 | Mod | San Diego | Main | 32.867 | -117.3 |
| 411 | 26 | Ferguson et al., 2013 | SD Mussel 2 | SD136-25 | | 1.00 | -0.64 | 23 | Mod | San Diego | Main | 32.867 | -117.3 |

| | | | | | | | | | | | | | |
|---|---|---|---|---|---|---|---|---|---|---|---|---|---|
| 411 | 26 | Ferguson et al., 2013 | SD Mussel 2 | SD136-26 | | 0.95 | -0.51 | 23 | Mod | San Diego | Main | 32.867 | -117.3 |
| 411 | 26 | Ferguson et al., 2013 | SD Mussel 2 | SD136-27 | | 0.88 | -0.40 | 23 | Mod | San Diego | Main | 32.867 | -117.3 |
| 411 | 26 | Ferguson et al., 2013 | SD Mussel 2 | SD136-27 | | 0.81 | -0.40 | 23 | Mod | San Diego | Main | 32.867 | -117.3 |
| 411 | 26 | Ferguson et al., 2013 | SD Mussel 2 | SD136-28 | | 0.70 | -0.29 | 23 | Mod | San Diego | Main | 32.867 | -117.3 |
| 411 | 26 | Ferguson et al., 2013 | SD Mussel 2 | SD136-29 | | 0.54 | -0.14 | 23 | Mod | San Diego | Main | 32.867 | -117.3 |
| 411 | 26 | Ferguson et al., 2013 | SD Mussel 2 | SD136-3 | | -0.18 | -1.08 | 23 | Mod | San Diego | Main | 32.867 | -117.3 |
| 411 | 26 | Ferguson et al., 2013 | SD Mussel 2 | SD136-30 | | 0.45 | -0.04 | 23 | Mod | San Diego | Main | 32.867 | -117.3 |
| 411 | 26 | Ferguson et al., 2013 | SD Mussel 2 | SD136-4 | | 0.03 | -1.22 | 23 | Mod | San Diego | Main | 32.867 | -117.3 |
| 411 | 26 | Ferguson et al., 2013 | SD Mussel 2 | SD136-5 | | 0.49 | -1.64 | 23 | Mod | San Diego | Main | 32.867 | -117.3 |
| 411 | 26 | Ferguson et al., 2013 | SD Mussel 2 | SD136-6 | | 0.64 | -1.81 | 23 | Mod | San Diego | Main | 32.867 | -117.3 |
| 411 | 26 | Ferguson et al., 2013 | SD Mussel 2 | SD136-7 | | 0.87 | -1.40 | 23 | Mod | San Diego | Main | 32.867 | -117.3 |
| 411 | 26 | Ferguson et al., 2013 | SD Mussel 2 | SD136-8 | | 0.99 | -1.29 | 23 | Mod | San Diego | Main | 32.867 | -117.3 |
| 411 | 26 | Ferguson et al., 2013 | SD Mussel 2 | SD136-9 | | 1.00 | -1.26 | 23 | Mod | San Diego | Main | 32.867 | -117.3 |

**Appendix 2.** Appendix to Chapter 3. Shell information and characteristics for all *M. californianus* specimens used and analyzed in Chapter 3. Shell ID was assigned by this study. Growth index refers to valve mass (g)/shell length (mm). Cross-sectional thickness was measured at the thickest point adjacent to the umbo. Standardized gray-value variance is an indicator of growth band contrast. Light band amount is an estimate of the portion of light bands in the inner calcite layer of each shell.

| Shell ID | Museum | Region | County | Locality | Lat | Long | Year | Length (mm) | Width (mm) | Valve mass (g) | Growth index (g/mm) | Cross-sec thickness (mm) | Std. gray-value variance | Light band amount |
|---|---|---|---|---|---|---|---|---|---|---|---|---|---|---|
| BLJ965 | Bullard | SD and Baja CA | San Diego | La Jolla Tide Pools | 32.84 | -117.3 | 1996 | 30 | 15 | 1.4 | 0.0467 | 2.27 | -0.7911 | 0.34 |
| BLJ964 | Bullard | SD and Baja CA | San Diego | La Jolla Tide Pools | 32.84 | -117.3 | 1996 | 31 | 15 | 1.4 | 0.0459 | 0.969 | -0.8821 | 0.46 |
| BLJ963 | Bullard | SD and Baja CA | San Diego | La Jolla Tide Pools | 32.84 | -117.3 | 1996 | 35 | 17 | 1 | 0.0284 | | | |
| BLJ962 | Bullard | SD and Baja CA | San Diego | La Jolla Tide Pools | 32.84 | -117.3 | 1996 | 53 | 27 | 3.6 | 0.0684 | 1.062 | 0.1527 | 0.39 |
| BLJ961 | Bullard | SD and Baja CA | San Diego | La Jolla Tide Pools | 32.84 | -117.3 | 1996 | 61 | 27 | 10 | 0.168 | 2.04 | 1.7084 | 0.45 |
| BSD961 | Bullard | SD and Baja CA | San Diego | | | | 1996 | 92 | 40 | 10 | 0.1122 | 1.74 | -0.177 | 0.52 |
| BCM20105 | Bullard | Greater LA | Orange County | Corona del Mar | 33.59 | -117.9 | 2010 | 18 | 9.9 | 0.2 | 0.0109 | | | |
| BCM20104 | Bullard | Greater LA | Orange County | Corona del Mar | 33.59 | -117.9 | 2010 | 26 | 14 | 0.5 | 0.0193 | | | |
| BCM20103 | Bullard | Greater LA | Orange County | Corona del Mar | 33.59 | -117.9 | 2010 | 43 | 20 | 2.3 | 0.0536 | 1.95 | 0.9572 | 0.07 |

| | | | | | | | | | | | | | | |
|---|---|---|---|---|---|---|---|---|---|---|---|---|---|---|
| BCM2 0102 | Bullard | Greater LA | Orange County | Corona del Mar | 33.59 | -117.9 | 2010 | 50 | 24 | 4.4 | 0.0885 | 1.82 | -0.9553 | 0.4 |
| BCM2 0101 | Bullard | Greater LA | Orange County | Corona del Mar | 33.59 | -117.9 | 2010 | 76 | 32 | 9.9 | 0.1304 | 1.744 | -1.2076 | 0.58 |
| BSIO2 0101 | Bullard | SD and Baja CA | San Diego | SIO Pier Pilings | 32.87 | -117.3 | 2010 | 73 | 32 | 9.7 | 0.1331 | 3.342 | 0.5855 | 0.54 |
| BTP20 1027 | Bullard | SD and Baja CA | San Diego | Dike Rock Tide Pools | 32.84 | -117.3 | 2010 | 20 | 12 | 0.3 | 0.0153 | | | |
| BTP20 1017 | Bullard | SD and Baja CA | San Diego | Dike Rock Tide Pools | 32.84 | -117.3 | 2010 | 20 | 11 | 0.2 | 0.0101 | | | |
| BTP20 1024 | Bullard | SD and Baja CA | San Diego | Dike Rock Tide Pools | 32.84 | -117.3 | 2010 | 21 | 11 | 0.3 | 0.0144 | | | |
| BTP20 1016 | Bullard | SD and Baja CA | San Diego | Dike Rock Tide Pools | 32.84 | -117.3 | 2010 | 30 | 15 | 0.8 | 0.0265 | | | |
| BTP20 103 | Bullard | SD and Baja CA | San Diego | Dike Rock Tide Pools | 32.84 | -117.3 | 2010 | 32 | 16 | 0.8 | 0.0247 | 0.96 | -0.2712 | 0.46 |
| BTP20 1025 | Bullard | SD and Baja CA | San Diego | Dike Rock Tide Pools | 32.84 | -117.3 | 2010 | 33 | 18 | 1 | 0.0302 | 0.982 | -0.1811 | 0.52 |
| BTP20 1022 | Bullard | SD and Baja CA | San Diego | Dike Rock Tide Pools | 32.84 | -117.3 | 2010 | 37 | 20 | 1 | 0.0273 | 1.35 | -0.8719 | 0.42 |
| BTP20 1015 | Bullard | SD and Baja CA | San Diego | Dike Rock Tide Pools | 32.84 | -117.3 | 2010 | 38 | 20 | 1.4 | 0.037 | 1.42 | -0.7842 | 0.44 |
| BTP20 1014 | Bullard | SD and Baja CA | San Diego | Dike Rock Tide Pools | 32.84 | -117.3 | 2010 | 41 | 21 | 1.9 | 0.0466 | 0.875 | -0.5748 | 0.45 |

| | | | | | | | | | | | | | | |
|---|---|---|---|---|---|---|---|---|---|---|---|---|---|---|
| BTP20104 | Bullard | SD and Baja CA | San Diego | Dike Rock Tide Pools | 32.84 | -117.3 | 2010 | 44 | 22 | 2.6 | 0.0586 | 2.104 | -0.4627 | 0.28 |
| BTP20102 | Bullard | SD and Baja CA | San Diego | Dike Rock Tide Pools | 32.84 | -117.3 | 2010 | 48 | 23 | 3 | 0.0629 | | | |
| BTP201013 | Bullard | SD and Baja CA | San Diego | Dike Rock Tide Pools | 32.84 | -117.3 | 2010 | 48 | 24 | 2.2 | 0.046 | | | |
| BTP201012 | Bullard | SD and Baja CA | San Diego | Dike Rock Tide Pools | 32.84 | -117.3 | 2010 | 50 | 24 | 3.1 | 0.0621 | | | |
| BTP201011 | Bullard | SD and Baja CA | San Diego | Dike Rock Tide Pools | 32.84 | -117.3 | 2010 | 52 | 24 | 3.4 | 0.0659 | | | |
| BTP201010 | Bullard | SD and Baja CA | San Diego | Dike Rock Tide Pools | 32.84 | -117.3 | 2010 | 57 | 29 | 5 | 0.0874 | 2.61 | -0.5425 | 0.54 |
| BTP20107 | Bullard | SD and Baja CA | San Diego | Dike Rock Tide Pools | 32.84 | -117.3 | 2010 | 59 | 31 | 6.8 | 0.1158 | 2.82 | 1.3496 | 0.45 |
| BTP20106 | Bullard | SD and Baja CA | San Diego | Dike Rock Tide Pools | 32.84 | -117.3 | 2010 | 64 | 31 | 5.6 | 0.087 | | | |
| BTP201021 | Bullard | SD and Baja CA | San Diego | Dike Rock Tide Pools | 32.84 | -117.3 | 2010 | 65 | 30 | 7.2 | 0.1101 | 2.112 | -1.2551 | 0.3 |
| BTP201018 | Bullard | SD and Baja CA | San Diego | Dike Rock Tide Pools | 32.84 | -117.3 | 2010 | 66 | 32 | 7.1 | 0.1084 | | | |
| BTP201020 | Bullard | SD and Baja CA | San Diego | Dike Rock Tide Pools | 32.84 | -117.3 | 2010 | 71 | 35 | 7.5 | 0.105 | | | |
| BTP20105 | Bullard | SD and Baja CA | San Diego | Dike Rock Tide Pools | 32.84 | -117.3 | 2010 | 73 | 35 | 8.2 | 0.1123 | 2.713 | 3.5266 | 0.43 |

| | | | | | | | | | | | | | | |
|---|---|---|---|---|---|---|---|---|---|---|---|---|---|---|
| BTP20109 | Bullard | SD and Baja CA | San Diego | Dike Rock Tide Pools | 32.84 | -117.3 | 2010 | 79 | 34 | 11 | 0.1356 | 3.221 | 1.4127 | 0.43 |
| BTP20108 | Bullard | SD and Baja CA | San Diego | Dike Rock Tide Pools | 32.84 | -117.3 | 2010 | 81 | 36 | 15 | 0.181 | 3.7 | -0.2956 | 0.46 |
| BTP201026 | Bullard | SD and Baja CA | San Diego | Dike Rock Tide Pools | 32.84 | -117.3 | 2010 | 82 | 33 | 20 | 0.2378 | 3.61 | 2.2266 | 0.33 |
| BTP201101 | Bullard | SD and Baja CA | San Diego | Dike Rock Tide Pools | 32.84 | -117.3 | 2010 | 85 | 33 | 20 | 0.2289 | | | |
| BTP201023 | Bullard | SD and Baja CA | San Diego | Dike Rock Tide Pools | 32.84 | -117.3 | 2010 | 86 | 35 | 18 | 0.2086 | 2.92 | 1.1942 | 0.42 |
| BTP201019 | Bullard | SD and Baja CA | San Diego | Dike Rock Tide Pools | 32.84 | -117.3 | 2010 | 94 | 41 | 19 | 0.2041 | | | |
| BLJ20101 | Bullard | SD and Baja CA | San Diego | La Jolla Tide Pools | 32.84 | -117.3 | 2010 | 71 | 35 | 8.6 | 0.1204 | 1.494 | 0.727 | 0.38 |
| CSMI19251 | CASIZ | Greater LA | Los Angeles | Santa Monica Beach | 34.01 | -118.5 | 1925 | 60 | 32 | 6.1 | 0.1025 | 1.391 | 0.0979 | 0.44 |
| CSMI19252 | CASIZ | Greater LA | Los Angeles | Santa Monica Beach | 34.01 | -118.5 | 1925 | 61 | 31 | 5 | 0.0824 | | | |
| CSMI19253 | CASIZ | Greater LA | Los Angeles | Santa Monica Beach | 34.01 | -118.5 | 1925 | 75 | 40 | 13 | 0.1722 | | | |
| CSMI19254 | CASIZ | Greater LA | Los Angeles | Santa Monica Beach | 34.01 | -118.5 | 1925 | 94 | 42 | 19 | 0.2045 | | | |
| CCB19601 | CASIZ | Greater LA | Los Angeles | Cabrillo Beach | 33.71 | -118.3 | 1960 | 56 | 29 | 5.7 | 0.1014 | | | |
| CCB19602 | CASIZ | Greater LA | Los Angeles | Cabrillo Beach | 33.71 | -118.3 | 1960 | 58 | 33 | 7.2 | 0.1246 | | | |
| CCB19603 | CASIZ | Greater LA | Los Angeles | Cabrillo Beach | 33.71 | -118.3 | 1960 | 63 | 32 | 8.6 | 0.1359 | 2.514 | -0.2777 | 0.42 |

| | | | | | | | | | | | | | | |
|---|---|---|---|---|---|---|---|---|---|---|---|---|---|---|
| CPF19601 | CASIZ | Greater LA | Los Angeles | Point Fermin | 33.7 | -118.3 | 1960 | 24 | 11 | 0.7 | 0.0294 | | | |
| CPF19602 | CASIZ | Greater LA | Los Angeles | Point Fermin | 33.7 | -118.3 | 1960 | 49 | 24 | 5 | 0.1004 | | | |
| CPF29603 | CASIZ | Greater LA | Los Angeles | Point Fermin | 33.7 | -118.3 | 1960 | 63 | 34 | 15 | 0.2317 | | | |
| CANI19611 | CASIZ | SB and Ventura | Ventura | Anacapa Island | 34.01 | -119.4 | 1961 | 35 | 14 | 2 | 0.0568 | 1.352 | -0.4926 | 0.35 |
| CANI19612 | CASIZ | SB and Ventura | Ventura | Anacapa Island | 34.01 | -119.4 | 1961 | 50 | 20 | 4.3 | 0.0867 | | | |
| CSJ1973 | CASIZ | SD and Baja CA | San Diego | La Jolla | 32.85 | -117.3 | 1973 | 162 | 59 | 84 | 0.5158 | | | |
| CSNI1981 | CASIZ | SB and Ventura | Ventura | Dutch Harbor San Nicolas Island | 33.22 | -119.5 | 1981 | 111 | 38 | 27 | 0.2477 | | | |
| SALG2003 | CASIZ | SB and Ventura | Santa Barbara | Alegria | 34.47 | -120.3 | 2003 | 50 | 25 | 3.1 | 0.0625 | | | |
| CSCI20032 | CASIZ | SB and Ventura | Santa Barbara | Fraser Point Santa Cruz Island | 34.06 | -119.9 | 2003 | 16 | 8.6 | | | | | |
| CSCI20031 | CASIZ | SB and Ventura | Santa Barbara | Fraser Point Santa Cruz Island | 34.06 | -119.9 | 2003 | 33 | 15 | | | 1.215 | 0.0293 | 0.39 |
| CJL20021 | CASIZ | SB and Ventura | Santa Barbara | Johnsons Lee Santa Rosa Island | 33.91 | -120.1 | 2002 | 29 | 15 | | | | | |
| CJL20022 | CASIZ | SB and Ventura | Santa Barbara | Johnsons Lee Santa Rosa Island | 33.91 | -120.1 | 2002 | 32 | 16 | 1.2 | 0.0377 | 1.258 | -0.8904 | 0.45 |

| | | | | | | | | | | | | | | |
|---|---|---|---|---|---|---|---|---|---|---|---|---|---|---|
| CJL20023 | CASIZ | SB and Ventura | Santa Barbara | Johnsons Lee Santa Rosa Island | 33.91 | -120.1 | 2002 | 47 | 21 | 3.4 | 0.0719 | | | |
| CJL20024 | CASIZ | SB and Ventura | Santa Barbara | Johnsons Lee Santa Rosa Island | 33.91 | -120.1 | 2002 | 52 | 23 | | | | | |
| LPB1915 | LACM | Greater LA | Los Angeles | Portuguese Bend, Palos Verdes Peninsula | 33.74 | -118.4 | 1915 | 56 | 22 | 6.1 | 0.1091 | | | |
| LV252 | LACM | Greater LA | Los Angeles | Venice Beach | 33.98 | -118.5 | 1925 | 35 | 16 | 1.5 | 0.0434 | 1.037 | -0.9048 | 0.38 |
| LV251 | LACM | Greater LA | Los Angeles | Venice Beach | 33.98 | -118.5 | 1925 | 93 | 39 | 12 | 0.1308 | | | |
| LWP22 | LACM | Greater LA | Los Angeles | White Point, Palos Verdes Peninsula | 33.71 | -118.3 | 1922 | 49 | 20 | 3.1 | 0.0629 | | | |
| LNB693 | LACM | Greater LA | Orange County | Newport Beach Jetty | 33.6 | -117.9 | 1969 | 18 | 7.3 | 0.3 | 0.017 | | | |
| LNB692 | LACM | Greater LA | Orange County | Newport Beach Jetty | 33.6 | -117.9 | 1969 | 35 | 15 | 1.5 | 0.0427 | 1.327 | -0.7798 | 0.42 |
| LNB691 | LACM | Greater LA | Orange County | Newport Beach Jetty | 33.6 | -117.9 | 1969 | 53 | 20 | 3.5 | 0.066 | | | |
| LBC766 | LACM | SD and Baja CA | Baja California | E Punta Azufre | 30.4 | -116 | 1976 | 71 | 30 | 14 | 0.1957 | | | |
| LBC763 | LACM | SD and Baja CA | Baja California | E Punta Azufre | 30.4 | -116 | 1976 | 71 | 31 | 14 | 0.1921 | | | |

| | | | | | | | | | | | | | | |
|---|---|---|---|---|---|---|---|---|---|---|---|---|---|---|
| LBC767 | LACM | SD and Baja CA | Baja California | E Punta Azufre | 30.4 | -116 | 1976 | 72 | 38 | 16 | 0.2284 | | | |
| LBC769 | LACM | SD and Baja CA | Baja California | E Punta Azufre | 30.4 | -116 | 1976 | 74 | 38 | 17 | 0.2254 | | | |
| LBC765 | LACM | SD and Baja CA | Baja California | E Punta Azufre | 30.4 | -116 | 1976 | 76 | 41 | 16 | 0.2079 | | | |
| LBC764 | LACM | SD and Baja CA | Baja California | E Punta Azufre | 30.4 | -116 | 1976 | 78 | 40 | 24 | 0.3082 | | | |
| LBC768 | LACM | SD and Baja CA | Baja California | E Punta Azufre | 30.4 | -116 | 1976 | 79 | 40 | 24 | 0.3057 | | | |
| LBC7610 | LACM | SD and Baja CA | Baja California | E Punta Azufre | 30.4 | -116 | 1976 | 79 | 41 | 16 | 0.203 | | | |
| LBC762 | LACM | SD and Baja CA | Baja California | E Punta Azufre | 30.4 | -116 | 1976 | 85 | 40 | 25 | 0.2981 | | | |
| LBC761 | LACM | SD and Baja CA | Baja California | E Punta Azufre | 30.4 | -116 | 1976 | 120 | 46 | 51 | 0.4239 | | | |
| LBCM722 | LACM | SD and Baja CA | Baja California | Rocas Pinaculo, Islas San Benito | 28.26 | -115.6 | 1972 | 42 | 22 | 3.3 | 0.078 | | | |
| LBCM723 | LACM | SD and Baja CA | Baja California | Rocas Pinaculo, Islas San Benito | 28.26 | -115.6 | 1972 | 54 | 27 | 6.3 | 0.116 | | | |
| LBCM721 | LACM | SD and Baja CA | Baja California | Rocas Pinaculo, Islas San Benito | 28.26 | -115.6 | 1972 | 80 | 39 | 18 | 0.2253 | | | |

| | | | | | | | | | | | | | | |
|---|---|---|---|---|---|---|---|---|---|---|---|---|---|---|
| LBC72 | LACM | SD and Baja CA | Baja California | Piedra Colorada, Isla Cedros | 28.14 | -115.4 | 1972 | 50 | 20 | 4.2 | 0.084 | | | |
| LBCS712 | LACM | Baja California Sur | Baja California Sur | Punta Rompiente | 27.72 | -115 | 1971 | 33 | 12 | 1 | 0.0306 | 1.634 | 0.6514 | 0.6 |
| LBCS711 | LACM | Baja California Sur | Baja California Sur | Punta Rompiente | 27.72 | -115 | 1971 | 51 | 24 | 4.2 | 0.0825 | 0.519 | 0.4653 | 0.56 |
| LBCS713 | LACM | Baja California Sur | Baja California Sur | Punta Rompiente | 27.72 | -115 | 1971 | 85 | 37 | 22 | 0.2611 | | | |
| LBCS715 | LACM | Baja California Sur | Baja California Sur | Punta Rompiente | 27.72 | -115 | 1971 | 86 | 36 | 20 | 0.2267 | | | |
| LBCS714 | LACM | Baja California Sur | Baja California Sur | Punta Rompiente | 27.72 | -115 | 1971 | 99 | 41 | 20 | 0.2053 | | | |
| LBCS79 | LACM | Greater LA | Los Angeles | Portuguese Bend, Palos Verdes Peninsula | 33.74 | -118.4 | 1979 | 58 | 27 | 10 | 0.1753 | | | |
| LSB774 | LACM | SB and Ventura | Santa Barbara | Carpinteria State Beach | 34.39 | -119.5 | 1977 | 71 | 32 | 19 | 0.2623 | 4.34 | 0.0547 | 0.42 |
| LSB776 | LACM | SB and Ventura | Santa Barbara | Carpinteria State Beach | 34.39 | -119.5 | 1977 | 86 | 41 | 19 | 0.2159 | | | |
| LSB775 | LACM | SB and Ventura | Santa Barbara | Carpinteria State Beach | 34.39 | -119.5 | 1977 | 97 | 43 | 32 | 0.3285 | | | |
| LSB772 | LACM | SB and Ventura | Santa Barbara | Carpinteria State Beach | 34.39 | -119.5 | 1977 | 101 | 46 | 36 | 0.3576 | | | |

| | | | | | | | | | | | | | | |
|---|---|---|---|---|---|---|---|---|---|---|---|---|---|---|
| LSB773 | LACM | SB and Ventura | Santa Barbara | Carpinteria State Beach | 34.39 | -119.5 | 1977 | 108 | 47 | 47 | 0.437 | | | |
| LSB771 | LACM | SB and Ventura | Santa Barbara | Carpinteria State Beach | 34.39 | -119.5 | 1977 | 136 | 54 | 85 | 0.6236 | | | |
| LPC882 | LACM | SB and Ventura | Santa Barbara | Government Point | 34.45 | -120.5 | 1988 | 27 | 12 | 0.7 | 0.0255 | 1.049 | -1.3983 | 0.6 |
| LPC883 | LACM | SB and Ventura | Santa Barbara | Government Point | 34.45 | -120.5 | 1988 | 28 | 11 | 1.2 | 0.0409 | | | |
| LPC881 | LACM | SB and Ventura | Santa Barbara | Government Point | 34.45 | -120.5 | 1988 | 66 | 30 | 9.1 | 0.1385 | 2.15 | -0.054 | 0.43 |
| SLJ1913 | SBMNH | SD and Baja CA | San Diego | La Jolla | 32.87 | -117.3 | 1913 | 43 | 21 | 3.1 | 0.0724 | 2.276 | 0.2993 | 0.55 |
| SPR1920 | SBMNH | Greater LA | Los Angeles | Playa del Rey | 33.95 | -118.4 | 1920 | 59 | 34 | 5.9 | 0.1005 | | | |
| SAL | SBMNH | Greater LA | Orange County | Anaheim Landing | 33.73 | -118.1 | 1920 | 40 | 24 | 2.4 | 0.0606 | 1.5 | 0.2411 | 0.55 |
| SCOR1936 | SBMNH | SD and Baja CA | San Diego | North Island Coronado Jetty | 32.68 | -117.2 | 1936 | 58 | 26 | 6.1 | 0.1052 | 2.056 | -0.9589 | 0.46 |
| SSLB1944 | SBMNH | Greater LA | Orange County | South Laguna Beach | 33.52 | -117.8 | 1944 | 60 | 28 | 3.8 | 0.0633 | 1.561 | -0.4554 | 0.47 |
| SPD1956 | SBMNH | Greater LA | Los Angeles | Point Dume | 34 | -118.8 | 1956 | 69 | 29 | 8.5 | 0.1232 | 2.466 | -0.3943 | 0.53 |
| SPV1956 | SBMNH | Greater LA | Los Angeles | Palos Verdes | 33.8 | -118.4 | 1956 | 98 | 44 | 29 | 0.2964 | 2.175 | 2.0322 | 0.52 |
| SWP1956 | SBMNH | Greater LA | Los Angeles | Whites Point | 33.72 | -118.3 | 1956 | 80 | 34 | 8.4 | 0.1054 | 1.515 | -0.3017 | 0.42 |

| | | | | | | | | | | | | | | |
|---|---|---|---|---|---|---|---|---|---|---|---|---|---|---|
| SCM1959 | SBMNH | Greater LA | Orange County | Corona del Mar | 33.58 | -117.9 | 1959 | 48 | 22 | 3 | 0.0625 | 1.646 | -0.6432 | 0.49 |
| SCM1957 | SBMNH | Greater LA | Orange County | Corona del Mar | 33.58 | -117.9 | 1957 | 54 | 26 | 3.9 | 0.0726 | 1.742 | -0.3814 | 0.38 |
| SPF19601 | SBMNH | Greater LA | Los Angeles | Point Fermin | 33.7 | -118.3 | 1960 | 46 | 21 | 4.4 | 0.0963 | | | |
| SPF19602 | SBMNH | Greater LA | Los Angeles | Point Fermin | 33.7 | -118.3 | 1960 | 66 | 31 | 11 | 0.1639 | | | |
| SPLEIS | SBMNH | Greater LA | Orange County | Newport Mesa | 33.63 | -117.9 | | 100 | 45 | 30 | 0.3034 | 2.6 | 1.1282 | 0.43 |
| UDM19391 | UCMP | SD and Baja CA | San Diego | Mission Bay | 32.78 | -117.2 | 1939 | 35 | 18 | 0.9 | 0.0258 | | | |
| UDM19392 | UCMP | SD and Baja CA | San Diego | Mission Bay | 32.78 | -117.2 | 1939 | 42 | 23 | 2.7 | 0.0646 | 1.84 | -0.7095 | 0.44 |
| UDM19393 | UCMP | SD and Baja CA | San Diego | Mission Bay | 32.78 | -117.2 | 1939 | 59 | 33 | 4.2 | 0.0718 | | | |
| USD19391 | UCMP | SD and Baja CA | San Diego | San Diego | 32.7 | -117 | 1939 | 41 | 20 | 2 | 0.0489 | 1.253 | -0.3626 | 0.48 |
| USD19392 | UCMP | SD and Baja CA | San Diego | San Diego | 32.7 | -117 | 1939 | 54 | 24 | 4.1 | 0.0762 | | | |
| USD19393 | UCMP | SD and Baja CA | San Diego | San Diego | 32.7 | -117 | 1939 | 56 | 26 | | | | | |
| USD19394 | UCMP | SD and Baja CA | San Diego | San Diego | 32.7 | -117 | 1939 | 66 | 30 | | | | | |

| | | | | | | | | | | | | | | |
|---|---|---|---|---|---|---|---|---|---|---|---|---|---|---|
| USD19395 | UCMP | SD and Baja CA | San Diego | San Diego | 32.7 | -117 | 1939 | 73 | 33 | 11 | 0.1431 | | | |
| UDM19481 | UCMP | SD and Baja CA | San Diego | Del Mar | 33 | -117 | 1948 | 57 | 27 | 2.7 | 0.0475 | | | |
| UBC19582 | UCMP | SD and Baja CA | Baja California | Punta Banda | 31.7 | -117 | 1958 | 34 | 16 | | | | | |
| UBC19581 | UCMP | SD and Baja CA | Baja California | Punta Banda | 31.7 | -117 | 1958 | 61 | 29 | 8.4 | 0.1382 | 2.956 | 0.5914 | 0.56 |
| UDP1955 | UCMP | Greater LA | Orange County | Dana Point | 33.5 | -118 | 1955 | 17 | 9.1 | 0.3 | 0.0148 | | | |
| USB19585 | UCMP | SD and Baja CA | San Diego | Solana Beach | 33 | -117 | 1958 | 15 | 7.1 | | | | | |
| USB19584 | UCMP | SD and Baja CA | San Diego | Solana Beach | 33 | -117 | 1958 | 38 | 21 | | | 1.92 | -1.1038 | 0.49 |
| USB19582 | UCMP | SD and Baja CA | San Diego | Solana Beach | 33 | -117 | 1958 | 45 | 24 | | | | | |
| USB19583 | UCMP | SD and Baja CA | San Diego | Solana Beach | 33 | -117 | 1958 | 46 | 23 | | | | | |
| USB19581 | UCMP | SD and Baja CA | San Diego | Solana Beach | 33 | -117 | 1958 | 63 | 33 | | | | | |
| UCB1961 | UCMP | Greater LA | Los Angeles | Cabrillo Beach | 34 | -119 | 1961 | 18 | 9.6 | 0.2 | 0.0113 | | | |
| UTB1960 | UCMP | Greater LA | Los Angeles | Topanga Beach | 34.04 | -118.6 | 1960 | 18 | 10 | 0.3 | 0.0139 | | | |
| UVB1961 | UCMP | Greater LA | Los Angeles | Venice Beach | 34 | -118 | 1961 | 61 | 32 | 5 | 0.0817 | 1.904 | -0.0711 | 0.5 |